Synthesis and Properties modulation of novel functional degradable polymers by means of fine tuning of their structure

Kamolchanok Sarisuta

RÉPUBLIQUE FRANÇAISE
Liberté Égalité Fraternité

Université de Toulouse

Doctorat de l'Université de Toulouse

délivré en co-tutelle avec Collège doctoral de sciences et techniques de Nara

préparé à l'Université Toulouse III - Paul Sabatier

Synthèse et Modulation des Propriétés de Nouveaux Polymères Dégradables Fonctionnels par le Contrôle Fin de Leur Structure

---

Thèse présentée et soutenue, le 23 juillet 2024 par

Kamolchanok SARISUTA

École doctorale
SDM - SCIENCES DE LA MATIERE - Toulouse

Spécialité
Chimie Macromoléculaire et Supramoléculaire

Unité de recherche
LHFA - Laboratoire Hétérochimie Fondamentale et Appliquée

Thèse dirigée par
Blanca MARTIN-VACA et Hiroharu AJIRO

Composition du jury
M. Gwénaël RAPENNE, Président, Université Toulouse III - Paul Sabatier
Mme Véronique BENNEVAULT, Rapporteure, Université d'Evry
M. BONDUELLE COLIN, Rapporteur, CNRS Aquitaine
Mme Catherine LEFAY, Examinatrice, Aix-Marseille Université
Mme Blanca MARTIN-VACA, Directrice de thèse, Université Toulouse III - Paul Sabatier
M. Hiroharu AJIRO, Co-directeur de thèse, Nara Institute of Science and Technology

Membres invités
M. Tsumoru MORIMOTO, Nara Institute of Science and Technology
Mme Nalinthip CHANTHASET, Nara Institute of Science and Technology

Synthesis and Properties Modulation of Novel Functional Degradable Polymers by Means of Fine Tuning of Their Structure

Kamolchanok SARISUTA

A thesis submitted in fulfillment of the requirements for
the degree of
Doctor of Philosophy (Engineering)

September 2024

Nara Institute of Science and Technology

Université Toulouse III - Paul Sabatier

Contents

List of Abbreviations ..... **i**
PREFACE ..... **v**
Materials and Instruments ..... **vi**
Acknowledgements ..... **xi**
General Introduction **1**
Reference 21
Chapter I **32**
The Design of pH-Responsive Functional Chain Ends of Polylactides for Trigged Aggregation *32*
1.1 Introduction 32
1.2 Results and Discussions 46
1.3 Conclusions 65
1.4 Experimental 66
1.5 References 69
Chapter II **77**
Copolymerization of Trimethylene Carbonate and 5-Methylene-1,3-Dioxane-2-One: Control of Functionalization in Perfect Random Copolymers via Thiol-Ene Reaction *77*
2.1 Introduction 77
2.2 Results and Discussions 99
2.3 Conclusions 137
2.4 Experimental 139
2.5 References 144
Chapter III **158**
Evaluation of Biocompatible Properties in Random Copolymers of Trimethylene Carbonate and 5-Methylene-1,3-Dioxane-2-One with Controlled Introduction of Diol and Carboxylic Acid *158*
3.1 Introduction 158
3.2 Results and Discussions 172
3.3 Conclusions 192
3.4 Experimental 194
3.5 References 197
Chapter IV **207**
The design of side chain crosslinking to modulate the properties of copolymers *207*
4.1 Introduction 207
4.2 Results and Discussions 218
4.3 Conclusions 232
4.4 Experimental 233
4.5 References 235
General Conclusion **240**

Résumé en Français 245
Abstract 287
Résumé 288

List of Abbreviations

5CCs	Five-membered-ring cyclic carbonates
6CCs	Six-membered-ring cyclic carbonates
7CCs	Seven-membered-ring cyclic carbonates
AM	Activated-monomer
ACE	Activated-chain-End
APCs	Aliphatic polycarbonates
APEs	Aliphatic polyesters
AIBN	Azobisisobutyronitrile
BDM	1,4-benzenedimethanol
BEMP	2-*tert*-butylimino-2-diethylamino-1,3-dimethylperhydro-1,3,2-diazaphosphorine
BnOH	Benzyl alcohol
BSA	Bovine serum albumins
BSL	Beckingham-Sanoja-Lynd method
BPF	Bovine plasma fibrinogen
bis-MPA	2,2-bishydroxy(methyl)propionic acid
$CaCO_3$	Calcium carbonate
CaO	Calcium Oxide
CCs	Cyclic carbonates
$CDCl_3$	Deuterated chloroform
CH_3CN	Acetonitrile
CO_2	Carbon dioxide
$Đ$	Polydispersity index
D_2O	Deuterium oxide
DBU	1,8-diazabicyclo[5.4.0]undec-7-ene
DCM	Dichloromethane
DFT	Density functional theory
DLLA	*D,L*-lactide
DMAP	4-*N,N*-dimethylaminopyridine
DMBA	3,5-dimethoxybenzyl alcohol
DMF	Dimethylformamide
DMPA	Medroxyprogesterone acetate
DOX	Doxorubicin
DP	Degree of polymerization

DPP	Diphenyl phosphate
DSC	Differential scanning calorimetry
Et_2O	Diethyl ether
EtOH	Ethanol
EtOAc	Ethyl acetate
ε-CL	ε-caprolactone
exTMC	5-Methylene-1,3-dioxane-2-one
Fe_2O_3	Ferric oxide
FT-IR	Fourier-transform infrared spectroscopy
Γ	Reactivity ratio
G'	Storage modulus
G"	Loss modulus
H_2	Hydrogen
H_2O	Water
HMF	5-hydroxymethylfurfural
HOTf	Trifluoromethanesulfonic acid
LA	Lactide
L-LA	L-lactide
MALDI-TOF	Matrix-Assisted Laser Desorption/Ionization- Time-of-Flight
m_d	Mass of thedried polymer samples
MeOH	Methanol
MS	Mass Spectrometry
MSA	Methanesulfonic acid
M_n	Number average molecular weight
m_w	Mass of the wet polymer samples
M_w	Weight average molecular weight
n	Average number of monomers per polymer chain
NEt_3	Triethylamine
NHCs	*N*-heterocyclic carbenes
NMR	Nuclear Magnetic Resonance
PBS	Phosphate-buffered saline solutions
PCL	Poly (ε-caprolactone)
PCs	Polycarbonates
$Pd(OAc)_2$	Palladium(II) Acetate
Pd/C	Palladium on carbon
PDLA	Poly (*D,D*-lactide)

PDO	1,3-propanediol
PEC	Poly (ethylene carbonate)
PEs	Polyesters
PEO	Poly (ethylene oxide)
PEF	Poly (ethylene furanoate)
PEG	Poly (ethylene glycol)
PGA	Poly (glycolic acid)
PHA	Poly (3-hydroxyalkanoate)
PLA	Poly (lactide)
PLGA	Poly (lactic acid-*co*-glycolic acid)
PLLA	Poly (*L*-lactic acid)
PPC	Poly(propylene carbonate)
PTMC	Poly (trimethylene carbonate)
PTX	Paclitaxel
PUEP	Polyurethane elastomer prepolymer
RcoOP	Ring-opening copolymerization
ROP	Ring-opening polymerization
SC	Stereo-complexation
SEC	Size-exclusion chromatography
SEM	Scanning electron microscope
$Sn(Oct)_2$	Tin(II) 2-ethylhexanoate
T_{10}	The temperature at which the weight loss is 10%
TBD	Triazabicyclodecene
T_c	Crystallization temperature
T_d	Degradation temperature
TGA	Thermal gravimetric analysis
T_g	Glass transition temperature
TOBnTMC	5-(((3-(benzyloxy)propyl)thio)methyl)-1,3-dioxan-2-one
THF	Tetrahydrofuran
TiO_2	Titanium dioxide
T_m	Melt temperature
TMC	Trimethylene carbonate
TMP	2,2,6,6-tetramethylpiperidine
TU	1-(3,5-bis(trifluoromethyl)phenyl)-3-cyclohexyl-2-thiourea
UV-Vis	UV-Vis spectroscopy
W_i	Initial weight before soaking

W_d	Dried weight of the films at specific day
XRD	X-ray diffraction
ZnO	Zinc oxide
$\Delta_r H$	Enthalpy

PREFACE

This PhD thesis is part of a joint supervision program leading to a double degree between the University of Toulouse 3, Paul Sabatier, (UPS) in Toulouse, France, and the Nara Institute of Science and Technology (NAIST) in Nara, Japan. The research was conducted at the Laboratoire de Hétérochimie Fondamentale et Appliquée (LHFA) with the Ligands Bifonctionnels et Polymères Biodégradables (LBPB) team at UPS, and at the Nanomaterials and Polymer Chemistry laboratory within the Division of Materials Science, Graduate School of Science and Technology, NAIST.

Chapter I details experiments conducted at the Nanomaterials and Polymer Chemistry laboratory (NAIST) and the results were published in Sarisuta, K.; Iwami, M.; Martín-Vaca, B.; Chanthaset, N.; Ajiro, H. pH Effect on Particle Aggregation of Vanillin End-Capped Polylactides Bearing a Hydrophilic Group Connected by a Cyclic Acetal Moiety. *Langmuir* **2023**, 39 (11), 3994–4004.
Chapter II encompasses work performed at LBPB (UPS) and the findings were published in Palenzuela, M.; Sarisuta, K.; Navarro, M.; Kumamoto, N.; Chanthaset, N.; Monot, J.; Ajiro, H.; Martín-Vaca, B.; Bourissou, D. 5-Methylene-1,3-Dioxane-2-One: A First-Choice Comonomer for Trimethylene Carbonate. *Macromolecules* **2023**, 56 (2).
Chapters III and IV present experiments conducted at the Nanomaterials and Polymer Chemistry laboratory (NAIST).

Materials and Instruments

Materials

Chapter I, all reactions were performed under an inert atmosphere of nitrogen, using standard Schlenk techniques. (*L,L*)-lactide (Tokyo Chemical Industry (TCI), Ltd., Japan) and (*D,D*)-lactide (Musashino Chemical Laboratory, Ltd.,) were recrystallized in ethyl acetate : hexane (3:1, (v/v) and then dried in vacuo at 40 °C overnight. Vanillin (Tokyo Chemical Industry (TCI), Ltd., Japan) was used without purification. Benzaldehyde and anhydrous toluene were purchased from wako pure chemical. *p*-Toluenesulfonic acid monohydrate, buffer solution pH 7.4 (KH_2PO_4-NaOH), trimethylolethane, epichlorohydrin, and $Sn(Oct)_2$ catalyst were also purchased from TCI and dried with molecular sieve 3A overnight. Sodium hydride, 5M Hydrochloric acid, 5M Sodium Hydroxide Solution, and *p*-Toluenesulfonyl Chloride were purchased from Nacalai tesque.

Chapter II, III, and IV, all reactions were performed under an inert atmosphere of argon, using standard Schlenk techniques. Tetrahydrofuran (THF), ethyl acetate (EtOAc), diethyl ether (Et_2O) and dichloromethane (DCM) were dried with a Braun solvent-purification system. $CDCl_3$ was dried over activated molecular sieves (3Å) and filtered. Trimethylene carbonate (TMC) (> 98%, TCI Europe), was dried in THF solution with activated molecular sieves (3Å), recrystallized and stored in a glovebox at -20°C. 5-methylene-1,3-dioxane-2-one (exTMC) was dried in DCM and Et_2O solution with activated molecular sieves (3Å), recrystallized and stored in a glovebox at -20°C. Methane sulfonic acid (MSA) (Fluka) was dried by azeotropic distillation in toluene with dean-stark and then stored under argon in a glovebox. Propane-1,3-diol (PDO) were dried by preparing dichloromethane solutions and addition of activated molecular sieves (3Å). After stirring overnight and filtration, the solvent was evaporated and the initiators/catalysts were stored under argon in a glovebox. Protic initiators and other organocatalysts (Dimethoxybenzyl alcohol (DMBA), 1,4-benzenedimethanol (BDM), propan-1,3-diol (PDO), 1,8-diazabicyclo[5.4.0]undec-7-ene (DBU), 1,5,7-triazabicyclo[4.4.0]dec-5-ene (TBD), 1-(3,5-bis(trifluoromethyl)phenyl)-3-cyclohexyl-2-thiourea (TU), diphenylphosphate (DPP)) were dried by preparing dichloromethane solutions and addition of activated molecular sieves (3Å). After stirring overnight and filtration, the solvent was evaporated and the initiators/catalysts were stored under argon in a glovebox. 2,2-dimethoxy-2-phenyl acetophenone (DMPA) was purchased from

Fujifilm Wako Pure Chemical (WAKO), Japan. Thioglycolic acid (TGA), thiolglycerol (TGC), magnesium acetate tetrahydrate, sodium acetate trihydrate, iron(II) acetate, and zinc(II) acetate were purchased from Tokyo Chemical Industry (TCI), Japan. Pierce™ BCA Protein Assay Kit was purchased by ThermoFisher scientific. Bovine serum albumins (BSA) and bovine plasma fibrinogen (BPF) were purchased from Sigma-Aldrich (St. Louis, U.S.A.).

Measurement

NAIST, Japan;

SEC analyses. The number-average and weight-average molar masses (M_n and M_w, respectively) and molar mass distributions ($Đ$) of the polymer samples were determined by size exclusion chromatography (SEC) with polystyrene standards at 40°C, equipped with RI-2031 and UV-2075 (Deuterium lamp wavelength 264 nm). Two commercial columns, TSKgel SuperH4000 and TSKgel GMHXL were connected in series and tetrahydrofuran (THF) was used as an eluent.

NMR analyses. ^{1}H NMR spectra were measured with JEOL ECX-400P, JNM-ECX500 at 400 MHz and 500MHz. at room temperature and chemical shifts are reported in ppm relative to Me_4Si as an external standard.

UV-Vis analyses. The aggregation rate of particles was measured by UV-2600 (Shimadzu Corporation, Japan) at 500 nm for chapter I and 481 nm for chapter III.

SEM analyses. The surface morphology of the polymers was observed using a scanning electron microscope (SEM) SU6600 (Hitachi Corporation, Ltd., Japan).

Mass analyses. Mass spectroscopy was determined by Bruker Autoflex II (Bruker Daltonics K. K., Japan) for MALDI-TOF and JEOL AccuTOF, JMS-T100LC (JEOL Ltd., Japan).

XRD analyses. Attenuated total reflection infrared (ATR-IR) spectroscopy were obtained by IRAffinity-1S (Shimadzu). X-ray diffraction (XRD) patterns were taken at 2θ = 5—35°, scan rate of 2°Cmin^{-1} and CuKα (λ = 0.154 nm) as the X-ray source at 50 kV and 300 mA with a Ni filter by a Rigaku RINT-TTRIII/NM.

DSC analyses. Differential scanning calorimetry (DSC) spectra were analyzed by Hitachi DSC6200 in the atmosphere with a temperature ramp rate of 10℃ min^{-1} in the range of 100 and 350℃

TGA analyses. The thermal stability of the polymer was determined by a thermo-gravimetric analyser TGA-50 (Shimadzu) under nitrogen atmosphere with 10°C/min flow rate to 500°C.

UPS, France;

SEC analyses. The number-average and weight-average molar masses (M_n and M_w, respectively) and molar mass distributions ($Đ$) of the polymer samples were determined by size exclusion chromatography (SEC) at 35 °C with a Waters 712 WISP high-speed liquid chromatograph equipped with a R410 refractometer detector. Tetrahydrofuran (THF) was used as the eluent and the flow rate was set up at 1.0 mL/min. A SHODEX pre-column (polystyrene AT806M/S M_w = 50 000 000 g/mol) and two STYRAGEL columns (HR1, 100 – 5 000 g/mol and HR 4E, 50 – 100 000 g/mol) were used. Calibrations were performed using polystyrene standards (400 – 100 000 g/mol).

NMR Analyses. ^1H and ^{13}C NMR Spectra were recorded in $CDCl_3$ on BRUKER Avance 300, 400 and 500 MHz spectrometers at room temperature and chemical shifts are reported in ppm relative to Me_4Si as an external standard. ^1H measurements were used to determine the monomer conversion, the degree of polymerization (DP_{NMR}), and the end group fidelity. Monomer conversion was determined from the relative intensities of the OCH_2 signals for the monomers (multiplet at δ 4.45 and 4.86 ppm for TMC and exTMC, respectively) and polymer (multiplet at δ 4.25 and 4.70 ppm for PTMC and PexTMC, respectively). DP_{NMR} was determined from the relative intensities of the OCH_2 signals for the polymer and the terminal CH_2OH signals (multiplet at δ 3.76 ppm for PTMC and doublet at δ 4.20 ppm for PexTMC). Initiation efficiency was determined from the relative intensities of the the benzyl terminal moiety (singlet at δ 5.13 ppm) and the terminal CH_2OH signals.

MALDI-TOF MS analyses. MALDI-TOF-MS analyses were performed on a MALDI MicroMX from Waters equipped with a 337 nm nitrogen laser. An accelerating voltage of 20 kV was applied. Mass spectra of 1000 shots were accumulated. The polymer sample was dissolved in THF at a concentration of 1 mg mL^{-1}. The cationization agent used was NaI dissolved in THF at a concentration of 1 mg mL^{-1}. The matrix used was dithranol and was dissolved in THF at a concentration of 10 mg mL−1. Solutions of matrix, salt, and polymer were mixed in a volume ratio of 10:1:1 respectively. The mixed solution was hand-spotted on a stainless steel MALDI target and left to dry. The spectrum wasrecorded in the reflectron mode. Baseline corrections and data analyses were performed using MassLynx version 4.1.

Differential Scanning Calorimetr (DSC) Thermal analyses were performed with

a Mettler Toledo DSC1 apparatus, equipped with a FRS6 sensor, a gas controller GC200, and a TC100 chiller. Dry nitrogen with a flow rate at 20 $mL.min^{-1}$ was used as purge gas. Samples were weighed in aluminum pans (40 µL), sealed under inert gas in a glovebox. Thermal analysis were performed between -30°C to 80°C on heating and cooling, at 3 different rates: 6 $K.min^{-1}$, 4 $K.min^{-1}$, and 2 $K.min^{-1}$. Transition temperatures were determined by extrapolation at zero speed of the onset value.

X-Ray diffraction study. Crystallographic data were collected at 193(2) K on a Bruker-AXS D8-Venture equipped with a PHOTON III detector, using MoK_α radiation (λ=0.71073 Å). Phi- and omega-scans were used. An empirical absorption correction was applied. The structures were solved using an intrinsic phasing method (SHELXT), and refined using the least-squares method on F^2. All non-H atoms were refined with anisotropic displacement parameters. All H atoms bonded to the carbon atoms were placed on calculated positions and refined isotropically using a riding model.

Crystallographic data (excluding structure factors) have been deposited to the Cambridge Crystallographic Data Centre as supplementary publication no. CCDC 2212167. These data can be obtained free of charge *via* www.ccdc.cam.uk/conts/retrieving.html (or from the CCDC, 12 Union Road, Cambridge CB2 1EZ, UK; fax: (+44) 1223-336-033; or deposit@ccdc.cam.ac.uk).

DFT Calculations. DFT calculations were done by Prof L Maron and Dr I Del Rosal from the University of Toulouse 3. They were carried out with the Gaussian 09 suite of programs. Geometries were fully optimized in chloroform, using SMD solvation model without symmetry constraints, employing the B3PW91 functional. The nature of the extrema was verified by analytical frequency calculations. The calculation of electronic energies and enthalpies of the extrema of the potential energy surface (minima and transition states) has been performed at the same level of theory as the geometry optimizations. For the H, C and O atoms a Pople's double-ζ basis set 6-31G(d,p) was used.

Acknowledgements

First and foremost, I extend my deepest gratitude to Prof. Hiroharu Ajiro and Prof. Blanca Martin-Vaca. Their invaluable support and guidance have been crucial throughout my research journey. I am especially thankful for their assistance, mentorship, and understanding during my academic tenure in the double degree program at the Nanomaterials and Polymer Chemistry Laboratory, Nara Institute of Science and Technology, Nara, Japan, and LHFA, Paul Sabatier University, Toulouse, France. I am extremely grateful to my advisors for their encouragement and support in every aspect of both my research and daily life during this PhD program. Without their expert guidance and supervision, this achievement would not have been possible.

I would also like to extend my sincere thanks to Assistant Prof. Nalinthip Chanthaset, Prof. Julien Monot, Dr. Didier Bourissou, and my co-supervisors; Prof. Gwenael Rapenne and Assoc. Prof. Tsumoru Morimoto, for their invaluable guidance and advice. Their kindness and contributions were instrumental to my success in this PhD program. I have gained immense knowledge from both, and I will remain forever grateful for their mentorship.

Additionally, my heartfelt appreciation goes to Assoc. Prof. Wanpen Tachaboonyakiat for encouraging me to pursue graduate studies and for providing the opportunity to work with Prof. Hiroharu Ajiro.

I would like to express my profound appreciation to all staff and technicians at both NAIST and UPS for their invaluable help and guidance throughout my studies.

This thesis would not have been successful without the genuine support, enriching academic discussions, and the welcoming environments provided by the members of the Nanomaterials and Polymer Chemistry Laboratory in Japan and LBPB in France. I am also grateful to NAIST and CNRS for their financial support, which was indispensable to the completion of my research.

In addition, I would like to sincerely thank all the members of the Nanomaterials and Polymer Chemistry Laboratory and the LBPB team for their warm welcome and the friendship they extended to me. Their collegiality greatly enriched my experience,

making my time both productive and enjoyable.

At Ajiro-lab, I am deeply grateful to:

Palmy: You're more than just a lab mate; you're like my ride or die. Thanks for being there through every high and low, and for all those impromptu trips that kept us sane! Thank you for always make me smile and also crying with me in every situation.
LeeYae: Your kindness has a unique way of lighting up my darkest days. I'm truly grateful for your constant presence and the smiles you've brought into my life. Thank you for never leaving me alone in any situation.
Tsujimoto: It has been an absolute pleasure to meet you. I am immensely appreciative of all your help and our shared moments, especially those delightful ramen outings.
Narukawa: I sincerely thank you for making my time at NAIST so enriching and for being there during those challenging days. Your support has meant the world to me.
Ayun: I could not have wished for a better companion throughout this journey. Your steadfast support in every situation has been a great comfort to me.
Sapto: Your humor and your culinary skills have truly lightened up our lab environment. I am deeply grateful for your friendship and technical assistance.
Ren: Thank you for making the effort to speak English, enhancing our lab's inclusive atmosphere and helping everyone feel more connected. I can tell that you are the initiator and catalyst that can make monomer (person) become polymer (group).
Shuga: Your support during challenging times and your invaluable help as my translator have been greatly appreciated.
Tojo: You've added some serious color to my life and been a huge help, especially with translating those tricky French or Japanese phrases.
Kanoko: Thank you for being an incredible sister throughout this journey, making every moment at NAIST worthwhile.
Nakanishi: Your consistent encouragement has been a key motivator throughout my PhD journey.

Special thanks also go to the LBPB team:
Miguel: Your guidance was crucial in navigating the complex pathways of my research. Your insights and expertise were invaluable.
Julien B.: Your invaluable guidance and suggestions were essential in navigating the complexities of my research. Thank you for imparting new knowledge and engaging in productive discussions.

Liyao: Thank you for making Toulouse feel like home and for caring for me at every step of this journey.
Marte: Your companionship on our weekend adventures has been a breath of fresh air, encouraging me to embrace the beauty of nature.
Maceline: Your kindness in helping me solve various issues and sharing the delightful tastes of French cuisine has enriched my experience immensely.

Moreover, also a great thanks to all of my international friends (Haiying, Chan, Jee, Enzo, Josh, Shumpei, Takaaki, Risa, Rae, Surgio, Uncle Lee, Andy, Tager, Aissam, Taichi, Alan, Nag, and the many others) and Thai student community (Tem, Bam, Eve, Bam, Pong, Man, Jamie, Anchan) at NAIST for creating a home away from home and reminding me that I am never alone.

Additional special thanks to:

Chihiro: for all those deep talks and fun times, and for always being my ready buddy to grab a drink and hit the road that anyone could ask for.
Boom: for being my personal secretary and always being ready to assist.
Tan: for the laughter and for staying by my side until the very last moment at NAIST.
Kanom: for your support and for being there whenever I needed you.
Lean: for always being willing to lend a hand.
Shiho: for the wonderful memories we shared both in France and Japan.
Sharhoor: for your unfailing support and care.
Pablo: for being a supportive friend and confidant through thick and thin.

Your collective support has shaped my PhD journey into an incredibly fulfilling experience, for which I am profoundly thankful.

Finally, I extend my heartfelt gratitude to my beloved family. To my parents, Kittiya SARISUTA and Mongkol SARISUTA, thank you for your unwavering support, love, and presence through every step of this journey. Additionally, I hold dear the memory of my beloved grandparent; though you are no longer here, I feel your encouragement and embrace, as if from beyond the stars.

April, 2024
Kamolchanok SARISUTA (Ann)

General Introduction

Nowadays, the plastic waste such as polyethylene, polypropylene, and polyvinylchloride pose a significant environmental problem due to increasing difficulties of managing plastic waste that resist microbial degradation.[1] Hence, biodegradable polymers are being developed to be used as an alternative for non-biodegradable polymer materials in a wide array of applications.[2] The use of biodegradable polymers offers significant environmental benefits, including the regeneration of raw materials, biodegradation, and a reduction in carbon dioxide emissions that contribute to global warming. Microorganisms such as bacteria and fungi can consume these polymers, converting them into H_2O, CO_2, and methane. Additionally, biodegradable polymers offer medical advantages due to their biocompatibility, making them suitable for use within the human body. These polymers are designed to degrade under physiological conditions, can be engineered to degrade at specific rates through controlled mechanisms, and their byproducts are readily eliminated *via* the body's metabolic pathways.[3 4] The biodegradation process depends on the composition of the material.[5] The polymer morphology, polymer structure, chemical and radiation treatments, and polymer molecular weight are all parameters that influence the biodegradation process.[6]

In general, biodegradable polymers are classified into two groups based on their origin which are natural biopolymers and synthetic biopolymers. Natural biopolymers are derived from renewable or biological sources such as animal, plant, marine, and microbial sources, while synthetic biodegradable polymers are manufactured chemically.[7] In recent years, synthetic biodegradable polymers have garnered significant attention due to their ease of manipulation and high batch-to-batch reproducibility. These polymers degrade into non-toxic, and environmentally friendly materials,[8] demonstrating potential across a wide range of applications in the biomedical field. Key applications include drug delivery vehicles,[9,10] support structures for both hard and soft tissues,[11,12] and cardiac therapy[13,14] (**Figure 1**). Gao et al. reported that poly(lactide-*co*-glycotide) (PLGA) microspheres, integrated into gelatin/chitosan/hyaluronan scaffolds, were fabricated using freeze-drying and subsequently crosslinked with 1-ethyl-3-(3-dimethylaminopropyl) carbodiimide). They found that scaffolds containing 50% PLGA microspheres exhibited improved physical performance and preserved biocompatibility.[9] Research efforts have investigated polymers such as poly(*L*-lactic acid) (PLLA), polyglycolic acid (PGA), poly[(*D,L*-lactide)-*co*-(glycolic acid)] copolymer (PDLGA), and ε-polycaprolactone (PCL) for use in bioabsorbable polymer-coated drug-eluting stents.[14]

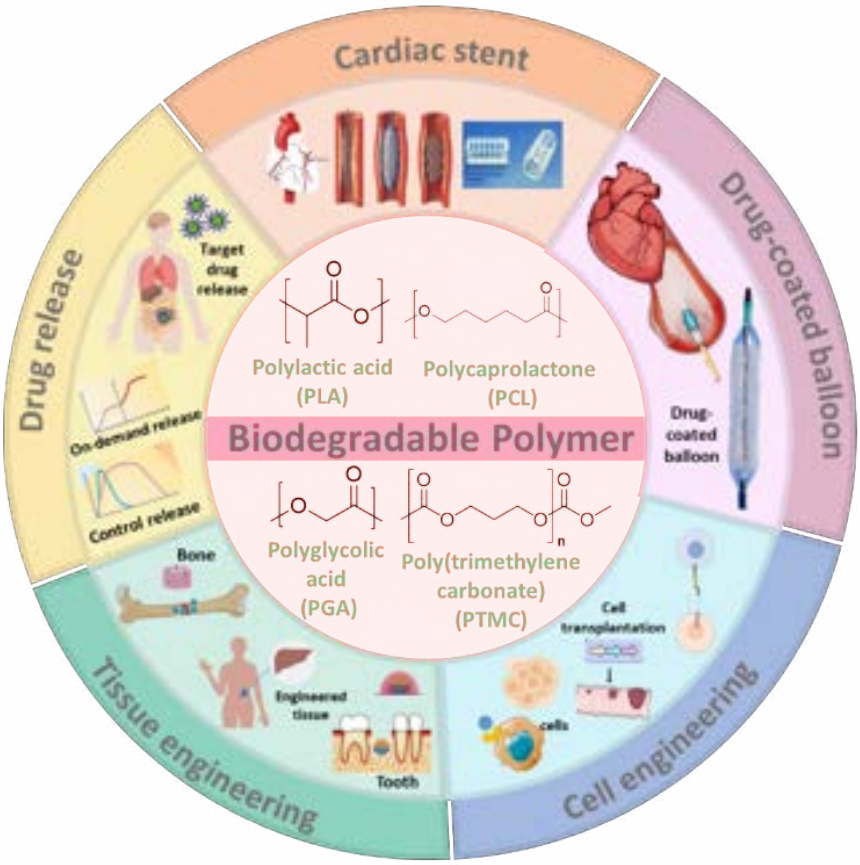

Figure 1. Major biodegradable polymer used in medical applications[15]

An important target in biomedical materials research is to develop materials that exhibit biocompatibility, controlled degradation, and high performance customized for their specific application. Recently, the polymer science advancement has emphasized the significance of designing molecular structures as a key method for material modification, where the branched structure offers rich structural designability and properties modifiability. Therefore, monomer and polymer designs are essential to produce various biomaterials and fostering development of alternative polymers that are fit-for-purpose, yet it is still currently have some limitations in practical use (**Figure 2**). The structure and properties of biodegradable polymer can be controlled by both physical and chemical modification. However, synthetic biodegradable polymers often belong to the polyester or polycarbonate families and include materials like poly(lactide) (PLA) and poly(trimethylene carbonate) (PTMC). Their diverse chemistry allows for the synthesis of polymers with adjustable physical and mechanical properties, making them more attractive than natural alternatives such as polysaccharides and proteins.[16]

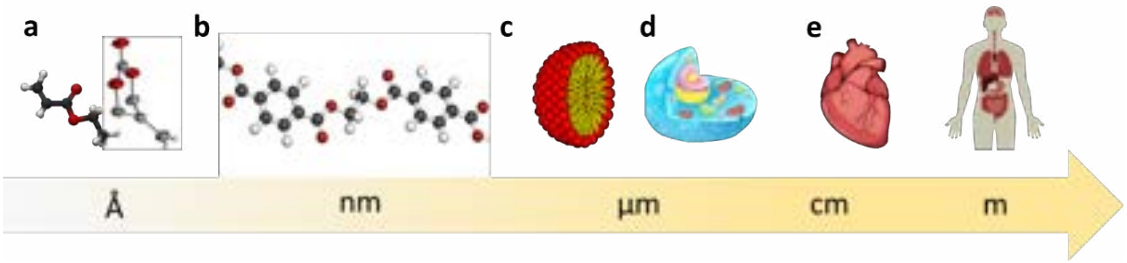

Figure 2. Illustration of scale difference from molecular design to biomedical application. (a) Monomer design with functional moieties and biocompatible structure. (b) Polymer structure control, including factors involving tacticity, block and random copolymers, graft polymers and star copolymers. (c) Nano structure control through polymer assembly, such as micelle and segregated films. (d) Cell experiments, such as particles for drug delivery and gene delivery. (e) Biomaterials for medical application to tissues and organs.

Aliphatic polyesters (APEs) and polycarbonates (APCs) serve as the cornerstone of biodegradable polymers and are potential candidates for clinical applications owing to their low toxicity, biocompatibility, and biodegradability. Monomeric precursors to polyesters and polycarbonates can be sourced from biomass or waste gas *via* various biological or chemical transformations.[17,18] For instance, carbon dioxide is from waste gas, combined with fossil-derived propylene oxide to create propylene carbonate polyols.[17,18] Triglycerides extracted from vegetable oils are transformed into long-chain aliphatic polyesters.[17,18] Moreover, starch, a natural carbohydrate polymer, is converted into glucose and subsequently used to synthesize polymers such as poly(ethylene furanoate) (PEF) and PLA[17,18]. A variety of polymerization methods are now available for polymer synthesis with diverse backbone topologies and side-chain functionalities. Additionally, the ester and carbonate linkages in novel polymer backbones can be enzymatically or chemically degraded, providing new options for the life cycle of these materials.[17,19] Enzymatic degradation naturally occurs in microorganisms through hydrolases that catalyze material hydrolysis. This process primarily involves esterases that hydrolyze ester bonds and proteases that cleave peptide bonds. The enzymatic degradation of polyesters generally occurs through surface erosion, meaning the bulk of the material remains unchanged while properties such as molar mass and crystallinity are preserved.[17,19] Concurrently, lower molar mass fragments are released from the surface. Chemical degradation of these materials is explored through acid- or base-catalyzed

hydrolysis. The overall degradation process is intricate, influenced by intrinsic degradation kinetics and water diffusion rates. Factors affecting water diffusion include the polymer's hydrophobicity, shape, and surface area, whereas intrinsic degradation kinetics are shaped by environmental conditions like pH, temperature, molecular weight, and polymer microstructures.[17,19] However, both ester and carbonate groups are susceptible to hydrolysis whereby polyesters typically undergo bulk degradation, whereas surface erosion predominates for polycarbonates (**Figure 3**).[20,21] When polymers undergo surface erosion, they gradually lose mass from the outer surface inward, maintaining their original shape. In contrast, bulk erosion results in the mass loss and degradation of the entire polymer, not limited to the surface.[20,21] Feijen et al. assessed the degradation behavior of poly(1,3-trimethylene carbonate) [poly(TMC)] and its copolymers with *D,L*-lactide (DLLA) or caprolactone (CL) by subcutaneously implanting polymer films in rats, monitoring the degradation over periods up to one year. Poly(TMC) primarily undergoes surface erosion driven by cellular-mediated processes. In contrast, the copolymers showed slower degradation than poly(TMC), due to autocatalyzed bulk hydrolysis, with a particular tendency to break down ester bonds. Notably, the TMC-DLLA copolymer degraded 20 times faster than its TMC-CL counterpart.[22] On top of their degradability, synthetic versatility and possibilities for diverse properties introduction have made APEs and APCs to be most widely studied compounds for biomedical application use.[20]

Figure 3. Degradation mechanisms of degradable polymers.

Ring-opening polymerization (ROP) allows for the synthesis of biodegradable polymers (mainly polyesters (PEs) and polycarbonates (PCs)) (**Figure 4**) *via* chain-growth mechanisms.[21,23,24] Besides, ROP offers the possibility of controlling the molecular weight (M_n), the distribution of molecular weights ($Đ$), the microstructure of the polymer, and the nature of its end groups.[21,23–25] A variety of catalysts and cyclic

monomers can be adopted, and it is possible to create macromolecules with tunable molecular weights in high yields by simply varying the monomer/initiator ratio. Initially, the synthesis of APEs and APCs utilized metal-based catalysts. $Sn(Oct)_2$ is one of the most widely used catalysts, not only in industry[26] for both PLA[27] and PTMC[28], but also in research for more sophisticated monomers. This versatile catalyst plays a crucial role in the polymerization processes, offering efficiency and reliability.[26] Vert et al. conducted the ring-opening polymerization of 3-(1,2-3,4-tetraoxobutyldiisopropylidene)dioxane-2,5-dione (DIPAGYL), a derivative of glycolic acid and partially protected gluconic acid, using $Sn(Oct)_2$ at 120°C. This process yielded a polymer with a high molecular weight, approximately 20,000 g/mol.[29] Subsequently, the detection of residual metals in the resulting polymers, which potentially induce cytotoxic effects, necessitated the development of more biocompatible alternatives. These alternatives include both metal-free and enzymatic catalysts. Despite their biocompatibility, metallo-organic catalysts continue to be favored for their high catalytic activity in APEs and APCs synthesis. However, while metal-free catalysts are extensively employed, their requirement for high loadings often impractically high for industrial scale applications limits their efficiency relative to that of metallo-organic analogues. [21,23–25] Guillaume et al. synthesized functionalized polycarbonates derived from 2,2-dimethoxytrimethylene carbonate ($TMC(OMe)_2$) using various binary catalyst systems that consist of (metallo)organic/alcohol (diol). These catalyst systems included the β-diiminate zinc complex [(BDIiPr)Zn($N(SiMe_3)_2$)], aluminium triflate, and organic bases such as 4-*N,N*-dimethylaminopyridine (DMAP), triazabicyclodecene (TBD), and 2-*tert*-butylimino-2-diethylamino-1,3-dimethylperhydro-1,3,2-diazaphosphorine (BEMP). In conjunction with benzyl alcohol (BnOH) or 1,3-propanediol (PDO), which served both as co-initiators and chain transfer agents, these catalysts facilitated the creation of well-defined *α*-hydroxy-*ω*-alkoxyester and α,ω-dihydroxy telechelic acetal-functionalized homopolycarbonates. Remarkably, these polymers were prepared with molar masses reaching up to 70,200 g/mol for the first time.[30] The selected cyclic monomers can each provide different properties and unique functionalities to the final polymers [21,23–25]. For example, Li et al. synthesized lipopolymers from PEG-*block*-poly(2-methyl-2-benzoxycarbonyl-propylene carbonate) (PEG-*b*-PBC) by using DBU as a catalyst . They modified the pendant benzyl group by substituting it with dodecanol to facilitate the attachment and delivery of the anticancer drug, embelin.[31]

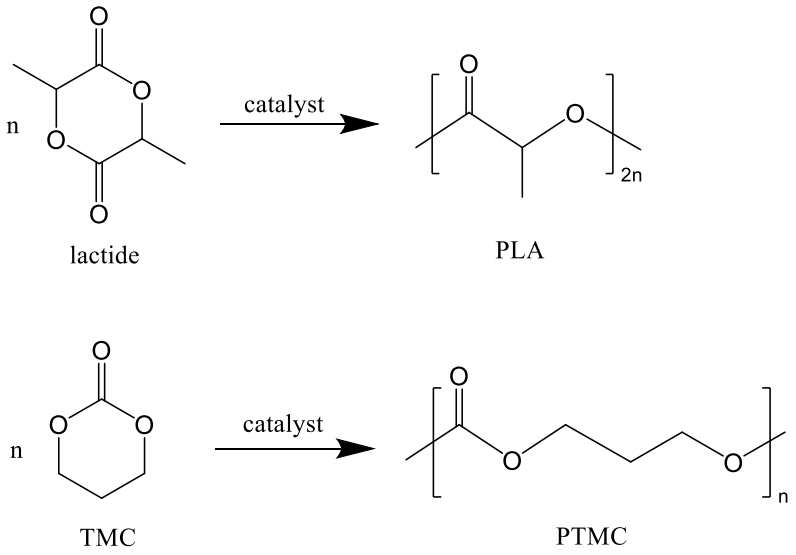

Figure 4. Aliphatic biodegradable polyesters and polycarbonates.

The polymerization of biodegradable polyesters (PEs) is achieved through the ring-opening polymerization (ROP) of cyclic lactones. Examples include PLA, [24,25] poly(butylene succinate) (PBS),[32] PGA,[33] and PCL[34]. Besides, the polymerization of biodegradable PCs involves ROP of cyclic carbonate (CCs) or copolymerization of CO_2 with epoxides.[35] Notable examples are poly(ethylene carbonate)(PEC),[36] PTMC,[37,38] poly(propylene carbonate) (PPC)[39] (**Figure 5**). However, the ROP of PEC [36] and PPC [39] is accompanied by a decarboxylation process.

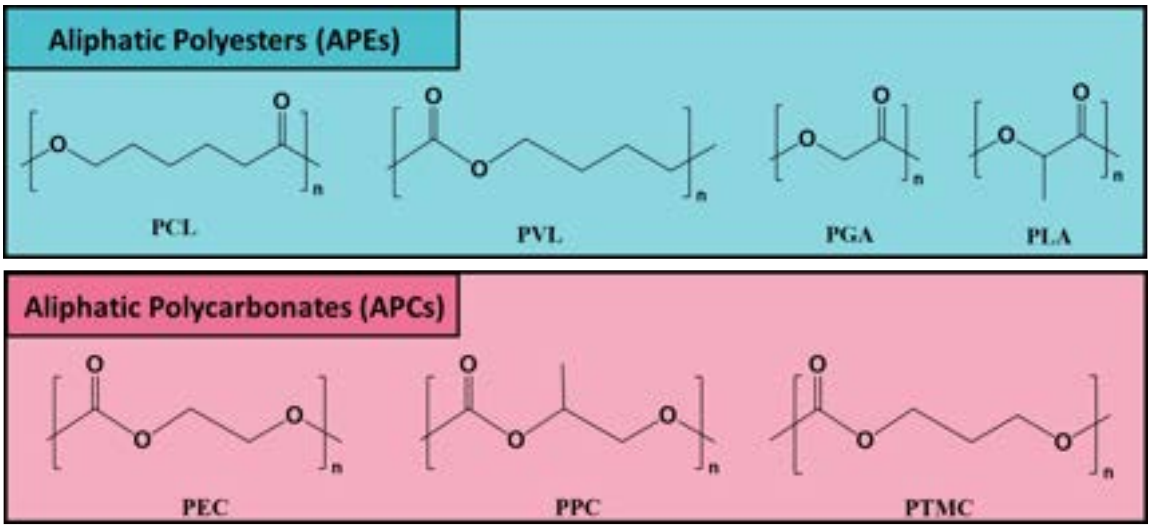

Figure 5. Chemical structures of the aliphatic biodegradable PEs and PCs that are applied most frequently in ROP.

In APEs, the hydrolysable ester bonds and the relatively short aliphatic chains have a predominant role in the degradability of the polymer, and its compatibility make it suitable to be broadly used in biomedical fields such drug delivery,[40] vascular grafts,[41] dental implants,[42] and bone screws.[43] There are three major routes for the synthesis of APEs. (I) polycondensation of a hydroxy acid or of a diol and a diacid (**Figure 6a).**[44] However, this method has some drawbacks including the low degree of polymerization resulting in low M_n polymers,[45] lack of control of the polymer structure and block copolymers cannot be synthesized. (II) ROP of the cyclic diesters under proper conditions can result in polyesters with high M_n and ROP is associated with limited side reactions such as racemization, leading a good control of the polymer structure (**Figure 6b).**[25] (III) Enzymatic polymerization can be carried out under mild conditions (70 — 80°C) avoiding the use of toxic reagents (**Figure 6c)**[46] and provide attractive possibilities for the direct synthesis of functional polyesters avoiding the use of protected monomers.[47] However, the major drawback of the enzymatic synthesis of polyesters is the relatively low M_n of the obtained polymers (5 — 40 kDa).[46]

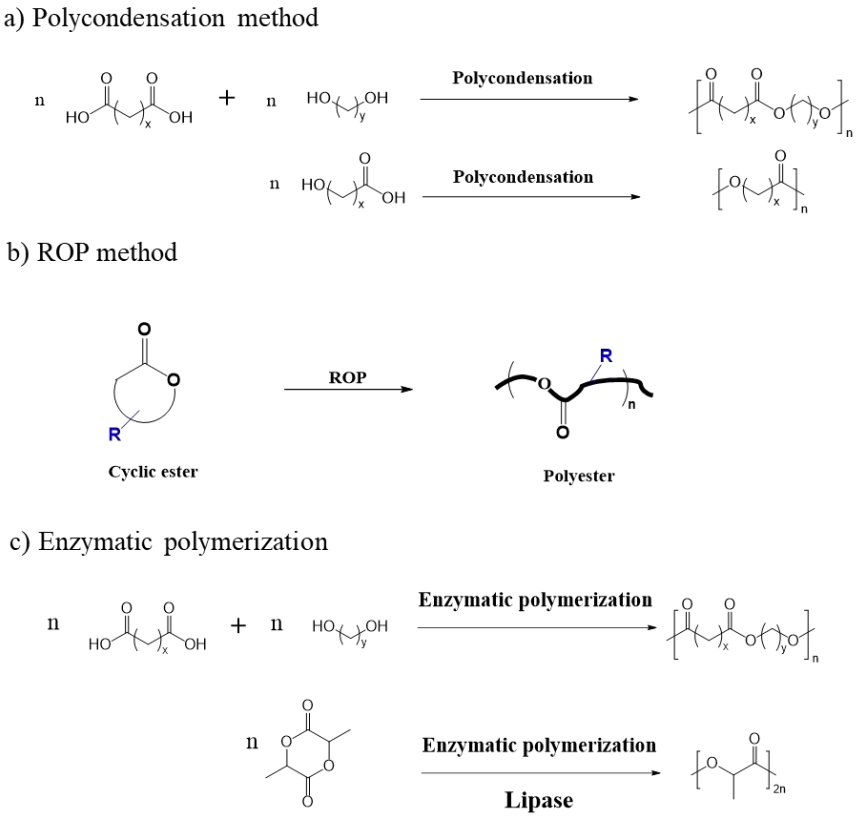

Figure 6. Synthesis routes for polyesters by a) polycondensation method, b) ROP method, and c) enzymatic polymerization.

To address the deficiencies in mechanical and physical properties of polymers, several strategies involving physical and chemical modifications have been developed. These approaches aim to enhance the material's performance and functionality. The main methods of physical modification include:(I) blending with plasticizer (e.g. cardanol, PEG)[48] ; (II) blending with nucleating agent (e.g. tetramethylene-dicarboxylic dibenzoyl-hydrazide, TMC-306)[49] ; (III) blending with inorganic filler (e.g. $CaCO_3$)[50] ; (IV) natural fiber composite (e.g. cellulose)[51]; (V) blending with biodegradable materials (e.g. PBS, ethylene-methyl acrylate-glycidyl methacrylate (EGMA))[52]; (VI) blending with other materials (e.g. polyurethane elastomer prepolymer (PUEP))[53] (**Figure 7**). The physical modification method is relatively simple and easy to realize industrialization, yet the compatibility and dispersion issues between materials need to be further improved.

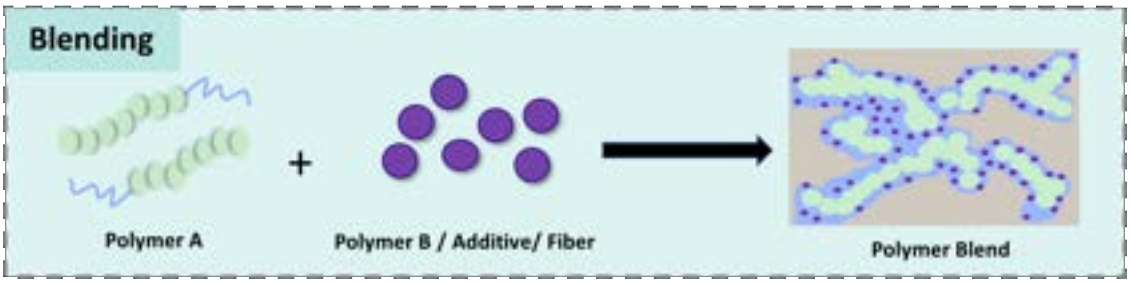

Figure 7. The physical modification by blending.

On the other hand, the chemical modification method involves modifying polyester through its molecular structure (monomer and polymer) resulting in a more stable structural design. The chemical modification mainly includes copolymerization[54] (**Figure 8a**). For instance, Devis et al. synthesized a series of AB block copolymers using a fixed PEG block (5 kDa) and a varying PLA segment (2—110 kDa) through the ring-opening polymerization of D,L-lactide, employing stannous octoate as a catalyst. [54] Secondly, crosslinking methods have been explored [55] (**Figure 8b**); Chen et al. prepared PLA cross-linked with biopolyamide (HDAPA) to produce a super tough material. Lastly, end-group modification has been utilized; Ajiro et al. prepared functionalized PLA at the chain end with anillin acetal-based initiators to impart pH-responsive properties (**Figure 8c**).[56,57]

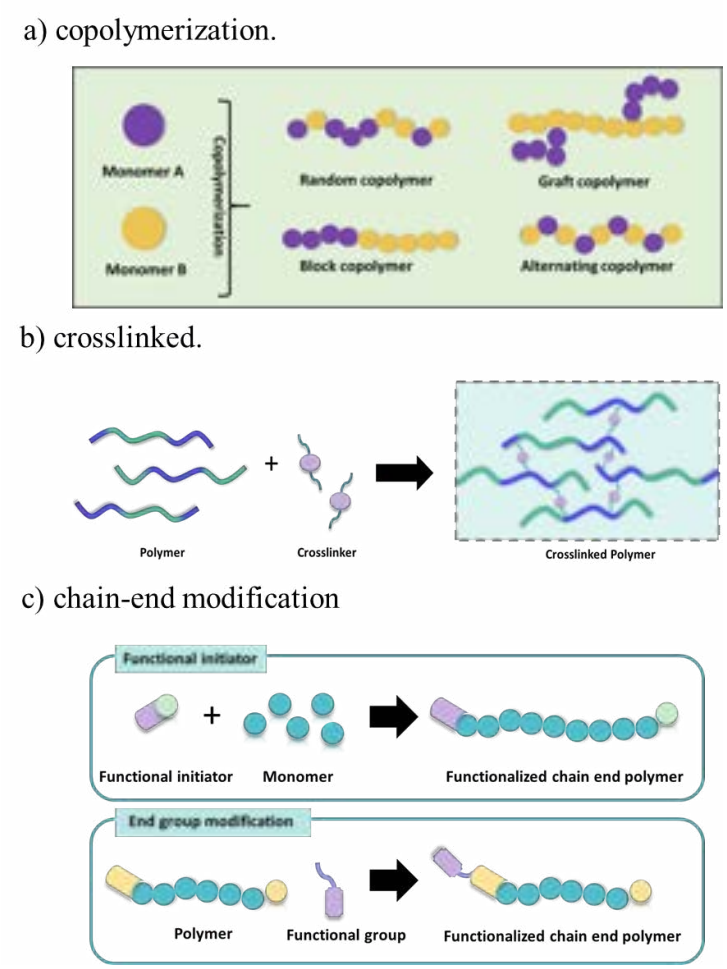

Figure 8. The chemical modification by a) copolymerization, b) crosslinked, and c) chain-end modification.

Previous studies[58,59] have employed introduction of functionality by chemical modification of the end-groups to improve mechanical and physical properties. In fact, introduction of the diversity of desired functionalities to the polyester macromolecules while retaining intrinsic properties of the matrix can be achieved by mean of this approach. This functional group introduction modulates various properties of polyester-based materials such as their degradation, self-assembly or interactions with nanoparticles. PEs such as PLA, PLLA, PCL, PGA, PLGA copolymers, or poly(hydroxyalkanoates) (PHA) are highly used in medical applications due to their wide range of custom properties, availability, tailoring capacity, cost-effectiveness, and easy processing. For example, PLGA end-groups modification has been extensively investigated for the drug release profiles which could be tuned to specific controlled delivery rates through gradients by altering the M_w and terminal functional groups,

especially acid-terminal functional groups, of PLGA.[60] Another example of an aliphatic biodegradable polyester is PCL which has been considerably used for the development of biomedical devices and tissue engineering scaffolds.[61] PCL shows long-term degradation of about 2 — 4 years depending on the molecular weight, which enables it to be used in long-term implants. The introduction of functional groups into polymer chains, commonly used at both the monomer[62,63] and polymer [56] levels of polyesters, provides polymers with tunable degradation behavior by suppressing crystallinity and enhancing hydrophilicity. This modification favors cell adhesion to surfaces, which is important for tissue engineering purposes. [64]Further, an increasing hydrophilicity results in a greater water absorbing capacity of the polymers, thereby increasing the degradation rate and probably preventing a pH drop inside the degrading matrices and hence prevent aggregation and incomplete release of encapsulated proteins.[65] Recently, PLA is a widely used biodegradable polyester has considered to be alternative commercially renewable polymer. PLA can be synthesized by the ROP of lactide (LA), which is derived from biomass such as corn or wheat. PLA is a bio-based polyester polymer with excellent biodegradability and biocompatible which have been developed in the biomedical field. However, PLA has some drawbacks that hinder its use for certain applications, such as its high crystallinity, low thermal stability, hydrophobic nature, and low degree of functionalization. In order to addressing these short coming, the recent research revealed that the properties of PLA can be easily modulated by modifying the end groups to achieve the desired functionality for the target application.[59]

Previous challenges with functionalized PLA have shown that chain-end modifications can alter the properties of PLA through the use of specially designed initiators. To facilitate dual dynamic interactions, vanillin (**Figure 9a**)[66] and 5-hydroxymethylfurfural (HMF) (**Figure 9b**)[67] have been reported to be functionalized for inducing an amine-imine reversible phenomenon. By controlling the formation of nanostructures, the hydrophilic moieties of a hydroxyl group at the chain end and PLA were demonstrated. As a result, the particles aggregated due to the detachment of the hydrophilic moiety (aldehyde-terminated PLA) after a change in pH.[66,67] However, the pH range below pH 2 in the previous study was not practical for medical therapy. With the consideration of a ketone acetal bond, it could be committed under physiological conditions (mildly acidic condition). It was noted that a six-membered ring diol-ketone acetal bond hydrolyzed faster than a five-membered ring.[68] Therefore, it is attractive to clarify whether the acetal bond can be hydrolyzed under physiological condition in the presence of aldehyde-hydroxyl derivatives, as proposed low-toxicity residues.

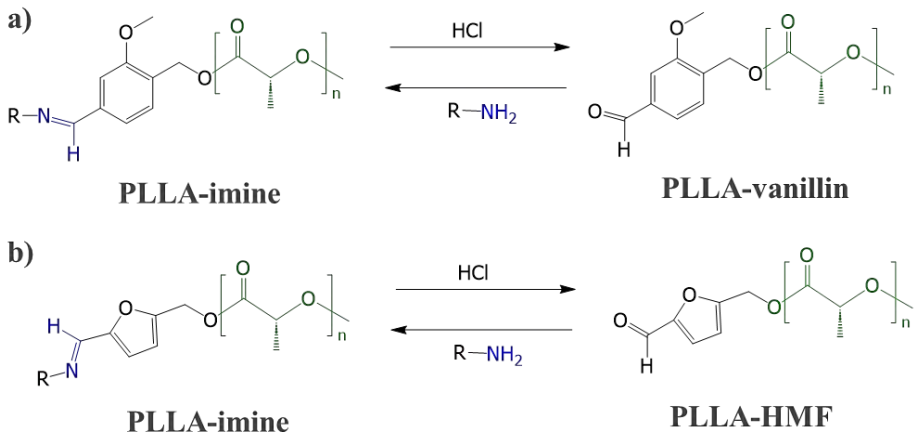

Figure 9. Chemical structure of a) PLLA-imine and PLLA-vanillin,[66] and b) PLLA-imine and PLLA-HMF. [67]

APCs are another fascinating class of degradable polymeric composites which have garnered increased attention as biomaterials primarily because they can be obtained from a range of resources, including natural and renewable sources. Additionally, their biocompatibility and tunable biodegradation characteristics contribute to their appeal in biomedical applications.[69] Furthermore, the capability to introduce functional groups in the polymer backbone through the careful design of cyclic carbonate monomers or copolymerization with other biodegradable polymers has significantly contributed to the interest in utilizing this class of materials for biomedical applications. The investigations have expanded the utility of aliphatic polycarbonates to a diverse range of applications in the biomedical field, including drug delivery,[38,70] tissue regeneration,[71] and the development of vascular grafts.[72]

Three synthetic routes have been explored for the synthesis of APCs. (I) polycondensation of aliphatic polyol and diallyl carbonates, (II)copolymerization of carbon dioxide (CO_2) with an epoxide, and (III) ROP of CC monomers, mainly six-membered-ring cyclic carbonates (6CCs) (from TMC) and seven-membered-ring cyclic carbonates (7CCs).[73] Nevertheless, the conventional synthesis of polycondensation involves the use of toxic and energy-intensive phosgene[74] (**Figure 10a**). New synthetic strategies involve the copolymerization of carbon dioxide with an epoxide, offering a greener alternative for polycarbonate synthesis (**Figure 10b**).[75] However, this polymerization technique has typically not been utilized for the synthesis of polycarbonates for biomedical applications, likely due to the requirement for high-pressure reactors (>2.0 MPa), competing formation of the corresponding five-membered-ring cyclic carbonates (5CCs) and limited reports of functional polymers produced using

this method.[76] Recently developed, the ROP of CCs has emerged as an attractive method for the introduction of functional groups into the polycarbonate backbone and well-defined polycarbonates with high molar masses (**Figure 10c**) by cationic,[77] anionic,[78] coordination−insertion,[79] organocatalytic,[80] and enzymatic methods.[81] Biomedically relevant polycarbonates can be accessed with high levels of control over polymer molar mass, dispersity, and end-group fidelity. This advancement has opened up the possibility of preparing functional polycarbonates for synthesizing biocompatible materials with tunable degradation rates and mechanical performance. The introduction of functional handles has been used as an alternative method to finely tune the properties of polycarbonates, precisely tailoring the polymer structure to enable specific interactions with cells or tissues.[82,83]

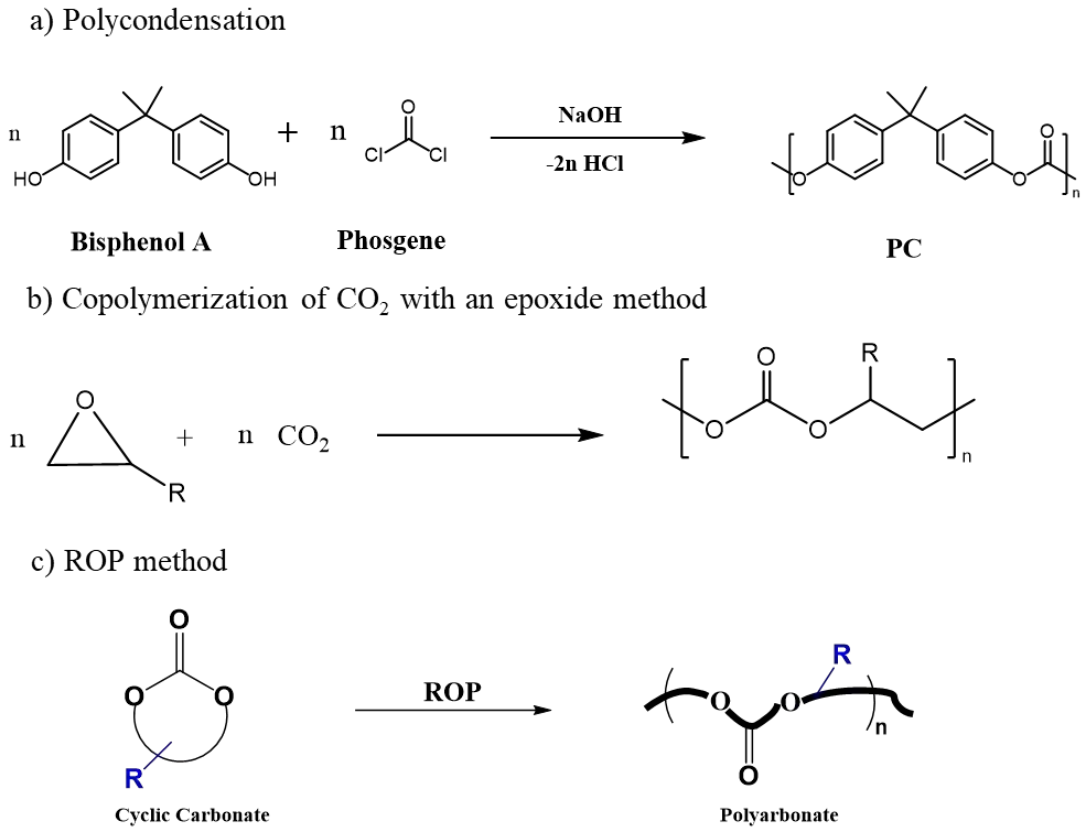

Figure 10. Synthesis routes for polycarbonates by a) polycondensation method, b) copolymerization of CO_2 with epoxide method, and c) ROP method.

Normally, the ROP of (CCs) is applied to prepare 6CCs. This preference is due to the synthetic challenges associated with the copolymerization of epoxides and CO_2, where the catalytic systems often exhibit low functional compatibility. Nevertheless,

significant progress has been made in the last decade in overcoming these challenges, particularly in the use of bio-sourced epoxides.[84,85] Therefore, the ROP of 6CCs, especially TMC, has received considerable attention.

Nowadays, PTMCs have recently attracted increasing attention as a soft biomaterial owing to their unique biodegradation behavior including surface erosion. It is advantageous that its versatility to introduction of functional pendant groups on the side chain of monomer to tune its properties for more advanced applications. The most common synthetic pathway for functional monomer TMC is using the versatile 2,2-bishydroxy(methyl)propionic acid (bis-MPA) as precursor to direct functionalization.[86] However, the preparation of functionalized TMC monomers requires several synthetic steps (typically 3—6 steps) (**Figure 11** and **Figure 12**), involving protection and deprotection reactions. [86] Moreover, some of these steps necessitate the use of toxic reagents.[86,87] This could serve as motivation to design TMC-derived monomers that enable the preparation of functionalized TMC monomers with as few steps as possible, while avoiding the use of toxic reagents.

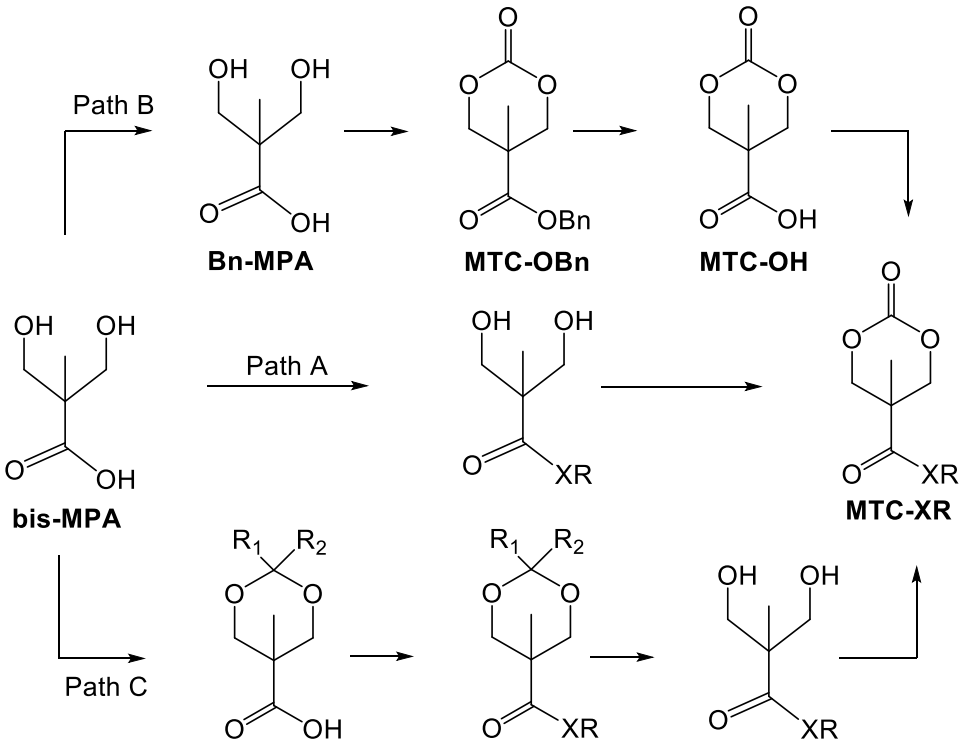

Figure 11. Reported synthetic routes to functionalized ester-based cyclic carbonate monomers.[88]

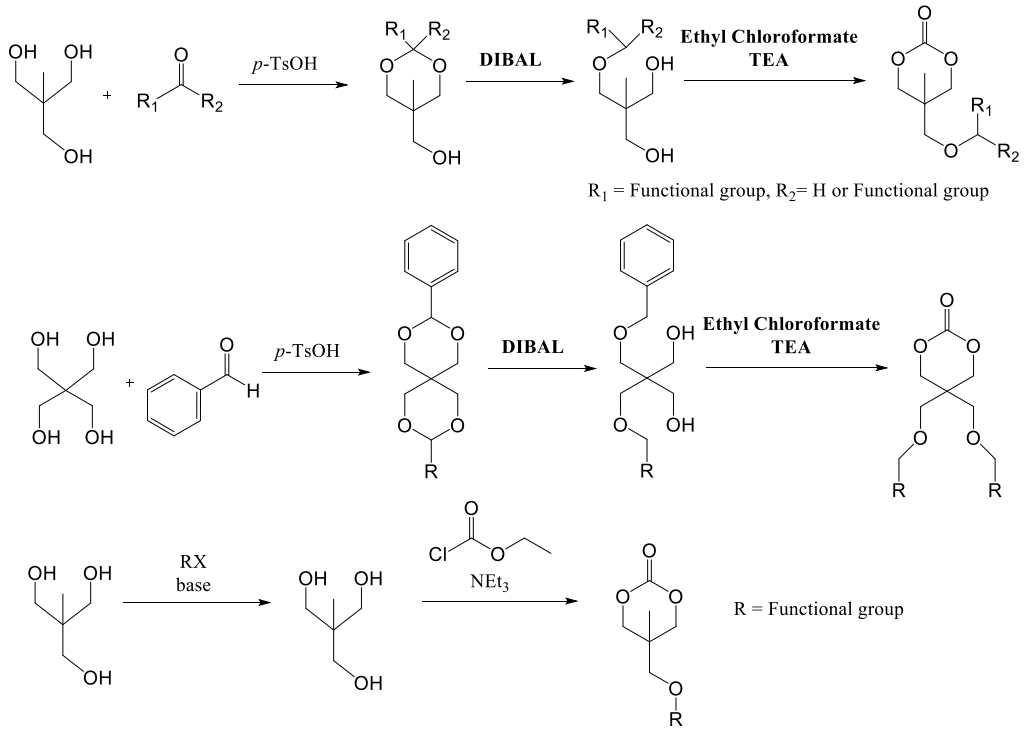

Figure 12. Reported synthetic routes to functionalized ester-free cyclic carbonate monomers.[89]

Normally, the efforts on modification PTMC have been achieved by functionalization at monomer level before polymerization. However, it is important to note that when the required functional group is protic, chemical compatibility issues appear either by quenching the organic or metallic-catalyst or acting as initiator which is compatible with the ROP such as the pendant functional group which contained amine, carboxylic acids and alcohols. To tackle this problem, one of the alternatives to ease without compromise the polymerization efficiency is to functionalize polycarbonates *via* post-polymerization modification pathway.[90,91] For instance, Hedrick et al. utilized monomer bearing pentafluorophenyl activated ester pendant groups that remain intact during the acid catalyzed polymerization, and were further modified with amines and alcohols in high yield in a post-polymerization modification step (**Figure 13).**[88] Also, Dove et al. studies reported polymerizing of cyclic monomers with allyl pendant group and further modified with host of thiols through thiol-ene 'click' chemistry.[86] This powerful methodology could be advantageous for preparing a series of randomly functionalized polycarbonates with tailored properties. [86,74] Based on a Thiol-ene reaction on the C=C group, a variety of functional groups can be introduced along the polymer chain without using any protective group. Thanks to the introduction of carboxylic

(COOH) or hydroxy (OH) functional groups, privileged interactions might be established with active ingredients in the domain of drug release. In addition, the hydrophilicity will be modified by the polar pendant groups, leading to higher degradation rates.[92] Therefore, focusing solely on precise structural design is not sufficient. It is worthwhile to pay attention on the impact of pendant groups after post-polymerization modification *via* thio-ene on polymer degradation or interaction with drugs in order to refine the application target at the molecular level precisely.

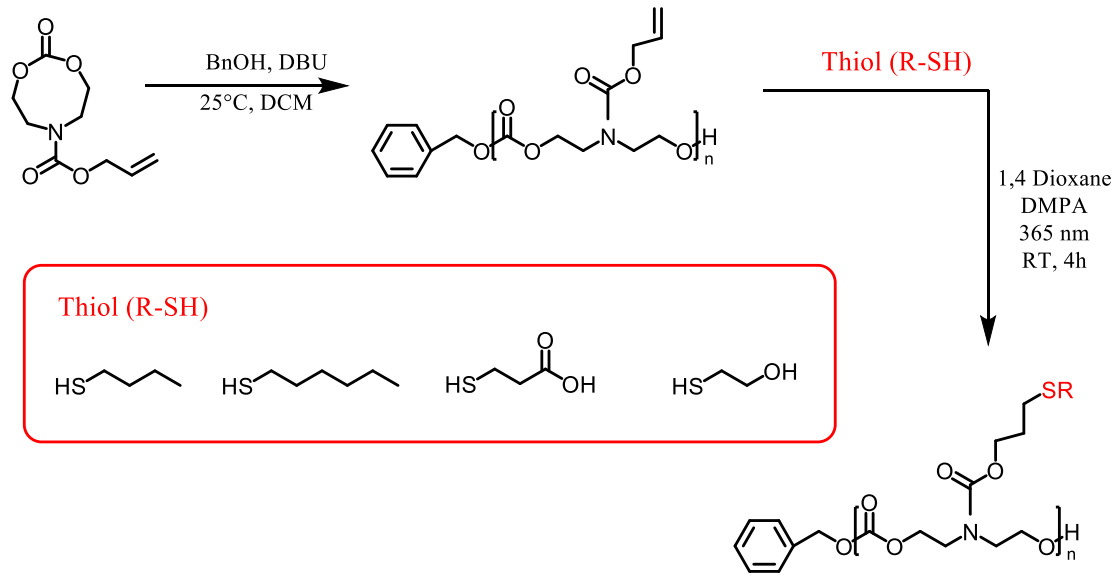

Figure 13. ROP of 8ACfm, an allyl bearing eight membered cyclic carbonate synthetic and radical addition of thiols onto polycarbonate on 8-ACfm. [88]

Expanding the versatility of PTMC to include a broader range of functionalities is highly desirable for achieving targeted applications. Similarly, the development of ionomers demonstrates the potential of specialized polymers in advanced applications. An ionomer is a polymer that incorporates a small percentage of ionic units, typically not exceeding 15 mol percent (**Figure 14**). These polymers are usually copolymers, consisting of both neutral and ionized units. Ionomers are distinguished by the profound influence of strong ionic interchain forces on their properties. Although only a minor proportion of bonded ionic groups are present within the main polymer structure, these groups tend to aggregate in the condensed phase, significantly altering the polymer's physical, mechanical, optical, and dynamic properties.[93]

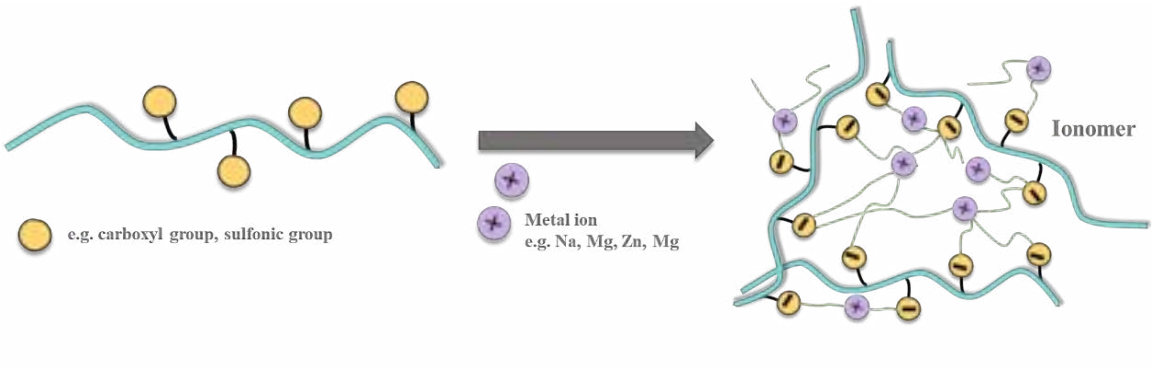

Figure 14. Illustration of Ionomer formation.

Besides, in biomedical applications, ionic units can be incorporated to impart dynamic surface and wettability properties that can be exploited for antifouling and protein delivery applications; while degradable ionomers bearing cationic units hold great promise for antimicrobial materials and coatings. The water dispersibility, swelling and hydrolytic degradation of degradable materials can also be substantially improved through the incorporation of just a small number of ionic units. Notably, the acceptance of blood contacting implants creating favorable conditions in vivo is decisively determined by their interaction with proteins that mediate inter cellular interactions with synthetic substrates.[94] For example, adsorption of fibrinogen onto a biomaterial surface may enhance platelet activation and ultimately trigger the haemostatic system.[95] Thus, one of the approaches to improve the acceptability of polymers for blood-contacting medical applications is by controlling the protein adsorption process. This may be achieved by reducing the total amount of proteins adsorbed to a surface or by the adsorption or covalent attachment of a specific protein. For example, immobilization of albumin was shown to reduce further adhesion of leucocytes and platelets, thus inhibiting thrombus formation.[96,97] F. Nederberg et al reported that PC ionomer have a strongly hydrophilic surface that prevents the adsorption of proteins and reduces the adhesion of cells (**Figure 15**).[98] With these inspirations, it is attractive to include the coordination bond between metal acetate and carboxylate functional group to build ionomer of PTMC derivatives.

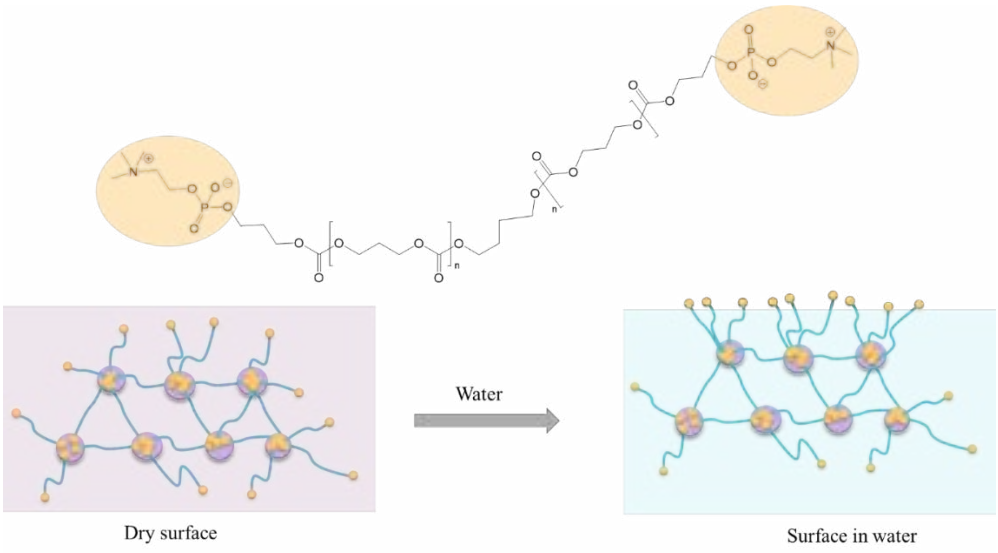

Figure 15. Molecular structure of the phosphorylcholine ionomers. [98]

Herein, the objective of this thesis is to focus on the precise structural design of novel biodegradable PEs and PCs featuring pendant functional groups, and to evaluate the properties that could impact their potential in various biomedical applications. Based on our developed strategy, the functionalized polyester at chain end is prepared by functionalized initiators to control pH-triggered degradation. The functionalized PCs at the side chain certainly controls the randomness in the polymer chain, adjusts the type, amount and distribution of functional group, and can be prepared through pre- or post-polymerization modification to control degradability within only three steps from monomer synthesis to functionalized polymer. However, the introduced functional groups may have an impact on the polymer properties, especially the degradation rates. To probe the degradability of these functionalized polymers, their degradation has been investigated in hydrolytic and enzymatic conditions. The scope of manuscript (**Figure 16**) is categorized in four chapters as illustrated hereafter:

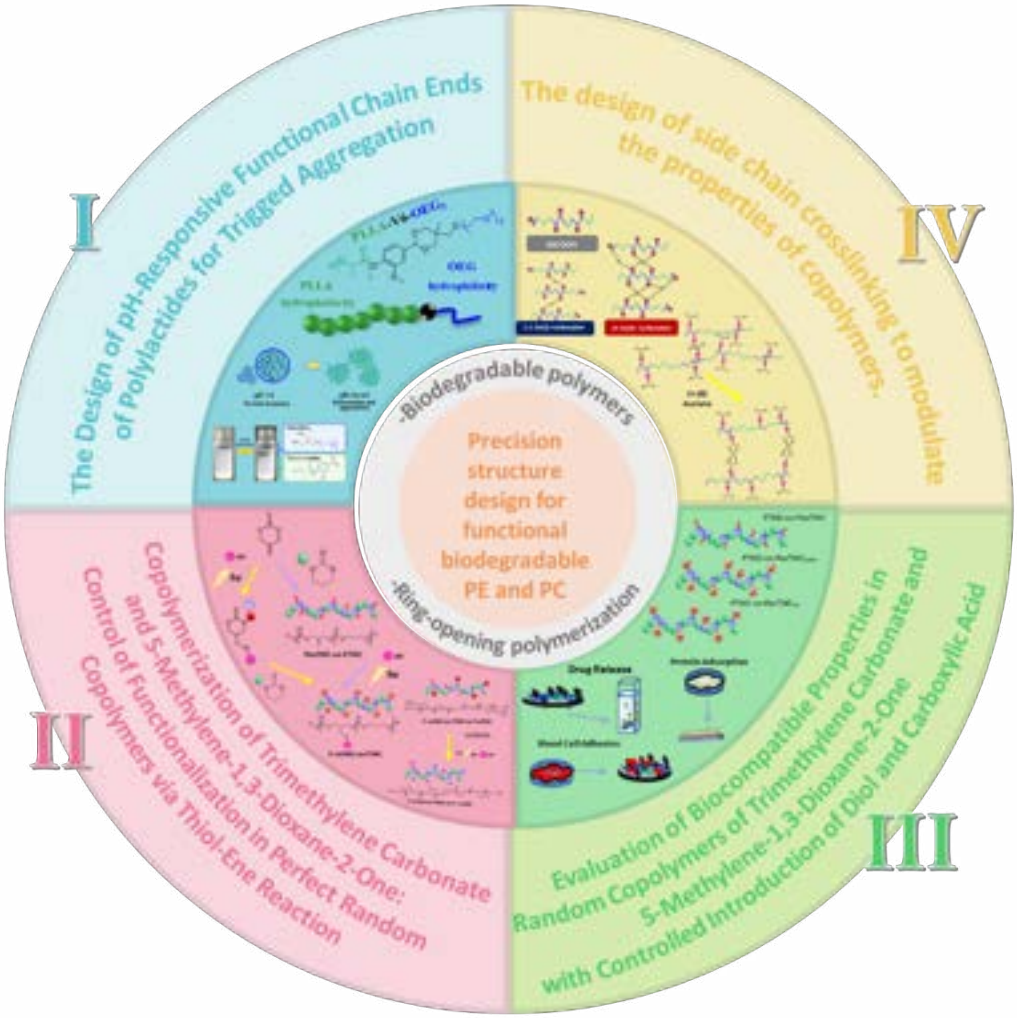

Figure 16. Overview illustration of the project represents the precision structure design for functional biodegradable PEs and PCs.

In Chapter I, we will explore an example of tuned structure by focusing on the chain end functionalization. The objective of this study is to functionalize the PLA chain end with six-membered ring ketone acetal unit through modification of a novel initiator diol-ketone acetal, to form particles from the resulting polymer and to study its pH responsive behavior towards degradation rate under physiological conditions. The effect of M_n, stereo-complexation (SC), pH range and chain end structure on the aggregation rate will be studied to reveal that it is mainly induced by the acetal hydrolysis process. Moreover, the effect on titanium dioxide addition as blending agent will be investigated as well. In this chapter, UV spectroscopy will be used to examine the aggregation rate as well as the resulting assembly morphology behavior.

In Chapter II, as an example of precision structure, attention will be given to homogeneous copolymer composition. The focus will be on the functionalization of PTMC at both the monomer and polymer levels by incorporating desired functional groups and controlling polymer structure design. 5-Methylene-1,3-dioxane-2-one (exTMC) and its functionalized derivatives were synthesized and investigated as comonomers with TMC with the aim of preparing functionalized PCs. The polymerization the organocatalyst and kinetics for the RcoOP of TMC and the comonomer (exTMC or the derived functionalized TMC) were explored to discover an alternative catalyst capable of promoting the ROP under mild conditions, while enabling easy control of the reaction to lead to copolymers with adjusted composition and high randomness (co-monomer regularly distributed along the polymer chains). Functionalization *via* thiol-ene reaction with thiols bearing the desired pendant functional group on the exomethylene group of exTMC by both pre- and post-polymerization modification means were explored in order to maximize fine tuning of the copolymer properties.

In Chapter III, was motivated by the successful preparation of homogeneous random copolymers in Chapter II to further investigate the various types of copolymer TMC structures and designs for biomaterial use. Copolymer of TMC and exTMC as well as copolymer of TMC and functionalized exTMC by thiol-ene click reaction with thioglycolic acid and thioglycerol were synthesized and used as potential biomaterial coating. The surface properties such as morphology, wettability, protein adsorption, palette-adhesion will be presented. Also, the water uptake, weight loss, and the interactive moiety of drug (doxorubicin) and copolymer were studied in order to investigate the effect of functional group on the drug releasing rate.

In Chapter IV, the attention is given to crosslinking structures as an example of precision in structural design. The research interest in this area arises from the successful preparation of a copolymer of TMC and functionalized exTMC through a thiol-ene click reaction with thioglycolic acid, which introduces carboxylic groups on the side chains. These groups can be strategically utilized to precisely place metal-carboxylates, thereby facilitating dynamic crosslinking to form ionomers. The copolymer of TMC and functionalized exTMC with carboxylic group were selected for crosslinking through the coordinating metallic ions to the carboxylate groups which target to control the gel strength, stability, and reducing protein adsorption. Herein, the series of the novel crosslinked polymers performance were examined in term of morphology, wettability, protein adsorption, thermal stability, rheology, swelling ratio, degradation behavior in details in this chapter.

Overall, compared to previous research, this thesis aimed to extend efforts in designing biodegradable polymers of precise structures for more targeted applications with easier modification midway and adjustability. Through this approach, the benefits of an efficient synthetic pathway and diverse improvements in polymer properties can be achieved more easily.

Reference

(1) Luckachan, G. E.; Pillai, C. K. S. Biodegradable Polymers- A Review on Recent Trends and Emerging Perspectives. *J. Polym. Environ.* **2011**, *19* (3), 637–676. https://doi.org/10.1007/s10924-011-0317-1.

(2) Zhong, Y.; Godwin, P.; Jin, Y.; Xiao, H. Biodegradable Polymers and Green-Based Antimicrobial Packaging Materials: A Mini-Review. *Adv. Ind. Eng. Polym. Res.* **2020**, *3*, 27–35. https://doi.org/10.1016/j.aiepr.2019.11.002.

(3) Azevedo, H.; Reis, R. Understanding the Enzymatic Degradation of Biodegradable Polymers and Strategies to Control Their Degradation Rate. *Biodegrad. Syst. Tissue Eng. Regen. Med.* **2004**, 177– 202. https://doi.org/10.1201/9780203491232.ch12

(4) Tiso, T.; Winter, B.; Wei, R.; Hee, J.; de Witt, J.; Wierckx, N.; Quicker, P.; Bornscheuer, U. T.; Bardow, A.; Nogales, J.; Blank, L. M. The Metabolic Potential of Plastics as Biotechnological Carbon Sources – Review and Targets for the Future. *Metabolic. Engineering*. **2022**, *71*, 77–98. https://doi.org/10.1016/j.ymben.2021.12.006.

(5) Künkel, A.; Becker, J.; Börger, L.; Hamprecht, J.; Koltzenburg, S.; Loos, R.; Schick, M. B.; Schlegel, K.; Sinkel, C.; Skupin, G.; Yamamoto, M. Polymers, Biodegradable. In *Ullmann's Encyclopedia of Industrial Chemistry*; Wiley-VCH GmbH: Weinheim, **2016**; pp 1– 29. https://doi.org/10.1002/14356007.n21_n01.pub2.

(6) Ghanbarzadeh, B.; Almasi, H. Biodegradable Polymers. *Biodegradation - Life of Science*; InTech, 2013. https://doi.org/10.5772/56230.

(7) Balaji, A. B.; Pakalapati, H.; Khalid, M.; Walvekar, R.; Siddiqui, H. Natural and Synthetic Biocompatible and Biodegradable Polymers. *Biodegradable and Biocompatible Polymer Composites: Processing, Properties and Applications*; Elsevier, **2017**; 3–32. https://doi.org/10.1016/B978-0-08-100970-3.00001-8.

(8) Jha, K.; Kataria, R.; Verma, J.; Pradhan, S. Potential Biodegradable Matrices and Fiber Treatment for Green Composites: A Review. *AIMS Materials Science* **2019**, *6* (1), 119–138. https://doi.org/10.3934/matersci.2019.1.119.

(9) Tran, V. T.; Benoît, J. P.; Venier-Julienne, M. C. Why and How to Prepare Biodegradable, Monodispersed, Polymeric Microparticles in the Field of Pharmacy? *Int. J. Pharm.* **2011**, *407*, 1–11. https://doi.org/10.1016/j.ijpharm.2011.01.027.

(10) Davoodi, P.; Lee, L. Y.; Xu, Q.; Sunil, V.; Sun, Y.; Soh, S.; Wang, C. H. Drug Delivery Systems for Programmed and On-Demand Release. *Adv. Drug Deliv. Rev*. **2018**, *132*, 104–138. https://doi.org/10.1016/j.addr.2018.07.002.

(11) Tan, H.; Wu, J.; Lao, L.; Gao, C. Gelatin/Chitosan/Hyaluronan Scaffold Integrated with PLGA Microspheres for Cartilage Tissue Engineering. *Acta Biomater.* **2009**, *5* (1), 328–337. https://doi.org/10.1016/j.actbio.2008.07.030.

(12) Wang, J.; Yang, Q.; Cheng, N.; Tao, X.; Zhang, Z.; Sun, X.; Zhang, Q. Collagen/Silk Fibroin Composite Scaffold Incorporated with PLGA Microsphere for Cartilage Repair. *Mater. Sci. Eng. C.* **2016**, *61*, 705–711. https://doi.org/10.1016/j.msec.2015.12.097.

(13) Toong, D. W. Y.; Toh, H. W.; Ng, J. C. K.; Wong, P. E. H.; Leo, H. L.; Venkatraman, S.; Tan, L. P.; Ang, H. Y.; Huang, Y. Bioresorbable Polymeric Scaffold in Cardiovascular Applications. *Int. J. Mol. Sci.* **2020**, *21*(10), 3444 https://doi.org/10.3390/ijms21103444.

(14) Abhilash Akinapelli; Jack P. Chen; Kristine Roy; Joseph Donnelly; Keith Dawkins; Barbara Huibregtse; Dongming Hou. Current State of Bioabsorbable Polymer-Coated Drug-Eluting Stents. *Curr. Cardiol Rev.* **2017**, *13*, 139–154.

(15) Kunduru, K. R.; Basu, A.; Domb, A. J. Biodegradable Polymers: Medical Applications. *Encyclopedia of Polymer Science and Technology*; **2016**; 1–22. https://doi.org/10.1002/0471440264.pst027.pub2.

(16) Kuperkar, K.; Atanase, L. I.; Bahadur, A.; Crivei, I. C.; Bahadur, P. Degradable Polymeric Bio(Nano)Materials and Their Biomedical Applications: A Comprehensive Overview and Recent Updates. *Polymers*. **2024**, *16*(2), 206 https://doi.org/10.3390/polym16020206.

(17) Zhang, X.; Fevre, M.; Jones, G. O.; Waymouth, R. M. Catalysis as an Enabling Science for Sustainable Polymers. *Chem. Rev.* **2017**, *118*(2), 839–885. https://doi.org/10.1021/acs.chemrev.7b00329.

(18) Zhu, Y.; Romain, C.; Williams, C. K. Sustainable Polymers from Renewable Resources. *Nature*. **2016**, *540* (7633), 354–362. https://doi.org/10.1038/nature21001.

(19) Tsuji, H.; Suzuyoshi, K. Environmental Degradation of Biodegradable Polyesters 1. Poly(e-Caprolactone), Poly[(R)-3-Hydroxybutyrate], and Poly(L-Lactide) Films in Controlled Static Seawater. *Polym. Degrad. Stab.* **2002**, *75*(2), 347–355. https://doi.org/10.1016/s0141-3910(01)00240-3.

(20) Anju, S.; Prajitha, N.; Sukanya, V. S.; Mohanan, P. V. Complicity of Degradable Polymers in Health-Care Applications. *Mater. Today Chem.* **2020**, *16*, 100236. https://doi.org/10.1016/j.mtchem.2019.100236.

(21) Yu, W.; Maynard, E.; Chiaradia, V.; Arno, M. C.; Dove, A. P. Aliphatic Polycarbonates from Cyclic Carbonate Monomers and Their Application as Biomaterials. *Chem. Rev.* **2021**, *121*(18), 10865–10907. https://doi.org/10.1021/acs.chemrev.0c00883.

(22) Pêgo, A. P.; Van Luyn, M. J. A.; Brouwer, L. A.; Van Wachem, P. B.; Poot, A. A.; Grijpma, D. W.; Feijen, J. *In Vivo* Behavior of Poly(1,3-Trimethylene Carbonate) and Copolymers of 1,3-Trimethylene Carbonate with *D,L*-Lactide or ε-Caprolactone: Degradation and Tissue Response. *J. Biomed. Mater Res. A.* **2003**, *67* (3), 1044–1054. https://doi.org/10.1002/jbm.a.10121.

(23) Guillaume, S. M.; Carpentier, J. F. Recent Advances in Metallo/Organo-Catalyzed Immortal Ring-Opening Polymerization of Cyclic Carbonates. *Catal. Sci. Technol.* **2012**, *2*(5), 898–906. https://doi.org/10.1039/c2cy00507g.

(24) Dove, A. P. Controlled Ring-Opening Polymerisation of Cyclic Esters: Polymer Blocks in Self-Assembled Nanostructures. *Chem. Commun.* **2008**, *48*, 6446–6470. https://doi.org/10.1039/b813059k.

(25) Pounder, R. J.; Dove, A. P. Towards Poly(Ester) Nanoparticles: Recent Advances in the Synthesis of Functional Poly(Ester)s by Ring-Opening Polymerization. *Polym. Chem*. **2010**, *1*(3), 260–271. https://doi.org/10.1039/b9py00327d.

(26) Rittinghaus, R. D.; Herres-Pawlis, S. Catalysts as Key Enablers for the Synthesis of Bioplastics with Sophisticated Architectures. *Chem. Eur. J.* **2023**, *29*, e202202222. https://doi.org/10.1002/chem.202202222.

(27) Rao, W.; Cai, C.; Tang, J.; Wei, Y.; Gao, C.; Yu, L.; Ding, J. Coordination Insertion Mechanism of Ring-Opening Polymerization of Lactide Catalyzed by Stannous Octoate. *Chin. J. Chem.* **2021**, *39* (7), 1965–1974. https://doi.org/10.1002/cjoc.202000519.

(28) Li, X.; Chen, H.; Xie, S.; Wang, N.; Wu, S.; Duan, Y.; Zhang, M.; Shui, L. Fabrication of Photo-Crosslinkable Poly (Trimethylene Carbonate)/Polycaprolactone Nanofibrous Scaffolds for Tendon Regeneration. *Int. J. Nanomedicine.* **2020**, *15*, 6373–6383. https://doi.org/10.2147/IJN.S246966.

(29) Benabdillah, K. M.; Coudane, J.; Boustta, M.; Engel, R.; Vert, M. Synthesis and Characterization of Novel Degradable Polyesters Derived from D-Gluconic and Glycolic Acids. *Macromolecules* **1999**, *32* (26), 8774–8780. https://doi.org/10.1021/ma991101o.

(30) Helou, M.; Brusson, J. M.; Carpentier, J. F.; Guillaume, S. M. Functionalized Polycarbonates from Dihydroxyacetone: Insights into the Immortal Ring-Opening Polymerization of 2,2-Dimethoxytrimethylene Carbonate. *Polym. Chem.* **2011**, *2* (12), 2789–2795. https://doi.org/10.1039/c1py00405k.

(31) Li, F.; Danquah, M.; Mahato, R. I. Synthesis and Characterization of Amphiphilic Lipopolymers for Micellar Drug Delivery. *Biomacromolecules* **2010**, *11* (10), 2610–2620. https://doi.org/10.1021/bm100561v.

(32) Serhan, M.; Sprowls, M.; Jackemeyer, D.; Long, M.; Perez, I. D.; Maret, W.; Tao, N.; Forzani, E. Total Iron Measurement in Human Serum with a Smartphone. *AIChE Annual Meeting, Conference Proceedings*; American Institute of Chemical Engineers, **2019**. https://doi.org/10.1039/x0xx00000x.

(33) Gautier, E.; Fuertes, P.; Cassagnau, P.; Pascault, J. P.; Fleury, E. Synthesis and Rheology of Biodegradable Poly(Glycolic Acid) Prepared by Melt Ring-Opening Polymerization of Glycolide. *J. Polym. Sci. A Polym. Chem.* **2009**, *47* (5), 1440–1449.

https://doi.org/10.1002/pola.23253.

(34) John, G.; Morita, M. Synthesis of polymer network scaffolds and microspheres based on poly(ε-caprolactone-co-glycolic acid-co-l-serine). *Mater. Sci. Eng. C.* **2000**, *13*, 91-95. https://doi.org/10.1016/S0928-4931(00)00181-8

(35) Wang, Y.; Darensbourg, D. J. Carbon Dioxide-Based Functional Polycarbonates: Metal Catalyzed Copolymerization of CO_2 and Epoxides. *Coord. Chem. Rev*. **2018**, *372*, 85–100. https://doi.org/10.1016/j.ccr.2018.06.004.

(36) Abdul-Karim, R.; Hameed, A.; Malik, M. I. Ring-Opening Polymerization of Ethylene Carbonate: Comprehensive Structural Elucidation by 1D & 2D-NMR Techniques, and Selectivity Analysis. *RSC Adv.* **2017**, *7*(19), 11786–11795. https://doi.org/10.1039/c7ra01113j.

(37) Palenzuela, M.; Sarisuta, K.; Navarro, M.; Kumamoto, N.; Chanthaset, N.; Monot, J.; Ajiro, H.; Martín-Vaca, B.; Bourissou, D. 5-Methylene-1,3-Dioxane-2-One: A First-Choice Comonomer for Trimethylene Carbonate. *Macromolecules* **2023,** *56*, 678-689. https://doi.org/10.1021/acs.macromol.2c02270.

(38) Nobuoka, H.; Nagasawa, M.; Chanthaset, N.; Yoshida, H.; Haramiishi, Y.; Ajiro, H. Synthesis of Amphiphilic Block Copolymer Using Trimethylene Carbonate Bearing Oligo(Ethylene Glycol) and Investigation of Thin Film Including Cilostazol. *J. Polym. Sci.* **2020**, *58* (17), 2347–2354. https://doi.org/10.1002/pol.20200390.

(39) Abdul-Karim, R.; Hameed, A.; Malik, M. I. Ring-Opening Polymerization of Propylene Carbonate: Microstructural Analysis of the Polymer and Selectivity of Polymerization by 2D-NMR Techniques. *Eur. Polym. J.* **2018**, *105*, 95–106. https://doi.org/10.1016/j.eurpolymj.2018.05.028.

(40) Mainardes, R. M.; Khalil, N. M.; Gremião, M. P. D. Intranasal Delivery of Zidovudine by PLA and PLA-PEG Blend Nanoparticles. *In.t J. Pharm.* **2010**, *395* (1–2), 266–271. https://doi.org/10.1016/j.ijpharm.2010.05.020.

(41) Sankaran, K. K.; Krishnan, U. M.; Sethuraman, S. Axially Aligned 3D Nanofibrous Grafts of PLA-PCL for Small Diameter Cardiovascular Applications. *J. Biomater. Sci. Polym. Ed.* **2014**, *25* (16), 1791–1812. https://doi.org/10.1080/09205063.2014.950505.

(42) Ohara, T.; Itaya, T.; Usami, K.; Ando, Y.; Sakurai, H.; Honda, M. J.; Ueda, M.; Kagami, H. Evaluation of Scaffold Materials for Tooth Tissue Engineering. *J. Biomed. Mater. Res. A.* **2010**, *94* (3), 800–805. https://doi.org/10.1002/jbm.a.32749.

(43) Mi, H. Y.; Salick, M. R.; Jing, X.; Jacques, B. R.; Crone, W. C.; Peng, X. F.; Turng, L. S. Characterization of Thermoplastic Polyurethane/Polylactic Acid (TPU/PLA) Tissue Engineering Scaffolds Fabricated by Microcellular Injection Molding. *Mater. Sci. Eng. C.* **2013**, *33* (8), 4767–4776. https://doi.org/10.1016/j.msec.2013.07.037.

(44) Albertsson, A.-C.; Varma, I. K. Aliphatic Polyesters: Synthesis, Properties and Applications. In: Degradable Aliphatic Polyesters. *Adv. Polym. Sci.* **2002**, *157*, 1-40. https://doi.org/10.1007/3-540-45734-8_1

(45) Hyon, S.-H.; Jamshidi, K.; Ikada, Y. Synthesis of Polylactides with Different Molecular Weights, *Biomaterials* **1997**, *16*, 1503-1508. https://doi.org/10.1016/S0142-9612(97)00076-8

(46) Kobayashi, S.; Uyama, H.; Kimura, S. Enzymatic Polymerization. *Chem. Rev*. **2001**, 101, *12*, 3793–3818 https://doi.org/10.1021/cr9901211.

(47) Loos, K.; Stadler, R. Synthesis of Amylose-Block-Polystyrene Rod-Coil Block Copolymers, *Macromolecules* **1997**, *30*(24), 7641–7643.

(48) Greco, A.; Ferrari, F. Thermal Behavior of PLA Plasticized by Commercial and Cardanol-Derived Plasticizers and the Effect on the Mechanical Properties. *J. Therm. Anal. Calorim.* **2021**, *146* (1), 131–141. https://doi.org/10.1007/s10973-020-10403-9.

(49) Gao, X.; Qi, S.; Yang, B.; Su, Y.; Li, J.; Wang, D. Synergistic Effect of Plasticizer and Nucleating Agent on Crystallization Behavior of Polylactide during Fused Filament Fabrication. *Polymer* **2021**, *215, 123426*. https://doi.org/10.1016/j.polymer.2021.123426.

(50) Brdlík, P.; Borůvka, M.; Běhálek, L.; Lenfeld, P. Biodegradation of Poly(Lactic Acid) Biocomposites under Controlled Composting Conditions and Freshwater Biotope. *Polymers* **2021**, *13* (4), 1–15. https://doi.org/10.3390/polym13040594.

(51) Wang, Y.; Ying, Z.; Xie, W.; Wu, D. Cellulose Nanofibers Reinforced Biodegradable Polyester Blends: Ternary Biocomposites with Balanced Mechanical Properties. *Carbohydr. Polym.* **2020**, *233,* 115845. https://doi.org/10.1016/j.carbpol.2020.115845.

(52) Xue, B.; He, H. Z.; Huang, Z. X.; Zhu, Z.; Xue, F.; Liu, S.; Liu, B. Fabrication of Super-Tough Ternary Blends by Melt Compounding of Poly(Lactic Acid) with Poly(Butylene Succinate) and Ethylene-Methyl Acrylate-Glycidyl Methacrylate. *Compos. B.Eng.* **2019**, *172*, 743–749. https://doi.org/10.1016/j.compositesb.2019.05.098.

(53) Zhang, H. C.; Kang, B. hao; Chen, L. S.; Lu, X. Enhancing Toughness of Poly (Lactic Acid)/Thermoplastic Polyurethane Blends *via* Increasing Interface Compatibility by Polyurethane Elastomer Prepolymer and Its Toughening Mechanism. *Polym. Test* **2020**, *87,* 106521. https://doi.org/10.1016/j.polymertesting.2020.106521.

(54) Riley, T.; Stolnik, S.; Heald, C. R.; Xiong, C. D.; Garnett, M. C.; Illum, L.; Davis, S. S.; Purkiss, S. C.; Barlow, R. J.; Gellert, P. R. Physicochemical Evaluation of Nanoparticles Assembled from Poly(Lactic Acid)-Poly(Ethylene Glycol) (PLA-PEG) Block Copolymers as Drug Delivery Vehicles. *Langmuir* **2001**, *17*(11), 3168–3174. https://doi.org/10.1021/la001226i.

(55) Liu, H.; Chen, N.; Shan, P.; Song, P.; Liu, X.; Chen, J. Toward Fully Bio-Based and Supertough PLA Blends *via* in Situ Formation of Cross-Linked Biopolyamide Continuity Network. *Macromolecules* **2019**, *52*(21), 8415–8429. https://doi.org/10.1021/acs.macromol.9b01398.

(56) Kost, B.; Basko, M.; Bednarek, M.; Socka, M.; Kopka, B.; Łapienis, G.; Biela, T.; Kubisa, P.; Brzeziński, M. The Influence of the Functional End Groups on the Properties of Polylactide-Based Materials. *Prog. Polym. Sci*. **2022**, *130*, 101556. https://doi.org/10.1016/j.progpolymsci.2022.101556.

(57) Sarisuta, K.; Iwami, M.; Martín-Vaca, B.; Chanthaset, N.; Ajiro, H. PH Effect on Particle Aggregation of Vanillin End-Capped Polylactides Bearing a Hydrophilic Group Connected by a Cyclic Acetal Moiety. *Langmuir* **2023**, *39*(11), 3994–4004. https://doi.org/10.1021/acs.langmuir.2c03303.

(58) Alba, A.; Du Boullay, O. T.; Martin-Vaca, B.; Bourissou, D. Direct Ring-Opening of Lactide with Amines: Application to the Organo-Catalyzed Preparation of Amide End-Capped PLA and to the Removal of Residual Lactide from PLA Samples. *Polym. Chem.* **2015**, *6* (6), 989–997. https://doi.org/10.1039/c4py00973h.

(59) Chanthaset, N.; Ajiro, H. Synthetic Biodegradable Polymers with Chain End Modification: Polylactide, Poly(Butylene Succinate), and Poly(Hydroxyalkanoate). *Chem. Lett.* **2021**, *50* (4), 767–777. https://doi.org/10.1246/CL.200859.

(60) Steele, T. W. J.; Huang, C. L.; Kumar, S.; Iskandar, A.; Baoxin, A.; Boey, F. Y. C.; Loo, J. S. C.; Venkatraman, S. S. Tuning Drug Release in Polyester Thin Films: Terminal End-Groups Determine Specific Rates of Additive-Free Controlled Drug Release. *NPG Asia Mater.* **2013**, *5* (4), e46. https://doi.org/10.1038/am.2013.9.

(61) Yildirim, E. D.; Ayan, H.; Vasilets, V. N.; Fridman, A.; Guceri, S.; Sun, W. Effect of Dielectric Barrier Discharge Plasma on the Attachment and Proliferation of Osteoblasts Cultured over Poly(ε-Caprolactone) Scaffolds. *Plasma Process. Polym.* **2008**, *5* (1), 58–66. https://doi.org/10.1002/ppap.200700041.

(62) Gerhardt, W. W.; Noga, D. E.; Hardcastle, K. I.; García, A. J.; Collard, D. M.; Weck, M. Functional Lactide Monomers: Methodology and Polymerization. *Biomacromolecules* **2006**, *7* (6), 1735–1742. https://doi.org/10.1021/bm060024j.

(63) Kaluzynski, K.; Pretula, J.; Lewinski, P.; Kaźmierski, S.; Penczek, S. Synthesis and Properties of Functionalized Poly(ϵ-Caprolactone); Chain Polymerization Followed by Polycondensation in One Pot with Initiator and Catalyst in One Molecule. Synthesis and Molecular Structures. *Macromolecules* **2022**, *55*(6), 2210–2221. https://doi.org/10.1021/acs.macromol.1c02325.

(64) Webb, K.; Hlady, V.; Tresco, P. A. Relative Importance of Surface Wettability and

Charged Functional Groups on NIH 3T3 Fibroblast Attachment, Spreading, and Cytoskeletal Organization. *J. Biomed. Mater. Res.* **1998**, *41*(3), 422–430. https://doi.org/10.1002/(SICI)1097-4636(19980905)41:3<422::AID-JBM12>3.0.CO;2-K.

(65) Ghassemi, A. H.; van Steenbergen, M. J.; Talsma, H.; van Nostrum, C. F.; Jiskoot, W.; Crommelin, D. J. A.; Hennink, W. E. Preparation and Characterization of Protein Loaded Microspheres Based on a Hydroxylated Aliphatic Polyester, Poly(Lactic-Co-Hydroxymethyl Glycolic Acid). *J. Control. Release.* **2009**, *138* (1), 57–63. https://doi.org/10.1016/j.jconrel.2009.04.025.

(66) Kan, K.; Akashi, M.; Ajiro, H. Polylactides Bearing Vanillin at Chain End Provided Dual Dynamic Interactions: Stereocomplex Formation and Nanostructure Control. *Macromol. Chem. Phys.* **2016**, *217* (24), 2679–2685. https://doi.org/10.1002/macp.201600395.

(67) Kan, K.; Akashi, M.; Ajiro, H. Dynamic Self-Assembly and Synthesis of Polylactide Bearing 5-Hydroxymethylfurfural Chain Ends. *ACS Appl. Polym. Mater.* **2019**, *1* (2), 267–274. https://doi.org/10.1021/acsapm.8b00185.

(68) Knowles, J. P.; Whiting, A. The Effects of Ring Size and Substituents on the Rates of Acid-Catalysed Hydrolysis of Five- and Six-Membered Ring Cyclic Ketone Acetals. *European J. Org. Chem.* **2007**, *20*, 3365–3368. https://doi.org/10.1002/ejoc.200700244.

(69) Chen, W.; Meng, F.; Cheng, R.; Deng, C.; Feijen, J.; Zhong, Z. Advanced Drug and Gene Delivery Systems Based on Functional Biodegradable Polycarbonates and Copolymers. *J. Control. Release*. **2014**, *190*, 398–414. https://doi.org/10.1016/j.jconrel.2014.05.023.

(70) Rosler, A.; Vandermeulen, G. W. M.; Klok, A. Advanced Drug Delivery Devices via Self-Assembly of Amphiphilic Block Copolymers. *Adv. Drug Deliv. Rev.* **2001**, *53* (1), 95–108. https://doi.org/10.1016/s0169-409x(01)00222-8.

(71) Weems, A. C.; Arno, M. C.; Yu, W.; Huckstepp, R. T. R.; Dove, A. P. 4D Polycarbonates *via* Stereolithography as Scaffolds for Soft Tissue Repair. *Nat. Commun.* **2021**, *12* (1). https://doi.org/10.1038/s41467-021-23956-6.

(72) Fukushima, K.; Inoue, Y.; Haga, Y.; Ota, T.; Honda, K.; Sato, C.; Tanaka, M. Monoether-Tagged Biodegradable Polycarbonate Preventing Platelet Adhesion and Demonstrating Vascular Cell Adhesion: A Promising Material for Resorbable Vascular Grafts and Stents. *Biomacromolecules* **2017**, *18* (11), 3834–3843. https://doi.org/10.1021/acs.biomac.7b01210.

(73) Guillaume, S. M.; Mespouille, L. Polycarbonates and Green Chemistry. *J. Appl. Polym. Sci.* **2013**, *131*(5). https://doi.org/10.1002/app.40081.

(74) Shaikh, A.-A. G.; Sivaram, S. Organic Carbonates. *Chem. Rev*. **1996**, *96*(3), 951–976. https://doi.org/10.1021/cr950067i.

(75) Gregory, G. L.; Ulmann, M.; Buchard, A. Synthesis of 6-Membered Cyclic Carbonates from 1,3-Diols and Low CO_2 Pressure: A Novel Mild Strategy to Replace Phosgene Reagents. *RSC Adv.* **2015**, *5* (49), 39404–39408. https://doi.org/10.1039/c5ra07290e.

(76) Lee, E. H.; Ahn, J. Y.; Dharman, M. M.; Park, D. W.; Park, S. W.; Kim, I. Synthesis of Cyclic Carbonate from Vinyl Cyclohexene Oxide and CO_2 Using Ionic Liquids as Catalysts. *Catal. Today* **2008**, *131*(1–4), 130–134. https://doi.org/10.1016/j.cattod.2007.10.012.

(77) Kricheldorp, H. R.; Dunsing, R.; Serra, A. Polylactones 12 a) Cationic Polymerization of 2,2dimethyltrimethylene Carbonate. *Die Makromolekulare Chemie.* **1987**, *188*(10), 2453–2466. https://doi.org/10.1002/macp.1987.021881020.

(78) Takojima, K.; Saito, T.; Vevert, C.; Ladelta, V.; Bilalis, P.; Watanabe, J.; Hatanaka, S.; Konno, T.; Yamamoto, T.; Tajima, K.; Hadjichristidis, N.; Isono, T.; Satoh, T. Facile Synthesis of Poly(Trimethylene Carbonate) by Alkali Metal Carboxylate-Catalyzed Ring-Opening Polymerization. *Polym. J.* **2020**, *52*(1), 103–110. https://doi.org/10.1038/s41428-019-0264-6.

(79) Kricheldorf, H. R.; Stricker, A. Polymers of Carbonic Acid, 28: SnOct2-Initiated Polymerizations of Trimethylene Carbonate (TMC, 1,3-Dioxanone-2). *Macromol. Chem. Phys.* **2000**, *201*(17), 2557–2565. https://doi.org/10.1002/1521-3935(20001101)201:17<2557::AID-MACP2557>3.0.CO;2-F.

(80) Delcroix, D.; Martín-Vaca, B.; Bourissou, D.; Navarro, C. Ring-Opening Polymerization of Trimethylene Carbonate Catalyzed by Methanesulfonic Acid: Activated Monomer versus Active Chain End Mechanisms. *Macromolecules* **2010**, *43* (21), 8828–8835. https://doi.org/10.1021/ma101461y.

(81) Kobayashi, S.; Kikuchi, H.; Uyama, H. Lipase-Catalyzed Ring-Opening Polymerization of 1,3-Dioxan-2-One. *Macromol. Rapid Commun.* **1997**, *18*(7), 575–579. https://doi.org/10.1002/marc.1997.030180707.

(82) Ma, Z.; Hong, Y.; Nelson, D. M.; Pichamuthu, J. E.; Leeson, C. E.; Wagner, W. R. Biodegradable Polyurethane Ureas with Variable Polyester or Polycarbonate Soft Segments: Effects of Crystallinity, Molecular Weight, and Composition on Mechanical Properties. *Biomacromolecules* **2011**, *12*(9), 3265–3274. https://doi.org/10.1021/bm2007218.

(83) Dargaville, B. L.; Vaquette, C.; Peng, H.; Rasoul, F.; Chau, Y. Q.; Cooper-White, J. J.; Campbell, J. H.; Whittaker, A. K. Cross-Linked Poly(Trimethylene Carbonate- Co - L - Lactide) as a Biodegradable, Elastomeric Scaffold for Vascular Engineering Applications. *Biomacromolecules* **2011**, *12*(11), 3856–3869. https://doi.org/10.1021/bm201291e.

(84) Diment, W. T.; Lindeboom, W.; Fiorentini, F.; Deacy, A. C.; Williams, C. K. Synergic Heterodinuclear Catalysts for the Ring-Opening Copolymerization (ROCOP) of Epoxides, Carbon Dioxide, and Anhydrides. *Acc. Chem. Res.* **2022**, *55* (15), 1997–2010. https://doi.org/10.1021/acs.accounts.2c00197.

(85) Brandolese, A.; Kleij, A. W. Catalyst Engineering Empowers the Creation of Biomass-Derived Polyesters and Polycarbonates. *Acc. Chem. Res.* **2022**, *55* (12), 1634–1645. https://doi.org/10.1021/acs.accounts.2c00204.

(86) Tempelaar, S.; Mespouille, L.; Coulembier, O.; Dubois, P.; Dove, A. P. Synthesis and Post-Polymerisation Modifications of Aliphatic Poly(Carbonate)s Prepared by Ring-Opening Polymerisation. *Chem. Soc. Rev.* **2013**, *42*(3), 1312–1336. https://doi.org/10.1039/c2cs35268k.

(87) Rokicki, G. Aliphatic Cyclic Carbonates and Spiroorthocarbonates as Monomers. *Prog. Polym. Sci.* **2000**, *25* (2), 259–342. https://doi.org/10.1016/s0079-6700(00)00006-x.

(88) Sanders, D. P.; Fukushima, K.; Coady, D. J.; Nelson, A.; Fujiwara, M.; Yasumoto, M.; Hedrick, J. L. A Simple and Efficient Synthesis of Functionalized Cyclic Carbonate Monomers Using a Versatile Pentafluorophenyl Ester Intermediate. *J. Am. Chem. Soc.* **2010**, *132* (42), 14724–14726. https://doi.org/10.1021/ja105332k.

(89) Nobuoka, H.; Ajiro, H. Novel Synthesis Method of Ester Free Trimethylene Carbonate Derivatives. *Tetrahedron Lett.* **2019**, *60*(2), 164–170. https://doi.org/10.1016/j.tetlet.2018.12.002.

(90) Yuen, A. Y.; Bossion, A.; Veloso, A.; Mecerreyes, D.; Hedrick, J. L.; Dove, A. P.; Sardon, H. Efficient Polymerization and Post-Modification of: N -Substituted Eight-Membered Cyclic Carbonates Containing Allyl Groups. *Polym. Chem.* **2018**, *9*(18), 2458–2467. https://doi.org/10.1039/c8py00231b.

(91) Thomas, A. W.; Dove, A. P. Postpolymerization Modifications of Alkene-Functional Polycarbonates for the Development of Advanced Materials Biomaterials. *Macromol. Biosci*. **2016**, *16*(12), 1762–1775. https://doi.org/10.1002/mabi.201600310.

(92) Yu, F.; Zhuo, R. Synthesis, Characterization, and Degradation Behaviors of End-Group-Functionalized Poly(Trimethylene Carbonate)s. *Polym. J.* **2003**, *35* (8), 671–676. https://doi.org/10.1295/polymj.35.671.

(93) Zhang, L.; Brostowitz, N. R.; Cavicchi, K. A.; Weiss, R. A. Perspective: Ionomer Research and Applications. *Macromol. React. Eng.* **2014**, *8*(2), 81–99. https://doi.org/10.1002/mren.201300181.

(94) Courtney, J. M.; Lamba, N. M. K.; Sundaram, S.; Forbes, C. D. Biomaterials for Blood-Contacting Applications. *Biomaterials* **1994**, *15*(10), 737–744. https://doi.org/10.1016/0142-9612(94)90026-4.

(95) Korneckq, E.; Niewiarowski, S.; Morinelli, T. A.; Kloczewiak, M. Effects of Chymotrypsin and Adenosine Diphosphate on the Exposure of Fibrinogen Receptors on Normal Human and Glanzmann's Thrombasthenic Platelets. *J. Biol. Chem.* **1981**, *256* (11), 5696–5701. https://doi.org/10.1016/s0021-9258(19)69261-6.

(96) Courtney, J. M.; Sundaram, S.; Qing, H.; Bioengineering, Y. Artificial Surfaces and Blood Interaction. *Vascular Medicine Review* **1994**, *5*, 47-49. https://doi.org/10.1177/1358863X9400500105.

(97) Engbers, G. H.; Feijen, J. Current Techniques to Improve the Blood Compatibility of Biomaterial Surfaces. *Int. J. Artif. Organs.* **1991**, *14* (4), 199–215.

(98) Nederberg, F.; Watanabe, J.; Ishihara, K.; Hilborn, J.; Bowden, T. Biocompatible and Biodegradable Phosphorylcholine Ionomers with Reduced Protein Adsorption and Cell Adhesion. *J. Biomater. Sci. Polym. Ed.* **2006**, *17*(6), 605–614. https://doi.org/10.1163/156856206777346304.

Chapter I

The Design of pH-Responsive Functional Chain Ends of Polylactides for Trigged Aggregation

1.1 Introduction

Biodegradable polymers have gained considerable attention in several decades due to low toxicity[1], biodegradability[2], and biocompatibility[3] compared to petroleum-based polymers. Recently, well-known aliphatic polyesters (APEs) such as poly(lactic-*co*-glycolic acid) (PLGA), poly(caprolactone) (PCL), and poly(lactic acid) (PLA) have been developed in the biomedical field.[4]

PLA is derived from lactic acid which is a product from renewable plant resources[5] and graded as safe by the US Food and Drug Administration (FDA).[6] With different configurations of PLA, the chiral molecules exist in two optically active polymers, poly(*L,L*-lactide) (PLLA) and poly(*D,D*-lactide) (PDLA) according to the enantiomer of the monomer.[7] However, the limited thermal and hydrolytic stability of PLA-based materials constrains their potential for long-term applications. Thankfully, stereocomplex crystallization of enantiomeric PLLA and PDLA offers a robust method to significantly enhance material properties such as stability and biocompatibility. This is achieved through strong intermolecular interactions between *L*-lactyl and *D*-lactyl units. This approach has become tone of the principal strategies for advancing PLA applications.[7] Currently, PLA is a candidate for various medical applications, including clinical devices,[8] tissue engineering,[9] and drug delivery[10] due to its bio-dissolvability in the human body.[11] However, the chemical structures of PLAs are inherently limited, resulting in properties that may lack the necessary versatility for diverse targeted applications. Many efforts have been focused on custom designing and synthesizing polymers with tailorable properties that can appropriately match the unique and particular requirements of each individual clinical application. Some of the important performances sought include degradation period that should match with the healing process, mechanical performances able to withstand on indicated application, and non-toxic degradation

products to avoid inflammatory or adverse effects upon implantation in the body.[4] Therefore, to enhance material properties, chemical modification of the polymer chains[12] is a valuable approach, along with processing[13] and blending.[14] The chemical modification methods for creating new functional biodegradable polymers are intriguing and have garnered significant attention because it allows for tunable properties and additional functions through molecular design. A commonly used route to functional polyesters involves homopolymerizing functional (protected) monomers or copolymerizing such monomers with commercially available non-functionalized monomers. This can be achieved through three major polymerization routes, as mentioned in the general introduction section.[15] Typically, the functional groups in the monomers are protected to prevent side reactions. Consequently, a deprotection step after polymerization is necessary to obtain polymers bearing functional groups (**Figure 1-1, Figure 1-2, and Figure 1-3).** [16–20]

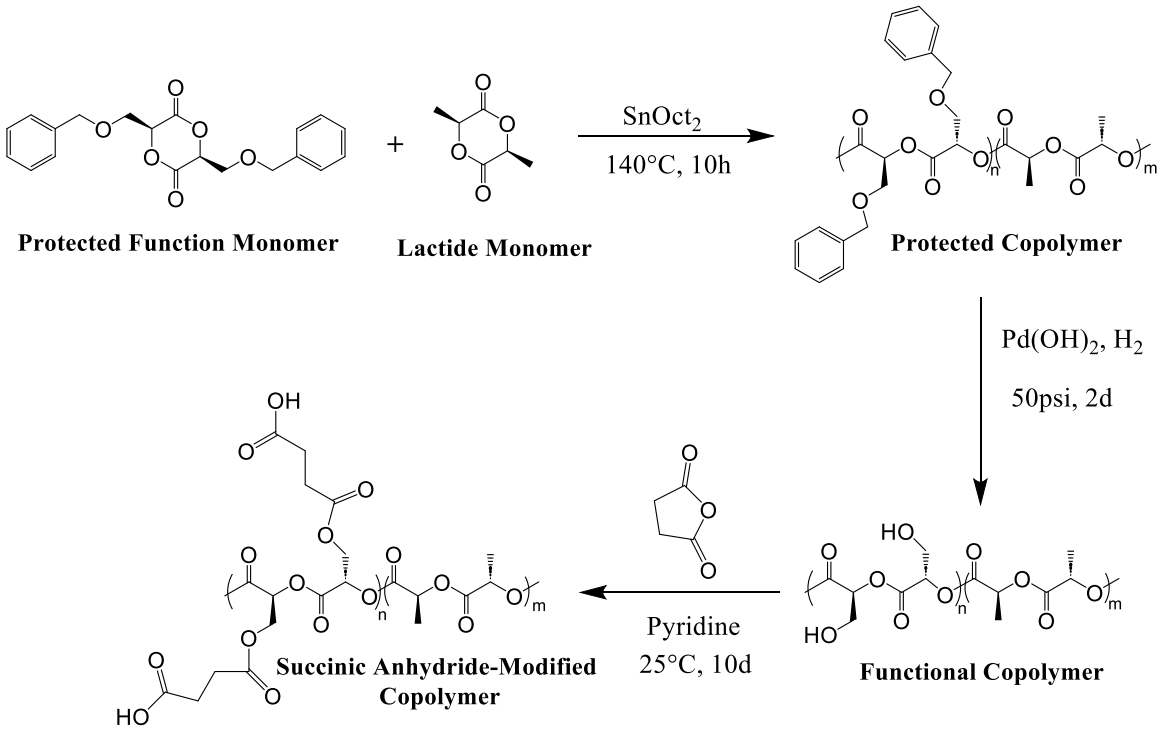

Figure 1-1. Copolymer synthesis, deprotection, and modification with succinic anhydride.[17]

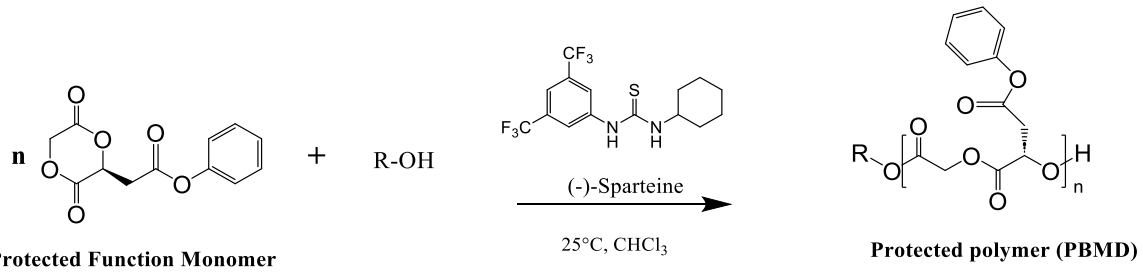

Figure 1-2. Ring-Opening Polymerization (ROP) of Cyclic Esters Derived from L-Malic Acid with protection group.[18]

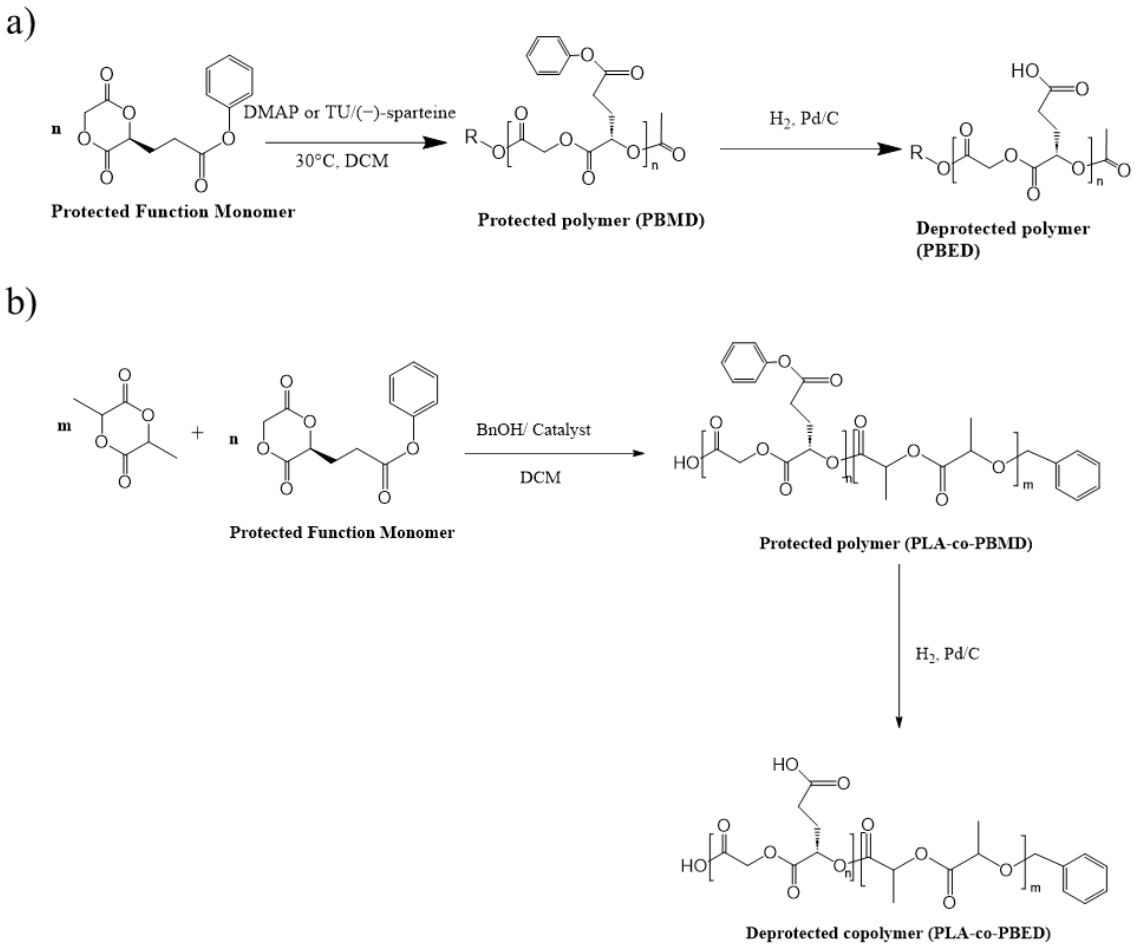

Figure 1-3. a) ROP of a 1,4-Dioxane-2,5-dione Deriving from Glutamic Acid and deprotection. [19] and b) The presentation of the synthesis of the investigated copolymers, based on: a *D,L*-lactide and *L*-3-(2-Benzyloxycarbonyl) Ethyl-1,4-Dioxane-2,5-dione (PLA-*co*-PBED).[20]

For example, Collard et al, synthesized a PLA copolymer with pendant benzyloxy groups by the copolymerization of a benzyl-ether substituted monomer with lactide. Debenzylation of the polymer to provide pendant hydroxyl groups followed by modification with succinic anhydride affords the corresponding carboxylic acid functionalized copolymer that is amenable to standard carbodiimide coupling conditions to attach amine-containing biological molecules.[17] Dove and co-workers successfully prepared functional polyesters with pendant benzyl-protected carboxylic acid groups, achieving high monomer conversions without transesterification side reactions. The protected functionalized polymer was then deprotected using Pd/C to obtain the desired functional groups (**Figure 1-2**).[18] Bourissou et al. synthesized the functionalized PLGA with protective group (*L*-3-(2-Benzyloxycarbonyl)Ethyl-1,4-Dioxane-2,5-dione (BED)) (**Figure 1-3a**). Copolymerization of these protected functionalized PLGA derivatives and PLA were polymerized. Then, the obtained protected functionalized copolymer was deprotected by Pd/C to obtain the desired functional group (**Figure 1-3b**).[20]

In another example, Hu et al. synthesized a functionalized polymer (PEG-*b*-P(LA-*co*-PTO)) through the copolymerization of a functionalized/protected monomer, [9-phenyl-2,4,8,10-tetraoxapiro[5,5]undecan-3-one] (PTO), with lactide (LA). This synthesis was conducted in the presence of monohydroxyl-poly(ethyleneglycol) (PEG) as a macro initiator and $Sn(Oct)_2$ as a catalyst. The benzylidene protecting groups of this polymer were removed by catalytic hydrogenation to obtain PEG-*b*-P(LA-*co*-DHP) (**Figure 1-4**).[21]

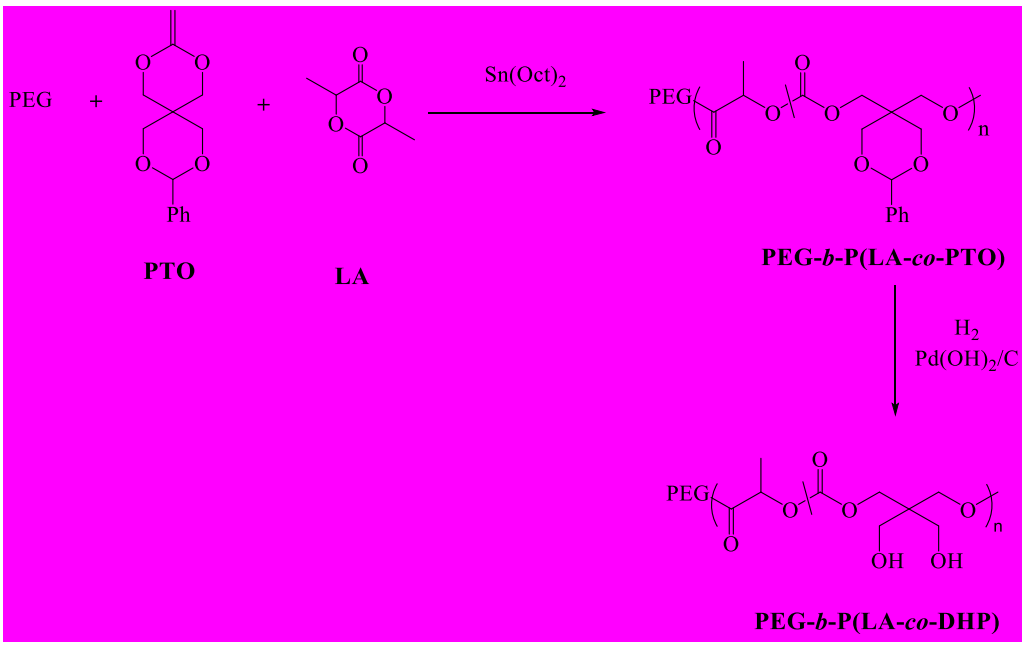

Figure 1-4. Synthesis of PEG-*b*-P(LA-*co*-PTO) and PEG-*b*-P(LA-*co*-DHP). [21]

Nevertheless, chemical modification using functionalized monomers can be both costly and time-consuming, as it frequently necessitates the creation of new monomers. This process generally includes additional steps to protect the reactive sites of the monomers during polymerization. Consequently, modifying the chain ends has proven to be an efficient method for introducing new functionalities while retaining the fundamental properties of the polymer. This approach can significantly influence various properties of the material such as degradation behavior, thermal property, contact angles, due to changes in molecular weights resulting from chain extension or degradation. There are two majority methods for chain end modifications: (I) end group modification and (II) functionalized initiators. Therefore, post-polymerization modification functionalization is not the preferred route to obtain functional polyesters. For instance, Bednarek et al. introduced several carboxylic moieties at the chain end of PLA in regard to the interaction with metal by using a propargyl group and mercaptosuccinic acid (**Figure 1-5**).[22] These end groups of PLA were then converted into ionic groups by neutralizing a polymer solution with metal oxides such as CaO, ZnO, and Fe_2O_3. In another example, lactose was efficiently incorporated using a specific technique: protected 2-aminoethanol was selected as an initiator for PLA preparation, followed by successive deprotection and ester interchange reaction of lactone with PLA bearing NH_2 (**Figure 1-6**).[23]

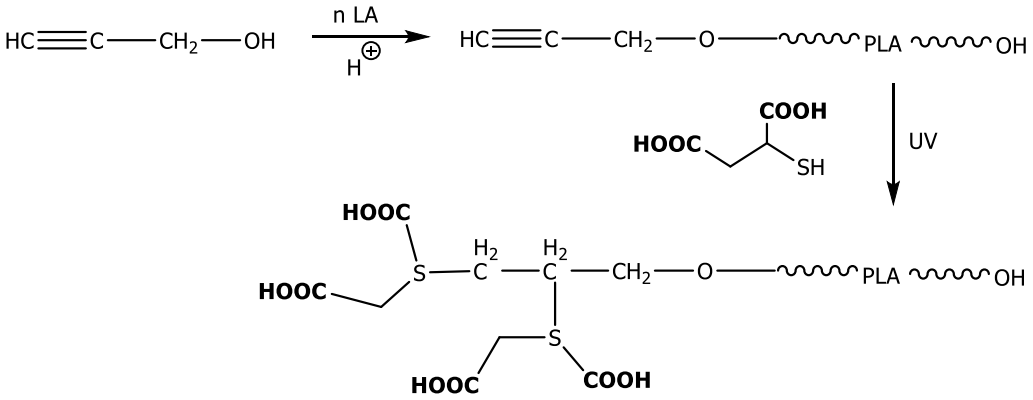

Figure 1-5. Schematic representation of the synthesis of PLA with several carboxyl groups at one chain end.[22]

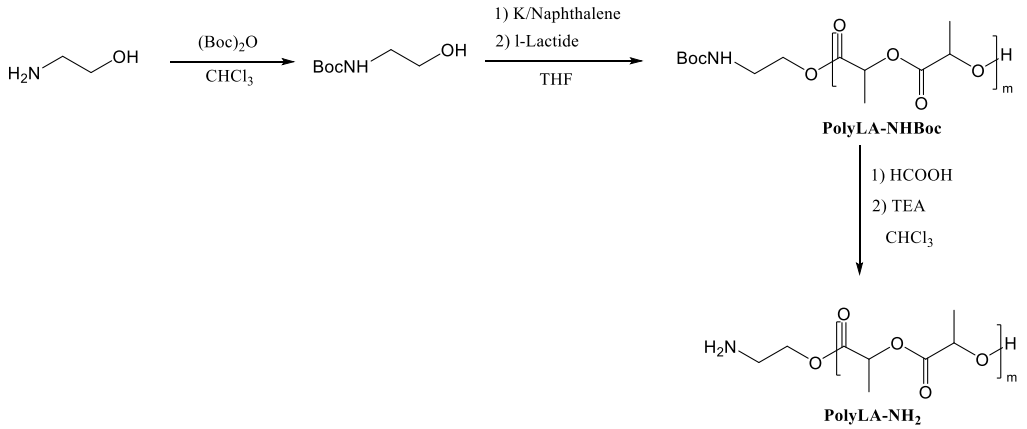

Figure 1-6. Synthetic Route of polyLA-NH_2 [23]

However, functionalizing PLAs through end group modification *via* post-polymerization modification functionalization has its drawbacks, such as the possibility of side reactions like chain scission and racemization.[15,24]

Alternatively, functionalizing PLAs through the use of functionalized initiators offers a simpler methodology. In this approach, the ring-opening polymerization of APEs is carried out using a functional alcohol compound as an initiator. This technique facilitates chemical modification at the chain end *via* a single polymerization reaction, thereby enabling the integration of diverse functionalities tailored specifically by selecting the appropriate functional alcohol compound to achieve desired properties such as. Notably, Kim et al. developed functionalized PLA with various end groups by modifying alcohol derivative compounds. Chloride (Cl), amine (NH_2-), and carboxyl (COOH-) terminated PLAs were synthesized from hydroxyl (OH-) terminated PLAs to control the degradation of the polymer (**Figure 1-7**).[25] Similarly, Sugimoto et al. highlighted the effectiveness of this approach by synthesizing PLLA with terminal *n*-alkyl groups of varying chain lengths (C_0-C_{22}) using a functional alcohol compound as the initiator. This significantly enhanced nucleation, attributed to the presence of long terminal *n*-alkyl groups.[26]

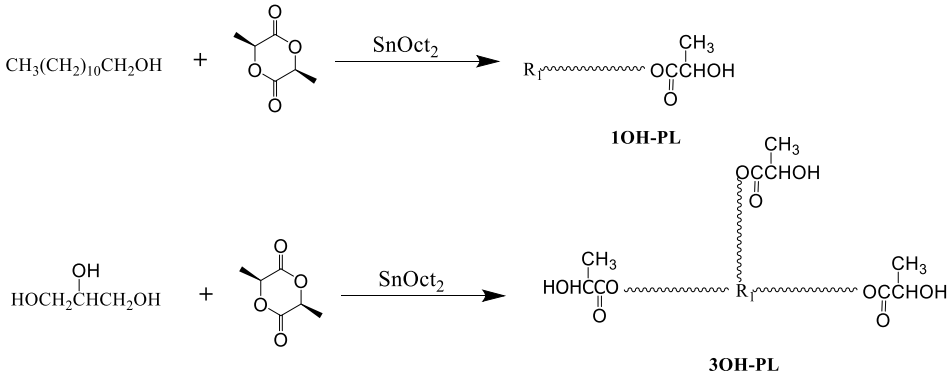

Figure 1-7. Synthesis of one-arm and three-arm PLAs.[25]

In light of using functional alcohol compounds as functionalized initiators, specific tailoring of polymer properties can be achieved. This approach may provide the potential to introduce pH-responsive functional groups at the initiation stage of polymerization. Additionally, pH-responsive biodegradable polymers[27,28] have been wildly developed due to their potential emerging *in vitro* and *in vivo* biomedical applications and the bio-relevance of pH modulation in living organisms. Their unique properties consequently make them practical in various medical applications such as targeted drug delivery systems,[29] tissue engineering, and cell culture.[30] The pH triggered could be advantage to set up targeted and localized delivery to achieve improved therapy (**Figure 1-8**). [31] For instance, the pH around tumor cells tends to be mildly acidic (~ 5.5–6.5) while physiological pH is essentially neutral (7.0–7.4).[32] The main design feature for pH-responsive nano-constructs are responsible to hydrophobic to hydrophilic transformation at low pH conditions. Widely explored in the different pH-responsive polymeric system have been studied by incorporating functional group such as hydrazone, imines, orthoesters, vinylether and acetals (**Figure 1-9**) as there can behave as acid labile linkages in the core-forming block polymeric nano-systems.[33] Degradation of these linkages leads to the disassembly of structure by pH triggered manner while the hydrolysis rate can be modified by altering the chemical structure. To overcome the targeted drug delivery systems, pH level and carrier plays the important role to achieve targeted delivery. The carrier from biodegradable polymer is essential to encapsulate and release drugs to a certain site with time limitation. Therefore, biodegradable polymeric particles could play a superior degradation under physiological condition (mild pH change) with a unique strategy. Recently, PLA nanoparticle has a promising application in nano-medicine carriers and encapsulations for drugs, proteins, hormones and genes.[34,35]

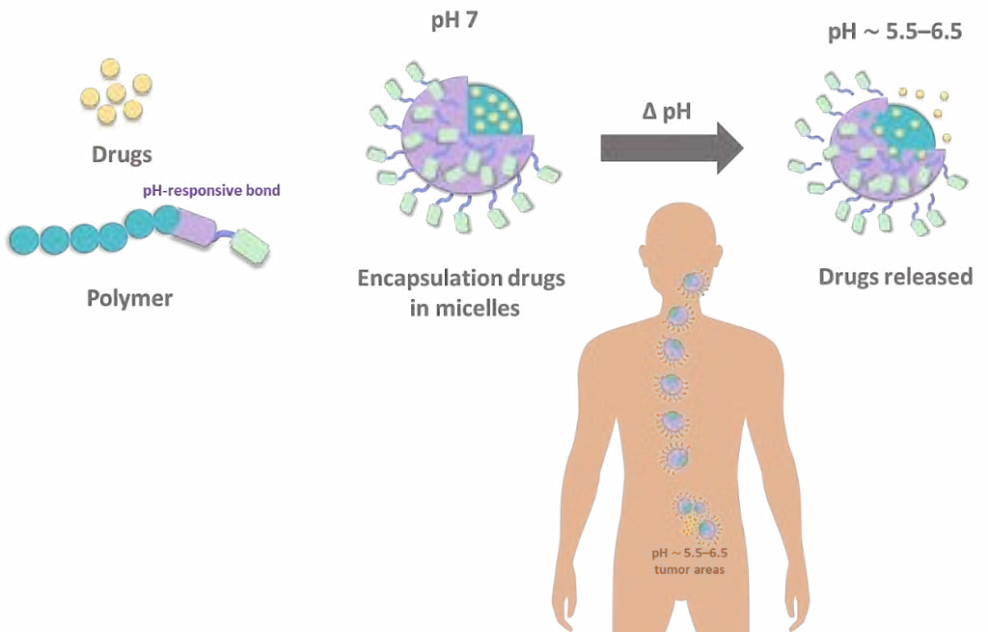

Figure 1-8. The advantage of pH-responsive for targeted and localized drug delivery

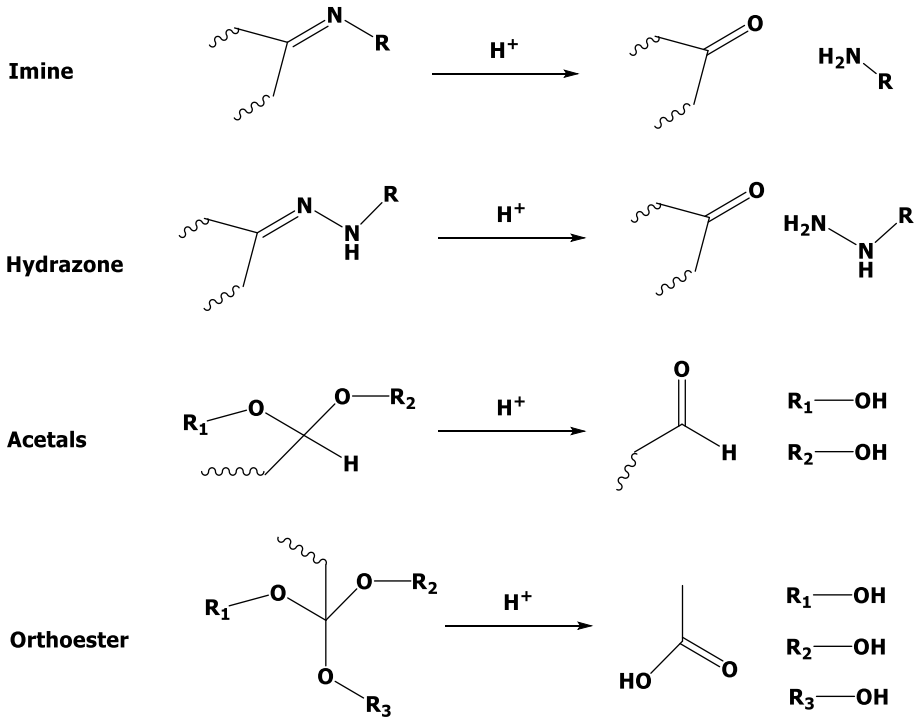

Figure 1-9. pH-sensitive chemical bonds and release mechanisms in the acidic conditions.

To form self-assembled micelles by emulsion solvent diffusion, a core-shell structure requires the balancing of hydrophobic and hydrophilic segments[36,37] (**Figure 1-10**). Poly(ethylene glycol) (PEG) is a popular hydrophilic moiety because of its superior biocompatibility, including linearity, neutral, immunogenicity, low toxicity and high water solubility.[38,39] For instance, PEG could prevent the adsorption of bioactive species of PLA encapsulation.[40]

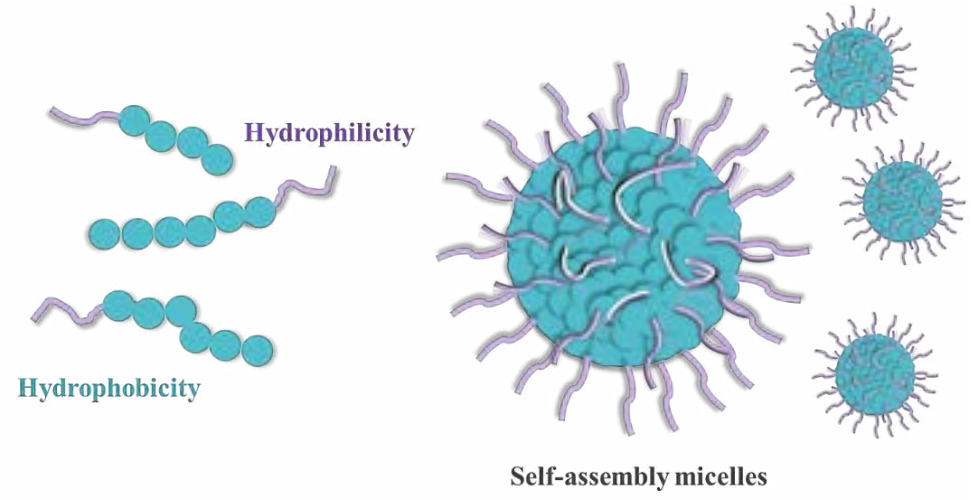

Figure 1-10. Self-assembled micelles forming by balancing between hydrophobic and hydrophilic segment.

With the light up on the design of pH-responsive polymeric particles, it requires a functional group which can undergo a bonding/de-bonding under pH change such as imines-amines, and ketone-diol acetal structure.[41] All these pH-sensitive bonds find their applications in drug delivery owing to their rapid hydrolysis rate at the acidic environment relative to neutral physiological environment, which could be used in the construction of drug-polymer conjugations *via* pH-labile bonds, and/or fabrication of crosslinking polymer networks *via* pH-sensitive bonds as dynamic linkages.[42] For example, the pH-responsive imine bond formed by the conjugation between primary amine and aldehyde has attracted much attention for the design of drug delivery system since amine bonds have been existed frequently in drug-molecules.[43,44] Moreover, a biodegradable micellar drug delivery system with a pH-responsive sheddable PEG shell was developed using an acetal-linked PEG-*block*-PLA copolymer (**Figure 1-11**) and applied to the tumoral release of paclitaxel (PTX).[45] Another example of acetal-linked, Griset et al. cross-linked NPs using acrylate-based hydrophobic polymers with hydroxyl groups that were masked by pH-labile protecting groups (**Figure 1-12**). The NPs were stable at neutral pH,

but the protecting group was cleaved and the hydroxyl groups were exposed at mildly acidic pH (pH ~5) due to hydrolysis of acetal bond.[46]

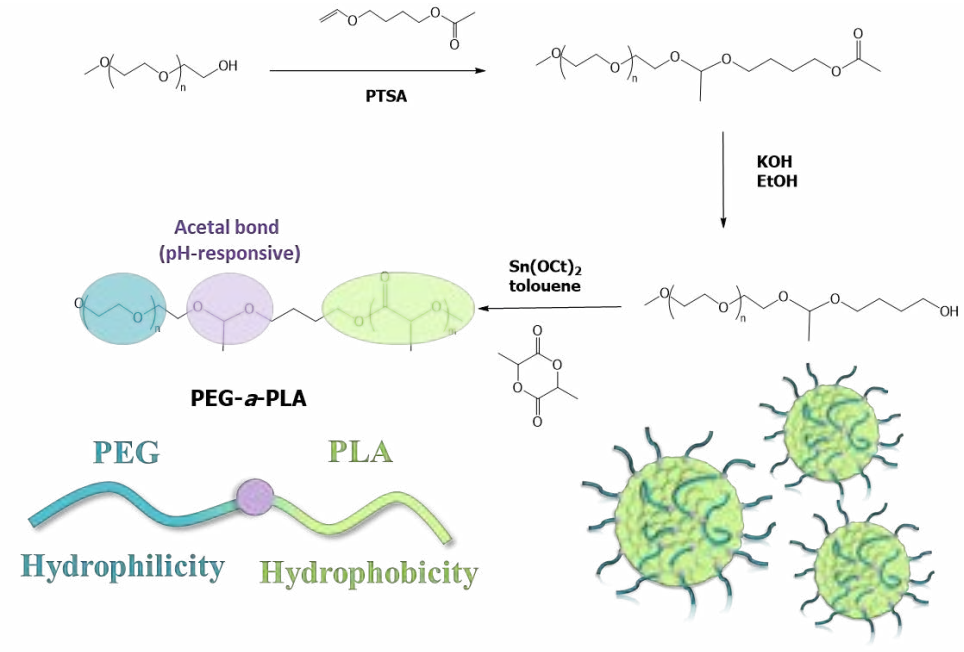

Figure 1-11. An acetal-linked PEG-*block*-PLA copolymer.[45]

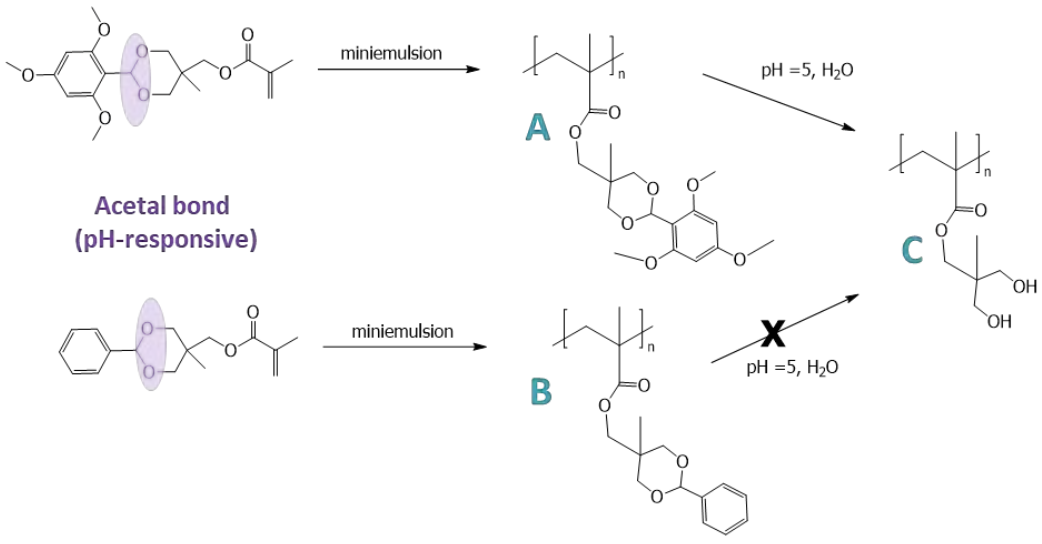

Figure 1-12. Synthesis of nanoparticles with differing pH responsiveness. The protecting group of nanoparticle A but not B is cleaved at a pH of~5. This transformation reveals the hydrophilic hydroxyl groups and formation of nanoparticle C with resulting expansion of the hydrogel nanoparticle in water.[46]

Likewise, Greenfield et al.[47] have explored diverse hydrazone connections for attaching the ketone group of doxorubicin to hydrazides. The half-lives of these linkages typically span several hours at pH 4.5, varying with the particular structure.[47,48] *cis*-Aconityl connections have been employed to attach the amino group of doxorubicin to polymers and antibodies,[49,50] with a reported half-life of 3 hours at pH 4.[49] Trityl groups have been utilized for attaching amine-bearing components to carriers, with half-lives ranging from 2 to 26 hours at pH 5.4, depending on the substitution on the aromatic groups of the trityl linkage.[51,52] Ortho esters have been employed in the creation of acid-sensitive polymers.[53] Recently, acetals are considered promising for the development of acid-sensitive connections for hydroxyl groups because their hydrolysis generally follows first-order kinetics with respect to the hydronium ion, leading to an expected hydrolysis rate that is 10 times faster with each pH unit decrease.[54] Additionally, acetals can be formed with various types of hydroxyl groups, including primary, secondary, tertiary, and syn-1,2- and -1,3-diols, and the hydrolysis rate can be adjusted by altering the acetal structure.[46,54] In general, the hydrolysis rate increases with a higher degree of substitution at the central carbon of each functional group. For example, substituting a hydrogen atom with an alkyl or an alkoxy group leads to a marked increase in the rate (**Figure 1-13**). This acceleration can be attributed to a steric decompression factor as tetrahedral intermediates transition to trigonal structures or to the increased stability of the corresponding alkoxy carbenium ion intermediate, which is directly related to the stability of the final hydrolysis product. Therefore, the relative rate follows the order formaldehyde (CH_2O), aldehyde (RCHO),ketone (RCOR), ester (RCOOR).[55,56]

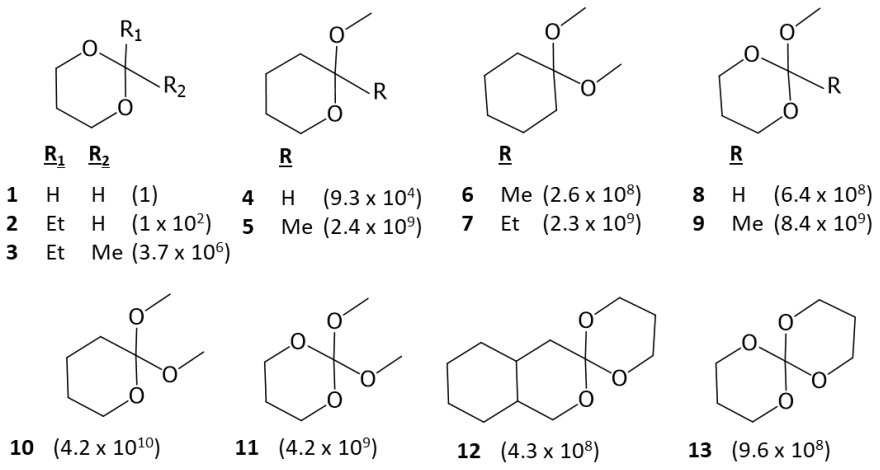

Figure 1-13. The relative rate of hydrolysis of the series of acetal compounds.[55]

With previous obstacles of functionalized PLA, it was found that chain-end modifications can be a complementary, and supplementary the properties by specially designed initiator. For example, to enhance thermal properties, natural aromatic moieties have been introduced, such as benzyl alcohol (**Figure 1-14a**)[57] and 3,4-diacetoxycinnamic acid (DACA) (**Figure 1-14b**).[58] To control molecular weight and narrow polydispersity, 2-ureido-4-pyrimidinone (UPy) (**Figure 1-14c**)[59] and polyhedral oligomeric silsesquioxane (POSS) (**Figure 1-14d**)[60] have been introduced as initiators. In addition, a catechol moiety has been addressed to polymer in order to improve adhesion properties (**Figure 1-14e**).[61]

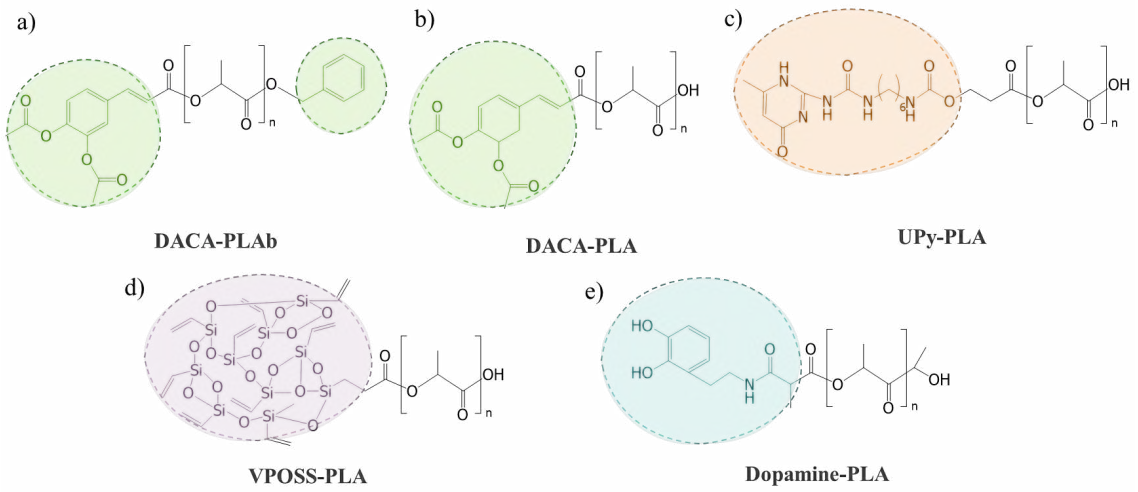

Figure 1-14. PLA with different end-capped; a) DACA and benzyl alcohol [57], b) DACA [58], c) UPy [59], d) POSS [60], and e) dopamine. [61]

Previously it was suggested that vanillin containing aldehyde and hydroxyl groups was implemented as a key building-block initiator.[62,63] To conduct the dual dynamic interactions, it has reported vanillin[64] (**Figure 1-15**) and 5-hydroxymethylfurfural (HMF)[65] were functionalized for inducing an amine-imine reversible phenomenon. By controlling the nanostructure formation, the hydrophilic moieties of a hydroxyl group at chain end and PLA were exhibited. As a result, the particles were aggregated due to the detachment of the hydrophilic moiety (aldehyde-terminated PLA) after pH change.[64,65] However, a pH range below pH 2 was needed in the previous study which is not compatible to reach a practical medical therapy. With the light of ketone acetal bond, it could be committed under physiological conditions (mild acidic condition).[45,54] Xiao et al have reported that micelles composed of an acetal-linked PEG-*block*-PLA copolymer were stable at pH 7.4, began to shed their shell and aggregate slowly at pH 6.5, and

disintegrated more rapidly at pH 5.5.[45] Nonetheless, this acetal linkage was not a cyclic acetal[45]. It has been reported that the hydrolysis rates of acyclic compounds are generally slower than those of cyclic acetals. [55] Specifically, it was noted that a six-membered ring diol-ketone acetal bond hydrolyzes faster than its five-membered ring counterpart. [66] Consequently, it is of interest to determine whether a 6-ring cyclic acetal moiety could improve the hydrolysis rate under higher pH conditions (approximately pH 5.5 to 6.5, which are physiological conditions) in a shorter timeframe, particularly in the presence of aldehyde-hydroxyl derivatives, which are considered to produce low-toxicity residues.

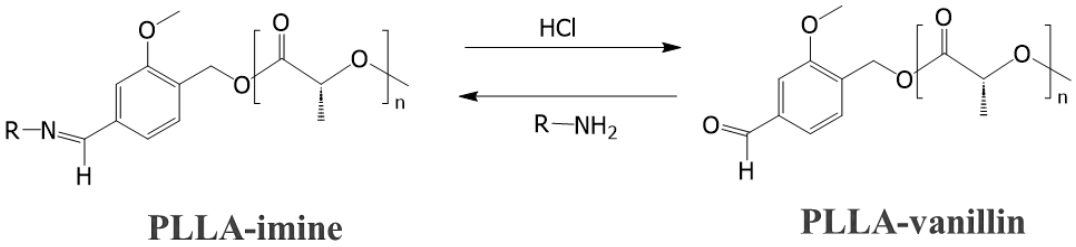

Figure 1-15. Chemical structure of PLLA-imine and PLLA-vanillin.[55]

To improve the aggregation rate of the polymer particles, the strategy of inorganic blending with polymer might be alternatively considered. Titanium and calcium dioxide nanoparticles (TiO_2/ CaO NPs) are well-known blending agents in various personal care products (PCPs) such as cosmetics, sunscreens, toothpastes, and skin care products. Luo et al. recently reported that degradation rate of PLA was accelerated by adding the TiO_2 nanofillers.[67] For this reason, TiO_2 was selected as blending agent candidate in our study (**Figure 1-16**).

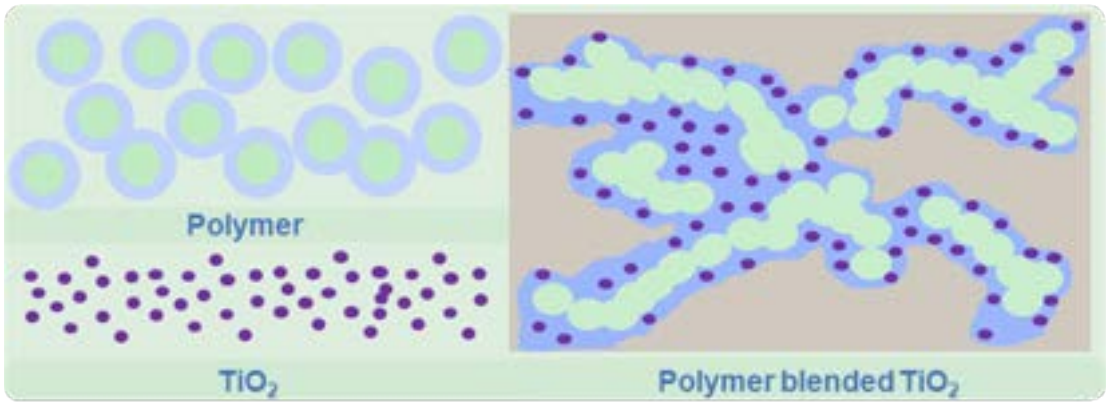

Figure 1-16. Illustrate of blended polymer with TiO_2.

In this work, novel initiators based on the diol-ketone acetal and vanillin units were designed and synthesized, for use at around pH 5.5—6.5 in aqueous solution for medical applications. The preparation of PLA particles with a six-membered ring ketone acetal unit was conducted to optimize the performance. Furthermore, the aggregation rates of stereo-complex (SC) blended with titanium dioxide were also investigated. To examine the aggregation, not only UV spectroscopy was performed, to observe the rate, but the behaviors of assembly morphology were analyzed by SEM. Aiming to study the effect of pH-induced on the aggregation rate, the hydrolysis of acetal bonds warrants further discussion. by the effects of the polymer molecular weight, pH range and chain end structure as shown in **Figure 1-17**. Notwithstanding, this work has been published in Sarisuta, K.; Iwami, M.; Martín-Vaca, B.; Chanthaset, N.; Ajiro, H. pH Effect on Particle Aggregation of Vanillin End-Capped Polylactides Bearing a Hydrophilic Group Connected by a Cyclic Acetal Moiety. *Langmuir* **2023**, 39 (11), 3994–4004.[68]

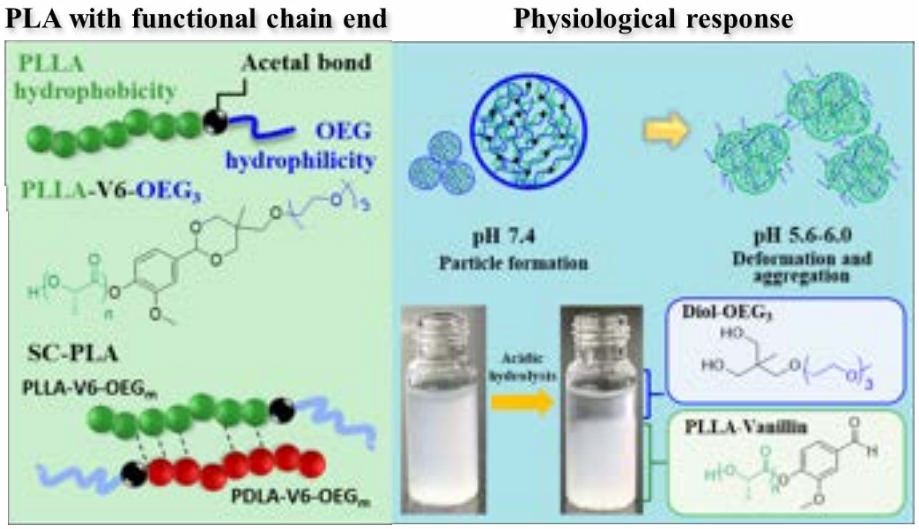

Figure 1-17. Preparation of PLA with functional chain-end *via* functionalized initiator.

1.2 Results and Discussions

1.2.1 Initiator syntheses

To enhance a control of pH-responsiveness between pH 5.5—6.2, the acetal-based initiators were designed and synthesized as previous hint.[66] In order to balance hydrophobicity and hydrophilicity of SC, the synthetic initiators with oligoethylene glycol chain end of different length were successfully prepared as vanillin-6-OEG_3 and vanillin-6-OEG_4. The syntheses of vanillin-6-ring cyclic is shown in (**Scheme 1-1)**.

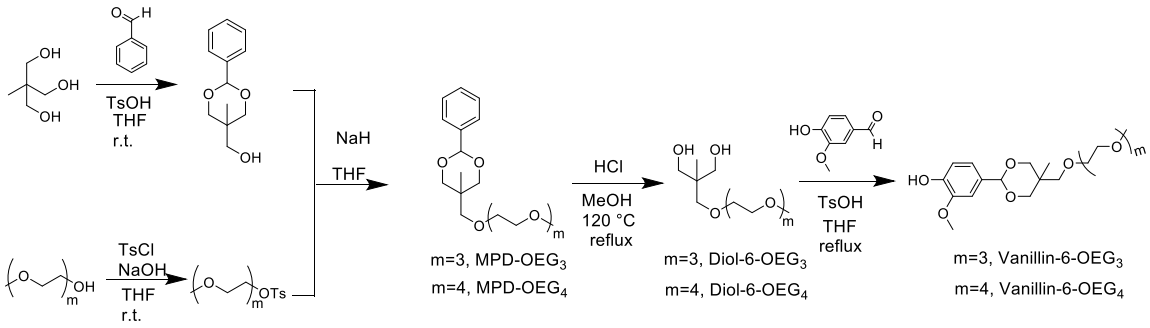

Scheme 1-1. Syntheses of vanillin-based initiatorsVanillin-6-OEG_m.

The chemical structure of the novel initiators, vanillin-6-OEG_3 and vanillin-6-OEG_4 were confirmed by ^{1}H NMR spectroscopy (**Figure 1-18**) The spectra confirmed the disappearance of the aldehyde signal around 9 ppm and the appearance of an acetal bond peak of 6-member cyclic rings at around 5.6 ppm. In addition, chemical shifts both of vanillin-6-OEG_3 and vanillin-6-OEG_4 were indicated by signals at 3.7—3.9, 5.7, 6.8—7.1 ppm (**Figure 1-18**), which were attributed to the OEG unit, acetal bond, and vanillin aromatic, respectively. Therefore, novel vanillin initiators were characterized not only by ^{1}H NMR but also mass spectrometry (**Figure 1-19**) and FT-IR spectroscopy, which confirms the disappearance of the CO band of the aldehyde (**Figure 1-20**).

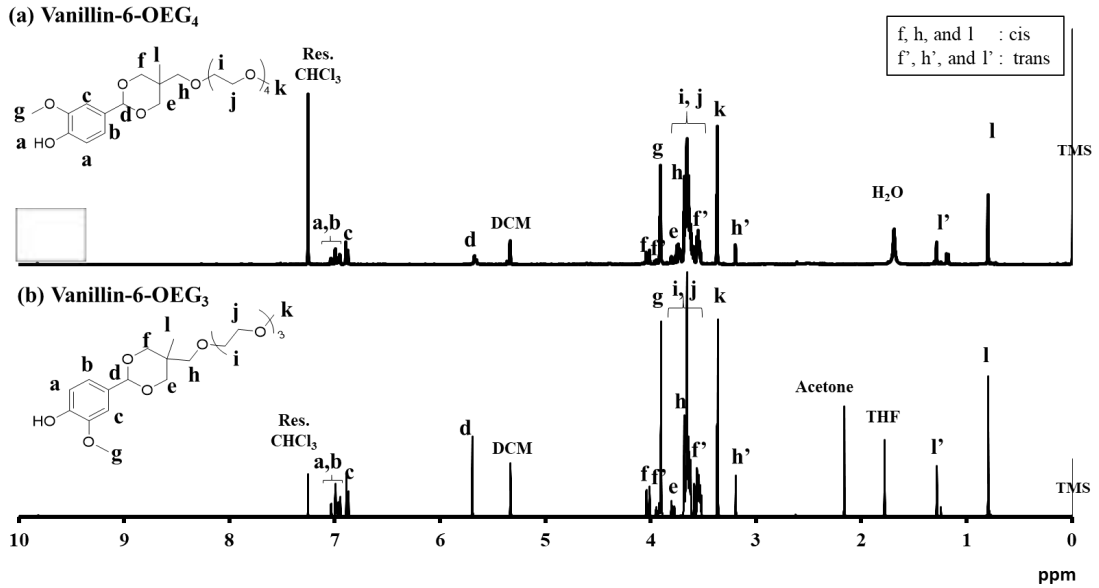

Figure 1-18. ^{1}H NMR and integrated ratio of (a) Vanillin-6-OEG_4 and (b) Vanillin-6-OEG_3 (400 MHz, r.t., in $CDCl_3$).

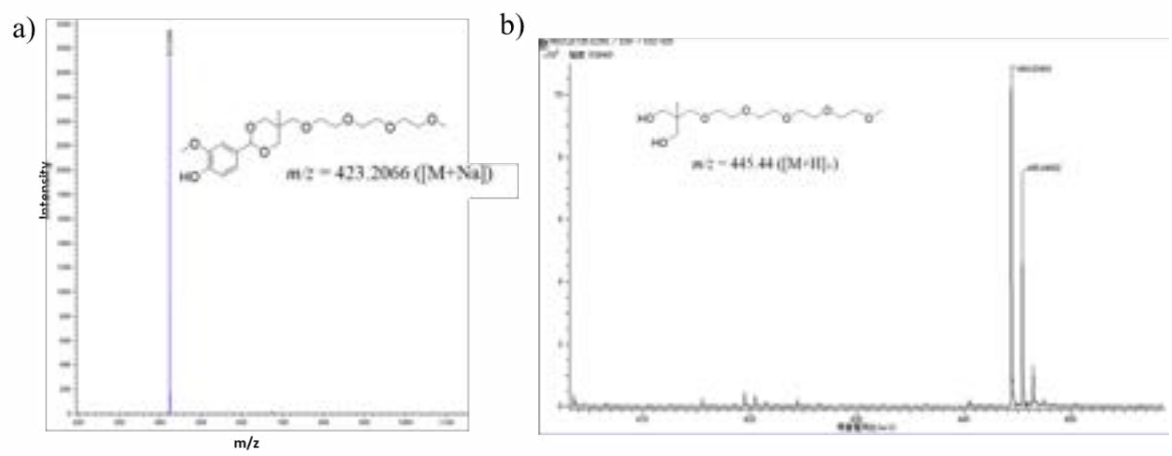

Figure 1-19. MASS spectrum of a) Vanillin-V6-OEG_3 and b) Vanillin-V6-OEG_4.

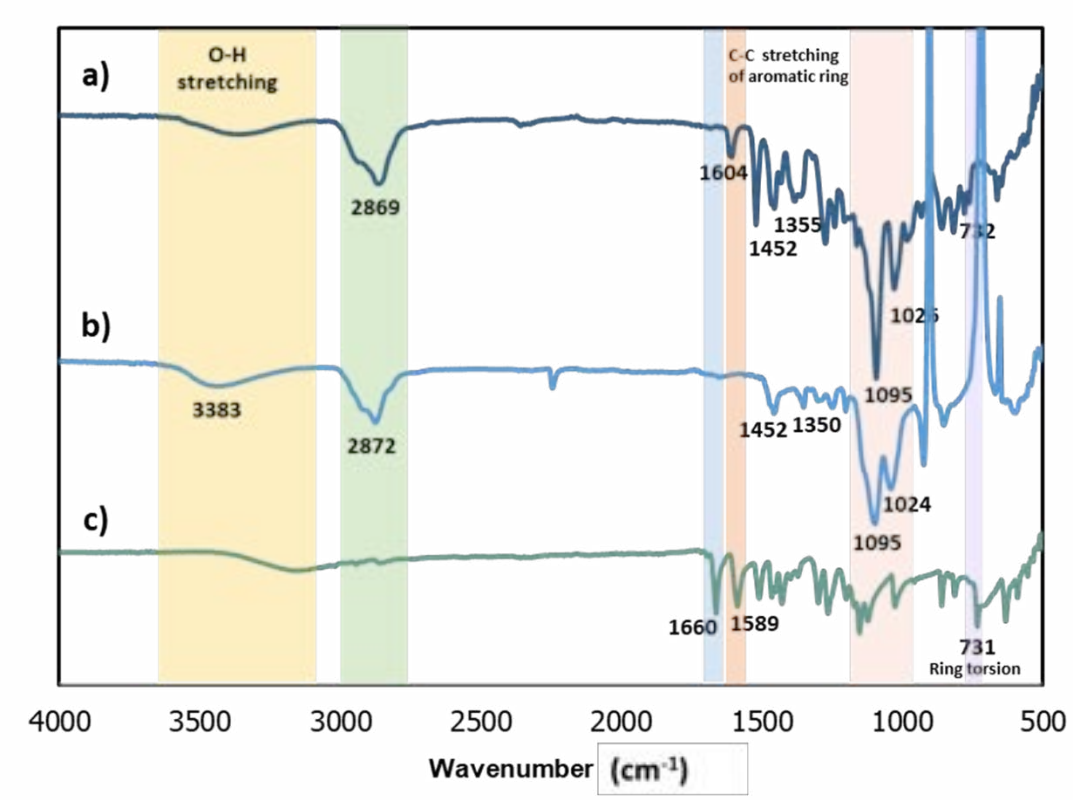

Figure 1-20. FT-IR spectra of (a) Vanillin-V6-OEG$_3$, (b) Diol-6-OEG$_3$, and (c) Vanillin.

1.2.2 Polymerization

The polymerization of PLA was initiated using a vanillin-6-OEG$_3$ initiator and catalysed by the Sn(Oct)$_2$ catalyst. The reaction was conducted over a period ranging from 0.5 to 24 hours at 40°C in 1M Toluene. As shown in **Table 1-1**, M_n, and dispersity ($Đ$) of the synthetic PLA were observed by SEC and ^{1}H NMR. To control the PLA molecular weight, there were various [M]:[I]$_{V6}$ feeding ratios of 20:1, 10:1 and 5:1 yielded $M_{n(SEC)}$ of 4,800, 2,400-4,600 and 2,600 g/mol (**Table 1-1, entries 1-6**), respectively. However, it was found that in the case of [M]:[I]$_{V6}$, 10:1, the molecular weight of PLA could not be controlled by feeding ratio alone but also by time dependence and monomer concentration.

Table 1. Polymerization of LA using Tin(II) octanoate catalyst and vanillin-based initiators.

Entry	Sample	Initiator	[M]/[I]	Time (h)	Yield (%)	M_n^{SECe} (kDa)	M_n^{SECf} (kDa)	DP	$Đ^e$
1[a, c]	$PLLA_{63}$-V6-OEG_3	Vanillin-6-OEG_3	20:01	24	76	4.8	3.3	63	1.8
2[a, c]	$PLLA_{61}$-V6-OEG_3	Vanillin-6-OEG_3	10:01	3	67	4.6	3.1	61	1.8
3[a, c]	$PLLA_{33}$-V6-OEG_3	Vanillin-6-OEG_3	10:01	0.5	84	2.4	1.6	33	1.3
4[a, c]	$PLLA_{34}$-V6-OEG_3	Vanillin-6-OEG_3	10:01	0.5	76	2.5	1.7	34	1.1
5[b, c]	$PLLA_{35}$-V6-OEG_3	Vanillin-6-OEG_3	5:01	2	74	2.6	1.8	35	1.2
6[b, c]	$PDLA_{35}$-V6-OEG_3	Vanillin-6-OEG_3	5:01	2	69	2.2	1.5	30	1.3
7[b, d]	$PLLA_{25}$-V6-OEG_4	Vanillin-6-OEG_4	10:01	0.5	76	1.9	1.3	25	1.2
8[b, c]	$PDLA_{23}$-V6-OEG_4	Vanillin-6-OEG_4	10:01	0.5	67	1.7	1.2	23	1.2

a) Monomer = 1.0 g; b) Monomer = 2.0 g; c) Concentration [M] Toluene = 1 mg/mL; d) Concentration [M] Toluene = 3 mg/mL; e)Determined by SEC by PS standard in THF; Catalyst = $Sn(Oct)_2$; f) Values corrected using the correction factor reported for PLA.[69]

To confirm the attachment of functional end group of PLA-V6-OEG_m, the structures were verified by ^1H NMR spectroscopy as shown in **Figure 1-21**. PLA-V6-OEG_3 spectra showed signals at 1.45—1.7, 3.2—4.2, and 5.04—5.25 ppm, referred to PLA and vanillin-6-OEG_3 (**Figure 1-21c**). It was found that a signal at 4.3 ppm is probably assigned to a methine group adjacent to the CHOH group terminal signal of PLA (**Figure 1-21**). In addition, the signal observed at 5.60 ppm and the absence of any signal around 9 ppm confirms that the acetal is compatible with the polymerization conditions. The molecular weights measured by SEC *via* UV detector at wavelength 264 nm were also examined to assure the presence of the aromatic group at the end-capping (**Figure 1-22)**. Finally, our findings confirmed the vanillin derivative initiators had already embedded at the PLA chain end, according to majority patterns of MALDI-TOF profiles (**Figure 1-23 and Figure 1-24**). Nevertheless, the observed differences in the SEC chromatograms patterns between UV and RI detection suggest that some PLA chains might not include the functional initiator (**Figure 1-22)**. This hypothesis is further substantiated by MALDI-TOF results (**Figure 1-23)**, which identified three distinct spectral patterns, two of which indicate minority PLA chains lacking the functional

initiator. Additionally, it has been suggested that the formation of cyclic polymer chains *via* intramolecular trans-esterification during polymerization is a possibility.

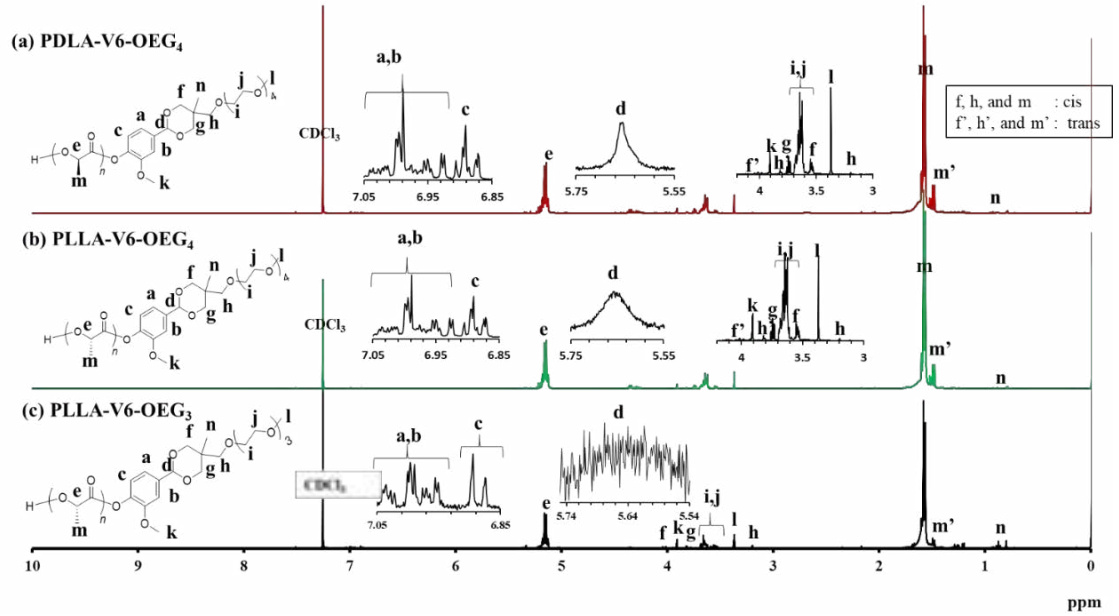

Figure 1-21. ^{1}H NMR of (a) PDLA$_{23}$-V5-OEG$_4$, (b) PLLA$_{25}$-V6-OEG$_4$ and (c) PLLA$_{33}$-V6-OEG$_3$ (400 MHz, r.t., in $CDCl_3$).

To balance hydrophilicity-hydrophobicity, PLLA-V6-OEG$_4$ and PDLA-V6-OEG$_4$ were polymerized successfully and confirmed by ^{1}H NMR (**Figure 1-21**). The spectra were showed signals at 1.45—1.7, 3.2—4.2, and 5.04—5.25 ppm that referred to PLA and V6-OEG$_4$ (**Figure 1-21a** and **1-21b)**. Also, MALDI-TOF patterns of PLLA-V6-OEG$_4$ and PDLA-V6-OEG$_4$ were exhibited the majority matching with aspect (**Figure 1-23)**.

From SEC results, PLLA-V6-OEG$_4$ and PDLA-V6-OEG$_4$ were confirmed the composition of aromatic ring at chain end which could be implied vanillin-6-OEG$_4$ moiety. The M_n of PLLA-V6-OEG$_4$ and PDLA-V6-OEG$_4$ were 1900 and 1700 g/mol, respectively (**Table 1-1, entries 6-7**).

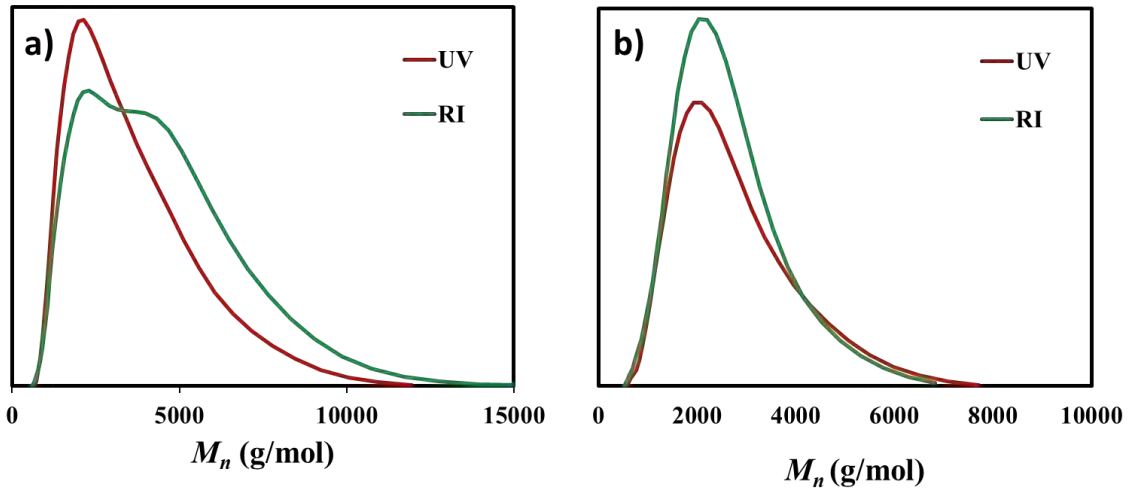

Figure 1-22. SEC molecular weight of a) $PLLA_{33}$-V6-OEG_3 and b) $PLLA_{25}$-V6-OEG_4 (UV detector wavelength 264 nm).

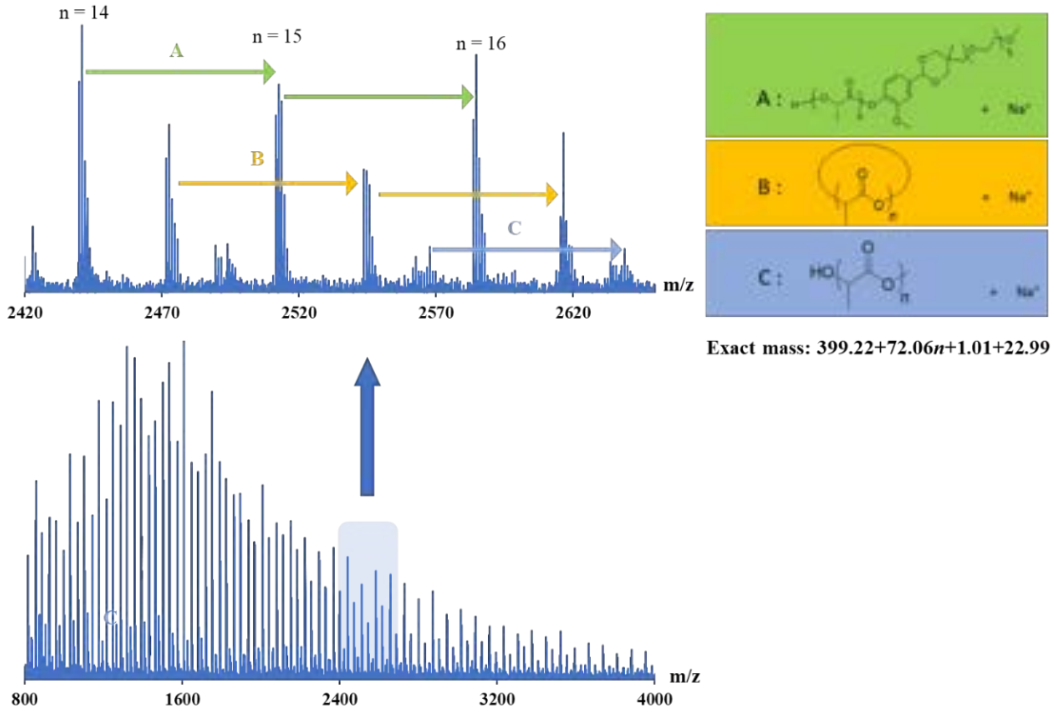

Figure 1-23. MALDI-TOF MS of $PLLA_{33}$-V6-OEG_3.

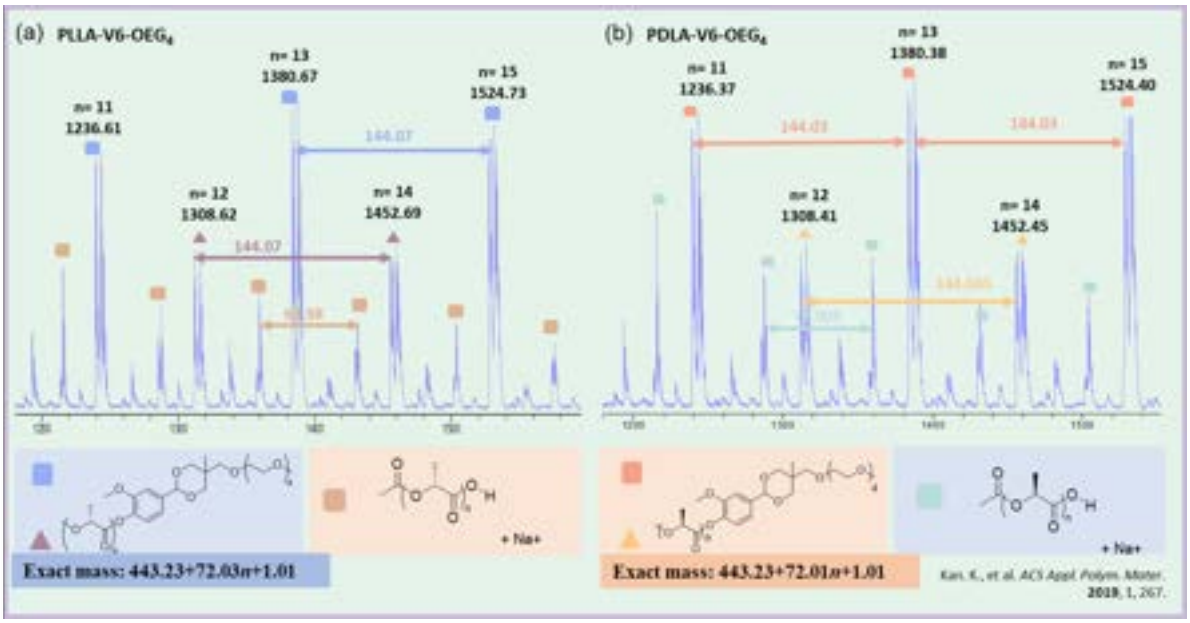

Figure 1-24. MALDI-TOF of (a)PLLA$_{25}$-6-OEG$_4$ and (b) PDLA$_{23}$-V6-OEG$_4$.

1.2.3 Particles preparation

Approaching to polymeric carriers as fabricated particles, the morphology of the synthetic polymers was characterized by SEM. The particles were prepared by precipitation method (**Figure 1-25a** and **1-25b**) and emulsion method (**Figure 1-25c** and **1-25d**). The PLA-V6-OEG$_3$ particles were prepared using the precipitation method with acetonitrile as the solvent. It was necessary to remove the solvent by freeze-drying to recover the precipitate. Alternatively, when the emulsion method was employed using ethyl acetate as the solvent, the particles were successfully isolated by centrifugation at 3500 rpm for 5 minutes. Then, the morphology of the particles was investigated by SEM measurement after the particles were dried for 2 weeks. It is notable that particle preparation by the precipitation methods could not yield well-defined the particles (**Figure 1-25a** and **1-25b**). In contrast, emulsion method was delivered entirely spherical shape for PLA-V6-OEG$_3$ particle as shown in **Figure 1-25c** and **1-25d**.

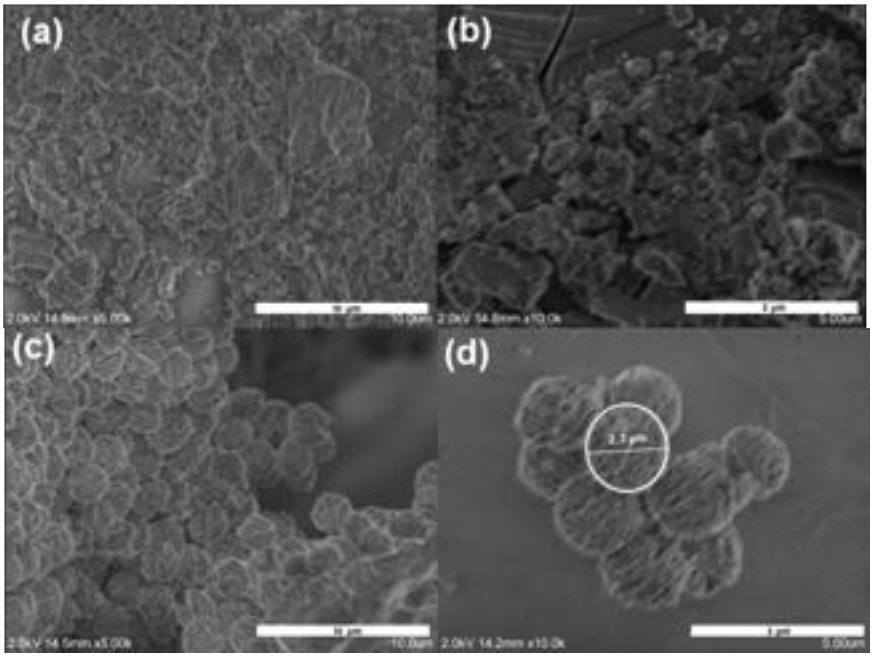

Figure 1-25. SEM image of the PLA-V6-OEG_3 after preparation as particles form: (a) 5k magnification by precipitation methods (no particles), (b) 10k magnification by precipitation methods (no particles) (c) 5k magnification by emulsion methods, and (d) 10k magnification by emulsion methods.

1.2.4 Particle aggregation

In order to control pH change from 7.0 to around 5.5 within 2—3 min. In demonstration of particle aggregation of $PLLA_{33}$-V6-OEG_3 was presented in the supporting video (Supporting Information of the published article; Sarisuta, K.; Iwami, M.; Martín-Vaca, B.; Chanthaset, N.; Ajiro, H. pH Effect on Particle Aggregation of Vanillin End-Capped Polylactides Bearing a Hydrophilic Group Connected by a Cyclic Acetal Moiety. *Langmuir* **2023**, 39 (11), 3994–4004.[68]). The particles of $PLLA_{33}$-V6-OEG_3 were prepared using the emulsion method and subsequently dispersed in a PBS solution at pH 7.0. The pH was then adjusted to 5.5, and a video was taken to observe the aggregation behaviour of the particles.

1.2.4.1 The aggregation rate of PLLA-V6-OEG_3 particles

To understand the influence of molecular weight on aggregation rates, the transmitted percentage were monitored (**Equation 1-1**) between 0 to 4.5 min during pH change from 7.4 to 6.2 (**Figure 1-26**). For particles of $PLLA_{33}$-V6-OEG_3 and $PLLA_{35}$-V6-OEG_3, the results showed that the aggregation behaviour expressed significantly at 3 min **(Figure 1-26a** and **1-26b**) while particles of $PLLA_{61}$-V6-OEG_3 and $PLLA_{63}$-V6-

OEG_3 were slightly increased less than 10% transmittance **(Figure 1-26c** and **1-26d**). A similar pattern of results was obtained under pH change from 7.4 to 5.5. It was suggested that the particles from short chain polymer ($PLLA_{33}$-V6-OEG_3) could provide readily deformation as the highest intensity compared to long chain polymer. Therefore, it is worth discussing these interesting facts which revealed by the relation of aggregation rate and pH strength at 5.6, 6.2, and 7.2 (**Figure 1-26**).

At pH 5.6, it was showed that $PLLA_{33}$-V6-OEG_3 particle were dramatically aggregated from 1.5 min as slope shown in **Figure 1-27a**, while at pH 6.2 was constant (**Figure 1-27b)**. It could be indicated that pH strength could influence the aggregation rate; however, this novel finding is promising to control under physiological conditions. At pH 7.4, the particles were dispersed homogeneously in PBS (**Figure 1-27c**). After the pH change to 5.6 or 6.2, the increased transmittance was supported the ideal of detachment of acetal bond by hydrolysis which may induce the separation between hydrophilic and hydrophobic residues. As a consequence, the hydrophobic residue will submerge at the bottom of the cuvette due to gravity-settling. The results showed that particles with high molecular weight ($PLLA_{61}$-V6-OEG_3, $PLLA_{63}$-V6-OEG_3) but lower than 40kDa in previous research [70], could exhibit a slow rate of aggregation due to M_n dependence. These results indicated that the particles with lower molecular weight of PLA have higher-density ratio of acetal bond in the structure, which means more hydrophilic terminal groups, thus it could be an advantage to easily hydrolyse the acetal bond by losing chain-packing in the amorphous area. These might be easier to be hydrolysed than high molecular weight of PLA, in which there is a lower-density ratio of acetal bond in the structure[71]. Therefore, lower molecular weight may induce faster separation between hydrophilic and hydrophobic residues affected on higher transmittance than higher molecular weight, although the experimental observation was UV-Vis transmittance change.

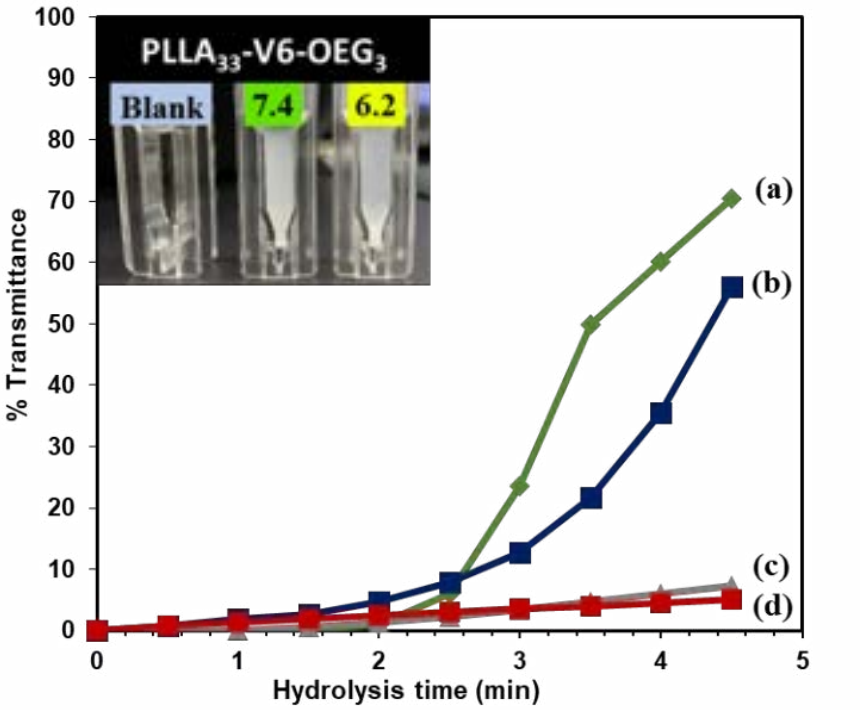

Figure 1-26. PLLA particles aggregation measuring by UV-visible when pH changed from 7.4 to 6.2. (a) $PLLA_{33}$-V6-OEG_3, (b) $PLLA_{35}$-V6-OEG_3, (c) $PLLA_{61}$-V6-OEG_3, (d) $PLLA_{63}$-V6-OEG_3 within 4.5 min.

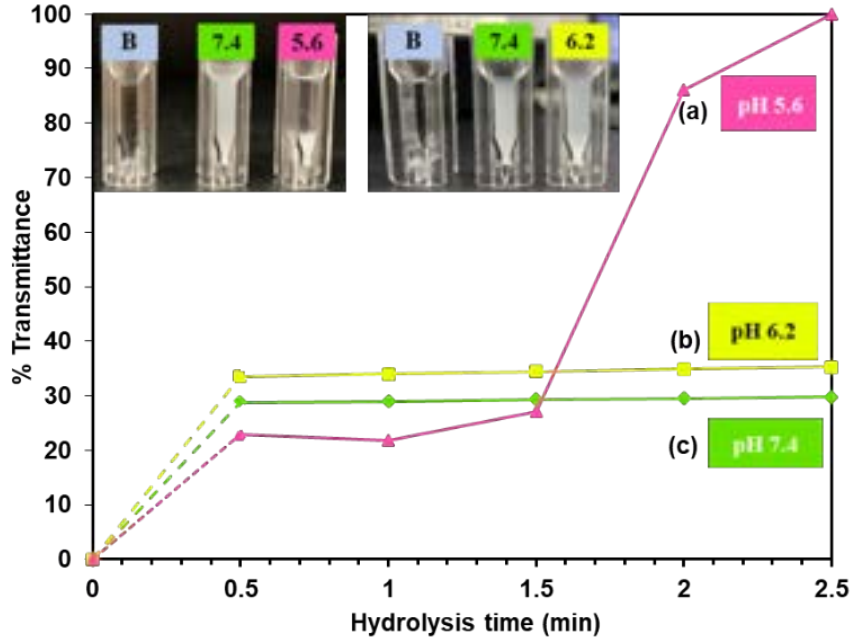

Figure 1-27. $PLLA_{33}$-V6-OEG_3 particles (M_n 2400) aggregation measuring by UV-visible at pH (a) pH 5.6, (b) pH 6.2, and (c) pH 7.4. within 2.5 min.

1.2.4.2 Morphology of the particles

I illustrated the particle shapes to confirm the aggregation before/after hydrolysis. Herein, $PLLA_{33}$-V6-OEG_3 particles were selected as candidates to be examined by SEM. PLLA-V6-OEG_3 particles at pH 7.4 were found to have a regular round shape (**Figure 1-28a**). The images of the PLLA-V6-OEG_3 tended to be featured a melted, re-size and merging together after the pH changed to 5.6 (**Figure 1-28b**). The irregular shape of particles was found which supported the occurrence of degradation. There promising results suggest that the ketone acetal bond might be hydrolysed by the acid condition and presented residues of the hydrophilic part as well as the merging particle.

To support the hydrolysis of the acetal moiety, the insoluble part after transmittance and pH changes to 5.6 within 4.5 min was analysed by ^{1}H NMR. The chemical structure confirmed the hydrolysis of acetal bond (**Figure 1-29**). Our strategy is aggregation of particles (after acetal bond was hydrolysed) the hydrophobic part will be precipitated to the bottom which is proportional to the turbidity *via* UV-Vis transmittance. ^{1}HNMR of vanillin-6-OEG_3 initiator and PLLA-V6-OEG_3 presented no a peak of aldehyde around 9.8 ppm (**Figure 1-29a** and **1-29b**). After the pH changed to 5.6 (within 4.5 min), the aldehyde peak at 9.8 appeared and the acetal signal at 5.6 ppm disappeared, which may be assigned to the hydrolysis of the acetal bond became aldehyde and diol as shown in **Figure 1-30c**. Also, the comparison of integral ratios before and after hydrolysis was shown in **Figure 1-30**. Other results to confirm the breakage of particle, the M_n of the polymer before and after pH change were determined by SEC. The observed decrease in M_n from approximately 2,400 to 2,200 g/mol suggests that the OEG_3 unit was removed. (**Figure 1-31**). Correspondingly, the trace profile changed to bimodal, as illustrated in **Figure 1-31a**. At this stage of understanding, we believe that the decreased M_n around 200 g/mol referred to the disappearance of diol-6-OEG_3 of which the exact mass was 267 g/mol. Alternatively, a higher molecular weight of 5,700 g/mol was observed which may feasibly indicate the particles melting and agglomerating together (**Figure 1-28b**). Moreover, Kurokawa et al. have reported that the weight loss of PLLA films in PBS solution (pH 7.4) 60°C, was slightly lost weight around 2–4 wt % of the initial film. The weight loss of the films was relatively small, the M_n value of PLLA sample drastically reduced from the initial stage of degradation[72]. It might suggest that a possibility of other reactions, such as partial degradation of a main chain.

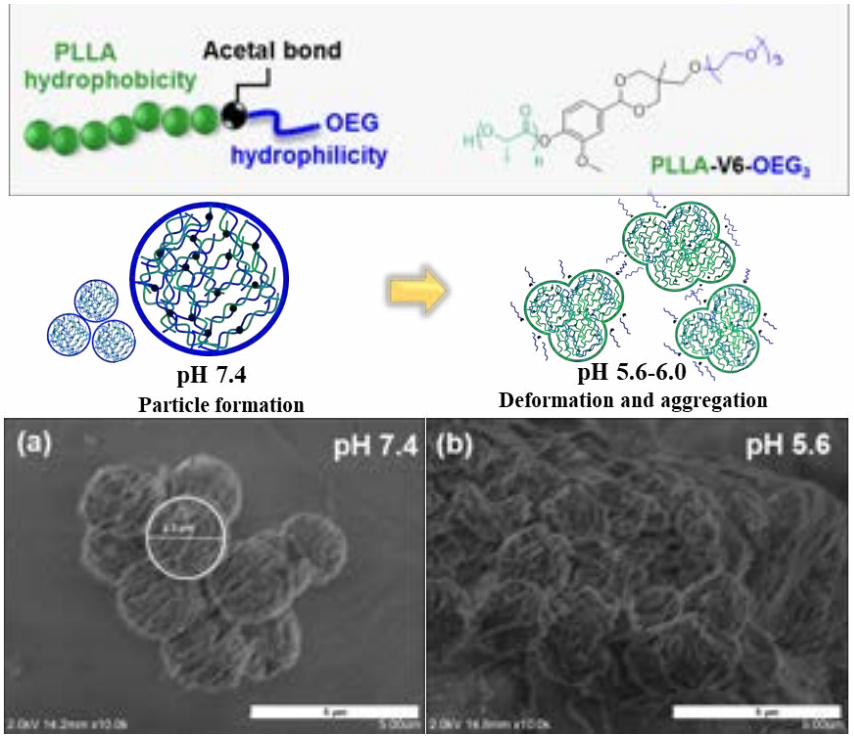

Figure 1-28. SEM images of microstructure (a)PLA-V6-OEG$_3$ at pH 7.4, and (b) aggregate-structures of PLA-V6-OEG$_3$ at pH 5.6. (White bar indicates 5 μm.)

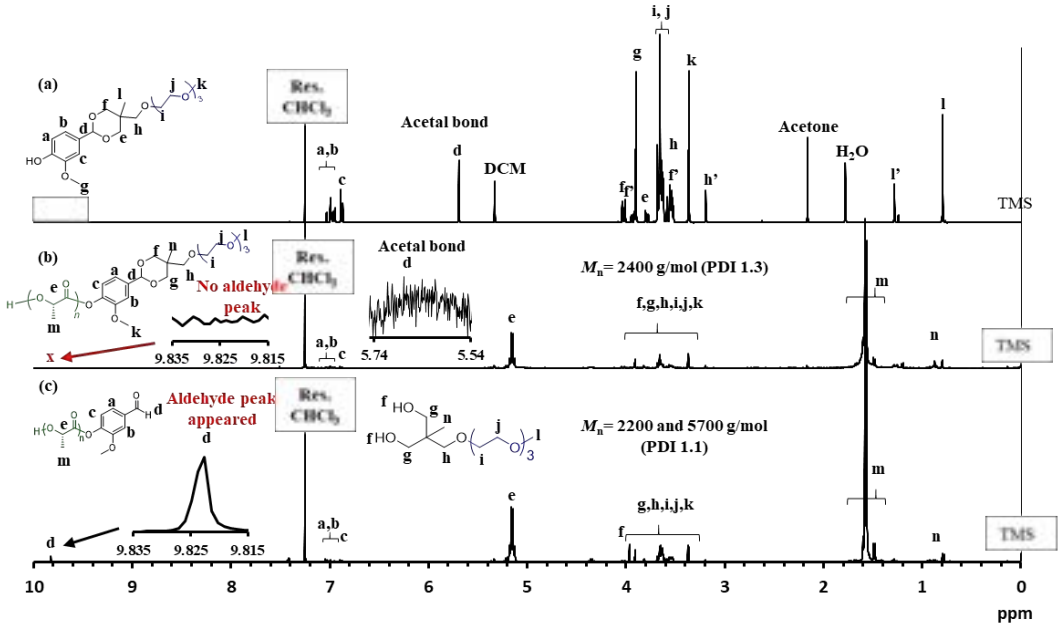

Figure 1-29. ^{1}H NMR of (a) Vanillin-6-OEG$_3$, (b) PLLA$_{33}$-V6-OEG$_3$, and (c) PLLA$_{33}$-V6-OEG$_3$ particles at pH5.6 and SEC before and after hydrolysis 4.5 min (400 MHz, r.t., 1024 scan, in $CDCl_3$).

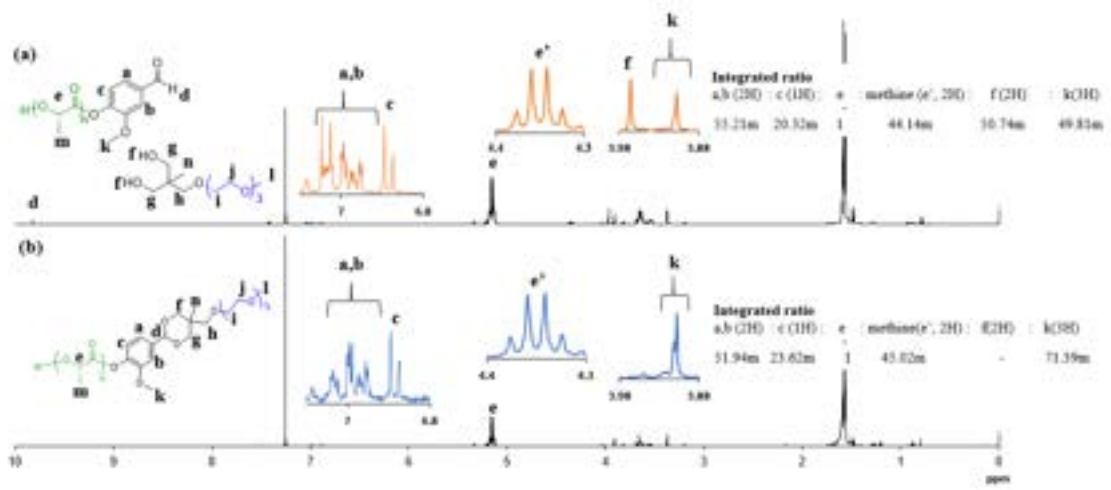

Figure 1-30. ^{1}H NMR and integrated ratio of (a) $PLLA_{33}$-V6-OEG_3 particles at pH5.6, and (b) $PLLA_{33}$-V6-OEG_3.

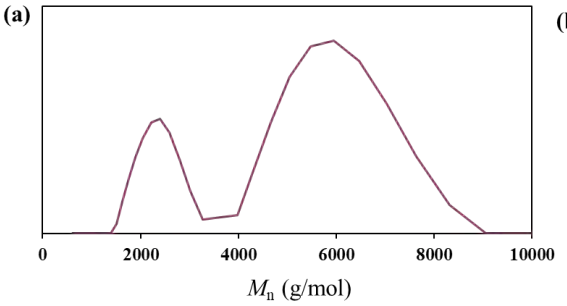

(b)

Status	pH	$M_{n,GPC}$ (n) ($\times 10^3$)RI	Đ
Before	7.4	2.4	1.3
After	5.6	2.2	1.0
		5.7	1.0

Figure 1-31. (a) SEC molecular weight after (pH 5.6) hydrolyzed by RI detector and (b) SEC results of PLLA-V6-OEG_3 before (pH7.4) and after (pH 5.6) hydrolyzed.

1.2.5 SC formation of PLA using V6-OEG_m modified initiators (SC-PLA-V6-OEG_m)

For the SC formation, we had synthesized several PLA derivatives such as PDLA-benzyl, PLLA-V6-OEG_3, PDLA-V6-OEG_3, PLLA-V6-OEG_4 and PDLA-V6-OEG_4. Then, its structure was confirmed by FT-IR, XRD, and DSC. FT-IR confirmed the formation of SC of SC-PLA-V6-OEG_4 which C=O peak was shifted from 1755 in PLLA or PDLA to 1745 cm^{-1} because of transition dipole coupling of the ester groups in the crystalline state (**Figure 1-32A**).[57,64] XRD profile were shown that after SC, 2θ was appeared identical peak at 11.97 and 20.69 compared with a peak of homopolymer at 16.7 (**Figure 1-32B**).[7,57,64] DSC heating curves were shown that after SC, melting temperature (T_m) was increased to 194° C (**Figure 1-32C**).

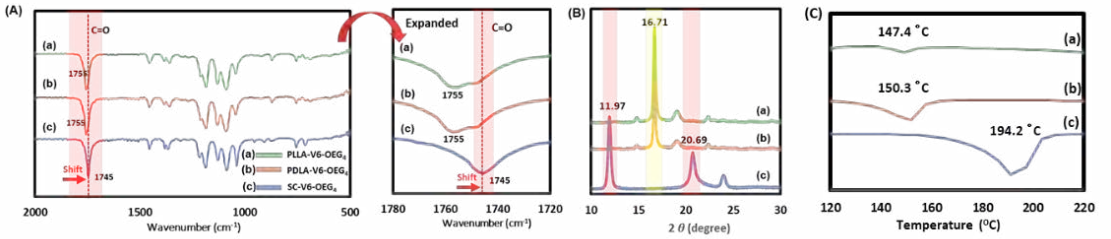

Figure 1-32. (A) FT-IR spectra to confirm stereo-complex. (B) XRD patterns to confirm stereo-complex (C) DSC heating curves to confirm SC formed by T_m. (a) $PLLA_{25}$-V6-OEG_4, (b) $PDLA_{23}$-V6-OEG_4, and (c) SC-V6-OEG_4.

1.2.6 Aggregation of SC particles

In this part, the effect of chain end could be discriminated with three kinds of pairing samples as following:

SC (1); PLLA-V6-OEG_3/ PDLA-benzyl (**Figure 1-33a).**

SC (2); PLLA-V6-OEG_3/ PDLA-V6-OEG_3 (**Figure 1-33b)**

SC (3); PLLA-V6-OEG_4/ PDLA-V6-OEG_4 (**Figure 1-33c)**

1.2.6.1 Study of chain end effect

The transmitted percentage were monitored (**Equation 1-1**) between 0 to 4.5 min during pH change 7.4 to 5.6. The results showed that SC (3) OEG_4/OEG_4 was expressed around 10% transmittance after 3 min when changing pH from 7.4 to 5.6 (**Figure 1-33c**). It was indicated that a significant difference of transmitted gap contributing to aggregation rate. While, SC (1) OEG_3-benzyl was around 0.01%, transmittance (**Figure 1-33a**) and SC (2) OEG_3/OEG_3 (**Figure 1-33b**) was around 3%. Therefore, it could be supposed that vanillin-6-OEG_4 initiator may induce the aggregation rate due to it more hydrophilic moiety and enhancing of water molecules. Moreover, SC (3) OEG_4/OEG_4 (**Figure 1-33c**) had two positions of acetal bond both PLLA/PDLA chain which could give a potential to be hydrolyzed in acidic condition. The obtained results imply that the effect of chain end can influence on the aggregation rate.

In this section, to confirm the aggregation after hydrolysis, the particle shapes were investigated by SEM. The particles residue after UV measurement were picked up and dried to observe the aggregation morphologies in several end-capping patterns as shown in **Figure 1-34** The results shown that SC(1) (**Figure 1-34a)**, SC(2) (**Figure 1-34b)**, and SC(3) (**Figure 1-34c)** at pH 7.4 were observed regular round shape of particles. After pH changed to 5.6, SC(1) particles still remained the round shape (**Figure 1-34d**)

as at pH 7.4 which could indicated that particles did not aggregate and agglomerate together within 3 minutes. Contrary, SC(2) and SC(3) tended to be featured a melted and merging together after the pH changed to 5.6. These results suggested that SC(2) and SC(3) particles had more high density of acetal bonds which benefit to be easily to hydrolysis of acetal bond than SC(1). Subsequently, some of the particles' shape could not be observed due to their aggregation and agglomeration (**Figure 1-34e** and **1-34f**). Compared to SC(2), SC(3) showed more aggregation or merging state at pH 5.6 (**Figure 1-34f**). This obtained results suggest that there was longer hydrophilic moiety in SC(3), thus it was advantageous for water penetration in the amorphous phase and resulted on faster hydrolysis. Moreover, it was reported that the micelles could grow in size to a greater length for longer hydrophobic.[50] It indicated that SC(3) might have smaller particles size than SC(2) which results in more surface area of particles. As the results, it seemed to be readily hydrolysis depending on not only hydrophilicity of chain-end but also number of acetal bonds.

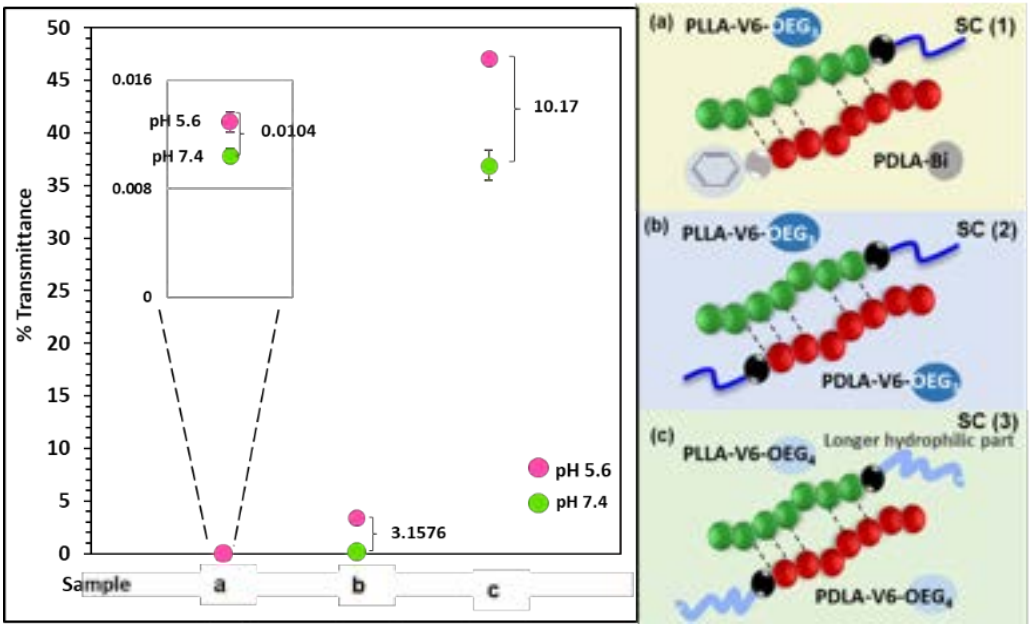

Figure 1-33 Effect of chain end on particle aggregation of (a) one position of acetal bond with OEG_3 (SC (1)), (b) two position of acetal bond with OEG_3 (SC (2)), and (c) two position of acetal bond with OEG_4 (SC (3)) measured by UV-Vis spectra at pH5.6, 2.5 min.

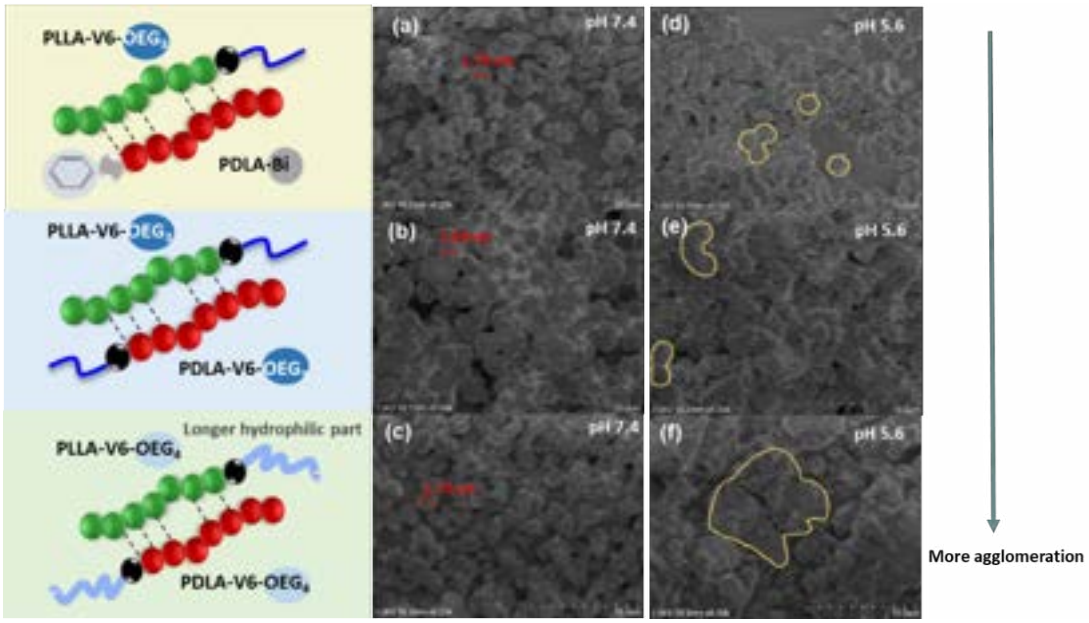

Figure 1-34. SEM images of (a)one position of acetal bond with OEG_3 at pH 7.4, (b) two position of acetal bond with OEG_3 at pH 7.4, (c) two position of acetal bond with OEG_4 at pH 7.4, (d) one position of acetal bond with OEG_3at pH 5.6, (e) two position of acetal bond with OEG_3 at pH 5.6, and (f) two position of acetal bond with OEG_4 at pH 5.6.

1.2.6.2 Study of molecular weight effect

SC-PLA were examined an effect of molecular weight on aggregation rate by controlling of polymer chain length (M_n) when changing pH from 7.4 to 5.6. The transmitted percentage were monitored (**Equation 1-1**) between 0 to 2.5 min. From the results, SC-PLA particles with one acetal bond (SC (1) OEG_3-benzyl) were formed by pairing various molecular weight of PLLA-V6-OEG_3. It was found that short chain M_n 1200 g/mol was exhibited the fastest aggregation rate compared with the M_n 2400 within 2.5 min (**Figure 1-35a**).

Moreover, the tendency of molecular weight effect on aggregation rate with two acetal bonds (SC (3) OEG_4/OEG_4) were presented in **Figure 1-35B**. SC-PLA consisting of short chain PDLA-V6-OEG_4 (M_n 1700)/PLLA-V6-OEG_4 (M_n 1800) (SC(3)) was exhibited the fastest aggregation rate compared with SC-PLA from PLLA-V6-OEG_4 M_n 2000. Considering the results, we may commit with the relation of low molecular weight with molecular mobility. Moreover, it was expected that hydrophilic terminal groups such as hydroxyl or carbonyl group may increase the water diffusion rate, and catalyzing degradation.[47,48] Concerning the impact of aggregation rate, the number of acetal bond also has an influence. Therefore, the comparison of SC-PLA was elucidated by pairs of PLLA-V6-OEG_3 (M_n 1200) / PDLA-Benzyl (M_n 5100) (SC(1)) and PLLA-V6-OEG_4 (M_n

1800) / PDLA-V6-OEG$_4$ (M_n 1700) (SC(3)). From the experiment, there was a clue with contributing design of hydrophilic/hydrophobic balance. Corresponding to aggregation rate, it seemed that transmittance percentage may induced by number of acetal bonds, hydrophilicity moiety, and molecular weight.

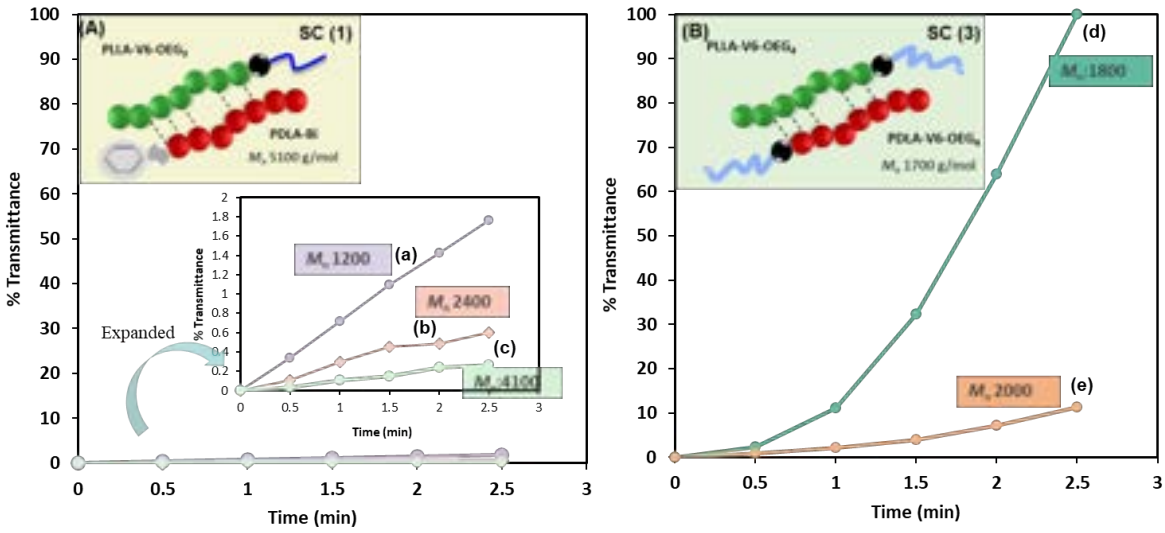

Figure 1-35. Effect of molecular weight on SC particles aggregation of (A) one arm of acetal bond with OEG$_3$ (SC (1)) various M_n of PLLA-V6-OEG$_3$ (a) M_n 1800 (b) M_n 24000, and (c) M_n 4100 at pH 5.6. (B) two arm of acetal bond with OEG$_4$ (SC (3)) various M_n of PLLA-V6-OEG$_4$ (d) M_n 1800, and (e) M_n 2000 at pH 5.6.

1.2.7 Titanium dioxide-blended PLLA-V6-OEG$_3$

PLLA-V6-OEG$_3$, M_n 2400 were selected as candidates to conduct the blended experiment. In this section, the PLA particles will be blended with TiO_2 by varying polymer concentration and 2.5 mg TiO_2 concentration ([P]:[Ti]) (**Figure 1-36A**). The transmitted percentage were monitored (**Equation 1-1**) between 0 to 2.5 min. From UV-Vis results, it was found that the ratio [P]:[Ti], 2.5 mg/mL: 2.5 mg (**Figure 1-36e**) presented optimum ratio for particles aggregation compared to those without TiO_2 (**Figure 1-36c**).

Besides, the experiment was continued by 2.5mg/mL polymer concentration and varying TiO_2 concentration (**Figure 1-36B**). It was found that 2.5 mg/mL polymer concentration to 2.5 mg of TiO_2 was also exhibited optimum ratio for particles aggregation within 3 min (**Figure 1-36h**). As previous research reported that the excessive content of TiO_2 is not conducted the higher rate of hydrolysis[41] which is also convinced to our results and could discuss in term of gravity-settling.

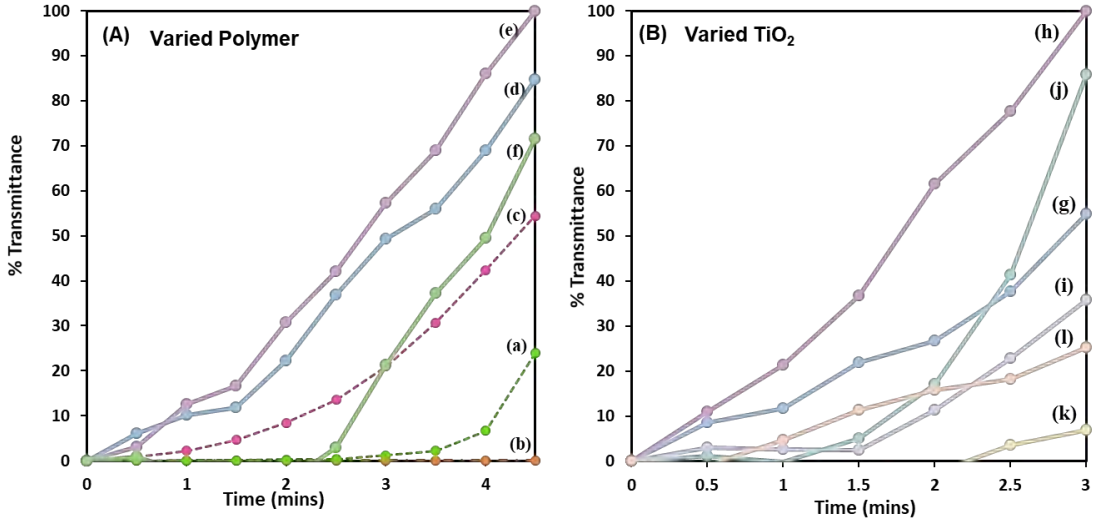

Figure 1-36. (A) UV-Vis results of PLLA-V6-OEG_3 various concentration blended with TiO_2 concentration 2.5mg at pH 7.4 (a) 2.5P, at pH 5.6 (b) 2.5Ti, (c) 2.5P, (d) 1P2.5Ti, (e) 2.5P2.5Ti, and (f) 5P2.5Ti. (B) UV-Vis results of PLLA-V6-OEG3 concentration 2.5 blended with TiO_2 various concentration at pH 5.6 (g)2.5P1Ti, (h) 2.5P2.5Ti, (i) 2.5P3.75Ti, (j) 2.5P5Ti, (k) 2.5P7.5Ti, and (l) 2.5P10Ti. (P = polymer concentration (mg/mL), Ti= TiO_2 (mg))

1.2.8 SC particles blended with Titanium dioxide

Herein, SC-PLA particles of PLLA-V6-OEG_4 (M_n 1800)/PDLA-V6-OEG_4 (M_n 1700) were selected as a candidate to be blended with TiO_2. This choice was based on their demonstrated ability to achieve aggregation within three minutes in previous experiments. The transmittance percentage of aggregation rate after pH change from 7.4 to 5.6 were analyzed (**Figure 1-37 and Equation 1-1**). With TiO_2 blend, it was perceived that transmittance changed 40% after 30 sec, 41% at 3 min, and notwithstanding at 58% after 15 min (**Figure 1-37b**). Contrastingly, at pH 7.4 transmittance changed 22% after 30 sec, and kept maintain even after 3 min and 15 min passed (**Figure 1-37a**). Regarding the results (**Figure 1-37** and **1-38**), it could be indicated that TiO_2-blends SC-PLA particles could not be reached to control pH responsive under physiological condition which seemed to be more benefit of stability.

To comprehend the gravity-settling phenomenon, the presence and absence of TiO_2 were examined (**Figure 1-38).** The results of transmittance percentage were shown TiO_2 existence (**Figure 1-38a**) and no TiO_2 (**Figure 1-38b**) at pH 5.6. It was discovered that the absence of TiO_2 resulted in more percentage of transmittance (**Figure 1-38b**)

which meant faster particle aggregation than TiO_2 existence system (**Figure 1-38a**). Regarding the result, it may contribute in term of stability of SC-PLA particles over the gravity-settling (weight and size inducing).

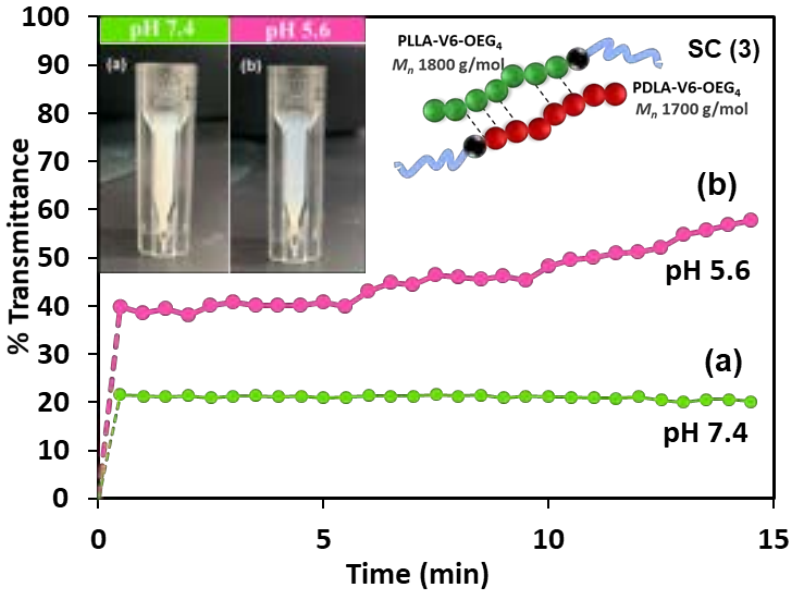

Figure 1-37. UV-Vis results of effect of TiO_2 on SC particles (a) at pH 7.4, (b) at pH 5.6.

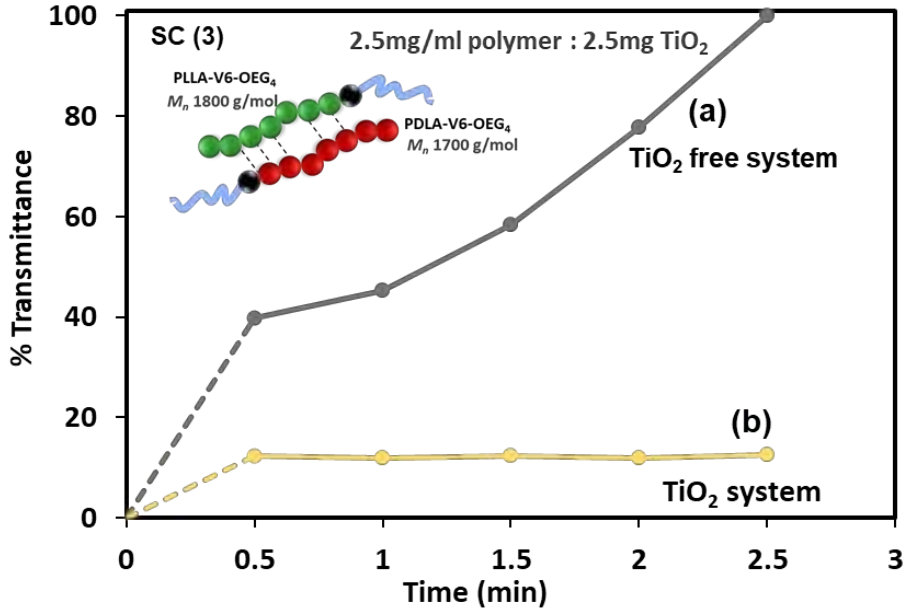

Figure 1-38. UV-Vis results of transmittance percentage at pH 5.6 (a) in TiO_2 system and (b) no TiO_2 of SC (3).

1.3 Conclusions

The desired vanillin acetal-based initiators including cyclic-membered ring diol-ketone acetal were synthesized and initiated novel functional PLA at the end-capping. PLLA-V6-OEG_3 particles were appropriated to achieve pH-responsive behaviour under physiological condition within 3 min. The particles from short chain polymer (M_n 2400) could provide readily deformation than long chain polymer (M_n > 4800). Moreover, PLLA-V6-OEG_3 was hydrolysed within 2.5 min at pH 6.2 and 1.5 min at pH 5.6, it could be indicated that pH strength could accurate to aggregation. Taking account to balance hydrophilicity/hydrophobicity for SC-PLA particles, PLLA-V6-OEG_4 and PDLA-V6-OEG_4 were successfully synthesized. The aggregation rate of SC-PLA-OEG_m particles were affected by molecular weight, hydrophilicity of chain-end, and number of acetal bond. PLLA-V6-OEG_3 particles blended with TiO_2 exhibited accelerated aggregation compared without TiO_2-blended. SC-PLA particles blended with TiO_2 could not reached to achievepH responsiveness under physiological condition (**Figure 39**). I believe that our promising PLA-V6-OEG_m particle could be addressed further for clinical applications.

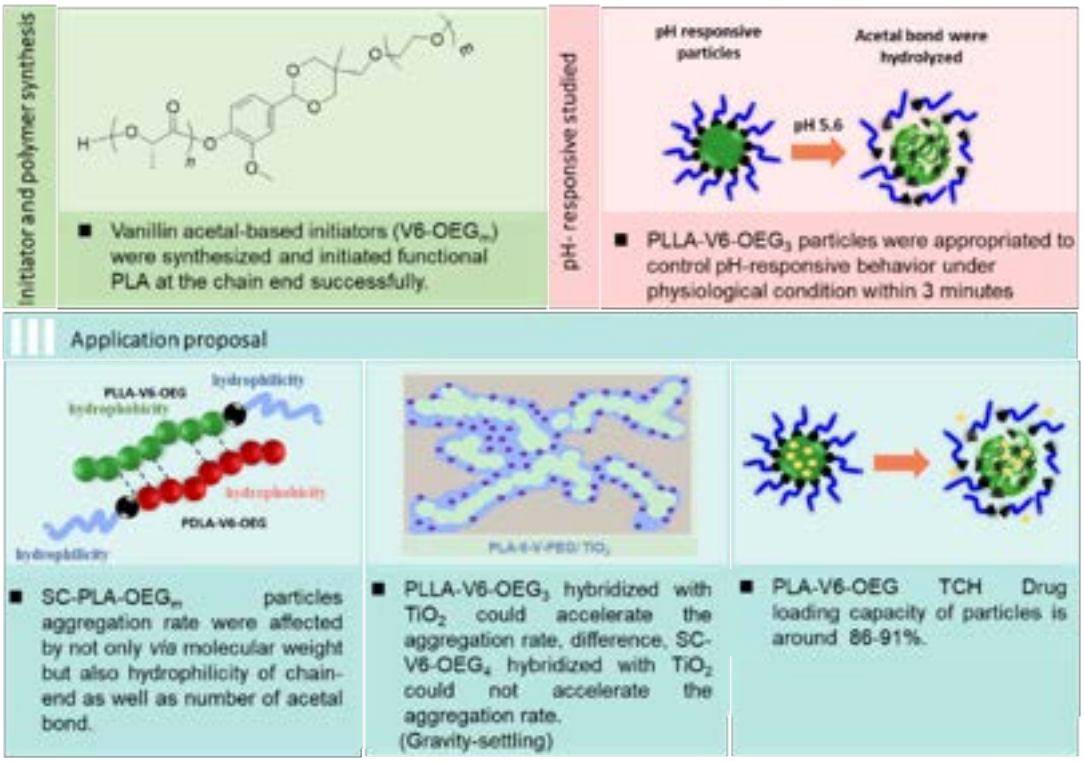

Figure 1-39. Summary of Conclusions for Chapter I

1.4 Experimental

1.4.1 Synthesis

1.4.1.1 Synthesis of Vanillin-6-OEG$_m$

The tosylation of 2-{2-(2-methoxyethoxy)ethoxy}ethyl tosylate was carried out according to literature [73] with a yield of 98%. The protection of the diol derivative was succeeded to obtain 52% yield of 5-hydroxymethyl-5-methyl-2-phenyl-1,3-dioxane (HMPD) using reported the method[74]. Next, the following synthesis of 5-[2-{2-(2-methoxyethoxy)ethoxy}- ethoxymethyl]-5-methyl-2-phenyl-1,3-dioxane (MPD-OEG$_3$) has been done as the previous literature,[75] as well as the deprotection of 2-[2-{2-(2-methoxyethoxy)ethoxy}-ethoxymethyl]-2-methylpropan-diol (Diol-OEG$_3$).[74,75]

1.4.1.1.1 *Synthesis of 2-methoxy-4-(5-((2-methoxyethoxy)methyl)-5-methyl-1,3-dioxan-2-yl)phenol (Vanillin-6-OEG$_3$)*

Diol-OEG$_3$ (21.3 mg, 79.9 mmol) was added into a round bottom flask and the solution of vanillin (15.5 mg, 101.57 mmol) and *p*-toluenesulfonic acid monohydrate (1.83g, 10.6 mmol) in THF (150 mL) was slowly added into the reaction flask. The reaction was proceeded under refluxing at 70°C and stirred 24 h. The reaction mixture was extracted with CH_2Cl_2 and water to recover the Vanillin-6-OEG$_3$ initiator. Then, the target was purified by column chromatography using hexane: acetone (10.3 g, yield 32%). ^{1}H NMR (400 MHz, CDCl3, δ): 6.99 (s, 2H, CH), 6.88 (s, 1H, CH), 5.66 (s, 1H, CH), 4.04-4.01 (d, *J* = 12 Hz, 2H, CH_2), 3.96-3.90 (d, *J* = 24 Hz, 4H, CH_2), 3.68-3.58 (d, *J* = 40 Hz, 12H, CH_2), 3.56-3.52 (t, *J* = 16 Hz, 3H; CH_3), 3.39-3.35 (t, *J* = 16 Hz, 3H; CH_3), 1.84-0.76(t, *J* = 12 Hz, 3H; CH_3) ; IR : ν = 3396, 2858, 1607, 1452, 1355, 1026, 732; MASS: m/z : $[M+Na]^+$ 423.2.

1.4.1.1.2 *Synthesis of 2-methoxy-4-(5-methyl-5-(2,5,8,11,14-pentaoxapentadecyl)-1,3-dioxan-2-yl)phenol (Vanillin-6-OEG$_4$)*

Vanillin-6-OEG$_4$, it was prepared using the same synthetic path of Vanillin-6-OEG$_3$. The target was purified by column chromatography using hexane: acetone: ethyl acetate (3.16 g, yield 45%).

^{1}H NMR (400 MHz, $CDCl_3$, δ): δ 6.99 (s, 2H, CH), 6.88 (s, 1H, CH), 5.66 (s, 1H, CH), 4.05—4.03 (d, *J* = 8 Hz, 2H, CH_2), 3.93—3.90 (d, *J* = 12 Hz, 4H, CH_2), 3.70—3.58 (d, *J* = 48 Hz, 16H, CH_2), 3.56—3.53 (t, *J* = 12 Hz, 3H; CH_3), 3.39—3.34 (t, *J* = 12 Hz, 3H; CH_3), 1.84—0.76(t, *J* = 12 Hz, 3H; CH_3) ; IR : ν = 3396, 2858, 1607, 1452, 1355, 1026, 732; MASS: m/z : $[M+H]^+$ 445.44.

1.4.1.2 Synthesis of PLA-V6-OEG$_m$

Under neat nitrogen conditions, (*L,L*)-lactide or (*D,D*)-lactide (2 g, 13.9 mmol) were dried in thermal desiccator at 40℃ for 24 h. Then, the (*L,L*)-lactide or (*D,D*)-lactide, initiator, and Sn(Oct)$_2$ (885 µL, 0.021 mmol) were combined with 13.9 mL toluene (1M) in the gloves box. Then, the reaction media was heated up to 100℃ with various reaction time. After that, the product was precipitated by hexane and isopropanol ratio 9:1 (450 mL) to obtain PLLA-V6-OEG$_3$, PDLA-V6-OEG$_3$, PLLA-V6-OEG$_4$, and PDLA-V6-OEG$_4$. The ratios of the initiators to monomer, vanillin-6-OEG$_3$, and vanillin-6-OEG$_4$ were proceeded as 1:20, 1:10, 1:5, and 1:1 in order to control the molecular weight of the polymer as shown in **Table 1**.

1.4.1.3 SC preparation

PLLA (various the chain-end type) (500 mg) in THF (10 mL) was dissolved at 37°C. PDLA (various the chain-end type) (500 mg) in THF (10 mL) was dissolved at 37°C. Then, the solutions of PLLA and PDLA which already dissolved were mixed together and sonicated 30 seconds. After that leave it overnight. Finally, the nanoparticles were filtrated and formation of the SC was confirmed by FT-IR and XRD.

1.4.1.4 Particles preparation PLA-V6-OEG$_m$

PLLA-V6-OEG$_3$ and SC-PLA nanoparticles were prepared by the emulsion technique[76]. PLA-V6-OEG$_m$ (50 mg) in ethyl acetate (1 mL) was sonicated 30 seconds. Then, 2 ml of pH 7.4 buffer solution was added slowly to the solution with stirring and sonicated 30 seconds. After that, 100 mL of pH 7.4 buffer solution was added slowly with stirring and then the organic solvent was rapidly eliminated by rotary evaporation. Finally, the nanoparticles were recovered by centrifugation at 3500 rpm for 5 min and the precipitant was washed with buffer solution three times.

1.4.1.5 Particles aggregation

1.4.1.5.1 *Observation of the particle aggregation behavior*

The PLLA-V6-OEG$_3$ and their SC-PLA particles were dispersed in pH 7.4 buffer solution (the concentration depends on each polymer) and then 1 mL of particles disoersion were picked up and was added 45 µL of 5M HCl to adjust pH at 5.6 and 28 µL of 5M HCl for pH 6.0. In order to determine the aggregation rate, the transmittance intensity of the samples was measured by UV-Vis spectroscopy at 500 nm for 3—5 min. However, the plotting of transmittance percentage was compromised with the optimum aggregation rate by using **Equation 1-1.**

$$\%\text{Transmittance} = \frac{[T_x]}{[T_{ref}]} \text{X } 100$$

Equation 1-1

T_x is Transmittance of particle in each pH or Mn or time

T_{ref1} is Transmittance of $PLA33-V6-OEG3$particles at pH 5.6 $(2.5$ mins$)$ Homopolymer

T_{ref2} isTransmittance of SC (3) Mn 1800 at pH 5.6 $(2.5$ mins$)$ Stereocomplex

T_{ref3} is Transmittance of $2.5P2.5Ti$ at pH 5.6 $(2.5$ mins$)$ Blended-TiO_2

In order to confirm the decomposed structure after hydrolysis, the liquid layer and solid layer were separated immediately after measuring particles aggregation rate by UV-Visible transmittance. Then, the solid layer was dissolved homogenously in $CDCl_3$ and in THF to measure by ^{1}HNMR and SEC, respectively.

1.4.1.5.2 *Morphology of particles*

PLA-V6-OEG_m and their SC-PLA particles in pH 7.4 buffer solution and after pH adjustment at pH 5.6 were dropped in foil and dried it for 2 weeks. After that, it was measured by Low Vacuum Scanning Electron Microscope in condition, accelerating voltage: 1—5 kV magnification: 5000X and 10,000X without metal coating of SEM signal.

1.4.1.5.3 *Titanium dioxide-blended*

PLLA-V6-OEG_3 particles and their SC-PLA particles were dispersed in pH 7.4 buffer solution (various concentration) from 1 to 5 mg/mL and then added TiO_2 (various weight) from 1 to 10 mg. After that it was sonicated 180 second. Then, 1 mL of particles solution were picked up and was added 45 µL of 5M HCl adjusting to pH 5.6 and 28 µL of 5M HCl for pH 6.0. In order to determine the aggregation rate, the samples were measured the transmitted intensity by UV-Vis spectroscopy at 500 nm for 3—15 min.

1.5 References

(1) Chivere, V. T.; Kondiah, P. P. D.; Choonara, Y. E.; Pillay, V. Nanotechnology-Based Biopolymeric Oral Delivery Platforms for Advanced Cancer Treatment. *Cancers* **2020**, *12* (2), 522. https://doi.org/10.3390/cancers12020522.

(2) Maiti, S. Nanometric Biopolymer Devices for Oral Delivery of Macromolecules with Clinical Significance. *Multifunctional Systems for Combined Delivery, Biosensing and Diagnostics*; Elsevier, **2017**, 109–138. https://doi.org/10.1016/B978-0-323-52725-5.00006-X.

(3) Williams, D. F. On the Mechanisms of Biocompatibility. *Biomaterials* **2008**, *29* (20), 2941–2953. https://doi.org/10.1016/j.biomaterials.2008.04.023.

(4) Bano, K.; Pandey, R. NEW ADVANCEMENTS OF BIOPLASTICS IN MEDICAL APPLICATIONS. *Int. J. Pharm. Sci. Res.* **2018**, *9* (2), 402. https://doi.org/10.13040/IJPSR.0975-8232.9(2).402-16.

(5) Avella, M.; Buzarovska, A.; Errico, M. E.; Gentile, G.; Grozdanov, A. Eco-Challenges of Bio-Based Polymer Composites. *Materials* **2009**, *2* (3), 911–925. https://doi.org/10.3390/ma2030911.

(6) Nair, L. S.; Laurencin, C. T. Biodegradable Polymers as Biomaterials. *Prog. Polym. Sci.* **2007**, *32* (8-9), 762–798. https://doi.org/10.1016/j.progpolymsci.2007.05.017.

(7) Tsuji, H.; Hyon, S.-H.; Ikada, Y. Stereocomplex Formation between Enantiomeric Poly(Lactic Acid)s. 4. Differential Scanning Calorimetric Studies on Precipitates from Mixed Solutions of PolyCn-Lactic Acid) and Poly(L-Lactic Acid). *Biomacromolecules* **2004**, *5* (4), 1181–1186. https://doi.org/10.1021/bm049835i.

(8) Singhvi, M. S.; Zinjarde, S. S.; Gokhale, D. V. Polylactic Acid: Synthesis and Biomedical Applications. *J. Appl. Microbiol*. **2019**, 127(6), 1612–1626. https://doi.org/10.1111/jam.14290.

(9) Santoro, M.; Shah, S. R.; Walker, J. L.; Mikos, A. G. Poly(Lactic Acid) Nanofibrous Scaffolds for Tissue Engineering. *Adv. Drug Deliv. Rev.* **2016**, *107*, 206–212. https://doi.org/10.1016/j.addr.2016.04.019.

(10) Mura, S.; Nicolas, J.; Couvreur, P. Stimuli-Responsive Nanocarriers for Drug Delivery. *Nat. Mater*. **2013**, *12*(11), 991–1003. https://doi.org/10.1038/nmat3776.

(11) Gonçalves, C.; Gonçalves, I. C.; Magalhães, F. D.; Pinto, A. M. Poly(Lactic Acid) Composites Containing Carbon-Based Nanomaterials: A Review. *Polymers* **2017**, *9*(12), 269. https://doi.org/10.3390/polym9070269.

(12) Tschan, M. J. L.; Brulé, E.; Haquette, P.; Thomas, C. M. Synthesis of Biodegradable Polymers from Renewable Resources. *Polym. Chem.* **2012**, *3* (4), 836–851. https://doi.org/10.1039/c2py00452f.

(13) Mahmood, H.; Moniruzzaman, M.; Yusup, S.; Welton, T. Ionic Liquids Assisted Processing of Renewable Resources for the Fabrication of Biodegradable Composite Materials. *Green Chem*. **2017**, *19* (9), 2051–2075. https://doi.org/10.1039/c7gc00318h.

(14) Yu, L.; Dean, K.; Li, L. Polymer Blends and Composites from Renewable Resources. *Prog. Polym. Sci.* **2006**, *31* (6), 576–602. https://doi.org/10.1016/j.progpolymsci.2006.03.002.

(15) Seyednejad, H.; Ghassemi, A. H.; Van Nostrum, C. F.; Vermonden, T.; Hennink, W. E. Functional Aliphatic Polyesters for Biomedical and Pharmaceutical Applications. *J. Control. Release*. **2011**, *152*(1), 168–176. https://doi.org/10.1016/j.jconrel.2010.12.016.

(16) Leemhuis, M.; Van Nostrum, C. F.; Kruijtzer, J. A. W.; Zhong, Z. Y.; Ten Breteler, M. R.; Dijkstra, P. J.; Feijen, J.; Hennink, W. E. Functionalized Poly(α-Hydroxy Acid)s via Ring-Opening Polymerization: Toward Hydrophilic Polyesters with Pendant Hydroxyl Groups. *Macromolecules* **2006**, *39* (10), 3500–3508. https://doi.org/10.1021/ma052128c.

(17) Noga, D. E.; Petrie, T. A.; Kumar, A.; Weck, M.; García, A. J.; Collard, D. M. Synthesis and Modification of Functional Poly(Lactide) Copolymers: Toward Biofunctional Materials. *Biomacromolecules* **2008**, *9* (7), 2056–2062. https://doi.org/10.1021/bm800292z.

(18) Pounder, R. J.; Dove, A. P. Synthesis and Organocatalytic Ring-Opening Polymerization of Cyclic Esters Derived from l-Malic Acid. *Biomacromolecules* **2010**, *11* (8), 1930–1939. https://doi.org/10.1021/bm1004355.

(19) Du Boullay, O. T.; Saffon, N.; Diehl, J. P.; Martin-Vaca, B.; Bourissou, D. Organo-Catalyzed Ring Opening Polymerization of a 1,4-Dioxane-2,5-Dione Deriving from Glutamic Acid. *Biomacromolecules* **2010**, *11* (8), 1921–1929. https://doi.org/10.1021/bm100433c.

(20) Regnier-Delplace, C.; Thillaye Du Boullay, O.; Siepmann, F.; Martin-Vaca, B.; Demonchaux, P.; Jentzer, O.; Danède, F.; Descamps, M.; Siepmann, J.; Bourissou, D. PLGAs Bearing Carboxylated Side Chains: Novel Matrix Formers with Improved Properties for Controlled Drug Delivery. *J. Control. Release.* **2013**, *166* (3), 256–267. https://doi.org/10.1016/j.jconrel.2012.12.024.

(21) Hu, X.; Liu, S.; Chen, X.; Mo, G.; Xie, Z.; Jing, X. Biodegradable Amphiphilic Block Copolymers Bearing Protected Hydroxyl Groups: Synthesis and Characterization. *Biomacromolecules* **2008**, *9* (2), 553–560. https://doi.org/10.1021/bm701092j.

(22) Bednarek, M.; Basko, M.; Biedroń, T.; Kubisa, P.; Pluta, M. Aggregation of Polylactide with Carboxyl Groups at One Chain End in the Presence of Metal Cations. *Polym. Bull.* **2014**, *71* (8), 1891–1907. https://doi.org/10.1007/s00289-014-1162-x.

(23) Ouchi, T.; Uchida, T.; Arimura, H.; Ohya, Y. Synthesis of Poly(L-Lactide) End-Capped with Lactose Residue. *Biomacromolecules* **2003**, *4* (3), 477–480. https://doi.org/10.1021/bm020110t.

(24) Saulnier, B.; Ponsart, S.; Coudane, J.; Garreau, H.; Vert, M. Lactic Acid-Based Functionalized Polymers via Copolymerization and Chemical Modification. *Macromol. Biosci.* **2004**, *4*(3), 232–237. https://doi.org/10.1002/mabi.200300087.

(25) Lee, S. H.; Hyun Kim, S.; Han, Y. K.; Kim, Y. H. Synthesis and Degradation of End-Group-Functionalized Polylactide. *J. Polym. Sci. A Polym. Chem.* **2001**, *39* (7), 973–985. https://doi.org/10.1002/1099-0518(20010401)39:7<973::AID-POLA1073>3.0.CO;2-8.

(26) Tsuji, H.; Sugimoto, S. Long Terminal Linear Alkyl Group as Internal Crystallization Accelerating Moiety of Poly(l-Lactide). *Polymer* **2014**, *55* (18), 4786–4798. https://doi.org/10.1016/j.polymer.2014.07.012.

(27) Xu, L.; Qiu, L.; Sheng, Y.; Sun, Y.; Deng, L.; Li, X.; Bradley, M.; Zhang, R. Biodegradable PH-Responsive Hydrogels for Controlled Dual-Drug Release. *J. Mater. Chem. B.* **2018**, *6* (3), 510–517. https://doi.org/10.1039/c7tb01851g.

(28) Huang, C. K.; Lo, C. L.; Chen, H. H.; Hsiue, G. H. Multifunctional Micelles for Cancer Cell Targeting, Distribution Imaging, and Anticancer Drug Delivery. *Adv. Funct. Mater.* **2007**, *17* (14), 2291–2297. https://doi.org/10.1002/adfm.200600818.

(29) Soppimath, K. S.; Kulkarni, A. R.; Aminabhavi, T. M. Chemically Modified Polyacrylamide-g-Guar Gum-Based Crosslinked Anionic Microgels as PH-Sensitive Drug Delivery q Systems: Preparation and Characterization. *J. Control. Release* **2001**, *75*(3), 331-345. https://doi.org/10.1016/s0168-3659(01)00404-7.

(30) Hoffman, A. S. Stimuli-Responsive Polymers: Biomedical Applications and Challenges for Clinical Translation. *Adv. Drug Deliv. Rev*. **2013**, *65*(1), 10–16. https://doi.org/10.1016/j.addr.2012.11.004.

(31) Liu, M.; Du, H.; Zhang, W.; Zhai, G. Internal Stimuli-Responsive Nanocarriers for Drug Delivery: Design Strategies and Applications. *Materials Science and Engineering C*. Elsevier Ltd February 1, 2017, pp 1267–1280. https://doi.org/10.1016/j.msec.2016.11.030.

(32) Swietach, P.; Vaughan-Jones, R. D.; Harris, A. L.; Hulikova, A. The Chemistry, Physiology and Pathology of PH in Cancer. *Philos. Trans. R. Soc. B: Biol. Sci.* **2014**, *369*(1638). https://doi.org/10.1098/rstb.2013.0099.

(33) Wu, W.; Luo, L.; Wang, Y.; Wu, Q.; Dai, H. Bin; Li, J. S.; Durkan, C.; Wang, N.; Wang, G. X. Endogenous PH-Responsive Nanoparticles with Programmable Size Changes for Targeted Tumor Therapy and Imaging Applications. *Theranostics*. **2018**,

8(11), 3038–3058. https://doi.org/10.7150/thno.23459.

(34) Hu, Q.; Gao, X.; Gu, G.; Kang, T.; Tu, Y.; Liu, Z.; Song, Q.; Yao, L.; Pang, Z.; Jiang, X.; Chen, H.; Chen, J. Glioma Therapy Using Tumor Homing and Penetrating Peptide-Functionalized PEG-PLA Nanoparticles Loaded with Paclitaxel. *Biomaterials* **2013**, *34* (22), 5640–5650. https://doi.org/10.1016/j.biomaterials.2013.04.025.

(35) Hamad, K.; Kaseem, M.; Yang, H. W.; Deri, F.; Ko, Y. G. Properties and Medical Applications of Polylactic Acid: A Review. *Express. Polym. Lett.* **2015**, *9* (5), 435–455. https://doi.org/10.3144/expresspolymlett.2015.42.

(36) Lee, B. K.; Yun, Y.; Park, K. PLA Micro- and Nano-Particles. *Adv. Drug Deliv. Rev.*, **2016**, *107*, 176–191. https://doi.org/10.1016/j.addr.2016.05.020.

(37) Letchford, K.; Burt, H. A Review of the Formation and Classification of Amphiphilic Block Copolymer Nanoparticulate Structures: Micelles, Nanospheres, Nanocapsules and Polymersomes. *Eur. J. Pharm. Biopharm*. **2007**, *65*(3), 259–269. https://doi.org/10.1016/j.ejpb.2006.11.009.

(38) Knop, K.; Hoogenboom, R.; Fischer, D.; Schubert, U. S. Poly(Ethylene Glycol) in Drug Delivery: Pros and Cons as Well as Potential Alternatives. *Angew. Chem. - Int. Ed*. **2010**, *49*(36), 6288–6308. https://doi.org/10.1002/anie.200902672.

(39) Li, C.; Wallace, S. Polymer-Drug Conjugates: Recent Development in Clinical Oncology. *Adv. Drug Deliv. Rev*. **2008**, 60(8), 886–898. https://doi.org/10.1016/j.addr.2007.11.009.

(40) Wang, J.; Li, S.; Han, Y.; Guan, J.; Chung, S.; Wang, C.; Li, D. Poly(Ethylene Glycol)-Polylactide Micelles for Cancer Therapy. *Front. Pharmacol*. **2018**, 9. https://doi.org/10.3389/fphar.2018.00202.

(41) Ciesielski, A.; El Garah, M.; Haar, S.; Kovaříček, P.; Lehn, J. M.; Samorì, P. Dynamic Covalent Chemistry of Bisimines at the Solid/Liquid Interface Monitored by Scanning Tunnelling Microscopy. *Nat. Chem.* **2014**, *6* (11). https://doi.org/10.1038/NCHEM.2057.

(42) Yoshida, T.; Lai, T. C.; Kwon, G. S.; Sako, K. PH-and Ion-Sensitive Polymers for Drug Delivery. *Expert Opin. Drug Deliv*. **2013**, *10*(11), 1497–1513. https://doi.org/10.1517/17425247.2013.821978.

(43) Gao, W.; Chan, J. M.; Farokhzad, O. C. PH-Responsive Nanoparticles for Drug Delivery. *Mol. Pharm*. **2010**, 7(6), 1913–1920. https://doi.org/10.1021/mp100253e.

(44) Feng, X.; Li, D.; Han, J.; Zhuang, X.; Ding, J. Schiff Base Bond-Linked Polysaccharide–Doxorubicin Conjugate for Upregulated Cancer Therapy. *Mater. Sci. Eng. C.* **2017**, *76*, 1121–1128. https://doi.org/10.1016/j.msec.2017.03.201.

(45) Xiao, L.; Huang, L.; Moingeon, F.; Gauthier, M.; Yang, G. PH-Responsive

Poly(Ethylene Glycol)-Block-Polylactide Micelles for Tumor-Targeted Drug Delivery. *Biomacromolecules* **2017**, *18* (9), 2711–2722. https://doi.org/10.1021/acs.biomac.7b00509.

(46) Griset, A. P.; Walpole, J.; Liu, R.; Gaffey, A.; Colson, Y. L.; Grinstaff, M. W. Expansile Nanoparticles: Synthesis, Characterization, and in Vivo Efficacy of an Acid-Responsive Polymeric Drug Delivery System. *J. Am. Chem. Soc.* **2009**, *131* (7), 2469–2471. https://doi.org/10.1021/ja807416t.

(47) Kaneko, T.; Willner, D.; Monkovic, I.; Braslawsky, G. R.; Greenfield, R. S.; Vyas, D. M. New Hydrazone Derivatives of Adriamycin and Their Immunoconjugates—a Correlation between Acid Stability And. *Bioconjug. Chem.* **1991**, *2* (3), 133–141.

(48) Rodrigues, P. C. A.; Beyer, U.; Schumacher, P.; Roth, T.; Fiebig, H. H.; Unger, C.; Messori, L.; Orioli, P.; Paper, D. H.; Muè, R.; Kratz, F. Acid-Sensitive Polyethylene Glycol Conjugates of Doxorubicin: Preparation, In Vitro Efficacy and Intracellular Distribution. *Bioorg. Med. Chem.* **1999**, *7* (11), 2517–2524. https://doi.org/10.1016/s0968-0896(99)00209-6.

(49) Shen, W.-C.; Hugues J.-P. Ryser. Cis-Aconityl Spacer between Daunomycin and Macromolecular Carriers: A Model of PH-Sensitive Linkage Releasing Drug from a Lysosomotropic Conjugate. *Biochem. Biophys. Res. Commun.* **1981**, *102* (3), 1048–1054. https://doi.org/10.1016/0006-291x(81)91644-2.

(50) Hudecz, F.; Ross, H.; Price, M. R.; Baldwin, R. W. Immunoconjugate Design: A Predictive Approach for Coupling of Daunomycin to Monoclonal Antibodies. *Bioconjug. Chem.* **1990**, *1* (3), 197–204. https://doi.org/10.1021/bc00003a004.

(51) Patel, V. F.; Hardin, J. N.; Mastro, J. M.; Law, K. L.; Zimmermann, J. L.; Ehlhardt, W. J.; Woodland, J. M.; Starling, J. J. Novel Acid Labile COL1 Trityl-Linked Difluoronucleoside Immunoconjugates: Synthesis, Characterization, and Biological Activity 1. *Bioconjug. Chem*. **1996**, *7* (4), 497–510. https://doi.org/10.1021/bc960038u.

(52) Timmers, M.; Weterings, J.; Van Geijn, M.; Bell, R.; Lenting, P. E.; Rijcken, C. J. F.; Vermonden, T.; Hennink, W. E.; Liskamp, R. M. J. A New Class of Tunable Acid-Sensitive Linkers for Native Drug Release Based on the Trityl Protecting Group. *Bioconjug. Chem.* **2022**, *33* (9), 1707–1715. https://doi.org/10.1021/acs.bioconjchem.2c00310.

(53) Heller, J.; Barr, J.; Ng, S. Y.; Abdellauoi, K. S.; Gurny, R. Poly(Ortho Esters): Synthesis, Characterization, Properties And. *Adv. Drug Deliv. Rev.* **2002**, *54*, 1015–1039.

(54) Fife, T. H.; Jao, L. K.; Br, N.; K Wynne, W. F.; Bunton, C. A.; Lewis, T. A.; Llewellyn, R.; Vernon, C. A.; Hammett, L. P.; Xii, H.; Xiii, C. Structure and Mechanism in

Organic Chemistry; *Cornell University Press*. **1929**, *30*.

(55) Deslongchamps, P.; Dory, Y. L.; Li, S. The Relative Rate of Hydrolysis of a Series of Acyclic and Six-Membered Cyclic Acetals, Ketals, Orthoesters, and Orthocarbonates. *Tetrahedron* **2000**, *56* (22), 3533–3537. https://doi.org/10.1016/s0040-4020(00)00270-2.

(56) Tamura, Y.; Kanomata, K.; Kitaoka, T. Interfacial Hydrolysis of Acetals on Protonated TEMPO-Oxidized Cellulose Nanofibers. *Sci. Rep.* **2018**, *8* (1). https://doi.org/10.1038/s41598-018-23381-8.

(57) Ajiro, H.; Hsiao, Y. J.; Thi, T. H.; Fujiwara, T.; Akashi, M. A Stereocomplex of Poly(Lactide)s with Chain End Modification: Simultaneous Resistances to Melting and Thermal Decomposition. *Chem. Commun.* **2012**, *48* (68), 8478–8480. https://doi.org/10.1039/c2cc33589a.

(58) Hang Thi, T.; Matsusaki, M.; Akashi, M. Thermally Stable and Photoreactive Polylactides by the Terminal Conjugation of Bio-Based Caffeic Acid. *Chem. Commun.* **2008**, *33*, 3918–3920. https://doi.org/10.1039/b803615b.

(59) Bao, J.; Chang, X.; Shan, G.; Bao, Y.; Pan, P. Synthesis of End-Functionalized Hydrogen-Bonding Poly(Lactic Acid)s and Preferential Stereocomplex Crystallization of Their Enantiomeric Blends. *Polym. Chem.* **2016**, *7* (30), 4891–4900. https://doi.org/10.1039/c6py00976j.

(60) Zhang, W. Bin; Li, Y.; Li, X.; Dong, X.; Yu, X.; Wang, C. L.; Wesdemiotis, C.; Quirk, R. P.; Cheng, S. Z. D. Synthesis of Shape Amphiphiles Based on Functional Polyhedral Oligomeric Silsesquioxane End-Capped Poly(l -Lactide) with Diverse Head Surface Chemistry. *Macromolecules* **2011**, *44* (8), 2589–2596. https://doi.org/10.1021/ma200268u.

(61) Sadaba, N.; Salsamendi, M.; Casado, N.; Zuza, E.; Muñoz, J.; Sarasua, J. R.; Mecerreyes, D.; Mantione, D.; Detrembleur, C.; Sardon, H. Catechol End-Functionalized Polylactide by Organocatalyzed Ring-Opening Polymerization. *Polymers* **2018**, *10* (2). https://doi.org/10.3390/polym10020155.

(62) Fache, M.; Darroman, E.; Besse, V.; Auvergne, R.; Caillol, S.; Boutevin, B. Vanillin, a Promising Biobased Building-Block for Monomer Synthesis. *Green Chem.* **2014**, *16* (4), 1987–1998. https://doi.org/10.1039/c3gc42613k.

(63) Fache, M.; Boutevin, B.; Caillol, S. Vanillin, a Key-Intermediate of Biobased Polymers. *Eur. Polym. J.* **2015**, *68*, 488–502. https://doi.org/10.1016/j.eurpolymj.2015.03.050.

(64) Kan, K.; Akashi, M.; Ajiro, H. Polylactides Bearing Vanillin at Chain End Provided Dual Dynamic Interactions: Stereocomplex Formation and Nanostructure Control. *Macromol. Chem. Phys.* **2016**, *217* (24), 2679–2685.

https://doi.org/10.1002/macp.201600395.

(65) Kan, K.; Akashi, M.; Ajiro, H. Dynamic Self-Assembly and Synthesis of Polylactide Bearing 5-Hydroxymethylfurfural Chain Ends. *ACS Appl. Polym. Mater.* **2019**, *1* (2), 267–274. https://doi.org/10.1021/acsapm.8b00185.

(66) Knowles, J. P.; Whiting, A. The Effects of Ring Size and Substituents on the Rates of Acid-Catalysed Hydrolysis of Five- and Six-Membered Ring Cyclic Ketone Acetals. *European J. Org. Chem.* **2007**, No. 20, 3365–3368. https://doi.org/10.1002/ejoc.200700244.

(67) Luo, Y. B.; Wang, X. L.; Wang, Y. Z. Effect of TiO 2 Nanoparticles on the Long-Term Hydrolytic Degradation Behavior of PLA. *Polym. Degrad. Stab.* **2012**, *97* (5), 721–728. https://doi.org/10.1016/j.polymdegradstab.2012.02.011.

(68) Sarisuta, K.; Iwami, M.; Martín-Vaca, B.; Chanthaset, N.; Ajiro, H. PH Effect on Particle Aggregation of Vanillin End-Capped Polylactides Bearing a Hydrophilic Group Connected by a Cyclic Acetal Moiety. *Langmuir* **2023**, *39* (11), 3994–4004. https://doi.org/10.1021/acs.langmuir.2c03303.

(69) Kowalski, A.; Duda, A.; Penczek, S. Mechanism of Cyclic Ester Polymerization Initiated with Tin(II) Octoate. 2. 1 Macromolecules Fitted with Tin(II) Alkoxide Species Observed Directly in MALDI-TOF Spectra. *Macromolecules* **2000**, *33* (3), 689–695. https://doi.org/10.1021/ma9906940.

(70) Saha, S. K.; Tsuji, H. Effects of Molecular Weight and Small Amounts of D-Lactide Units on Hydrolytic Degradation of Poly(l-Lactic Acid)s. *Polym. Degrad. Stab.* **2006**, *91* (8), 1665–1673. https://doi.org/10.1016/j.polymdegradstab.2005.12.009.

(71) Gorrasi, G.; Pantani, R. Hydrolysis and Biodegradation of Poly(Lactic Acid). *Adv. Polym. Sci.* **2018**, *279*, 119–151. https://doi.org/10.1007/12_2016_12.

(72) Kurokawa, K.; Yamashita, K.; Doi, Y.; Abe, H. Structural Effects of Terminal Groups on Nonenzymatic and Enzymatic Degradations of End-Capped Poly(L-Lactide). *Biomacromolecules* **2008**, *9* (3), 1071–1078. https://doi.org/10.1021/bm701259r.

(73) Chen, W.; Yang, H.; Wang, R.; Cheng, R.; Meng, F.; Wei, W.; Zhong, Z. Versatile Synthesis of Functional Biodegradable Polymers by Combining Ring-Opening Polymerization and Postpolymerization Modification via Michael-Type Addition Reaction. *Macromolecules* **2010**, *43* (1), 201–207. https://doi.org/10.1021/ma901897y.

(74) Ajiro, H.; Takahashi, Y.; Akashi, M. Thermosensitive Biodegradable Homopolymer of Trimethylene Carbonate Derivative at Body Temperature. *Macromolecules* **2012**, *45* (6), 2668–2674. https://doi.org/10.1021/ma300183t.

(75) Zhu, D.; Tao, W.; Zhang, H.; Liu, G.; Wang, T.; Zhang, L.; Zeng, X.; Mei, L. Docetaxel (DTX)-Loaded Polydopamine-Modified TPGS-PLA Nanoparticles as a Targeted Drug

Delivery System for the Treatment of Liver Cancer. *Acta Biomater.* **2016**, *30*, 144–154. https://doi.org/10.1016/j.actbio.2015.11.031.

(76) Tobío, M.; Sánchez, A.; Vila, A.; Soriano, I.; Evora, C.; Vila-Jato, J. L.; Alonso, M. J. The Role of PEG on the Stability in Digestive Fluids and in Vivo Fate of PEG-PLA Nanoparticles Following Oral Administration. *Colloids Surf. B: Biointerfaces.* **2000**, *18* (3-4), 315–323. https://doi.org/10.1016/s0927-7765(99)00157-5.

Chapter II

Copolymerization of Trimethylene Carbonate and 5-Methylene-1,3-Dioxane-2-One: Control of Functionalization in Perfect Random Copolymers *via* Thiol-Ene Reaction

2.1 Introduction

Recently, aliphatic polycarbonates (APCs) are among the most investigated synthetic polymers in a wide range of biomedical applications,[1,2] thanks to their potential in custom designing and synthesizing polymers with tailorable properties that can appropriately match the unique and particular requirements of each application. In turn, alongside new functional monomers, have enabled the preparation of a wide range of APCs with diverse chemical compositions and structures. Moreover, APCs possess the additional advantage of being in some cases accessible from natural and/or renewable sources.[3,4] As a consequence, APCs are receiving growing attention as biodegradable and biocompatible materials. There are several domains of application for APCs, not only for biomedical applications such as drug delivery or tissue engineering **(Figure 2-1)**, but also for other application such as packaging, adhesives, automotive, etc.[5–7] Additionally, APCs are increasing demanded for more versatile degradable biomaterials for biomedical applications due to their degradability, low glass transition temperatures (T_g) and elasticity.[8,9] APCs are degraded in *vivo* mainly by enzymes *via* surface erosion.[1, 5,10,11] In marked contrast, polyesters are degraded both enzymatically and hydrolytically *via* bulk erosion which leads to higher degradation rates compared to APCs. An attractive advantage of APCs over polyesters is that upon degradation, there is no release of acidic residues that may be hazardous to loaded drugs or living cells and tissues.[12,13]

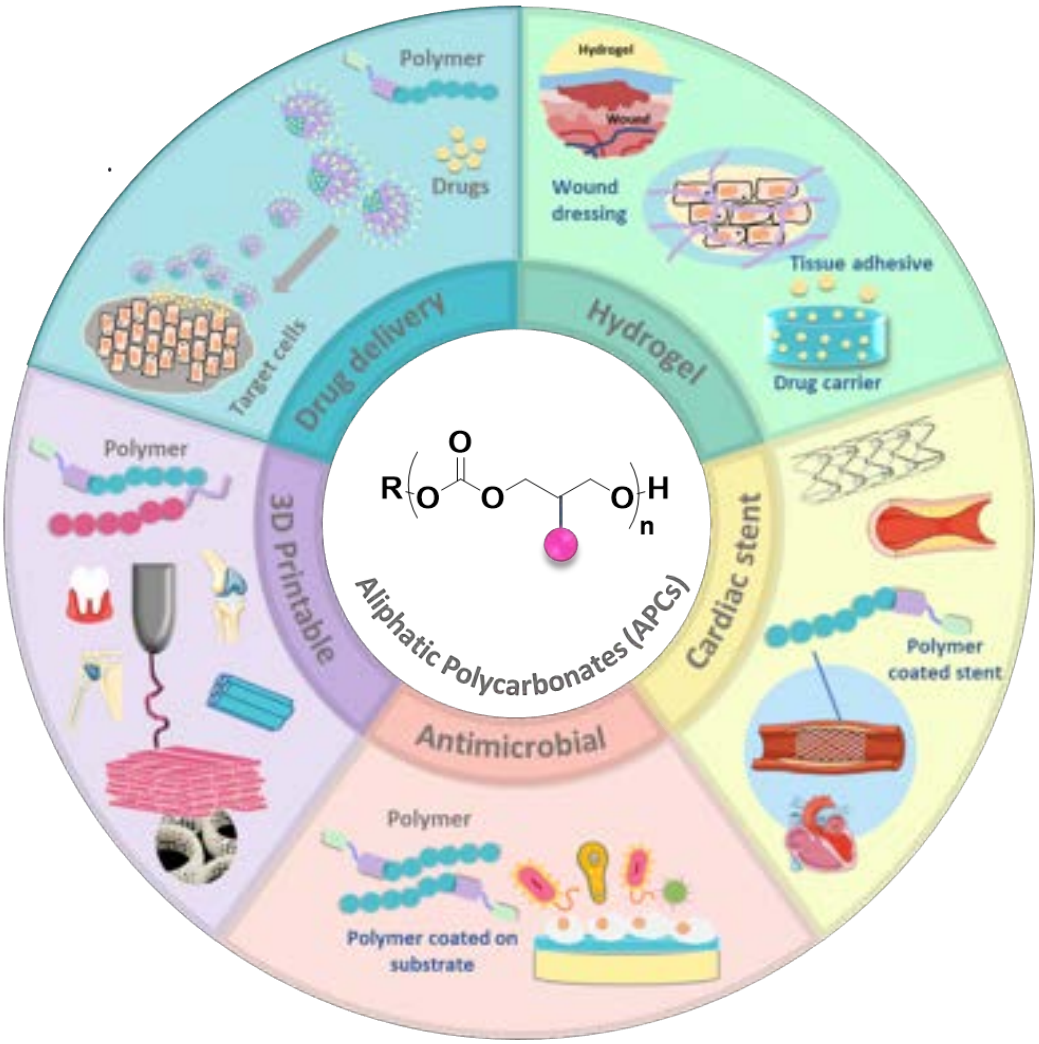

Figure 2-1. Biomedical applications of APCs: Drug delivery[14] Hydrogel dressing for wound healing,[15] 3D Printable,[16] Antimicrobial,[17] and A prototype stent fabricated[18].

As mentioned in the general introduction, APCs are typically prepared by using one of the three major polymerization techniques routes: (I) polycondensation between aliphatic polyol with dialkyl carbonate (**Figure 2-2a**); (II) copolymerization of carbon dioxide with epoxides (**Figure 2-2b**); (III) ring-opening polymerization (ROP) of cyclic carbonate monomers (**Figure 2-2c**).

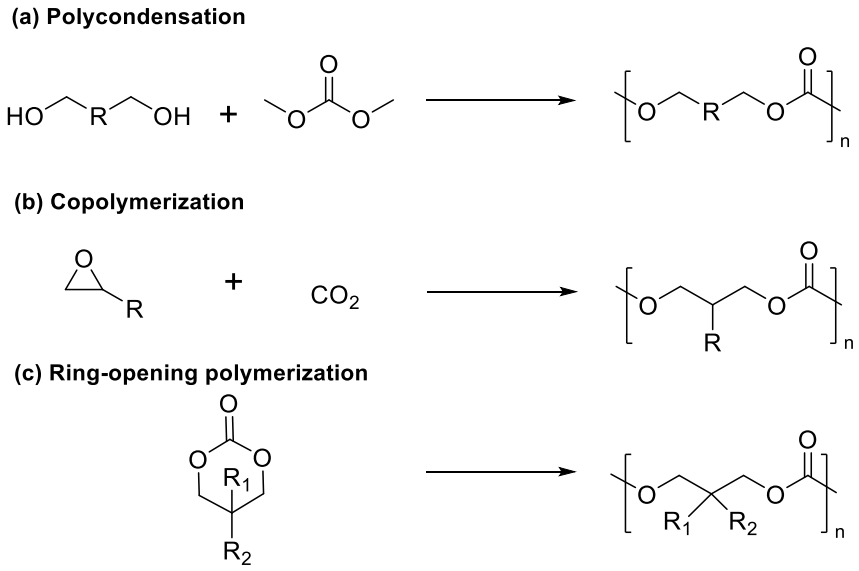

Figure 2-2. Polymerization techniques for the preparation of APCs. (a) polycondensation between polyols with dimethyl carbonate; (b) copolymerization of carbon dioxide with epoxides; (c) ring-opening polymerization of cyclic carbonate monomers.

I. Polycondensation

Polycondensation is performed by using active carbonylation derivatives (phosgene-like compound, carbonates …) with diphenols or diols *via* a step-growth mechanism.[19] The advantage of the polycondensation technique is that it enables straightforward preparation of APCs with different aliphatic linkages between the carbonates by simply using diols of different lengths during the polymerization.[20,21] However, it may involve toxic phosgene-like derivatives and the obtained polymers suffer from poor controls over the molecular weight (M_n) and broad dispersity ($Đ$).[22,23] Polycondensation techniques can also be catalysed by enzyme catalysts.[20,24] Enzymes offer significant advantages over conventional catalysts in the synthesis of functional polymers due to their mild reaction conditions, high tolerance for functional groups, and enhanced selectivity, which allows for control over branching. However, enzyme-catalysed polycondensations typically requires a high catalyst loading and a long reaction time. Additionally, the resulting polycarbonates often exhibit relatively low M_n and broad $Đ$.[20]

II. Alternating copolymerization of carbon dioxide and epoxy compounds

This method to synthesis APCs was firstly discovered by Inoue et al in 1969.[25] There is the advantage of using CO_2 as feedstock regarded as a promising green and

sustainable route to polycarbonates.[25–28] The former strategy is a synthetic challenge as the used catalytic selective systems may suffer from low functional compatibility. There is a wide range of catalysts that have been investigated in this field which contain metals, with Zn(II), Co(III) and Cr(III) being particularly common (**Figure 2-3**).[29–32] The polymerization is initiated by coordination of an epoxide molecule to the metal center and the subsequent ring opening by the nucleophilic attack of a carbonate group or ligand initiator, so as to form a metal alkoxide intermediate. During chain propagation, carbon dioxide inserts into the metal alkoxide intermediate to form a metal carbonate species. The metal coordinates another molecule of epoxide, and nucleophilic attack by the carbonate group leads to the ring opening of the epoxide and formation of a new metal alkoxide species. Propagation therefore involves the 'cycling' between metal alkoxide and carbonate intermediates. The polymerization is terminated by exposure to conditions/reagents that lead to hydrolysis of the metal-O bond of the growing polymer chain and formation of a polymer chain end-capped with a hydroxyl group. There are also side reactions within this process whose impact depend on the conditions, substrate and catalyst selected. The principal side reaction in many cases is the formation of the corresponding five membered-ring cyclic carbonates (5CCs) by depolymerization or 'back-biting' reactions that can be in competition with polymerization.[33,34] Thus, working at high CO_2 pressure (up to 35 bar) is often required for selective polymerization to take place. The equilibrium ratio of copolymer to cyclic carbonate decreases with the increase of the steric hindrance of the substituent on the epoxide.[32] Nevertheless, important progresses have been achieved over the last decade in this regard, as well as in the utilization of bio-resourced epoxides.[35]

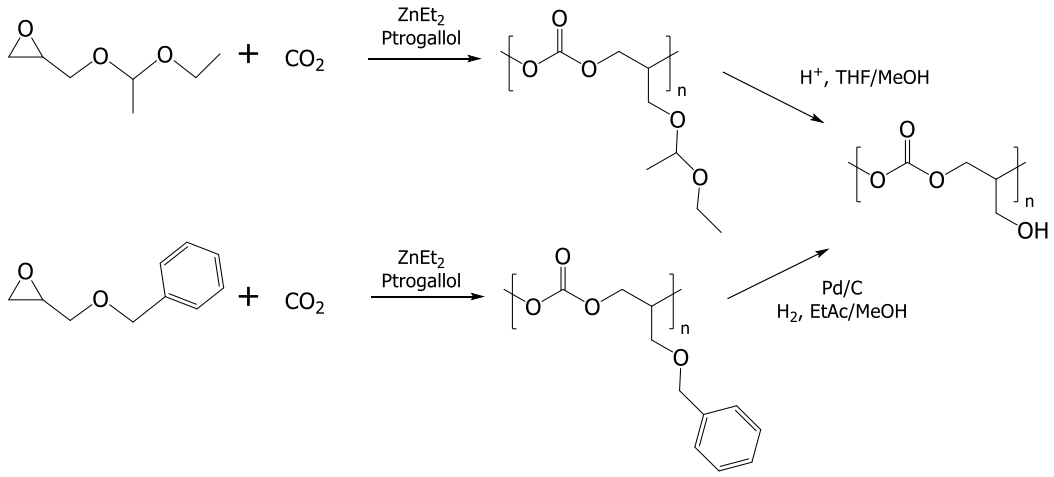

Figure 2-3. Synthetic strategies for the preparation of functional APCs by the copolymerization of CO_2 and epoxides.[36]

III. Ring-opening polymerization (ROP) of cyclic carbonate monomers.

ROP of cyclic carbonates (CCs) to prepare APCs was reported in early 1932 when the monomer trimethylene carbonate (TMC) was discovered.[37] ROP of CCs (mainly six and seven membered rings, 6CCs and 7CCs) has enhanced the most effective method to fabricate APCs with good reproducibility and high quality because ROP offers the possibility to promote living and control polymerization enabling to finely control the M_n, $Đ$ and chain-ends.[19] ROP of 6CCs, has also received great attention in biomedical applications as a consequence of their controlled polymer structure and tunable hydrolytic degradation[38] not only with TMC, but also with a variety of substituted / functionalized 6CCs, which is crucial to obtain materials with properties tailored to the desired application. As a consequence, numerous CCs, mainly 6CCs with a variety of functional groups, have been prepared and polymerized by ROP.[8,9] The functionalities can be introduced *via* post-polymerization modification or by the synthesis of substituted 6CCs when the functional groups are compatible with polymerization conditions.

ROP with a preferred catalyst and/or initiator can be conducted *via* different mechanisms including cationic[38], anionic[39], coordination-insertion[40], and enzymatic activation.[41–43] Catalysts available for ROP of CCs include not only metal-based catalysts, but also alkyl halides, basic and acidic organocatalysts, and enzyme catalysts.[42,43] Due to concerns over the toxic metal residues in polymerization for society and humanity, metal-free organocatalytic ROP have extended scope in order to get access to a wide range of polymer structures. Thus, controlled ROP of these 6CCs under mild conditions has strongly benefited from the major progress done in organocatalytic ROP. A variety of organocatalysts with complementary activation modes are now available to promote the controlled polymerization of CCs[44,45]. Lewis/Brönsted bases such as tertiary amines (4-(dimethylamino)pyridine (DMAP)[46] (**Figure 2-4a**) allowing controlled nucleophilic activation of the monomer and/or basic activation of the initiating/ propagating group were the first organo-catalyst to be shown as a good choice to promote controlled ROP. *N*-heterocyclic carbenes (NHCs)[47], and bicyclic amidines (1,8-diazabicyclo[5.4.0]undec-7-ene DBU)[48], as well as Brönsted acidic catalysts such as diphenyl phosphate (DPP)[49], trifluoromethanesulfonic acid (HOTf)[50], methanesulfonic acid (MSA)[51,52], and triflic acid(TFA)[53], (**Figure 2-4b**) that allow electrophilic activation of the monomer, have been also reported as efficient organocatalysts. Lastly, bifunctional systems such as amine/thiourea combinations[47] and bicyclic guanidine (such as 1,5,7-triazabicyclo[4.4.0]dec-5-ene (TBD))[54] (**Figure 2-4c**), combining a Lewis base and a hydrogen-bond donor allow concomitantly basic activation of the initiating/propagating

group and electrophilic activation of the monomer, have been found significantly higher effective in catalyzing the ROP of cyclic carbonates. Furthermore, Lipases as a class of bio-friendly enzyme catalysts have also been explored for ROP.[55] However, lipases are generally less efficient and have poorer control over polydispersity than organo-catalyst.

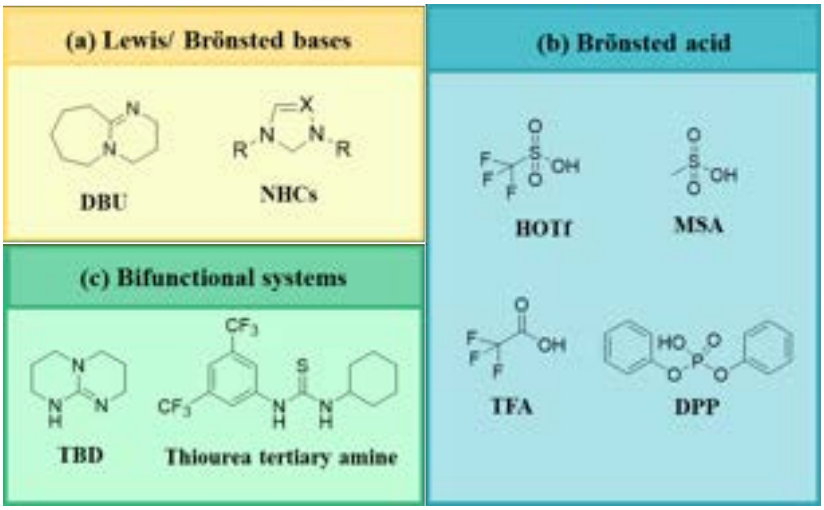

Figure 2-4. Organocatalysts used for ROP of APCs; (a) Lewis/ Brönsted bases; (b) Brönsted acids; (c) Bifunctional systems.

One advantage of TMC is its versatility to introduce various kind of functionalities on the side chain of PTMC to tune its properties for more advanced applications such as tailored drug delivery systems like targeted drug delivery[56], gene delivery[57,58], stimuli-responsive systems[59], polymer-drug conjugates[60], and delivery of immunological moieties[61]. The functionalized PTMC can be prepared by two main approaches: (I) ROP of functionalized 6CCs monomers (Pre-functionalized with a "neutral" or innocent function) and (II) the introduction of the functional groups onto the PTMC backbone (post-polymerization modification) (**Figure 2-5**).

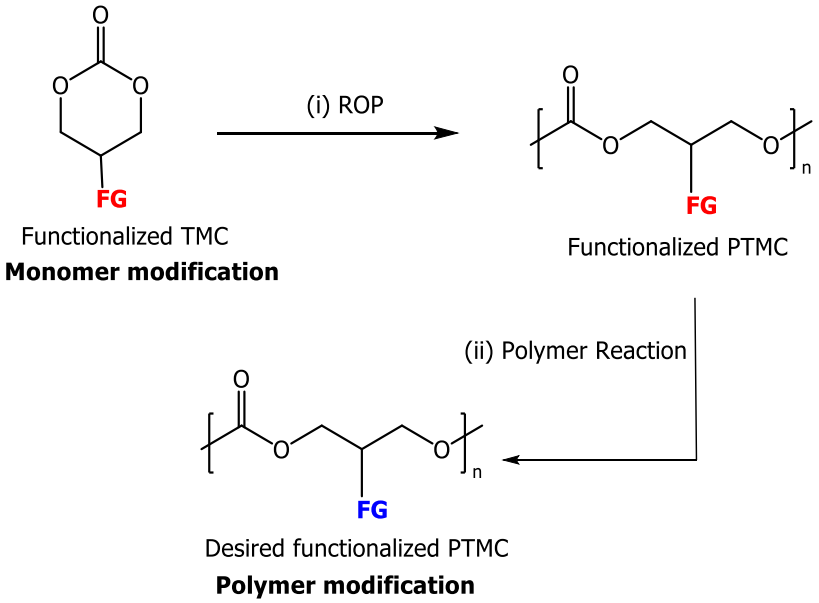

Figure 2-5. The strategies for the preparation of functionalized PTMC.

(I) ***Functionalized TMC monomers (Pre-functionalized)***

They are of prime interest, as far as they can be subjected to ROP process achieving high molecular weights with the desired grafting in a single-step polymerization. In case of protic functions, a protecting group needs to be used. The most common synthetic pathway for functional monomer trimethylene carbonate (TMC) is using the versatile 2,2-bishydroxy(methyl)propionic acid (bis-MPA) as precursor to direct functionalization (**Figure 2-6**).[2,8]

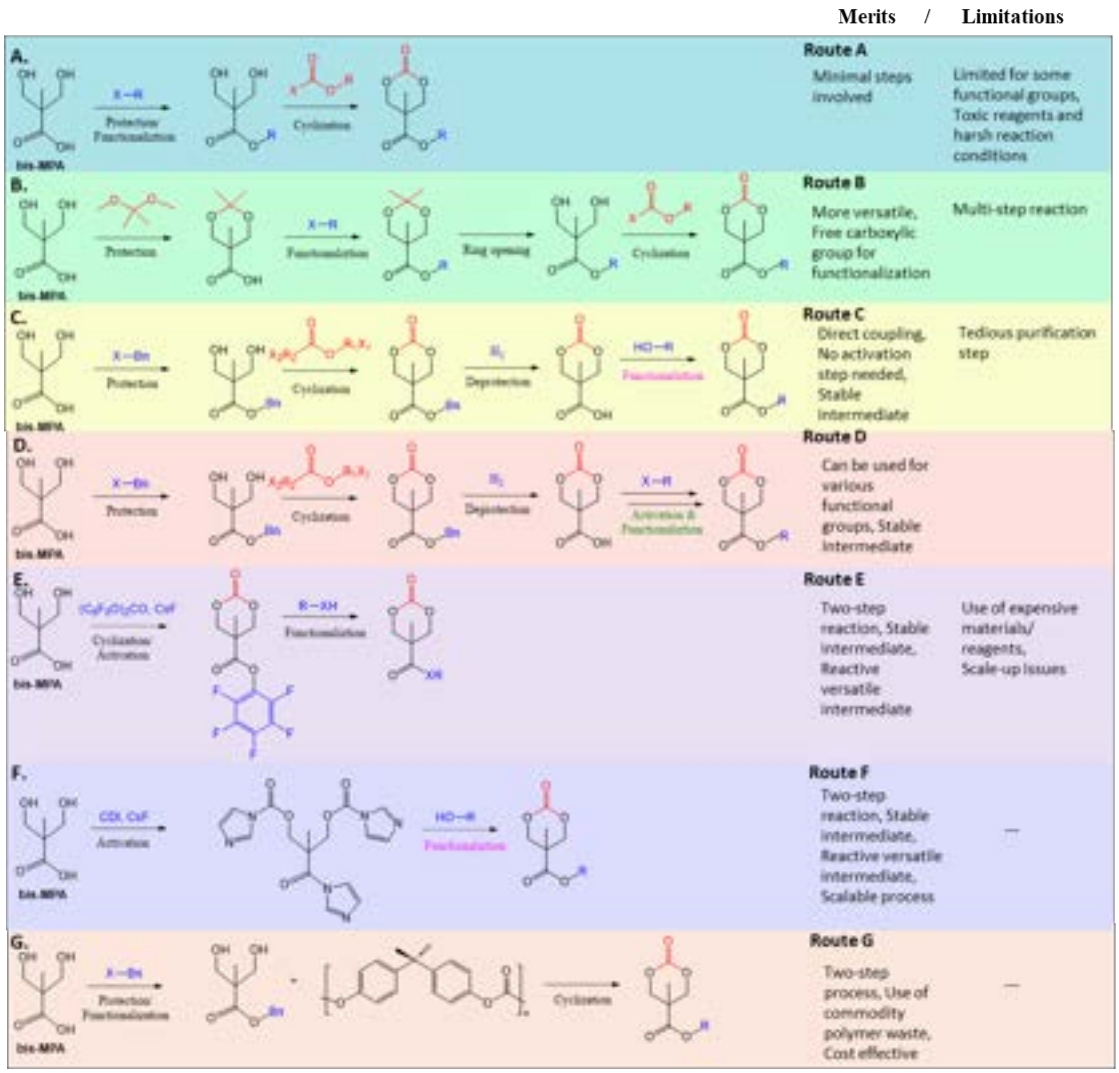

Figure 2-6. Routes for the synthesis of cyclic carbonate monomers from bis-MPA. (A) Route A (two-step method), (B) Route B (acetonide protection-deprotection method); (C) Route C (direct coupling method using DCC), (D) Route D (direct coupling method using acyl chloride), (E) Route E (pentafluorophenyl ester intermediate method), (F) Route F (reactive imidazole intermediate method), (G) Route G (BPA-PC; bisphenol A-based polycarbonate method).[2]

Recently, ester-based TMC have been focused for functionalized TMC monomer due to the simplicity of the synthetic route.[62] Functionalities such as as allyl,[62] alkyl,[63] acryl,[53] alkene,[64] alkyne,[65,66] halogen,[65,66] amino,[65] azide,[67] and urea[68] moieties have been incorporated into the side chain of the TMC monomer through ester linkages (**Figure 2-7**). However, concerns on acidic residues which might be generated due to by–product could possibly occur in the body after degradation. Alternative route to

functionalization of ester-free TMC derivatives is seeking to replace either ester-based PTMC or polyesters.

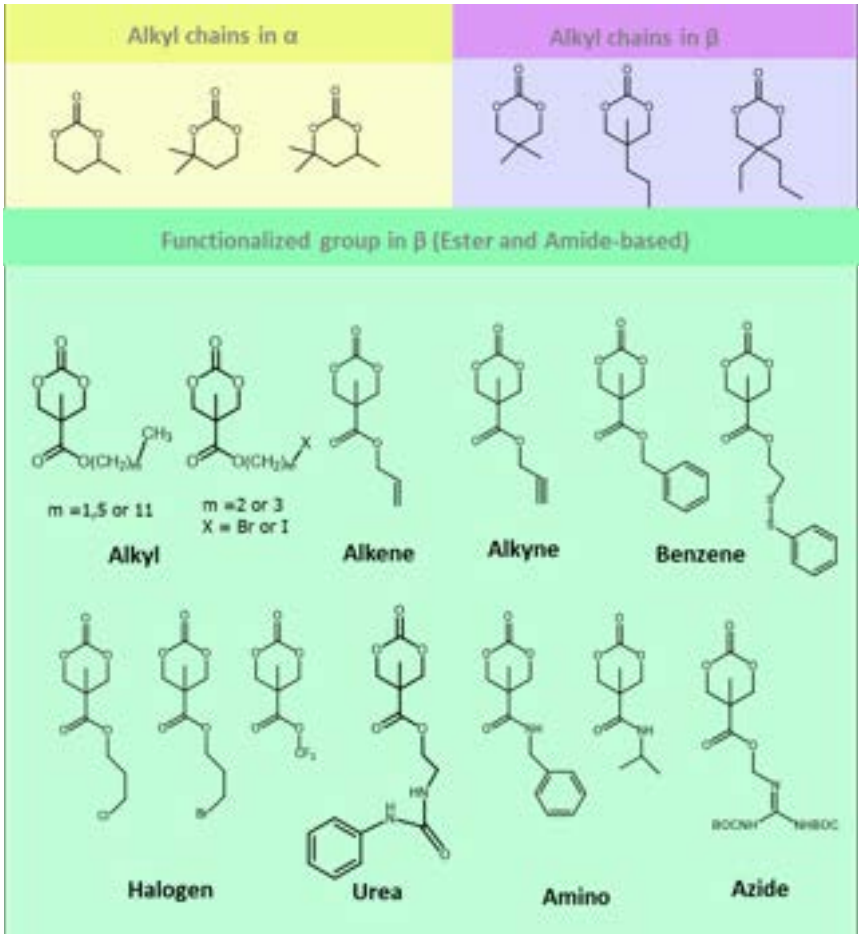

Figure 2-7. Chemical structures of functional 6 ring cyclic carbonate monomers (ester and amide-based).

Thus, the functionalization of ester-free TMC have gained potentials for fabrication diverse PTMC derivatives as we believe the ether linkage is promising to be generation no acidic compounds after decomposition.[69] The most common synthetic route for ester-free TMC derivatives involves introducing a substituent in the side chain in the form of an ether bond using an aldehyde or ketone as a starting substance. This has made it possible to introduce a substituent derived from a secondary alcohol into the side chain. There are several potential functional groups enable to introduce into PTMC *via* ether-linkage. Ajiro and coworkers have reported that ester-free base PTMC derivatives bearing oligoethylene glycol (OEG) in the side chain showed thermosensitive at body temperature (**Figure 2-8**).[70] In order to improve thermal property, various substituent functional groups were introduced (**Figure 2-9**)

such as aromatic groups,[71] cycloalkyl groups,[72] triphenylmethyl group,[73] and vinyl-aromatic (**Figure 2-10**), [74] coumarin.[75] To enhance mechanical properties, Tan et al. synthesized vinyl-aromatic as a pendant reactive functional groups in CCs were incorporated with vinyl benzyl and the cross-linker.[74] In order to achieve the antibacterial biomaterials applications, PTMC derivatives containing cinnamyl group has been synthesized.[17] Nobuoka et al. reported that a block copolymer composed of TMC and TMC derivatives with OEG was used to study cilostazol drug eluting by adjusting composition ratio of the block polymer.[76] Chanthaset et al. prepared a series of particles and thin films of poly(trimethylene carbonate) (PTMC) bearing diphenyl-, bis-phenyl, and trityl pendants *via* using hydrophilic initiators.[77]

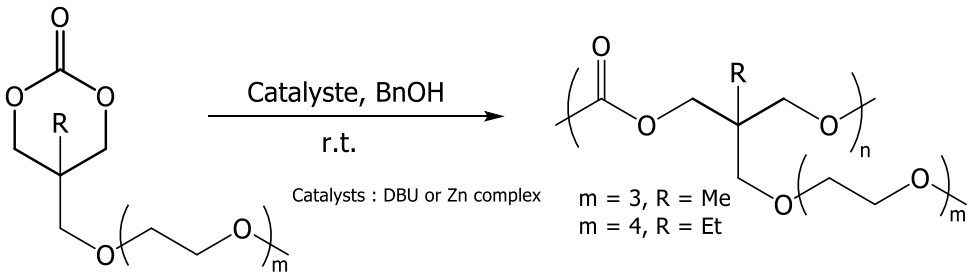

Figure 2-8. Synthesis of poly(TMCR-MOEmOM).[70]

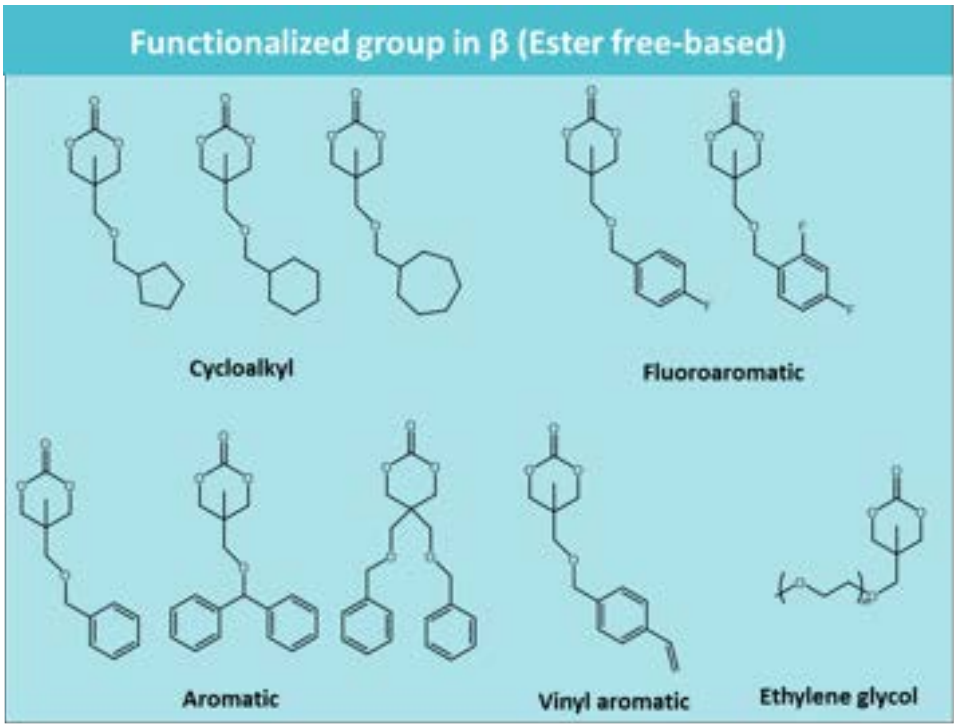

Figure 2-9. Chemical structures of functional 6 ring cyclic carbonate monomers (ester free-based).

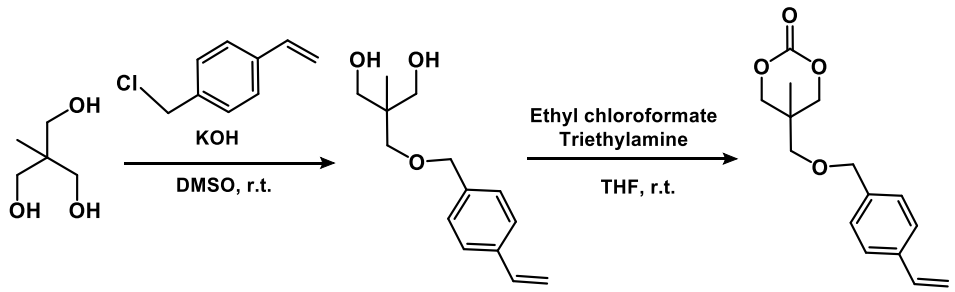

Figure 2-10. Synthesis of functionalized TMC with vinyl-aromatic as a pendant reactive functional group. [74]

However, the synthetic routes for functionalizing TMC derivatives, both ester-based and ester-free, require multi-step of synthesis (at least 3 steps), and some reactions need to utilize toxic reagents.[2,8,72] Besides, it is important to note that when the required functional group is protic, chemical compatibility issues appear either by quenching the organocatalyst or acting as initiator, which is compatible with the ROP such as the pendant functional group that contains amines, carboxylic acids and alcohols. This functional incompatibility imposes the utilization of protecting groups, which adds protection and deprotection steps to the synthetic process or requires relatively expensive/toxic reagents.[64] As referring to the literature of potential modifications, arylbenzyl-functional polymers might need deprotection by hydrogenolysis (**Figure 2-11**) to yield alcohol and carboxylic acid functionalities, which was incompatible in a ROP process (which may then be further modified themselves, e.g., by esterification) (**Figure 2-11**),[61,78–81] Recently, the introduction of pendant unsaturated groups in PTMC prepared by the ring-opening of TMC monomers has drawn many attentions because it could ease the introduction of functional groups to PTMC side chain (**Figure 2-12**). This approach could apply either before or after polymerization through a thiol-ene reaction to eliminate the requirement of protection and deprotection reactions.[82]

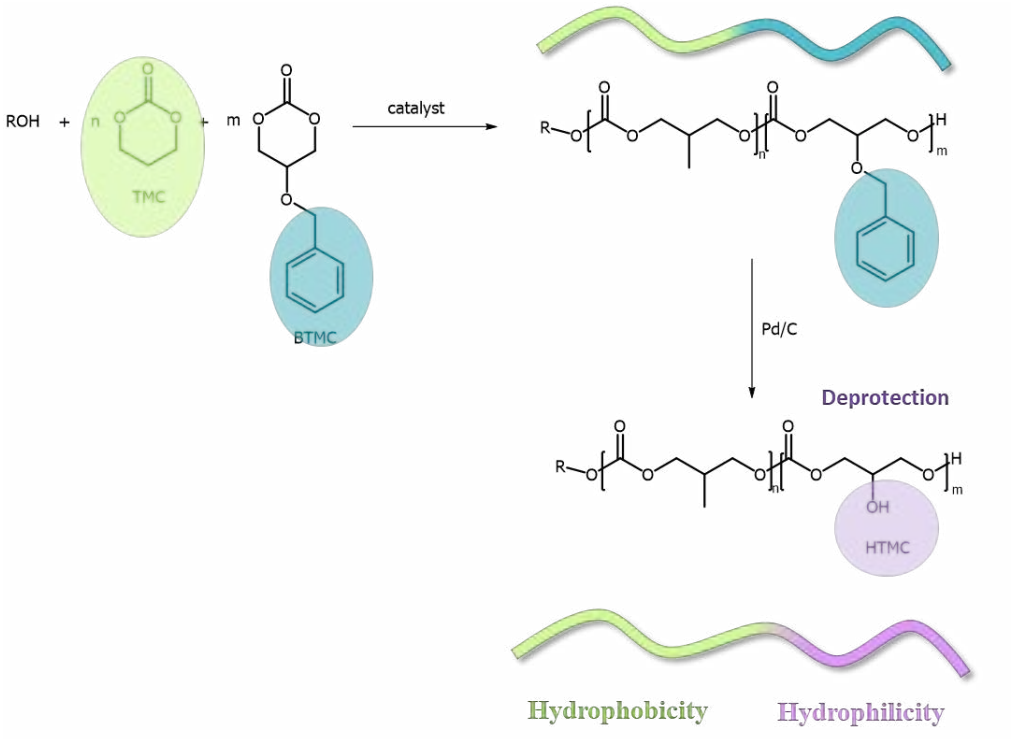

Figure 2-11. Synthesis route to P(TMC−HTMC) by first polymerizing BTMC with TMC followed by debenzylation.[81]

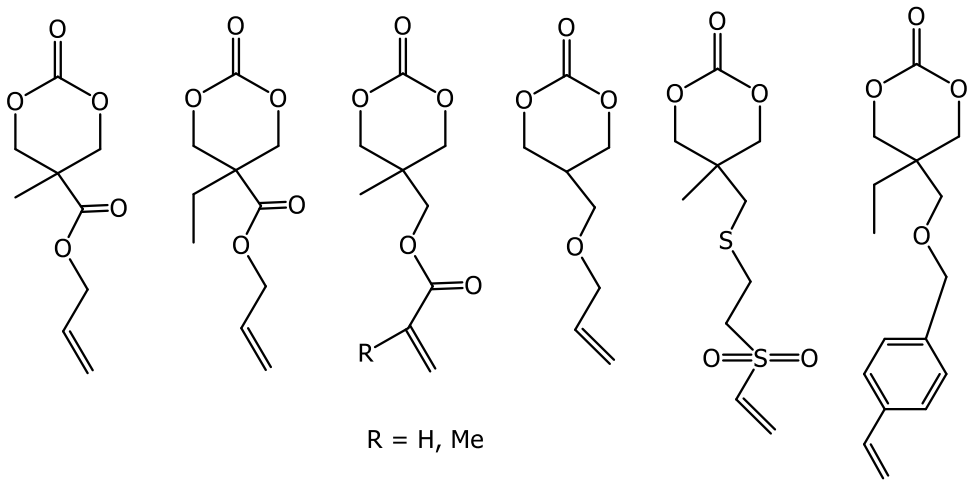

Figure 2-12. Cyclic carbonates bearing pendent alkene-terminated functionality.

(II) ***The introduction of the functional groups onto the PTMC backbone (Post-polymerization modification Functionalization)***

TMC bearing reactive functionalities such as aryl, allyl, halide, and azide moieties provide a route for post-polymerization modification of PTMC.[67,78,79,83] While the number of pendent functionalities compatible with ROP is not limited to the functionalities listed above post-polymerization modification of PTMC bearing such these simple functionalities could also be employed to modify its characteristic with wider range of functional groups.[78,79] For example, pendent halide functionalities may undergo reaction with nucleophiles,[83–86] **(Figure 2-13)** alkene groups could be modified to provide a wide range of additional functionalities through Michael addition or radical thiol-ene coupling reactions**(Figure 2-14)**,[87–89] and alkyne and azidefunctional polymers may be modified through copper or strain-promoted azide-alkyne click chemistry **(Figure 2-15)**.[67,90,91] Incorporation of multiple functionalities or sequential modification can be used to produce materials bearing multiple functionalities that would normally be incompatible with ROP (**Figure 2-16 and Figure 2-17**).[92–96]

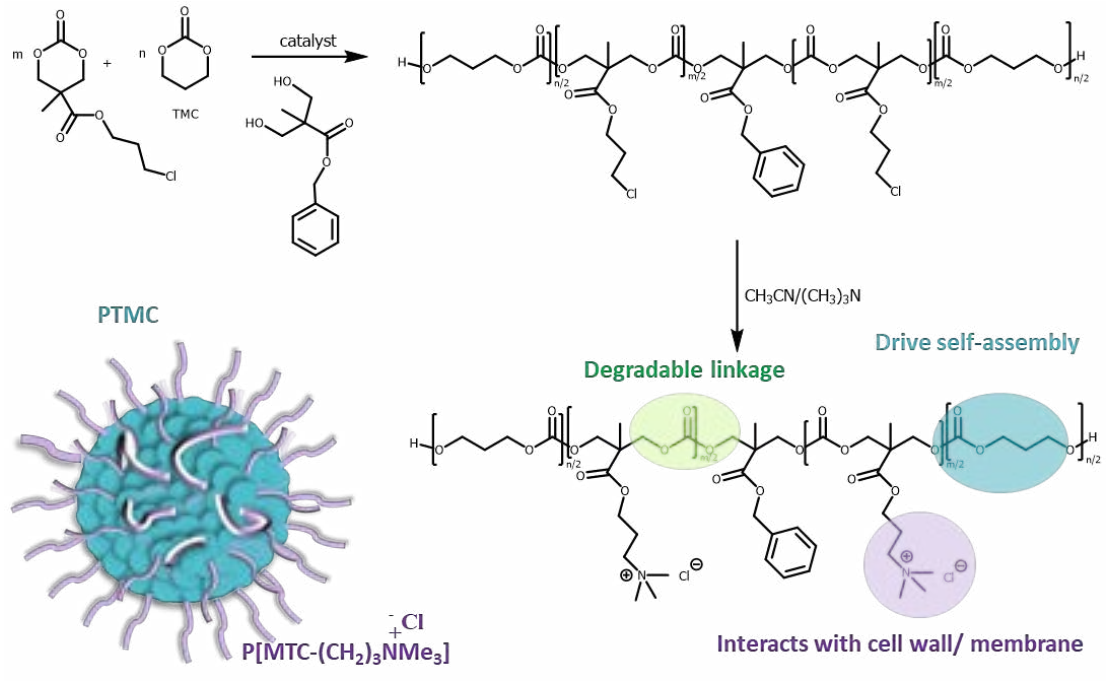

Figure 2-13. Synthesis and micelle formation of cationic amphiphilic polycarbonates.[84]

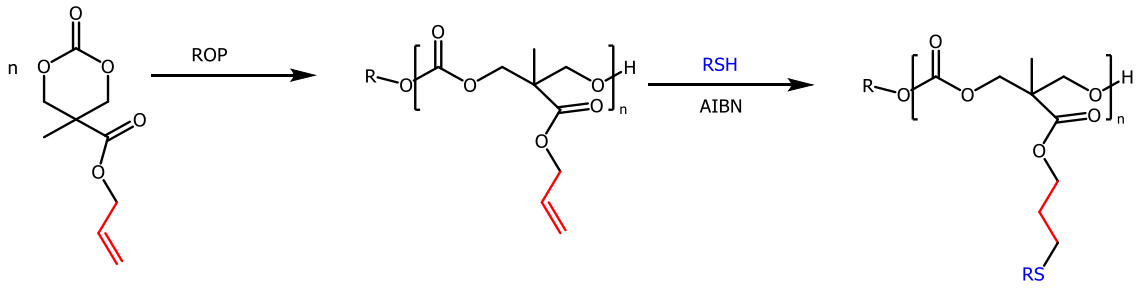

Figure 2-14. Radical Addition of a Thiol (RSH) to the PMAC.[62]

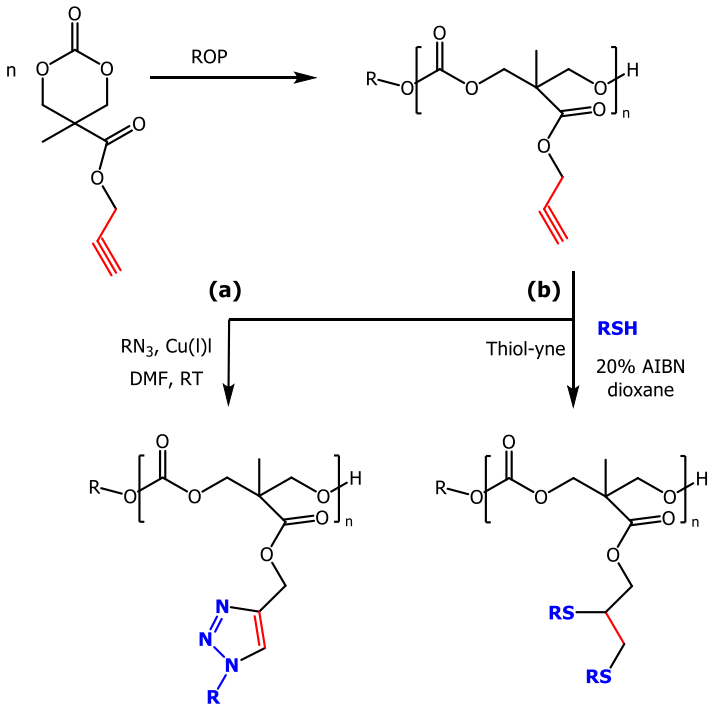

Figure 2-15. (a) Huisgen cycloaddition of azides (N_3R) to PMPC homopolymers; (b) radical addition of thiols (RSH) to PMPC homopolymers.[91]

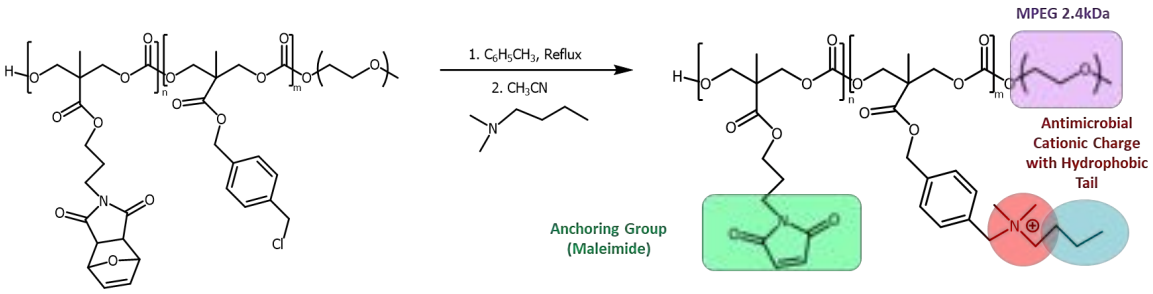

Figure 2-16. Synthesis of triblock copolymers of PEG, cationic, and maleimide-functionalized polycarbonates.[92]

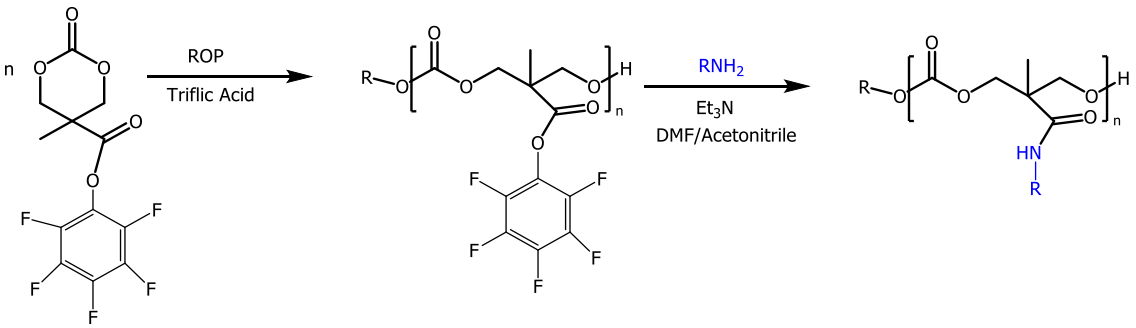

Figure 2-17. Synthesis of poly(*N*-(2-hydroxypropyl)methacrylamide).[95]

One of the most versatile groups for post-polymerization modification of PTMC is the vinyl group because functionalization can be carried out after polymerization, typically by thiol-ene reaction without resorting to protecting groups.[62,74,97,98] Thiol-ene reaction has high potential in many applications, especially for materials and biomedical sciences, due to its outstanding features as a "click-type" reaction, e.g., full atom economy reaction, tolerant of various solvents and functional groups, and generally free of side-products from the reactions.[99,100] In particular, there are two different pathways to carry out the thiol-ene addition: (I) base/nucleophilic-catalyzed Michael addition and (II) free-radical addition.[99,100]

(I) Base/nucleophilic-catalyzed Michael addition.

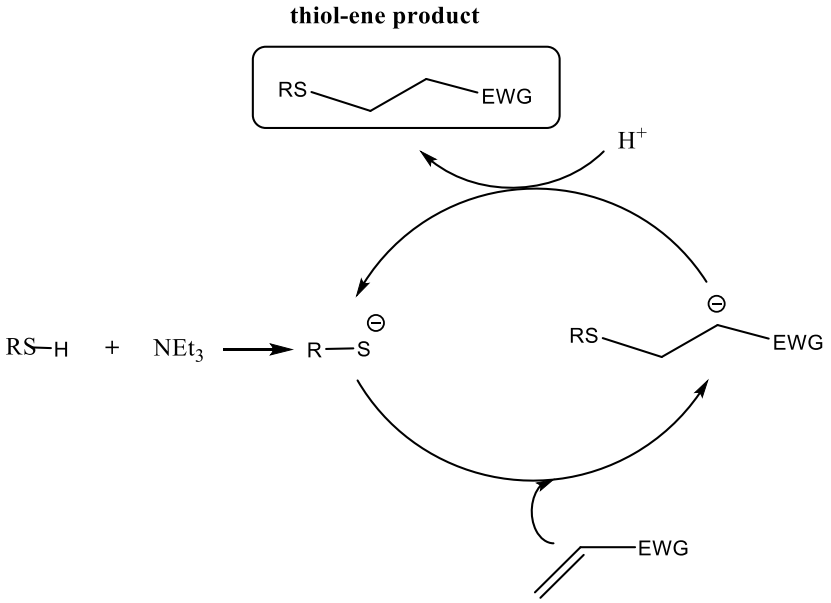

Figure 2-18. Base-catalyzed mechanism for the hydrothiolation of an activated C=C bond, EWG = ester, amide, or cyano.[99,101]

Michael addition reactions can be used to confer additional functionality to alkene-functional polycarbonates by addition of mercaptans to the alkene moiety activated by an EWG. Base-catalyzed Michael thiol-ene addition principally requires a catalytic amount of a base, e.g., an amine, to facilitate the specific coupling reaction of an electron-deficient alkene with a thiol (**Figure 2-18**).[99,101] Chen et al. have demonstrated that a wide range of different functionalities can be introduced on polycarbonates bearing pendent acryloyl groups. Copolymers of acryloyl or methacryloyl carbonate (AC) with ε-CL or *L*-LA prepared by ring-opening polymerization. P(CL-*co*-AC) and P(LA-*co*-AC) were then modified with a wide range of thiol-containing compounds, including 2-mercaptoethanol, 2-mercaptoethylamine hydrochloride, 3-mercaptopropanoic acid, *l*-cysteine, and arginine-glycine-aspartic acid-cysteine (RGDC) peptide (**Figure 2-19**). By using pyridine as catalyst to activate the thiol functionality, and a ten-molar excess of thiol relative to AC groups, the copolymers were successfully endowed with functionalities including hydroxyl, amino, carboxyl, amino acid, and peptide groups.[89] Another example, Li et al. have utilized the Michael addition of thiol-containing compounds to prepare biodegradable polymer with ionizable membranes for pH-responsive drug delivery applications. Diblock copolymers of mPEG-*b*-P(TMC-*co*-AC) were functionalized with carboxylic acid and amine functionality through Michael addition of 3-mercaptopropionic acid and cysteamine hydrochloride, respectively **(Figure 2-20)**.[102]

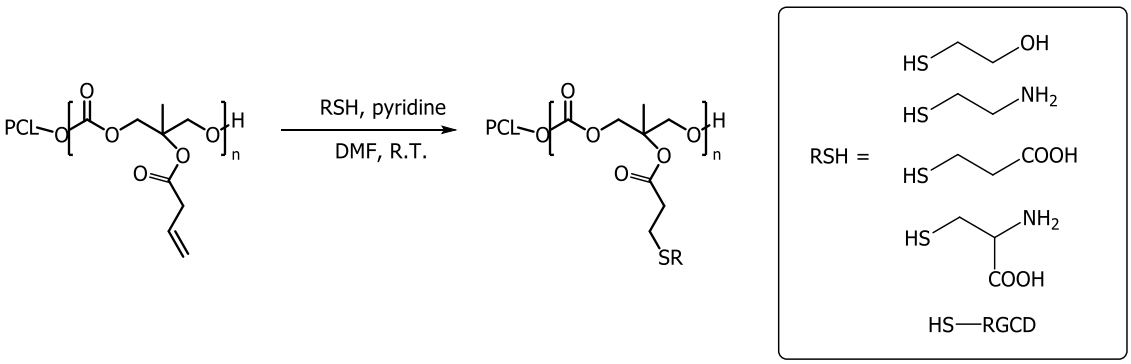

Figure 2-19. Base-catalysed Functionalization of P(CL-*co*-AC) with mercaptans *via* Michael-type addition.[89]

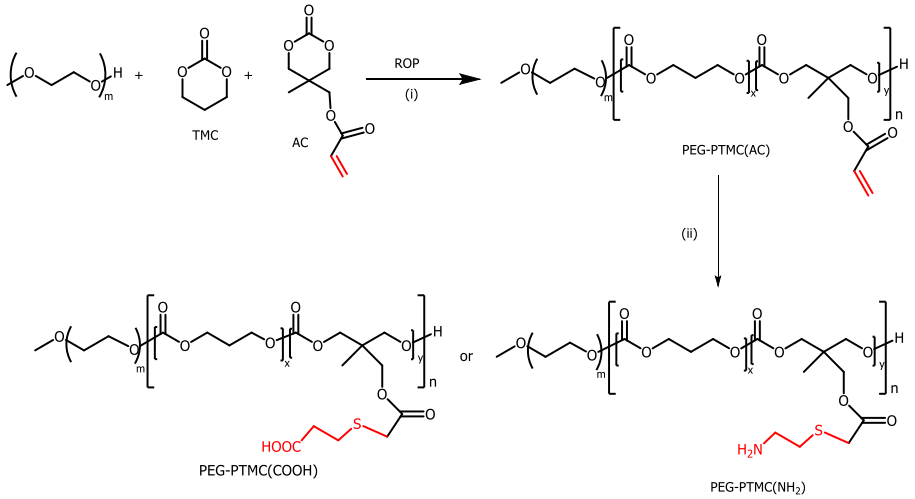

Figure 2-20. Synthesis of PEG–PTMC(AC), PEG–PTMC(COOH), and PEG–PTMC(NH_2) copolymers. Conditions: (i) CH_2Cl_2, zinc bis[bis(trimethylsilyl)amide], 40 °C, 24 h; (ii) 3-mercaptopropionic acid or cysteamine hydrochloride, DMF, r.t., 48 h.[102]

(II) Radical Thiol-Ene Addition

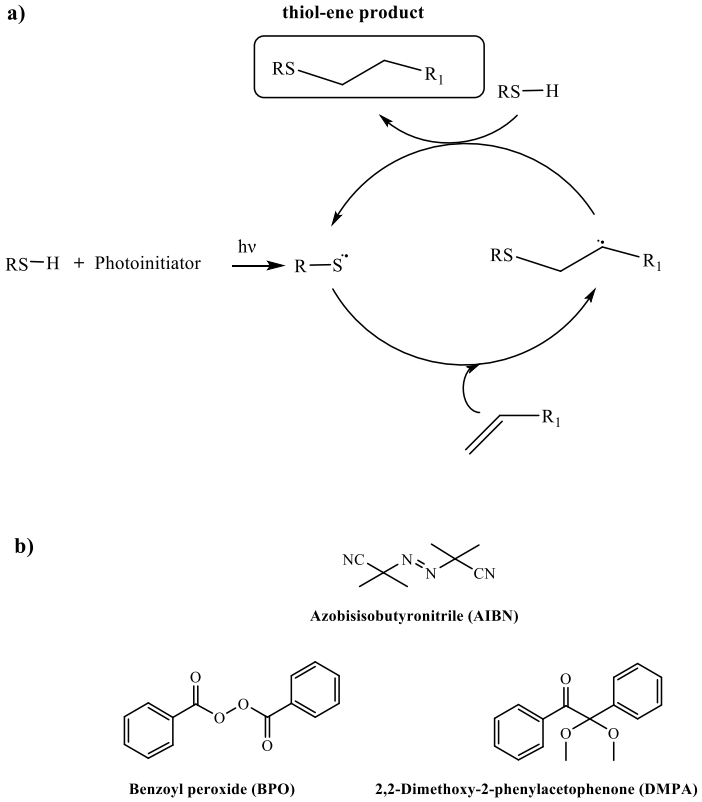

Figure 2-21. a)Free radical hydrothiolation of a C=C bond in the presence of a photoinitiator.[99] and b) Selected radical initiators such as AIBN (thermal), BPO (photo), and DMPA (photo).[102]

The most popular method of modifying alkene-functional polycarbonates is by the conjugation of thiol-bearing compounds to the polymer through thermally or photochemically initiated radical thiol-ene addition reactions. Radical thio-ene reaction is typically encountered with electron rich alkenes **(Figure 2-21a)**. Using this method, a wide range of different chemical functionalities have been conferred onto alkene-functional polymers. For instance, thermally initiated radical thiolene chemistry has been utilized by Tempelaar et al. to attach several different thiols to a polycarbonate backbone. Using poly(5-methyl-5-allyloxycarbonyl-1,3-dioxan-2-one) (PMAC) as the alkene-functional polycarbonate platform, azobis(isobutyronitrile) as a radical initiator and two equivalents of thiol per alkene group to avoid unwanted crosslinking, 1-dodecanethiol, benzyl mercaptan, 1-thioglycerol, mercaptoethanol, and mercaptoacetic acid (**Figure 2-21b**).were all successfully attached to the polymer backbone with near quantitative conversion of the allyl groups (**Figure 2-22**).[62] Tan et al. have reported that an aromatic PTMC derivative bearing a vinyl moiety (PTMCM-VB) can be used as precursor for further post-polymerization modification with urea group through facile photoinitiated radical thiol-ene addition to obtain PTMCM-SU, using ten equivalents of 1-(2-mercaptoethyl)urea (SU) per allyl group and DMPA as a photoinitiator (**Figure 2-23**).[74]

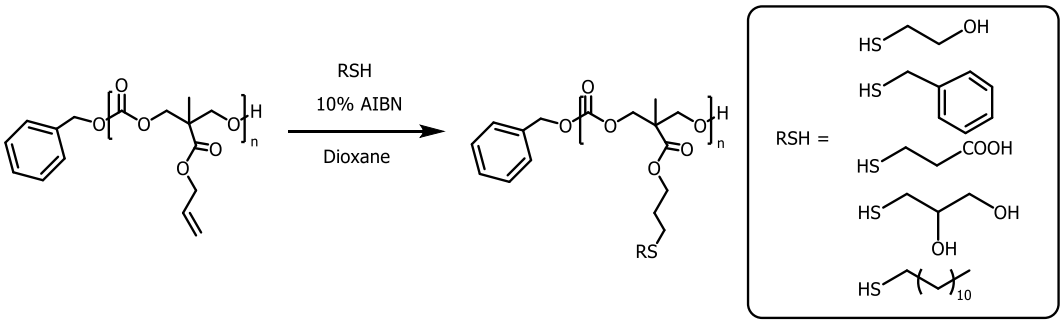

Figure 2-22. Post-polymerization modification of PMAC with mercaptans *via* radical thiol-ene addition.[62]

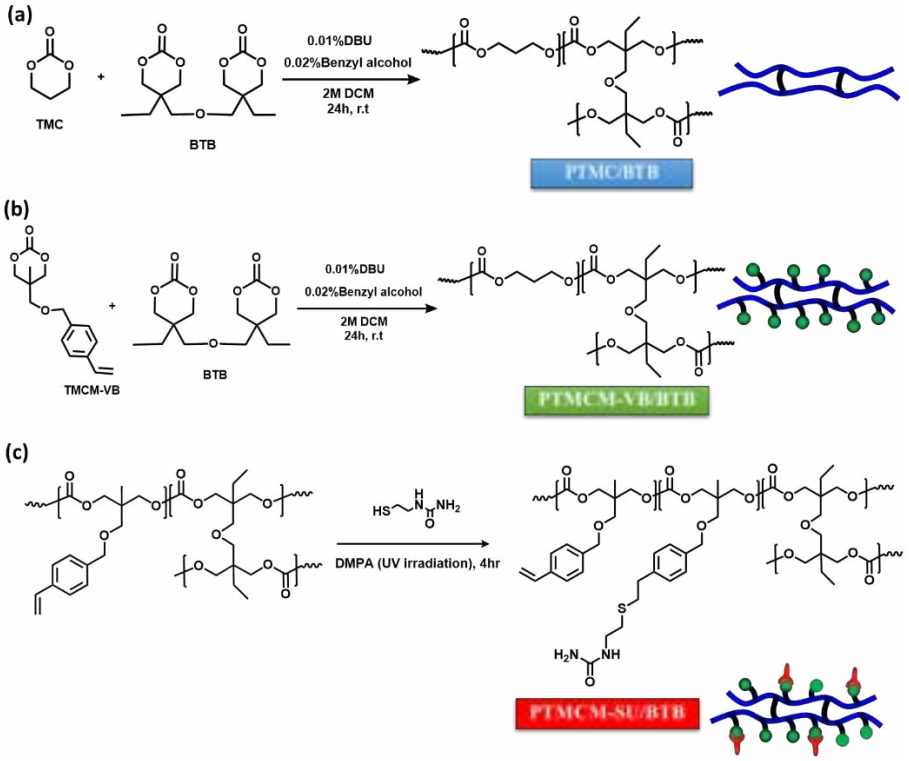

Figure 2-23. Synthesis of TMCM-VB monomer (a), preparation of PTMCM-VB/20%BTB and TMCM-VB/50%BTB films (b), and proposed post-polymerization modification pathway for attachment urea group into PTMCM-VB/20%BTB and PTMCM-VB/50%BTB (c).[74]

Typically, there are two major approaches for applying the thiol-ene chemistry to the synthesis of functionalized PTMC. The first strategy is post-polymerization modification with a thiol bearing functional groups as side groups/chains to the preformed polymer. The other way is to use the monomers bearing thiol pendant groups that are functionalized by thiol-ene reaction prior to polymerizations. As mentioned before, the pendant functional group which contained amine, carboxylic acids and alcohols appeared the chemical compatibility issues for ROP. Therefore, pre-polymerization modification, the thiols bearing the desired functional group, in protected form is required. Nevertheless, this opens the possibility to simply introducing multiple functionalities onto polymers bearing pendent allkene functionality.[103]

As for the microstructure of the functionalized APCs, the distribution of the functional groups along the copolymer chains is generally gradient-type. Indeed, functionalized TMC and TMC usually display different reactivities in organocatalytic ROP and the balance between the two comonomers depends on the organocatalyst. The functionalized TMC are typically more reactive than TMC when organocatalysts

such as TBD or the association DBU/1-(3,5-bis(trifluoromethyl)phenyl)-3-cyclohexyl-2-thiourea (TU) are used to promote the copolymerization.[62] On the contrary, they are less reactive when Brönsted acids such as MSA are used.[103] As a consequence, simultaneous copolymerization leads to the formation of gradient copolymers, with a higher concentration of functional groups on one side of the polymer chain. The achievement of random copolymerization of functionalized TMC with TMC is therefore a challenge so that APCs featuring adjustable amounts of functional groups regularly distributed along the polymer chains can be prepared.

Functional carbonates have been copolymerized with nonfunctional cyclic esters and TMC as a method of incorporating functionality and conferring favorable mechanical properties on materials. Carbonates bearing nonreactive pendant groups such as methyl groups or alkyl chains are generally employed to tailor mechanical properties and degradation rates or are copolymerized with carbonates bearing reactive functionalities in order to tailor the percentage of reactive groups present in a material.[104,105]

In this chapter, aiming at developing a way to prepare functionalized polycarbonates of tuned structure (functional compatibility with the organocatalyst and random copolymerization with TMC) with the idea of nontoxic chemicals usage, simple reaction, and high productivity (**Figure 2-24**).

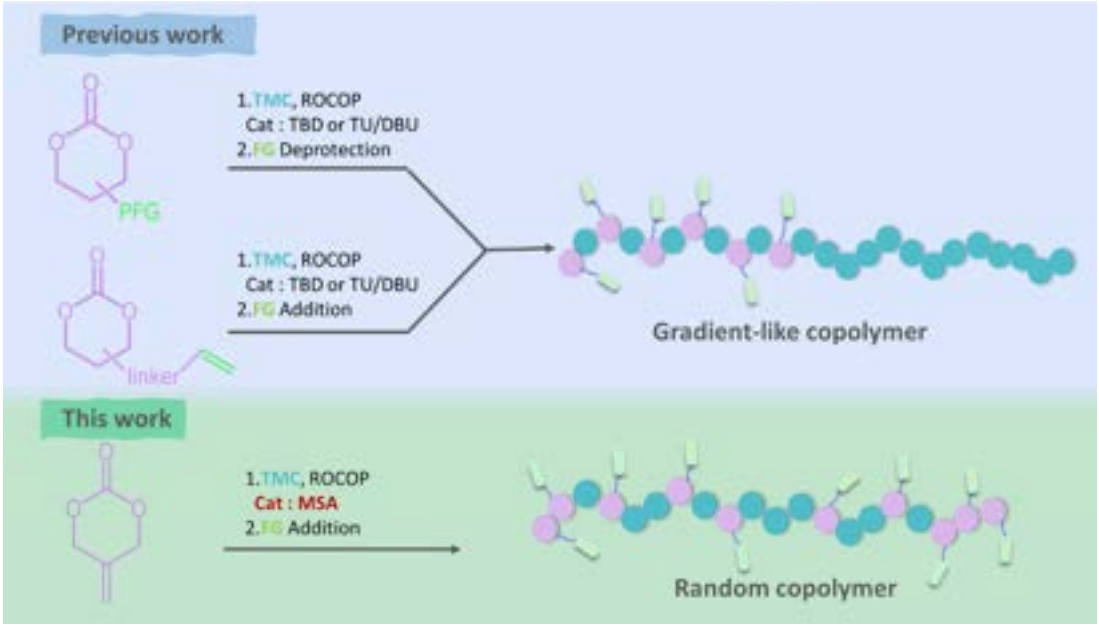

Figure 2-24. Different strategies for the preparation of functionalized aliphatic polycarbonates (FG = functional group, PFG = protected functional group, ROCOP = ring-opening copolymerization).

Thus, 5-methylene-1,3-dioxane-2-one (exTMC), a 6CC featuring the reactive methylene group embedded in the ring skeleton as an exocyclic C=CH_2 moiety was proposed as comonomer. exTMC could be potentially enough to apply with functionalized PTMC either before or after polymerization through a thiol-ene reaction, and this strategy could be extended to the terpolymerization of PTMC with multiple functional groups. Besides opening the way for post-polymerization modification functionalization, it differs from the other comonomers in the presence of a sp^2-hybridized carbon within the ring that may induce a different polymerization profile. The ROP of exTMC was briefly investigated in the 1990's by T. Endo et al using strong Lewis or Brönsted acids as polymerization promotors[106,107], but the polymerization exhibited low control and to the best of our knowledge, and there has been no other report on exTMC (co)polymerization since then. In addition, Delcroix et al. reported that methanesulfonic acid was found to be a better organocatalyst than trifluoromethanesulfonic acid for the ROP of TMC.[108] The results shown the good control of molar mass and end-group fidelity.

In this chapter, a comonomer of TMC, exTMC or functionalized exTMC (5-(((3-(benzyloxy)propyl)thio)methyl)-1,3-dioxan-2-one (TOBnTMC)) were chosen to access random copolymers by the investigation of the appropriate organocatalyst and a protic initiator to control the reactivity ratios in copolymerization reactions, leading to copolymers with high randomness ($R \approx 1$) and well-controlled structures. The synthetic pathway of the functionalized TMC and TMC copolymer could be differentiated in two path: (I) ROCOP of TMC and exTMC followed by functionalization of copolymer *via* thio-ene reaction. (II) Functionalization of exTMC *via* thio-ene reaction followed by ROCOP with TMC. These routes could give access to APCs with adjustable amounts of functional groups uniformly distributed along the polymer chains without requiring protection and deprotection step. This work was conducted at UPS, Toulouse, France, as part of a double degree program collaboration (**Figure 2-25**) and have resulted in a publication in Palenzuela, M.; Sarisuta, K.; Navarro, M.; Kumamoto, N.; Chanthaset, N.; Monot, J.; Ajiro, H.; Martín-Vaca, B.; Bourissou, D. 5-Methylene-1,3-Dioxane-2-One: A First-Choice Comonomer for Trimethylene Carbonate. *Macromolecules* **2023**, 56 (2).

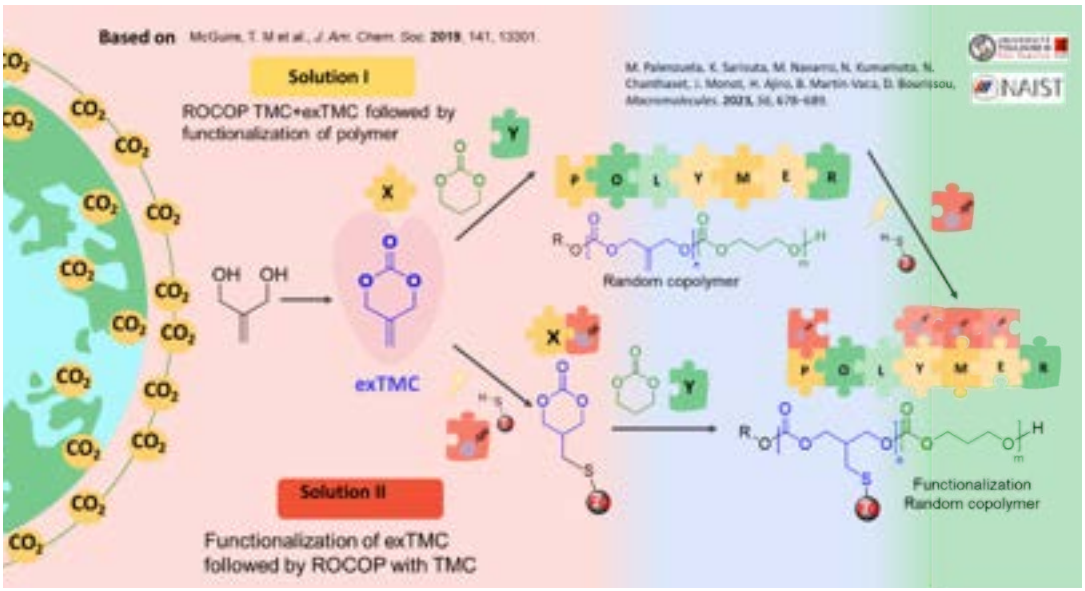

Figure 2-25. Different strategies for the preparation of functionalized aliphatic copolymer of TMC and TOBnTMC.

2.2 Results and Discussions

2.2.1 Preparation functionalized 6CCs

2.2.1.1 Preparation of exTMC

The most direct method to prepare exTMC reported so far consists in reacting 2-methylidene-1,3-propanediol **1** (derived from renewable glycerol)[109,110] with triphosgene in the presence of triethyl amine (24%—80% yield) (**Figure 2-26**). [110–112] However, seeking for a more sustainable procedure avoiding the use of phosgene derivatives, it was decided to test the CO_2-based methodology recently introduced by A. Buchard et al.[113–116] Gratifyingly, **1** (2-Methylene-1,3-propanediol (25 g, 284 mmol)) and tosyl chloride (TsCl) (54.1g, 284 mmol, 1 equiv.) was charged in a 5 L reactor followed by anhydrous acetonitrile (1.5 L). The atmosphere of the flask is exchanged for CO_2 and the solution saturated with CO_2 by bubbling 91 atm). Under a continuous feed of gas, 2,2,6,6-tetramethylpiperidine (TMP) (96 mL, 568 mmol, 2 equiv.) was added dropwise at 0 °C and the reaction is left to reach room temperature with stirring. After approximately 20 minutes, a bright white precipitate forms and CO_2 stopped being fed to the reactor. After overnight, the liquid phase was separated by centrifugation (5 minutes at 5000 rpm). The solid was then extracted with acetone and separated again by centrifugation (5 minutes at 5000 rpm). The combined solvent phases were then removed in vacuo. Tosyl salts were precipitated by adding ethyl acetate (3 mL per g) to the crude. The filtrate was then placed at -30°C to further eliminate traces of tosyl salts. After filtration, exTMC was purified twice by crystallization in DCM/Et_2O (1:20) at -80°C affording 18 g (yield ~56 %) of exTMC (up to about 300 mmol scale) (**Figure 2-26a**). The structure was confirmed by ^1H NMR with the characteristic signals of (-CH_2-) at 4.86 and (=CH_2) at 5.36 ppm (**Figure 2-27**).

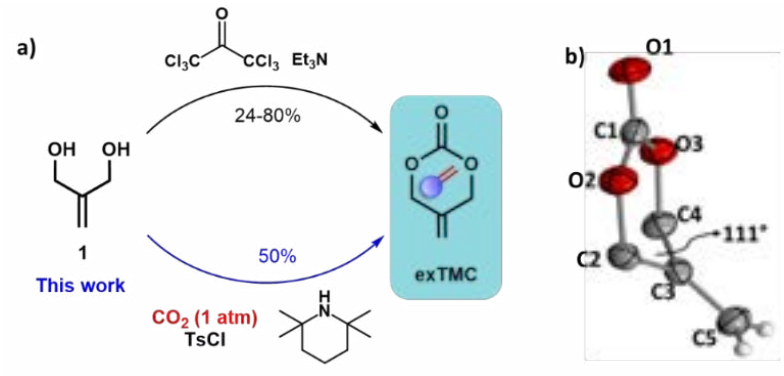

Figure 2-26. a) Preparation of exTMC according to two different routes. b) Molecular structure of exTMC (H-atoms, except the one at the exocyclic C=CH_2 moiety are omitted for clarity).

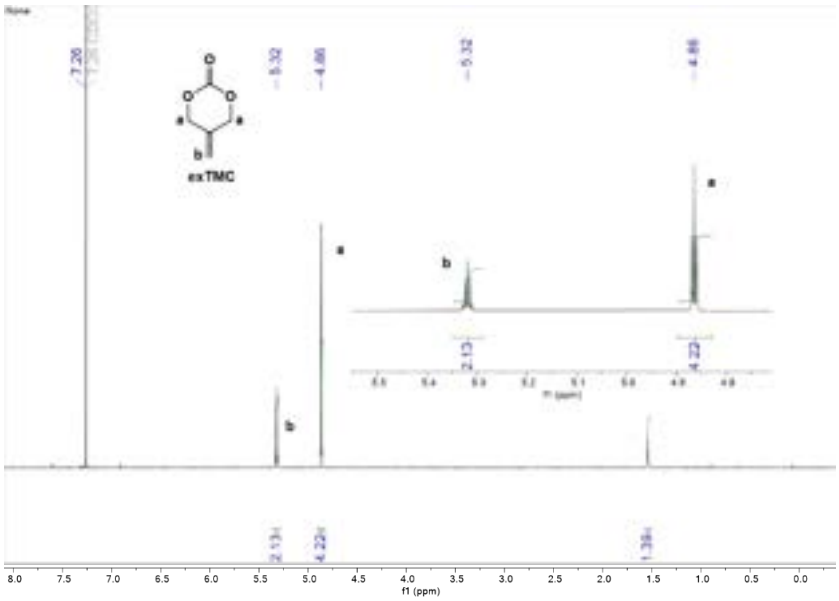

Figure 2-27. ^{1}H NMR spectrum of exTMC ($CDCl_3$, 300 MHz, r.t.).

In order to better understand the behavior of exTMC in ROP, crystals suitable for X-ray diffraction were grown and the solid-state structure of exTMC was compared with that of TMC and representative substituted 6CCs (**Figure 2-28**). The diffraction study revealed the typical envelope conformation of 6CCs (**Figure 2-26b**). The bending of the envelope (angle between the O_1-C_1-O_3-O_2 and C_2-C_3-C_4-C_5 mean planes, 137.8°) is very close to that of TMC (135.6°) and falls in the typical range of those observed in substituted 6CCs (126-141°). The other structural data are relatively close to those of TMC and substituted 6CCs. The main differences result from the presence of a C_{sp2} in the ring (C_3), in particular, the endocyclic C_2-C_3-C_4 angle. The typical values for this angle in 6CCs are in the range 105.5—107.4°, deviating only slightly from the expected 109° of a C_{sp3}. For exTMC, the observed value (111°) shows larger deviation from the expected 120° for a C_{sp2}. Since this constrain could affect the behavior of exTMC in ROP by impacting the ring strain, the ring-opening of exTMC was studied by DFT calculations and compared to that of TMC. As model reactions, we considered the ring-opening of the H-bonded adducts between the monomer and ethanol, and refered to the most stable conformations of the ensuing products (**Figure 2-29**).[116] The obtained $\Delta_r H$ values for the two monomers are very close (–2.3 / –3.5 kcal/mol), indicating that the presence of the $C{=}CH_2$ moiety in exTMC does not induce noticeable ring strain, as to compare with TMC.

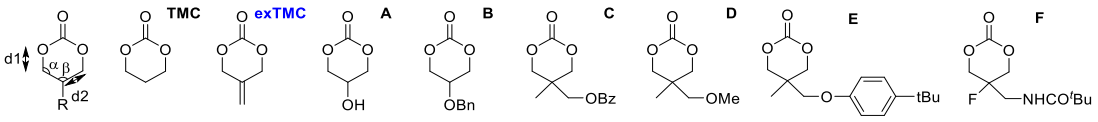

	TMC	exTMC	A	B	C	D	E	F
d1	1.458 / 1.46	**1.459 / 1.462**	1.458 / 1.460	1.459 / 1.460	1.453 / 1.460	1.461 / 1.481	1.457 / 1.453	1.438 / 1.435
d2	1.500 / 1.502	**1.478 / 1.489**	1.506 / 1.503	1.493 / 1.518	1.515 / 1.521	1.512 / 1.521	1.516 / 1.515	1.497 / 1.500
α	109.8 / 110.8	**110.6 / 111.1**	110.46 / 109.1	111.1 / 109.4	111.1 / 111.3	111.2 / 113	111.8 / 112.8	110.1 / 111.6
β	107.4	**111.3**	106.8	107.3	105.5	105.8	105.1	107.4
bending angle	135.66	**137.81**	132.55	126.46	134.2	141.45	140.44	129.35

Figure 2-28. Main structural data for a selection of 6CCs (including TMC).[34,117–120]

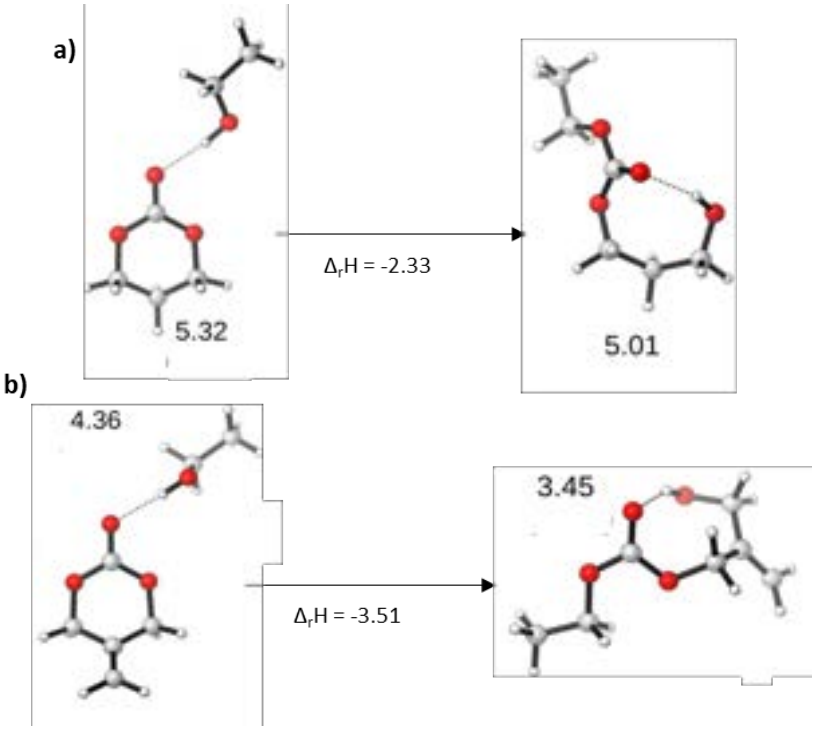

Figure 2-29. Δ_rH values computed by DFT for the ring-opening of TMC (a) and exTMC (b) by ethanol.

2.2.1.2 Preparation of TMC-COOH and TOBnTMC

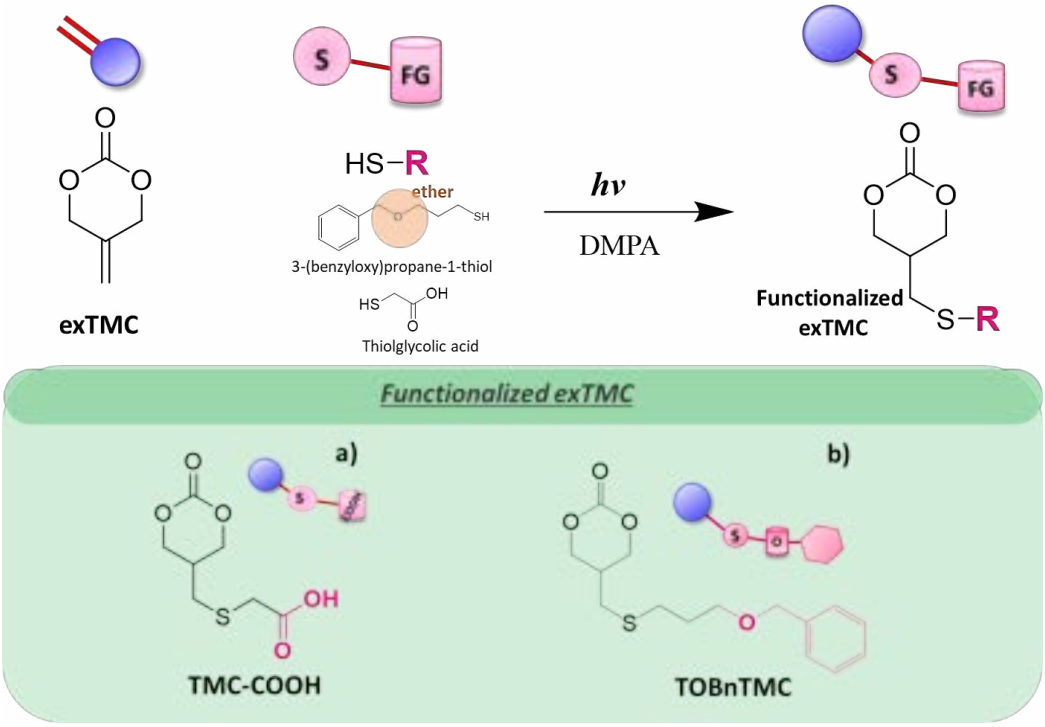

Figure 2-30. The modification of functionalized TMC by functionalized exTMC with thiol derivatives.

The results cast new light on a novel functionalized TMC monomer, introduced for thiol-ene click reactions in a one-step process using UV light (365 nm) irradiation. With the aid of a 2% *w/w* DMPA photoinitiator, 1 equivalent of thiolglycolic acid in THF at room temperature, the monomer was isolated by precipitation in diethyl ether and placed at -30°C overnight to further eliminate the excess thiol and initiator, as shown in **Figure 2-30.** Thiolglycolic acid comprising a carboxylic acid moiety was selected for introduction into the exTMC monomer (TMC-COOH) to enhance the hydrophilicity and bioactive properties (**Figure 2-30a**). After thiolglycolic acid modification, the structure was confirmed by the ^{1}H NMR spectrum (**Figure 2-31a**). The double bond and CH_2 peak of exTMC at 5.37 and 4.92 ppm disappeared. The new signals at 4.55, 4.42, 3.37, 2.68, and 2.48 appeared which is attributed to CH_2 and CH groups deriving from thioglycolic acid**,** indicating successful modification of TMC-COOH (**Figure 2-31b**).

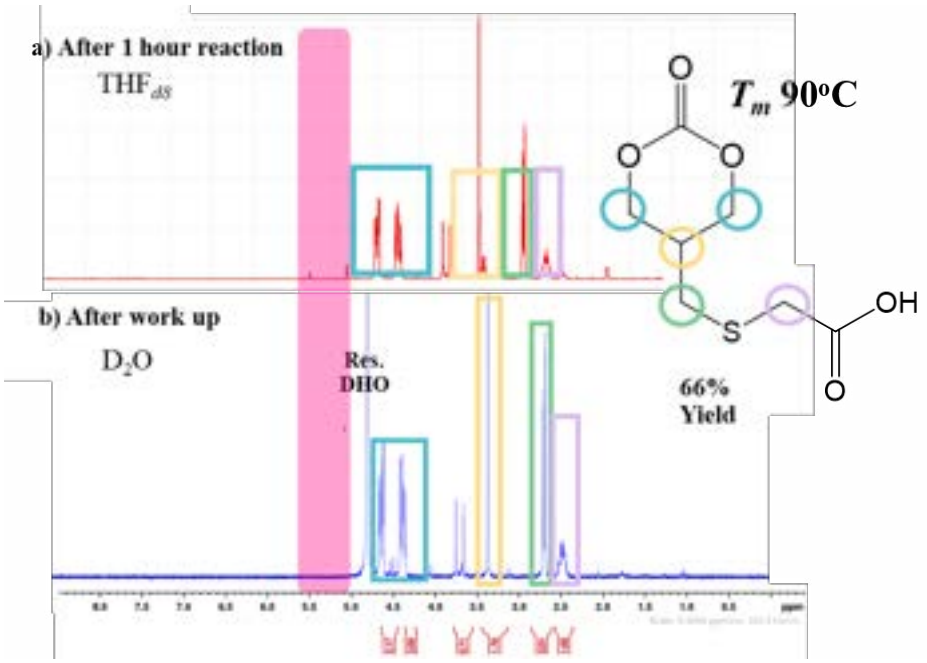

Figure 2-31. ^{1}H NMR spectra of TMC-COOH: (a) after 1 hour reaction in THF-d_8 and (b) after worked up reaction in D_2O (300 MHZ, r.t).

However, it was found that the polymerization of TMC-COOH was incompatible with the ROP due to the carboxylic functional group which will be discussed later.[64] Accordingly, it was necessary to protect the protic functional group before polymerization when working with functionalized exTMC. Thus, the thiol derivatives with a protected ether group (3-(benzyloxy)propane-1-thiol (TOBn))[121] was finally chosen (**Figure 2-30b**). Using a 4% *w/w* DMPA photoinitiator and 3 equivalents of TOBn in DCM at room temperature, the monomer was isolated by precipitation in diethyl ether. Subsequently, it was stored at -30°C overnight to further remove any excess thiol and initiator. It was necessary to use an excess of TOBn (3 equivalents to exTMC) to achieve more than 95% modification, because TOBn is less reactive than thiolglycolic acid. However, the excess TOBn could be recovered and recycled for use in subsequent reactions without any side reactions. The chemical structure of TOBnTMC was confirmed by ^{1}H NMR spectrum (**Figure 2-32**). The signal at 5.37 ppm corresponding to the double bond =CH_2 of exTMC disappeared. The appearance of new signals at 7.37 ppm, attributed to the phenyl group of 3-(benzyloxy)propane-1-thiol, indicates successful modification of TOBnTMC. This is further confirmed by ^{13}C NMR the presence of the new signals at 138.2, 128.4 and 127.6 ppm, attributed to the phenyl group of 3-(benzyloxy)propane-1-thiol (**Figure 2-32b**). The signal at 110.5 ppm corresponding to the double bond =CH_2 of exTMC

disappeared. Since the TMC was successfully functionalized *via* the thiol-ene reaction, the next step will be to evaluate the homopolymerization of the functionalized TMCs as well as their copolymerization with TMC.

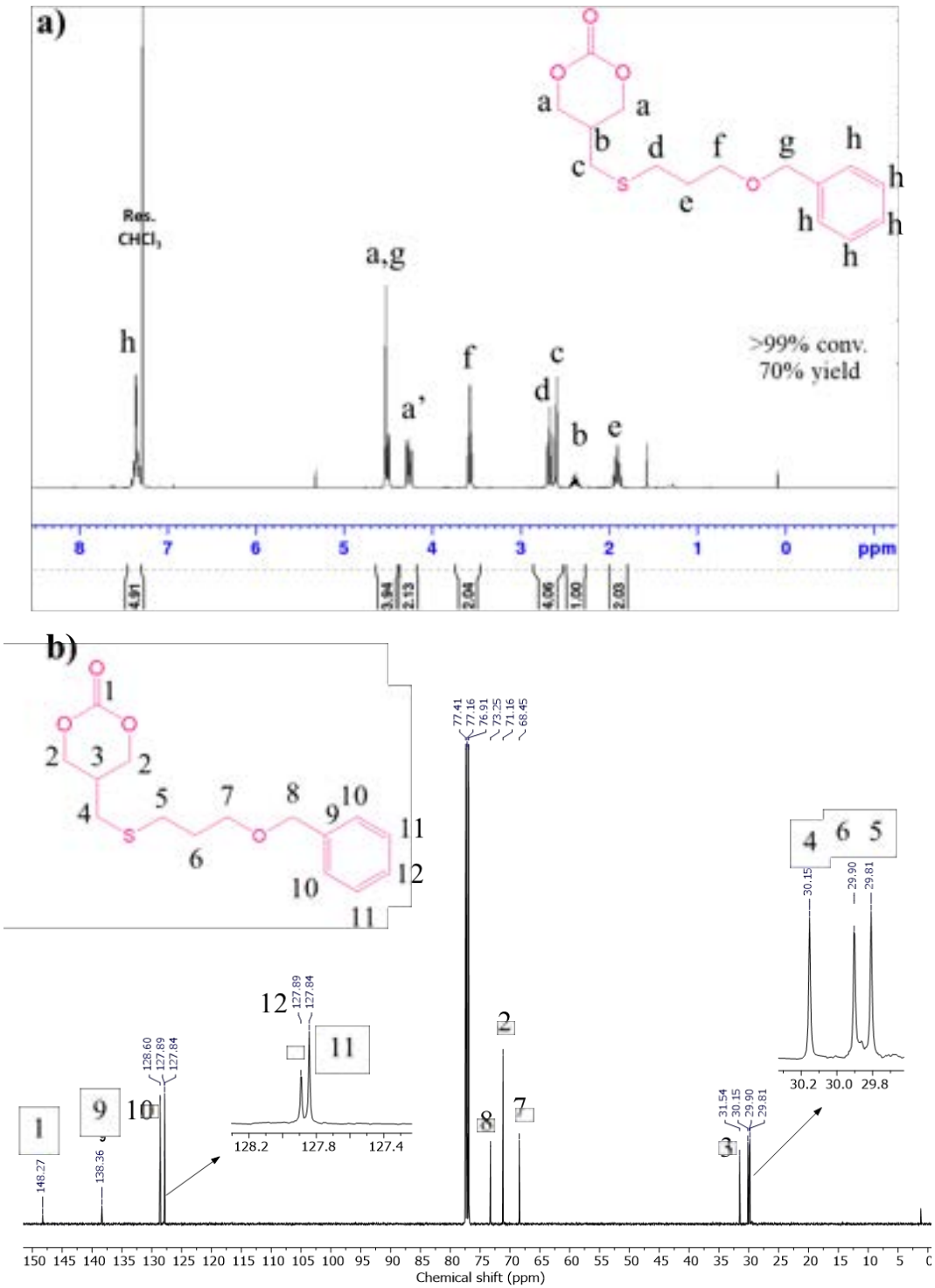

Figure 2-32. a) ^{1}H and b) ^{13}C NMR spectra of TOBnTMC ($CDCl_3$, 300 MHz, r.t).

2.2.2 Organocatalyzed homopolymerization of exTMC and TOBnTMC

2.2.2.1 *Organocatalyzed homopolymerization of exTMC*

The feasibility of exTMC ROP with efficient incorporation of a protic initiator was then explored using different types of organocatalysts: TBD, DBU, TU/DBU, DPP, and MSA. Dimethoxybenzyl alcohol (DMBA) was used as the protic initiator at a monomer / initiator ratio = 30/1 and with a monomer concentration of 0.5—1 M in chloroform (**Table 2-1**).

Table 2-1. ROP of exTMC with different organocatalysts and DMBA as intitiator[a]

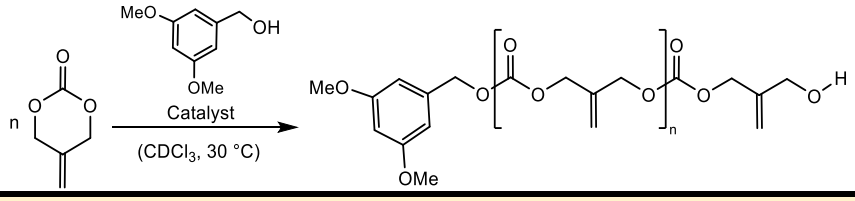

Run	Catalyst	[exTMC]/ [I]/[Cat]	Time (h)	Conv (%)	$M_{n\text{theo}}$	$M_{n\text{SEC}}$[b]	$Đ$
1	TBD	30/1/0.3	0.5	> 96	3591	3550	1.23
2	DBU	30/1/0.3	90	80	3591	2760	1.35
3	TU/DBU	30/1/1/1	1.5	85	3591	3100	1.22
4	DPP[c]	30/1/1	70	93	3591	2890	1.16
5	MSA	30/1/0.4	5	96	3591	3000	1.07

[a]Reaction conditions: 0.5-1 mol/L in $CDCl_3$ at 30°C. [b]In THF with calibration over PS standards, non-corrected values. [c]T = 60°C.

In all cases, the ROP occurred to give the corresponding polymer with incorporation of the initiator as the carbonate chain end (detected by ^{1}H NMR). However, important differences in reaction rate and control were observed. As could be expected, the polymerization is very fast with TBD at rt (30°C) (less than 30 minutes with DMBA/TBD = 1/0.3). Using DBU alone as catalyst (DMBA/DBU = 1/0.3), the polymerization is rather slow (41 % conversion after 20h, and 80 % after 90h) but associating it to TU speeds up the reaction significantly (85% conversion within only 1h for DMBA/TU/DBU = 1/1/1). Concerning Brönsted acids, DPP is the less active of all the catalysts. Heating at 60 °C (DMBA/DPP = 1/1) was necessary to reach 92% conversion after 70h. In marked contrast, MSA (DMBA/MSA = 1/1) led to full conversion in 5 h at 30 °C. Although this is a longer time that using TBD or TU/DBU as

catalyst, NMR spectrocopy, SEC and MALDI-TOF MS analyses suggest a better control of the polymer structure. SEC analysis on the polymer samples revealed M_n in the range 2760 and 3500 g/mol, depending on the organocatalyst. Notably, samples obtained with TBD or DBU as catalysts led to samples with broader molar distributions ($Đ$ 1.23 and 1.22, respectively) than those prepared with DPP or MSA ($Đ$ 1.07 and 1.16, respectively). MSA thus appears to be a good compromise between activity and selectivity. According to homopolymerization of exTMC with MSA as catalyst, typical procedure is exTMC (100 mg, 0.87 mmol, 30 equiv.) was dissolved in $CDCl_3$ ([exTMC] = 1 mol/L, 0.8 mL). The initiator, DMBA (5 mg, 3 10-2 mmol, 1 equiv.) and methane sulfonic acid (84 µL, 1.2 10-2 mmol, 0.4 equiv.) were successively added. The reaction mixture was stirred at 30 °C. The conversion of the monomer was monitored by ^{1}H NMR spectroscopy. An excess of diisopropylethylamine was added to neutralize the catalyst after 5 hours of stirring, and the reaction media was concentrated by solvent evaporation under vacuum. The polymer was then precipitated in cold methanol, filtered and dried under vacuum. Yield: 85 %. SEC (THF): M_n = 3000 g/mol; $Đ$ = 1.07.

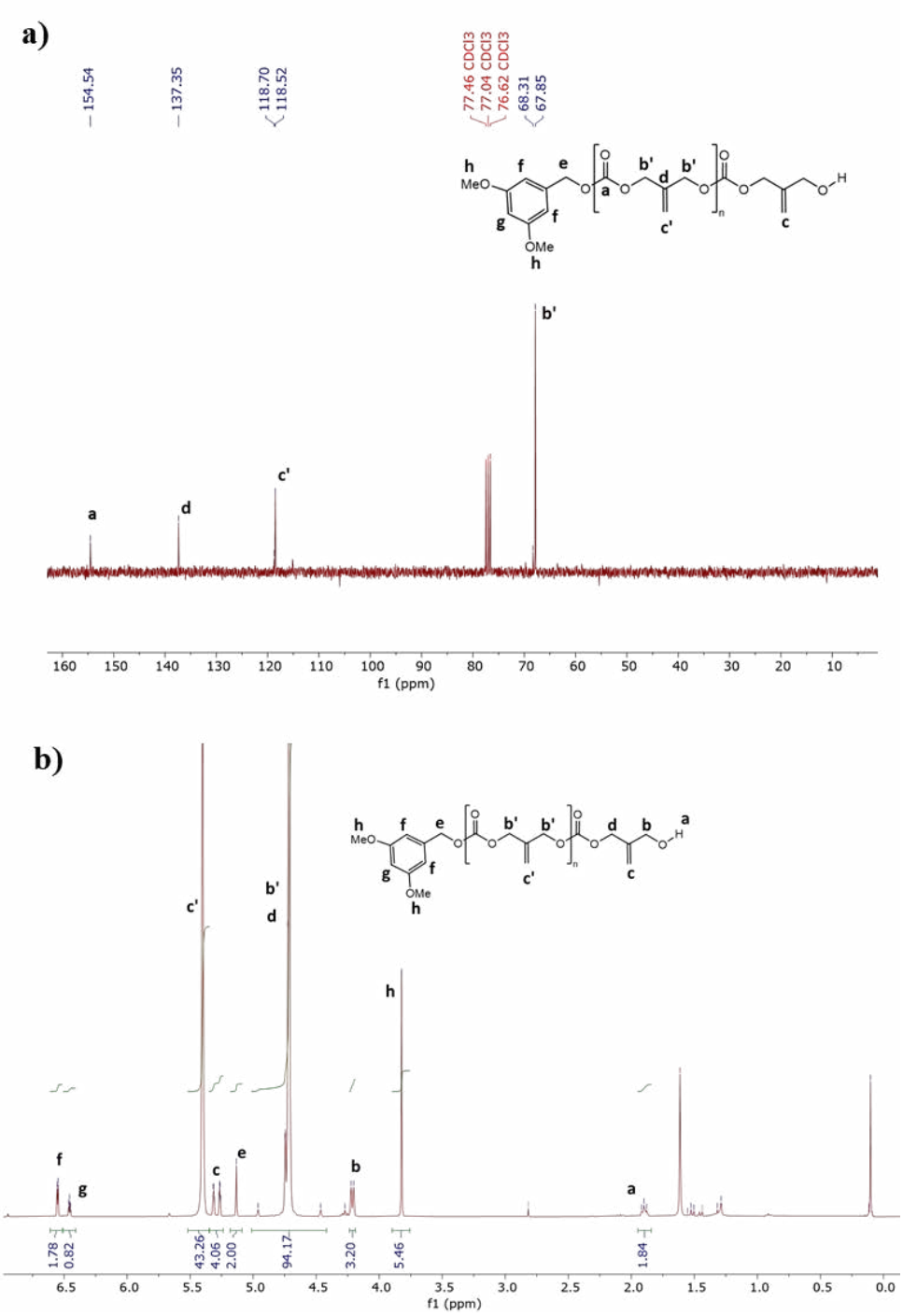

Figure 2-33. a) ^{1}H and b) ^{13}C NMR spectra ($CDCl_3$, 300MHz) of of Poly(exTMC) (DP30) prepared with MSA as catalyst.

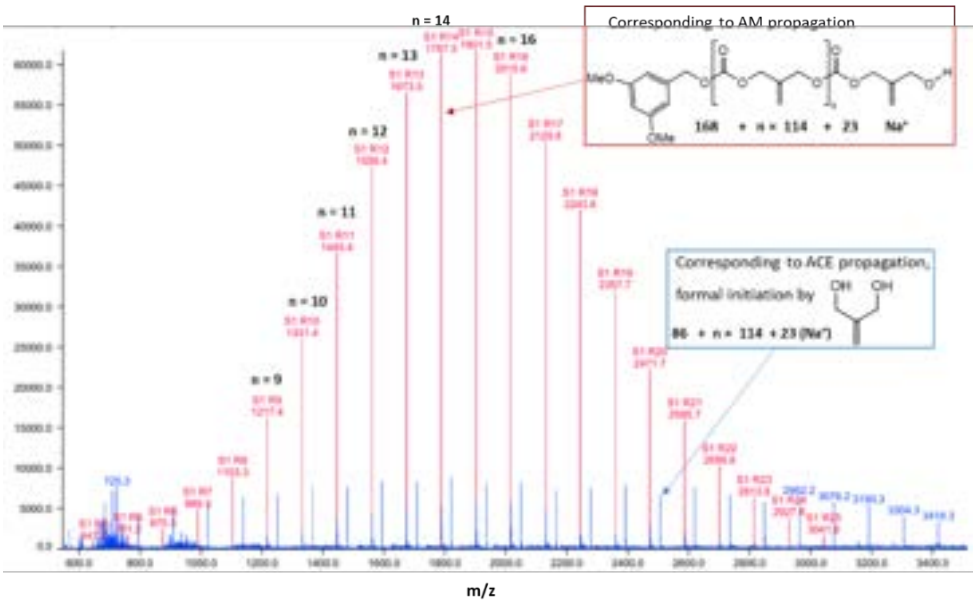

Figure 2-34. MALDI-TOF MS analysis of a Poly(exTMC) (DP30) prepared with MSA as catalyst

Poly(exTMC) homopolymer obtained with MSA as catalyst (DP30) was confirmed by ^{1}H NMR and $^{13}C\{^{1}H\}$ spectrum in **Figure 2-33a** and **Figure 2-33b**, respectively. The ^{1}H NMR signals corresponding to the repeating OCH_2 (b') and $=CH_2$ (c') groups are observed at 4.72 and 5.45 ppm, respectively. The $C=CH_2$ moiety is thus not affected by the polymerization process and is incorporated as is in the polymer chains. This is further confirmed by the presence of the C_{sp2} signals at 137.3 and 118.6 ppm in the $^{13}C\{^{1}H\}$ spectrum, **Figure 2-33a**. The ^{1}H NMR spectrum shows in addition signals corresponding to the carbonate and the hydroxy chain-ends. A doublet (4.21 ppm, 2H, b) and a triplet (1.90 ppm, 1H, a) are attributed to the CH_2OH chain end, whereas signals e, f, g and h correspond to the dimethoxybenzyl carbonate chain end. The presence of these signals confirms the incorporation of the protic initiator as the carbonate chain-end. However, the integration value of the signal b corresponding to the CH_2OH chain-end is higher than expected (3.2 instead of 2.0, integrals calibrated based on signal e), suggesting the presence of a second population. MALDI-TOF MS analysis (**Figure 2-34**) shows a main population corresponding to the targeted polymer chains that contain the initiator DMBA.$nC_5H_6O_3$ + Na^+), resulting from the typical Activated-Monomer (AM) mechanism reported for ROP of cyclic monomers with MSA as catalyst. A second minor population is also observed, corresponding to telechelic polymer chains formally initiated by the 2-methylenepropanediol ($H_2C=C(CH_2OH)_2$.$nC_5H_6O_3$ + Na^+). This is in fact consistent with the occurrence of some Activated-Chain-End (ACE) mechanism in

competition with the desired AM, but in a minor extent (in line with the deviation of the integration value noticed by ^{1}H NMR for the CH_2OH chain-end). Competition between these two propagating mechanisms is reminiscent of the situation it previously reported for TMC (**Figure 2-35**).[51,122,123]

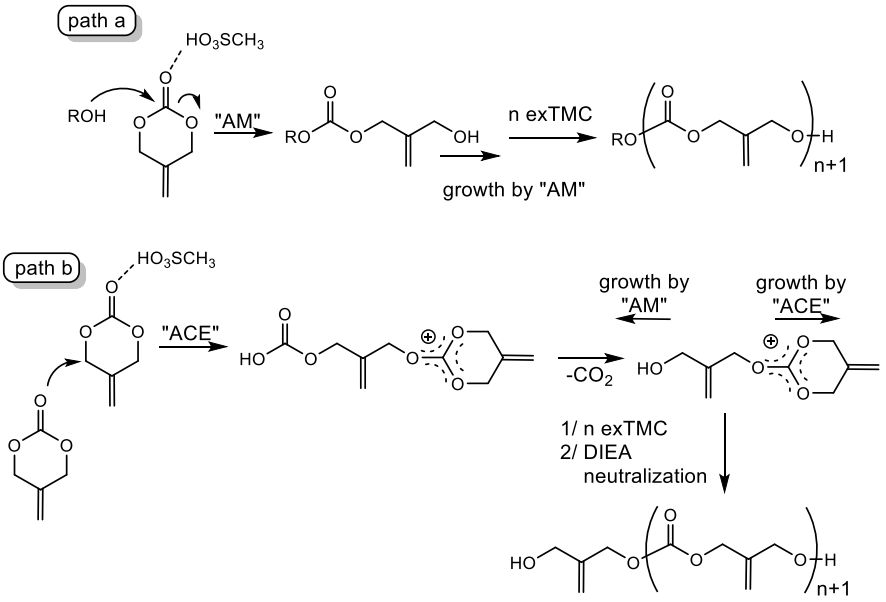

Figure 2-35. Illustration of the competing AM and ACE mechanisms in the MSA catalyzed ROP of exTMC and structure of the corresponding resulting polymers[51]

2.2.2.2 *Organocatalyzed homopolymerization of TOBnTMC*

TMC-COOH was evaluated for copolymerization with TMC utilizing DP of 60 and 10% TMC-COOH, with MAS serving as the catalyst and BDM as the initiator, in DCM at 30°C for 5 hours. However, it was found that the polymerization of TMC-COOH was incompatible with the ROP due to the carboxylic functional group.[57] The obtained SEC results showed a broad *Đ*, which could imply that the polymerization process could not be controlled. This might be because the carboxylic group on the monomer quenches the catalyst or acts as an initiator. To ensure successful polymerization when using functionalized exTMC, it was essential to protect the protic functional group beforehand. Consequently, the thiol derivatives featuring a protected ether group, specifically 3-(benzyloxy)propane-1-thiol, were ultimately selected for the next experiment.

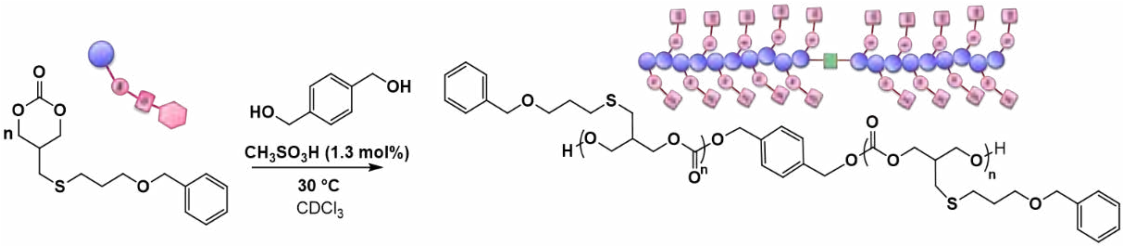

According to homopolymerization of exTMC with MSA as catalyst, appears to be a good compromise between activity and selectivity with BDM initiator. Therefore, the homopolymerization of TOBnTMC was set in the same condition to observe the compatibility between monomer, catalyst, and initiator. Poly(TOBnTMC) homopolymer obtained with MSA as catalyst and BDM as initiator at 30°C for 5 hours (DP60) was confirmed by ^{1}H NMR spectrum in **Figure 2-36**. The kinetics of monomer conversion were determined from the integrated peak areas at 4.55 and 2.87 ppm in the ^{1}H NMR **(Figure 2-36).** After 3 hours, the conversion exceeded 90% **(Figure 2-37)**. The ^{1}H NMR signals corresponding to the repeating OCH_2 (h) and CH (g) groups are observed at 4.37 and 2.29 ppm, respectively. The multiplet signals at 7.37, 4.54, 3.52, 2.64, and 1.85 ppm corresponding to the phenyl group and to the different CH_2 groups deriving from 3-(benzyloxy)propane-1-thiol are also observed. Additionally, the ^{1}H NMR spectrum shows in addition signals corresponding to the carbonate central unit deriving from the initiator and the hydroxy chain-end at 5.2 and 3.6, respectively. The presence of these signals confirms the incorporation of the protic initiator as a carbonate similarly to what was observed for Poly(exTMC). However, the relative integration of these two signals is different, which could imply that there is the occurrence of some ACE mechanism in competition with the desired AM. In addition, SEC analysis of the polymer samples revealed an M_n 2.2 kDa and $Đ$ 1.37, which is lower than the theoretical M_n 17.9 kDa. These results suggested that TOBnTMC might be problematic for controlled ROP.

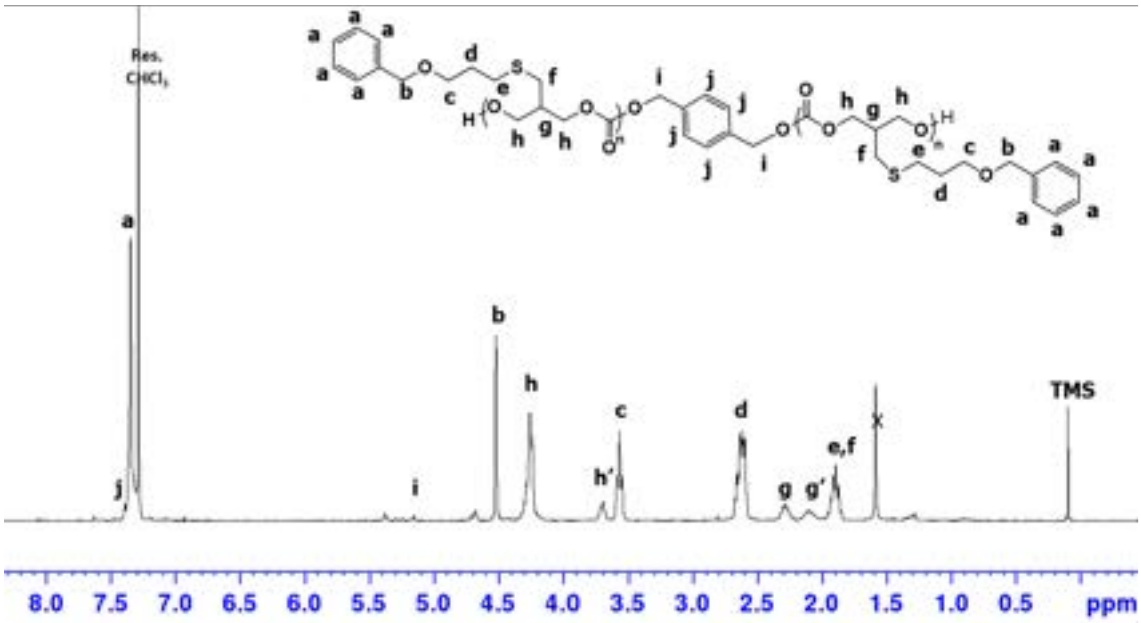

Figure 2-36. ^{1}H NMR spectra of Poly(TOBnTMC) ($CDCl_3$, 300 MHZ, r.t).

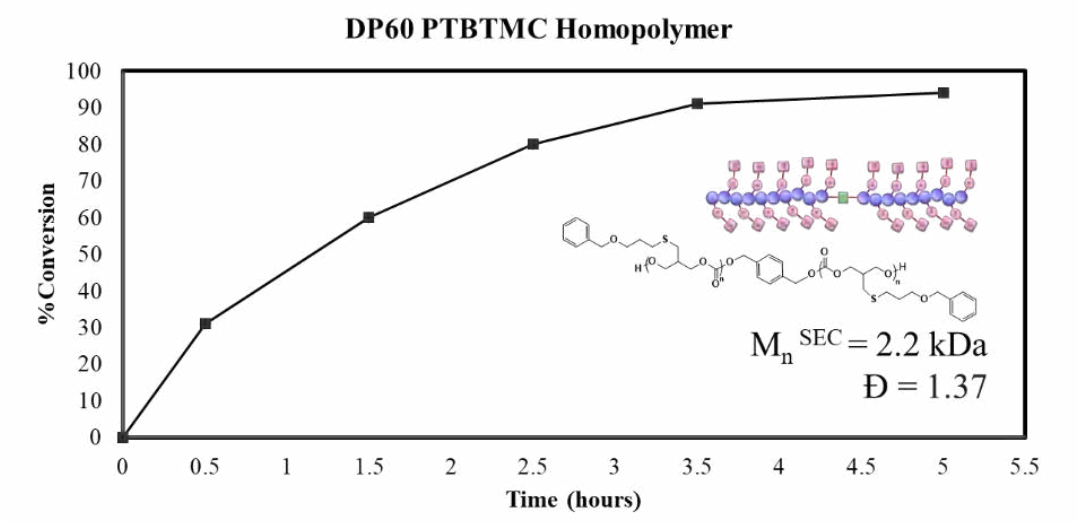

Figure 2-37. The kinetics of TOBnTMC conversion (DP60).

2.2.3 Random Copolymerization of TMC and exTMC and Random Copolymerization of TMC and the functionalized exTMC

2.2.3.1 *Random Copolymerization of TMC and exTMC*

To determine the appropriate catalyst for both TMC and exTMC monomers, with the aim of controlling the randomness of the copolymer, the conversion of TMC and exTMC was systematically observed using various organocatalysts, namely TBD, TU/DMAP, DPP and MSA (**Table 2-2**)

Table 2-2. Investigation of exTMC/TMC copolymerization with different organocatalysts[a]

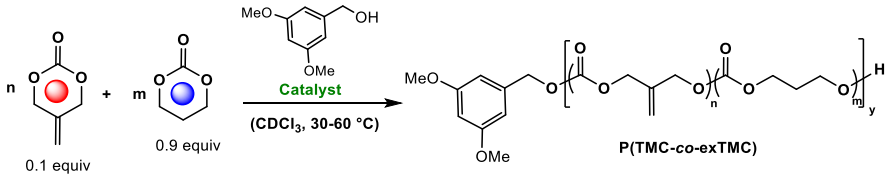

Run	Catalyst	Time(h)	$Conv_{TMC}$	$Conv_{exTMC}$	M_n^{Theo} (Da)	$M_n^{SEC,b}$(Da)	$Đ^b$
1	TBD	1	>96	>96	3267	4000	1.42
2	TU/DBU	2.5[c]	63	94	3267	4680	1.27
3	DPP	18[d]	91	94	3267	3600	1.15
4	MSA	5	>96	>96	3267	3566	1.12

[a]Reaction conditions: M/I = 30, 0.5-1 mol/L in $CDCl_3$ at 30°C. [b]In THF with calibration over PS standards, non-corrected values. [c]Full conv exTMC, 60% conv TMC. Full conv of TMC is reached overnight. [d]60 °C

Simultaneous copolymerization of exTMC and TMC (TMC/exTMC = 90/10) was next explored with DMBA as initiator (monomer/DMBA = 30/1). The organocatalysts TBD (DMBA/TBD = 0.3), TU/DBU (DMBA/TU/DBU = 1/1/1), DPP (DMBA/DPP = 1/2) and MSA (DMBA/MSA = 1/1) were used to draw a rapid comparison. All the reactions were carried out at 30 °C except for the one with DPP (60 °C) (**Table 2-2**). As in the case of the exTMC homopolymerization, the far faster reaction occurs with TBD as catalyst (full conversion in less than 1h) and the slowest one with DPP. TU/DBU and MSA are in between, leading to full conversion in less than 5h. NMR monitoring of the copolymerization reactions was very informative concerning monomer conversions, with two different situations. The ^{1}H NMR spectra showed that

with TBD and TU/DBU (**Figure 2-38a** for TBD),[123] exTMC is consumed more rapidly than TMC (TBD: 86 % conversion after 20 min *vs* 50% for TMC; TU/DBU: 94 *vs* 63 % after 2.5h). This behavior is in line with what has been previously reported for 4-substituted 6CCs with the same catalysts,[65] as well as in enzymatic conditions.[124] In marked contrast, with DPP and MSA, the conversions of the two monomers track each other (DPP: 94% and 91%, respectively, after 18h; MSA: 55% exTMC and 57% for TMC after 2.5 h, **Figure 2-38b**),[123] suggesting close reactivity of the two monomers. Another diagnostic data is the fact that at the end of the polymerization, the copolymer prepared with TBD as catalyst shows only TMC-hydroxyl chain-ends (**Figure 2-38b**, signal g'),[123] whereas the one prepared with MSA also shows some exTMC-hydroxyl chain-ends (**Figure 2-39b**, signal a').[123] SEC analysis shows unimodal traces in all cases, but molar distributions are narrower for the sample obtained with DPP (despite the higher reaction temperature, 60°C *vs* rt) and MSA ($Đ$ 1.12—1.15)

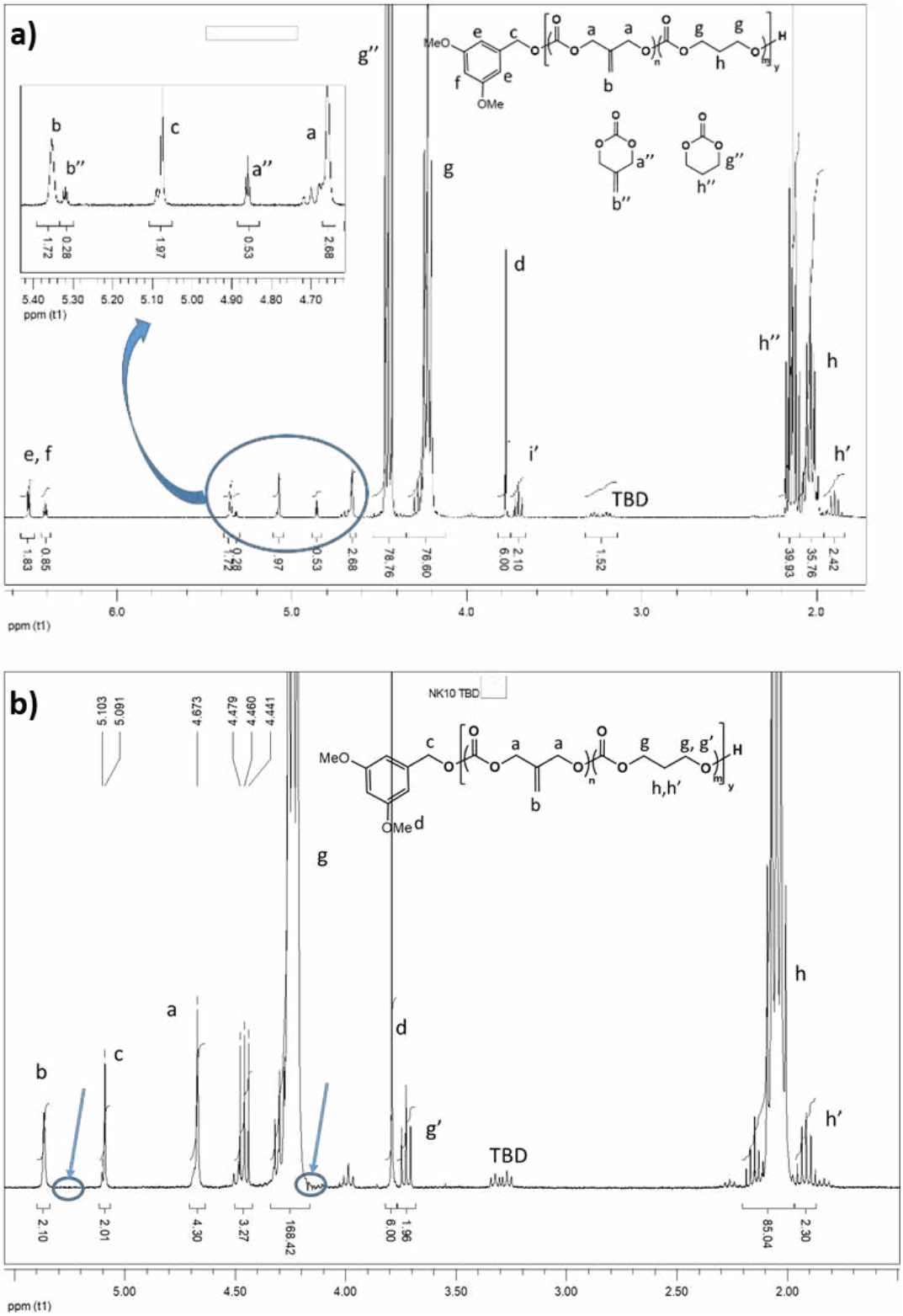

Figure 2-38. ^{1}H NMR spectra ($CDCl_3$, 300 MHz) for the TMC/exTMC copolymerization catalyzed with TBD. During copolymerization (a) and after full conversion (b).

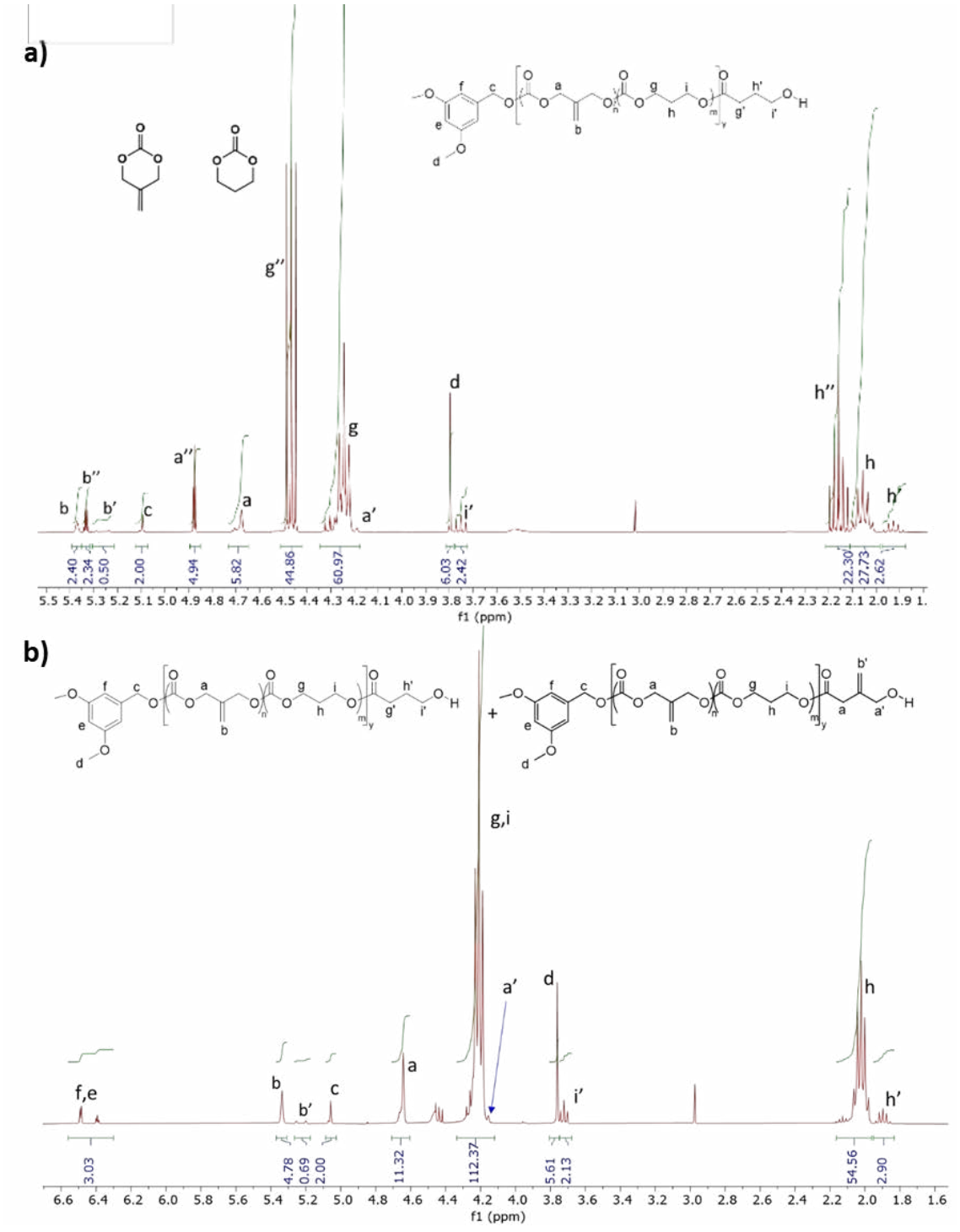

Figure 2-39. ^{1}H NMR spectra ($CDCl_3$, 300 MHz) for the TMC/exTMC copolymerization catalyzed with MSA. During copolymerization (a) and after full conversion (b).

As ROCOP with MSA as organocatalyst (1.3 mol%) leads to a more random incorporation of two comonomers within the polymer chains than TBD or TU/DBU, while maintaining good control of the polymerization, the study was followed with this organocatalyst. In addition, MSA is easy to remove and is reported to be ecofriendly.[125] In order to get higher molar masses and minimize the impact of the ACE mechanism, the diol 1,4-benzenedimethanol (BDM) was chosen to further explore the copolymerization of exTMC and TMC. Typical procedure for the copolymerization of TMC and exTMC with MSA as catalyst (DP = 60). exTMC (112 mg, 0.98 mmol, 30 equiv.) and TMC (100 mg, 0.98 mmol, 30 equiv.) were dissolved in $CDCl_3$ ([exTMC] = 1 mol/L, 2 mL). The initiator, DMBA (4.5 µg, 3.3 10-2 mmol, 1 equiv.) and methane sulfonic acid (190 µL, 2.6 10-2 mmol, 0.8 equiv.) were successively added. The reaction mixture was stirred at 30 °C. The conversion of the comonomers was monitored by ^{1}H NMR spectroscopy. An excess of diisopropylethylamine was added to neutralize the catalyst after 8 hours, and the solvent was evaporated under vacuum. The polymer was precipitated in cold methanol, then filtered and dried under vacuum. Yield: 93 %. SEC (THF): M_n = 5 300 g/mol; $Đ$ = 1.08.

Table 2-3. TMC/exTMC copolymerization catalyzed by MSA: variation of DP and composition.

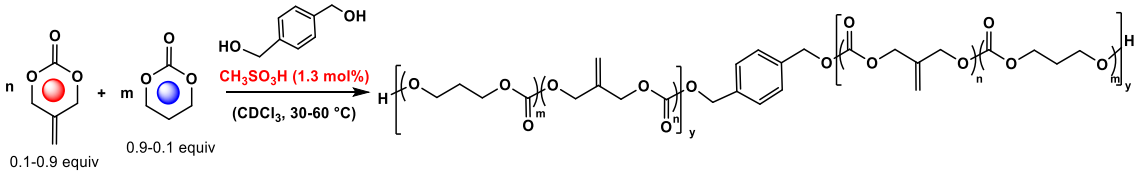

Run	Ref Code	M/I	mol% exTMC	time (h)	$M_{n\text{theo}}$ (Da)	$M_{n\text{SEC}}$[b] (Da)	$M_{n\text{SEC}}$[C] (Da)	$Đ$
1	P1	15	10	2	1900	2700	1539	1.08
2	P2	30	10	4	3400	4400	2508	1.08
3	P3	60	10	6	6500	6410	4700	1.07
4	P4	90	10	7	9600	10300	9100	1.08
5	P4	120	10	7	12700	12300	10800	1.09
6	P6	60	30	7	6500	7600	5500	1.12
7	P7	60	50	8	6600	7200	5300	1.08
8[e]	P8	120	10	7	12700	11400	10000	1.21
9[d]	P9	120	10	8	12700	13700	12100	1.10
10[e]	P10	60	50	5	6600	7900	5800	1.09
11	P11	120	30	7	12800	12400	10900	1.13
12[e,f]	P12	120	30	3	12800	12700	11200	1.15
13[e,f]	P13	120	10	3	12700	10600	9300	1.14
14[e,g]	P14	120	30	5	15800	13400	11800	1.15

[a]Reaction conditions: 1.3 % in catalyst, 1 mol/L in $CDCl_3$ at 30°C. [b]In THF with calibration over PS standards, non-corrected values. [c]Values corrected using the correction factor reported for PTMC. [d]Multi-feed experiment 4×30 equiv. [e]In bulk, 60°C. [f]With propane-1,3-diol as initiator. [g]With PBD H as macroinitiator, M_n PBD H = 5 600 g/mol, $Đ$ = 1.10.

ROCOP with an exTMC/TMC monomer ratio of 10/90 and increasing DP (from 15 to 120) was first explored at 1.3% catalyst loading (relative to the monomer) in 1 mol/L chloroform solutions (**Table 2-3, Entry 1-5**). The exTMC content was then increased to 30-50% for a DP of 60 (**Table 2-3, Entry 6 and 7**), leading to results close to those 10% content in exTMC. The ratio of functionalization can thus be easily adjusted. Conversions >96% were observed in 2-7 h and the copolymers were isolated in 85-95% yields by precipitation in cold methanol after catalyst quenching with diethylisopropyl amine (DEIA).

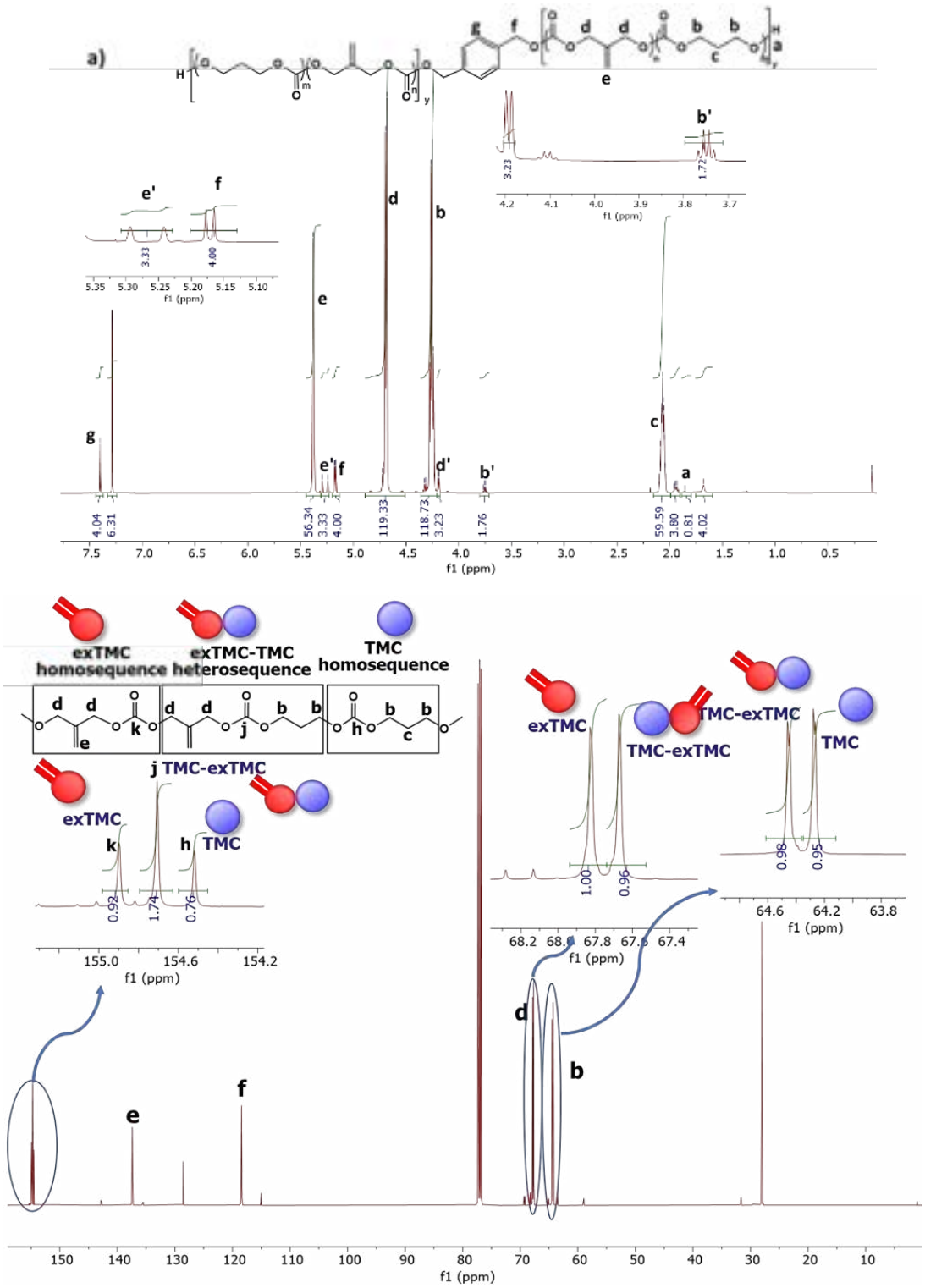

Figure 2-40. (a)^{1}H NMR and (b)^{13}C NMR spectra of a copolymer with DP = 60 and a TMC/exTMC monomer ratio of 50/50 ($CDCl_3$, 300 MHZ, r.t).

According to the results in **Figure 2-40a** shown the ^{1}H NMR spectrum of a copolymer with DP = 60 and a TMC/exTMC monomer ratio of 50/50 (**P7, Table 2-3**). Efficient incorporation of the difunctional initiator BDM in the core of the polymer chains is confirmed by the presence of the signals f and g, corresponding to the methylene and aromatic groups of the initiator, at 5.16 and 7.40 ppm respectively. As the obtained result, DMBA was tested in order to observe for the copolymerization behavior, two different CH_2OH chain-ends are observed (b' at 3.75 ppm and d' at 4.19 ppm) corresponding to the TMC and exTMC CH_2OH terminal units, respectively. Signal d' overlaps with signal b, associated with the CH_2O moieties of the TMC units, which impedes accurate integration. The relative integrals of signals b, d (corresponding to the CH_2O moieties of TMC and exTMC units, respectively), f and g (associated with the initiator) agree nicely with the initial monomer ratio (50/50) and monomer feed (DP60). Signals b and d are splitted due to the presence of homo- and heterodiades (TMC–TMC, exTMC–exTMC and TMC–exTMC sequences). The signals are very close in intensity, which denotes a high randomness of the copolymer, but accurate integration to determine the average sequence lengths (L_{exTMC} and L_{TMC}) was not possible due to overlapping. It was however possible using $^{13}C\{^{1}H\}$ NMR spectroscopy (**Figure 2-40b**), in which integration of the corresponding signals to the homo- and heterosequences was possible (after assignment of the signals by 2D NMR analysis and comparison with the respective homopolymers). The relative integrations of the signals CH_2O and C=O signals give L values close to 2 for both exTMC and TMC (L_{exTMC} = $1+I_{exTMC}/(I_{exTMC}+I_{TCM})$, L_{TMC} = $1+I_{exTMC}/(I_{TMC}+I_{TCM})$), which corresponds to an almost perfect randomness ($R = 1/L_{exTMC} + 1/L_{TMC} \approx 1$).[123]

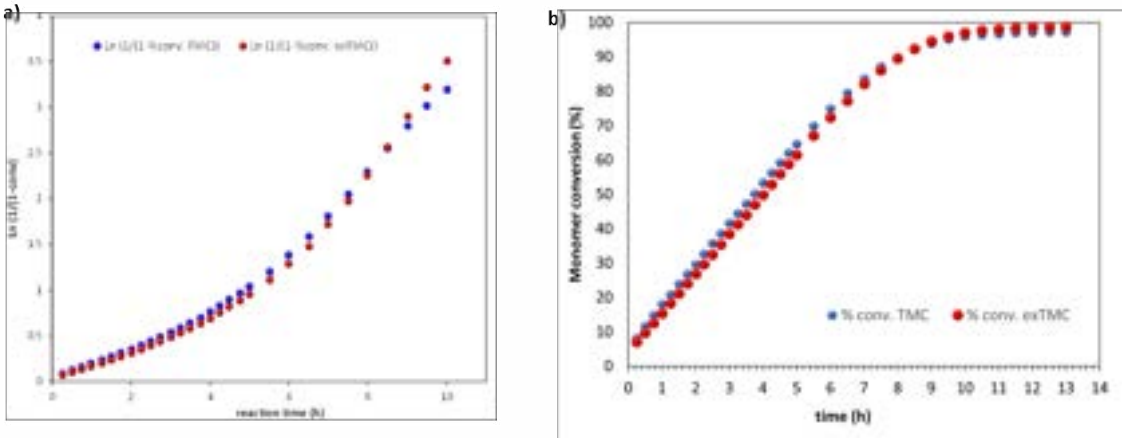

Figure 2-41. (a) Semilogarithmic plots of the two monomer conversions *vs* reaction time, and (b) Monomer conversion *vs* time for an exTMC/TMC copolymerization (30/30/1 exTMC/TMC/initiator ratio).

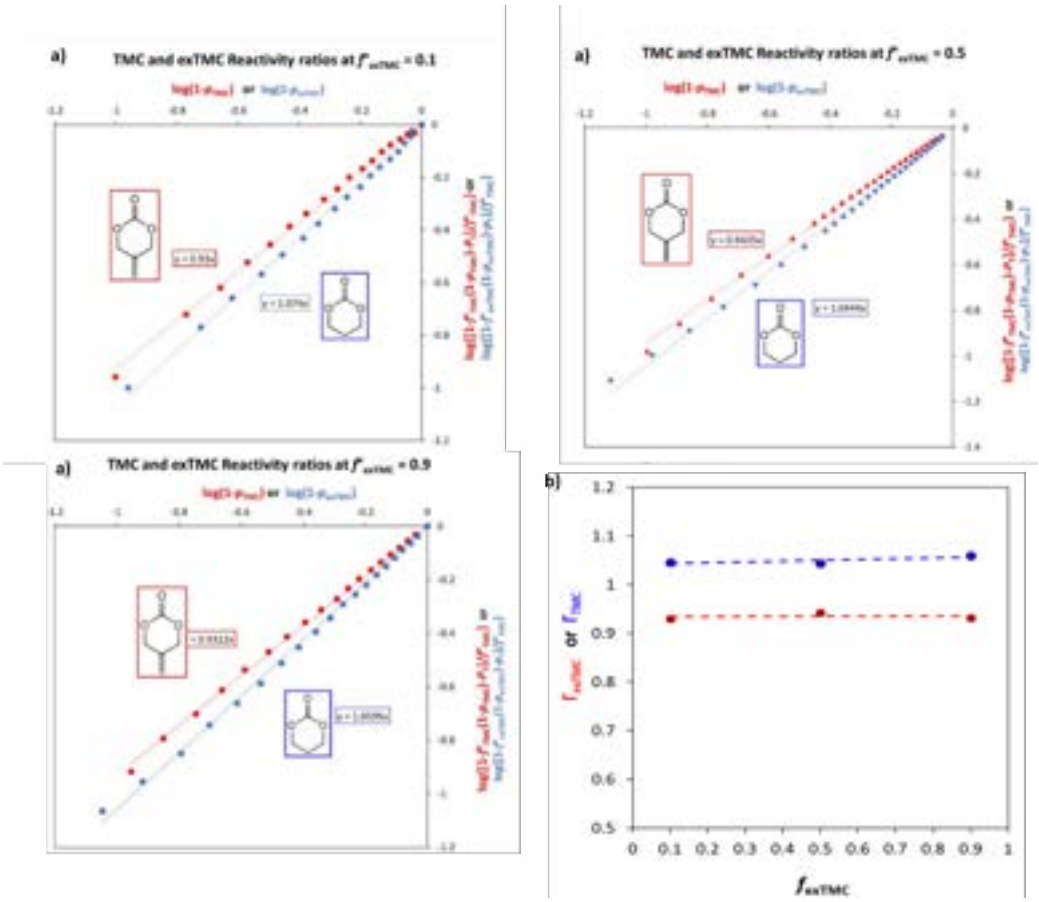

Figure 2-42. a) Determination of the reactivity ratios of the two monomers by Beckingham-Sanoja-Lynd (BSL) [123] method from the in situ ^{1}H NMR monitoring of copolymerizations at different monomer ratios. The slope coefficient of the straight lines (Y) represents the reactivity ratio. b) Fit of the determined reactivity ratios at different TMC/exTMC ratios.

This nearly perfect randomness of the TMC/exTMC copolymer is in line with the ^{1}H NMR monitoring of the monomer conversions. The semi-logarithmic plot of the copolymerization reaction with a 50/50 monomer ratio and DP = 60 shows almost overlapped conversion curves for the two monomers (**Figure 2-41a**, see **Figure 2-41b** for the plot of the monomer conversions). The curves show an upward deviation from linearity (quasi zero-order in monomer rather than classical first-order) as already reported for the ROP of lactones and 6CCs with acid catalysts such as MSA or DPP[125–129], and in line with the higher basicity of the carbonate moieties in the cyclic monomer compared to those of the polymer chains (due to their different conformation). To confirm the close reactivity of the two monomers in copolymerization, ^{1}H NMR monitoring was also carried out for copolymerizations with exTMC/TMC monomer

ratios of 10/90 and 90/10 and DP = 60, and the relative reactivity ratios were determined for TMC and exTMC applying the Beckingham-Sanoja-Lynd (BSL) method from the in situ ^{1}H NMR monitoring of copolymerizations at different monomer ratios. Fitting curves from equations **E3** and **E4** obtained from the non-terminal model for ionic or pseudo-ionic catalytic copolymerizations (according to **Equations E1** and **E2**). The slope coefficient of the straight lines (Y) represent the reactivity ratio. (**Figure 2-42a**).[123] Whatever the monomer ratio, reactivity ratios of 0.95-0.98 and 1.00-1.06 were obtained for exTMC and TMC (**Figure 2-42b**),[123] respectively, confirming the very close reactivity of the two monomers and supporting the high randomness of the obtained copolymers.

Equations

p_T =global monomer conversion; p_{TMC} =TMC conversion; p_{exTMC} =exTMC conversion
$f°_{TMC}$ = initial molar fraction in TMC; $f°_{extMC}$ = initial molar fraction in exTMC

(E1) $$p_T = 1 - f°_{TMC}(1-p_{TMC}) - f°_{exTMC}(1-p_{TMC})^{\Gamma_{exTMC}}$$

(E2) $$p_T = 1 - f°_{TMC}(1-p_{exTMC})^{\Gamma_{TMC}} - f°_{exTMC}(1-p_{TMC})$$

(E3) $$[\log((1-p_{TMC})]_{\mathbf{exTMC}} = \log\left[\frac{1 - f°_{TMC}(1-p_{TMC}) - p_T}{f°_{exTMC}}\right]$$

(E4) $$[\log((1-p_{exTMC})]_{\mathbf{TMC}} = \log\left[\frac{1 - f°_{exTMC}(1-p_{exTMC}) - p_T}{f°_{TMC}}\right]$$

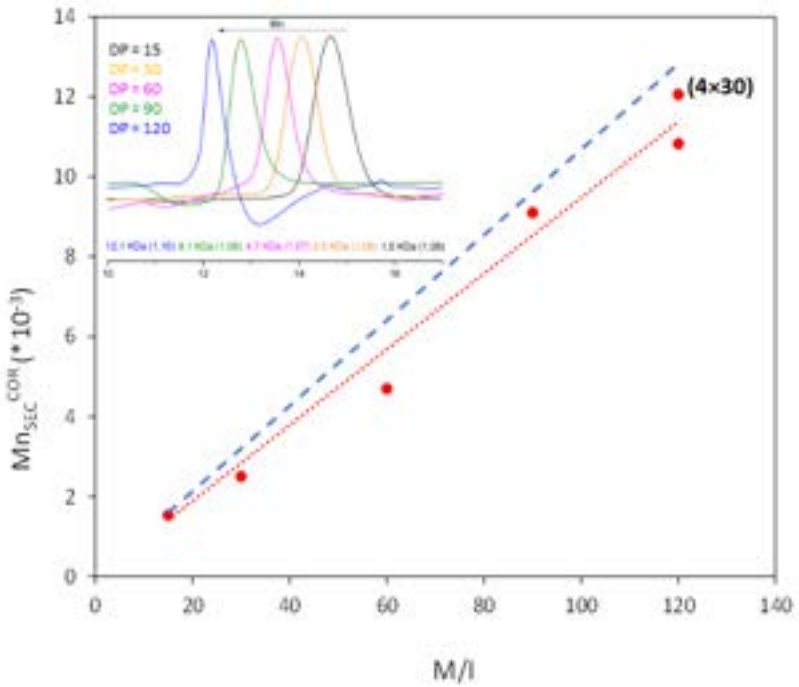

Figure 2-43. $M_{n\ SEC}$ *vs*. monomer/initiator ratio plot for copolymerizations with a TMC/exTMC ratio of 90/10.

As shown in **Figure 2-43**, M_n, and $Đ$ of copolymer were observed by SEC. The obtained data indicated that the linear increase of M_n with DP, up to 10800 g/mol for DP 120 (applying the correction factor reported for PTMC),[130] and narrow molecular distributions ($Đ$ < 1.12), supporting the possibility of adjusting the M_n of the copolymer by the monomer/initiator ratio.

In order to minimize the competing ACE mechanism, two variations of the polymerization conditions were explored: (i) bulk polymerization and (ii) multi-feed of the monomers, so that the activated-monomer / monomer ratio is decreased (it is a known way to decrease the impact of the ACE mechanism).[51,122] Bulk polymerization (**Table 2-3, entry 8**) led to similar results than in solution. As for the multi-feed test (**Table 2-3, entry 9**), a polymerization was set up in reaction conditions similar to those of DP30 (**Table 2-3, entry 2**), and subsequent additions of 30 equivalents of a 10/90 mixture of comonomers (3 times at 3h time intervals, to reach DP = 120 ultimately). SEC analysis shown a clear increase of the M_n (from 10800 to 12100 g/mol) while maintaining narrow molar distributions, in agreement with a lower impact of the competitive ACE propagation mechanism.

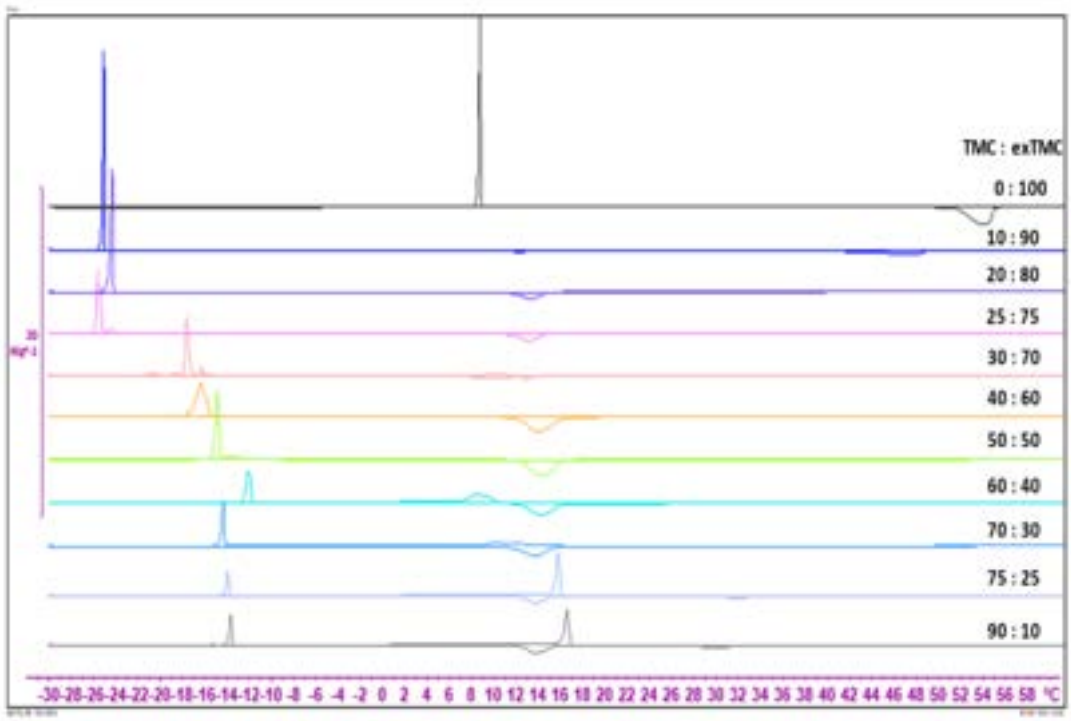

Figure 2-44. Stacking of the thermograms obtained for different TMC/exTMC mixtures at 2°C/min.

It is interesting to note that while performing the copolymerization reaction in bulk conditions, the formation of an eutectic melt was observed when the content in exTMC was higher than 30%. The mixture of monomers was thereupon melt at room temperature occurred (the two monomers are white solids with $T_{m,TMC}$ = 48 °C and $T_{m,exTMC}$ = 53.7 °C). DSC analysis of TMC/exTMC mixtures of different compositions, from 90/10 to 10/90 (**Figure 2-44** for the stacking of the thermograms obtained at 2°C/min), were carried out and revealed a melting point of ~14 °C for the eutectic (**Figure 2-45a**) with a composition close to 50/50 (**Figure 2-45b)** for the estimation of the eutectic composition by plotting the relative melting enthalpy of the eutectic as a function of the content in exTMC). The formation of eutectic melts is not common in ROCOP. It was reported previously when mixing TMC with L-lactide[131] and a 6CC deriving from desoxy-D-ribose.[132] Copolymerizations of exTMC and TMC were performed in bulk with propane-1,3-diol and dihydroxylated polybutadiene as initiators and monomer to initiator (OH group) ratios of 120 (**Table 2-3, entries 12-14**). The reactions proceeded efficiently and with good control ($Đ$ < 1.15).

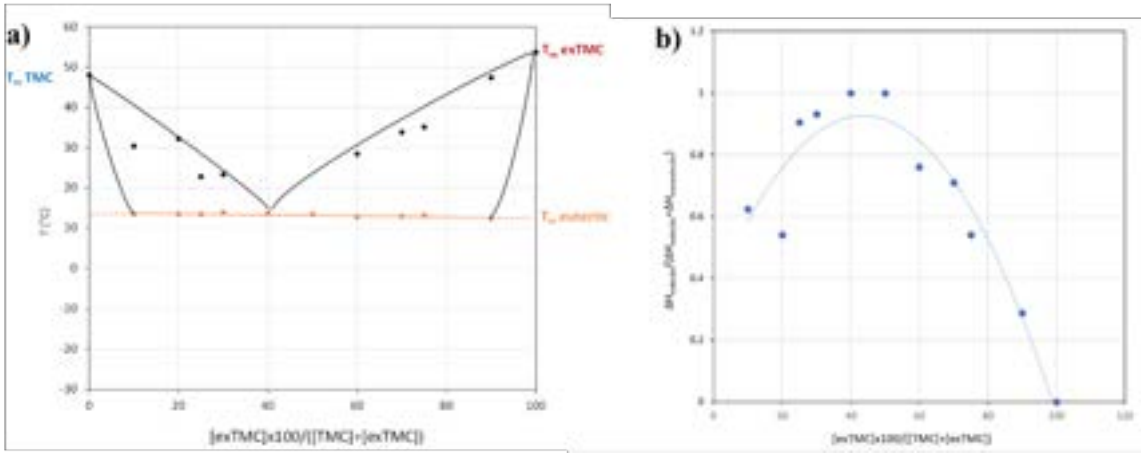

Figure 2-45. a) Melting points of different TMC/exTMC mixtures and b) Estimation of the eutectic composition by plotting the relative meting enthalpy of the eutectic as a function of the content in exTMC.

All these results show that, thanks to the controlled character of the MSA-catalyzed copolymerization and reactivity ratios values close to 1, it is possible to prepare P(TMC-*r*-exTMC) copolymers with almost perfect randomness and well-defined structures. Accordingly, copolymers with a defined content of methylidene groups distributed along the polymer chain in a highly uniform manner can be readily obtained.

2.2.3.2 *Random Copolymerization of TMC and the functionalized exTMC*

Table 2-4. Investigation of TOBnTMC/TMC copolymerization with different organocatalysts at DP60 with 30%TOBnTMC[a]

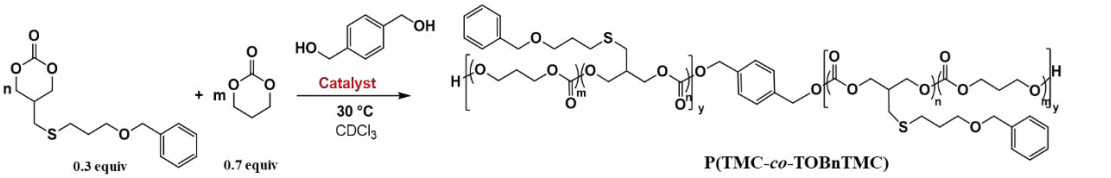

Run	Catalyst	time(h)	Conv^{TMC}	Conv^{TOBnTMC}	M_{nSEC},[b] (kDa)	$Đ$[b]
1	TBD	4	94	99	7.1	1.62
2	TU/DBU	30	89	100	4.3	1.28
3	DPP[c]	20	99	99	4	1.46
4	MSA	5	94	96	5.2	1.15

[a]Reaction conditions: 0.5-1 mol/L in $CDCl_3$ at 30°C. [b]In THF with calibration over PS standards, non-corrected values. [c]T = 60°C.

Simultaneous copolymerization of TOBnTMC and TMC (TMC/ TOBnTMC = 70/30) was next explored with BDM as initiator (monomer/BDM = 60/1). The organocatalysts TBD (BDM/TBD = 0.3), TU/DBU (BDM /TU/DBU = 1/1/1), DPP (BDM /DPP = 1/2) and MSA (BDM/MSA = 1/1) were used to draw a rapid comparison. All the reactions were carried out at 30°C with the exception of the one with DPP (60°C) (**Table 2-4**). The kinetics of monomer global conversion against time show that with TBD and MSA (**Figure 2-46a**), the conversion of both TOBnTMC and TMC monomers can exceed 90% within 5 hours. Nevertheless, the monomer conversion rate of the TBD was exceptionally rapid, achieving over 90% consumption within one hour. In contrast, TU/DBU and DPP showed less activity than TBD and MSA. It requires more than 20 hours to achieve 99% conversion.

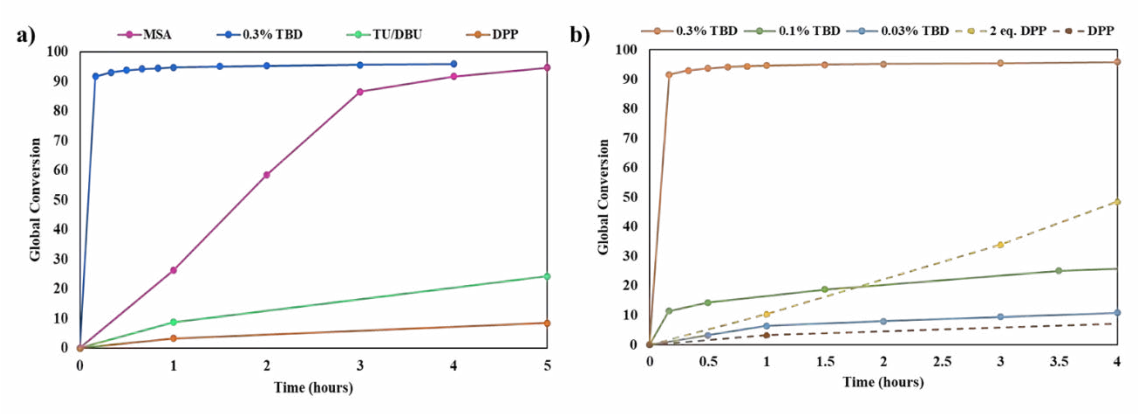

Figure 2-46. a) Monomer global conversion *vs* time for an TOBnTMC/TMC copolymerization with difference catalyst and b) Demonstrates the effects of using different ratios of TBD and DPP.

Table 2-5. Investigation of TOBnTMC/TMC copolymerization with different ratio of TBD and DPP organocatalysts at DP60 with 30%TOBnTMC[a]

Run	Catalyst	Time (h)	Mn [SEC,b] (kDa)	*Đ*
1	0.03TBD	120	2.7	1.38
2	0.1TBD	44	3.2	1.45
3	0.3TBD	4	7.1	1.62
4	1%DPP[c]	48	3.3	1.23
5	2 eq DPP[c]	20	4	1.46

[a]Reaction conditions: 0.5-1 mol/L in $CDCl_3$ at 30°C. [b]In THF with calibration over PS standards, non-corrected values. [c]T = 60°C.

The impact of varying TBD and DPP ratios is demonstrated in **Table 2-5 and Figure 2-46b.** Both of them shown increasing catalyst ratio affected on faster monomer conversion and higher M_n but boarder *Đ*. However, compared TBD and MSA, MSA appears to be more moderate in its behavior (appropriate M_n with narrow *Đ)*. Additionally, ROCOP of TMC and exTMC with MSA as the organocatalyst (1.3 mol%) leads to a more random incorporation of the two comonomers within the polymer chains compared to TBD, while maintaining good control over the polymerization and easy to remove. Therefore, continuing the experiment with MSA as the organocatalyst may be advantageous for working on tercopolymerization.

Table 2-6. TMC/TOBnTMC copolymerization catalyzed by MSA: variation of DP and composition[a]

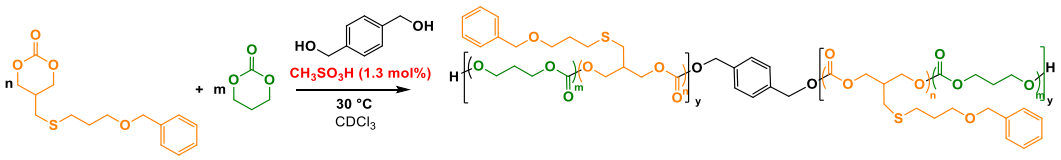

Entry	*M/I*	mol%TOBnTMC	M_{ntheo}	M_{nSEC}[b]	M_{nSEC}[c]	*Đ*
1	60	10	7.4	6.4	4.7	1.06
2	60	20	8.6	5.7	4.2	1.15
3	60	30	9.8	5.2	3.8	1.15
4	60	50	12.1	4.0	2.9	1.31
5	60	80	15.6	3.3	2.4	1.31
6	60	100	17.9	2.2	1.6	1.37
7	90	10	11.4	7.9	5.8	1.11
8	120	10	14.7	8.8	6.2	1.12

[a]Reaction conditions: 0.5-1 mol/L in $CDCl_3$ at 30°C. [b]In THF with calibration over PS standards, non-corrected values. [c]Values corrected using the correction factor reported for PTMC.[i]

ROCOP with an TOBnTMC/TMC monomer at DP 60 with increasing ratios of TOBnTMC from10-100 was first explored at 1.3% catalyst loading (relative to the monomer) in 1 mol/L chloroform solutions at 30 °C (**Table 2-6 entries 1-6**) using BDM as bifunctional initiator. The obtained results showed that an increasing ratio of TOBnTMC resulted in lower M_n and broader *Đ*, in particular for content in TOBnTMC > 30%. This indicates that utilizing a reduced content of TOBnTMC, with MSA as the catalyst and BDM as the initiator, could enhance the outcomes. The DP was increased from 30 to 120 with 10% of TOBnTMC (**Table 2-6, entries 7-8**). The results showed that M_n increased with DP, but could not reach 10 kDa by using BDM as initiator. However, it maintained a narrow *Đ* (*Đ* < 1.12).

Table 2-7. TMC/TOBnTMC (108/12) copolymerization catalyzed by MSA: variation of initiator and temperature (DP 120)[a]

Entry	Initiator	Temp (°C)	Time (h)	DP	M_n SEC,b	Đ
1	BDM	30	24	120	8.8	1.12
2	PDO	60	24	120	12.7	1.64
3	PDO	30	15	120	5.9	1.52
4	PDO[c]	30	6	120 (Bulk)	2.1	1.08
5	PDO[c]	60	7	120 (Bulk)	7.7	1.63

[a]Reaction conditions: 0.5-1 mol/L in $CDCl_3$ at 30°C. [b]In THF with calibration over PS standards, non-corrected values. [c] at 60°C.

PTMC-*co*-PTOBnTMC copolymers were synthesized with the desired M_n, ranging from 6 to 13 kDa, suitable for coating applications, thanks to the substitution of the initiator from BDM to PDO (**Table 2-7, entries 1 and 2**). However, reducing the temperature from 60 °C to 30 °C resulted in a decreased M_n when PDO was used as the initiator (**Table 2-7, entries 2, 3, and 5**). This effect was similarly observed in PTMC-*co*-PexTMC. Nevertheless, the bulk polymerization method proved unsuitable for the copolymerization of TMC and TOBnTMC, although it is effective for copolymerizing TMC and exTMC (**Table 2-7, entries 3 and 5**).

The ^{1}H NMR spectrum of a copolymer with DP = 60 and a TMC/TOBnTMC monomer ratio of 90/10 is shown in **Figure 2-47**. Efficient incorporation of the difunctional initiator BDM in the core of the polymer chains is confirmed by the presence of the signals k and l, corresponding to the methylene and aromatic groups of the initiator, at 5.16 and 7.40 ppm respectively. The signal (g) at 2.25 ppm is attributed to the CH moieties of TOBnTMC. CH_2OH chain-ends are observed at i' at 3.75 ppm corresponding to the TMC $C\underline{H}_2OH$ terminal units. Signal a associated with the aromatic group, signal c associated with the CH_2O groups of the thioether, and signal b, d, e, and f associated with the CH_2 of the TOBnTMC units, which impedes accurate integration. The relative integrals of signals h, and i (corresponding to the CH_2O moieties of TOBnTMC and TMC units, respectively), k and l (associated with the initiator) agree nicely with the initial monomer ratio (90/10) and monomer feed (DP60). Signals i and h are split due to the presence of homo- and heterodiades (TMC–TMC, TOBnTMC–TOBnTMC and TMC–TOBnTMC sequences).

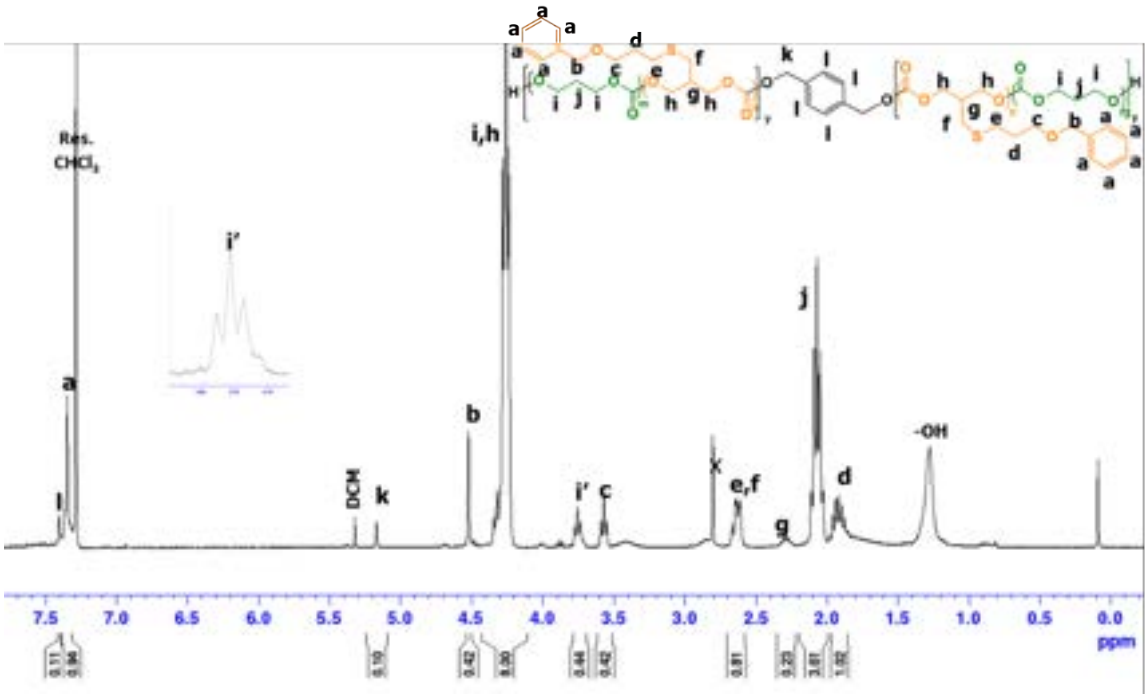

Figure 2-47. ^{1}H NMR spectra of a copolymer with DP = 60 and a TMC/TOBnTMC ($CDCl_3$, 300 MHZ, r.t).

The semi-logarithmic plot of the copolymerization reaction, utilizing monomer ratios of 80/20, 50/50, and 20/80 with DP 60, displays nearly overlapping conversion curves for the two monomers (**Figure 2-48**). These curves deviate upward from linearity, exhibiting quasi zero-order kinetics in the monomer rather than the classical first-order, a phenomenon previously reported for the ROP of lactones and 6CCs with acid catalysts such as MSA or DPP. [125–129] This behavior aligns with the higher basicity of the carbonate moieties in the cyclic monomer compared to those in the polymer chains, attributable to their differing conformations. To verify the similar reactivity of the two monomers in copolymerization, ^{1}H NMR monitoring was conducted for copolymerizations at TOBnTMC/TMC monomer ratios of 80/20, 50/50, and 20/80 with DP = 60. The relative reactivity ratios for TMC and TOBnTMC were determined using the Beckingham-Sanoja-Lynd (BSL) (**Figure 2-49a**) method from in situ ^{1}H NMR monitoring at various monomer ratios, similar to the procedures used for exTMC. The fitting curves from equations **E3** and **E4**, derived from the non-terminal model for ionic or pseudo-ionic catalytic copolymerizations (according to **Equations E1** and **E2**), indicate the reactivity ratio through the slope coefficient of the straight lines (Y) (**Figure 2-49b**). [125–129] Regardless of the monomer ratio, reactivity ratios between 0.95 and 0.99 for TOBnTMC and between 1.01 and 1.05 for TMC were observed (**Figure 2-49b**), confirming their

nearly identical reactivity ($\Gamma_{TOBnTMC} \approx \Gamma_{TMC} \approx 1$) and supporting the high randomness of the resulting copolymers. Furthermore, these findings suggest the feasibility of polymerizing a terpolymer consisting of TMC, exTMC, and TOBnTMC, given that their reactivity ratios are close to 1 ($\Gamma_{exTMC} \approx \Gamma_{TMC} \approx 1$ and $\Gamma_{TOBnTMC} \approx \Gamma_{TMC} \approx 1$). This proximity in reactivity facilitates the incorporation of two complementary pendant groups, thereby expanding potential applications.

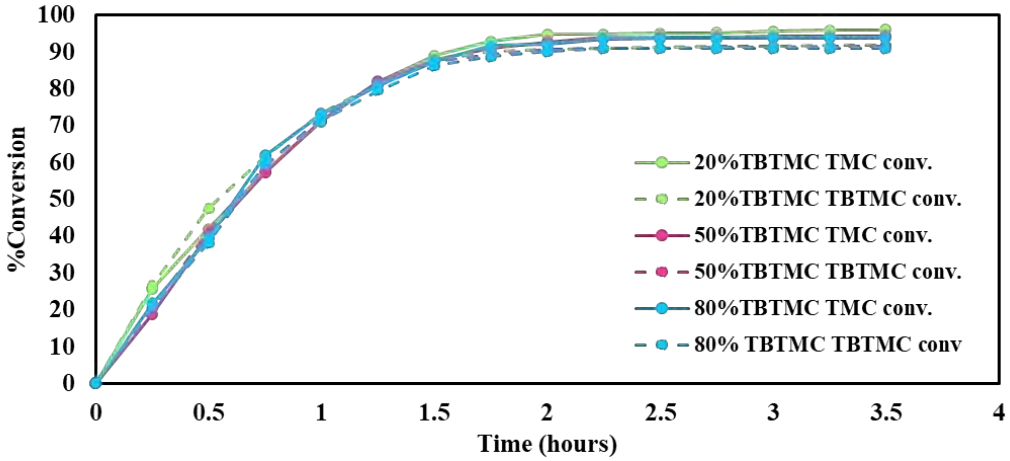

Figure 2-48. Monomer conversion *vs* time for an exTMC/TMC copolymerization (30/30/1 exTMC/TMC/initiator ratio).

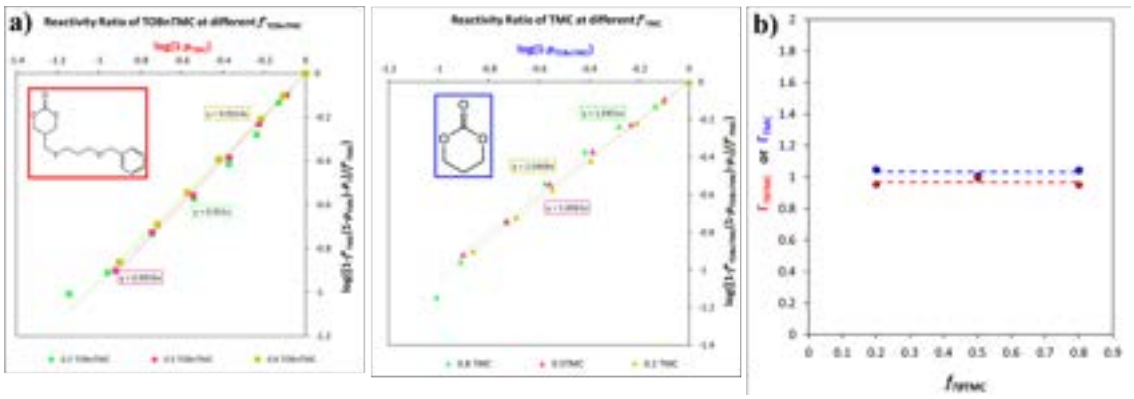

Figure 2-49. a) Determination of the reactivity ratios of the TMC and TOBnTMCmonomers by the Beckingham-Sanoja-Lynd (BSL) method.[123] and b) The fit of the determined reactivity ratios at different TMC/TOBnTMC ratios.

2.2.4 Tercopolymerization of TMC, exTMC, and functionalized exTMC

Given that $\Gamma_{exTMC} \approx \Gamma_{TMC} \approx 1$ and $\Gamma_{TOBnTMC} \approx \Gamma_{TMC} \approx 1$, this indicates potential for successful terpolymerization. Hence, simultaneous terpolymerization of exTMC, TOBnTMC and TMC (TMC/ exTMC/ TOBnTMC = 80/20/20) was next explored with BDM as initiator and MSA as catalyst in the same condition with copolymerization at DP120.

The ^{1}H NMR spectrum of a terpolymer with DP = 120 and a TMC/exTMC/TOBnTMC monomer ratio of 80/20/20 was shown in **Figure 2-50**. Efficient incorporation of the difunctional initiator BDM in the core of the polymer chains is confirmed by the presence of the signals m and n, corresponding to the methylene and aromatic groups of the initiator, at 5.16 and 7.40 ppm respectively. Two different CH_2OH chain-ends are observed (i' at 3.75 ppm and k' at 4.02 ppm) corresponding to the TMC, and exTMC C$\underline{H_2}$OH terminal units, respectively. Signal a associated with the aromatic group, signal c associated with the CH_2O groups of the thioether, and signal b, d, e, and f associated with the CH_2 of the TOBnTMC units, which impedes accurate integration. The signal at 5.38 and 2.25 ppm was attributed from CH_2 moieties of exTMC units and CH moieties of TOBnTMC, respectively. The relative integrals of signals h, i, and k (corresponding to the CH_2O moieties of TOBnTMC and TMC units, respectively), m and n (associated with the initiator) agree nicely with the initial monomer ratio (80/20/20) and monomer feed (DP120). Signals g', i', and l' are splitted due to the presence of homo- and heterodiades (TMC–TMC, TOBnTMC–TOBnTMC, exTMC-exTMC, TMC-exTMC, exTMC-TOBnTMC, and TMC–TOBnTMC sequences).

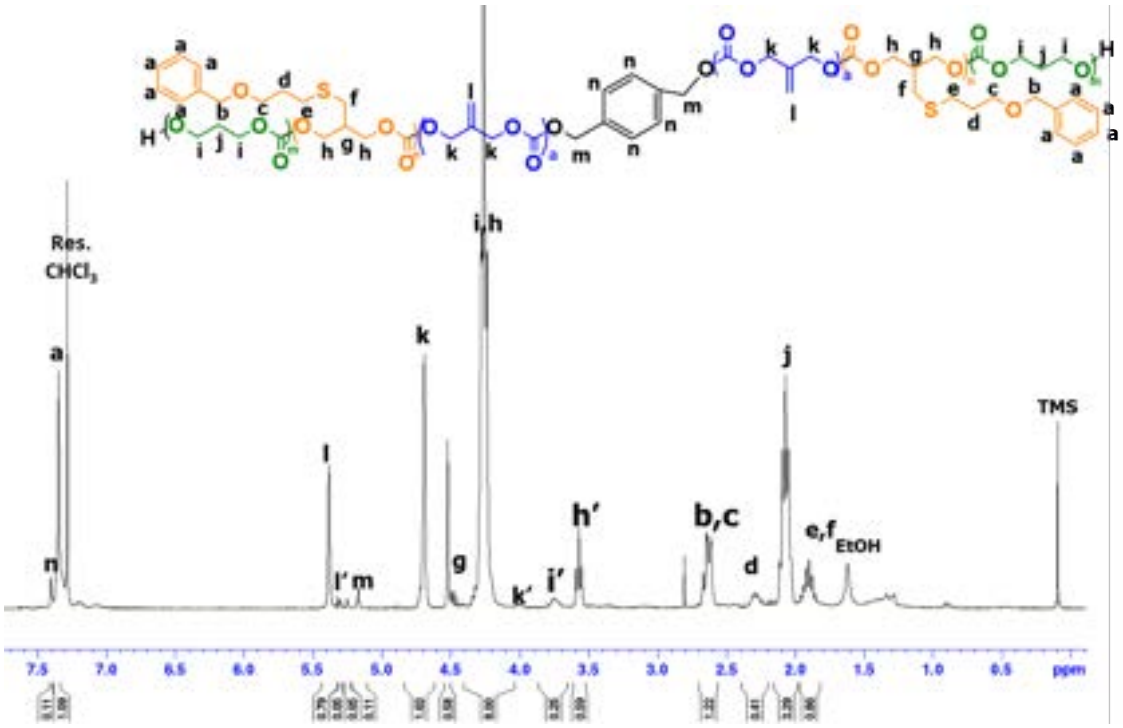

Figure 2-50. ^{1}H NMR spectra of a terpolymer with DP = 120 and a TMC/exTMC/TOBnTMC monomer ratio of 80/20/20 ($CDCl_3$, 300 MHZ, r.t).

Table 2-8. TMC/exTMC/TOBnTMC terpolymerization catalyzed by MSA: variation of initiator, DP, and monomer ratio[a]

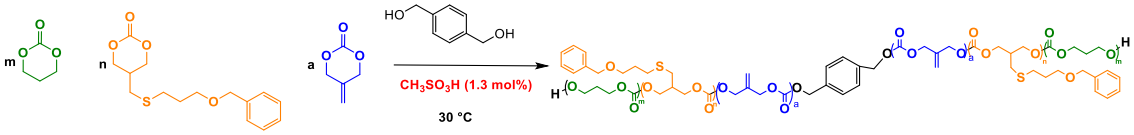

Entry	DP	Initiator	TMC : exTMC : TBTMC	M_n [SEC,b]	$Đ$
1	60	BDM	20:20:20	5.6	1.48
2	60	BDM	40:10:10	10	1.09
3	120	BDM	80:20:20	7.8	1.81
4	120	PDO[c]	80:20:20	12.6	2.07

[a]Reaction conditions: 0.5-1 mol/L in $CDCl_3$ at 30°C. [b]In THF with calibration over PS standards, non-corrected values. [c] at 60°C.

Poly(TOBnTMC)-*co*-Poly(TMC)-*co*-Poly(exTMC) were successfully prepared by using MSA as a catalyst. It was found that the monomer conversion rate of the three monomers was almost the same (**Table 2-8, entry 1** and **Figure 2-51**) which could suggest that $\Gamma_{TBTMC} \sim \Gamma_{TMC} \sim \Gamma_{exTMC} \sim 1$. Therefore, it could be confirmed that the terpolymer of exTMC, TMC, and TOBnTMC is Random terpolymer. The substitution of the initiator from BDM to PDO resulted in a higher M_n, a result consistent with the

Poly(TOBnTMC)-*co*-Poly(TMC)-*co*-Poly(exTMC). These results provide the opportunity to engage in multifunctional polymer design, aiming to achieve properties that are adjustable for specific applications. However, the low M_n of the obtained terpolymers, as well as their rather broad $Đ$ (up to 2) suggest that side-reaction occur.

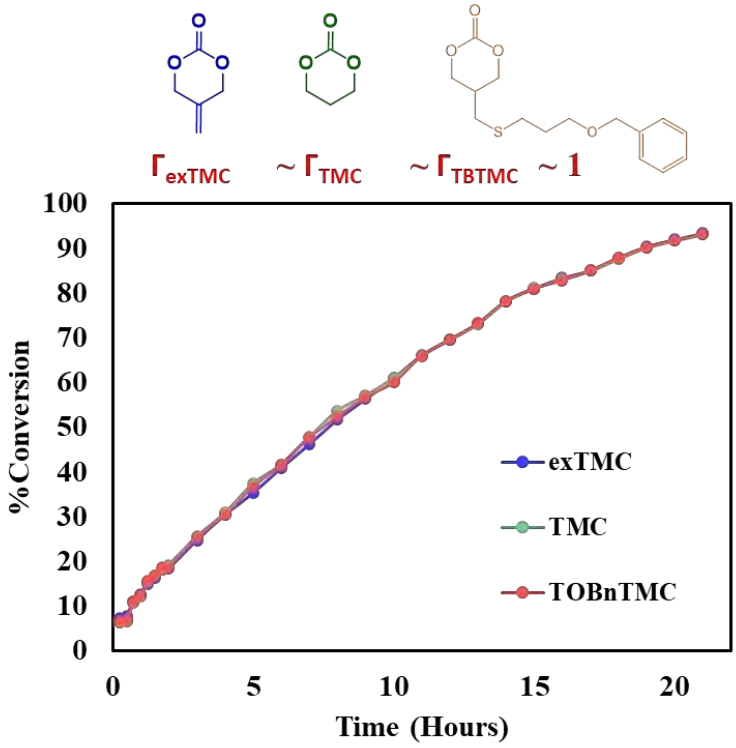

Figure 2-51. The monomer conversion of TMC, exTMC, and TOBnTMC tercopolymer (DP60 : TMC/ exTMC/ TOBnTMC = 20/20/20).

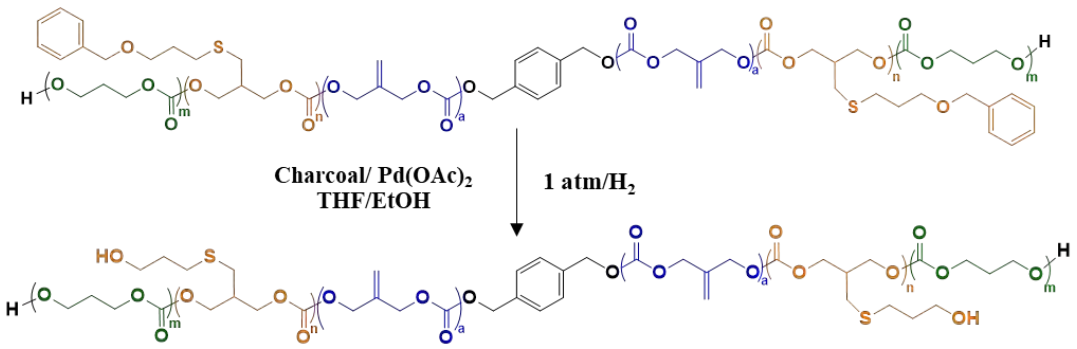

Figure 2-52. The debenzylation of Poly(TOBnTMC)-*co*-Poly(TMC)-*co*-Poly(exTMC) containing TOBn groups using charcoal/ $Pd(OAc)_2$ as a catalyst.

To enhance the versatility of the tercopolymer for acquiring protic multifunctional groups, the functional groups in the synthesized copolymers were initially protected. Consequently, the subsequent deprotection of these groups is crucial. The successful demonstration of benzyl group deprotection in TOBnTMC within the Poly(TOBnTMC)-*co*-Poly(TMC)-*co*-Poly(exTMC) **(Figure 2-52)**, which aimed to release hydroxyl groups, underscores the effectiveness of this approach. Notably, palladium on carbon (Pd/C) serves as an efficient catalyst for both hydrogenolysis and debenzylation processes, as documented in recent studies.[108,133] An innovative approach has been developed involving Pd/C nanoparticles, which have been reported to effectively catalyze hydrogenolysis of *O*-benzyl groups.[134] The *in situ* generation of an active Pd^0/C catalyst was accomplished by combining charcoal (90 wt% relative to Pd) and $Pd(OAc)_2$ (0.05 mol%) in a THF solution, with the mixture stirred for 30 minutes prior to application. Using this methodology, the hydrogenolysis of 10% TOBnTMC in Poly(TOBnTMC)-*co*-Poly(TMC)-*co*-Poly(exTMC) was conducted under controlled conditions (50% w/w Pd nanoparticles, room temperature, under an H_2 atmosphere, THF/EtOH ratio 9:1). After the complete removal of benzyl protecting groups, an excess Pd/C was removed by filtration over Celite and washing by DCM 3 times following by solvent evaporation. The crude was dissolved in DCM, precipitated in cold diethyl ether, and dried under vacuum overnight to yield a sticky material. The complete removal of the benzyl protecting groups (–OBn) is easily verified from the disappearance of all aromatic signals belonging to the –OBn in the ^{1}H NMR spectrum, compared to the ^{1}H NMR spectra of protected copolymers (**Figure 2-53**). Although debenzylation was achieved within 4 hours, inadvertent hydrogenation of the double bond in exTMC was also observed. Consequently, it is essential to modify exTMC through a thiol-ene reaction to secure the intended functional group before proceeding with debenzylation using Pd/C.

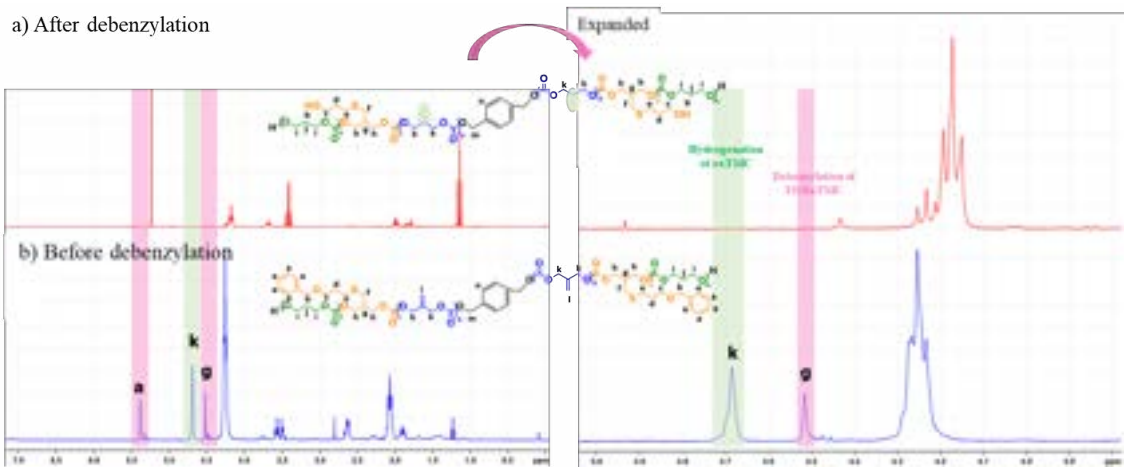

Figure 2-53. ^{1}H NMR spectra ($CDCl_3$, 300 MHz) of Poly(TOBnTMC)-*co*-Poly(TMC)-*co*-Poly(exTMC) containing 10% of TOBn; a) after deprotected copolymer (Hydrogenolysis), b) before deprotected copolymer (with protection TOBn).

2.2.5 Preparation of functionalized polycarbonates by thiol-ene reaction (post-polymerization functionalization)

To illustrate the feasibility of post-polymerization modification functionalization, we turned to the thiol-ene reaction.[132] Reactions were carried out with two different thiols bearing *non-protected protic functional* groups (hydroxyl and carboxylic), namely thioglycerol and thioglycolic acid. 1.51 g of copolymer **P12** (30% content in exTMC, DP 120, M_n = 12700 g/mol) was dissolved in dry THF (2.5 mL), DMPA (30 mg, 2%wt) and thioglycerol (0.41 mL, 4.7 mmol, ~1 equiv.) were added and the reaction media was irradiated at 365 nm with a UV-lamp. After complete disappearance of the vinylic signals, the solvent was evaporated, and the polymer isolated by precipitation on cold methanol.

Table 2-9. Thiol-ene click reactions with non-protected functionalized thiols.[a]

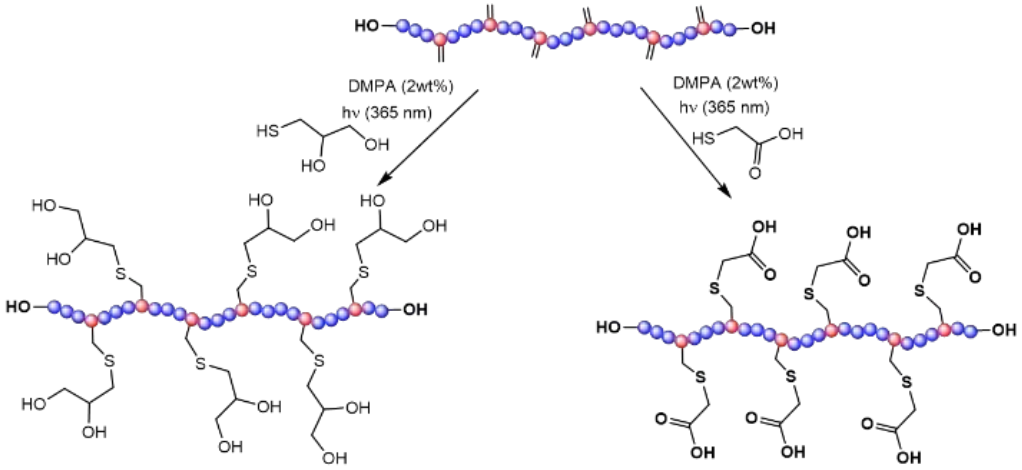

Starting copolymer	% exTMC	Thiol	%function[b]	$M_n^{SEC,c}$	$Đ^c$
P12[c]	30	Thioglycolic acid	29	12800	1.20
P13[d]	10	Thioglycolic acid	9	10800	1.19
P12[c]	30	Thioglycerol	27	11600	1.12
P13[d]	10	Thioglycerol	9	9390	1.23

[a]Reaction conditions: [b] Determined by ^{1}H NMR. [c] THF with calibration PS standard non-corrected. [c] 30% content in exTMC, M_n = 12700 g/mol, $Đ$ = 1.15. [d] 10% content in exTMC, M_n = 10600 g/mol, $Đ$ = 1.14.

Click addition reactions were carried out on two copolymers with DP120 and different monomer compositions (**Table2-9, P12 and P13** with 30 and 10 % contents in exTMC, respectively) under radical conditions, using DMPA (2,2-dimethoxy-2-phenyl acetophenone) as initiator (2 wt%) and irradiation at 365 nm. After few hours of reaction at room temperature, ^{1}H NMR monitoring showed almost complete disappearance of the signals at 4.70 and 5.40 ppm, corresponding to the O-CH_2-C(=CH_2)CH_2-O sequences of the exTMC units after post-polymerization modification by thiolglycerol (**Figure 2-54a**) and thioglycolic acid(**Figure 2-55a**),[123] and the appearance of new broad multiplet signals: (i) at 2.80, 3.50-3.60 and 3.65-3.90 ppm corresponding to the CH_2 and CH groups deriving from thioglycerol (e, f and g), (ii) at 2.35 and 2.70-2.80 ppm for the new CH and CH_2 groups resulting from the thio-ene addition to the C=CH_2 moiety (c and d). All these data are consistent with clean chemo- and regio-selective addition of the functionalized thiol to the C=CH_2 moieties.

Moreover, SEC analysis confirms that the thiol-ene reaction occurs without affecting the integrity of the polymer chains or causing reticulation, since M_n and $Đ$ values are in the same range than the starting copolymers after post-modification by thiolglycerol (**Figure 2-54b** and **Table 2-9**) and thioglycolic acid (**Figure 2-55b** and **Table 2-9**).

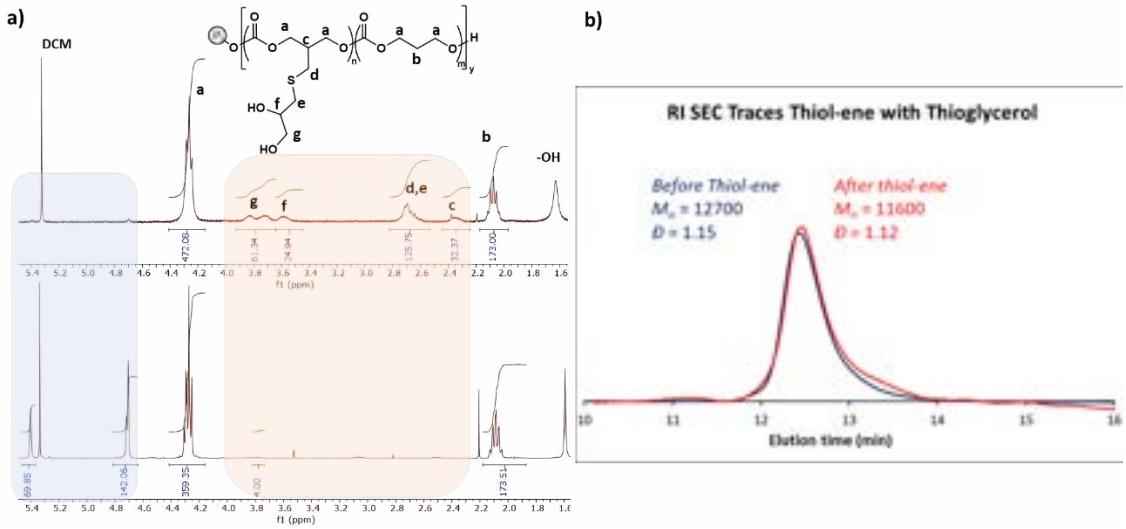

Figure 2-54. a) Stacking of the ^{1}H NMR spectra of a TMC/exTMC copolymer (30% exTMC) before (bottom) and after (top) post-polymerization modification functionalization by thiol-ene reaction with thioglycerol. b) SEC traces of the corresponding copolymers

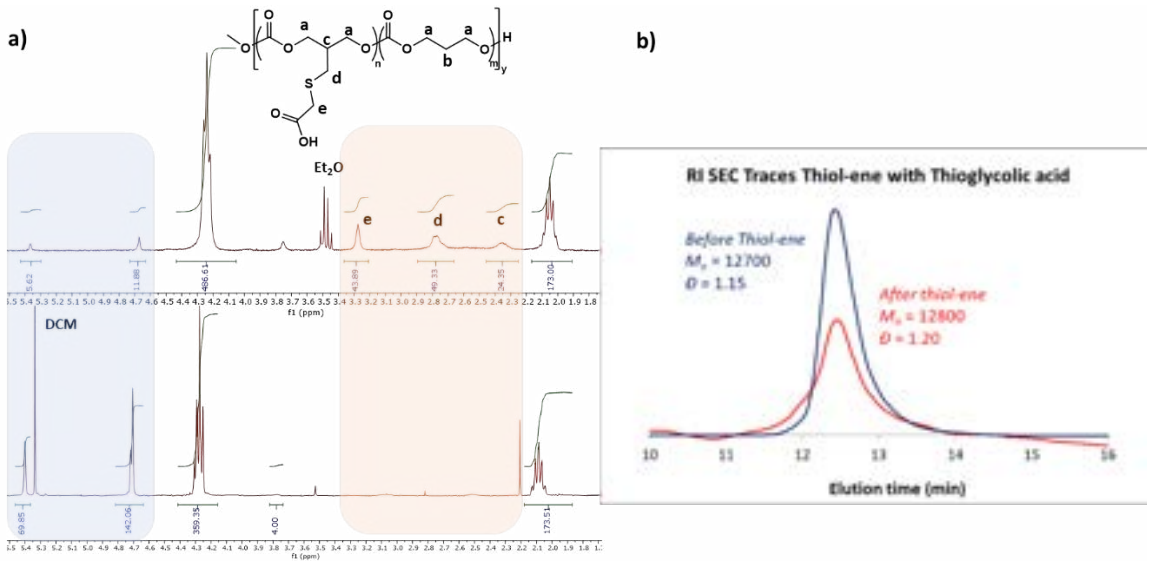

Figure 2-55. a) Stacking of the ^{1}H NMR spectra of a TMC/exTMC copolymer (30% exTMC) before (bottom) and after (top) post-polymerization modification functionalization by thiol-ene reaction with thioglycolic acid. b) SEC traces of the corresponding copolymers.

2.3 Conclusions

The aim of this research topic is presented with the development of new biodegradable material with low toxicity and degradability adjustable based on the advanced functionalities by pre or post modification *via* thio-en reaction. This study demonstrates that exTMC, a sustainable 6CCs derived from glycerol and CO_2, along with its functionalized variants, are preferred comonomers for achieving random copolymerization with TMC under mild conditions. To achieve the purpose, Poly(TMC)-*co*-Poly(exTMC) was prepared by using MSA as organocatalyst with different exTMC content, in order to adjust the functionalities. exTMC and TMC copolymerize in a controlled manner and with relative reactivity ratios close to 1. Copolymers of well-defined structures (M_n, composition, molecular distributions) and high randomness can thereby be easily prepared. The methylene groups distributed along the polymer chains were then transformed by thiol-ene click reaction with thioglycolic acid or thioglycerol to give access to APCs with adjustable amounts of COOH or OH functional groups uniformly distributed along the polymer chains with DP120 and functional group content from 1-30%. Polycarbonates with highly regular distribution of functional groups along the polymer chains can be prepared in a controlled and efficient manner thanks to this approach (only 3 steps from 1, a biobased diol, and CO_2), without using any protecting group. This achievement will give us the opportunity to investigate the impact of the amount and distribution (gradient vs random) of functional groups on the copolymer (APCs) properties. Additionally, TOBnTMC was successfully prepared *via* click thiol-ene on exTMC, followed by copolymerization with TMC monomers to assess polymerization conditions and kinetics. The copolymerization of TOBnTMC and TMC, catalyzed by MSA, achieved reactivity ratios close to 1. However, the copolymer displayed broader dispersity. It was also observed that ACE acted competitively in the polymerization process, significantly enhancing the integration at the chain end. Furthermore, the terpolymerization of TMC, exTMC, and TOBnTMC demonstrated that the monomer conversion rates of the three monomers were nearly identical, which could indicate that $\Gamma_{TBTMC} \sim \Gamma_{TMC} \sim \Gamma_{exTMC} \sim 1$. Consequently, it can be concluded that Poly(TOBnTMC)-*co*-Poly(TMC)-*co*-Poly(exTMC) is Random terpolymer. These findings enable the pursuit of multifunctional polymer design, targeting to develop adjustable properties with controlled randomness of monomers along the polymer chain, specifically tailored for designated applications. (**Figure 2-57**). In order to convince to fulfill biomedical materials applications, thermal properties and multifunctionalities, such as drug release control, biological function, animal test, and degradation experiment were performed and discussion in the Chapter III.

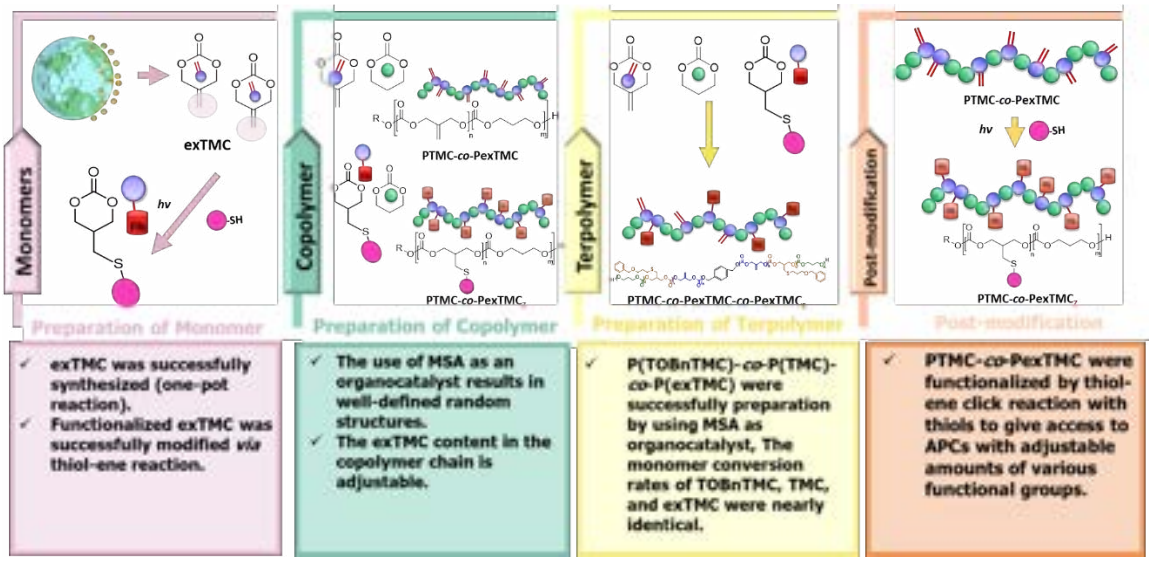

Figure 2-57. Summary of Conclusions for Chapter II

2.4 Experimental

2.4.1 Synthesis

2.4.1.1 Preparation functionalized 6CCs

2.4.1.1.1 *Preparation of exTMC*

2-Methylene-1,3-propanediol (25 g, 284 mmol) and tosylchloride (54.1g, 284 mmol, 1 equiv.) were charged in a 5 L reactor followed by anhydrous acetonitrile (1.5 L). The atmosphere of the flask was exchanged for CO_2 and the solution saturated with CO_2 by bubbling. Under a continuous feed of gas, 2,2,6,6-tetramethylpiperidine (96 mL, 568 mmol, 2 equiv.) was added dropwise at 0 °C and the reaction was left to reach room temperature with stirring. After approximately 20 minutes, a bright white precipitate forms and CO_2 stopped being fed to the reactor. After overnight, the liquid phase was separated by centrifugation (5 minutes at 5000 rpm). The solid was then extracted with acetone and separated again by centrifugation (5 minutes at 5000 rpm). The combined solvent phases were then removed in vacuo. Tosyl salts were precipitated by adding ethyl acetate (3 mL per g) to the crude. The filtrate was then placed at -30°C to further eliminate traces of tosyl salts. After filtration, exTMC was purified twice by crystallization in DCM/Et_2O (1:20) at -80°C affording 18 g (yield ~56 %) of exTMC. **^{1}H–NMR (300 MHz, $CDCl_3$):** δ ppm 5.32 (quint., *J* = 1.4 Hz, 2H, =C*H*$_2$), 4.86 (t, *J* = 1.4 Hz, 4H, OCH_2). Spectroscopic data are in accordance with the literature.[114]

2.4.1.1.2 *Preparation of functionalized exTMC*

Functionalized exTMC by thioglycolic acid (TMC-COOH)

exTMC (529 mg, 4.64 mmol) was dissolved in dry THF (4.5 mL), DMPA (10 mg, 2%wt) and thioglycolic acid (471 mg, 5.10 mmol, ~1.1 equiv.) were added and the reaction media was irradiated at 365 nm with a UV-lamp. After complete disappearance of the vinylic signals, the solvent was evaporated and the monomer isolated by precipitation on diethyl ether and placed at -30°C overnight to further eliminate the excess thiol and initiator. Then, the diethyl ether layer was removed, and the obtained solid compound was washed with diethyl ether three times affording 592 mg (yield ~66 %) of TMC-COOH. **^{1}H–NMR (300 MHz, D_2O):** 4.61 and 4.37 (d, *J* = 6 Hz, 4H, OCH_2), 3.36 (m, 1H, CH), 2.68 (d , *J* = 4.2 Hz, 2H, CH_2S), and 2.48 (m , 2H, SCH_2CO).

Functionalized exTMC by 3-(benzyloxy)propane-1-thiol (TOBnTMC)

exTMC (500 mg, 4.35 mmol) was dissolved in dry DCM (5 mL), DMPA (20 mg, 4%wt) and 3-(benzyloxy)propane-1-thiol[121] (2378 mg, 13.05 mmol, ~3 equiv.) were added and the reaction media was irradiated at 365 nm with a UV-lamp. After complete

disappearance of the vinylic signals, the solvent was evaporated and the monomer isolated by precipitation on diethyl ether and placed at -30°C overnight to further eliminate the excess thiol and initiator for 3 times. Then purification the obtained compound by column chromatography (using diethyl ether and cyclohexane) affording 901 mg (yield ~70 %) of TOBnTMC. Notably, the excess 3-(benzyloxy)propane-1-thiol could be recycled for use again in subsequent reactions. **^{1}H–NMR (300 MHz, $CDCl_3$):** 7.32 (s, 5H, CH_{Ar}), 4.58 (s, 2H, OCH_2Ar), 4.45 and 4.25 (d, J = 6 Hz, 2H, OCH_2), 3.58 (t, J = 6 Hz, 2H, CH_2O), 2.71 (t, J = 6 Hz, 2H, SCH_2), 2.62 (d, J = 6 Hz, 2H, CH_2S), 2.35 (m, J = 6 Hz, 1H, CH), and 1.86 (m, J = 6 Hz, 2H, CH_2) **^{13}C NMR ($CDCl_3$, 300 MHz):** 148.1 (s, C), 138.2 (s, C), 128.4 (s, C-CH), 127.6 (s, CH-CH), 73.1 (s, OCH_2-C), 71.0 (s, CH-CH_2S) , 68.3 (s, CH_2-CH_2O) , 31.3 (s, CH-CH_2S) , 29.9 (s, SCH_2-CH_2) , 29.7 (s, CH) , 29.6 (s, CH_2).

2.4.1.2 Organocatalyzed homopolymerization of exTMC and the functionalized exTMC

2.4.1.2.1 *Organocatalyzed homopolymerization of exTMC (DP30)*

exTMC (100 mg, 0.87 mmol, 30 equiv.) was dissolved in $CDCl_3$ ([exTMC] = 1 mol/L, 0.8 mL). The initiator, DMBA (7 mg, 3 10^{-2} mmol, 1 equiv.) and methane sulfonic acid (MSA) (0.78 µL, 1.2 10^{-2} mmol, 0.4 equiv.) were successively added. The reaction mixture was stirred at 30 °C. The conversion of the monomer was monitored by ^{1}H NMR spectroscopy. An excess of diisopropylethylamine was added to neutralize the catalyst after 5 hours of stirring, and the reaction media was concentrated by solvent evaporation under vacuum. The polymer was then precipitated in cold methanol, filtered and dried under vacuum. The theoretical number-average molecular weight (M_n,^{theo}) of PexTMC was calculated using the following equation:

M_n,^{theo}(Da)= Mass of initiator + (m×114.1)

Where: m = Degree of polymerization of exTMC

Yield: 85 %. SEC (THF): M_n = 3 000 g/mol; $Đ$ = 1.07. **^{1}H NMR ($CDCl_3$, 300 MHz):** 6.55 (d, J = 2.3 Hz, 2H, CH_{Ar}), 6.46 (t, J = 2.3 Hz, 1H, CH_{Ar}), 5.40 (s, 22x2H, $=CH_{2,polymer}$), 4.31 and 4.26 (s, 1H each, $=CH_{2,chain\text{-}end}$), 5.13 (s, 2H, $ArCH_2O$), 4.70 (s, 24x4H, $OCH_{2polymer}$), 4.20 (d, J = 5.9 Hz, 2H CH_2OH), 3.82 (s, 6H, OCH3), 1.9 (m, 1H, OH). **^{13}C NMR ($CDCl_3$, 300 MHz):** 154.5 (s, CO), 137.4 (s, C=), 118.5 (s, $=CH_2$), 67.8 (s, OCH_2).

2.4.1.2.2 *Organocatalyzed homopolymerization of TOBnTMC (DP60)*

TOBnTMC (150 mg, 0.51 mmol, 60 equiv.) was dissolved in $CDCl_3$ ([TOBnTMC] = 1 mol/L, 0.5 mL). The initiator, BDM (1.16 mg, 0.84 10^{-2} mmol, 1 equiv.) and MSA (0.54 µL, 0.83 10^{-2} mmol, 0.4 equiv.) were successively added. The reaction mixture was stirred at 30 °C. The conversion of the monomer was monitored by ^{1}H NMR spectroscopy. An excess of diisopropylethylamine was added to neutralize the catalyst after 7 hours of stirring, and the reaction media was concentrated by solvent evaporation under vacuum. The polymer was then precipitated in cold methanol, filtered and dried under vacuum. M_n,^{theo} of POBnTMC was calculated using the following equation:

M_n,^{theo}(Da)= Mass of initiator + (p ×182.3)

Where: p = Degree of polymerization of TOBnTMC

Yield: 56 %. SEC (THF): M_n = 2 200 g/mol; $Đ$ = 1.37. **^{1}H NMR ($CDCl_3$, 300 MHz):** 7.46 (d, J = 6 Hz, 4H, CH_{Ar}), 7.32 (s, 5H, CH_{Ar}), 5.18 (s, 2H, OCH_2), 4.51 (s, 2H, OCH_2Ar), 4.25 (t, J = 6 Hz, 4H, $OCH_{2polymer}$), 3.71 (t, J = 6 Hz, 2H, 1H each, $CH_2OH_{,chain-end}$),3.55 (t, J = 6 Hz, 2H, CH_2O), 2.62 (pen, J = 6 Hz, 2H, CH_2), 2.23 (m, J = 6 Hz, 1H, CH), 1.89 (m, J = 6 Hz, 2H, CH_2S), and 1.84 (pen, J = 6 Hz, 2H, SCH_2)

2.4.1.3 Random copolymerization of TMC and exTMC and random copolymerization of TMC and the functionalized exTMC

2.4.1.3.1 *Random Copolymerization of TMC and exTMC (DP60 with 50%exTMC)*

exTMC (112 mg, 0.98 mmol, 30 equiv.) and TMC (100 mg, 0.98 mmol, 30 equiv.) were dissolved in $CDCl_3$ ([exTMC] = 1 mol/L, 2 mL). The initiator, DMBA (4.5 µg, 3.3 10^{-2} mmol, 1 equiv.) and MSA (1.68 µL, 2.6 10^{-2} mmol, 0.8 equiv.) were successively added. The reaction mixture was stirred at 30 °C. The conversion of the comonomers was monitored by ^{1}H NMR spectroscopy. An excess of diisopropylethylamine was added to neutralize the catalyst after 8 hours, and the solvent was evaporated under vacuum. The polymer was precipitated in cold methanol, then filtered and dried under vacuum. The M_n,^{theo} of PTMC-*co*-PexTMC was calculated using the following equation:

M_n,^{theo}(Da)= Mass of initiator + (n×102.09) + (m×114.1)

Where: n = Degree of polymerization of TMC

m = Degree of polymerization of exTMC

Yield: 93 %. SEC (THF): M_n = 5 300 g/mol; $Đ$ = 1.08. **^{1}H NMR ($CDCl_3$, 300 MHz):** 7.40 (s, *4*H, CH_{Ar}), 5.40 (s, 28x2H, $=CH_{2,polymer}$), 4.31 and 4.26 (s, 1H each, $=CH_{2,chain\text{-}end}$), 5.13 (s, 2H, $ArCH_2O$), 4.70 (s, 29x4H, $OCH_{2polymer}$), 4.25 (m, 29x4H, $OCH_{2polymer}$), 4.20 (d, J = 5.9 Hz, 2H CH_2OH_{exTMC}), 3.76 (m, 2H, CH_2OH_{TMC}), 2.05 (m, 29x2H, CH_2), 1.9 (m, 2H, OH). **^{13}C NMR ($CDCl_3$, 300 MHz):** 154.9 (s, $CO_{TMC\text{-}TMC}$), 154.8 (s, $CO_{TMC\text{-}exTMC}$), 154.5 (s, CO_{exTMC}), 137.4 (s, C=), 128.5 (s, Ar), 118.5 (s, $=CH_2$), 67.8 (s, $OCH_{2exTMC\text{-}exTMC}$), 67.7 (s, $OCH_{2exTMC\text{-}TMC}$), 64.4 (s, $OCH_{2TMC\text{-}exTMC}$), 64.4(s, $OCH_{2TMC\text{-}TMC}$), 28.0 (s, CH_{2TMC}).

2.4.1.3.2 *Random Copolymerization of TMC and TOBnTMC (DP60 with 10% TOBnTMC)*

TOBnTMC (32.31 mg, 0.11 mmol, 6 equiv.) and TMC (100 mg, 0.98 mmol, 54 equiv.) were dissolved in $CDCl_3$ ([exTMC] = 1 mol/L, 1 mL). The initiator, BDM (2.5 mg, 1.8 10^{-2} mmol, 1 equiv.) and MSA (0.92 µL, 1.42 10^{-2} mmol, 0.8 equiv.) were successively added. The reaction mixture was stirred at 30 °C. The conversion of the comonomers was monitored by ^{1}H NMR spectroscopy. An excess of diisopropylethylamine was added to neutralize the catalyst after 8 hours, and the solvent was evaporated under vacuum. The polymer was precipitated in cold methanol, then filtered and dried under vacuum. $M_{n,}^{theo}$ of PTMC-*co*-PTOBnTMC was calculated using the following equation:

$M_{n,}^{theo}$(Da)= Mass of initiator + (n×102.09) + (p×182.3)

Where: n = Degree of polymerization of TMC

p = Degree of polymerization of TOBnTMC

Yield: 87 %. SEC (THF): M_n = 6 400 g/mol; $Đ$ = 1.06 **^{1}H NMR ($CDCl_3$, 300 MHz):** 7.46 (d, J = 6 Hz, 4H, CH_{Ar}), 7.32 (s, 5H, CH_{Ar}), 5.18 (s, 2H, OCH_2), 4.51 (s, 2H, OCH_2Ar), 4.25 (t, J = 6 Hz, 8H, $OCH_{2polymer}$), 3.74 (t, J = 6 Hz, 2H, CH_2OH_{TMC}), 3.55 (t, J = 6 Hz, 2H, $CH_2OH_{TOBnTMC}$), 2.62 (pen, J = 6 Hz, 2H, CH_2O), 2.57 (t, J = 6 Hz, 2H, CH_2), 2.23 (m, J = 6 Hz, 1H, CH), 2.05 (pen, J = 6 Hz, 2H, CH_2), 1.89 (m, J = 6 Hz, 2H, CH_2S), and 1.84 (m, J = 6 Hz, 2H, SCH_2)

2.4.1.4 Tercopolymerization of TMC, exTMC, and functionalized exTMC (DP120 with 20%exTMC, 20%TOBnTMC, and 80%TMC)

exTMC (27.95 mg, 0.24 mmol, 20 equiv.), TOBnTMC (72.60 mg, 0.24

mmol, 20 equiv.) and TMC (100 mg, 0.98 mmol, 80 equiv.) were dissolved in $CDCl_3$ ([exTMC] = 1 mol/L, 2 mL). The initiator, BDM (1.7 mg, 1.2 10^{-2} mmol, 1 equiv.) and MSA (0.92 µL, 1.42 10^{-2} mmol, 0.8 equiv.) were successively added. The reaction mixture was stirred at 30 °C. The conversion of the comonomers was monitored by ^{1}H NMR spectroscopy. An excess of diisopropylethylamine was added to neutralize the catalyst after 8 hours, and the solvent was evaporated under vacuum. The polymer was precipitated in cold methanol, then filtered and dried under vacuum. M_n,^{theo} of PTMC-*co*-PexTMC-*co*-PTOBnTMC was calculated using the following equation:

M_n,^{theo}(Da)= Mass of initiator + (n×102.09) + (m×114.1) + (p ×182.3)

Where: n = Degree of polymerization of TMC

m = Degree of polymerization of exTMC

p = Degree of polymerization of TOBnTMC

Yield: 91 %. SEC (THF): M_n = 7 800 g/mol; $Đ$ = 1.81. **^{1}H NMR ($CDCl_3$, 300 MHz):** 7.46 (d, J = 6 Hz, 4H, CH_{Ar}), 7.32 (s, 5H, CH_{Ar}), 5.39 (s, 4H, OCH_{2exTMC}), 5.18 (s, 2H, OCH_2), 4.68 (s, 2H, $=CH_{2exTMC}$), 4.51 (s, 2H, OCH_2Ar), 4.25 (t, J = 6 Hz, 8H, $OCH_{2polymer}$), 4.31 (t, J = 6 Hz, 2H, CH_2OH_{exTMC}), 3.74 (t, J = 6 Hz, 2H, CH_2OH_{TMC}), 3.55 (t, J = 6 Hz, 2H, $CH_2OH_{TOBnTMC}$), 2.62 (pen, J = 6 Hz, 2H, CH_2O), 2.57 (t, J = 6 Hz, 2H, CH_2), 2.23 (m, J = 6 Hz, 1H, CH), 2.05 (pen, J = 6 Hz, 2H, CH_2), 1.89 (m, J = 6 Hz, 2H, CH_2S), and 1.84 (m, J = 6 Hz, 2H, SCH_2)

2.4.1.5 Preparation of functionalized polycarbonates by Thiol-ene reaction (Post-polymerization modification)

1.51 g of Copolymer P12 (30% content in exTMC, DP 120, M_n = 12 700 g/mol) was dissolved in dry THF (2.5 mL), DMPA (30 mg, 2%wt) and Thioglycerol (0.41 mL, 4.7 mmol, ~1 equiv.) were added and the reaction media was irradiated at 365 nm with a UV-lamp. After complete disappearance of the vinylic signals, the solvent was evaporated and the polymer isolated by precipitation on cold methanol. Yield: 1.51 g (75%). SEC (THF): M_n = 9 400 g/mol; $Đ$ = 1.23. **^{1}H NMR ($CDCl_3$, 300 MHz):** 4.25 (m, 118x4H, $OCH_{2polymer}$), 3.90−3.65 (m, 30x2H, CH_2OH), 3.60−3.50 (m, 25x1H, C*H*OH), 2.80−2.55 (m, 30x4H, CH_2-S-CH_2), 2.30 (m, 30x1H, $CH_{polymer}$), 2.15−2.00 (m, 86x2H, $CH_{2polymer}$).

2.5 References

(1) Yu, W.; Maynard, E.; Chiaradia, V.; Arno, M. C.; Dove, A. P. Aliphatic Polycarbonates from Cyclic Carbonate Monomers and Their Application as Biomaterials. *Chem. Rev.* **2021**, 10865–10907. https://doi.org/10.1021/acs.chemrev.0c00883.

(2) Ansari, I.; Singh, P.; Mittal, A.; Mahato, R. I.; Chitkara, D. 2,2-Bis(Hydroxymethyl) Propionic Acid Based Cyclic Carbonate Monomers and Their (Co)Polymers as Advanced Materials for Biomedical Applications. *Biomaterials* **2021**, *275*, 120953–120953. https://doi.org/10.1016/j.biomaterials.2021.120953.

(3) Tamura, M.; Nakagawa, Y.; Tomishige, K. Direct CO2 Transformation to Aliphatic Polycarbonates. *Asian J. Org. Chem*. **2022**, *11*(11). https://doi.org/10.1002/ajoc.202200445.

(4) Huang, J.; Jehanno, C.; Worch, J. C.; Ruipérez, F.; Sardon, H.; Dove, A. P.; Coulembier, O. Selective Organocatalytic Preparation of Trimethylene Carbonate from Oxetane and Carbon Dioxide. *ACS Catal.* **2020**, *10* (10), 5399–5404. https://doi.org/10.1021/acscatal.0c00689.

(5) Deacy, A. C.; Kilpatrick, A. F. R.; Regoutz, A.; Williams, C. K. Understanding Metal Synergy in Heterodinuclear Catalysts for The Copolymerization of CO_2 and Epoxides. *Nat. Chem.* **2020**, *12* (4), 372–380. https://doi.org/10.1038/s41557-020-0450-3.

(6) Sulley, G. S.; Gregory, G. L.; Chen, T. T. D.; Peña Carrodeguas, L.; Trott, G.; Santmarti, A.; Lee, K. Y.; Terrill, N. J.; Williams, C. K. Switchable Catalysis Improves the Properties of CO2-Derived Polymers: Poly(Cyclohexene Carbonate- b-ϵ-Decalactone- b-Cyclohexene Carbonate) Adhesives, Elastomers, and Toughened Plastics. *J. Am. Chem. Soc.* **2020**, *142* (9), 4367–4378. https://doi.org/10.1021/jacs.9b13106.

(7) Hauenstein, O.; Agarwal, S.; Greiner, A. Bio-Based Polycarbonate as Synthetic Toolbox. *Nat. Commun.* **2016**, *7*(1). https://doi.org/10.1038/ncomms11862.

(8) Tempelaar, S.; Mespouille, L.; Coulembier, O.; Dubois, P.; Dove, A. P. Synthesis and Post-Polymerization Modifications of Aliphatic Poly(Carbonate)s Prepared by Ring-Opening Polymerization. *Chem. Soc. Rev.* **2013**, *42* (3), 1312–1336. https://doi.org/10.1039/c2cs35268k.

(9) Feng, J.; Zhuo, R. X.; Zhang, X. Z. Construction of Functional Aliphatic Polycarbonates for Biomedical Applications. *Prog. Polym. Sci.* **2012**, *37* (2), 211–236. https://doi.org/10.1016/j.progpolymsci.2011.07.008.

(10) Zhang, X.; Fevre, M.; Jones, G. O.; Waymouth, R. M. Catalysis as an Enabling Science for Sustainable Polymers. *Chem. Rev*. **2017**, *118*(2), 839–885.

https://doi.org/10.1021/acs.chemrev.7b00329.

(11) Wu, L.; Wang, Y.; Zhao, X.; Mao, H.; Gu, Z. Investigating the Biodegradation Mechanism of Poly(Trimethylene Carbonate): Macrophage-Mediated Erosion by Secreting Lipase. *Biomacromolecules* **2023**, *24* (2), 921–928. https://doi.org/10.1021/acs.biomac.2c01350.

(12) Zhang, Z.; Kuijer, R.; Bulstra, S. K.; Grijpma, D. W.; Feijen, J. The in Vivo and in Vitro Degradation Behavior of Poly(Trimethylene Carbonate). *Biomaterials* **2006**, *27* (9), 1741–1748. https://doi.org/10.1016/j.biomaterials.2005.09.017.

(13) Amsden, B. In Vivo Degradation Mechanisms of Aliphatic Polycarbonates and Functionalized Aliphatic Polycarbonates. *Macromo.l Biosc.i* **2021**, *21* (7). https://doi.org/10.1002/mabi.202100085.

(14) Wang, Y.; Xi, L.; Zhang, B.; Zhu, Q.; Su, F.; Jelonek, K.; Orchel, A.; Kasperczyk, J.; Li, S. Bioresorbable Hydrogels Prepared by Photo-Initiated Crosslinking of Diacrylated PTMC-PEG-PTMC Triblock Copolymers as Potential Carrier of Antitumor Drugs. *Saudi. Pharm. J.* **2020**, *28* (3), 290–299. https://doi.org/10.1016/j.jsps.2020.01.008.

(15) Zong, Q.; Peng, X.; Ding, Y.; Wu, H.; Lu, C.; Ye, J.; Sun, W.; Zhang, J.; Zhai, Y. Multifunctional Hydrogel Wound Dressing with Rapid On-Demand Degradation Property Based on Aliphatic Polycarbonate and Chitosanchitosan. *Int. J. Biol. Macromol.* **2023**, *244*. https://doi.org/10.1016/j.ijbiomac.2023.125138.

(16) Welle, A.; Kröger, M.; Döring, M.; Niederer, K.; Pindel, E.; Chronakis, I. S. Electrospun Aliphatic Polycarbonates as Tailored Tissue Scaffold Materials. *Biomaterials* **2007**, *28* (13), 2211–2219. https://doi.org/10.1016/j.biomaterials.2007.01.024.

(17) Tan, L. Y.; Chanthaset, N.; Fadlan, A.; Ajiro, H. Synthesis of Ester-Free Poly(Trimethylene Carbonate) Bearing Cinnamyl Moiety for Antibacterial Biomaterials Applications. *React. Funct. Polym.* **2023**, *186*. https://doi.org/10.1016/j.reactfunctpolym.2023.105563.

(18) Dong, J.; Liao, L.; Shi, L.; Tan, Z.; Fan, Z.; Li, S.; Lu, Z. A Bioresorbable Cardiovascular Stent Prepared from L-Lactide, Trimethylene Carbonate and Glycolide Terpolymers. *Polym. Eng. Sci.* **2014**, *54* (6), 1418–1426. https://doi.org/10.1002/pen.23662.

(19) Yokoe, M.; Keigo, A. O. I.; Okada, M. Biodegradable Polymers Based on Renewable Resources.VII. Novel Random and Alternating Copolycarbonates From1,4:3,6-Dianhydrohexitols and Aliphatic Diols. *J. Polym. Sci. A Polym. Chem.* **2003**, *41* (15), 2312–2321. https://doi.org/10.1002/pola.10772.

(20) Foy, E.; Farrell, J. B.; Higginbotham, C. L. Synthesis of Linear Aliphatic Polycarbonate

MacroglycolsUsing Dimethylcarbonate. *J. Appl. Polym. Sci.* **2009**, *111* (1), 217–227. https://doi.org/10.1002/app.28887.

(21) Sun, J.; Kuckling, D. Synthesis of High-Molecular-Weight Aliphatic Polycarbonates by Organo-Catalysis. *Polym. Chem.* **2016**, *7* (8), 1642–1649. https://doi.org/10.1039/c5py01843a.

(22) Brunelle, D. J. Advances in Polycarbonates An Overview. *ACS Symp. Ser.* **2005**, *898*, 1–5. https://doi.org/10.1021/bk-2005-0898.ch001.

(23) Ono, Y. Dimethyl Carbonate for Environmentally Benign Reactions. *Catal. Today* **1997**, *35* (1–2), 15–25.

(24) Zhu, W.; Huang, X.; Li, C.; Xiao, Y.; Zhang, D.; Guan, G. High-Molecular-Weight Aliphatic Polycarbonates by Melt Polycondensation of Dimethyl Carbonate and Aliphatic Diols Synthesis and Characterization. *Polym. Int.* **2011**, *60* (7), 1060–1067. https://doi.org/10.1002/pi.3043.

(25) Shohei Inoue; Hideomi Koinuma; Teiji Tsuruta. Copolymerization of Carbon Dioxide and Epoxide. *J. Polym. Sci. B.* **1969**, *7* (4), 287–292.

(26) Fukuoka, S.; Kawamura, M.; Komiya, K.; Tojo, M.; Hachiya, H.; Hasegawa, K.; Aminaka, M.; Okamoto, H.; Fukawa, I.; Konno, S. A Novel Non-Phosgene Polycarbonate Production Process Using By-Product CO2 as Starting Material. *Green Chem.* **2003**, *5* (5), 497–507. https://doi.org/10.1039/b304963a.

(27) Darensbourg, D. J.; Mackiewicz, R. M.; Phelps, A. L.; Billodeaux, D. R. Copolymerization of CO2 and Epoxides Catalyzed by Metal Salen Complexes. *Acc. Chem. Res.* **2004**, *37* (11), 836–844. https://doi.org/10.1021/ar030240u.

(28) D'Alessandro, D. M.; Smit, B.; Long, J. R. Carbon Dioxide Capture: Prospects for New Materials. *Angew. Chem. - Int. Ed.* **2010**, *49* (35), 6058–6082. https://doi.org/10.1002/anie.201000431.

(29) Darensbourg, D. J. Making Plastics from Carbon Dioxide: Salen Metal Complexes as Catalysts for the Production of Polycarbonates from Epoxides and CO2. *Chem. Rev.* **2007**, *107* (6), 2388–2410. https://doi.org/10.1021/cr068363q.

(30) Darensbourg, D. J.; Yeung, A. D. A Concise Review of Computational Studies of The Carbon Dioxide-Epoxide Copolymerization Reactions. *Polym. Chem.* **2014**, *5* (13), 3949–3962. https://doi.org/10.1039/c4py00299g.

(31) Klaus, S.; Lehenmeier, M. W.; Anderson, C. E.; Rieger, B. Recent Advances in CO2/Epoxide Copolymerization-New Strategies and Cooperative Mechanisms. *Coord. Chem. Rev.* **2011**, *255* (13–14), 1460–1479. https://doi.org/10.1016/j.ccr.2010.12.002.

(32) Darensbourg, D. J.; Ganguly, P.; Choi, W. Metal Salen Derivatives as Catalysts for the Alternating Copolymerization of Oxetanes and Carbon Dioxide To Afford

Polycarbonates. *Inorg. Chem.* **2006**, *45* (10), 3831–3833. https://doi.org/10.1021/ic052109j.

(33) Darensbourg, D. J.; Wei, S. H. Depolymerization of Polycarbonates Derived from Carbon Dioxide and Epoxides to Provide Cyclic Carbonates. A Kinetic Study. *Macromolecules* **2012**, *45* (15), 5916–5922. https://doi.org/10.1021/ma301110c.

(34) Darensbourg, D. J.; Moncada, A. I.; Wei, S. H. Aliphatic Polycarbonates Produced from the Coupling of Carbon Dioxide and Oxetanes and Their Depolymerization via Cyclic Carbonate Formation. *Macromolecules* **2011**, *44* (8), 2568–2576. https://doi.org/10.1021/ma2002323.

(35) Diment, W. T.; Lindeboom, W.; Fiorentini, F.; Deacy, A. C.; Williams, C. K. Synergic Heterodinuclear Catalysts for the Ring-Opening Copolymerization (ROCOP) of Epoxides, Carbon Dioxide, and Anhydrides. *Acc. Chem. Re.s* **2022**, *55* (15), 1997–2010. https://doi.org/10.1021/acs.accounts.2c00197.

(36) Geschwind, J.; Frey, H. Poly(1,2-Glycerol Carbonate): A Fundamental Polymer Structure Synthesized from CO2 and Glycidyl Ethers. *Macromolecules* **2013**, *46* (9), 3280–3287. https://doi.org/10.1021/ma400090m.

(37) Wallace H. Carothers; G. L. Dorough; F. J. van Natta. Studies of Polymerization and Ring Formation. X. The Reversible Polymerization of Six-Membered Cyclic Esters. *J. Am. Chem. Soc.* **1932**, *54* (2), 761–772.

(38) Ariga, T.; Takata, T.; Endo, T. Cationic Ring-Opening Polymerization of Cyclic Carbonates with Alkyl Halides To Yield Polycarbonate without the Ether Unit by Suppression of Elimination of Carbon Dioxide. *Macromolecules* **1997**, *30* (4), 737–744.

(39) Jacques Penelle; Philippe Dubois; Olivier Coulembier; Jean-Marie Raquez. Polymerization of Cycloalkanes. In *Handbook of Ring-Opening Polymerization*; Wiley-VCH, 2009; Vol. 12, pp 329–353.

(40) Kricheldorf, H. R.; Stricker, A. Polymers of Carbonic Acid, 28: SnOct2-Initiated Polymerizations of Trimethylene Carbonate (TMC, 1,3-Dioxanone-2). *Macromol. Chem. Phys.* **2000**, *201* (17), 2557–2565. https://doi.org/10.1002/1521-3935(20001101)201:17<2557::AID-MACP2557>3.0.CO;2-F.

(41) He, F.; Jia, H. L.; Liu, G.; Wang, Y. P.; Feng, J.; Zhou, R. X. Enzymatic Synthesis and Characterization of Novel Biodegradable Copolymers of 5-Benzyloxy-Trimethylene Carbonate with 1,4-Dioxan-2-One. *Biomacromolecules* **2006**, *7* (8), 2269–2273. https://doi.org/10.1021/bm060070j.

(42) Soeda, Y.; Toshima, K.; Matsumura, S. Enzymatic Synthesis and Chemical Recycling of Poly(Carbonate-Urethane). *Macromol. Biosci.* **2004**, *4* (8), 721–728. https://doi.org/10.1002/mabi.200400042.

(43) Albertsson, A. C.; Srivastava, R. K. Recent Developments in Enzyme-Catalyzed Ring-Opening Polymerization. *Adv. Drug Deliv. Rev*. **2008**, 1077–1093. https://doi.org/10.1016/j.addr.2008.02.007.

(44) Fukushima, K.; Nozaki, K. Organocatalysis: A Paradigm Shift in the Synthesis of Aliphatic Polyesters and Polycarbonates. *Macromolecules* **2020**, *53* (13), 5018–5022. https://doi.org/10.1021/acs.macromol.0c00582.

(45) Ottou, W. N.; Sardon, H.; Mecerreyes, D.; Vignolle, J.; Taton, D. Update and Challenges in Organo-Mediated Polymerization Reactions. *Prog. Polym. Sci.* **2016**, *56*, 64–115. https://doi.org/10.1016/j.progpolymsci.2015.12.001.

(46) Nederberg, F.; Connor, E. F.; Möller, M.; Glauser, T.; Hedrick, J. L. New Paradigms for Organic Catalysts: The First Organocatalytic Living Polymerization. *Angew. Chem. - Int. Ed.* **2001**, *40* (14), 2712–2715.

(47) Lohmeijer, B. G. G.; Pratt, R. C.; Leibfarth, F.; Logan, J. W.; Long, D. A.; Dove, A. P.; Nederberg, F.; Choi, J.; Wade, C.; Waymouth, R. M.; Hedrick, J. L. Guanidine and Amidine Organocatalysts for Ring-Opening Polymerization of Cyclic Esters. *Macromolecules* **2006**, *39* (25), 8574–8583. https://doi.org/10.1021/ma0619381.

(48) Dove, A. P.; Pratt, R. C.; Lohmeijer, B. G. G.; Culkin, D. A.; Hagberg, E. C.; Nyce, G. W.; Waymouth, R. M.; Hedrick, J. L. N-Heterocyclic Carbenes: Effective Organic Catalysts for Living Polymerization. *Polymer (Guildf)* **2006**, *47* (11), 4018–4025. https://doi.org/10.1016/j.polymer.2006.02.037.

(49) Makiguchi, K.; Ogasawara, Y.; Kikuchi, S.; Satoh, T.; Kakuchi, T. Diphenyl Phosphate as an Efficient Acidic Organocatalyst for Controlled/Living Ring-Opening Polymerization of Trimethylene Carbonates Leading to Block, End-Functionalized, and Macrocyclic Polycarbonates. *Macromolecules* **2013**, *46* (5), 1772–1782. https://doi.org/10.1021/ma4000495.

(50) Thillaye Du Boullay, O.; Marchal, E.; Martin-Vaca, B.; Cossío, F. P.; Bourissou, D. An Activated Equivalent of Lactide toward Organocatalytic Ring-Opening Polymerization. *J. Am. Chem. Soc.* **2006**, *128* (51), 16442–16443. https://doi.org/10.1021/ja067046y.

(51) Delcroix, D.; Martín-Vaca, B.; Bourissou, D.; Navarro, C. Ring-Opening Polymerization of Trimethylene Carbonate Catalyzed by Methanesulfonic Acid: Activated Monomer versus Active Chain End Mechanisms. *Macromolecules* **2010**, *43* (21), 8828–8835. https://doi.org/10.1021/ma101461y.

(52) Campos, J. M.; Ribeiro, M. R.; Ribeiro, M. F.; Deffieux, A.; Peruch, F. A New Insight Into the Mechanism of the Ring-Opening Polymerization of Trimethylene Carbonate Catalyzed by Methanesulfonic Acid. *Macromol. Chem. Phys* .**2013**, *214* (1), 85–93. https://doi.org/10.1002/macp.201200433.

(53) Nemoto, N.; Sanda, F.; Endo, T. Cationic Ring-Opening Polymerization of Six-Membered Cyclic Carbonates with Ester Groups. *J. Polym. Sci. A. Polym. Chem.* **2001**, *39* (9), 1305–1317.

(54) Mahmood, Q.; Xu, G.; Zhou, L.; Guo, X.; Wang, Q. Chiral 1,5,7-Triazabicyclo[4.4.0]Dec-5-Ene (TBD)-Catalyzed Stereoselective Ring-Opening Polymerization of Rac-Lactide: High Reactivity for Isotactic Enriched Polylactides (PLAs). *Polymers (Basel)* **2020**, *12* (10), 1–10. https://doi.org/10.3390/polym12102365.

(55) Wu, R.; Al-Azemi, T. F.; Bisht, K. S. Functionalized Polycarbonate Derived from Tartaric Acid: Enzymatic Ring-Opening Polymerization of a Seven-Membered Cyclic Carbonate. *Biomacromolecules* **2008**, *9* (10), 2921–2928. https://doi.org/10.1021/bm800696q.

(56) Hu, X.; Chen, X.; Liu, S.; Shi, Q.; Jing, X. Novel Aliphatic Poly(Ester-Carbonate) with Pendant Allyl Ester Groups and Its Folic Acid Functionalization. *J. Polym. Sci. A. Polym. Chem.* **2008**, *46* (5), 1852–1861. https://doi.org/10.1002/pola.22530.

(57) Wang, C. F.; Lin, Y. X.; Jiang, T.; He, F.; Zhuo, R. X. Polyethylenimine-Grafted Polycarbonates as Biodegradable Polycations for Gene Delivery. *Biomaterials* **2009**, *30* (27), 4824–4832. https://doi.org/10.1016/j.biomaterials.2009.05.053.

(58) Ong, Z. Y.; Yang, C.; Cheng, W.; Voo, Z. X.; Chin, W.; Hedrick, J. L.; Yang, Y. Y. Biodegradable Cationic Poly(Carbonates): Effect of Varying Side Chain Hydrophobicity on Key Aspects of Gene Transfection. *Acta Biomater.* **2017**, *54*, 201–211. https://doi.org/10.1016/j.actbio.2017.03.027.

(59) Leong, J.; Chin, W.; Ke, X.; Gao, S.; Kong, H.; Hedrick, J. L.; Yang, Y. Y. Disease-Directed Design of Biodegradable Polymers: Reactive Oxygen Species and PH-Responsive Micellar Nanoparticles for Anticancer Drug Delivery. *Nanomedicine* **2018**, *14* (8), 2666–2677. https://doi.org/10.1016/j.nano.2018.06.015.

(60) Liu, S.; Ono, R. J.; Yang, C.; Gao, S.; Ming Tan, J. Y.; Hedrick, J. L.; Yang, Y. Y. Dual PH-Responsive Shell-Cleavable Polycarbonate Micellar Nanoparticles for in Vivo Anticancer Drug Delivery. *ACS Appl. Mater. Interfaces.* **2018**, *10* (23), 19355–19364. https://doi.org/10.1021/acsami.8b01954.

(61) Shi, M.; Wosnick, J. H.; Ho, K.; Keating, A.; Shoichet, M. S. Immuno-Polymeric Nanoparticles by Diels–Alder Chemistry. *Angew. Chem. - Int. Ed.* **2007**, *46* (32), 6126–6131. https://doi.org/10.1002/anie.200701032.

(62) Tempelaar, S.; Mespouille, L.; Dubois, P.; Dove, A. P. Organocatalytic Synthesis and Postpolymerization Functionalization of Allyl-Functional Poly(Carbonate)s. *Macromolecules* **2011**, *44* (7), 2084–2091. https://doi.org/10.1021/ma102882v.

(63) Bartolini, C.; Mespouille, L.; Verbruggen, I.; Willem, R.; Dubois, P. Guanidine-Based

Polycarbonate Hydrogels: From Metal-Free Ring-Opening Polymerization to Reversible Self-Assembling Properties. *Soft Matter.* **2011**, *7* (20), 9628–9637. https://doi.org/10.1039/c1sm05581j.

(64) Sanders, D. P.; Fukushima, K.; Coady, D. J.; Nelson, A.; Fujiwara, M.; Yasumoto, M.; Hedrick, J. L. A Simple and Efficient Synthesis of Functionalized Cyclic Carbonate Monomers Using a Versatile Pentafluorophenyl Ester Intermediate. *J. Am. Chem. Soc.* **2010**, *132* (42), 14724–14726. https://doi.org/10.1021/ja105332k.

(65) Pratt, R. C.; Nederberg, F.; Waymouth, R. M.; Hedrick, J. L. Tagging Alcohols with Cyclic Carbonate A Versatile Equivalent of (Meth)Acrylate for Ring-Opening Polymerization. *Chemical Communications* **2008**, No. 1, 114–116. https://doi.org/10.1039/b713925j.

(66) He, F.; Wang, C. F.; Jiang, T.; Han, B.; Zhuo, R. X. Poly[(5-Methyl-5-Allyloxycarbonyl-Trimethylene Carbonate)-Co-(5,5-Dimethyl-Trimethylene Carbonate)] with Grafted Polyethylenimine as Biodegradable Polycations for Efficient Gene Delivery. *Biomacromolecules* **2010**, *11* (11), 3028–3035. https://doi.org/10.1021/bm1008525.

(67) Xu, J.; Prifti, F.; Song, J. A Versatile Monomer for Preparing Well-Defined Functional Polycarbonates and Poly(Ester−carbonates). *Macromolecules* **2011**, *44* (8), 2660–2667. https://doi.org/10.1021/ma200021m.

(68) Kim, S. H.; Tan, J. P. K.; Nederberg, F.; Fukushima, K.; Colson, J.; Yang, C.; Nelson, A.; Yang, Y. Y.; Hedrick, J. L. Hydrogen Bonding-Enhanced Micelle Assemblies for Drug Delivery. *Biomaterials* **2010**, *31* (31), 8063–8071. https://doi.org/10.1016/j.biomaterials.2010.07.018.

(69) Chanthaset, N.; Ajiro, H. Preparation of Thermosensitive Biodegradable Hydrogel Using Poly(5-[2-{2-(2-Methoxyethoxy)Ethyoxy}-Ethoxymethyl]-5-Methyl-1,3-Dioxa-2-One) Derivatives. *Materialia (Oxf)* **2019**, *5*. https://doi.org/10.1016/j.mtla.2018.11.027.

(70) Ajiro, H.; Takahashi, Y.; Akashi, M. Thermosensitive Biodegradable Homopolymer of Trimethylene Carbonate Derivative at Body Temperature. *Macromolecules* **2012**, *45* (6), 2668–2674. https://doi.org/10.1021/ma300183t.

(71) Nobuoka, H.; Ajiro, H. Novel Synthesis Method of Ester Free Trimethylene Carbonate Derivatives. *Tetrahedron Lett.* **2019**, *60* (2), 164–170. https://doi.org/10.1016/j.tetlet.2018.12.002.

(72) Nobuoka, H.; Miyake, R.; Choi, J.; Yoshida, H.; Chanthaset, N.; Ajiro, H. Synthesis of Ester-Free Type Poly(Trimethylene Carbonate) Derivatives Bearing Cycloalkyl Side Groups. *Eur. Polym. J.* **2021**, *160*. https://doi.org/10.1016/j.eurpolymj.2021.110782.

(73) Miyake, R.; Maehara, A.; Chanthaset, N.; Ajiro, H. Thermal Property Control by Copolymerization of Trimethylene Carbonate and Its Derivative Bearing Triphenylmethyl Group. *ChemistrySelect* **2022**, *7* (11). https://doi.org/10.1002/slct.202104326.

(74) Tan, L. Y.; Chanthaset, N.; Nanto, S.; Soba, R.; Nagasawa, M.; Ohno, H.; Ajiro, H. Synthesis and Preparation of Cross-Linked Films with Ester-Free Poly(Trimethylene Carbonate) Bearing Aromatic Urea Moiety. *Macromolecules* **2021**, *54* (12), 5518–5525. https://doi.org/10.1021/acs.macromol.1c00339.

(75) Chanthaset, N.; Takahashi, Y.; Haramiishi, Y.; Akashi, M.; Ajiro, H. Control of Thermoresponsivity of Biocompatible Poly(Trimethylenecarbonate) with Direct Introduction of Oligo(Ethylene Glycol) under Various Circumstances. *J. Polym. Sci. A Polym. Chem.* **2017**, *55* (20), 3466–3474. https://doi.org/10.1002/pola.28728.

(76) Nobuoka, H.; Nagasawa, M.; Chanthaset, N.; Yoshida, H.; Haramiishi, Y.; Ajiro, H. Synthesis of Amphiphilic Block Copolymer Using Trimethylene Carbonate Bearing Oligo(Ethylene Glycol) and Investigation of Thin Film Including Cilostazol. *Journal of Polymer Science* **2020**, *58* (17), 2347–2354. https://doi.org/10.1002/pol.20200390.

(77) Chanthaset, N.; Maehara, A.; Ajiro, H. Particles and Film Preparation of Ester-Free Type Poly(Trimethylene Carbonate) Derivatives Bearing Aromatic Groups Initiated with Hydrophilic Initiators. *Colloids Surf. A Physicochem. Eng. Asp.* **2023**, *667*. https://doi.org/10.1016/j.colsurfa.2023.131413.

(78) Hansell, C. F.; O'Reilly, R. K. A "Mix-and-Click" Approach to Double Core–Shell Micelle Functionalization. *ACS Macro.Lett.* **2012**, *1* (7), 896–901. https://doi.org/10.1021/mz300230c.

(79) Nederberg, F.; Zhang, Y.; Tan, J. P. K.; Xu, K.; Wang, H.; Yang, C.; Gao, S.; Guo, X. D.; Fukushima, K.; Li, L.; Hedrick, J. L.; Yang, Y. Y. Biodegradable Nanostructures with Selective Lysis of Microbial Membranes. *Nat. Chem.* **2011**, *3* (5), 409–414. https://doi.org/10.1038/nchem.1012.

(80) Xu, J.; Liu, Z. L.; Zhuo, R. X. Synthesis and In Vitro Degradation of Novel Copolymers of Cyclic Carbonate and D,L-Lactide. *J. Appl. Polym. Sci.* **2006**, *101* (3), 1988–1994. https://doi.org/10.1002/app.23719.

(81) Mohajeri, S.; Chen, F.; De Prinse, M.; Phung, T.; Burke-Kleinman, J.; Maurice, D. H.; Amsden, B. G. Liquid Degradable Poly(Trimethylene-Carbonate- Co-5-Hydroxy-Trimethylene Carbonate): An Injectable Drug Delivery Vehicle for Acid-Sensitive Drugs. *Mol. Pharm.* **2020**, *17* (4), 1363–1376. https://doi.org/10.1021/acs.molpharmaceut.0c00064.

(82) Becker, G.; Wurm, F. R. Functional Biodegradable Polymers: Via Ring-Opening

Polymerization of Monomers without Protective Groups. *Chemical Society Reviews*. Royal Society of Chemistry October 21, 2018, pp 7739–7782. https://doi.org/10.1039/c8cs00531a.

(83) Al-Azemi, T. F.; Harmon, J. P.; Bisht, K. S. Enzyme-Catalyzed Ring-Opening Copolymerization of 5-Methyl-5-Benzyloxycarbonyl-1,3-Dioxan-2-One (MBC) with Trimethylene Carbonate (TMC): Synthesis and Characterization. *Biomacromolecules* **2000**, *1* (3), 493–500. https://doi.org/10.1021/bm005552o.

(84) Engler, A. C.; Tan, J. P. K.; Ong, Z. Y.; Coady, D. J.; Ng, V. W. L.; Yang, Y. Y.; Hedrick, J. L. Antimicrobial Polycarbonates: Investigating the Impact of Balancing Charge and Hydrophobicity Using a Same-Centered Polymer Approach. *Biomacromolecules* **2013**, *14* (12), 4331–4339. https://doi.org/10.1021/bm401248t.

(85) Ono, R. J.; Liu, S. Q.; Venkataraman, S.; Chin, W.; Yang, Y. Y.; Hedrick, J. L. Benzyl Chloride-Functionalized Polycarbonates: A Versatile Platform for the Synthesis of Functional Biodegradable Polycarbonates. *Macromolecules* **2014**, *47* (22), 7725–7731. https://doi.org/10.1021/ma501734y.

(86) Park, N. H.; Cheng, W.; Lai, F.; Yang, C.; Florez De Sessions, P.; Periaswamy, B.; Wenhan Chu, C.; Bianco, S.; Liu, S.; Venkataraman, S.; Chen, Q.; Yang, Y. Y.; Hedrick, J. L. Addressing Drug Resistance in Cancer with Macromolecular Chemotherapeutic Agents. *J. Am. Chem. Soc.* **2018**, *140* (12), 4244–4252. https://doi.org/10.1021/jacs.7b11468.

(87) Onbulak, S.; Tempelaar, S.; Pounder, R. J.; Gok, O.; Sanyal, R.; Dove, A. P.; Sanyal, A. Synthesis and Functionalization of Thiol-Reactive Biodegradable Polymers. *Macromolecules* **2012**, *45* (3), 1715–1722. https://doi.org/10.1021/ma2019528.

(88) Hassan, M.; Bhat, G. A.; Darensbourg, D. J. Post-Polymerization Functionalization of Aliphatic Polycarbonates Using Click Chemistry. *Polym. Chem.* **2024**. https://doi.org/10.1039/D4PY00174E.

(89) Chen, W.; Yang, H.; Wang, R.; Cheng, R.; Meng, F.; Wei, W.; Zhong, Z. Versatile Synthesis of Functional Biodegradable Polymers by Combining Ring-Opening Polymerization and Postpolymerization Modification via Michael-Type Addition Reaction. *Macromolecules* **2010**, *43* (1), 201–207. https://doi.org/10.1021/ma901897y.

(90) Shi, Y.; Wang, X.; Graff, R. W.; Phillip, W. A.; Gao, H. Synthesis of Degradable Molecular Brushes via a Combination of Ring-Opening Polymerization and Click Chemistry. *J. Polym. Sci. A Polym. Chem.* **2015**, *53* (2), 239–248. https://doi.org/10.1002/pola.27307.

(91) Tempelaar, S.; Barker, I. A.; Truong, V. X.; Hall, D. J.; Mespouille, L.; Dubois, P.; Dove, A. P. Organocatalytic Synthesis and Post-Polymerization Functionalization of

Propargyl-Functional Poly(Carbonate)s. *Polym. Chem.* **2013**, *4* (1), 174–183. https://doi.org/10.1039/c2py20718d.

(92) Williams, R. J.; Barker, I. A.; OReilly, R. K.; Dove, A. P. Orthogonal Modification of Norbornene-Functional Degradable Polymers. *ACS Macro. Lett.* **2012**, *1* (11), 1285–1290. https://doi.org/10.1021/mz300496q.

(93) Voo, Z. X.; Khan, M.; Narayanan, K.; Seah, D.; Hedrick, J. L.; Yang, Y. Y. AntimicrobialAntifouling Polycarbonate Coatings: Role of Block Copolymer Architecture. *Macromolecules* **2015**, *48* (4), 1055–1064. https://doi.org/10.1021/ma5022488.

(94) Engler, A. C.; Chan, J. M. W.; Coady, D. J.; O'Brien, J. M.; Sardon, H.; Nelson, A.; Sanders, D. P.; Yang, Y. Y.; Hedrick, J. L. Accessing New Materials through Polymerization and Modification of a Polycarbonate with a Pendant Activated Ester. *Macromolecules* **2013**, *46* (4), 1283–1290. https://doi.org/10.1021/ma4001258.

(95) Engler, A. C.; Ke, X.; Gao, S.; Chan, J. M. W.; Coady, D. J.; Ono, R. J.; Lubbers, R.; Nelson, A.; Yang, Y. Y.; Hedrick, J. L. Hydrophilic Polycarbonates: Promising Degradable Alternatives to Poly(Ethylene Glycol)-Based Stealth Materials. *Macromolecules* **2015**, *48* (6), 1673–1678. https://doi.org/10.1021/acs.macromol.5b00156.

(96) Park, N. H.; Voo, Z. X.; Yang, Y. Y.; Hedrick, J. L. Convergent Approach to Boronic Acid Functionalized Polycarbonates: Accessing New Dynamic Material Platforms. *ACS Macro. Lett.* **2017**, *6* (3), 252–256. https://doi.org/10.1021/acsmacrolett.6b00875.

(97) Durand, P. L.; Brège, A.; Chollet, G.; Grau, E.; Cramail, H. Simple and Efficient Approach toward Photosensitive Biobased Aliphatic Polycarbonate Materials. *ACS Macro. Lett.* **2018**, *7* (2), 250–254. https://doi.org/10.1021/acsmacrolett.8b00003.

(98) Stevens, D. M.; Tempelaar, S.; Dove, A. P.; Harth, E. Nanosponge Formation from Organocatalytically Synthesized Poly(Carbonate) Copolymers. *ACS Macro. Lett.* **2012**, *1* (7), 915–918. https://doi.org/10.1021/mz300179r.

(99) Lowe, A. B. Thiol-Ene Click Reactions and Recent Applications in Polymer and Materials Synthesis. *Polym. Chem.* **2010**, *1* (1), 17–36. https://doi.org/10.1039/b9py00216b.

(100) Hoyle, C. E.; Bowman, C. N. Thiol–Ene Click Chemistry. *Angew. Chem. - Int. Ed.* **2010**, *49* (9), 1540–1573. https://doi.org/10.1002/anie.200903924.

(101) Nair, D. P.; Podgórski, M.; Chatani, S.; Gong, T.; Xi, W.; Fenoli, C. R.; Bowman, C. N. The Thiol-Michael Addition Click Reaction: A Powerful and Widely Used Tool in Materials Chemistry. *Chem. Mater*. **2014**, 724–744. https://doi.org/10.1021/cm402180t.

(102) Li, S.; Meng, F.; Wang, Z.; Zhong, Y.; Zheng, M.; Liu, H.; Zhong, Z. Biodegradable

Polymersomes with An Ionizable Membrane: Facile Preparation, Superior Protein Loading, and Endosomal PH-Responsive Protein Release. *Eur. J. Pharm. Biopharm.* **2012**, *82* (1), 103–111. https://doi.org/10.1016/j.ejpb.2012.05.009.

(103) Sardon, H.; Engler, A. C.; Chan, J. M. W.; García, J. M.; Coady, D. J.; Pascual, A.; Mecerreyes, D.; Jones, G. O.; Rice, J. E.; Horn, H. W.; Hedrick, J. L. Organic Acid-Catalyzed Polyurethane Formation via a Dual-Activated Mechanism: Unexpected Preference of N-Activation over O-Activation of Isocyanates. *J. Am. Chem. Soc.* **2013**, *135* (43), 16235–16241. https://doi.org/10.1021/ja408641g.

(104) Yasuda, H.; Aludin, M. S.; Kitamura, N.; Tanabe, M.; Sirahama, H. Syntheses and Physical Properties of Novel Optically Active Poly(Ester−carbonate)s by Copolymerization of Substituted Trimethylene Carbonate with ε-Caprolactone and Their Biodegradation Behavior. *Macromolecules* **1999**, *32* (19), 6047–6057. https://doi.org/10.1021/ma981904w.

(105) Yang, L.; Li, J.; Li, M.; Gu, Z. The in Vitro and in Vivo Degradation of Cross-Linked Poly(Trimethylene Carbonate)-Based Networks. *Polymers (Basel)* **2016**, *8* (4). https://doi.org/10.3390/polym8040151.

(106) Sanda, F.; Fueki, T.; Endo, T. Cationic Ring-Opening Polymerization of an Exomethylene Group Carrying Cyclic Carbonate. Pseudo-Living Polymerization of 5-Methylene-1,3-Dioxan-2-One by the Assistance of the Exomethylene Group. *Macromolecules* **1999**, *32* (13), 4220–4224. https://doi.org/10.1021/ma981947c.

(107) Toshikazu Takata; Michito Igarashi; Takeshi Endo. Synthesis and Cationic Ring-Opening Polymerization of a Cyclic Carbonate, 5-Methylene-1,3-Dioxan-2-One. *J. Polym. Sci. A Polym. Chem.* **1991**, *29* (5), 781–784.

(108) Entwistle, I. D.; Wood, W. W. *Hydrogenolysis of Allyl and Benzyl Halides and Related Compounds*, eds Trost B.M. and Fleming I. Pergamon Press, Oxford, **1991**, *8,* 955–981.

(109) Painter, R. M.; Pearson, D. M.; Waymouth, R. M. Selective Catalytic Oxidation of Glycerol to Dihydroxyacetone. *Angew. Chem. - Int. Ed.* **2010**, *49* (49), 9456–9459. https://doi.org/10.1002/anie.201004063.

(110) Shintani, R.; Moriya, K.; Hayashi, T. Guiding The Nitrogen Nucleophile to The Middle: Palladium-Catalyzed Decarboxylative Cyclopropanation of 2-Alkylidenetrimethylene Carbonates with Isocyanates. *Chemical Communications* **2011**, *47* (11), 3057–3059. https://doi.org/10.1039/c0cc05308b.

(111) Olsén, P.; Morvan, J.; Sawadjoon, S.; Shatskiy, A.; 2017

, E. V.; Åkermark, B. Cyclic Allylic Carbonates as a Renewable Platform for Protecting Chemistry in Water. *Green Chem.* **2018**, *20* (14), 3186–3190. https://doi.org/10.1039/c8gc01622d.

(112) Zhang, S. S.; Zheng, Y. C.; Zhang, Z. W.; Chen, S. Y.; Xie, H.; Shu, B.; Song, J. L.; Liu, Y. Z.; Zeng, Y. F.; Zhang, L. Access to Branched Allylarenes via Rhodium(III)-Catalyzed C-H Allylation of (Hetero)Arenes with 2-Methylidenetrimethylene Carbonate. *Org. Lett.* **2021**, *23* (15), 5719–5723. https://doi.org/10.1021/acs.orglett.1c01832.

(113) McGuire, T. M.; López-Vidal, E. M.; Gregory, G. L.; Buchard, A. Synthesis of 5- to 8-Membered Cyclic Carbonates from Diols and CO2 A One-Step, Atmospheric Pressure and Ambient Temperature Procedure. *J. CO2 Util.* **2018**, *27*, 283–288. https://doi.org/10.1016/j.jcou.2018.08.009.

(114) McGuire, T. M.; Pérale, C.; Castaing, R.; Kociok-Köhn, G.; Buchard, A. Divergent Catalytic Strategies for the Cis/Trans Stereoselective Ring-Opening Polymerization of a Dual Cyclic Carbonate/Olefin Monomer. *J. Am. Chem. Soc.* **2019**, *141* (34), 13301–13305. https://doi.org/10.1021/jacs.9b06259.

(115) Tang, S.; Nozaki, K. Advances in the Synthesis of Copolymers from Carbon Dioxide, Dienes, and Olefins. *Acc Chem. Res.* **2022**, *55* (11), 1524–1532. https://doi.org/10.1021/acs.accounts.2c00162.

(116) Ngassam Tounzoua, C.; Grignard, B.; Detrembleur, C. Exovinylene Cyclic Carbonates: Multifaceted CO2-Based Building Blocks for Modern Chemistry and Polymer Science. *Angew. Chem. - Int. Ed*. **2022**, *61*(22). https://doi.org/10.1002/anie.202116066.

(117) Darensbourg, D. J.; Moncada, A. I.; Choi, W.; Reibenspies, J. H. Mechanistic Studies of the Copolymerization Reaction of Oxetane and Carbon Dioxide to Provide Aliphatic Polycarbonates Catalyzed by (Salen)CrX Complexes. *J. Am. Chem. Soc.* **2008**, *130* (20), 6523–6533. https://doi.org/10.1021/ja800302c.

(118) Tryznowski, M.; Zołek-Tryznowska, Z.; ̨widerska, A.; Parzuchowski, P. G. Synthesis, Characterization and Reactivity of A Six-Membered Cyclic Glycerol Carbonate Bearing A Free Hydroxyl Group. *Green Chem.* **2016**, *18* (3), 802–807. https://doi.org/10.1039/c5gc01688f.

(119) Wang, H. Y.; Zhang, K.; Zheng, C. W.; Chai, Z.; Cao, D. D.; Zhang, J. X.; Zhao, G. Asymmetric Dual-Reagent Catalysis Mannich-Type Reactions Catalyzed by Ion Pair. *Angew. Chem. - Int. Ed.* **2015**, *54* (6), 1775–1779. https://doi.org/10.1002/anie.201409342.

(120) Rintjema, J.; Guo, W.; Martin, E.; Escudero-Adán, E. C.; Kleij, A. W. Highly Chemoselective Catalytic Coupling of Substituted Oxetanes and Carbon Dioxide. *Chem. Eur. J.* **2015**, *21* (30), 10754–10762. https://doi.org/10.1002/chem.201501576.

(121) Hauser, A. W.; Hayward, R. C. Random Photografting of Polymers to Nanoparticles for Well-Dispersed Nanocomposites. *J Polym Sci B Polym Phys* **2016**, *54* (2), 152–158.

https://doi.org/10.1002/polb.23803.

(122) Penczek, S.; Pretula, J. Activated Monomer Mechanism (AMM) in Cationic Ring-Opening Polymerization. The Origin of the AMM and Further Development in Polymerization of Cyclic Esters. *ACS Macro. Let*. **2021**, 1377–1397. https://doi.org/10.1021/acsmacrolett.1c00509.

(123) Lynd, N. A.; Ferrier, R. C.; Beckingham, B. S. Recommendation for Accurate Experimental Determination of Reactivity Ratios in Chain Copolymerization. *Macromolecules* **2019**, *52* (6), 2277–2285. https://doi.org/10.1021/acs.macromol.8b01752.

(124) Albertsson, A. C.; Srivastava, R. K. Recent Developments in Enzyme-Catalyzed Ring-Opening Polymerization. *Adv. Drug Deliv. Rev.* **2008**, *60* (9), 1077–1093. https://doi.org/10.1016/j.addr.2008.02.007.

(125) Palden, T.; Onghena, B.; Regadío, M.; Binnemans, K. Methanesulfonic Acid: A Sustainable Acidic Solvent for Recovering Metals from The Jarosite Residue of The Zinc Industry. *Green Chem.y* **2019**, *21* (19), 5394–5404. https://doi.org/10.1039/c9gc02238d.

(126) Baśko, M.; Kubisa, P. Cationic Copolymerization of ε-CaprolactoneandL,L-Lactide by an Activated Monomer Mechanism. *J. Polym. Sci. A Polym. Chem.* **2006**, *44* (24), 7071–7081. https://doi.org/10.1002/pola.21712.

(127) Batiste, D. C.; Meyersohn, M. S.; Watts, A.; Hillmyer, M. A. Efficient Polymerization of Methyl-ϵ-Caprolactone Mixtures to Access Sustainable Aliphatic Polyesters. *Macromolecules* **2020**, *53* (5), 1795–1808. https://doi.org/10.1021/acs.macromol.0c00050.

(128) Schneiderman, D. K.; Hillmyer, M. A. Aliphatic Polyester Block Polymer Design. *Macromolecules* **2016**, *49* (7), 2419–2428. https://doi.org/10.1021/acs.macromol.6b00211.

(129) Delcroix, D.; Couffin, A.; Susperregui, N.; Navarro, C.; Maron, L.; Martin-Vaca, B.; Bourissou, D. Phosphoric and Phosphoramidic Acids As Bifunctional Catalysts for The Ring-Opening Polymerization of ε-Caprolactone: A Combined Experimental and Theoretical S. *Polym. Chem.* **2011**, *2* (10), 2249–2256. https://doi.org/10.1039/c1py00210d.

(130) Palard, I.; Schappacher, M.; Belloncle, B.; Soum, A.; Guillaume, S. M. Unprecedented Polymerization of Trimethylene Carbonate Initiated by a Samarium Borohydride Complex: Mechanistic Insights and Copolymerization with e-Caprolactone. *Chem. Eur. J.* **2007**, *13* (5), 1511–1521. https://doi.org/10.1002/chem.200600843.

(131) Coulembier, O.; Lemaur, V.; Josse, T.; Minoia, A.; Cornil, J.; Dubois, P. Synthesis of

Poly(l-Lactide) and Gradient Copolymers from A L-Lactidetrimethylene Carbonate Eutectic Melt. *Chem. Sci.* **2012**, *3* (3), 723–726. https://doi.org/10.1039/c2sc00590e.

(132) Chen, X.; Michinobu, T. Postpolymerization Modification: A Powerful Tool for the Synthesis and Function Tuning of Stimuli-Responsive Polymers. *Macromol. Chem. Phys.* **2022**, *223* (1). https://doi.org/10.1002/macp.202100370.

(133) Safaei Nikouei, N.; Lavasanifar, A. Characterization of the Thermo- and PH-Responsive Assembly of Triblock Copolymers Based on Poly(Ethylene Glycol) and Functionalized Poly(ε-Caprolactone). *Acta Biomater.* **2011**, *7* (10), 3708–3718. https://doi.org/10.1016/j.actbio.2011.05.035.

(134) Felpin, F. X.; Fouquet, E. A Useful, Reliable and Safer Protocol for Hydrogenation and the Hydrogenolysis of o-Benzyl Groups: The in Situ Preparation of an Active Pd 0/C Catalyst with Well-Defined Properties. *Chem. Eur. J.* **2010**, *16* (41), 12440–12445. https://doi.org/10.1002/chem.201001377.

Chapter III

Evaluation of Biocompatible Properties in Random Copolymers of Trimethylene Carbonate and 5-Methylene-1,3-Dioxane-2-One with Controlled Introduction of Diol and Carboxylic Acid

3.1 Introduction

One of the most rapidly evolving area in materials science is the development of biodegradable polymers for medical applications. Biodegradable polymers have been extensively investigated for biomedical and pharmaceutical applications including implanted medical devices[1–5], drug delivery systems[6,7], nerve guides[8] and temporary three-dimensional (3D) scaffolds in tissue engineering.[9,10] In the design of biodegradable biomaterials, many important properties must be considered. These materials must: (I) avoid eliciting a sustained inflammatory response; (II) exhibit a degradation time that aligns with their intended function; (III) possess mechanical properties suitable for their specific applications; (IV) yield non-toxic degradation products that can be easily resorbed or excreted; and (V) demonstrate appropriate permeability and processability for the designated application (**Figure 3-1**).[11] These properties are greatly affected by a number of monomer composition features of degradable polymeric biomaterials including, but not limited to: material chemistry, molecular weight, hydrophobicity, surface charge, water adsorption, and degradation and erosion mechanisms.

Reflecting these key design principles, Poly(trimethylene carbonate) (PTMC) stands out among biodegradable polymers due to its excellent degradability and biocompatibility..[12,13] PTMC is one of the most important biodegradable polymers due to its favorable characteristics, such as excellent degradability and biocompatibility.[12,13] PTMC generally possess longer degradation times than their polyester counterparts, as the degradation of polyesters can be autocatalyzed by the formation of acidic end groups as a product of hydrolysis, resulting in a lowering of the local pH and accelerated degradation. For PTMC, the degradation mechanism is mainly through surface erosion

and possess slower resorbable rate as well as loss of mass and dimensions proportional to the surface area as compared to polyester that undergo bulk erosion. As a result, PTMC preserve their structural integrity and mechanical properties for a longer time Therefore, these materials are able to support complete tissue formation or biomedical application requiring longer service periods. Also, the degradation products of PTMC are not acidic, which can be an advantage compared to polyesters in avoiding the inflammation provoked by acidic degradation products. [14–16]

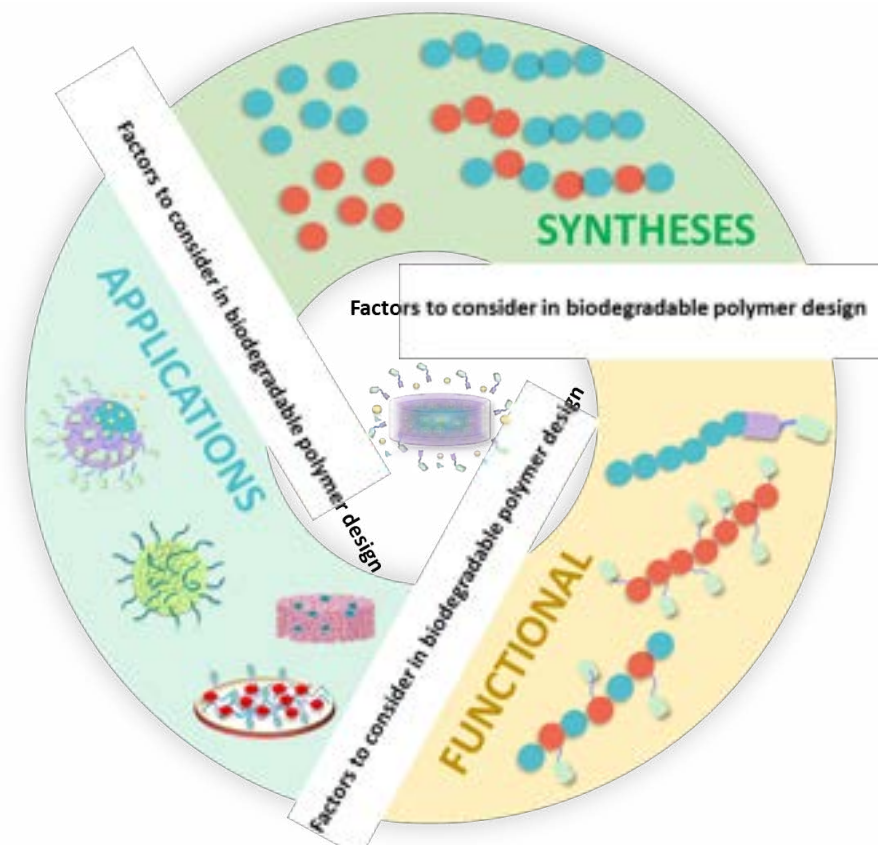

Figure 3-1. Factors to consider in polymer design.

However, the progress in current medical technologies leads to the requirement for more complex and higher level of functional materials. Non-functionalized PTMC lacks specific functionalities or interactions with biological surroundings, which can limit its applicability in certain biomedical contexts. Thus, the integration of multiple functions has been explored for PTMC by various approaches, including composites,[17] copolymerization,[18,19] polymer blends, and the incorporation of functional pendant groups[20] (**Figure 3-2**), in order to respond to a broad range of applications.[21]

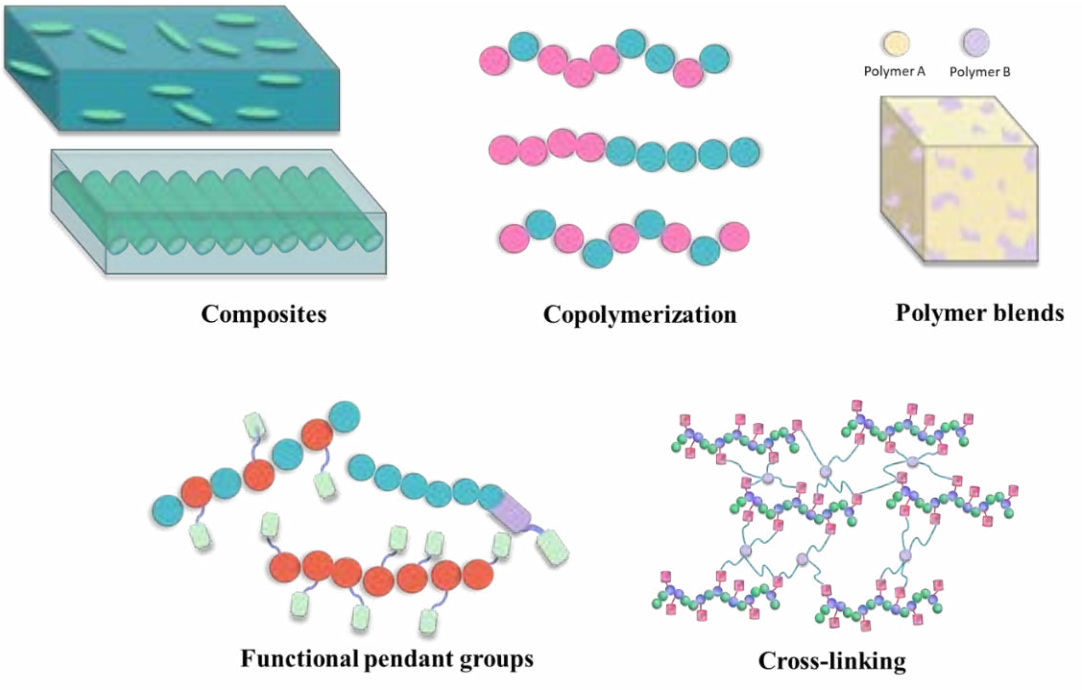

Figure 3-2. The method for integrating multiple functions into PTMC.[21]

Currently, there have been many efforts to utilize the benefits of PTMC while incorporating functionality into biodegradable polymers used as biomaterials. In bone regeneration, hydroxyapatite and bioglass particles are used as the "gold standard" scaffold materials.[22,23] They are biodegradable and favorable to biomineralization and compatible with osteoblast cells. However, their brittle nature is an issue for their mechanical strength that needs to be improved. Therefore, efforts have been made to explore composites with biodegradable polymers such as PTMC as scaffold polymeric materials matrix for bone regeneration due to its elastomeric, extended degradation span and able to resorbable without creating acidic environment as calcium phosphate ceramics and bone more promptly to dissolve in acidic environment. Annie and coworkers have prepared a composite of the high molecular weight PTMC with 50 wt% (30 vol%) of biphasic calcium phosphate (BCP) and its laminate with poly(*D,L*-lactide) (PDLLA). Subsequently, it was tested for the reconstruction of bone defects in a sheep model (**Figure 3-3**).[24] As a consequence of the excellent bone formation and retained mechanical stability 9 months after implantation, the PTMC-BCP composite and its laminate with PDLLA were proven appropriate as an osteoinductive material for the orbital floor reconstruction.

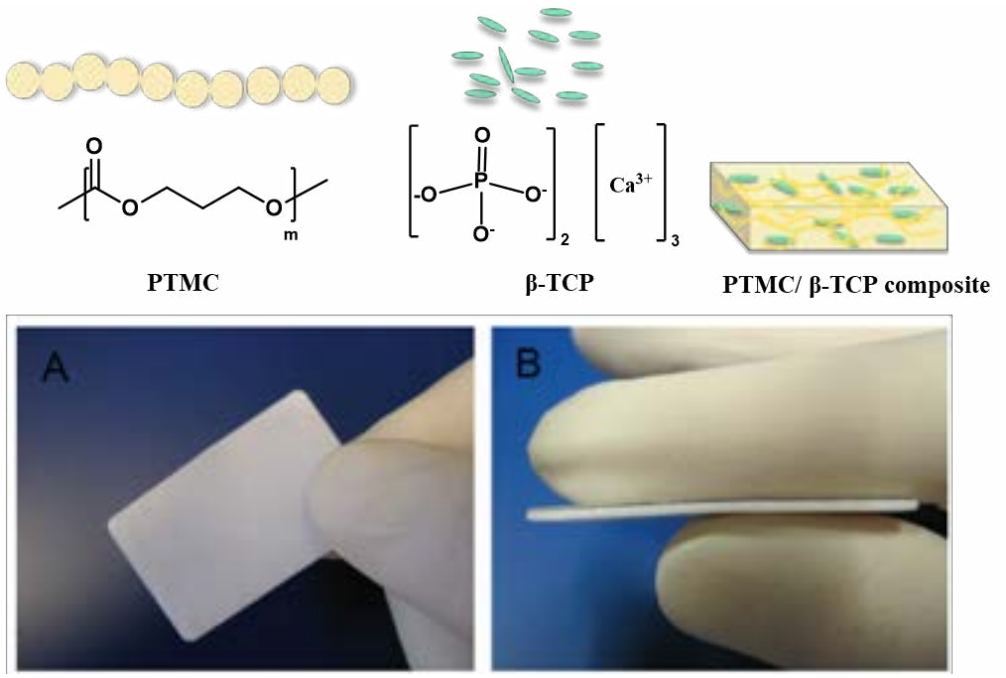

Figure 3-3. Images of the prepared PTMC/ β -TCP composite (A) and the laminated PTMC/ β -TCP composite sheets (B).[24]

By means of copolymer, the desired properties such as degradation rate, hydrophilicity or mechanical properties can be adjusted to desired requirement based on a specific biomaterial application. Major candidates of these copolymers are PLA-*co*-PTMC,[25] poly(glycolide-*co*-trimethylene carbonate)[12] and poly(caprolactone-*co*-trimethylene carbonate).[26] PLA-*co*-PTMC has been proposed for application as small diameter vascular grafts.[25] Copolymers with varying trimethylene carbonate (TMC)/lactide (LA) ratios 20/80, 30/70, and 40/60 were submitted to electrospinning and the resulting scaffolds were evaluated in terms of their physicochemical and biological properties. Poly(glycolide-*co*-TMC) is a commercial monofilament used for suture with slow biodegradation rate which allows maintenance of high mechanical strength compatible with the surgical recovery.[27] Poly(caprolactone-*co*-TMC) has been proposed as biomaterial for conduits in the regeneration of central nervous system (**Figure 3-4**).[26]

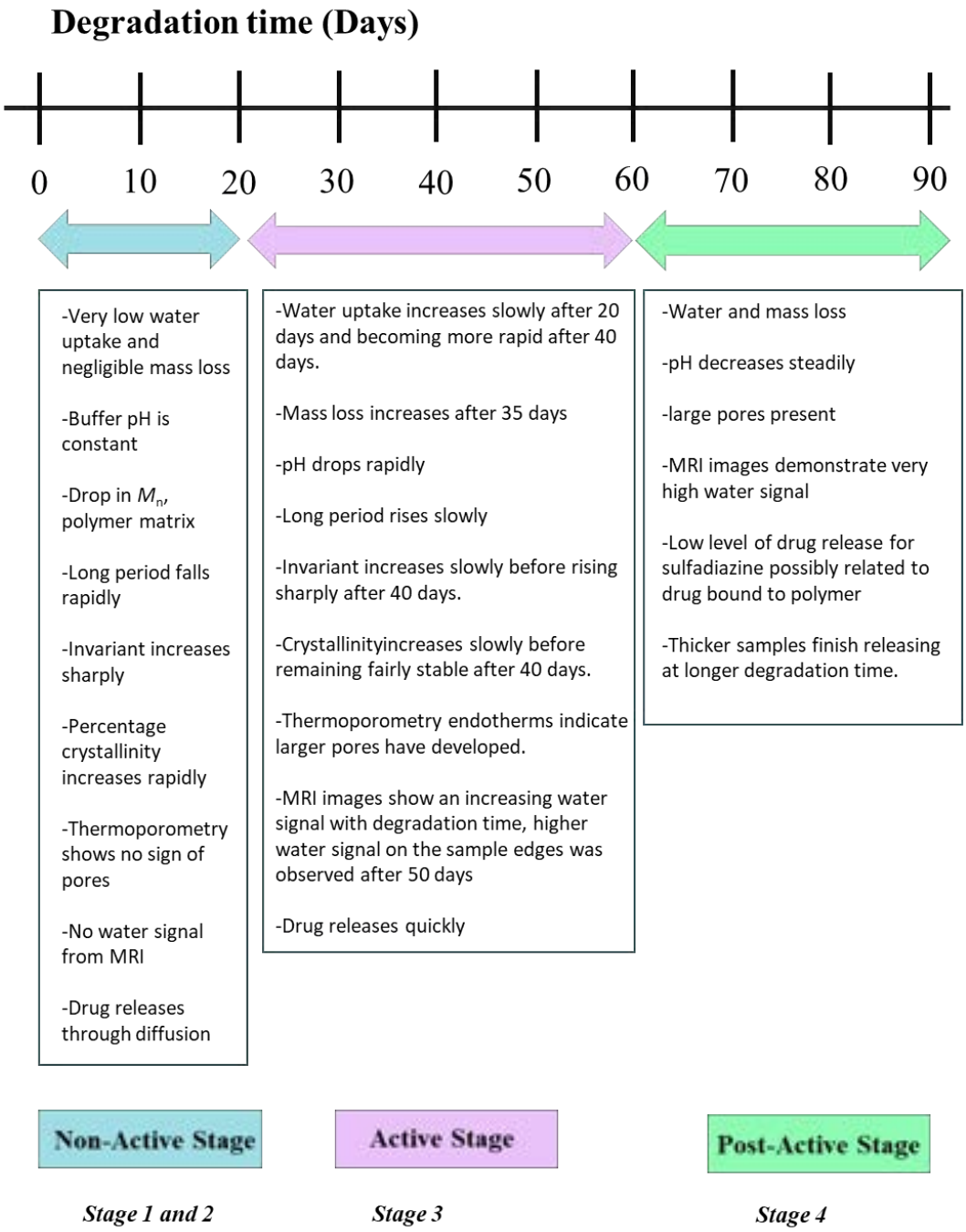

Figure 3-4. Timeline summary of the degradation and drug release of polycarbonate containing copolymers.[26]

Besides, therapeutics is the largest areas for which biodegradable polymers are studied for in biomedical applications at the experimental level. The unique properties of PTMC rendered it a promising candidate to form amphiphilic copolymer for drug delivery systems. PTMC which act as a hydrophobic part is used as an amphiphilic block

copolymers to form spherical carriers, including micelles and vesicles.[26] It has been published that its combination with hydrophilic groups such as oligo(ethylene glycol) and poly(ethylene glycol) (PEG) would offer a useful approach to vary the PTMC properties and their ability to suppress the adsorption of non-specific proteins are attractive properties for biomedical applications. Diblock copolymers and triblock copolymers, as well as star-shaped polymers, are most often prepared through ring-opening polymerization of hydroxyl groups in PEG at chain ends (**Figure 3-5**).[28] mPEG–PTMC forms micelles and nanoparticles that are incorporated into hydrophobic compounds, such as pyrene,[29] dexamethasone[30] and paclitaxel has been studied.[31] Zhang et al. prepared PTMC and monomethoxy PEG-*block*-PTMC (mPEG–PTMC) nanoparticles and were loaded at high efficiencies with dexamethasone, a poorly water soluble, anti-inflammatory and immuno-suppressive drug.[30] The stability of the drug-loaded nanoparticles and the release profiles of dexamethasone were evaluated. It is found that the release of dexamethasone from these nanoparticles was diffusion-controlled and could be sustained for 14 to 60 days.

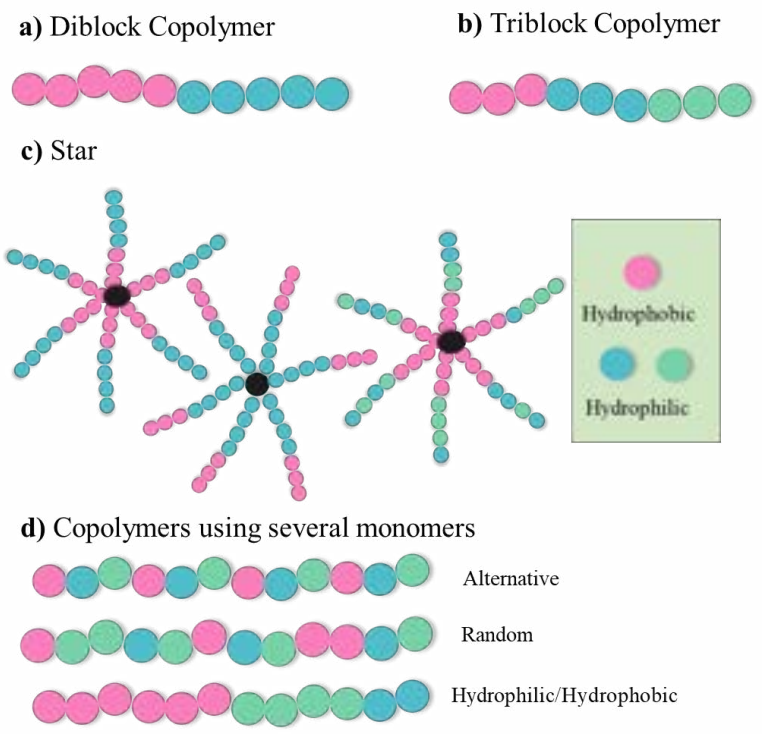

Figure 3-5. Types of amphiphilic polymers.[28]

In the practice of biodegradable biomaterial, very often PTMC polymers and their copolymers cannot satisfy the requirements for particular applications, due to their high

hydrophobicity, improper degradation profile, and/or lack of reactive centers in the polymer chain for the covalent immobilization of bioactive molecules such as drugs, peptides and proteins. In the past decade, the design of functional cyclic carbonate monomers has received more and more interest, and various functional aliphatic polycarbonate-based polymers and copolymers containing such as hydroxyl, carboxyl, and amine pendant groups have been reported.[32–35] These functional polymers on the one hand show improved physicochemical properties, including wettability, surface free energy, surface charge, stiffness, topography and the presence of specific chemical functionalities, surface bound water appears to bear an instrumental role in the biological response induced by the synthetic polymers.

Up-to-date, there are many functional PTMC that have been investigated and designed seeking for more advanced biomaterial development. Fukushima et al, have introduced methoxy group into PTMC which have prevented platelet adhesion that is 93% and 89% lower than those of poly(ethylene terephthalate) and PTMC, respectively (**Figure 3-6**).[36] Hydration (contact angle) and viscoelasticity (estimated from glass transition temperature (T_g) of polymers) have been utilized to elucidate the differing cell adhesion behaviors between platelets and vascular cells. Hydration and its effect on decreasing T_g appeared to be associated with the preventing platelet adhesion. Also, selective cell adhesion for vascular cell is contributed to the slightly denatured of fibrinogen by the monoether-tagged PTMC and the activation of fibronectin to exposed the RGD motif have favorable vascular cell adhesion and appeared to be promising in resorbable vascular grafts and stents.

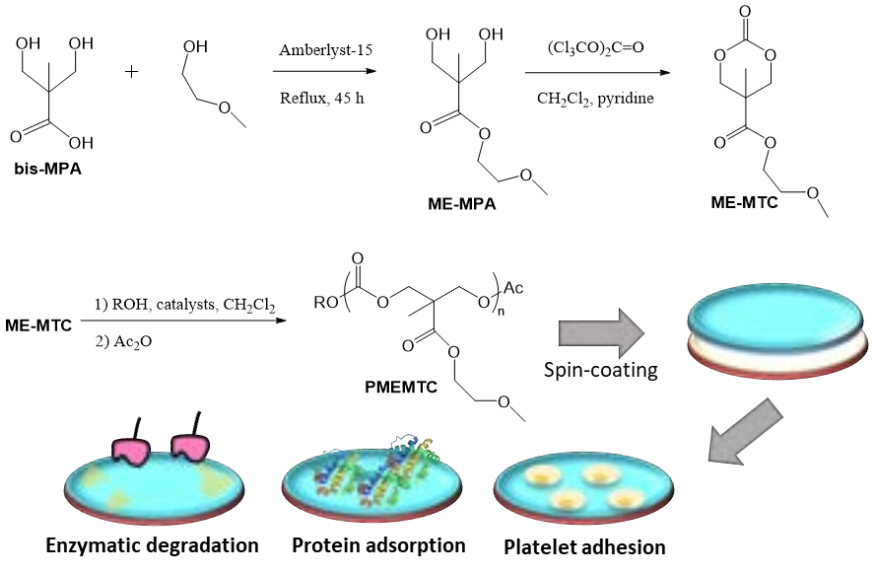

Figure 3-6. Outline of Synthesis and Biological Evaluation of a Monoether-Tagged Polycarbonate.[36]

PTMC bearing pendant amide, amino, amido and urea functionalities have also been reported.[37–40] Cooley and her coworkers incorporated guanidinium side chains into PTMC and this functionalization have showed their ability to intracellularly deliver and release the bioluminescent small molecule-probe luciferin, confirming the intracellular availability of the free cargo to interact with its target enzyme.[41] Kim and co-workers have studied that introducing a urea-bearing functional group into a copolymer for forming stable micelle for drug delivery(**Figure 3-7**).[42] Presence of urea-functional groups lowered critical micelle concentration and enhanced kinetic stability of the micelles. Urea is associated with hydrogen bonding as a strategy for improving physical-chemical properties and desired intermolecular interaction such as drug release control. The increase of urea content led to a slight decrease in doxorubicin release rate.

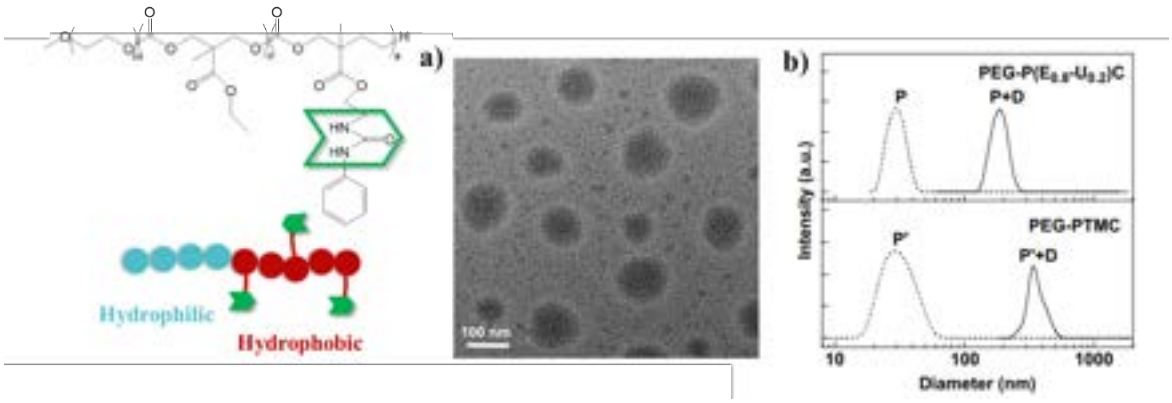

Figure 3-7. (a) Stability of PEG-P(E-B)C block copolymers micelles. (b) TEM images of PEG-P(E0.6-U0.4)C, (c) critical micelle concentration (cmc).[42]

In particularly, introducing hydroxyl (–OH) and carboxylic acid (–COOH) functionalities into PTMC chains is considered an attractive approach for tuning the properties of biodegradable polymers. This method controls the balance between the hydrophilic (–OH and –COOH groups) and the hydrophobic segments of the polymer backbone, thereby altering interactions with the physiological environment, degradation behavior, and wettability to meet specific biomedical application requirements. Feng et al, have demonstrated that hydroxyl-enriched polycarbonates possessed high cell-biocompatibility using COS 7 cells as shown by the MTT assay.[43] The typical degradation rate of aliphatic polycarbonates is considerably lower than that of most aliphatic polyesters, which restricts their use as short-term implant biomaterials. Due to the improved hydrophilicity and the autocatalytic effect of the hydroxyl groups, hydroxyl-enriched polycarbonates have a much faster degradation rate than that of the non-

functionalized PTMC analog, with a similar structure differing merely by the absence of pendant hydroxyl groups.[43–45] It is assumed that the fast degradation also involves an intra-molecular nucleophilic attack by the pendant hydroxyl groups on the carbonate linkages of the main chain.[46] These hydroxyl containing functional polycarbonates and copolymers can be easily constructed to advanced nano carriers for drug delivery.

Furthermore, Yu et al, studied the impact of COOH and OH side groups of PTMC on the degradation behaviors of the functionalized polymers.[47] In the study, PTMC with different number of arms terminated by hydroxyl group or carboxylic group and it is appeared that COOH-PTMCs were hydrolyzed faster than the OH-PTMCs. Introducing COOH end group into polycarbonate, the end group of COOH may catalyze the degradation by virtue of the hydrolytic degradation mechanism of polycarbonate catalyzed by both acid and base. The multi-arm structure polymers have higher concentration of COOH end group and higher acidity than the linear polymers of the same molecular weight, thus they should degrade faster. This was in line with our observation that the one-, two-, and three-arm structures terminated by COOH degraded increasingly in order (**Figure 3-8**).[47]

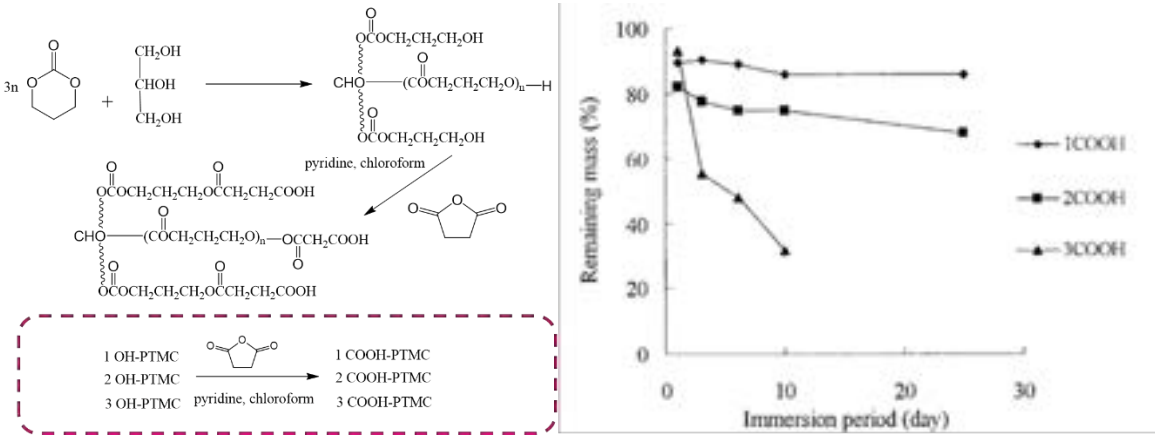

Figure 3-8. Synthesis of multi-arm COOH-terminated PTMCs and Mass remaining after the hydrolytic degradation of COOH-terminated multiarm PTMCs.[47]

In order to design newly bioresorbable polymeric materials for medical application, how to control degradation and behavior is a necessary factor that should be considered to prevent any biologically adverse effects. Recently, Amsden and coworker reported that copolymers consisting of randomly 5-hydroxy-trimethylene carbonate (HTMC) backbone with TMC could be degraded over 4 months *in vitro* by manipulating the HTMC content, Mn of the copolymer, and initiator (**Figure 3-9**).[48] Moreover, the

result of degradation residues showed appreciable changes upon buffer solution nor caused significant cytotoxicity towards fibroblasts and macrophages in vitro.[48]

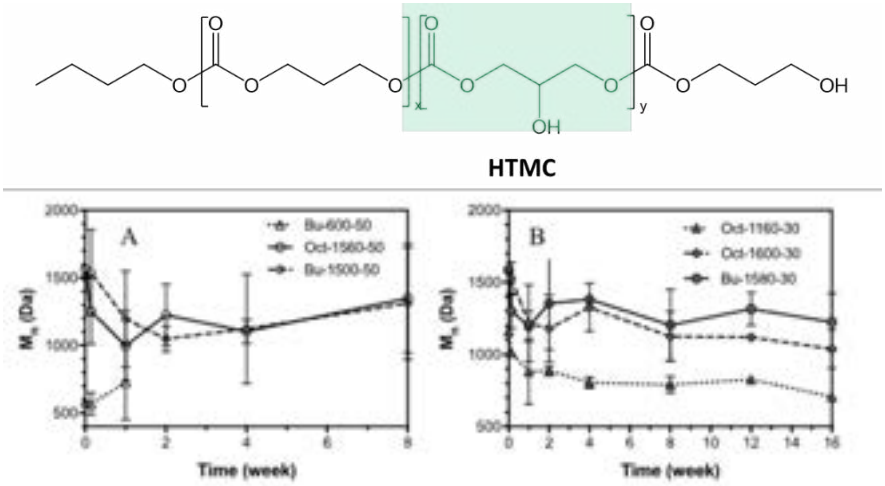

Figure 3-9. Change in copolymer M_n with time during in vitro degradation in PBS (pH 7.4) at 37°C for copolymers initially containing (A) 50 mol% HTMC and (B) 30 mol % HTMC (n= 3).[48]

Interestingly, mussel-inspired hydrogels, which comprised of catechol group on 3,4-Dihydroxyphenyl-L-alamine, has been found to have remarkable function for various engineering application such as tissue adhesives, drug delivery carriers, self healing hydrogels and coating materials. Thus, there are some studies to introduce DOPA and its analogues into PTMC and have successfully prepared self-healing gel materials (**Figure 3-10**). [49,50]

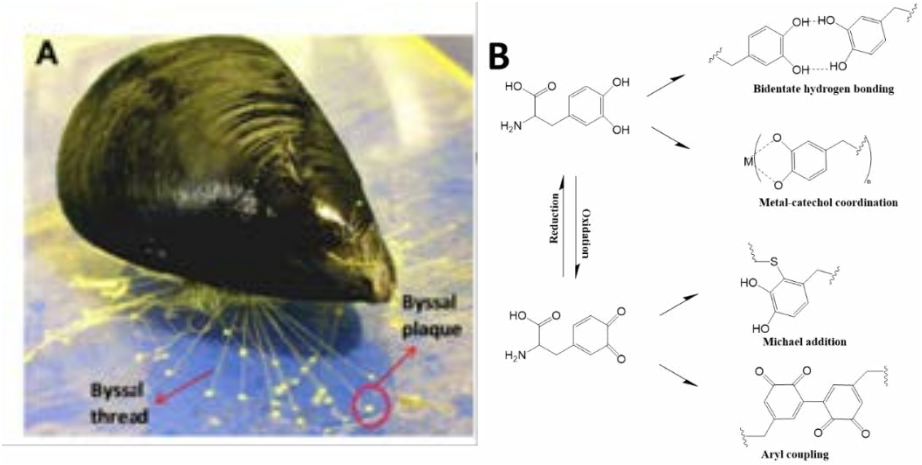

Figure 3-10. (A) A mussel (M. edulis) attached to a sheet of mica through byssal 70 thread and byssal plaque. (B) Schematic illustration of the various interactions involved with DOPA and dopaquinone in constructing mussel-inspired hydrogels.[50]

Despite the fact that the merit of hydroxyl and carboxylic group into PTMC in biomedical application has been evidenced, there are difficulties in introducing the pendant functionalities at monomer level, in particular due to the incompatibility of these protic functional groups with the polymerization. They require thus the use of protecting groups. It is imperative that the functionalized biodegradable polymeric material is not only scientifically sound but also of feasible synthesis and viable. The synthesis must be adaptable to facilitate the easy incorporation of a variety of functionalities. It is well known that thiol-ene reaction has been consistently held a preferable technique in introducing new functionality to the polymer with ease, avoiding the need to use protecting groups and able to post-polymerization modification with functional group that is arduous to incorporate before polymerization. More attractively, through thiol-ene couple chemistry, it facilitates the attachment of biomolecules, prodrugs and targeting ligands for appropriate medical applications.[51] Besides, it have been reported that substituted TMCs exhibit higher reactivity than TMC when organocatalysts such as 1,5,7-triazabicyclo[4.4.0]dec-5-ene (TBD) or the association of 1,8-diazabicyclo[5.4.0]undec-7-ene (DBU) and 1-(3,5-bis(trifluoromethyl)phenyl)-3-cyclohexyl-2-thiourea (TU) are employed to promote copolymerization.[52,53] Conversely, it demonstrates lower reactivity when Brönsted acids such as methane sulfonic acid (MSA) are used.[54] This observation underscores the interest in using 5-Methylene-1,3-Dioxane-2-One (exTMC), which exhibits reactivity comparable to TMC, for introducing functional groups *via* post-polymerization modification through thiol-ene reactions. Consequently, simultaneous copolymerization leads to the formation of gradient copolymers, characterized by a higher concentration of functional groups on one side of the polymer chain.

Introduction of carboxylic acid into PEG-*block*-PTMC has been realized by post-polymerization modification with 3-mercaptopropionic acid through thiol-ene reaction (**Figure 3-11**).[55] It is found that functionalized polymer formed nano-sized polymersomes had remarkably high protein loading efficiencies for FITC-labeled bovine serum albumin (FITC-BSA) and exhibit a pH-dependant protein release behavior, that is, inhibited protein release at physiological pH while fast release at endosomal pH. This pH-dependant release behavior of ‘‘charged’’ polymersomes is likely contributed by the weakened interactions between protein and polymersome membrane at mildly acidic pH. This biodegradable polymersome is promising for tumor-targeting delivery of various therapeutic proteins.

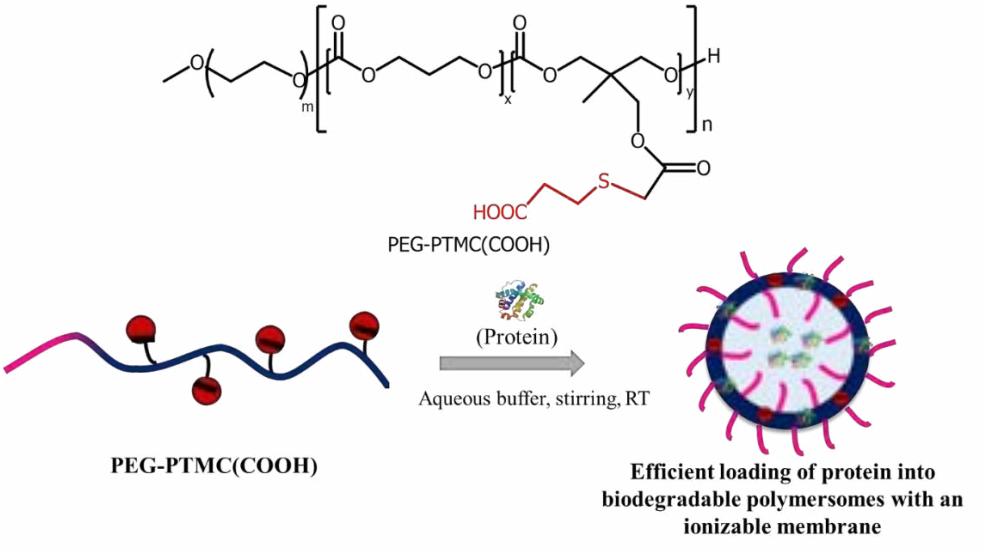

Figure 3-11. Biodegradable polymersomes with an ionizable membrane allow efficient loading of proteins.[55]

Olofsson and co-workers used thiol-ene chemistry to introduced synthetic mussel foot proteins analogues into PTMC through thiol-functionalized derivative of dopamine *via* UV-initiated thiol-ene coupling with ally-PTMC has successfully prepare self-healing gel materials with catechol functionality (**Figure 3-12**).[49] Gels were formed by addition of Fe3+, as a result of the high affinity of the catechol functionality for these ions. Increasing pH resulted in a higher degree of complexation of Fe^{3+} ions with the catechol group, ranging from monocomplexes at pH 5, to bis and tris complexes at higher pH. A solution of catecholfunctional polymer with $FeCl_3 \cdot 6H_2O$ (catechol:Fe^{3+} ratio of 3:1) was prepared in a solution of 2M NaOH in methanol, resulting in the production of free-standing gels. Application of strain to the gels resulted in a drop in elastic modulus and viscosity, and a consequent loss in gel properties. However, when the strain was removed, the gel-like character of the material was fully regained. The reliability of this self-healing property was demonstrated by repeated application and removal of strain, with the complete reformation of the gel shown to occur in under 6 s after each test. DOPA-functionalized PMAC therefore demonstrates the possibility of developing biomedical devices based on aliphatic polycarbonates which are capable of self-healing following damage resulting from the application of excess strain.[49]

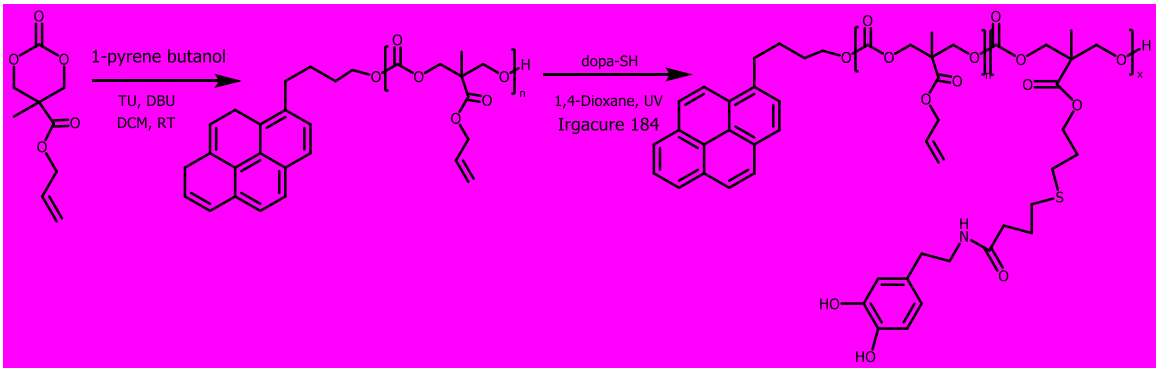

Figure 3-12. Reaction scheme for the ring-opening polymerization of MAC and UV-initiated TEC postpolymerization functionaliza-tion with dopa-thiol leading to pMAC(allyl/dopa).[49]

In this study in Chapter III, I aim to clarify the fundamental relationship between the biocompatible property of polymers and the chemical structure of polymeric biomaterials. Notably, PTMC-*co*-PexTMC exhibits considerable potential to modulate the number of functional groups and to subsequently modify these with a diverse array of thiol derivatives through thiol-ene click reactions, all achieved without the necessity for protective groups. This study extends to a detailed examination of various TMC copolymer structures, specifically tailored for applications in biomaterials. Synthesized copolymers of TMC with exTMC and TMC with functionalized exTMC through thiol-ene reactions involving thioglycolic acid and thioglycerol, have been employed as coatings for biomaterials. Comprehensive investigations have been undertaken to assess the influence of structural and functional group variations in PTMC-*co*-PexTMC on several parameters including thermal stability, contact angle, initial degradation patterns, drug release kinetics, protein adsorption, and blood platelet adhesion, as depicted in (**Figure 3-13**).

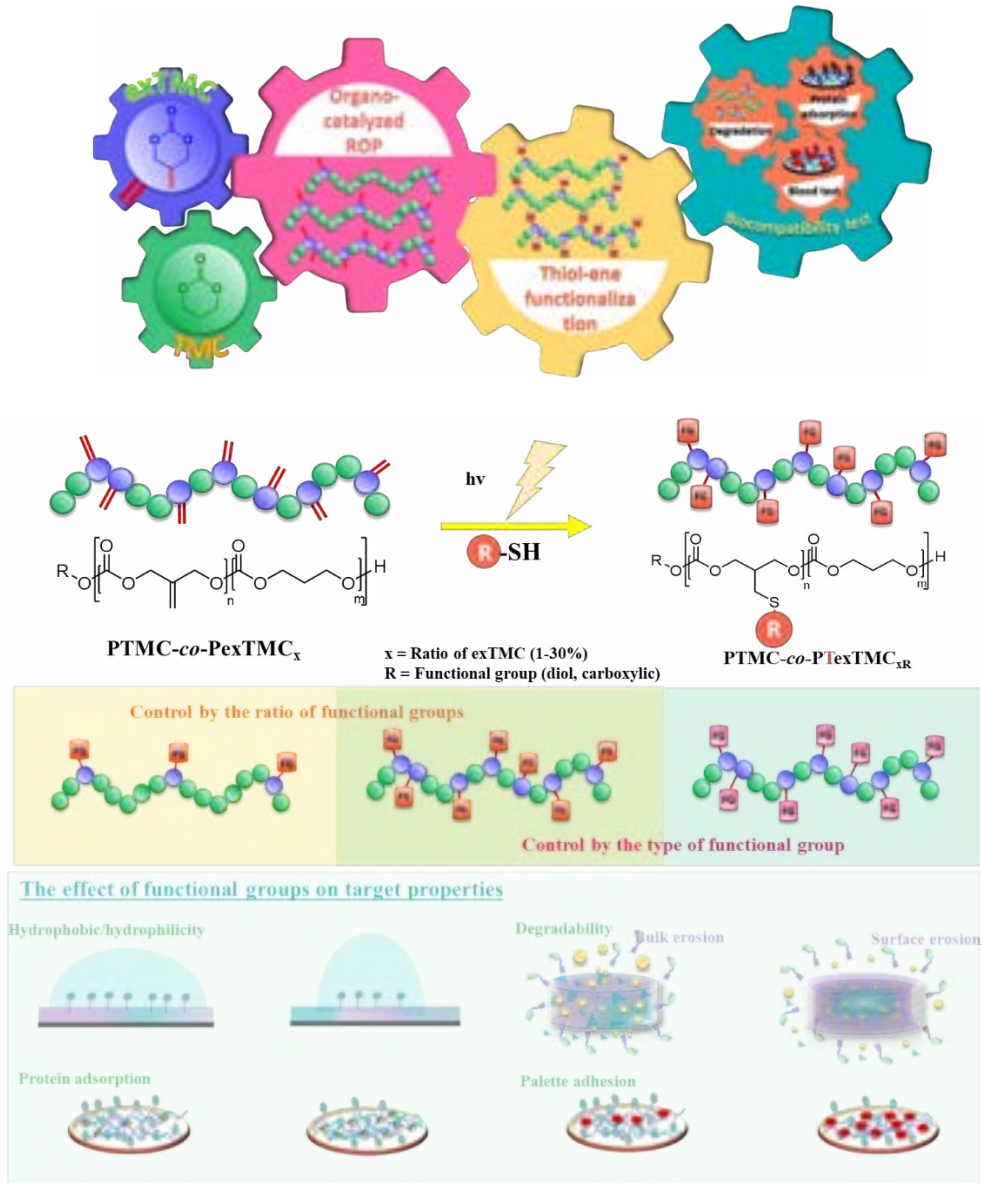

Figure 3-13. Preparation of PTMC-*co*-PexTMC derivatives by post-polymerization modification *via* thiol-ene reaction to study the effect of functional groups.

3.2 Results and Discussions

3.2.1 Synthesis of copolymer of TMC and exTMC with MSA as catalyst

As was reported in chapter 2 MSA-catalyst could control the copolymerization of TMC and exTMC with reactivity ratios values close to 1, leading to PTMC-*co*-exTMC copolymers with almost perfect randomness and well-defined structures.[56] To adjust the methylidene groups content distributed along the polymer chain, exTMC monomer was controlled by feeding ratios of 1,5,10 and 30% for a global DP of 120.

Table 3-1. M_n of copolymer before and after post-polymerization modification by thiol-ene reaction

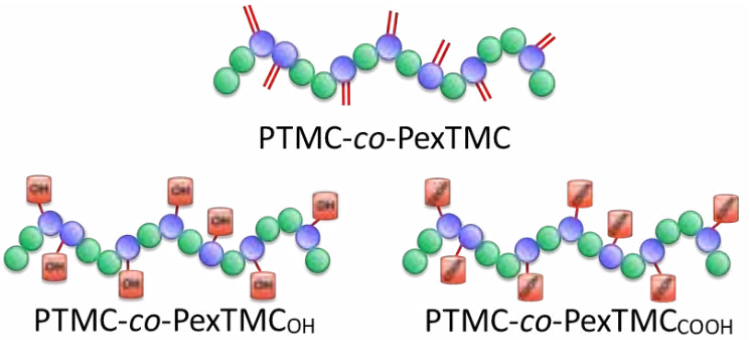

Entry	Name	M_{nTheo} (kDa)	M_{nSEC} [a,b] (kDa)	M_{nCOR} [c] (kDa)	$Đ$	Contact angle (°)	T_{10} (°C)
1	PTMC-co-PexTMC$_1$	12.7	10.6	9.3	1.25	53.3±1.6	266
2	PTMC-co-PexTMC$_{1OH}$		11.7		1.18	43.0±1.4	331
3	PTMC-co-PexTMC$_{1COOH}$		12.6		1.37	43.9±0.6	330
4	PTMC-co-PexTMC$_5$	12.7	12.1	10.6	1.17	50.8±0.7	282
5	PTMC-co-PexTMC$_{5OH}$		10.4		1.28	39.8±0.7	310
6	PTMC-co-PexTMC$_{5COOH}$		12.4		1.3	45.2±1.2	320
7	PTMC-co-PexTMC$_{10}$	12.7	10.3	9.1	1.12	55.5±2.1	301
8	PTMC-co-PexTMC$_{10OH}$		10.8		1.18	37.1±1.2	248
9	PTMC-co-PexTMC$_{10COOH}$		11.3		1.23	39.6±1.3	283
10	PTMC-co-PexTMC$_{30}$	12.7	12.9	11.4	1.14	68.7±2.5	317
11	PTMC-co-PexTMC$_{30OH}$		12.9		1.23	35.8±2.3	198
12	PTMC-co-PexTMC$_{30COOH}$		15.1		1.31	31.5±0.7	206

[a] Determined by SEC by polystyrene (PS) standard in THF, 40 °C. [b]Bulk, 60°C with propane-1,3-diol as initiator.

[c]Values corrected using the correction factor reported for PTMC.[57]

The exTMC content along the polymer chain were confirmed by ^{1}H NMR (**Figure 3-14**). The obtained results in **Figure 3-14** indicated that it is possible to control TMC and exTMC content in the copolymer chain. The linear difunctional initiator propan-1,3-diol (DPO) in the core of the polymer chains cannot be differentiated from signals c and d corresponding to the OCH_2-CH_2-CH_2-O of the TMC units. Two different CH_2OH chain-ends are observed b' at 3.75 ppm and d' at 4.19 ppm corresponding to the TMC and exTMC CH_2OH terminal units, respectively. The relative integrals of signals b, c corresponding to the CH_2O moieties and signals a, d corresponding to the CH_2 moieties of exTMC and TMC units, respectively, agree nicely with the initial TMC:exTMC monomer ratio 118.8:1.2 (**Figure 3-14a**), 114:6 (**Figure** 3-**14b**), 108:12 (**Figure 3-14c**), and 84:36 (**Figure 3-14d**). The molecular weights of PTMC-*co*-PexTMC$_1$, PTMC-*co*-PexTMC$_5$, PTMC-*co*-PexTMC$_{10}$, and PTMC-*co*-PexTMC$_{30}$ were confirmed by SEC analysis which are detailed in **Entry 1, Entry 4, Entry 7, and Entry 10** (**Table 3-1)**, respectively. The obtained results shown that the M_n of PTMC-*co*-exTMC copolymers at DP 120 with various TMC and exTMC monomer content are close to the expected values (around 10 kDa) while maintaining narrow $Đ$ (1.12-1.25), in agreement with a lower impact of the competitive ACE propagation mechanism.

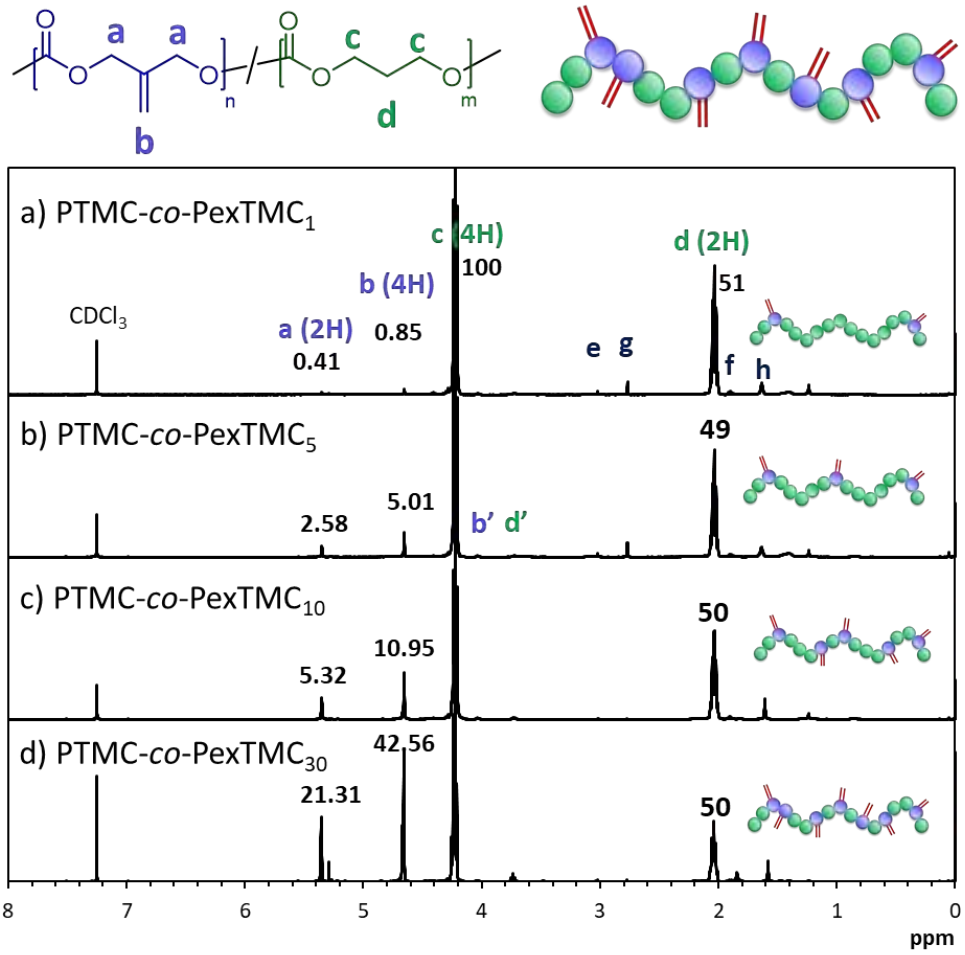

Figure 3-14 ^{1}H NMR spectra of PTMC-*co*-PexTMC with DP = 120 by various TMC/exTMC monomer ratio of a) 118.8:1.2, b) 114:6, c)108:12, and d) 84:36 ($CDCl_3$, 300 MHz).

3.2.2 Post-polymerization modification of Thiol-ene of PTMC-*co*-PexTMC with thioglycolic acid (TGA) or thiolglycerol (TGC) moiety

Then post-polymerization modification was performed by thiol-ene reaction *via* UV light (365 nm) which was used for irradiation with the aid of a DMPA photo-initiator. Reactions were carried out on four copolymers with DP120 and different monomer compositions (1-30% contents in exTMC) with two different thiol derivatives bearing non-protected protic functional groups (hydroxyl and carboxylic), namely thioglycerol (TGA) and thioglycolic acid (TGC). Thus, hydrophobicity and hydrophilicity could be controlled by not just only functionality but also methylidene groups content (exTMC

content) in the polymer chains. The structure after post-polymerization modification was confirmed by the ^{1}H NMR spectrum (**Figure 3-15**) and FT-IR spectrum (**Figure 3-16**). ^{1}H NMR monitoring showed almost complete disappearance of the signals at 4.70 and 5.40 ppm, corresponding to the O-CH_2-C(=CH_2)CH_2-O sequences of the exTMC units (**Figure 3-15a and 3-15b**), and the appearance of new broad multiplet signals: (i) at 2.35, 2.65—2.90, 3.36—3.60, and 3.60—3.90 ppm corresponding to the CH_2 and CH groups deriving from TGA (l, k, b', j, and i) (**Figure 3-15b**), (ii) at 2.35 and 2.72—2.80, and 3.20—3.60 ppm for the new CH and CH_2 groups deriving from TGC (j,b', and i) resulting from the thio-ene addition to the C=CH_2 moiety (**Figure 3-15a**) . Additionally, FTIR spectrum (**Figure 3-16**) indicated that thio-ene addition to the C=CH_2 moiety because appeared of S-C stretching peak at 668 cm^{-1}. Moreover, SEC analysis confirms that the thiol-ene reaction occurs without affecting the integrity of the polymer chains or causing reticulation, since M_n and $Đ$ values are in the same range than the starting copolymers (**Figure 3-17a** and **Table 3-1**). However, increasing the exTMC content in copolymer chain influenced to increase of M_n and broader $Đ$ after post-polymerization modification *via* thiol-en reaction (**Figure 3-17b** and **Table 3-1**). It could be implied that the thiol derivatives had been incorporated into the side chain of PTMC-*co*-exTMC copolymers whereas the broadening of polydispersity was possibly due to either a side reaction for attachment of thiol at different positions on the vinyl or chain scission that occurred during UV irradiation.

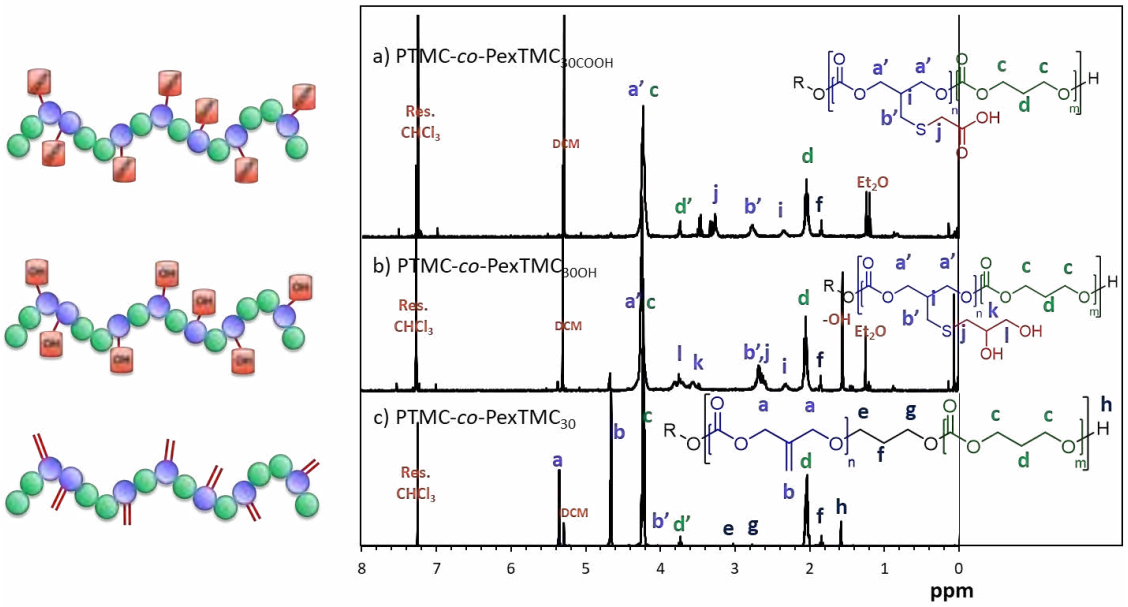

Figure 3-15 ^{1}H NMR spectra of PTMC-*co*-PexTMC a) after post-polymerization modification by glycolic acid, b) after post-polymerization modification by thiolglycerol,

and c) before post-polymerization modification with DP = 120 and TMC/exTMC monomer ratio 84:36 ($CDCl_3$, 300 MHz).

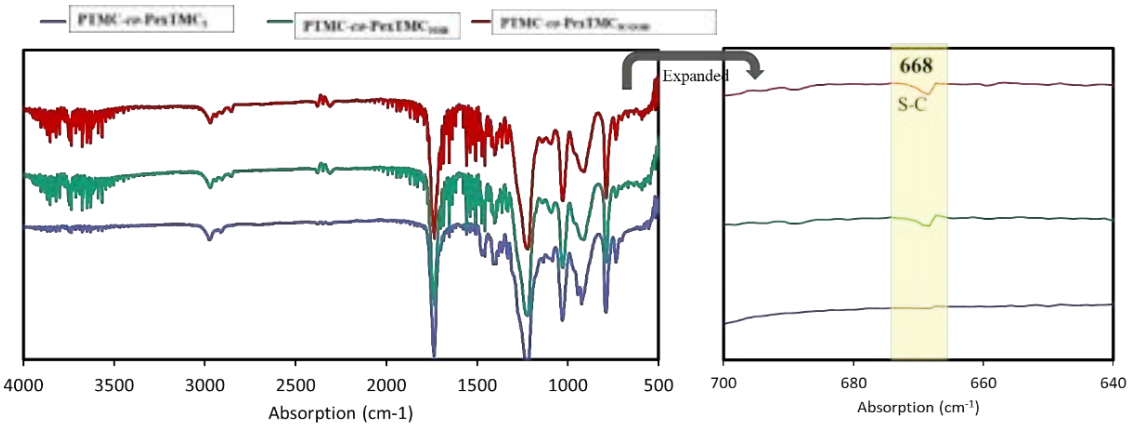

Figure 3-16. FT-IR spectra of PTMC-*co*-PexTMC before and after post-polymerization modification by TGA or TGC with DP = 120 and TMC/exTMC monomer ratio 114:6.

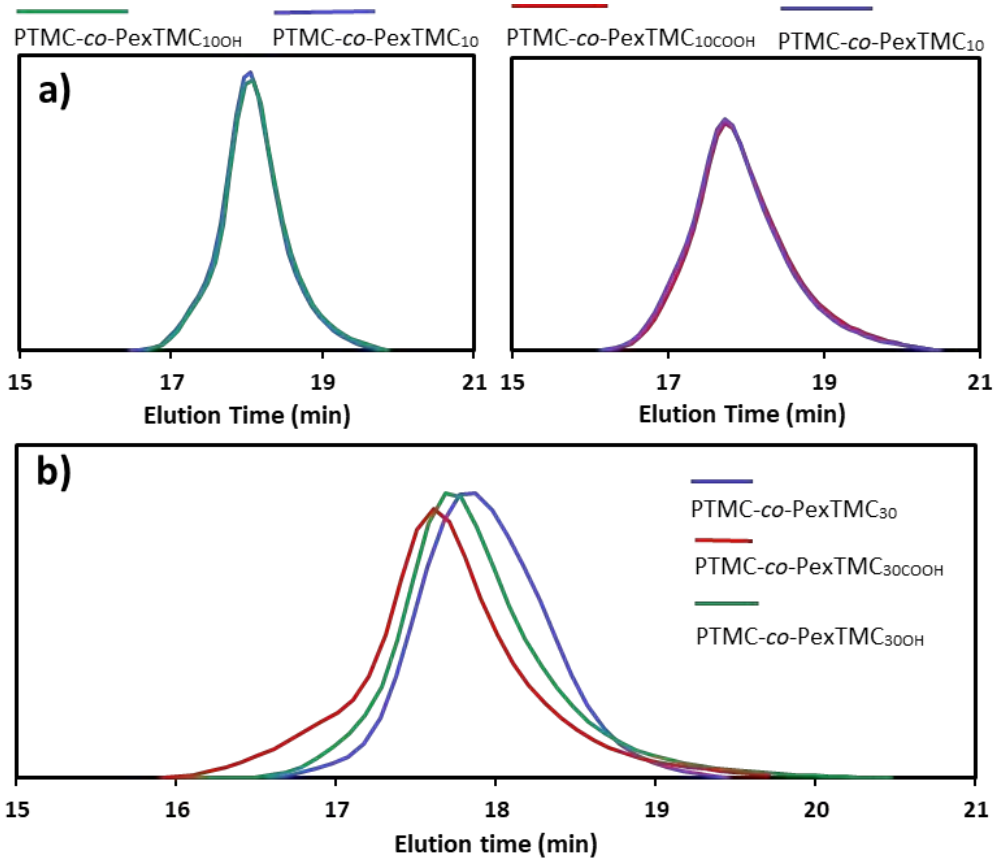

Figure 3-17. SEC traces of the copolymers before and after post-polymerization modification; a) TMC/exTMC monomer ratio 108:12 and b) TMC/exTMC monomer ratio 84:36.

In this experiment, PTMC-*co*-PexTMC was synthesized using MSA as an organocatalyst to adjust functionalities, achieving controlled copolymerization of exTMC and TMC with relative reactivity ratios near 1. This process enabled the preparation of copolymers with well-defined structures and high randomness. Through thiol-ene click reactions with thioglycolic acid or thioglycerol, methylene groups on the polymer chains were modified to uniformly distribute COOH or OH functional groups, with degrees of polymerization at 120 and functional group content from 1—30%. This method efficiently produced polycarbonates with a regular functional group distribution.

3.2.3 Thermal stabilities

In order to achieve biomedical application as considering the sterilization and processing-related temperature, thermal stability of polymeric materials is considered. Herein, TGA thermograms and measurements of PTMC-*co*-PexTMC and their derivatives were evaluated in the relevant temperature profile (**Figure 3-18**).

In this chapter, the onset decomposition temperatures at 10% weight loss (T_{10}) were evaluated. Comparing to increase exTMC content on copolymer chain appeared higher T_{10} (**Figure 3-18b**). This obtained results suggested that increased of exTMC (hydrophobicity), might influence on thermal stability due to increase of C=C bond on side chains. Contrarily, after post-polymerization modification *via* thio-ene reaction and increasing of hydroxyl (**Figure 3-18c**) or carboxyl (**Figure 3-18d**) content in copolymer chains, it appeared lower T_{10}. The side chain groups after post-polymerization modification are considered to make polymer less resistant of thermal stability. However, it was sufficient for sterilization in clinical field by autoclaving (120 °C). It was reported T_{10} as 317°C for PTMC-*co*-PexTMC$_{30}$, 198°C for PTMC-*co*-PexTMC$_{30OH}$, and 206°C for PTMC-*co*-PexTMC$_{30COOH}$ (**Figure 3-18a**). The obtained results shown that after PTMC-*co*-PexTMC$_{30}$ was post-polymerization modification *via* thio-en reaction, the polymers have lower T_{10} compared to before post-polymerization modification. This might be due to the incorporation of hydroxyl or carboxy functional groups that probably contribute to the thermal degradation of the polymers after post-polymerization modification.[58]

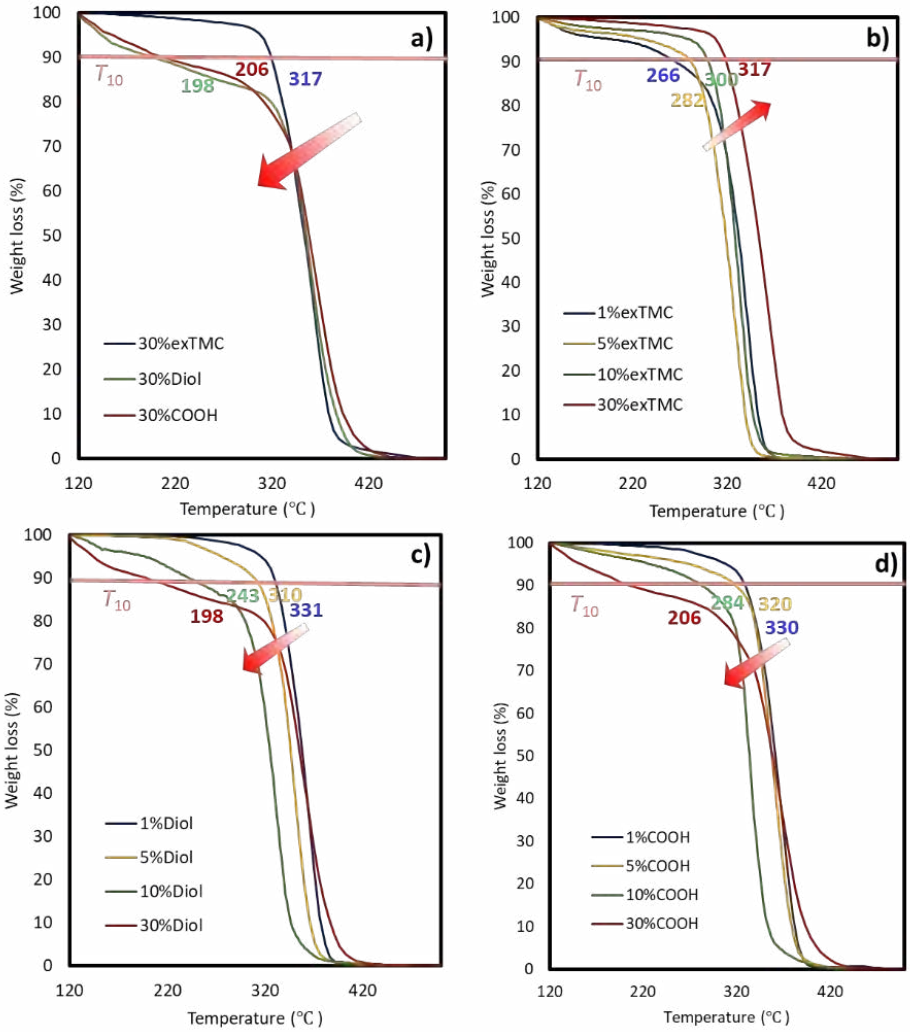

Figure 3-18 TGA thermogram of PTMC-*co*-PexTMC before and after post-polymerization modification by TGA or TGC; a) various types of copolymers with 30%modification, b) various exTMC content, c) various diol content, and d) various carboxylic content.

3.2.4 Wettability

To evaluate whether the surface has a hydrophobic or hydrophilic characteristic, which plays an important role in the material behaviour with biological molecules in physiological environment, the wettability of the polymers was evaluated. To simulate the conditions found in blood vessels, which are surrounded by blood (liquid), the captive bubble method was employed. This technique was used to analyse the water contact angle of coated polymers on glass, as detailed in **Table 3-1** and **Figure 3-19**. Copolymers were

coated on the glass substrates (diameter 0.8 mm). The concentration of copolymers solution in DCM was 20 mg/ml and dropped 40 µl of polymeric solution to the substrate for four time-repeated coating. The coated substrates were then dried under vacuum before testing. Then, the coated samples were soaked in DI water 3 minutes, then, the air 40 µl was dropped on coated surface with three replicates at different locations to obtain mean value of the contact angle.

The contact angles were 53.3 ° ± 1.6, 50.8° ± 0.7, 55.5° ± 2.1 and 68.7° ± 2.5 for PTMC-*co*-PexTMC$_1$, PTMC-*co*-PexTMC$_5$, PTMC-*co*-PexTMC$_{10}$, and PTMC-*co*-PexTMC$_{30}$, respectively. As the results, it seems that increasing of exTMC content might have a significant impact on increasing the hydrophobicity. Conversely, the contact angles of copolymer modified by TGC were 43.0 ° ± 1.4, 39.8° ± 0.7, 37.1° ± 1.2 and 35.8° ± 2.3 for PTMC-*co*-PexTMC$_{1OH}$, PTMC-*co*-PexTMC$_{5OH}$, PTMC-*co*-PexTMC$_{10OH}$, and PTMC-*co*-PexTMC$_{30OH}$, respectively. The contact angles of copolymer modified by TGA were 43.9 ° ± 0.6, 45.2° ± 1.2, 39.6° ± 1.3 and 31.5° ± 1.7 for PTMC-*co*-PexTMC$_{1COOH}$, PTMC-*co*-PexTMC$_{5COOH}$, PTMC-*co*-PexTMC$_{10COOH}$, and PTMC-*co*-PexTMC$_{30COOH}$, respectively. Regarding the results, the contact angles exhibited different trend after post-polymerization modification *via* thio-ene reaction, as could be expected. The increase in protic function improves hydrophilicity. However, the presence of carboxylic functional groups can enhance hydrophilicity more effectively than diols at equivalent concentrations.

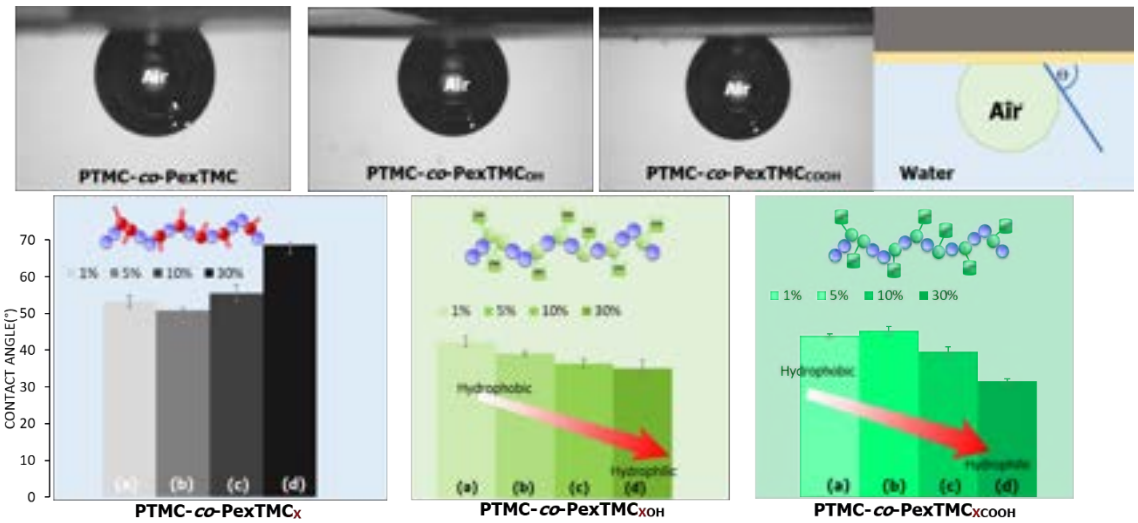

Figure 3-19 Contact angle measuring by captive bubble method of PTMC-*co*-PexTMC before and after post-polymerization modification by thiol-glycerol and glycolic acid with a) 1, b) 5, c) 10, and c) 30% of functional groups.

3.2.5 Degradation behavior

Approaching to biomedical materials, it is important to study the biological response of different polymeric biomaterials. Surfaces with different functional group have different chemically and physically properties in term of wettability, roughness, hydrophobicity-hydrophilicity, and these could correlate to biodegradability, blood and tissue-interaction, and compatibility. Custom designing and synthesizing polymers with tailorable properties are essential to control the degradability of polymers for clinical applications. These properties must match the unique requirements of each application, such as a degradation period that aligns with the healing process. Additionally, the mechanical performance should be sufficient to withstand the stresses of the intended application. It is also critical that the degradation products are non-toxic to avoid inflammatory or adverse effects upon implantation in the body.

Therefore, the degradation behaviour of the prepared copolymers was studied and the results are shown in **Figure 3-20.** In this chapter, copolymers were coated on the glass substrates (diameter 0.8 mm). The concentration of copolymers solution in DCM was 20 mg/ml and dropped 40 µl of polymeric solution to the substrate for four time-repeated coating. The coated substrates were then dried under vacuum before testing. Then, the coated samples were assessed in degradation study under circumstances 2 ml which are 5mg/ml of lipase enzyme solution, and PBS solution at 37 °C. The polymer amount on the substrate was approximately 3-5 mg. %weight loss (**Figure 3-20**) and % water uptake (**Figure 3-22**) were dependent on copolymer composition and were examined at every 1, 5, 20, 35, 50, 60, 80, and 90 days. The results indicated that PexTMC-*co*-TMC_{30COOH} showed the highest %weight loss after 90 days both in lipase and PBS solution (100 % (**Figure 3-20b**) and 78.50 ± 5.03% (~3.7 mg) (**Figure 3-20a**), respectively. It appeared that PTMC-*co*-$PexTMC_{30COOH}$ and PTMC-*co*-$PexTMC_{30OH}$ experienced accelerated weight loss more rapidly than PTMC-*co*-$exTMC_{30}$ in lipase, which contrasts with previous reports stating that increasing the composition of TMC in the copolymer chain enhances degradation. This confirms the higher propensity of the carbonate bonds and hydrophobic surfaces to undergo enzymatic degradation more rapidly than those with greater hydrophilicity.[59,60] However, Maria et al. reported that carboxylic acids in lipase can catalyse esterification reactions,[61] which could agree with our results; PTMC-*co*-$PexTMC_{30COOH}$ obtained the highest weight loss due to the carboxylic pendant catalysed the esterification of the polymer chain in lipase.

Additionally, PTMC-*co*-$PexTMC_{30COOH}$ showed faster %weight loss not only than PTMC-*co*-$PexTMC_{30}$ but also than PTMC-*co*-$PexTMC_{30OH}$ in PBS solution. It is well known that acid could play a role as a degradation catalyst, which accelerates the

hydrolysis of ester bonds in the polymer backbone. [47] Yu et al. have reported that PTMC modified with carboxylic group were hydrolysed faster than PTMC modification with hydroxyl group.[47] Moreover, the obtained results could imply that increasing of hydroxyl content in copolymer chains caused a higher %weight loss due to improvement of hydrophilicity as shown in **Figure 3-19.** It was the same trend which have been reported by Amsden and co-worker that increasing of hydroxyl content in copolymer chains has the greatest impact on the degradation rate.[48] Furthermore, Andriani et al. reported that an increase in the hydrophilic moieties within the copolymer chains can accelerate hydrolytic degradation, as water molecules more readily penetrate the polymer structure.[56] In lipase, PTMC-*co*-PexTMC$_{30}$, PTMC-*co*-PexTMC$_{1OH}$, and PTMC-*co*-PexTMC$_{5OH}$ exhibited less %weight loss; 10% (~1.1 mg), 19% (~1.5 mg), and 25% (~2.1 mg), respectively over 90 days compared to their degradation in PBS conditions. This reduced interaction between polymer and lipase may be attributed to the presence of hydrophilic properties within the polymers.[62] However, functional groups such as hydroxyl and carboxylic acids continue to play a crucial role in the degradation behavior, suggesting that functionalization of PTMC-*co*-PexTMC leads to increased weight loss. It is important to note, that the PTMC-*co*-PexTMC with low content of post-polymerization modification exhibited lower % weight loss against the lipase compared with PBS. Nevertheless, PTMC-*co*-PexTMC with high content of post-polymerization modification such as PTMC-*co*-PexTMC$_{30COOH}$, PTMC-*co*-PexTMC$_{30OH}$ exhibited higher % weight loss in lipase. As shown in **Figure 3-20b,** PTMC-*co*-PexTMC$_{30COOH}$ could not be observed in substrate after 50 days in lipase (fully degraded). Moreover, it was observed by optical microscopy that the surface morphology was observed that it changed from smooth to rough surface within 20 days for lipase and 50 days for PBS (**Figure 3-21**). Besides, the M_n of coated polymer was observed by SEC. It was found that the M_n of PTMC-*co*-PexTMC$_{30}$ and PTMC-*co*-PexTMC$_{30OH}$ did not change significantly during the degradation experiment. In contrast, the M_n of PTMC-*co*-PexTMC$_{30COOH}$ was reduced from the first day of the experiment in both PBS and lipase solution (**Figure 3-20c**). These results might indicate that PTMC-*co*-PexTMC$_{30COOH}$ initial weight loss could be due to the PTMC bulk erosion process. Also, this may support the crucial modification on the PTMC side chain with ether linkage. This variation could be explained to the presence of functionalization.

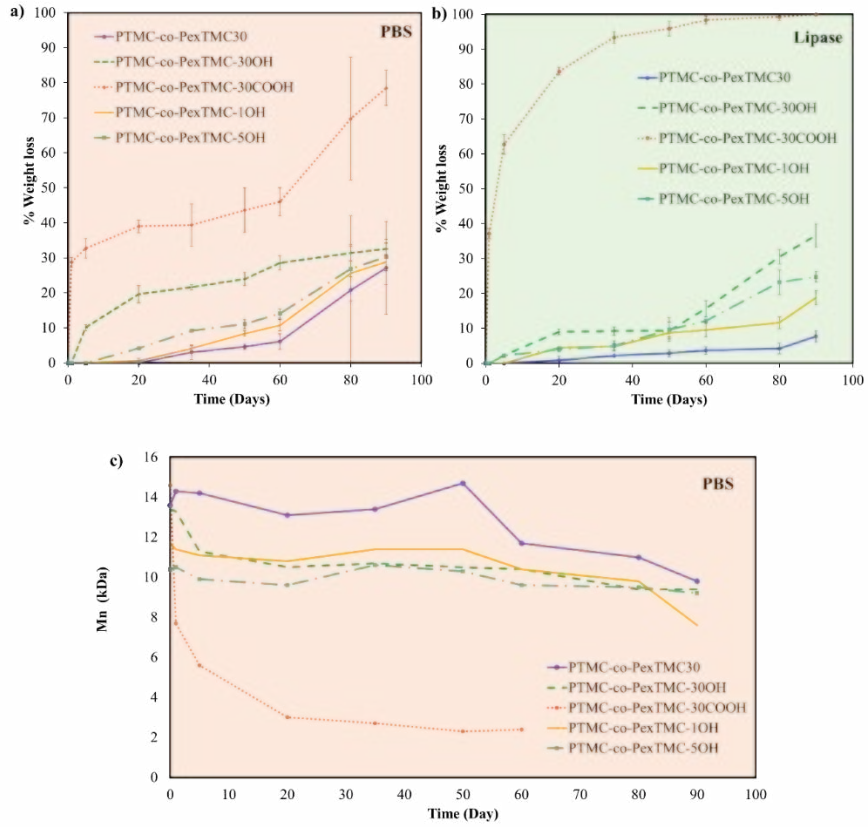

Figure 3-20 The plots of PTMC-*co*-PexTMC derivatives (a) % weight loss over time in PBS circumstances, (b) % weight loss over time in lipase circumstances, and (c) M_n after degradation over time in PBS.

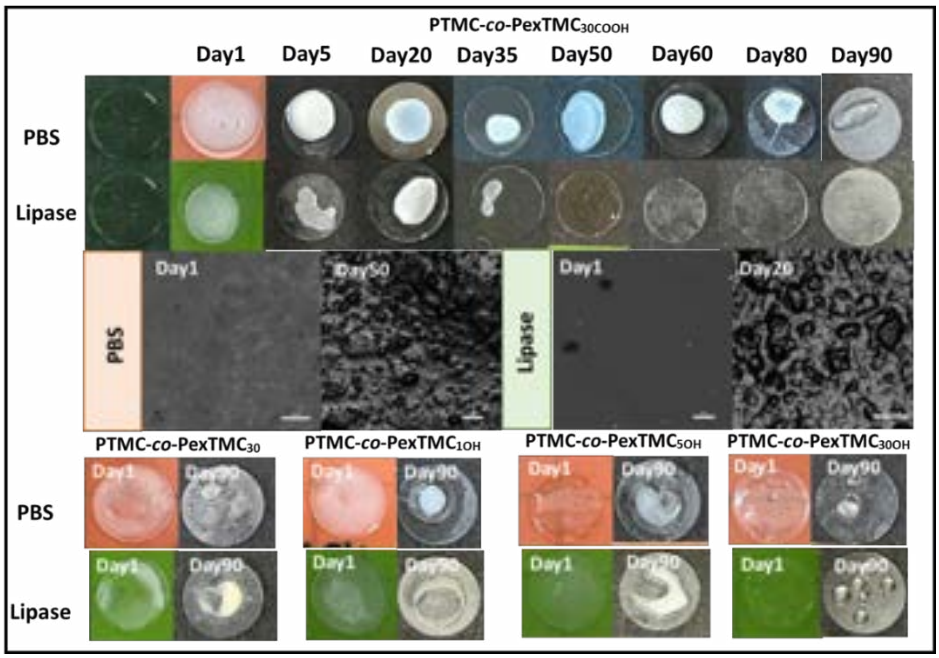

Figure 3-21 Surface morphology of PTMC-*co*-PexTMC derivatives.

The water uptake of polymeric materials plays an important role in evaluation of bioresorbable materials as it is related to the degradability. Therefore, water uptake occurred during the degradation seems to be an important factor in the degradation of the PTMC. The absorbed water molecules could lead to plasticization of the polymer and thus facilitate enzymatic attack. Consequently, PTMC variants with higher water absorption exhibited accelerated degradation rates compared to those with lesser water uptake.[63] Moreover, water infiltration into the amorphous regions of the copolymer prompts cleavage of carbonate linkages, yielding hydroxyl and carboxyl end groups. These end groups may exert an autocatalytic effect, further expediting the cleavage and disentanglement of the polymer chains.[64] Furthermore, the presence of hydrophilic functional groups could increase water absorption into the polymer matrix. PTMC-*co*-PexTMC$_{30COOH}$ showed the highest % water uptake both in lipase and PBS (**Figure 3-22b** and **Figure 3-22a**). The obtained results could imply that PTMC-*co*-PexTMC$_{30COOH}$ absorbed highest water content over 1300% within 35 days and 570% within 80 days in lipase and PBS, respectively. After showing the highest %water uptake, the trend of the curve was decreased due to degradation of the polymer chains, as shown in **Figure 3-20c** which was confirmed by the decrease of M_n observed by SEC analysis on the solid residue. In conclusion, it could be indicated that after post-polymerization modification of copolymer *via* thiol-en reaction, hydrophilicity functional groups were introduced to polymer chains, thus, hydrophilic groups such as hydroxyl or carbonyl group may increase the water diffusion rate, and catalysing degradation.[47,65,66]The obtained results is in agreement with previous studies suggesting that the water uptake could contribute to copolymer degradation. Introducing hydrophilic groups to the polymer chain might therefore lead to more water absorption, which could increase the cleavage of carbonate linkages and promote autocatalytic degradation.[63]

Nonetheless, the escalation in water uptake may be ascribed to the alterations in the surface morphology of the copolymer consequent to in vivo degradation. **Figure 3-21** illustrates the surface morphology of PTMC-*co*-PexTMC$_{30COOH}$ in PBS solution for 50 days and Lipase solution for 20 days, revealing a transition to a rough and pitted appearance. This increased roughness provides a greater capacity for water retention compared to smoother surfaces, thus correlating with the observed augmentation in water uptake. Moreover, the progressive increase in surface roughness over the degradation period further corroborates the occurrence of degradation.[63]

The obtained results suggest that carboxylic group modification of PTMC-*co*-PexTMC accelerates copolymer weight loss and water uptake more effectively than diol group modification or no modification. Therefore, PTMC-*co*-PexTMC$_{30COOH}$ emerges as

a promising candidate for coating medical devices that demand precise degradation timing, particularly for drug delivery applications that span 1-50 days. This finding is especially pertinent to the development of outer-layer drug-eluting stent coatings designed to control drug release and prevent excessive cellular proliferation, with an optimal release duration of approximately 30 days.[67,68] Additionally, controlling drug release over various durations may be achieved by adjusting the ratio of carboxylic and hydroxyl groups or by opting for non-modification. The customization of functional groups in type and quantity is key to meeting specific application requirements.

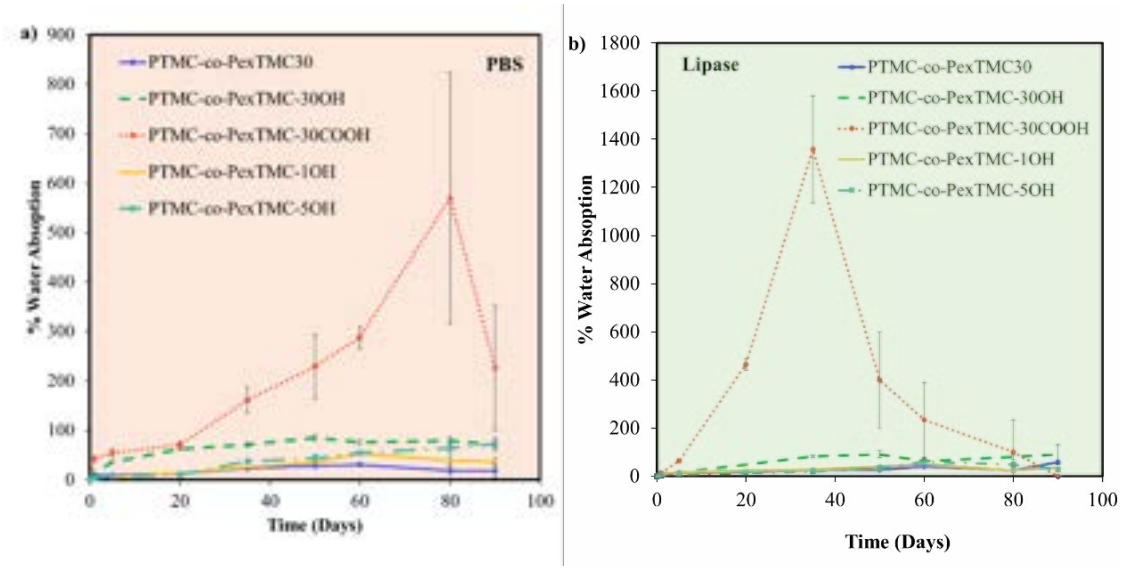

Figure 3-22 The plots of PTMC-*co*-PexTMC derivatives (a) % water uptake in PBS circumstances and (b) % water uptake in lipase circumstances over time.

3.2.6 *In vitro* drug released

We decided then to assess the potential of the polymers in drug release in a controlled manner to achieve a therapeutic goal for the effective treatment. A controlled release formulation over an extended period offers prolonged efficacy, decreased toxicity, and more compliance to the patient. The control of the release of drug could be achieved by polymer degradability which is adjustable by balancing hydrophobicity and hydrophilicity. The release profiles of doxorubicin from multifunctional copolymer were evaluated for 35 days at 37° C. DOX release profile of PTMC-*co*-PexTMC$_{30}$, PTMC-*co*-PexTMC$_{30OH}$, and PTMC-*co*-PexTMC$_{30COOH}$ samples are illustrated in **Figure 3-24.** To investigate the drug release behavior of copolymer, PTMC-*co*-PexTMC$_{30}$, PTMC-*co*-PexTMC$_{30OH}$, and PTMC-*co*-PexTMC$_{30COOH}$ were applied for incorporation with doxorubicin drugs. In vitro drug release measurements were carried out by circle round

shape of glass with dimension of 0.8 mm size. The drug loaded polymers were prepared by solubilizing drug (0.3 mg, 0.55mmol) and polymer 20mg in 1 ml of DCM. The drug-polymeric solution was sonicated for homogenous solution prior to coat by dropped 40 µl of polymeric solution to the substrate for four time-repeated coating. The coated substrates were then dried under vacuum. The coated samples were immersed in PBS (pH 7.4) as release medium and incubated at 37°C. At predetermined time points, the solution was detected the doxorubicin concentration by using UV spectrophotometry at wavelength 481 nm. It was found that DOX loading in one sample was accurate, at approximately 0.042 mg/mL (**Figure 3-23c**). This value was calculated by fitting the absorption data at 481nm (UV-Vis) from PTMC-*co*-PexTMC$_{30}$, PTMC-*co*-PexTMC$_{30OH}$, and PTMC-*co*-PexTMC$_{30COOH}$ (**Figure 2-23b**) to the DOX calibration curve equation shown in Figure **3-23a**.

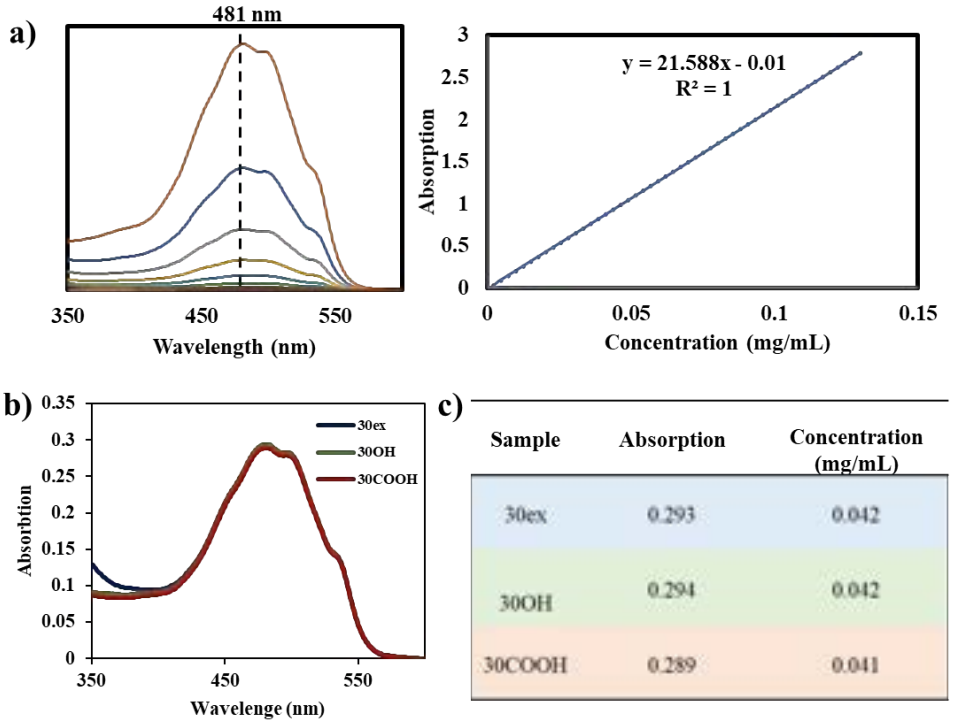

Figure 3-23 a) DOX calibration curve in DMSO, b) Absorption of DOX in copolymer, and c) concentration of DOX in copolymer.

Compared with PTMC-*co*-PexTMC$_{30COOH}$, the release rate of PTMC-*co*-PexTMC$_{30OH}$ was similar over a period of 1 to 14 days. Indeed, PTMC-*co*-PexTMC$_{30COOH}$ and PTMC-*co*-PexTMC$_{30OH}$ showed almost the same profile of releasing on 14 days which is 16.4 ± 1.2% and 15.5 ± 1.2%, respectively (**Figure 3-24**). After 14 days, PTMC-*co*-PexTMC$_{30COOH}$ expressed the highest DOX releasing profiles over 68.0 ± 19.6 %

within 28 days. On the other hand, the PTMC-*co*-PexTMC$_{30}$ and PTMC-*co*-PexTMC$_{30OH}$ showed gradually and sustained release profiles around 5.9 ± 1.3 % and 18.9 ± 2.8 % after 35 days. PTMC-*co*-PexTMC$_{30COOH}$ was abruptly released up over 126.9 ± 42.1% within 35 days. The possibility of PTMC-*co*-PexTMC$_{30COOH}$ -DOX over released might be the degradation of polymer effected on the transparency of the solution (**Figure 3-24**). The DOX release profile trend was the same as the degradation experiment which showed PTMC-*co*-PexTMC$_{30COOH}$ obtained highest %weight loss, it could then be implied that PTMC-*co*-PexTMC$_{30COOH}$ demonstrated the fastest DOX release profile due to degradation of copolymer. This observation is in agreement with the work of Fu et al which suggested that the drug release involved two different mechanisms: drug molecules diffusion and polymer matrix degradation.[69] Besides, SEC analysis confirmed that M_n of PTMC-*co*-PexTMC$_{30}$ remained the same (**Table 3-2** and **Figure 3-25b**) after 35 days which could be implied about stability of copolymer, thus, it was influent on the slowest DOX release profile. Conversely, M_n of PTMC-*co*-TPexMC$_{30OH}$ and PTMC-*co*-PexTMC$_{30COOH}$ was decreased after 35 days from 12.9 to 9.9 kDa and from 15.1 to 5.9 kDa (**Table 3-2** and **Figure 3-25b**), respectively. The obtained results indicate that introducing functional groups to improve hydrophilicity might improve the degradability of the polymer, which is related to drug release.

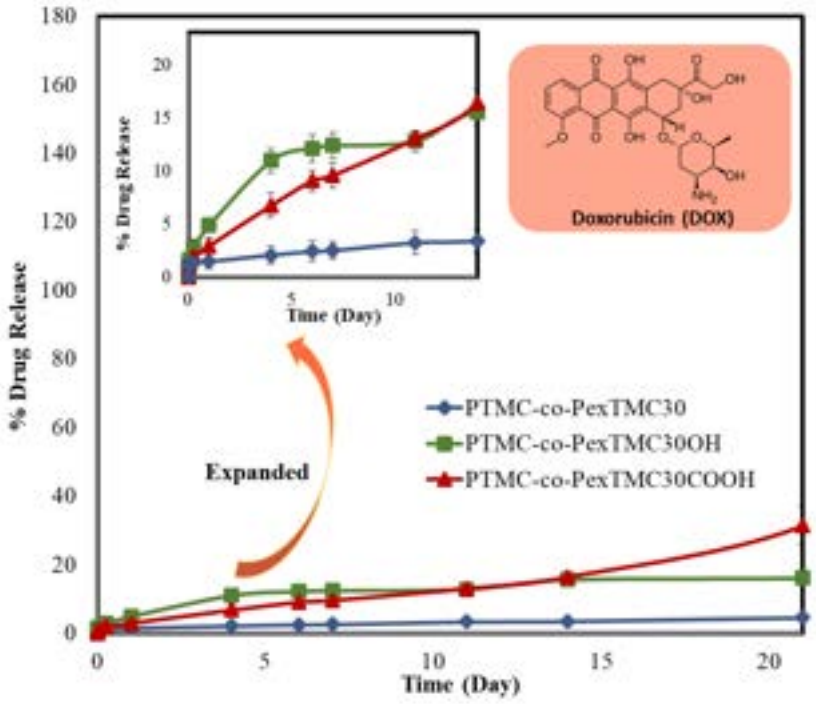

Figure 3-24. Doxorubicin drug release profile of PTMC-*co*-PexTMC$_{30}$, PTMC-*co*-PexTMC$_{30OH}$, and PTMC-*co*-PexTMC$_{30COOH}$.

Table 3-2. SEC curves before and after DOX control released of PTMC-*co*-PexTMC$_{30}$, PTMC-*co*-PexTMC$_{30OH}$, and PTMC-*co*-PexTMC$_{30COOH}$.

Sample	$M_n^{Before,a}$ (kDa)	Đ	$M_n^{After\ 35\ D,a}$ (kDa)	Đ
PTMC-*co*-PexTMC$_{30}$	12.9	1.14	**13.0**	**1.22**
PTMC-*co*-PexTMC$_{30OH}$	12.9	1.23	**9.9**	**1.59**
PTMC-*co*-PexTMC$_{30COOH}$	15.1	1.31	**5.9**	**2.08**

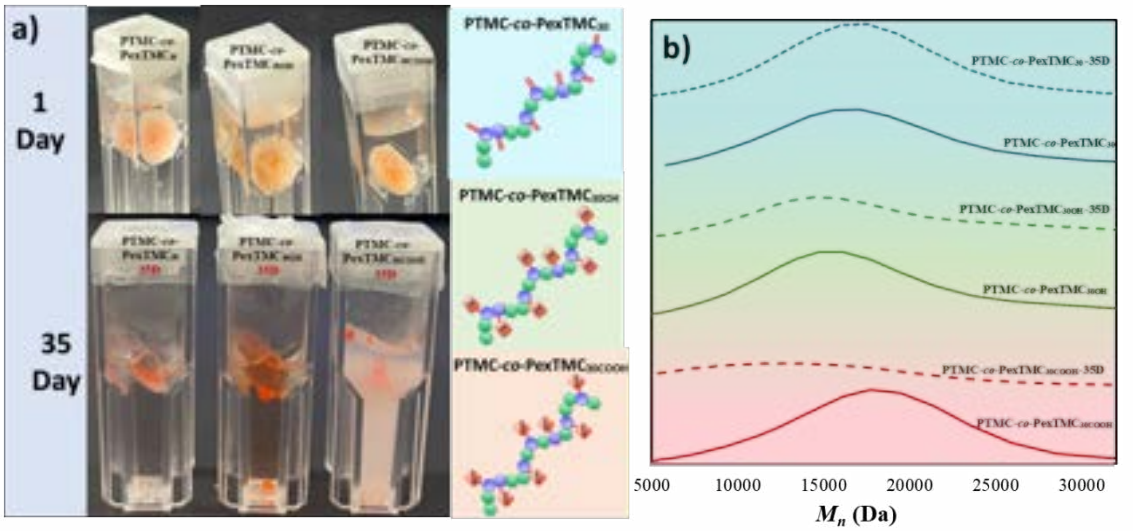

Figure 3-25. Observations from days 1 and 35: a) Image displaying PTMC-*co*-PexTMC$_{30}$, PTMC-*co*-PexTMC$_{30OH}$, and PTMC-*co*-PexTMC$_{30COOH}$ combined with DOX; b) SEC chromatograms or traces overlay of PTMC-*co*-PexTMC$_{30}$, PTMC-*co*-PexTMC$_{30OH}$, and PTMC-*co*-PexTMC$_{30COOH}$.

3.2.7 Biocompatibilities

3.2.7.1 Protein adsorption

Protein adsorption of a coating biomaterial is important for determining its biocompatibility when exposed to the physiological environment. It is believed that interaction between the proteins and biomaterials may mediate cellular adhesion that affect the long-term performance of the medical device. Thus, investigating the surface

modification of a coating polymers are a matter of concern. The protein behaviours in response to PTMC-*co*-PexTMC before and after post-polymerization modification with various content of exTMC on glass substrate is shown in **Figure 3-26**. Albumin and fibrinogen, the major protein of human blood plasma, were used in this chapter.

The albumin adsorption on non- post-polymerization modification PTMC-*co*-PexTMC coated on glass by varying exTMC content from 1—30% were 0.64 μg/cm^2 ± 0.001, 0.72 μg/cm^2 ± 0.23, and 0.93 μg/cm^2 ± 0.001 for PTMC-*co*-PexTMC$_1$, PTMC-*co*-PexTMC$_5$, and PTMC-*co*-PexTMC$_{10}$, respectively (**Figure 3-26a**). After post-polymerization modification by TGA, the protein adsorption increased to 3.38 μg/cm^2 ± 0.04, and 16.73 μg/cm^2 ± 1.71 for PTMC-*co*-PexTMC$_{1COOH}$, PTMC-*co*-PexTMC$_{5COOH}$, respectively (**Figure 3-26a**). The protein adsorption after post-polymerization modification by TGC were 1.68 μg/cm^2 ± 0.28, 3.54 μg/cm^2 ± 1.67, and 4.50 μg/cm^2 ± 0.56 for PTMC-*co*-PexTMC$_{1OH}$, PTMC-*co*-PexTMC$_{5OH}$, and PTMC-*co*-PexTMC$_{10OH}$, respectively (**Figure 3-26a**). The result was same trend with fibrinogen (**Figure 3-26b**). The fibrinogen adsorption of non- post-polymerization modification PTMC-*co*-PexTMC were 0.70 μg/cm^2 ± 0.11, 1.02 μg/cm^2 ± 0.01, and 1.10 μg/cm^2 ± 0.10 for PTMC-*co*-PexTMC$_1$, PTMC-*co*-PexTMC$_5$, and PTMC-*co*-PexTMC$_{30}$, respectively (**Figure 3-26a**). After post-polymerization modification by TGA, the protein adsorption was 1.86 μg/cm^2 ± 0.08, and 15.78 μg/cm^2 ± 2.43 for PTMC-*co*-PexTMC$_{1COOH}$, PTMC-*co*-PexTMC$_{5COOH}$, respectively. The protein adsorption after post-polymerization modification by TGC were 1.30 μg/cm^2 ± 0.02, 5.58 μg/cm^2 ± 0.20, and 10.27 μg/cm^2 ± 0.18 for PTMC-*co*-PexTMC$_{1OH}$, PTMC-*co*-PexTMC$_{5OH}$, and PTMC-*co*-PexTMC$_{30OH}$, respectively. Based on the obtained result, there is a marked difference in protein adsorption for functionalized PTMC-*co*-PexTMC depending on the function that is introduced on polymer chains (hydroxyl or carboxylic group). This is attributed to their high affinity to adsorb protein compared to non-functionalized PTMC-*co*-PexTMC in this study. It was found that affinity to adsorb protein of non-functionalized PTMC-*co*-PexTMC was not significantly changed by modifying the exTMC content. However, the results expressed significantly changed affinity to adsorb protein of functionalized PTMC-*co*-PexTMC by introduced different content of both hydroxy and carboxylic group. It showed that increasing the content of both hydroxy and carboxylic group is attributed to its high affinity to adsorb protein compared to lower content of functional groups (**Figure 3-26**). According to Arima et al, the effects of surface functional groups such as amines, hydroxy, and carboxylic showed higher protein adsorption compared to methyl group.[70] Moreover, Thevenot et al. have reported that carboxyl (–COOH) groups could interact preferentially with fibronectin and albumin more than hydroxyl (-OH) groups due to their

negatively charged and hydrophilic.[71] A similar pattern of results was obtained in **Figure 3-26a** and **Figure 3-26b** that after introducing carboxyl groups has significantly more increased affinity to adsorb protein for both of fibrinogen and albumin compared with hydroxyl (-OH). Furthermore, the effect of wettability could contribute to inducing favourable conditions for protein adsorbed on the surface. Cells effectively adhere onto a polymer surface with moderate wettability with water contact angles. The contact angles of PTMC-*co*-PexTMC after post-polymerization modification *via* thio-en reaction (**Table 3-1**), shown increasing of post-polymerization modification content increased hydrophilicity of polymer chain. Thus, it might affect of greater protein interaction with the polymer surface.

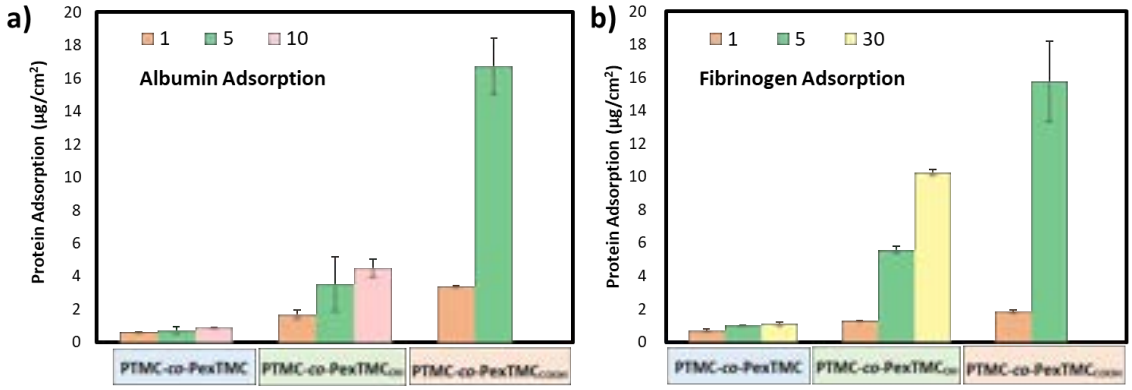

Figure 3-26. a) Albumin (BSA) protein adsorption and b) Fibrinogen (BPF) on PTMC-*co*-PexTMC, PTMC-*co*-PexTMC$_{OH}$, and PTMC-*co*-PexTMC$_{COOH}$.

3.2.7.2 Platelet adhesion

To assess the materials for blood vessel disorder, *in vitro* platelet adhesion was investigated to the coated surfaces because platelet adhesion could trigger fibrin production, resulting in blood clot formation. The platelet adhesion on the coated surfaces was characterized by SEM. The magnified SEM images indicated that the morphology of platelets adherent on surfaces depends on the coatings. PTMC-*co*-PexTMC$_{COOH}$ coated surface induced some platelets formed lamellipodia, which induced aggregation of platelets to adhere firmly onto the surface. On the other hand, each platelet seems to be isolated rather than aggregated for most of the polymer coatings. To quantify the platelet adhesion, the number of adherent platelets on the coatings was determined from the SEM images (**Figure 3-27**). Interestingly, the number of platelets that adhered to PTMC-*co*-PexTMC$_{OH}$ (**Figure 3-27c**) surface was significantly smaller than non-coated glass, PTMC-*co*-PexTMC, and PTMC-*co*-PexTMC$_{COOH}$. The adhered platelet number on substrate were 531 cell/mm^2 ± 126, 509 cell/mm^2 ± 112, 99 cell/mm^2 ± 33, and 881

cell/mm^2 ± 95 for Bear glass, PTMC-*co*-PexTMC$_{30COOH}$, PTMC-*co*-PexTMC$_{30OH}$, and PTMC-*co*-PexTMC$_{30}$, respectively (**Figure 3-28**). The obtained results seem to reflect the higher hydrophilicity of PTMC-*co*-PexTMC$_{OH\ and}$ PTMC-*co*-PexTMC$_{COOH}$ than PTMC-*co*-PexTMC, determined from the air-bubble contact angle in water (**Table 3-1**). Although the wettability of PTMC-*co*-PexTMC$_{OH}$ and PTMC-*co*-PexTMC$_{COOH}$ were almost similar. However, the functional groups and surface charges were different. Roach et al has reported the potential of protein, platelet and cell adhesion related to the hydrophilicity, charge, morphology, and chemical component on surface.[72] Methyl (–CH_3) is neutral and hydrophobic groups, thus, it is tightly binding fibrinogen (a protein involved in blood clotting). Hydroxyl groups (–OH) could increase the hydrophilicity of a material surface and neutral charge, thus, reduce the affinity of plasma proteins. Carboxyl (–COOH) groups are negatively charged in blood serum and other aqueous protein solutions, are hydrophilic, and interact preferentially with fibronectin and albumin.[71–74] Combining our results and the literatures indicate that PTMC-*co*-PexTMC$_{OH}$ could prevent platelet adhesion more effectively than PTMC-*co*-PexTMC, and PTMC-*co*-PexTMC$_{COOH}$.

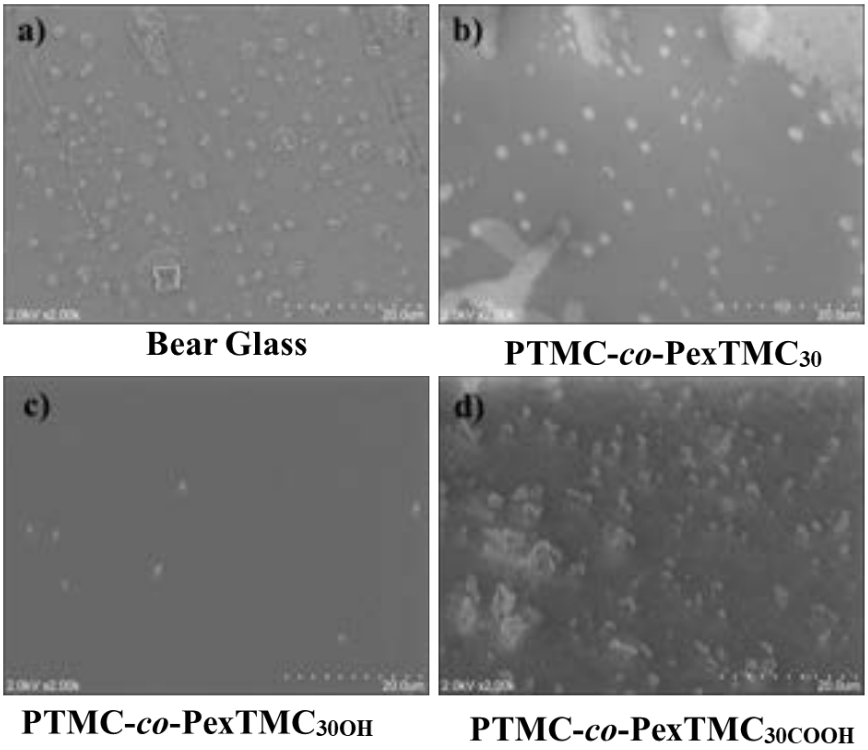

Figure 3-27. SEM images of platelet adhesion on materials surface; bear glass (a), PTMC-*co*-PexTMC30(b), PTMC-*co*-PexTMC30OH (c), PTMC-*co*-PexTMC30COOH (d) (n=5, 2 kV at 2000x magnification, scale bar 20 μm).

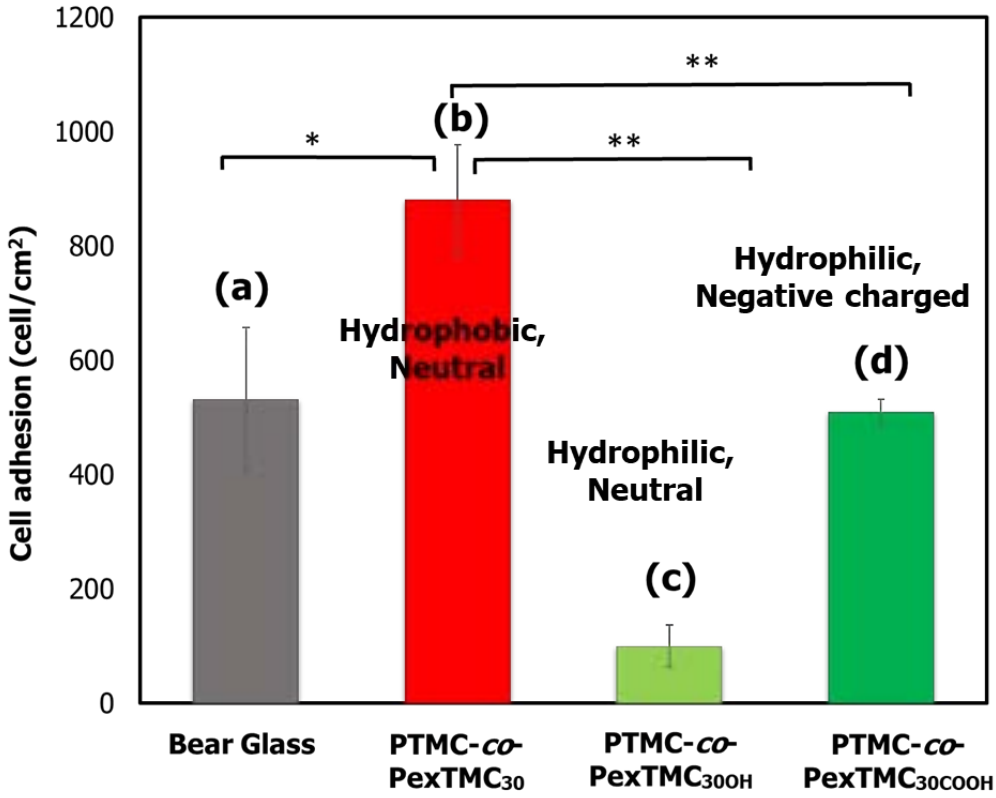

Figure 3-28. Quantitative plot the adhered platelet number on materials surface (n = 5, *p < 0.03, **p < 0.003).

The overall findings suggest that functionalized PTMC-*co*-PexTMC with different functional groups significantly alters its properties. The introduction of carboxylic groups has been shown to accelerate mass loss, enhance water uptake, and increase hydrophilicity, platelet adhesion, drug release, and protein absorption more than the addition of hydroxyl groups. For biomedical applications, specifically drug-eluting stent coatings, PTMC-*co*-PexTMC$_{COOH}$ is more suitable for the outer layer, offering controlled drug release to limit cell overgrowth, with an ideal release time of around 30 days.[67,68] Meanwhile, PTMC-*co*-PexTMC$_{OH}$ could be better for inner-layer coatings, providing longer-term drug release and more effective prevention of platelet adhesion after the outer layer's drug is released or degraded.

3.3 Conclusions

In this study, a series of PTMC-*co*-PexTMC copolymers were precisely grafted through the click thiol-ene reaction, featuring DP 120 and functional group contents ranging from 1% to 30% along the copolymer chain, incorporating either diol or carboxylic functional groups. Thermal stability analysis revealed that copolymers modified with over 10% thiol-ene content consistently exhibited a lower T_{10} compared to their unmodified counterparts. Additionally, an increased percentage of thiol-ene modification further reduced T_{10} values. The presence of diol and carboxylic pendant tended to increase hydrophilicity of copolymer. PTMC-*co*-PexTMC with increased exTMC content, both before and after thiol-ene post-polymerization modification, exhibited greater affinity for both of albumin and fibrinogen. Additionally, it was observed that post-polymerization modification with carboxylic groups led to increased proteins adsorption more than PTMC-*co*-PexTMC$_{OH}$ and PTMC-*co*-PexTMC, likely due to enhanced hydrophilicity. Besides, PTMC-*co*-PexTMC$_{OH}$ could prevent platelet adhesion more effectively than PTMC-*co*-PexTMC, and PTMC-*co*-PexTMC$_{COOH}$. The water absorption shown PTMC-*co*-PexTMC$_{30COOH}$ could adsorb water better than PTMC-*co*-PexTMC and PTMC-*co*-PexTMC$_{30OH}$, thus, it could degrade faster than both of PTMC-*co*-PexTMC and PTMC-*co*-PexTMC$_{30OH}$ which was proved by SEC and % weight loss. Besides, the carboxylic group effect on polymer to degradation by bulk erosion instead of the typically observed surface erosion. Consistent with the trend observed in drug release experiments, PTMC-*co*-PexTMC$_{COOH}$ demonstrated an accelerated release of doxorubicin (DOX) compared to both the non-modified copolymer and PTMC-*co*-PexTMC$_{OH}$. Conversely, the non-modified PTMC-*co*-PexTMC exhibited the slowest DOX release, attributable to its hydrophobic properties (**Figure 3-25**). These compelling findings underscore the profound potential of these specially designed copolymers and functional group for diverse biomedical applications.

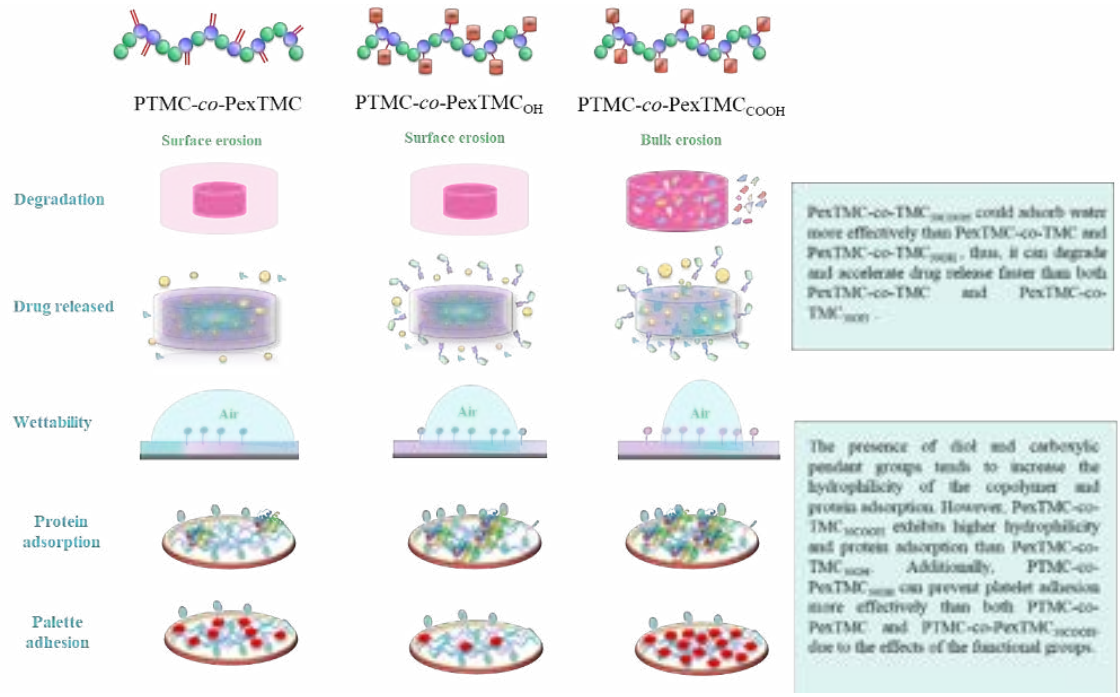

Figure 3-25. Summarized of Chapter III

3.4 Experimental

3.4.1 Synthesis of copolymerization of TMC and exTMC with MSA as catalyst and post modification by thiol-ene reaction with TGA or TGC

(DP = 120, 30%exTMC)

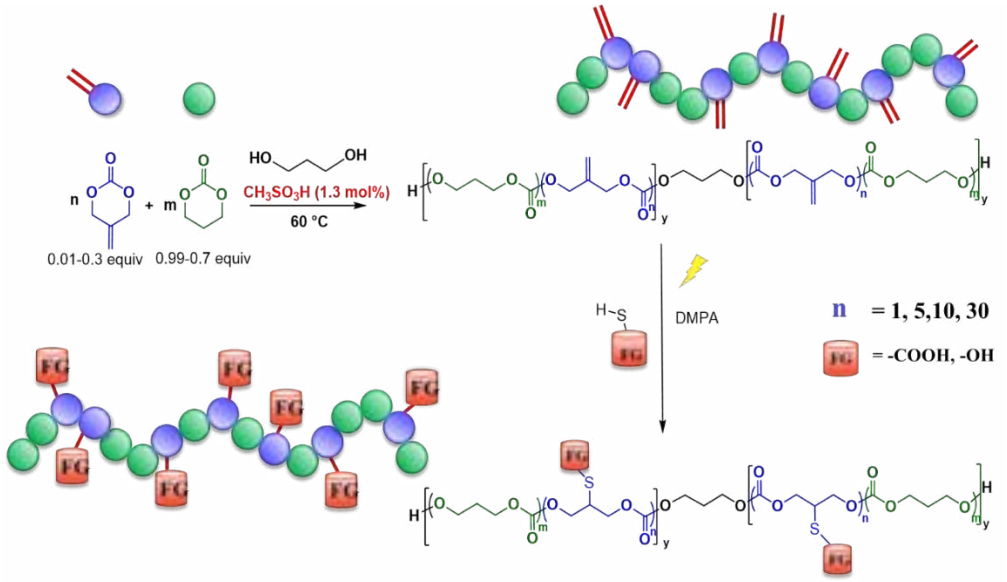

Scheme 1. Syntheses of PTMC-*co*-PexTMC and functionalization *via* thiol-ene reaction

The copolymerization of TMC and exTMC has been done as the previous literature (**Scheme 1**).[56] exTMC (234 mg, 2.1 mmol, 84 equiv.) and TMC (500mg, 4.9 mmol, 36 equiv.) were mixed. The initiator, DPO (4.2 µg, 55.3 µmol, 1 equiv.) and methane sulfonic acid (6.1 mL, 93.5 µmol, 1.3 equiv.) were successively added. The reaction mixture was stirred at 60 °C. The conversion of the comonomers was monitored by 1H NMR spectroscopy. An excess of diisopropylethylamine was added to neutralize the catalyst after 3 hours, and the solvent was evaporated under vacuum. The polymer was precipitated in cold methanol, then filtered and dried under vacuum. Yield: 93 %. SEC (THF): M_n = 5 300 g/mol; $Đ$ = 1.08. ^{1}H NMR ($CDCl_3$, 300 MHz): 5.40 (s, 28x2H, =CH_2,polymer), 4.31 and 4.26 (s, 1H each, =CH_2,chain-end), 4.70 (s, 29x4H, OCH_2,polymer), 4.25 (m, 29x4H, OCH_2polymer), 4.20 (d, J = 5.9 Hz, 2H CH_2OH_{exTMC}), 3.76 (m, 2H, CH_2OH_{TMC}), 2.05 (m, 29x2H, CH_2), 1.9 (m, 2H, OH). ^{13}C NMR ($CDCl_3$, 300 MHz): 154.9 (s, COTMC-TMC), 154.8 (s, COTMC-exTMC), 154.5 (s, CO exTMC), 137.4 (s, C=), 118.5 (s, =CH_2), 67.8 (s, OCH_2exTMC-exTMC), 67.7 (s, OCH_2exTMC-TMC), 64.4 (s, OCH_2TMC-exTMC), 64.4(s, OCH_2TMC-TMC), 28.0 (s, CH_2TMC).

Post-polymerization modification was performed under nitrogen atmosphere (**Scheme 1**). The PTMC-*co*-PexTMC (2000 mg, 0.16 mmol, ~1-30 vinyl units per chain) was dissolved in 2 ml of THF until homogenous solution. TGA (0.36mL, 5.1mmol) or TGC (0.30mL, 5.1mmol) and 2% wt DMPA as photo-initiator (40mg, 156.1 mmol) were added into the mixture. The mixture was stirred at room temperature under UV light (365 nm). The reaction was monitored at specific time interval by ^{1}H NMR. After 1h, the UV light was turned off and the mixture was vacuum evaporated to remove solvent. The obtained compound was purification by MeOH and Et_2O to remove unreactive thiol-derivative. After that, the mixture was vacuum dried at 60°C for overnight to obtain post-polymerization modification polymer (PTMCM-*co*-PexTMC$_{COOH}$ or PTMCM-*co*-PexTMC$_{OH}$) (86% yield). ^{1}H NMR ($CDCl_3$, 300 MHz): 4.25 (m, 118x4H, OCH_2polymer), 3.90-3.65 (m, 30x2H, CH_2OH), 3.60-3.50 (m, 25x1H, CHOH), 2.80-2.55 (m, 30x4H, CH_2-S-CH_2), 2.30 (m, 30x1H, CHpolymer), 2.15-2.00 (m, 86x2H, CH_2polymer).

3.4.2 Coating procedure

The concentration of synthetic polymer solution in DCM was 20 mg/ml. The synthetic polymers were applied on the glass substrates (diameter 0.8 mm) by dropped 40 µl of polymeric solution to the substrate for four time-repeated coating. The coated substrates were then dried under vacuum before testing.

3.4.3 Thermal resistance

The thermal stability of the polymer was determined by a thermo-gravimetric analyser TGA-50 (Shimadzu) under nitrogen atmosphere with 10°C/min flow rate to 500°C. Differential scanning calorimetry (DSC) spectra were also analyzed by a Hitachi DSC6200 in the atmosphere with temperature ramp rate 10°C/min in range 70°C — 200°C.

3.4.4 Wettability test

The static water contact angle of coated substrates was measured by CropMaster DM-301/501/707/901 (Kyowa Interface Science Co., Ltd.). Image were taken after sample were soaked in DI water 3 minutes, then, the air 40 µl was dropped on coated surface with three replicates at different locations to obtain mean value of the contact angle.

3.4.5 Degradation behavior

PTMC-*co*-PexTMC$_{30}$, PTMC-*co*-PexTMC$_{1OH}$, PTMC-*co*-PexTMC$_{5OH}$, PTMC-*co*-PexTMC$_{30OH}$, and PTMC-*co*-PexTMC$_{30COOH}$ were coated on circle round shape of glass with dimension of 0.8 mm and demonstrated with 3 replicates. The concentration of synthetic polymer solution in DCM was 20 mg/ml. The synthetic polymers were applied on the glass substrates (diameter 0.8mm) by dropped 40 µl of polymeric solution to the substrate for four time-repeated coating. The coated substrates were then dried under vacuum before testing. The samples were then soaked in 2 ml of lipase solution (5mg/ml), or PBS solution. The samples were monitored weight simultaneously at 1, 5, 20, 35, 50, 60, 80, and 90 days and calculated % weight loss as the following equation.

$$\% \text{ Weight loss} = \frac{Wi - Wd}{Wi} \times 100\%$$

Where w_i; initial weight before soaking and w_d; dried weight of the films at specific day.

Water uptake

The water uptake of samples were determined as the following equation:

$$\%\text{Water uptake} = \frac{mw - md}{Wmd} \times 100\%$$

Where m_w and m_d are the mass of the wet and dried polymer samples, respectively.

3.4.6 In vitro drug release test

To investigate the drug release behavior of copolymer, PTMC-*co*-PexTMC$_{30}$, PTMC-*co*-PexTMC$_{30OH}$, and PTMC-*co*-PexTMC$_{30COOH}$ were applied for incorporation with doxorubicin drugs. In vitro drug release measurements were carried out by circle round shape of glass with dimension of 0.8 mm size. Before coating, all the bare samples were pre-treated with ethanol for cleaning the surface. The drug loaded polymers were prepared by solubilizing drug (0.3 mg, 0.55mmol) and polymer 20mg in 1 ml of DCM. The drug-polymeric solution was sonicated for homogenous solution prior to coat by dropped 40 µl of polymeric solution to the substrate for four time-repeated coating. The coated substrates were then dried under vacuum. The coated samples were immersed in PBS (pH 7.4) as release medium and incubated at 37°C. At predetermined time points, the solution was detected the doxorubicin concentration by using UV spectrophotometry at wavelength 481 nm. DOX loading in sample was observed by UV-Vis at 481 nm and fitting with DOX calibration curve in DMSO.

3.4.7 Protein Adsorption

Biocompatibility could be defined as the surface properties of the coated polymeric to prolife or adhere by protein or blood platelet cell. Protein adsorption was examined using bovine serum albumin (BSA) with concentration of 4.5 mg/ ml and bovine plasma fibrinogen (BPF) with concentration of 0.3 mg/ ml detecting by bicinchoninic acid (BCA) protein assay reagent. The samples and reference samples were soaked in PBS (pH 7.4) at 37 °C overnight. Then, each sample was immersed into 900 μL of each protein solution and incubated 4 h at 37 °C. After rinsing with PBS, adsorbed protein was detached by 1 wt% of n-sodium dodecyl sulfate (SDS) for 4 h. Bicinchoninic acid (BCA) protein assay reagent was used as indicator for protein adsorption on the samples. UV measurement at 562 nm for protein on sample surface was interpreted by absorbance microplate reader (MTP-310lab, Corona Electric) based on standard control and calibration curve of the protein.

3.4.8 Platelet adhesion

To advance our purpose, platelet adhesion test is essential for preliminary testing. The procedure was following reference.[75] A fresh blood sample was drawn from a healthy cow. The mixture of 3.24% sodium citrate and blood was centrifuged at 2000 rpm for 7 min to obtain heterogeneous supernatant, platelet-rich plasma (PRP) and platelet poor plasma (PPP). PRP layer was diluted 40- fold with PBS and then platelet concentration (5.0×10^3 cells μL^{-1}) in diluted PRP was determined using fluorescence microscope. The coated sample (diameter 0.8 mm) were placed at the center of glass petri dish and washed with deionized water 3 times and soaked in PBS for 24 h at 37 °C. The PRP solution was added onto samples and incubated at 37 °C 60 min. the sample was washed by PBS solution 3 times and then 2 ml of 20% glutaraldehyde in PBS at 4 °C 2 h. The samples were finally cleansed with 2 ml PBS (3 times) and water, and dried under vacuum overnight. The number of adhered platelets on gel surface was counted and averaged by SEM image. Low Vacuum Scanning Electron Microscope (SU6600, Hitachi) was used in condition, accelerating voltage: 2 kV magnification: 2000x without metal coating of SE signal. Five different areas of the sample were captured and counted as average value with standard deviation.

3.5 References

(1) Mehdikhani-Nahrkhalaji, M.; Fathi, M. H.; Mortazavi, V.; Mousavi, S. B.; Hashemi-Beni, B.; Razavi, S. M. Novel Nanocomposite Coating for Dental Implant Applications in Vitro and in Vivo Evaluation. *J. Mater. Sci. Mater. Med.* **2012**, *23* (2), 485–495. https://doi.org/10.1007/s10856-011-4507-0.

(2) Yang, L. Q.; Yang, D.; Guan, Y. M.; Li, J. X.; Li, M. Random Copolymers Based on Trimethylene Carbonate and ε-Caprolactone for Implant Applications: Synthesis and Properties. *J. Appl. Polym. Sci.* **2012**, *124* (5), 3714–3720. https://doi.org/10.1002/app.35355.

(3) Bok, O.; Pihlajamak, H. Clinical Biocompatibility of Biodegradable Orthopaedic Implants for Internal Fixation: A Review. *Biomaterials* **2000**, *21*, 2615–2621.

(4) Weiler, A.; Hoffmann, R. F. G.; Stähelin, A. C.; Helling, H.-J.; Südkamp, N. P. Biodegradable Implants in Sports Medicine: The Biological Base. *Arthrosc. - J. Arthrosc. Relat. Surg.* **2000**, *16* (3), 305–321. https://doi.org/10.1053/ay.2000.4374.

(5) Witte, F.; Calliess, T.; Windhagen, H. Degradable Synthetische Implantatmaterialien Klinische Applikationen Und Immunologische Aspekte. *Orthopade.* **2008**, *37* (2), 125–130. https://doi.org/10.1007/s00132-008-1193-9.

(6) Zhang, Y.; Zhuo, R. X. Synthesis and Drug Release Behavior of Poly(Trimethylene Carbonate)–Poly(Ethylene Glycol)–Poly(Trimethylene Carbonate) Nanoparticles. *Biomaterials* **2005**, *26* (14), 2089–2094. https://doi.org/10.1016/j.biomaterials.2004.06.004.

(7) Brzeziński, M.; Socka, M.; Makowski, T.; Kost, B.; Cieślak, M.; Królewska-Golińska, K. Microfluidic-Assisted Nanoprecipitation of Biodegradable Nanoparticles Composed of PTMC/PCL (Co)Polymers, Tannic Acid and Doxorubicin for Cancer Treatment. *Colloids Surf. B. Biointerfaces* **2021**, *201*. https://doi.org/10.1016/j.colsurfb.2021.111598.

(8) Pêgo, A. P.; Poot, A. A.; Grijpma, D. W.; Feijen, J. Copolymers of Trimethylene Carbonate and ε-Caprolactone for Porous Nerve Guides: Synthesis and Properties. *J. Biomater. Sci. Polym. Ed.* **2001**, *12* (1), 35–53. https://doi.org/10.1163/156856201744434.

(9) Song, Y.; Wennink, J. W. H.; Kamphuis, M. M. J.; Vermes, I.; Poot, A. A.; Feijen, J.; Grijpma, D. W. Effective Seeding of Smooth Muscle Cells into Tubular Poly(Trimethylene Carbonate) Scaffolds for Vascular Tissue Engineering. *J. Biomed. Mater. Res. A.* **2010**, *95 A* (2), 440–446. https://doi.org/10.1002/jbm.a.32859.

(10) Brossier, T.; Volpi, G.; Vasquez-Villegas, J.; Petitjean, N.; Guillaume, O.; Lapinte, V.; Blanquer, S. Photoprintable Gelatin-Graft-Poly(Trimethylene Carbonate) by Stereolithography for Tissue Engineering Applications. *Biomacromolecules* **2021**, *22*

(9), 3873–3883. https://doi.org/10.1021/acs.biomac.1c00687.

(11) Ulery, B. D.; Nair, L. S.; Laurencin, C. T. Biomedical Applications of Biodegradable Polymers. *J. Polym. Sci. B. Polym. Phys.* **2011**, *49* (12), 832–864. https://doi.org/10.1002/polb.22259.

(12) Zhang, Z.; Kuijer, R.; Bulstra, S. K.; Grijpma, D. W.; Feijen, J. The in Vivo and in Vitro Degradation Behavior of Poly(Trimethylene Carbonate). *Biomaterials* **2006**, *27* (9), 1741–1748. https://doi.org/10.1016/j.biomaterials.2005.09.017.

(13) Pêgo, A. P.; Van Luyn, M. J. A.; Brouwer, L. A.; Van Wachem, P. B.; Poot, A. A.; Grijpma, D. W.; Feijen, J. In Vivo Behavior of Poly(1,3-Trimethylene Carbonate) and Copolymers of 1,3-Trimethylene Carbonate with D,L-Lactide or ε-Caprolactone: Degradation and Tissue Response. *J. Biomed. Mater. Res. A.* **2003**, *67* (3), 1044–1054. https://doi.org/10.1002/jbm.a.10121.

(14) Chanthaset, N.; Ajiro, H. Preparation of Thermosensitive Biodegradable Hydrogel Using Poly(5-[2-{2-(2-Methoxyethoxy)Ethyoxy}-Ethoxymethyl]-5-Methyl-1,3-Dioxa-2-One) Derivatives. *Materialia (Oxf)* **2019**, *5*. https://doi.org/10.1016/j.mtla.2018.11.027.

(15) Albertsson, A.-C.; Eklund, M. Influence of Molecular Structure on the Degradation Mechanism of Degradable Polymers: In Vifro Degradation of Poly(Trimethy1ene Carbonate), Poly(Trimethy1ene Carbonate-Co-Caprolactone), and Poly(Adipic Anhydride). *J. Appl. Polym. Sci.* **1995**, *57* (1), 87–93.

(16) Karp, J. M.; Shoichet, M. S.; Davies, J. E. Bone Formation on Two-Dimensional Poly(DL-Lactide-Co-Glycolide) (PLGA) Films and Three-Dimensional PLGA Tissue Engineering Scaffolds in Vitro. *J. Biomed. Mater. Res. A.* **2003**, *64* (2), 388–396. https://doi.org/10.1002/jbm.a.10420.

(17) Dienel, K. E. G.; Van Bochove, B.; Seppälä, J. V. Additive Manufacturing of Bioactive Poly(Trimethylene Carbonate)/β-Tricalcium Phosphate Composites for Bone Regeneration. *Biomacromolecules* **2020**, *21* (2), 366–375. https://doi.org/10.1021/acs.biomac.9b01272.

(18) Nobuoka, H.; Nagasawa, M.; Chanthaset, N.; Yoshida, H.; Haramiishi, Y.; Ajiro, H. Synthesis of Amphiphilic Block Copolymer Using Trimethylene Carbonate Bearing Oligo(Ethylene Glycol) and Investigation of Thin Film Including Cilostazol. *J. Polym. Sci.* **2020**, *58* (17), 2347–2354. https://doi.org/10.1002/pol.20200390.

(19) Haramiishi, Y.; Kawatani, R.; Chanthaset, N.; Ajiro, H. Preparation of Block Copolymer of Poly(Trimethylene Carbonate) with Oligo(Ethylene Glycol) and the Surface Properties of the Dip Coated Film. *Polym. Test* **2020**, *86*. https://doi.org/10.1016/j.polymertesting.2020.106484.

(20) Mohajeri, S.; Amsden, B. G. In Vivo Degradation Mechanism and Biocompatibility of a Biodegradable Aliphatic Polycarbonate: Poly(Trimethylene Carbonate-Co-5-Hydroxy Trimethylene Carbonate). *ACS Appl. Bio. Mater.* **2021**, *4* (4), 3686–3696. https://doi.org/10.1021/acsabm.1c00160.

(21) Fukushima, K. Poly(Trimethylene Carbonate)-Based Polymers Engineered for Biodegradable Functional Biomaterials. *Biomater. Sci.* **2016**, *4* (1), 9–24. https://doi.org/10.1039/c5bm00123d.

(22) Talebian, S.; Mehrali, M.; Mohan, S.; Balaji Raghavendran, H. R.; Mehrali, M.; Khanlou, H. M.; Kamarul, T.; Afifi, A. M.; Abass, A. A. Chitosan (PEO)/Bioactive Glass Hybrid Nanofibers for Bone Tissue Engineering. *RSC Adv.* **2014**, *4* (90), 49144–49152. https://doi.org/10.1039/c4ra06761d.

(23) Pyhältö, T.; Lapinsuo, M.; Pätiälä, H.; Pelto, M.; Törmälä, P.; Rokkanen, P. Fixation of Distal Femoral Osteotomies with Self-Reinforced Polymer/Bioactive Glass Rods: An Experimental Study on Rabbits. *Biomaterials* **2005**, *26* (6), 645–654. https://doi.org/10.1016/j.biomaterials.2004.03.007.

(24) Van Leeuwen, A. C.; Bos, R. R. M.; Grijpma, D. W. Composite Materials Based on Poly(Trimethylene Carbonate) and β-Tricalcium Phosphate for Orbital Floor and Wall Reconstruction. *J. Biomed. Mater. Res. B. Appl. Biomater*.**2012**, *100 B* (6), 1610–1620. https://doi.org/10.1002/jbm.b.32729.

(25) Braghirolli, D. I.; Caberlon, B.; Gamba, D.; Petry, J. F. T. C.; Dias, M. L.; Pranke, P. Poly(Trimethylene Carbonate-Co-l-Lactide) Electrospun Scaffolds for Use as Vascular Grafts. *Braz. J. Med. Biol. Res.* **2019**, *52* (8). https://doi.org/10.1590/1414-431X20198318.

(26) Rocha, D. N.; Brites, P.; Fonseca, C.; Pêgo, A. P. Poly(Trimethylene Carbonate-Co-ε-Caprolactone) Promotes Axonal Growth. *PLoS. One* **2014**, *9* (2). https://doi.org/10.1371/journal.pone.0088593.

(27) Noorsal, K.; Mantle, M. D.; Gladden, L. F.; Cameron, R. E. Degradation and Drug-Release Studies of a Poly(Glycolideco-Trimethylene Carbonate) Copolymer (Maxon). *J. Appl. Polym. Sci.* **2005**, *95* (3), 475–486. https://doi.org/10.1002/app.21108.

(28) Ajiro, H.; Haramiishi, Y.; Chanthaset, N.; Akashi, M. Polymer Design Using Trimethylene Carbonate with Ethylene Gycol Units for Biomedical Applications. *Polym. J.* **2016**, *48* (7), 751–760. https://doi.org/10.1038/pj.2016.35.

(29) Hyun, H.; Lee, J. W.; Cho, J. S.; Kim, Y. H.; Lee, C. R.; Kim, M. S.; Khang, G.; Lee, H. B. Polymeric Nano-Micelles Using Poly(Ethylene Glycol) and Poly(Trimethylene Carbonate) Diblock Copolymers as A Drug Carrier. *Colloids Surf. A. Physicochem. Eng. Asp.* **2008**, *313–314*, 131–135. https://doi.org/10.1016/j.colsurfa.2007.05.078.

(30) Zhang, Z.; Grijpma, D. W.; Feijen, J. Poly(Trimethylene Carbonate) and Monomethoxy Poly(Ethylene Glycol)-Block-Poly(Trimethylene Carbonate) Nanoparticles for The Controlled Release of Dexamethasone. *J. Control. Release* **2006**, *111* (3), 263–270. https://doi.org/10.1016/j.jconrel.2005.12.001.

(31) Jiang, X.; Xin, H.; Sha, X.; Gu, J.; Jiang, Y.; Law, K.; Chen, Y.; Chen, L.; Wang, X.; Fang, X. PEGylated Poly(Trimethylene Carbonate) Nanoparticles Loaded with Paclitaxel for The Treatment of Advanced Glioma: In Vitro and in Vivo Evaluation. *Int. J. Pharm.* **2011**, *420* (2), 385–394. https://doi.org/10.1016/j.ijpharm.2011.08.052.

(32) Suriano, F.; Coulembier, O.; Hedrick, J. L.; Dubois, P. Functionalized Cyclic Carbonates: From Synthesis and Metal-Free Catalyzed Ring-Opening Polymerization to Applications. *Polym. Chem.* **2011**, *2* (3), 528–533. https://doi.org/10.1039/c0py00211a.

(33) Feng, J.; Zhuo, R. X.; Zhang, X. Z. Construction of Functional Aliphatic Polycarbonates for Biomedical Applications. *Prog. Polym. Sci.* **2012**, *37* (2), 211–236. https://doi.org/10.1016/j.progpolymsci.2011.07.008.

(34) Tempelaar, S.; Mespouille, L.; Coulembier, O.; Dubois, P.; Dove, A. P. Synthesis and Post-Polymerisation Modifications of Aliphatic Poly(Carbonate)s Prepared by Ring Opening Polymerisation. *Chem. Soc. Rev.* **2013**, *42* (3), 1312–1336. https://doi.org/10.1039/c2cs35268k.

(35) Guillaume, S. M.; Mespouille, L. Renaissance of Aliphatic Polycarbonates New Techniques AndBiomedical Applications. *J. Appl. Polym. Sci.* **2014**, *131* (5). https://doi.org/10.1002/app.40081.

(36) Fukushima, K.; Inoue, Y.; Haga, Y.; Ota, T.; Honda, K.; Sato, C.; Tanaka, M. Monoether-Tagged Biodegradable Polycarbonate Preventing Platelet Adhesion and Demonstrating Vascular Cell Adhesion: A Promising Material for Resorbable Vascular Grafts and Stents. *Biomacromolecules* **2017**, *18* (11), 3834–3843. https://doi.org/10.1021/acs.biomac.7b01210.

(37) Sanders, D. P.; Fukushima, K.; Coady, D. J.; Nelson, A.; Fujiwara, M.; Yasumoto, M.; Hedrick, J. L. A Simple and Efficient Synthesis of Functionalized Cyclic Carbonate Monomers Using a Versatile Pentafluorophenyl Ester Intermediate. *J. Am. Chem. Soc.* **2010**, *132* (42), 14724–14726. https://doi.org/10.1021/ja105332k.

(38) Sanda, F.; Kamatani, J.; Endo, T. Synthesis and Anionic Ring-Opening Polymerization Behavior of AminoAcid-Derived Cyclic Carbonat. *Macromolecules* **2001**, *34* (6), 1564–1569. https://doi.org/10.1021/ma0013307.

(39) Hu, X.; Chen, X.; Xie, Z.; Cheng, H.; Jing, X. Aliphatic Poly(Ester-Carbonate)s Bearing Amino Groupsand Its RGD Peptide Grafting. *J. Polym. Sci. A. Polym. Chem.* **2008**, *46* (21), 7022–7032. https://doi.org/10.1002/pola.23008.

(40) Wang, H. F.; Su, W.; Zhang, C.; Luo, X. H.; Feng, J. Biocatalytic Fabrication of Fast-Degradable, Water-Soluble Polycarbonate Functionalized with Tertiary Amine Groups in Backbone. *Biomacromolecules* **2010**, *11* (10), 2550–2557. https://doi.org/10.1021/bm1001476.

(41) Cooley, C. B.; Trantow, B. M.; Nederberg, F.; Kiesewetter, M. K.; Hedrick, J. L.; Waymouth, R. M.; Wender, P. A. Oligocarbonate Molecular Transporters: Oligomerization-Based Syntheses and Cell-Penetrating Studies. *J. Am. Chem. Soc.* **2009**, *131* (45), 16401–16403. https://doi.org/10.1021/ja907363k.

(42) Kim, S. H.; Tan, J. P. K.; Nederberg, F.; Fukushima, K.; Colson, J.; Yang, C.; Nelson, A.; Yang, Y. Y.; Hedrick, J. L. Hydrogen Bonding-Enhanced Micelle Assemblies for Drug Delivery. *Biomaterials* **2010**, *31* (31), 8063–8071. https://doi.org/10.1016/j.biomaterials.2010.07.018.

(43) Feng, J.; Wang, X. L.; He, F.; Zhuo, R. X. Non-Catalyst Synthesis of Functionalized Biodegradable Polycarbonate. *Macromol. Rapid Commun.* **2007**, *28* (6), 754–758. https://doi.org/10.1002/marc.200600774.

(44) Vandenberg, E. J.; Tian, D. A New, Crystalline High Melting Bis(Hydroxymethyl)Polycarbonate and Its Acetone Ketal for Biomaterial Applications. *Macromolecules* **1999**, *32* (11), 3613–3619. https://doi.org/10.1021/ma9816822.

(45) Li, Z. M.; Yan, G. P.; Ai, C. W.; Zhang, Q.; Li, L.; Liu, F.; Yu, X. H.; Zhao, B. Synthesis and Properties of Polycarbonate Copolymers of Trimethylene Carbonate and 2-Phenyl-5,5-Bis(Hydroxymethyl) Trimethylene Carbonate. *J. Appl. Polym.Sci.* **2012**, *124* (5), 3704–3713. https://doi.org/10.1002/app.35386.

(46) Acemoglu, M.; Bantle, S.; Mindt, T.; Nimmerfall, F. Novel Bioerodible Poly(Hydroxyalkylene Carbonates)s: A Versatile Class of Polymers for Medical and Pharmaceutical Applications. *Macromolecules* **1995**, *28*, 3030–3037.

(47) Yu, F.; Zhuo, R. Synthesis, Characterization, and Degradation Behaviors of End-Group-Functionalized Poly(Trimethylene Carbonate)s. *Polym. J.* **2003**, *35* (8), 671–676. https://doi.org/10.1295/polymj.35.671.

(48) Mohajeri, S.; Chen, F.; De Prinse, M.; Phung, T.; Burke-Kleinman, J.; Maurice, D. H.; Amsden, B. G. Liquid Degradable Poly(Trimethylene-Carbonate- Co-5-Hydroxy-Trimethylene Carbonate): An Injectable Drug Delivery Vehicle for Acid-Sensitive Drugs. *Mol. Pharm.* **2020**, *17* (4), 1363–1376. https://doi.org/10.1021/acs.molpharmaceut.0c00064.

(49) Olofsson, K.; Malkoch, M.; Hult, A. Facile Synthesis of Dopa-Functional Polycarbonates *Via* Thiol-Ene-Coupling Chemistry towards Self-Healing Gels. *J. Polym. Sci. A Polym. Chem.* **2016**, *54* (15), 2370–2378.

https://doi.org/10.1002/pola.28111.

(50) Li, L.; Smitthipong, W.; Zeng, H. Mussel-Inspired Hydrogels for Biomedical and Environmental Applications. *Polym. Chem*. **2015**, 353–358. https://doi.org/10.1039/c4py01415d.

(51) Thomas, A. W.; Dove, A. P. Postpolymerization Modifications of Alkene-Functional Polycarbonates for The Development of Advanced Materials Biomaterials. *Macromol. Biosci*. **2016**, 1762–1775. https://doi.org/10.1002/mabi.201600310.

(52) Pratt, R. C.; Nederberg, F.; Waymouth, R. M.; Hedrick, J. L. Tagging Alcohols with Cyclic Carbonate A Versatile Equivalent of (Meth)Acrylate for Ring-Opening Polymerization. *Chem. Commun.* **2008**, *1*, 114–116. https://doi.org/10.1039/B713925J.

(53) Al-Azemi, T. F.; Harmon, J. P.; Bisht, K. S. EnzymeCatalyzed Ring-Opening Copolymerization of 5-Methyl-5-benzyloxycarbonyl-1,3-dioxan-2-one (MBC) with Trimethylene Carbonate (TMC): Synthesis and Characterization. *Biomacromolecules* **2000**, *1*, 493-500. https:// 10.1021/bm005552o

(54) Coady, D. J.; Horn, H. W.; Jones, G. O.; Sardon, H.; Engler, A. C.; Waymouth, R. M.; Rice, J. E.; Yang, Y. Y.; Hedrick, J. L. Polymerizing Base Sensitive Cyclic Carbonates Using Acid Catalysis. *ACS Macro. Lett*. **2013**, *2*, 306-312. https://doi.org/10.1021/mz3006523

(55) Li, S.; Meng, F.; Wang, Z.; Zhong, Y.; Zheng, M.; Liu, H.; Zhong, Z. Biodegradable Polymersomes with An Ionizable Membrane: Facile Preparation, Superior Protein Loading, and Endosomal PH-Responsive Protein Release. *Eur. J. Pharm. Biopharm.* **2012**, *82* (1), 103–111. https://doi.org/10.1016/j.ejpb.2012.05.009.

(56) Palenzuela, M.; Sarisuta, K.; Navarro, M.; Kumamoto, N.; Chanthaset, N.; Monot, J.; Ajiro, H.; Martín-Vaca, B.; Bourissou, D. 5-Methylene-1,3-Dioxane-2-One: A First-Choice Comonomer for Trimethylene Carbonate. *Macromolecules* **2022**, *56* (2), 678–689. https://doi.org/10.1021/acs.macromol.2c02270.

(57) Palard, I.; Schappacher, M.; Belloncle, B.; Soum, A.; Guillaume, S. M. Unprecedented Polymerization of Trimethylene Carbonate Initiated by a Samarium Borohydride Complex Mechanistic Insights and Copolymerization with ε-Caprolactone. *Chem. Eur. J.* **2007**, *13* (5), 1511–1521. https://doi.org/10.1002/chem.200600843.

(58) Haramiishi, Y.; Kawatani, R.; Chanthaset, N.; Ajiro, H. Preparation of Block Copolymer of Poly(Trimethylene Carbonate) with Oligo(Ethylene Glycol) and The Surface Properties of The Dip Coated Film. *Polym. Test* **2020**, *86*. https://doi.org/10.1016/j.polymertesting.2020.106484.

(59) Andriani, F.; Fuoco, T. Statistical Enchainment of Ester/Ether and Carbonate Cleavable Bonds to Control Copolymers' Erosion Rate and Trigger Environment-Specific

Degradation. *Eur. Polym. J.* **2022**, *178*. https://doi.org/10.1016/j.eurpolymj.2022.111457.

(60) Wu, L.; Wang, Y.; Zhao, X.; Mao, H.; Gu, Z. Investigating the Biodegradation Mechanism of Poly(Trimethylene Carbonate): Macrophage-Mediated Erosion by Secreting Lipase. *Biomacromolecules* **2023**, *24* (2), 921–928. https://doi.org/10.1021/acs.biomac.2c01350.

(61) Domínguez de María, P.; Fernández-Álvaro, E.; ten Kate, A.; Bargeman, G. Role of Apparent PKa of Carboxylic Acids in Lipase-Catalyzed Esterifications in Biphasic Systems. *J. Mol. Catal. B. Enzym.* **2009**, *59* (1–3), 220–224. https://doi.org/10.1016/j.molcatb.2009.03.004.

(62) Haramiishi, Y.; Chanthaset, N.; Kan, K.; Akashi, M.; Ajiro, H. Contrast Effect on Hydrolysis of Poly(Trimethylene Carbonate) Depending on Accelerated Species Due to the Hydrophilic Oligo(Ethylene Glycol) Units at Side Groups. *Polym. Degrad. Stab.* **2016**, *130*, 78–82. https://doi.org/10.1016/j.polymdegradstab.2016.05.027.

(63) Yang, L.; Li, J.; Zhang, W.; Jin, Y.; Zhang, J.; Liu, Y.; Yi, D.; Li, M.; Guo, J.; Gu, Z. The Degradation of Poly(Trimethylene Carbonate) Implants: The Role of Molecular Weight and Enzymes. *Polym. Degrad. Stab.* **2015**, *122*, 77–87. https://doi.org/10.1016/j.polymdegradstab.2015.10.016.

(64) Ma, Z.; Wu, Y.; Wang, J.; Liu, C. In Vitro and in Vivo Degradation Behavior of Poly(Trimethylene Carbonate-Co-D,L-Lactic Acid) Copolymer. *Regen. Biomater.* **2017**, *4* (4), 207–213. https://doi.org/10.1093/rb/rbx003.

(65) Saha, S. K.; Tsuji, H. Effects of Molecular Weight and Small Amounts of D-Lactide Units on Hydrolytic Degradation of Poly(l-Lactic Acid)s. *Polym. Degrad. Stab.* **2006**, *91* (8), 1665–1673. https://doi.org/10.1016/j.polymdegradstab.2005.12.009.

(66) Gorrasi, G.; Pantani, R. Hydrolysis and Biodegradation of Poly(Lactic Acid). In *Adv. Polym. Sci*. **2017**, *279*, 119–151. https://doi.org/10.1007/12_2016_12.

(67) Xu, B.; Gao, R.; Yang, Y.; Cao, X.; Qin, L.; Li, Y.; Li, Z.; Li, X.; Lin, H.; Guo, Y.; Ma, Y.; Wang, an; Nie, S.; Xu, L.; Cao, E.; Guan, C.; Stone, G. W. Biodegradable Polymer-Based Sirolimus-Eluting Stents With Differing Elution and Absorption Kinetics. *J. Am. Coll. Cardiol*. **2016**, *67*(19), 2249-2258. https://doi.org/10.1016/j.jacc.2016.03.475.

(68) Koźlik, M.; Harpula, J.; Chuchra, P. J.; Nowak, M.; Wojakowski, W.; Gąsior, P. Drug-Eluting Stents: Technical and Clinical Progress. *Biomimetics*. **2023**, *8* (1), 72. https://doi.org/10.3390/biomimetics8010072.

(69) Fu, Y.; Kao, W. J. Drug Release Kinetics and Transport Mechanisms of Non-Degradable and Degradable Polymeric Delivery Systems. *Expert Opin. Drug Deliv.* **2010**, *7* (4), 429–444. https://doi.org/10.1517/17425241003602259.

(70) Arima, Y.; Iwata, H. Effects of Surface Functional Groups on Protein Adsorption and Subsequent Cell Adhesion Using Self-Assembled Monolayers. *J. Mater. Chem.* **2007**, *17* (38), 4079–4087. https://doi.org/10.1039/b708099a.

(71) Thevenot, P.; Hu, W.; Tang, L. Surface Chemistry Influences Implant Biocompatibility. *Current topics in medicinal chemistry* **2008**, *8* (4), 270–280. https://doi.org/10.2174/156802608783790901.

(72) Sivaraman, B.; Latour, R. A. The Adherence of Platelets to Adsorbed Albumin by Receptor-Mediated Recognition of Binding Sites Exposed by Adsorption-Induced Unfolding. *Biomaterials* **2010**, *31* (6), 1036–1044. https://doi.org/10.1016/j.biomaterials.2009.10.017.

(73) Xu, L. C.; Bauer, J. W.; Siedlecki, C. A. Proteins, Platelets, and Blood Coagulation at Biomaterial Interfaces. *Colloids Surf. B. Biointerfaces* **2014**, *124*, 49–68. https://doi.org/10.1016/j.colsurfb.2014.09.040.

(74) Schmidt, D. R.; Waldeck, H.; Kao, W. J. Protein Adsorption to Biomaterials. *Biological Interactions on Materials Surfaces* **2009**, 1–18. https://doi.org/10.1007/978-0-387-98161-1_1.

(75) Totani, M.; Ando, T.; Terada, K.; Terashima, T.; Kim, I. Y.; Ohtsuki, C.; Xi, C.; Kuroda, K.; Tanihara, M. Utilization of Star-Shaped Polymer Architecture in The Creation of High-Density Polymer Brush Coatings for The Prevention of Platelet and Bacteria Adhesion. *Biomater. Sci.* **2014**, *2* (9), 1172–1185. https://doi.org/10.1039/c4bm00034j.

Chapter IV

The design of side chain crosslinking to modulate the properties of copolymers.

4.1 Introduction

Poly trimethylenecarbonate (PTMC) is an amorphous polymer, obtained by ring opening polymerization from the cyclic carbonate. Physically, PTMC exhibits a low glass transition temperature, ranging from −25 to −15 °C (depending on the molecular weight) and relatively low elastic modulus.[1] Low molecular weight PTMC is a rubbery polymer with poor dimensional stability, tackiness, and inadequate mechanical properties.[2] Due to poor physical properties, PTMC is generally used in the combination of copolymer, blending and cross-linking to overcome the dimensional stability issues that is vital for any practical application including biomedical realm. Copolymerization and blending with PTMC complement each other's properties and conceal PTMC limitations. Copolymer with poly(ε-caprolactone) (PCL),[3] poly(lactic acid) (PLA)[4] and poly(glycolic acid) (PGA)[5] have been well-studied over the past decade.

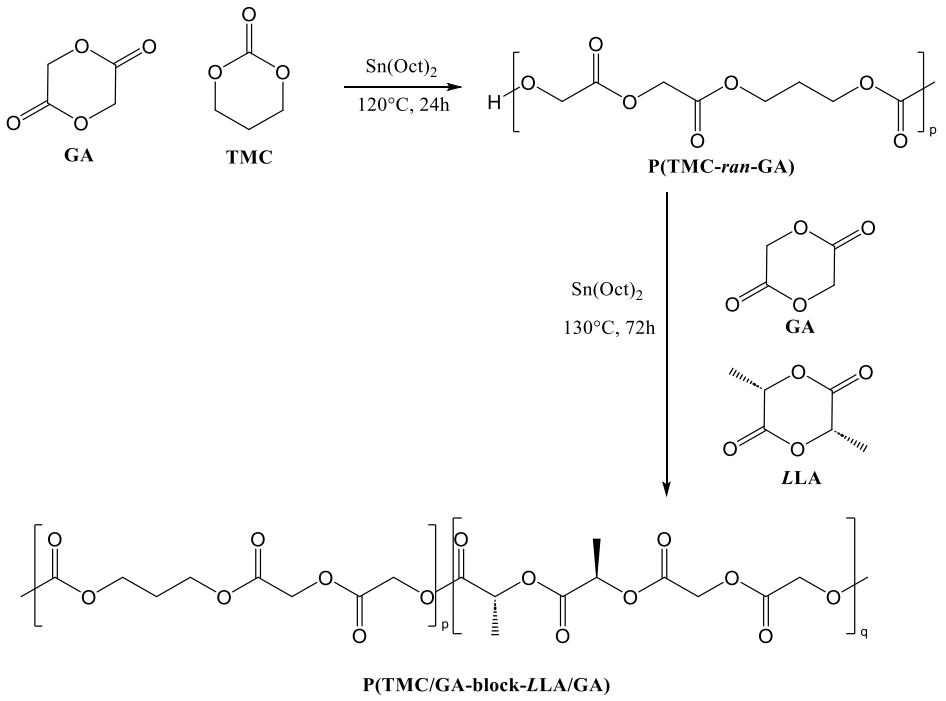

Figure 4-1. The pathway to synthesize P(TMC/GA-*block*-LLA/GA)[5]

Xiaomeng et al, have synthesized the poly(TMC/GA-*block*-LLA/GA)) block copolymers by ROP with high M_n (above 2.0 × 105 Da). The block copolymers composed of P(TMC-*ran*-GA) and P(LLA-*ran*-GA) segments show good mechanical properties and adjustable degradation rate (**Figure 4-1**).[5]

In an example of blending compound with PTMC, Jiang et al. demonstrated the use of blending techniques with PTMC by preparing a PLLA/PTMC electrospun fiber membrane. This material was created through the physical blending of PTMC and PLLA, employing electrospinning technology. The objective was to broaden the application range of biodegradable PLLA/PTMC materials within the biomedical sector. Potential applications include bio-absorbable sutures, implantable medical devices, tissue engineering scaffolds, and controlled drug delivery systems.[6] Irikura et al have successfully blended PTMC and its derivatives bearing pendant COOH in the form of flexible film with *N,N,N*-trimethylchitosan (TM-CS) by using a casting method. The obtained films were evaluated for their mechanical properties, contact angles, and thermal properties (**Figure 4-2**).[7]

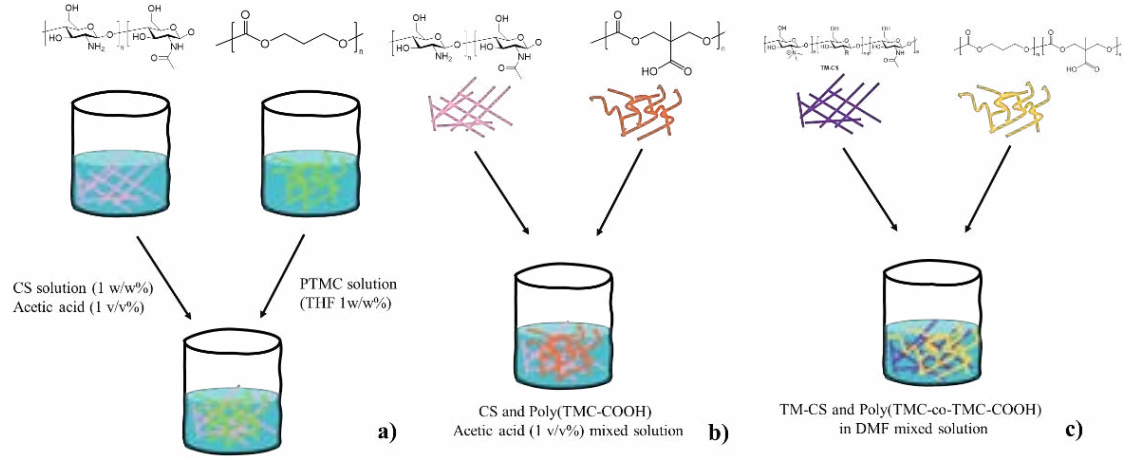

Figure 4-2. Preparation of the blend films: (a) CS and PTMC blend film, (b) CS and poly(TMC-COOH) film and (c) TM-CS and poly(TMC-*co*-TMC-COOH)/GA).[7]

Although copolymerization and blending are key techniques for improving the physical properties of polymers, they also introduce variables that can adversely affect the physicochemical properties of the resulting materials. Specifically, when a secondary component is integrated into a PTMC matrix, it can lead to undesired effects, such as material incompatibility or the generation of unwanted degradation by-products.[8]

Therefore, cross-linking is another alternative for improving chemical and physical stability of PTMC. The cross-linking reaction facilitates the formation of covalent, hydrogen, and ionic bonds, as well as van der Waals interactions between polymer chains. Additionally, this reaction is instrumental in modifying various characteristics of polymer materials, including their thermal, mechanical, and physicochemical properties.[9] These crosslinking mechanisms can be classified into two groups: physical involving non-covalent bonding or chemical involving covalent bonding (**Figure 4-3**).[10]

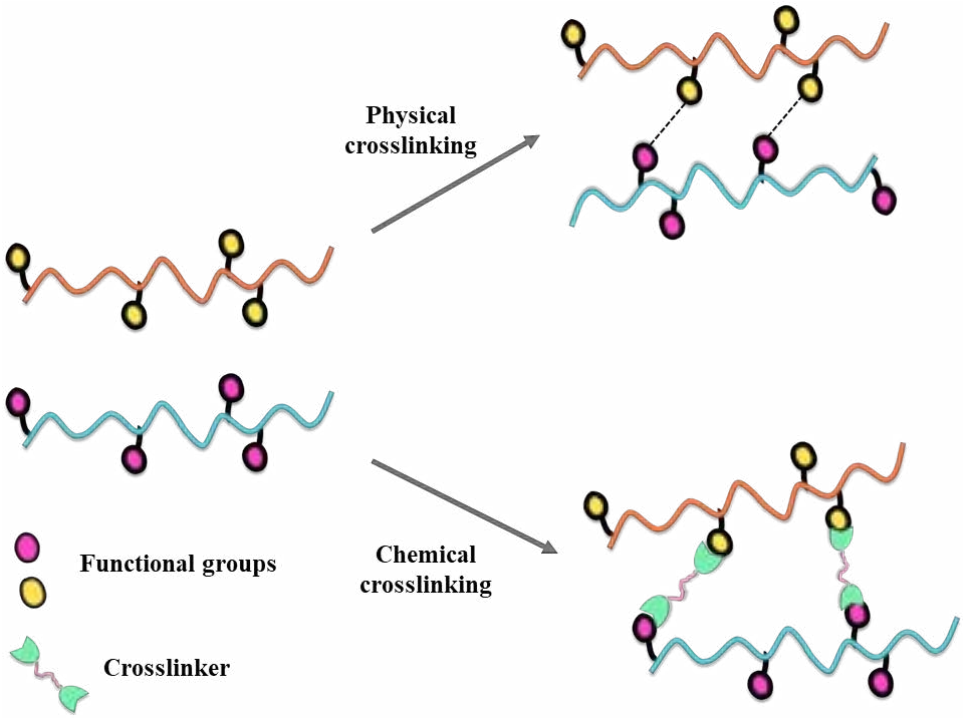

Figure 4-3. The effect of physical and chemical crosslinking on the type of bonds formed.

Cross-linking of PTMC have been performed using several methods, including chemical reactions,[11,12] gamma- and electron-beam irradiatio,[13] and UV photo-cross-linking.[14] These techniques are considered promising solutions for forming an intermolecular bonding network between polymer chains. Nobuoka et al, have synthesized 2,2'-bis(trimethylenecarbonate-5-yl)-butylether (BTB) as a crosslinking agent, incorporated with different ratios of hydrophilic and hydrophobic monomers with the aim to overcome the difficulty of handling polymers (**Figure 4-4**).[15] Oligo(ethylene glycol) (OEG) which acts as hydrophilic part with different ratio L-OEG-film (Low OEG), M-OEG-film (medium OEG), H-OEG-film(high OEG) has been created to study thermal properties, mechanical properties, surface properties, and protein adsorption.

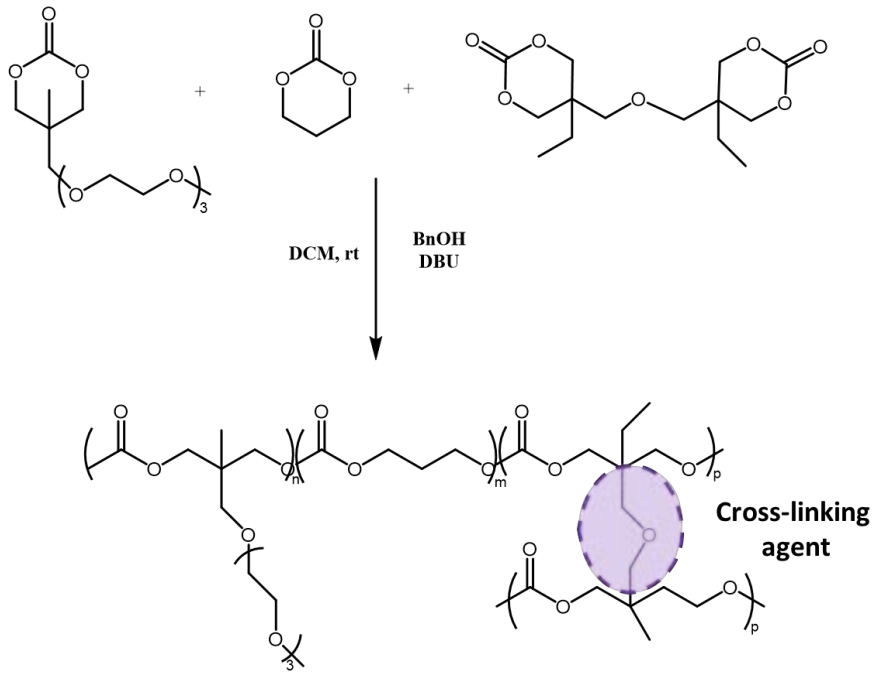

Figure 4-4. Synthesis of crosslinked trimethylene carbonate bearing Oligo(ethylene glycol).[15]

In particular, gamma- and electron beam irradiation enables rapid cross linking of the molded PTMC and the cross-linked. Liu et al. have used trimethylolpropane triacrylate (TMPTA), pentaerythritol triacrylate (PETA), and pentaerythritol tetraacrylate (PET4A) as crosslinking agents to prepare PTMC networks by gamma irradiation under vacuum to improve mechanical properties and resist creep (**Figure 4-5**).[16] The PTMC network containing the crosslinking agent did not deform significantly. It was a successful strategy for improving material shape stability through cross-linking. In the presence of porcine pancreatic lipase (PPL), the PTMC network also accelerated degradation. This could be due to the occurrence of chain scission that simultaneously occurs with cross-linking, which can make the molecular weight of PTMC decrease, and the resulting low-molecular weight segments will form defects in the three-dimensional network.

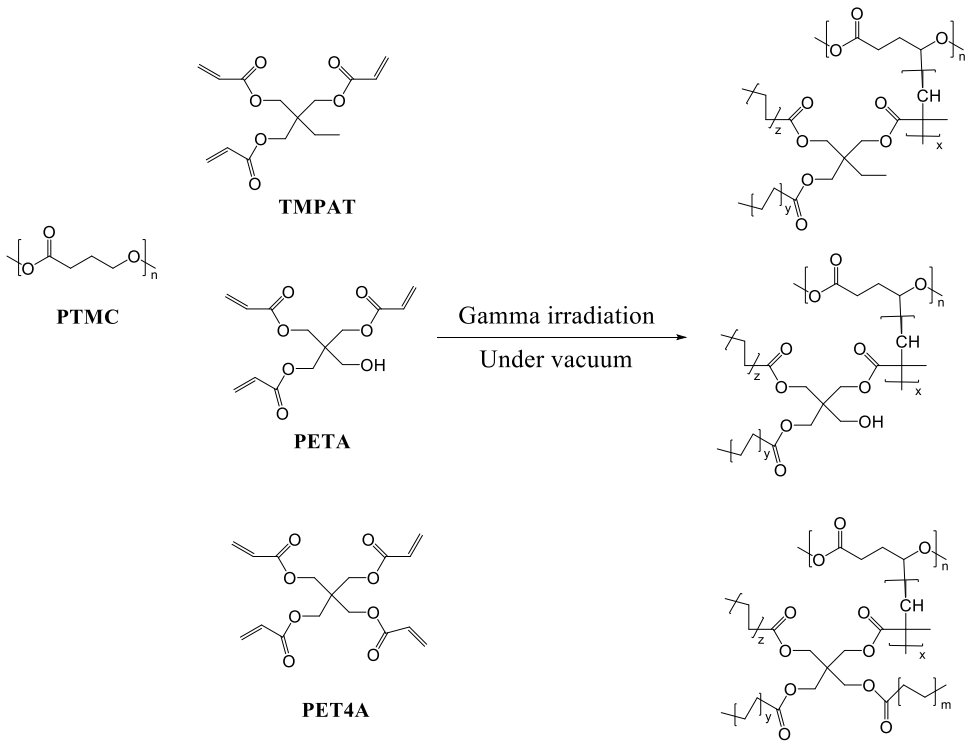

Figure 4-5. Preparation biodegradable elastic poly (1,3-trimethylene carbonate) network.[16]

Conversely, UV cross-linking offers more controllable outcomes, where the architecture and molecular weight of the prepolymers determine the cross-linking density. Allyl-functionalized PTMC can undergo thiol-ene click reactions with dithiol crosslinkers under UV irradiation (365 nm), resulting in the formation of insoluble, gel-like materials (**Figure 4-6**).[17] Hydrogels were formed with different sized crosslinkers in the presence or absence of a hydrophilic component, polyglycidol. The resulting four hydrogels were analyzed for their swelling capabilities, mechanical properties and degradation in phosphate buffered saline. Paclitaxel was chosen as a model drug to study the drug release from these two carriers and was incorporated during the crosslinking reaction.

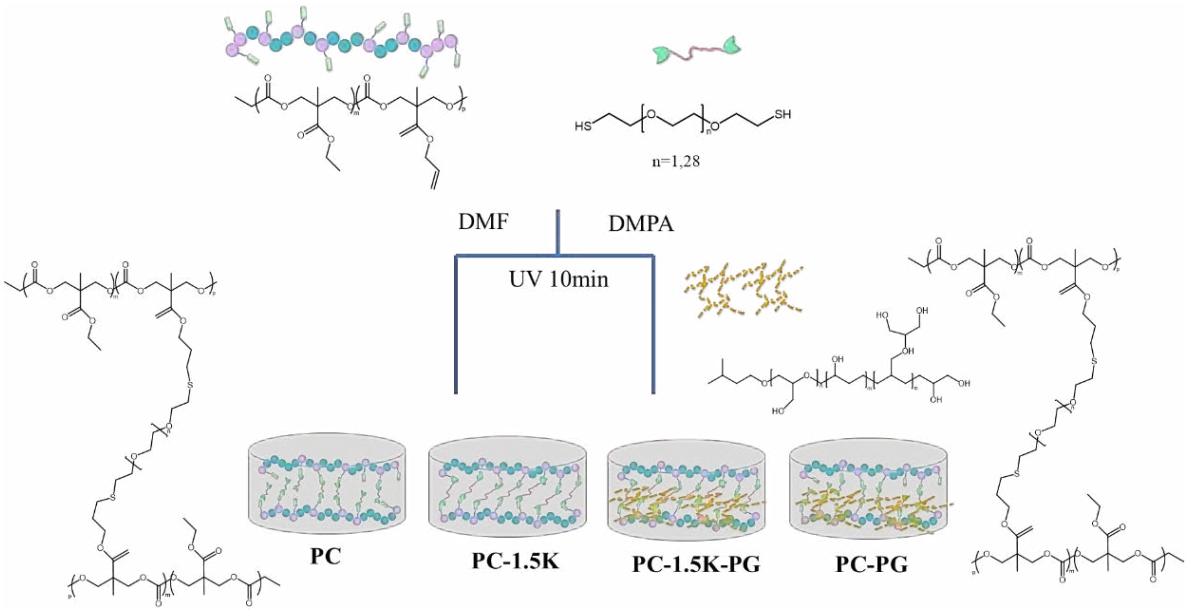

Figure 4-6. Synthesis of polycarbonate gels with short (PC, PC-PG) or long dithiol crosslinker (PC-1.5K, PC-1.5K-PG) in the presence (PC-PG, PC-1.5K-PG) or absence of polyglycidol (PC, PC-1.5K).[17]

Recently, there has been another considerable interest design in achieving stable dimensional polymer. The incorporation of an ionomer (typically 10-15 mol%)[18] either along the polymer backbone or as side chain groups markedly alters its physical properties. These modifications include enhanced mechanical properties, higher melt viscosity, and improved thermal stability. The improvements in rheological and mechanical properties can be attributed to the physical cross-linking effect, which is caused by thermally reversible intermolecular or intramolecular interactions. These interactions are contingent upon the ionic content and the polarity of the base polymer.

Extensive research has focused on enhancing the mechanical and thermal properties of degradable polymers.[19–25] Notably, Gregory et al. designed ABA-type block polymers utilizing ring-opening polymerization of ε-decalactone (derived from castor oil; B-block), followed by alternating ring-opening copolymerization of phthalic anhydride with 4-vinylcyclohexene oxide (A-blocks) (**Figure 4-7**).[19] These polyesters are efficiently functionalized *via* thiol-ene reaction to regularly incorporate carboxylic acid groups onto the A-blocks. By reacting the polymers with sodium or lithium hydroxide, the degree of ionization can be controlled (ranging from 0−100%), resulting in ionized polymers that exhibit enhanced tensile strength (20 MPa), elasticity (>2000%), and elastic recovery (>80%). This approach not only demonstrates the efficient synthesis of ABA block polymers but also the precise control of ionization in perfectly alternating monomer

sequences, offering a strategy that could be applied to a broad range of monomers, functional groups, and metals. Furthermore, the study revealed that neutralized metal carboxylate polymers display a lower glass transition temperature (T_g) of -51 °C corresponding to the PDL block and a higher T_g, corresponding to the aromatic polyester block, of 91 °C for lithium and 76 °C for sodium variants. The higher T_g observed with lithium carboxylate correlates with the stronger ionic associations typically formed by smaller cations.

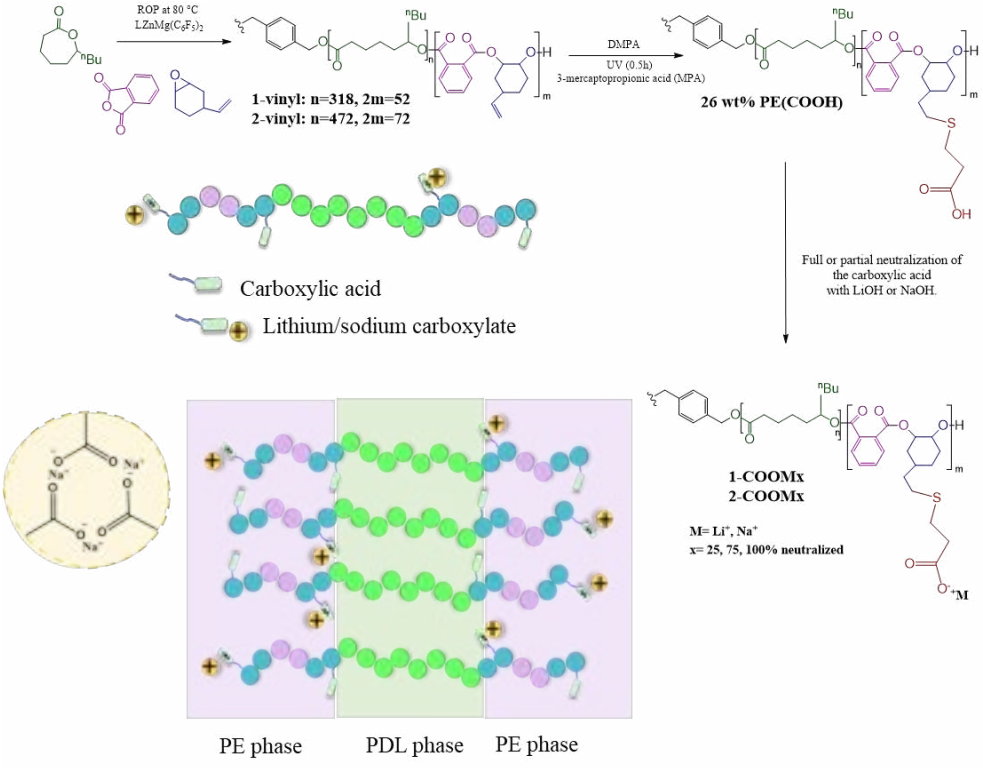

Figure 4-7. Synthesis of polyester ionomers (PE(COOH)-PDL-PE(COOH).[19]

On top of that, presence of ionomers in degradable polymer are expected to offer other advantages such as reduction in crystallinity may be achieved with the random distribution of a small number of ionic moieties. Also, considering the hydrophilic nature of ionic groups, the incorporation of ionic groups *via* the co-polymerization route or blending method might profoundly affect the biodegradation behavior of degradable polymer.

Han et al. synthesized poly(butylene adipate)-based ionomer (PBAi) and poly(butylene succinate) ionomer (PBSi) with varying concentrations of dimethyl 5-sulfoisophthalate sodium salt (DMSI).[20] They investigated the impact of the ionic group

on several properties, including dynamic mechanical properties, melt rheology, crystallization behavior, degradation behavior, and biocompatibility with human dermal cells. It was observed that water absorption in the polymers increased linearly with the ionic content. Notably, the hydrolytic degradation of PBSi was significantly accelerated as the ionic content increased. This enhanced hydrophilicity in polyester-based ionomer films is believed to increase the susceptibility of the surface to hydrolytic degradation.

In the biological context, ionomers utilize weak but abundant coordination bonds to create materials that are both rigid and healable. Lai et al. demonstrated that the rapid softening and hardening properties of the PDMSCOO-Zn polymer make it suitable for medical applications, such as orthopedic immobilization and external fixation systems (**Figure 4-8**).[21] This behavior is attributed to PDMS linear chains being crosslinked by Zn(II)-carboxylate interactions into a three-dimensional network. Upon heating, the Zn^{2+} +PDMS-COO^-↔Zn^{2+}($^-$OOC-PDMS) equilibrium shifts toward the dissociated state, resulting in an increase of non-crosslinked PDMS- PDMS-COO- chains. This shift reduces the mechanical strength and enhances polymer chain mobility, leading to a softer and more viscoelastic polymer. Conversely, upon cooling, the equilibrium shifts back to the associated state, which restores the densely crosslinked three-dimensional network.

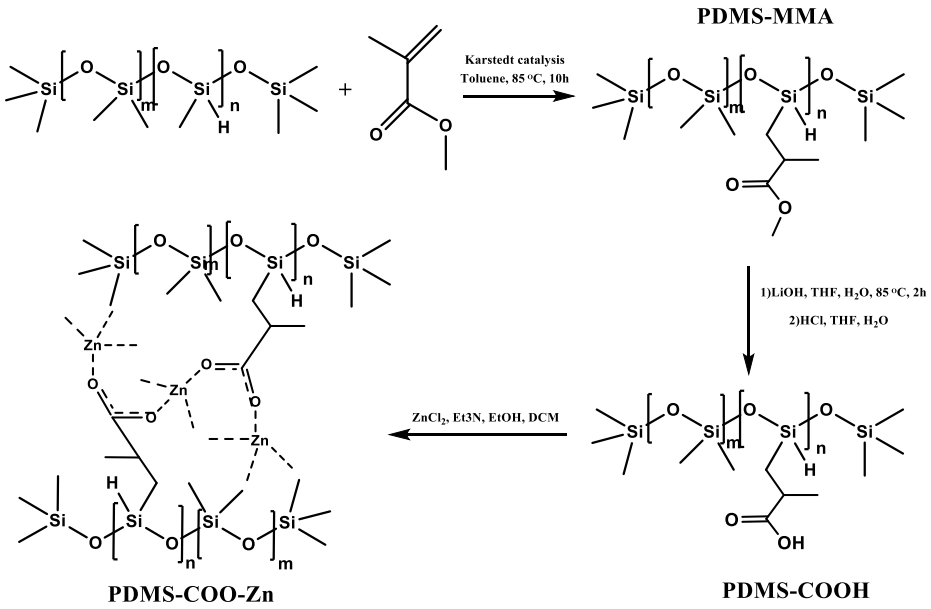

Figure 4-8. Synthesis of the highly crosslinked PDMS-COO-Zn polymer.[21]

Chen et al. prepared an imidazolium-based poly(ionic liquid)-b-PLA copolymer (ILA) and ionomers as toughening agents for PLA through an integrative approach.[22] By blending PLA with ILA and ionomers, enhanced PLA materials were obtained, featuring

combined properties of high toughness, good transparency, and antibacterial properties. The increase in imidazolium cation and anion groups' content was found to enhance the inhibition of *E. coli* and *S. aureus* growth. Furthermore, studies have explored PTMC modified with ionomers to develop elastomers that maintain high tensile strength without compromising elasticity or elastic recovery. Gregory et al. synthesized PTMC using phthalic anhydride (PA) and cyclohexene oxide, and further incorporated vinyl-substituted cyclohexene oxide in (ROCOP). This modification allows for subsequent interaction with Zn(II) salts to form Zn carboxylate moieties.[24] Results indicate that ionomers containing less than 1 wt% Zn benefit from PTMC's strain-induced crystallization, which is fully recoverable after stretching. Significantly, these elastomers are also reprocessable, retaining their thermal and mechanical properties, and can fully degrade into small molecules under aqueous alkaline conditions at the end of their use. Generally, the application of polymers and precision ionization in perfectly alternating monomer sequences is a concept that can be extended to various other monomers, functional groups, and metals.

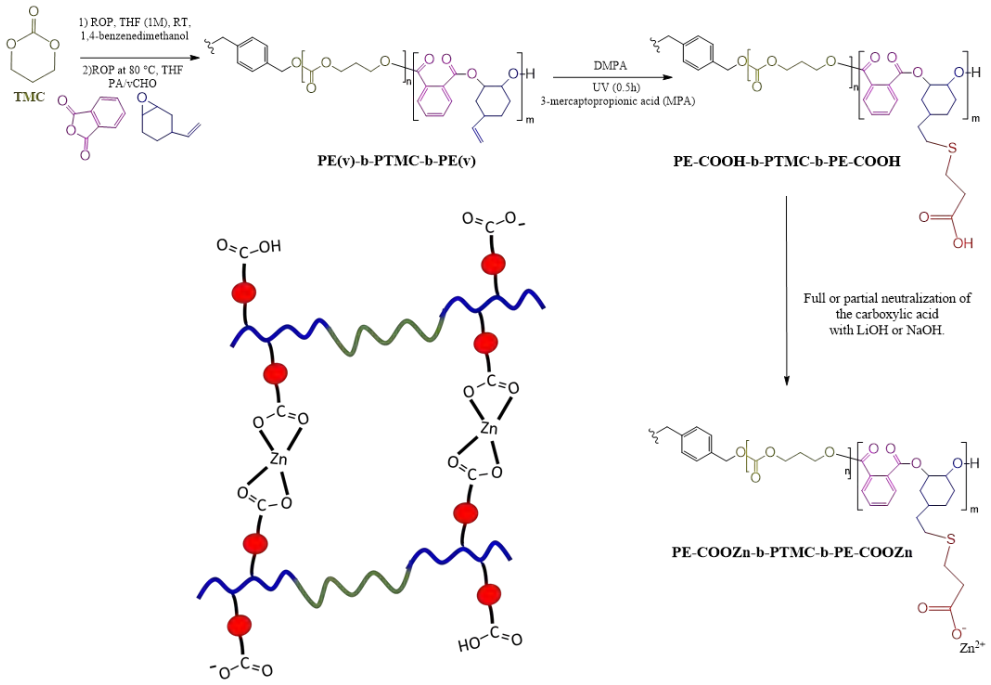

Figure 4-9. Synthesis of polycarbonate ionomers (PE(COO-Zn)-*b*-PTMC-*b*-PE(COO-Zn).[24]

In this chapter, we address the previously unexplored area of functionalizing PTMC with carboxylic groups on its side chains to create ionomers. This chapter is dedicated to designing and conducting a preliminary investigation into the effects of

ionomer crosslinking on the functionalized PTMC side chains. As highlighted earlier, PTMC-*co*-PexTMC$_{COOH}$ can be easily modified to incorporate carboxylic groups regularly distributed into its side chains without the need for a protective process. The carboxylic groups are crucial for precisely positioning . Magnesium acetate tetrahydrate, sodium acetate trihydrate, iron (II) acetate, and zinc (II) acetate were used as the metal-acetates to generate metal-carboxylated crosslinking, and the amounts of metal-acetate were also varied to study their effects. The degradation behavior, thermal properties, rheology, and water uptake of the metal-carboxylate crosslinked networks were discussed.

4.2 Results and Discussions

4.2.1 Preparation of PTMC-*co*-exTMC$_{30COOH}$ Ionomer

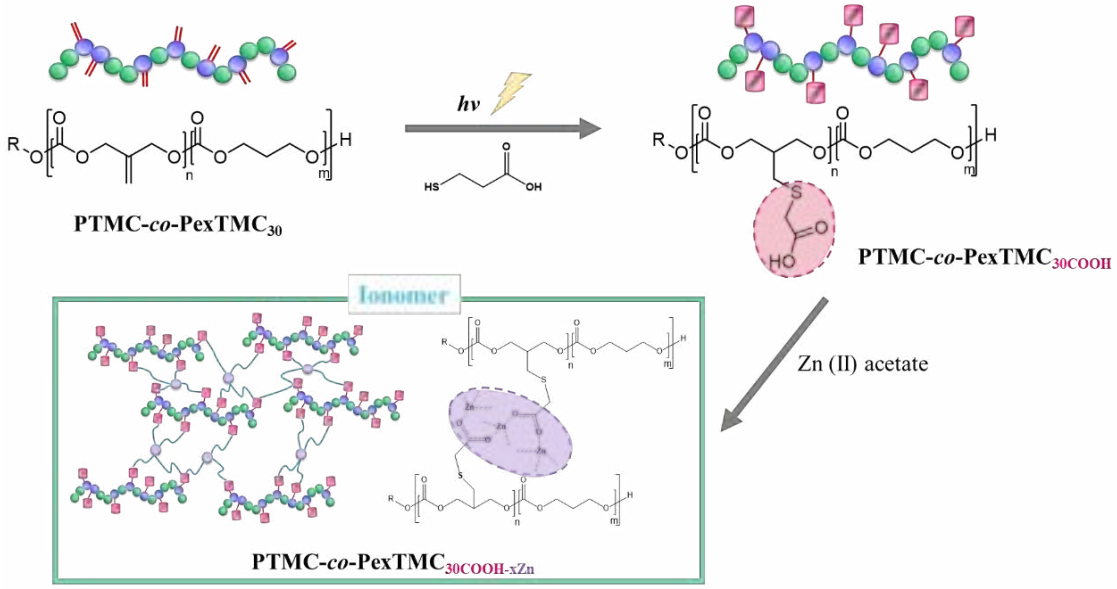

Table 4-1 Summary of the Mn and thermal stability of PTMC-*co*-PexTMC$_{30}$ before and after post-polymerization modification by Thiol-ene reaction and crosslinked by Zn (II) acetate.

Entry	Name	M_n[a] (kDa)	$Đ$	T_g (°C)	T_d (°C)	ΔH (J/g)
1	PTMC-*co*-PexTMC$_{30}$	12.9	1.14	-	234.78	-42.39
2	PTMC-*co*-PexTMC$_{30OH}$	12.9	1.14	-2.3	166.51	-24.04
3	PTMC-*co*-PexTMC$_{30COOH}$	15.1	1.31	-4.36	177.3	-21.52
4	PTMC-*co*-PexTMC$_{30COOH-2.5Zn}$	17.3	1.58	-4.82	199.41	-15.39
5	PTMC-*co*-PexTMC$_{30COOH-5Zn}$	16.7	1.76	-5.23	212.03	-15.77
6	PTMC-*co*-PexTMC$_{30COOH-10Zn}$	17.4	2.07	-4.29	206.11	-16.82
7	PTMC-*co*-PexTMC$_{30COOH-20Zn}$	16.6	2.16	-5.53	206.4	-17.29
8	PTMC-*co*-PexTMC$_{30COOH-30Zn}$	17.8	1.81	-5.92	205.99	-16.88

[a] Determined by SEC by polystyrene (PS) standard in THF, 40 °C.

To broaden their application fields, PTMC-*co*-exTMC$_{30COOH}$ was selected for crosslinking *via* abundant metal carboxylate interactions. This was achieved by coordinating metallic ions with the carboxylate groups to form metal complex ionomers. The ionomer coordination chemistry is investigated with sodium(I), magnesium(II),

zinc(II), and Fe (II). These metals are selected to be earth-abundant, inexpensive, low-weight, low toxicity and to feature strong bonding to carboxylic acids. This approach was chosen to utilize the resulting material as a biodegradable ionomer. The initial trial involved Zn(II)-carboxylate interactions. According to hard-soft-acid base theory in coordination chemistry, Zn(II) is a borderline acid while carboxylate is a hard base. Therefore, the coordination bond between Zn(II) and carboxylate is relatively weak but still stronger than a hydrogen bond. The experiment was set by various molar ratios of Zn(II) acetate to the molar ratio of carboxylic groups, ranging from 0 to 30%. After PTMC-*co*-PexTMC$_{30COOH\text{-}xZn}$ was formed, the Fourier-transform infrared (FTIR) spectroscopic analysis showed new absorbances characteristic of the carboxylate salt symmetric stretches at around 1583—1587 cm^{-1} after ionomer was formed, which shifted from the carboxylate salt symmetric stretches of PTMC-*co*-PexTMC$_{30COOH}$ at 1577 cm^{-1} (**Figure 4-10**).[19,26,27] Additionally, it was observable that with an increase in Zn-carboxylate content, the aspect of the copolymer became more opaque (**Figure 4-11**). SEC data indicated that after ionomer forming, the molar mass distribution of PTMC-*co*-PexTMC$_{30COOH\text{-}xZn}$ transitioned to a bimodal pattern with a higher M_n compared to PTMC-*co*-PexTMC$_{30COOH}$, which exhibited a monomodal distribution. Furthermore, an increase in Zn-carboxylate content corresponded with a rise in $Đ$ (**Table 4-1 and Figure 4-12**).

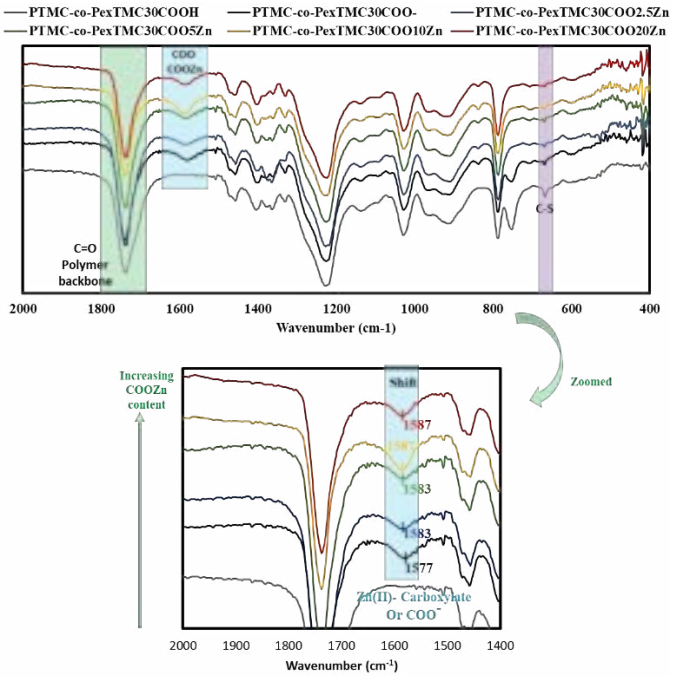

Figure 4-10 The FTIR spectra of PTMC-*co*-PexTMC$_{30}$ before and after post-polymerization modification by thiol-ene reaction and crosslinked by Zn (II) acetate.

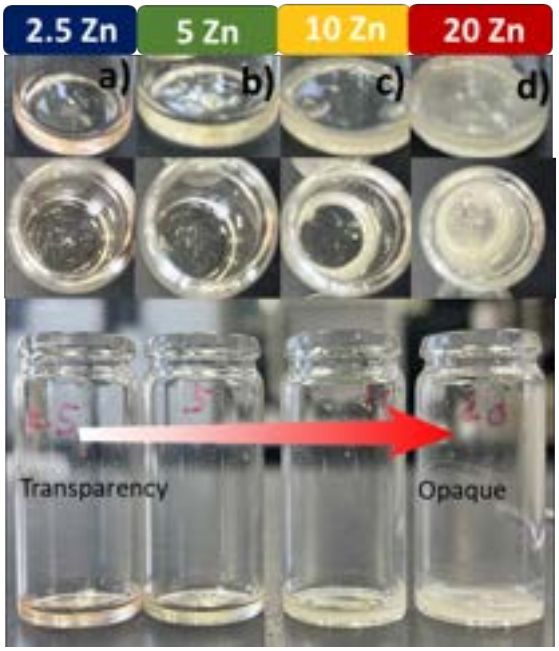

Figure 4-11 The images of PTMC-*co*-PexTMC$_{30COOH-xZn}$; a) 2.5Zn, b) 5Zn, c) 10Zn, and d) 20Zn.

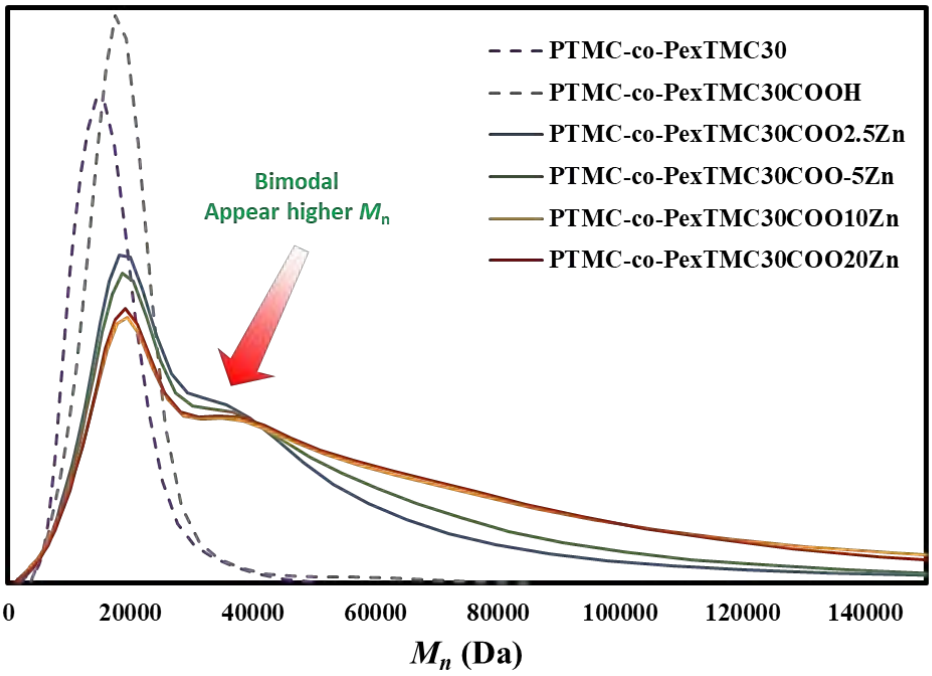

Figure 4-12 SEC traces of PTMC-*co*-PexTMC$_{30}$ before and after post-polymerization modification by Thiol-ene reaction and crosslinked by Zn (II) acetate.

4.2.2 Thermal stabilities

For biomedical applications, considering factors such as sterilization and processing-related temperatures, the thermal stability of polymeric materials is critical. Accordingly, the glass transition temperature (T_g) of the polymeric were studied by DSC as shown in **Table 4-1** and the thermal degradation profiles of PTMC-*co*-PexTMC and its derivatives were assessed using TGA (**Figure 4-13**) thermograms across the relevant temperature profile.

The T_g values of PTMC-*co*-PexTMC$_{30COOH}$, PTMC-*co*-PexTMC$_{30COOH\text{-}2.5Zn}$, PTMC-*co*-PexTMC$_{30COOH\text{-}5Zn}$, PTMC-*co*-PexTMC$_{30COOH\text{-}10Zn}$, and PTMC-*co*-PexTMC$_{30COOH\text{-}20Zn}$ were recorded at –4.36°C, –4.82°C, –5.23°C, –4.29°C and –5.53°C, respectively. A comparison of the T_g values before and after coordination with the Zn indicates no significant change in the thermal properties of PTMC-*co*-PexTMC$_{30COOH}$. Alternatively, the T_d values of PTMC-*co*-PexTMC$_{30}$, PTMC-*co*-PexTMC$_{30COOH}$, PTMC-*co*-PexTMC$_{30COOH\text{-}2.5Zn}$, PTMC-*co*-PexTMC$_{30COOH\text{-}5Zn}$, PTMC-*co*-PexTMC$_{30COOH\text{-}10Zn}$, and PTMC-*co*-PexTMC$_{30COOH\text{-}20Zn}$ were recorded at 234°C, 177°C, 199°C, 212°C, 206°C, and 206°C, respectively. These findings demonstrate that coordination with Zn-carboxylate enhances the T_d of PTMC-*co*-PexTMC$_{30COOH}$.

In this chapter, the onset decomposition temperatures at 10% weight loss (T_{10}) were evaluated and reported as 206°C for PTMC-*co*-PexTMC$_{30COOH}$, 289°C for PTMC-*co*-PexTMC$_{30COOH\text{-}2.5Zn}$, 292°C for PTMC-*co*-PexTMC$_{30COOH\text{-}5Zn}$, 297 °C for PTMC-*co*-PexTMC$_{30COOH\text{-}10Zn}$, and 299 °C for PTMC-*co*-PexTMC$_{30COOH\text{-}20Zn}$ (**Figure 4-13a**). The results demonstrated that upon coordination of PTMC-*co*-PexTMC$_{30COOH}$ with Zn(II) acetate, the thermal stability, as indicated by the increase in T_{10} values, was enhanced compared to the polymer prior to coordination with Zn. This observation may be attributed to the crosslinking effect of Zn ions coordinating with carboxylic groups, which likely alters the chemical structure of the polymer. This coordination-induced crosslinking potentially enhances the polymer's thermal properties by modifying its macromolecular architecture (**Figure 4-13**). These results may be beneficial for biomedical coating applications, particularly for sterilization in clinical settings through autoclaving at 120°C.

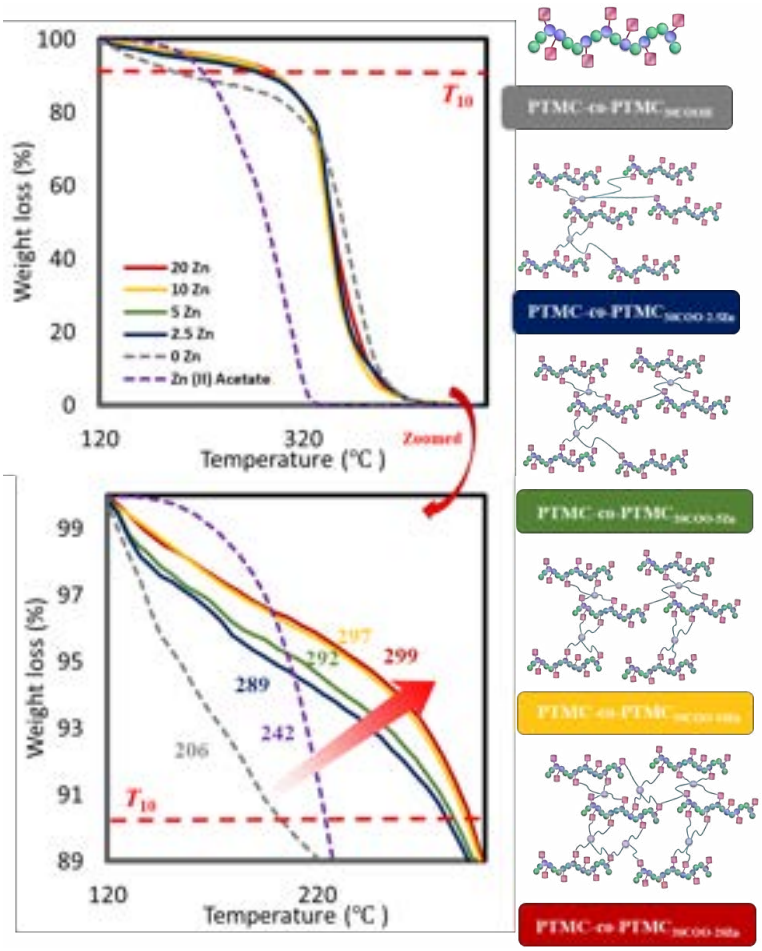

Figure 4-13 TGA curves of PTMC-*co*-PexTMC$_{30COO\text{-}xZn}$ by varied Zn (II) acetate ratio.

Table 4-2 The thermal stability of PTMC-*co*-PexTMC$_{30COO\text{-}30X}$ with different metal carboxylate

Entry	Name	T_{10} (°C)
1	30COONa	304
2	30COOMg	298
3	30COOZn	299
4	30COOFe	294

To investigate the influence of metal coordination on thermal stability, a series of metal complex ionomers were synthesized using sodium (I), magnesium (II), zinc (II), and iron (II) (**Table 4-2**). The results demonstrated that T_{10} of PTMC-*co*-PexTMC$_{30COOH\text{-}}$

$_{30Na}$, PTMC-*co*-PexTMC$_{30COOH-30Mg}$, PTMC-*co*-PexTMC$_{30COOH-30Zn}$, and PTMC-*co*-PexTMC$_{30COOH-30Fe}$ were 304°C, 298°C, 299°C, 294°C, respectively. This data suggests that variations in the type of metal complex ionomers do not significantly influence the thermal stability as indicated by the T_{10} values. This is likely because the crosslinking structure does not strongly impact on T_{10}, which primarily reflects the thermal degradation temperatures associated with the polymer main chain. The similarity in decomposition temperatures across different metal ions highlights the robustness of the PTMC-*co*-PexTMC$_{30COOH-30X}$ thermal properties irrespective of the specific metal ion incorporated.

4.2.3 Wettability

The surface enrichment behavior plays a crucial role in protein adsorption and cell adhesion, which are related to wettability. To simulate the human body conditions, the captive bubble method was employed to analyze the water contact angle of coated polymers on glass, as detailed in **Figure 4-14**.

The contact angles were 31.5 ° ± 0.7, 44.3° ± 0.3, 45.7° ± 0.3, 50.5° ± 0.26, and 58.9° ± 0.2 for PTMC-*co*-PexTMC$_{30COOH}$, PTMC-*co*-PexTMC$_{30COOH-2.5Zn}$, PTMC-*co*-PexTMC$_{30COOH-5Zn}$, PTMC-*co*-PexTMC$_{30COOH-10Zn}$, and PTMC-*co*-PexTMC$_{30COOH-20Zn}$, respectively. The results indicated that an increase in Zn(II) carboxylate content could significantly enhance the hydrophobicity of PTMC-*co*-PexTMC$_{30COOH}$. This reduction in hydrophilicity may be attributed to the formation of an ionomer, implying that increased crosslinking occurs. This is likely related to the reduction of available carboxylic groups which are essential for improving hydrophilicity.

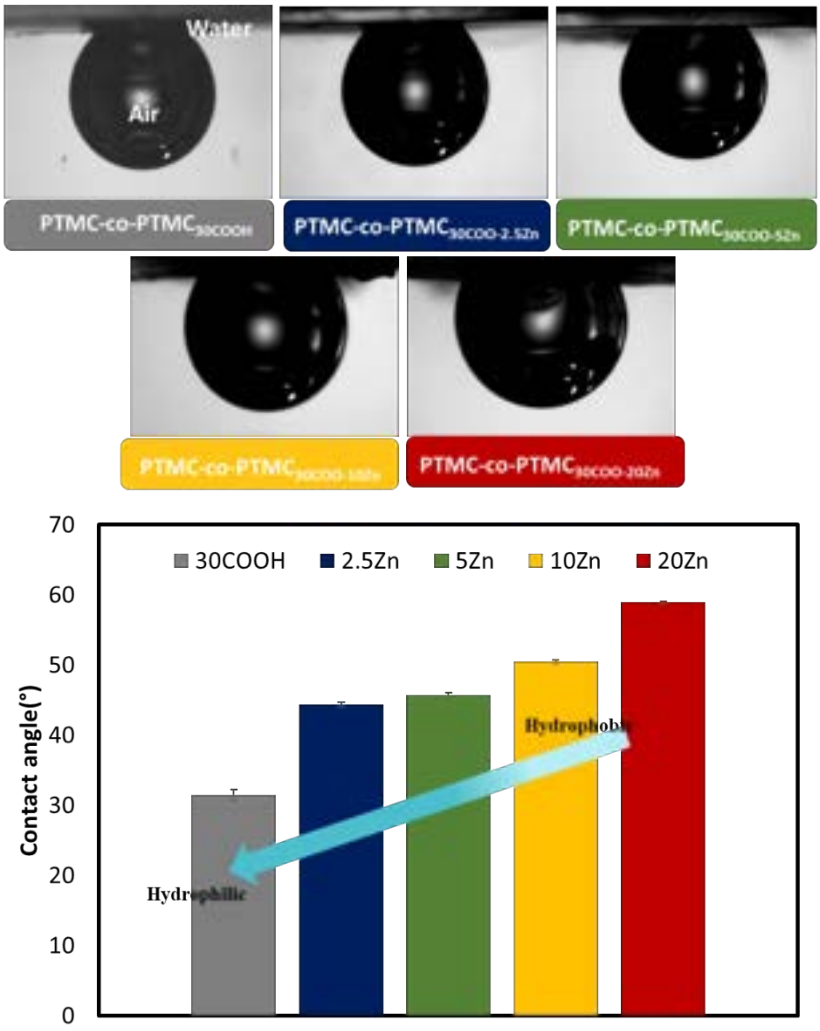

Figure 4-14 Contact angle measuring by captive bubble method of PTMC-*co*-PexTMC$_{30COO-xZn}$ by varied Zn (II) acetate ratio.

4.2.4 Degradation behavior

To evaluate their potential as the biomaterials, the degradation behavior of the polymer was studied and shown in **Figure 4-15 and Figure 4-16.** In this experiment, the main polymeric structure PexTMC$_{30COO-20Zn}$ coated on glass were assessed in degradation study under lipase enzyme solution at 37◦C. % water uptake (**Figure 4-15**) and %weight loss (**Figure 4-16**) were examined at every 1, 7, 14, 21, 28, and 42 days.

The obtained result indicated that PTMC-*co*-PexTMC$_{30COOH-30Zn}$ ionomer significantly reduced water uptake by nearly tenfold compared to PexTMC-*co*-TMC$_{30COOH}$, over the same period (**Figure 4-15**). Additionally, a similar trend was observed in the weight loss experiments. Over the same period, PTMC-*co*-PexTMC$_{30COOH-30Zn}$ exhibited lower weight loss percentages compared to PTMC-*co*-

PexTMC$_{30COOH}$. The results indicate that the formation of cross-linked networks effectively prevents degradation of PTMC-*co*-PexTMC$_{30COOH}$, which is in agreement with previous reports showing that crosslinking of PTMC can reduce enzymatic degradation.[28–30] Specifically, after 42 days, PTMC-*co*-PexTMC$_{30COOH}$ exhibited almost 90% weight loss, whereas after crosslinking with Zn(II) carboxylate reduced the weight loss to just 25%. It could be inferred that the carboxylic groups play a role in increasing water uptake and acting as catalysts for degradation,[31–33] which accelerates the hydrolysis of ester bonds in the polymer backbone. Yu et al. have reported that PTMC modification with carboxylic or hydroxy group could accelerate the hydrolysis faster than non-modified PTMC.[31] The results indicate that an increase in carboxylic content in the copolymer chains leads to a higher percentage of weight loss due to enhanced hydrophilicity, as previously discussed in Chapter III. Following the formation of ionomers, there may be a reduction in the availability of carboxylic groups, which in turn increases hydrophobicity (**Figure 4-16**), resulting in lower water uptake and weight loss. Additionally, as reported in Chapter III, the initial weight loss of PTMC-*co*-PexTMC$_{30COOH}$ could be attributed to the bulk erosion process. However, after forming the PTMC-*co*-PexTMC$_{30COOH-20Zn}$ ionomer, the initial weight loss pattern shifted to resemble the surface erosion process typical of normal PTMC.

Furthermore, the surface morphology of the PTMC-*co*-PexTMC$_{30COOH-30Zn}$ ionomer showed no significant changes over 42 days when exposed to lipase (**Figure 4-17**), in contrast to PTMC-*co*-PexTMC$_{30COOH}$. The latter exhibited a transformation from a smooth surface to a rough surface, with almost no polymer remaining on the substrate after 20 days. This variation could be attributed to the presence of carboxylic functionalization.

The results of the degradation rate study on PTMC-*co*-PexTMC30$_{COOH-30Zn}$ demonstrated that metal carboxylate cross-linking of the ionomer was an effective strategy to reduce the degradation rate of PTMC-*co*-PexTMC$_{30COOH}$. This reduction could potentially be controlled by manipulating the amount and type of cross-linker, thereby facilitating their extensive use in long-term biomedical applications.

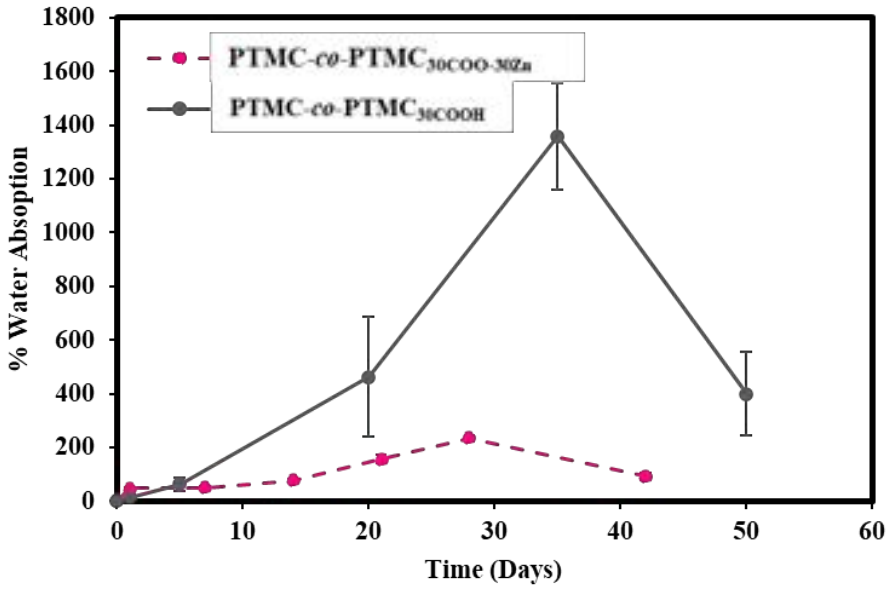

Figure 4-15 % water uptake in lipase circumstances plot of PTMC-*co*-PexTMC$_{30COOH}$ and PTMC-*co*-PexTMC$_{30COO-20Zn}$ over time.

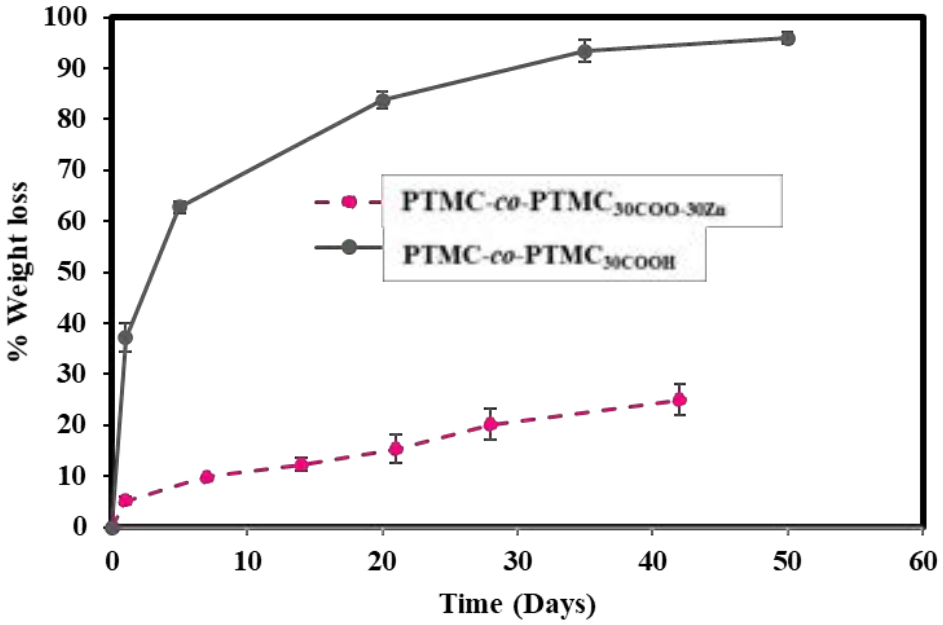

Figure 4-16 % weight loss in lipase circumstances plot of PTMC-*co*-PexTMC$_{30COOH}$ and PTMC-*co*-PexTMC$_{30COO-20Zn}$ over time.

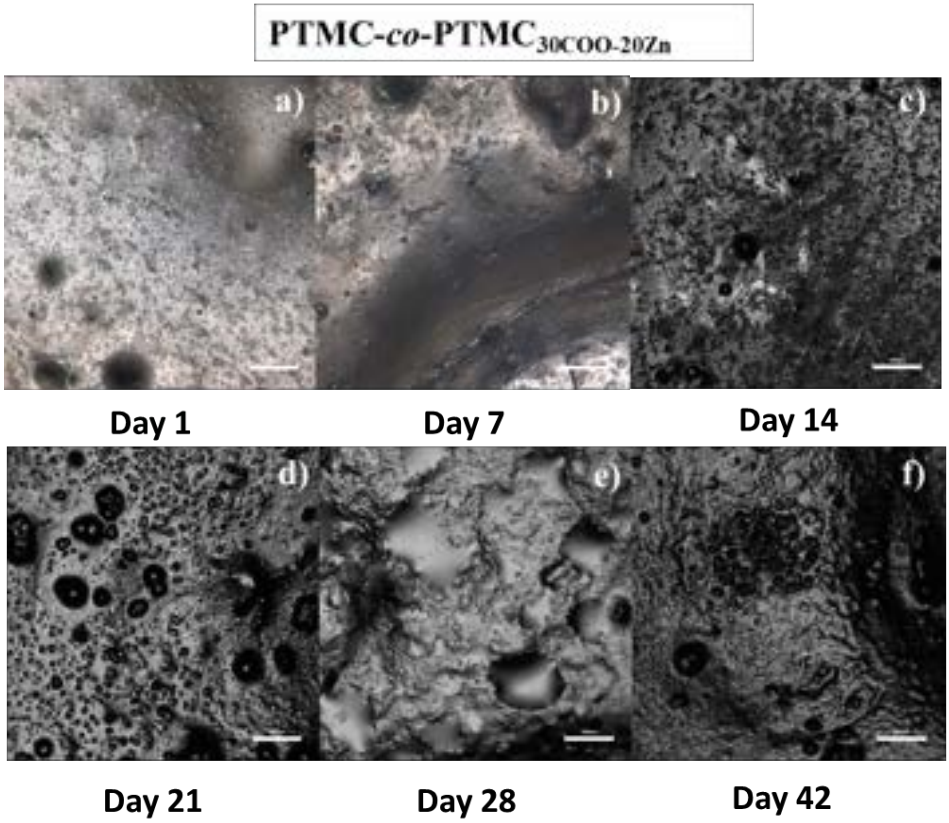

Figure 4-17 The surface morphology of PTMC-co-PexTMC$_{30COO-20Zn}$ in lipase at every 1, 7, 14, 21, 28, and 42 days.

4.2.5 Biocompatibilities

4.2.5.1 Protein adsorption

Protein adsorption on a coating biomaterial is crucial for determining its biocompatibility in a physiological environment. It is believed that interactions between proteins and biomaterials may mediate cellular adhesion, affecting the long-term performance of medical devices. Therefore, investigating surface modifications of coating polymers is a significant concern. The protein behaviours in response to PTMC-*co*-PexTMC$_{30COOH}$ before and after Zn(II) complex ionomer formed with various content of Zn(II) acetate content on glass substrate is shown in **Figure 4-18**. In this study, albumin, the primary protein in human blood plasma, was specifically chosen for experiment. The albumin adsorption of PTMC-*co*-PexTMC$_{30COOH}$, PTMC-*co*-PexTMC$_{30COOH-2.5Zn}$, PTMC-*co*-PexTMC$_{30COOH-5Zn}$, PTMC-*co*-PexTMC$_{30COOH-10Zn}$, and PTMC-*co*-PexTMC$_{30COOH-20Zn}$ coated on glass were 46.33 μg/cm^2 ± 0.03, 39.93 μg/cm^2

± 1.47, 38.77 µg/cm^2 ± 2.04, 37.02 µg/cm^2 ± 2.23, and 33.36 µg/cm^2 ± 0.02, respectively (**Figure 4-18**).

Based on the obtained results, it was observed that an increase in Zn(II) carboxylate content significantly reduced protein adsorption. This reduction may be attributed to the decreased availability of carboxylic groups, which are crucial for protein binding. Arima et al. noted that surface functional groups such as amines, hydroxy, and carboxylic typically exhibit higher protein adsorption compared to methyl groups[34]. Furthermore, another study reported that carboxyl (–COOH) groups tend to interact more effectively with fibronectin and albumin than hydroxyl (-OH) groups due to their negatively charged and hydrophilic nature.[34,35] Additionally, the effect of wettability could contribute to inducing favorable conditions for protein adsorbed on the surface. Cells effectively adhere onto a polymer surface with moderate wettability with water contact angles of around 40─70°.

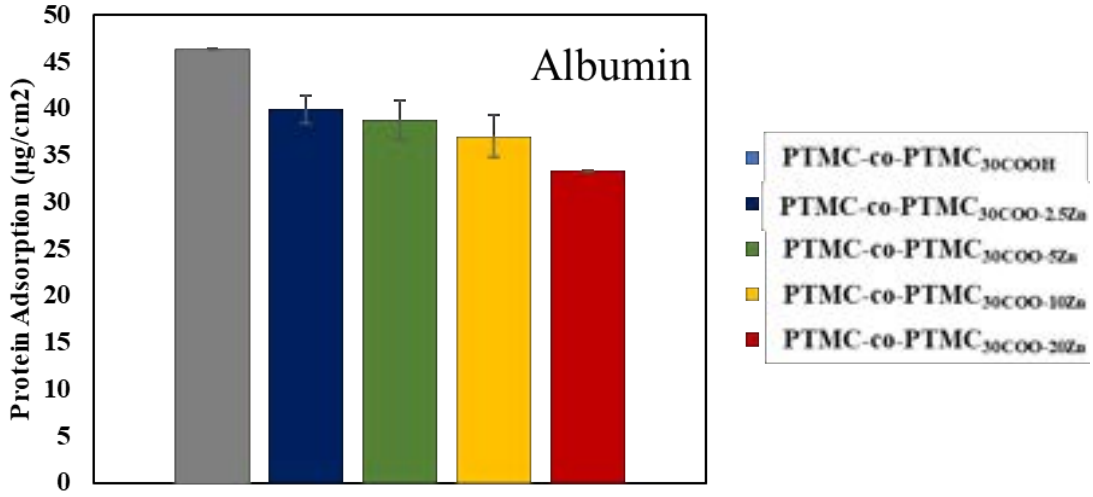

Figure 4-18. Albumin (BSA) protein adsorption on PTMC-co-PexTMC$_{30COO\text{-}xZn}$ by varied Zn (II) acetate ratio.

5.1.1 Rheology

The impact of metal coordination on the mechanical properties can be evaluated through rheological analysis. Additionally, for applications involving human body use, temperature is a crucial factor in studying polymer behavior. Thus, the temperature sweeps were employed to measure the rheological properties of PTMC-*co*-PexTMC$_{30COOH}$, both before and after metal coordination. This method is crucial for characterizing polymer structures, particularly for describing the internal superstructure and configuration of macromolecules. It helps evaluate their properties by analyzing the

storage modulus (G') and the loss modulus (G"), which are essential for determining the sol/gel transition temperature (T_{SG}) at the crossover point where G' equals G", and it can be related to the T_m. In the results presented in **Figure 4-19**, PTMC-*co*-PexTMC$_{30COOH}$ consistently exhibited a dominance of the G" over the G' across the entire experimental temperature range of 20—70°C (**Figure 4-19a**) which could be implied that T_{SG} of PTMC-*co*-PexTMC$_{30COOH}$ was lower than 20°C. In contrast, when the carboxylic groups of PTMC-*co*-PexTMC$_{30COOH}$ were coordinated with Zn(II) acetate, there was a noticeable increase in the T_{SG} (where G' equals G"). This transition temperature shift was directly correlated with the increasing content of metal coordination, achieving higher T_{SG} of 48°C for PTMC-*co*-PexTMC$_{30COOH-2.5Zn}$ (**Figure 4-19b**), 59°C for PTMC-*co*-PexTMC$_{30COOH-10Zn}$ (**Figure 4-19c**), 61°C for PTMC-*co*-PexTMC$_{30COOH-20Zn}$ (**Figure 4-19d**), and 70°C for PTMC-*co*-PexTMC$_{30COOH-30Zn}$ (**Figure 4-19e**), respectively. These results suggest that metal complex ionomers were formed and crosslinked, as indicated by G' over G" after Zn(II) acetate was introduced. Furthermore, higher concentrations of Zn(II) acetate lead to more extensive crosslinking, which can maintain the gel behavior at higher temperatures. Consequently, this affects the polymer structure, which in turn influences the variations in T_d, T_{10}, T_m, and enthalpy, as evidenced by DSC and TGA results.

To investigate the impact of metal coordination on rheology, a series of metal complex ionomers incorporating sodium (I), magnesium (II), zinc (II), and iron (II) were studied. The results indicated that varying the type of metal coordinated, at the same ratio, did not significantly alter the T_{SG} of PTMC-*co*-PexTMC$_{30COOH-30X}$. For PTMC-*co*-PexTMC$_{30COOH-30Na}$ (**Figure 4-20a**), PTMC-*co*-PexTMC$_{30COOH-30Mg}$ (**Figure 4-20c**), and PTMC-*co*-PexTMC$_{30COOH-30Zn}$ (**Figure 4-20d**), G' consistently dominated over G" up to around 70°C. However, PTMC-*co*-PexTMC$_{30COOH-30Fe}$ (**Figure 4-20b**) displayed a dominance of G' over G" across the entire experimental temperature range of 20-70°C, suggesting that the T_{SG} for PTMC-*co*-PexTMC$_{30COOH-30Fe}$ might exceed 70°C. This observation maybe be linked to the stronger coordination of Fe to the carboxylate moieties.[21] Moreover, the results suggested that PTMC-*co*-PexTMC$_{30COOH-30Fe}$ exhibited more elastic behavior (higher G') than PTMC-*co*-PexTMC$_{30COOH-30Na}$, PTMC-*co*-PexTMC$_{30COOH-30Mg}$, and PTMC-*co*-PexTMC$_{30COOH-30Zn}$ at the same measurement temperature.

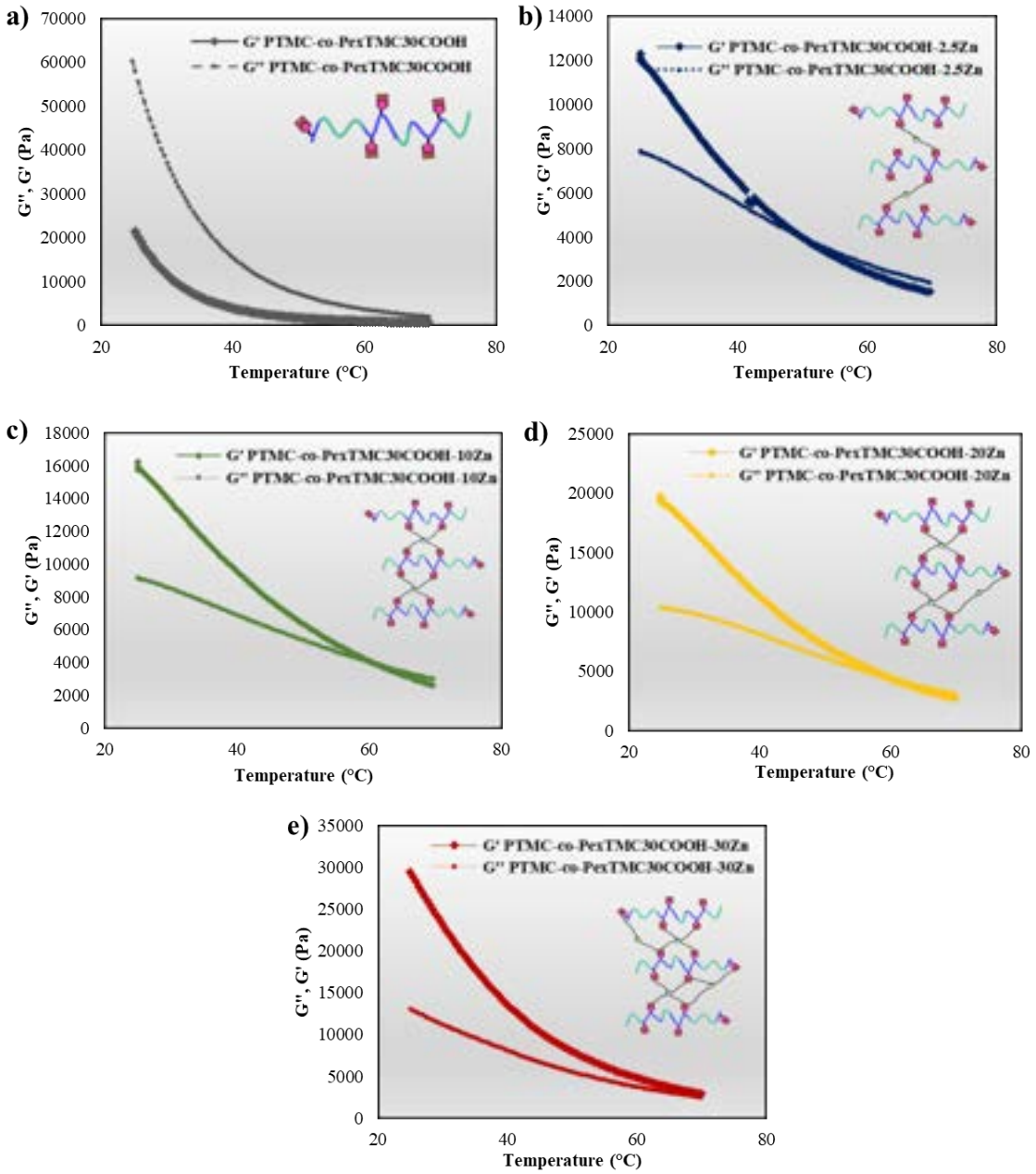

Figure 4-19. The plot of the temperature dependence of G' and G" during isochronal dynamic temperature sweeping by varied Zn (II) acetate ratio; a) PTMC-*co*-PexTMC$_{30COOH}$, b) PTMC-*co*-PexTMC$_{30COO\text{-}2.5Zn}$, c) PTMC-*co*-PexTMC$_{30COO\text{-}10Zn}$, d) PTMC-*co*-PexTMC$_{30COO\text{-}20Zn}$, and e) PTMC-*co*-PexTMC$_{30COO\text{-}30Zn}$

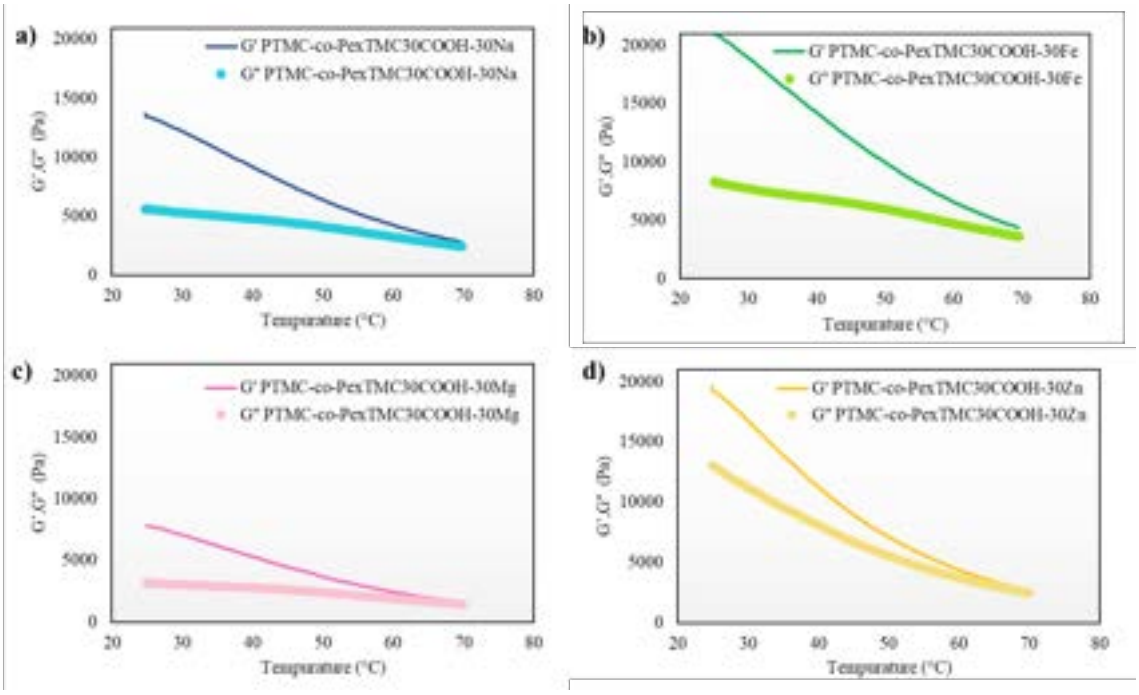

Figure 4-20. The plot of the temperature dependence of G' and G" during isochronal dynamic temperature sweeping by varied the type of metal coordinate; a) PTMC-*co*-PexTMC$_{30COO\text{-}30Na}$, b) PTMC-*co*-PexTMC$_{30COO\text{-}30Fe}$, c) PTMC-*co*-PexTMC$_{30COO\text{-}30Mg}$, and d) PTMC-*co*-PexTMC$_{30COO\text{-}30Zn}$.

Overall, the results indicate that the crosslinking of PTMC-*co*-PexTMC$_{30COOH}$ *via* metal-coordinated ionomers can be precisely controlled by varying the amount of carboxylic groups in the copolymer chain or by adjusting the input of metal acetate incorporated with the copolymer. The amount of metal carboxylate plays a pivotal role in tuning the polymer properties. Consequently, the strategic crosslinking of PTMC-*co*-PexTMC$_{30COOH}$ through metal-coordinated ionomers holds significant potential for expanding its biomedical applications.

4.3 Conclusions

The ionomers derived from PTMC-*co*-PexTMC$_{COOH\text{-}metal}$ have been synthesized with variable metal coordination levels and different metals. These ionomers exhibited enhanced thermal properties, including increased T_{10}, in comparison to PTMC-*co*-PexTMC$_{COOH}$. Furthermore, elevating the Zn(II) carboxylate content was found to significantly enhance the hydrophobicity of PTMC-*co*-PexTMC$_{30COOH}$. Accordingly, the presence of metal-carboxylate bonds in the PTMC-*co*-PexTMC$_{30COOH\text{-}30Zn}$ ionomer reduced both water adsorption and weight loss, thereby decelerating polymer degradation. These bonds also altered the degradation mechanism of PTMC-*co*-PexTMC$_{30COOH}$ from bulk erosion to surface erosion. Increased Zn(II) carboxylate content also led to a significant reduction in protein adsorption. From a mechanical perspective, PTMC-*co*-PexTMC$_{30COOH}$ exhibited plastic behavior (G'< G") before crosslinking *via* metal acetate throughout the tested temperature range of 20—70°C. After PTMC-*co*-PexTMC$_{30COOH}$ was cooperated with metal acetate, G' became greater than G", indicating that the PTMC-co-PexTMC$_{30COOH}$ ionomer was formed and crosslinked through metal carboxylation. Consequently, the ionomer exhibited elastic behavior. Additionally, the ionomers demonstrated that a higher metal coordination content could enhance their stability at elevated temperatures. Once the metal coordination bonds were established, the ionomer maintained elastic behavior throughout the tested temperature range of 20–70°C.

4.4 Experimental

4.4.1 Synthesis of PTMC-*co*-exTMC$_{30COOH-xMetal}$ Ionomer

The copolymerization of TMC and exTMC with DP120 (30%exTMC) was modified using thiolglycolic acid (TGC) in chapter 2. PTMC-*co*-PexTMC (2000 mg, 0.16 mmol, ~1-30 vinyl units per chain) was dissolved in 2 mL of THF until a homogeneous solution was achieved. TGC (0.30mL, 5.1mmol) and 2% wt DMPA as photo-initiator (40mg, 156.1 mmol) were added into the mixture. The mixture was stirred at room temperature under UV light (365 nm). The reaction was monitored at specific time interval by ^{1}H NMR. After 1h, the UV light was turned off and the mixture was vacuum evaporated to remove solvent. The obtained compound was purification by MeOH and Et_2O to remove unreactive thiol-derivative. After that, the mixture was vacuum dried at 60°C for overnight to obtain post-polymerization modification polymer (PTMC-*co*-PexTMC$_{COOH}$) (86% yield). ^{1}H NMR ($CDCl_3$, 300 MHz): 4.25 (m, 118x4H, $OCH_{2polymer}$), 3.90-3.65 (m, 30x2H, CH_2OH), 3.60-3.50 (m, 25x1H, CHOH), 2.80-2.55 (m, 30x4H, CH_2-S-CH_2), 2.30 (m, 30x1H, $CH_{polymer}$), 2.15-2.00 (m, 86x2H, $CH_{2polymer}$). Subsequently, PTMC-*co*-PexTMC$_{30COOH}$ (120 mg, 0.0079 mmol) was dissolved in 1 mL of THF. The experiment was set up with varying molar ratios of metal acetate to carboxylic groups, ranging from 0% to 30%. Metal acetates were prepared as stock solutions dissolved in DI water and added to the PTMC-*co*-PexTMC$_{30COOH}$ solution in different amounts, depending on the desired metal coordination ionomer ratio. The mixture was dried overnight to form the metal coordination ionomer. After complete solvent evaporation, the product was washed with DI water three times to remove acetic acid (by-product) and vacuum dried overnight. The metal acetates used in this experiment were sodium(I), magnesium(II), zinc(II), and iron(II).

4.4.2 Coating procedure

The concentration of ionomer solution in THF was 20 mg/ml. The ionomer was applied on the glass substrates (diameter 0.8 mm) by dropped 40 µl of polymeric solution to the substrate for four time-repeated coating. The coated substrates were then dried under vacuum before testing.

4.4.3 Thermal resistance

The thermal stability of the polymer was determined by a thermo-gravimetric analyser TGA-50 (Shimadzu) under nitrogen atmosphere with 10°C/min flow rate to 500°C. Differential scanning calorimetry (DSC) spectra were also analysed by a Hitachi DSC6200 in the atmosphere with temperature ramp rate 10°C/min in range 70°C—

200°C.

4.4.4 Wettability test

The static water contact angle of coated substrates was measured by CropMaster DM-301/501/707/901 (Kyowa Interface Science Co., Ltd.). Image were taken after sample were soaked in DI water 3 minutes, then, the air 40 µl was dropped on coated surface with three replicates at different locations to obtain mean value of the contact angle.

4.4.5 Degradation behavior

PTMC-*co*-PexTMC$_{30COOH-30Zn}$ was coated on circle round shape of glass with dimension of 0.8 mm and demonstrated with 5 replicates. Sample was soaked in 2 ml of lipase solution (5mg/ml), and. The samples were monitored weight simultaneously at 1, 7, 14, 21, 28, and 42, days and calculated % weight loss as the following equation.

$$\% \text{ Weight loss} = \frac{Wi - Wd}{Wi} \times 100\%$$

Where w_i; initial weight before soaking and w_d; dried weight of the films at specific day.

Water uptake

The water uptake of samples was determined as the following equation:

$$\%\text{Water uptake} = \frac{mw - md}{Wmd} \times 100\%$$

Where m_w and m_d are the mass of the wet and dried polymer samples, respectively.

4.4.6 Protein Adsorption

Biocompatibility could be defined as the surface properties of the coated polymeric to prolife or adhere by protein or blood platelet cell. Protein adsorption was examined using bovine serum albumin (BSA) with concentration of 4.5 mg/ ml detecting by bicinchoninic acid (BCA) protein assay reagent. The samples and reference samples were soaked in PBS (pH 7.4) at 37 °C overnight. Then, each sample was immersed into 900 µL of each protein solution and incubated 4 h at 37 °C. After rinsing with PBS, adsorbed protein was detached by 1 wt% of n-sodium dodecyl sulfate (SDS) for 4 h. Bicinchoninic acid (BCA) protein assay reagent was used as indicator for protein adsorption on the samples. UV measurement at 562 nm for protein on sample surface was interpreted by absorbance microplate reader (MTP-310lab, Corona Electric) based on standard control and calibration curve of the protein.

4.4.7 Rheology

To understand the mechanical properties of ionomer, rheological experiments were applied with a Kinexus pro+ rheometer (Malvern Panalytic) using a parallel plate geometry on a pettier plate. The diameter of the plate is 20 mm, the plate gap is 100 μm. Ionomer samples were measured in temperature sweeps mode with ramp rate 5°C / min, frequency 1 Hz, and shear strain 1%.

4.5 References

(1) Fukushima, K. Poly(Trimethylene Carbonate)-Based Polymers Engineered for Biodegradable Functional Biomaterials. *Biomater. Sci.* **2016**, 4(1), 9–24. https://doi.org/10.1039/c5bm00123d.

(2) Pêgo, A. P.; Grijpma, D. W.; Feijen, J. Enhanced Mechanical Properties of 1,3-Trimethylene Carbonate Polymers and Networks. *Polymer (Guildf)* **2003**, *44* (21), 6495–6504. https://doi.org/10.1016/S0032-3861(03)00668-2.

(3) Kuhnt, T.; Marroquín García, R.; Camarero-Espinosa, S.; Dias, A.; Ten Cate, A. T.; Van Blitterswijk, C. A.; Moroni, L.; Baker, M. B. Poly(Caprolactone -Co - Trimethylenecarbonate) Urethane Acrylate Resins for Digital Light Processing of Bioresorbable Tissue Engineering Implants. *Biomater. Sci.* **2019**, *7* (12), 4984–4989. https://doi.org/10.1039/c9bm01042d.

(4) Braghirolli, D. I.; Caberlon, B.; Gamba, D.; Petry, J. F. T. C.; Dias, M. L.; Pranke, P. Poly(Trimethylene Carbonate-Co-l-Lactide) Electrospun Scaffolds for Use as Vascular Grafts. *Braz. J. Med. Biol. Res.* **2019**, *52* (8). https://doi.org/10.1590/1414-431X20198318.

(5) Xiaomeng, W.; Xiaoyu, C.; Zhongyong, F. Totally Biodegradable Poly(Trimethylene Carbonate/Glycolide-Block-L-Lactide/Glycolide) Copolymers: Synthesis, Characterization and Enzyme-Catalyzed Degradation Behavior. *Eur. Polym. J.* **2018**, *101*, 140–150. https://doi.org/10.1016/j.eurpolymj.2018.02.028.

(6) Jiang, D.; Zou, H.; Zhang, H.; Zhao, W.; Lan, Y.; Yuan, M. Preparation and Properties of Electrospun PLLA/PTMC Scaffolds. *Polymers (Basel)* **2022**, *14* (20). https://doi.org/10.3390/polym14204406.

(7) Irikura, K.; Ekapakul, N.; Choochottiros, C.; Chanthaset, N.; Yoshida, H.; Ajiro, H. Fabrication of Flexible Blend Films Using a Chitosan Derivative and Poly(Trimethylene Carbonate). *Polym. J.* **2021**, *53* (7), 823–833. https://doi.org/10.1038/s41428-021-00470-6.

(8) Dorigato, A. Recycling of Polymer Blends. *Advanced Industrial and Engineering Polymer Research*. **2021**, 4(2), 53–69. https://doi.org/10.1016/j.aiepr.2021.02.005.

(9) Burdick, J. A.; Stevens, M. M. Biomedical Hydrogels. *Biomaterials, Artificial Organs and Tissue Engineering*. **2005**, 107–115. https://doi.org/10.1533/9781845690861.2.107.

(10) Sapuła, P.; Bialik-Wąs, K.; Malarz, K. Are Natural Compounds a Promising Alternative to Synthetic Cross-Linking Agents in the Preparation of Hydrogels? *Pharmaceutics*. **2023**, *15*(1), 253. https://doi.org/10.3390/pharmaceutics15010253.

(11) Yang, L. Q.; He, B.; Meng, S.; Zhang, J. Z.; Li, M.; Guo, J.; Guan, Y. M.; Li, J. X.; Gu, Z. W. Biodegradable Cross-Linked Poly(Trimethylene Carbonate) Networks for Implant Applications: Synthesis and Properties. *Polymer (Guildf)* **2013**, *54* (11), 2668–

2675. https://doi.org/10.1016/j.polymer.2013.03.059.

(12) Tan, L. Y.; Chanthaset, N.; Nanto, S.; Soba, R.; Nagasawa, M.; Ohno, H.; Ajiro, H. Synthesis and Preparation of Cross-Linked Films with Ester-Free Poly(Trimethylene Carbonate) Bearing Aromatic Urea Moiety. *Macromolecules* **2021**, *54* (12), 5518–5525. https://doi.org/10.1021/acs.macromol.1c00339.

(13) Bat, E.; van Kooten, T. G.; Feijen, J.; Grijpma, D. W. Macrophage-Mediated Erosion of Gamma Irradiated Poly(Trimethylene Carbonate) Films. *Biomaterials* **2009**, *30* (22), 3652–3661. https://doi.org/10.1016/j.biomaterials.2009.03.033.

(14) Zant, E.; Grijpma, D. W. Tough Biodegradable Mixed-Macromer Networks and Hydrogels by Photo-Crosslinking in Solution. *Acta Biomater.* **2016**, *31*, 80–88. https://doi.org/10.1016/j.actbio.2015.12.014.

(15) Nobuoka, H.; Ajiro, H. Biodegradable and Biocompatible Crosslinked Film with Trimethylene Carbonate Bearing Oligo(Ethylene Glycol). *Chem. Lett.* **2019**, *48* (3), 245–248. https://doi.org/10.1246/cl.180960.

(16) Liu, X.; Liu, S.; Li, K.; Feng, S.; Fan, Y.; Peng, L.; Wang, X.; Chen, D.; Xiong, C.; Bai, W.; Zhang, L. Preparation and Degradation Characteristics of Biodegradable Elastic Poly (1,3-Trimethylene Carbonate) Network. *Polym. Degrad. Stab.* **2021**, *193*. https://doi.org/10.1016/j.polymdegradstab.2021.109718.

(17) David M. Stevens; Anand Rahalkar; Benjamin Spears; Kelly Gilmore; Emily Douglas; Murugappan Muthukumar; Eva Harth. Semibranched Polyglycidols as “Fillers” in Polycarbonate Hydrogels to Tune Hydrophobic Drug Release. *Polym. Chem.* **2015**, *6*, 1096–1102. https://doi.org/10.1039/x0xx00000x.

(18) Johnston, P.; Adhikari, R. Synthesis, Properties and Applications of Degradable Ionomers. *Eur. Polym. J.* **2017**, *95*, 138–160. https://doi.org/10.1016/j.eurpolymj.2017.08.009.

(19) Gregory, G. L.; Williams, C. K. Exploiting Sodium Coordination in Alternating Monomer Sequences to Toughen Degradable Block Polyester Thermoplastic Elastomers. *Macromolecules* **2022**, *55* (6), 2290–2299. https://doi.org/10.1021/acs.macromol.2c00068.

(20) Han, S. Il; Yoo, Y.; Kim, D. K.; Im, S. S. Biodegradable Aliphatic Polyester Ionomers. *Macromol. Biosci.* **2004**, 4, 199–207. https://doi.org/10.1002/mabi.200300095.

(21) Lai, J. C.; Li, L.; Wang, D. P.; Zhang, M. H.; Mo, S. R.; Wang, X.; Zeng, K. Y.; Li, C. H.; Jiang, Q.; You, X. Z.; Zuo, J. L. A Rigid and Healable Polymer Cross-Linked by Weak but Abundant Zn(II)-Carboxylate Interactions. *Nat. Commun.* **2018**, *9* (1). https://doi.org/10.1038/s41467-018-05285-3.

(22) Chen, X.; Ding, Y.; Li, Y.; Li, J.; Sun, L.; Wei, X.; Wei, J.; Zhang, K.; Wang, H.; Pan,

L.; He, S.; Li, Y. Modification of Polylactide by Poly(Ionic Liquid)-b-Polylactide Copolymer and Bio-Based Ionomers: Excellent Toughness, Transparency and Antibacterial Property. *Int. J. Biol. Macromol.* **2022**, *221*, 1512–1526. https://doi.org/10.1016/j.ijbiomac.2022.08.122.

(23) Sai, T.; Ran, S.; Huo, S.; Guo, Z.; Song, P.; Fang, Z. Sulfonated Block Ionomers Enable Transparent, Fire-Resistant, Tough yet Strong Polycarbonate. *Chem. Eng. J.* **2022**, *433*. https://doi.org/10.1016/j.cej.2021.133264.

(24) Gregory, G. L.; Sulley, G. S.; Kimpel, J.; Łagodzińska, M.; Häfele, L.; Carrodeguas, L. P.; Williams, C. K. Block Poly(Carbonate-Ester) Ionomers as High-Performance and Recyclable Thermoplastic Elastomers. *Angew. Chem. - Int. Ed.* **2022**, *61* (47). https://doi.org/10.1002/anie.202210748.

(25) Saumer, A.; Mecking, S. Recyclable and Degradable Ionic-Substituted Long-Chain Polyesters. *ACS Sustain. Chem. Eng.* **2023**, *11* (33), 12414–12422. https://doi.org/10.1021/acssuschemeng.3c03141.

(26) Miwa, Y.; Kurachi, J.; Kohbara, Y.; Kutsumizu, S. Dynamic Ionic Crosslinks Enable High Strength and Ultrastretchability in a Single Elastomer. *Commun. Chem.* **2018**, *1* (1). https://doi.org/10.1038/s42004-017-0004-9.

(27) Kajita, T.; Tanaka, H.; Noro, A.; Matsushita, Y.; Nozawa, A.; Isobe, K.; Oda, R.; Hashimoto, S. Extremely Tough Block Polymer-Based Thermoplastic Elastomers with Strongly Associated but Dynamically Responsive Noncovalent Cross-Links. *Polymer (Guildf)* **2021**, *217*. https://doi.org/10.1016/j.polymer.2021.123419.

(28) Li, W.; Lin, M.; Wang, C.; Lu, Y.; Sui, Y.; Ni, X.; Guo, J.; Jiang, M.; Yang, L.; Cui, H. In Vitro Enzymatic Degradation of the PTMC/Cross-Linked PEGDA Blends. *Front Bioeng. Biotechnol.* **2023**, *11*. https://doi.org/10.3389/fbioe.2023.1253221.

(29) Zant, E.; Grijpma, D. W. Tough Biodegradable Mixed-Macromer Networks and Hydrogels by Photo-Crosslinking in Solution. *Acta Biomater.* **2016**, *31*, 80–88. https://doi.org/10.1016/j.actbio.2015.12.014.

(30) Hou, Z.; Hu, J.; Li, J.; Zhang, W.; Li, M.; Guo, J.; Yang, L.; Chen, Z. The in Vitro Enzymatic Degradation of Cross-Linked Poly(Trimethylene Carbonate) Networks. *Polymers (Basel)* **2017**, *9* (11). https://doi.org/10.3390/polym9110605.

(31) Yu, F.; Zhuo, R. Synthesis, Characterization, and Degradation Behaviors of End-Group-Functionalized Poly(Trimethylene Carbonate)s. *Polym. J.* **2003**, 35(8), 671-676. https://doi.org/10.1295/polymj.35.671.

(32) Gorrasi, G.; Pantani, R. Hydrolysis and Biodegradation of Poly(Lactic Acid). *Adv. Polym. Sci.* **2018**, *279*, 119–151. https://doi.org/10.1007/12_2016_12.

(33) Saha, S. K.; Tsuji, H. Effects of Molecular Weight and Small Amounts of D-Lactide

Units on Hydrolytic Degradation of Poly(l-Lactic Acid)s. *Polym. Degrad. Stab.* **2006**, *91* (8), 1665–1673. https://doi.org/10.1016/j.polymdegradstab.2005.12.009.

(34) Arima, Y.; Iwata, H. Effects of Surface Functional Groups on Protein Adsorption and Subsequent Cell Adhesion Using Self-Assembled Monolayers. *J. Mater. Chem.* **2007**, *17* (38), 4079–4087. https://doi.org/10.1039/b708099a.

(35) Thevenot, P.; Hu, W.; Tang, L. Surface Chemistry Influences Implant Biocompatibility. *Curr. Top. Med. Chem.* **2008**, *8* (4), 270–280. https://doi.org/10.2174/156802608783790901.

General Conclusion

The aim of this thesis entitled "*Synthesis and properties modulation of novel functional degradable polymers by means of fine tuning of their structure*" is to present the development of novel structural designs for functional PEs and polycarbonates PCs. These designs are intended to precisely control target properties from the molecular to the macromolecular level. The approach is grounded in the principles of low toxicity and ease of functionalization of pendant groups to achieve specific properties related to biomedical applications. To achieve the purpose, the strategic design and synthesis of functionalized biodegradable polyesters and polycarbonates has been carried out through the tuning of the macromolecular architecture to control specific physical and chemical properties,. Employing advanced synthetic strategies, this work systematically investigates four key aspects of biodegradable polymer design.

In Chapter I, "*The Design of pH-Responsive Functional Chain Ends of Polylactides for Trigged Aggregation*" - the concept of 'Functionalized Chain End' was presented as a concrete strategy for developing functionalized biodegradable polyesters through chain-end modification. Novel vanillin acetal-based initiators, including cyclic-membered ring diol-ketone acetal, were synthesized. These initiators were used to produce novel functional PLA with precise end-capping. PLLA-V6-OEG_3 particles were engineered to exhibit pH-responsive behavior under physiological conditions within 3 minutes, targeting specific medical applications. To balance hydrophilicity and hydrophobicity for SC-PLA particles, PLLA-V6-OEG_4 and PDLA-V6-OEG_4 were successfully synthesized. The aggregation rate of SC-PLA-OEG_m particles was influenced by molecular weight, the hydrophilicity of the chain-end, and the number of acetal bonds. Blending PLLA-V6-OEG_3 particles with TiO_2 accelerated aggregation compared to those without TiO_2. However, SC-PLA particles blended with TiO_2 did not achieve pH responsiveness under physiological conditions. Overall, Chapter I highlights the achievement of incorporating vanillin acetal-based initiators for PLA end-capping, which enables pH-responsive performance at the designed functionalized chain end. This advancement facilitates controlled aggregation within three minutes under physiological conditions.

In Chapter II, "*Copolymerization of Trimethylene Carbonate and 5-Methylene-1,3-Dioxane-2-One: Control of Functionalization in Perfect Random Copolymers via*

Thiol-Ene Reaction" - the strategy of 'Randomness Structure Control' is elucidated through detailed kinetic investigations as a fundamental approach. The preparation of polycarbonates with various functional groups was explored. This was achieved through organo-catalyzed copolymerization of newly functionalized CCs with TMC, designed to control the sequence distribution of monomers within copolymers *via* kinetics, thereby achieving desired randomness. Targeted functional groups such as carboxylic acid, alcohol, and amine were incorporated *via* pre- and post-polymerization modification strategies, which minimized the use of protective groups. To achieve the purpose, PTMC-*co*-PexTMC was prepared using MSA as an organocatalyst with varying exTMC content, allowing for the adjustability of functionalities. exTMC and TMC were copolymerized in a controlled manner, with relative reactivity ratios close to 1, facilitating the synthesis of copolymers with well-defined structures (molecular weight, composition, molecular distributions) and high randomness. The methylene groups distributed along the polymer chains were subsequently transformed by thiol-ene click reactions with thioglycolic acid or thioglycerol, yielding APCs with uniformly distributed COOH or OH functional groups across DP120 and functional group content ranging from 1—30%. Additionally, functionalized exTMC (TOBnTMC) was successfully prepared *via* click thiol-ene reaction on exTMC, followed by copolymerization with TMC monomers to evaluate polymerization conditions and kinetics. TOBnTMC and TMC also copolymerized in a rather controlled manner using MSA as a catalyst, with relative reactivity ratios again close to 1. Furthermore, the terpolymerization of TMC, exTMC, and TOBnTMC demonstrated that the monomer conversion rates for all three were nearly identical, suggesting that the terpolymer PTOBnTMC-*co*-PTMC-*co*-PexTMC is a random terpolymer. In summary, Chapter II highlights the successful control of randomness and the adjustable incorporation of functional groups along the polymer chain using MSA as organocatalyst under mild conditions. Furthermore, this chapter demonstrates that the introduction of functional groups can be achieved without the need for protecting groups. Additionally, the strategy outlined enables advancements in the development of terpolymers, which may enhance the introduction of multifunctional groups.

In Chapter III, "*Evaluation of Biocompatible Properties in Random Copolymers of Trimethylene Carbonate and 5-Methylene-1,3-Dioxane-2-One with Controlled Introduction of Diol and Carboxylic Acid*" - The behavior of side-chain functionalized biodegradable polycarbonate copolymer was investigated. The strategic incorporation of biodegradable linkages within PTMC derivatives facilitated precise degradation profiles, which are crucial for biomedical applications. A series of

functionalized PTMC-*co*-PexTMC copolymers were synthesized through the precise click thiol-ene reaction, featuring DP 120 and functional group contents ranging from 1% to 30% along the copolymer chain. These copolymers incorporated either diol or carboxylic functional groups. Thermal stability analysis indicated that copolymers with more than 10% thiol-ene content consistently displayed a lower T_{10}, indicating decreased thermal stability compared to their unmodified counterparts. Additionally, increasing the thiol-ene modification proportionately reduced the T_{10} values. The introduction of diol and carboxylic pendant groups was found to enhance the hydrophilicity of the copolymers. Enhanced hydrophilicity, particularly in PTMC-*co*-PexTMC variants with higher exTMC content, improved their affinity for protein binding, specifically albumin and fibrinogen, both before and after thiol-ene post-polymerization modification. Notably, post-polymerization modification with carboxylic groups resulted in significantly higher protein adsorption compared to the variants PexTMC-*co*-TMC_{OH} and PexTMC-*co*-TMC. Water absorption tests showed that PexTMC-*co*-TMC_{30COOH} absorbed water more efficiently than PexTMC-*co*-TMC and PexTMC-*co*-TMC_{30OH}, leading to faster degradation, as confirmed by SEC and percentage weight loss analyses. Moreover, the presence of carboxylic groups accelerated polymer degradation *via* bulk erosion. Drug release studies further validated the functional benefits of these modifications; PexTMC-*co*-TMC_{COOH} demonstrated accelerated release of doxorubicin (DOX) compared to the non-modified copolymer and PexTMC-*co*-TMC_{OH}. In contrast, the non-modified PTMC-*co*-PexTMC exhibited the slowest DOX release, attributed to its inherent hydrophobic properties. These findings collectively highlight the significant potential of these meticulously designed copolymers and their functional groups for a range of biomedical applications. The ability to tailor copolymer properties through strategic functionalization opens new avenues for the development of advanced biodegradable materials, specifically tailored for enhanced performance in targeted medical applications.

In Chapter IV, "*The design of side chain crosslinking to modulate the properties of copolymers*" - the focus was on utilizing the benefits of PTMC-*co*-$PexTMC_{COOH}$ for metal-carboxylate crosslinking. This chapter explored how functional side chains can facilitate ionomer crosslinking, a crucial technique for modifying the physical properties of polymers. By implementing targeted crosslinking strategies, the polymers developed exhibited improved mechanical properties and stability, significantly enhancing their applicability in various biomedical fields. To meet these objectives, an ionomer derived from PTMC-*co*-$PexTMC_{COOH\text{-}metal}$ was synthesized with varying levels

of metal coordination. This ionomer demonstrated superior thermal properties, including elevated T_g and T_{10}, compared to unmodified PTMC-*co*-PexTMC$_{COOH}$. Additionally, increasing the Zn(II) carboxylate content notably enhanced the hydrophobicity of PTMC-*co*-PexTMC$_{30COOH}$. The introduction of metal-carboxylate bonds in the PTMC-*co*-PexTMC$_{30COOH\text{-}30Zn}$ ionomer effectively reduced water adsorption and weight loss, slowing down the degradation process. These bonds also shifted the degradation mechanism of PTMC-*co*-PexTMC$_{COOH}$ from bulk back to surface erosion, further illustrating the impact of strategic crosslinking. Moreover, a higher content of Zn(II) carboxylate significantly reduced protein adsorption, underscoring the ionomer's potential in biomedical applications where reduced protein interactions are beneficial. From a mechanical standpoint, this ionomer proved that increased metal coordination could bolster stability at higher temperatures. Once established, the metal coordination bonds allowed the ionomer to maintain its elastic properties throughout a broad temperature range of 20—70°C. In contrast, bare PTMC-co-PexTMC$_{COOH}$ without metal coordination bonds exhibited plastic behavior throughout the same temperature range. These results indicate that crosslinking occurs through the formation of metal coordination bonds. These findings underscore the transformative potential of using functionalized side chains for crosslinking in biopolymer design, paving the way for the development of advanced biodegradable materials tailored for specific medical uses.

In summary, the work presented in this Thesis not only demonstrates the power of precise molecular design in biodegradable polymer field but also demonstrates how nuanced control at the molecular level can lead to significant enhancements in polymer functionality. The developed methodologies and synthesized biodegradable polymer not only push the boundaries of current biodegradable polymers applications but also open new avenues for future research. The main objective of the thesis has found valuable characteristics for further research in more sophisticated prospects. The insights gained from this research contribute to the broader goal of advancing polymer science to meet contemporary challenges in biomaterial sustainability and functionality. Furthermore, the outcomes of this research have been published as a platform to facilitate the exchange of knowledge and to further the development of biodegradable polymers for future generations.

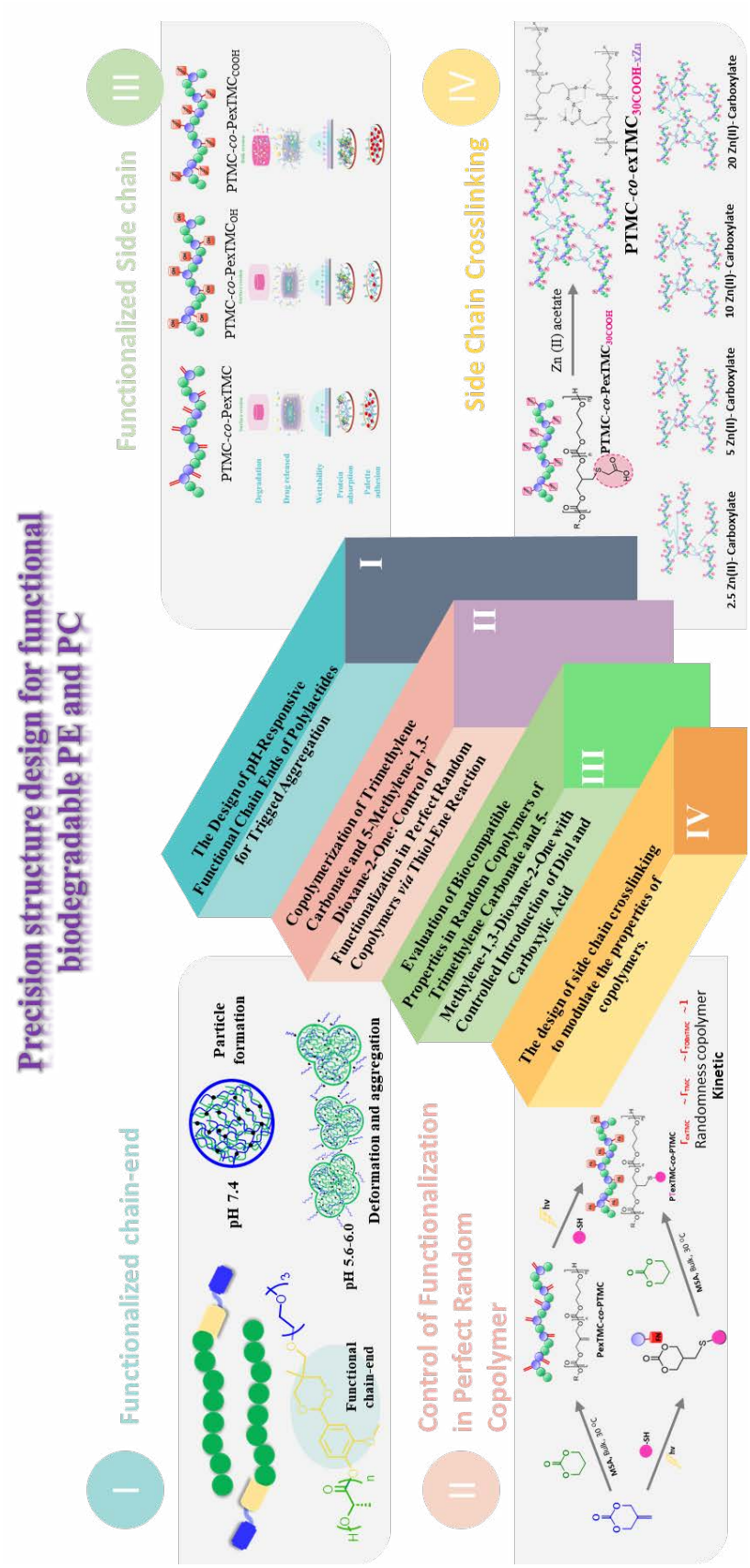
Precision structure design for functional biodegradable PE and PC
I
Functionalized chain-end
Functional chain-end
pH 7.4
Particle formation
pH 5.6-6.0
Deformation and aggregation
II
Control of Functionalization in Perfect Random Copolymer
Randomness copolymer
Kinetic
III
Functionalized Side chain
PTMC-co-PexTMC
PTMC-co-PexTMCOH
PTMC-co-PexTMCCOOH
Degradation
Drug released
Wettability
Protein absorption
Platelet adhesion
IV
Side Chain Crosslinking
Zn (II) acetate
PTMC-co-PexTMC30COOH
PTMC-co-exTMC30COOH-xZn
2.5 Zn(II)- Carboxylate
5 Zn(II)- Carboxylate
10 Zn(II)- Carboxylate
20 Zn(II)- Carboxylate
The Design of pH-Responsive Functional Chain Ends of Polylactides for Trigged Aggregation
Copolymerization of Trimethylene Carbonate and 5-Methylene-1,3-Dioxane-2-One: Control of Functionalization in Perfect Random Copolymers via Thiol-Ene Reaction
Evaluation of Biocompatible Properties in Random Copolymers of Trimethylene Carbonate and 5-Methylene-1,3-Dioxane-2-One with Controlled Introduction of Diol and Carboxylic Acid
The design of side chain crosslinking to modulate the properties of copolymers.

Résumé en Français

Les polymères biodégradables suscitent un grand intérêt en raison de leurs avantages médicaux significatifs, en particulier leur biocompatibilité, qui les rend aptes à être utilisés dans le corps humain. Ces polymères sont conçus pour se dégrader dans des conditions physiologiques et peuvent être adaptés pour se dégrader à des vitesses spécifiques grâce à des mécanismes contrôlés. En outre, les sous-produits de dégradation sont facilement éliminés par les voies métaboliques de l'organisme.[1,2] Le processus de biodégradation est influencé par la composition du matériau.[3] Des paramètres tels que la morphologie du polymère, la structure du polymère, les traitements chimiques et radiologiques et le poids moléculaire du polymère jouent un rôle crucial dans la détermination du processus de biodégradation.[4]

En général, les polymères biodégradables sont classés en deux groupes en fonction de leur origine : les biopolymères naturels et les biopolymères synthétiques. Les biopolymères naturels sont dérivés de sources renouvelables ou biologiques telles que les sources animales, végétales, marines et microbiennes, tandis que les polymères biodégradables synthétiques sont fabriqués chimiquement.[5] Ces dernières années, les polymères biodégradables synthétiques ont fait l'objet d'une attention particulière en raison de leur facilité de manipulation et de leur grande reproductibilité d'un lot à l'autre. Ces polymères se dégradent en matériaux non toxiques et respectueux de l'environnement,[6] démontrant leur potentiel dans une large gamme d'applications dans le domaine biomédical (**Figure I**).[7]

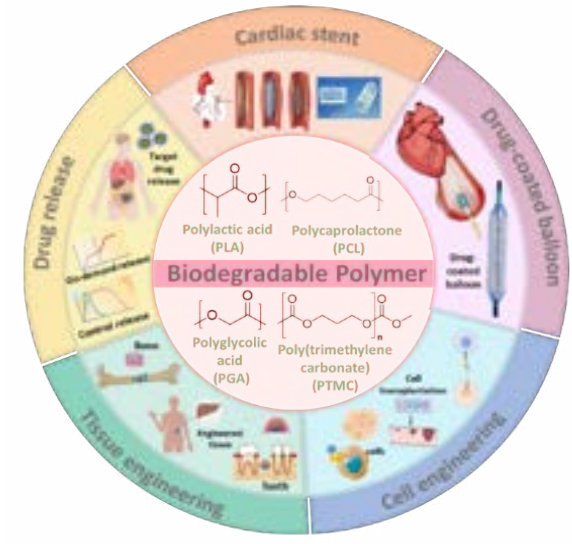

Figure I. Principaux polymères biodégradables utilisés dans les applications médicales[15]

Un objectif important de la recherche sur les matériaux biomédicaux est de développer des matériaux qui présentent une biocompatibilité, une dégradation contrôlée et des performances élevées adaptées à leur application spécifique. Récemment, les progrès de la science des polymères ont mis l'accent sur l'importance de la conception de structures moléculaires en tant que méthode clé pour la modification des matériaux, où la structure ramifiée offre une grande capacité de conception structurelle et de modification des propriétés. Par conséquent, la conception de monomères et de polymères est essentielle pour produire divers biomatériaux et favoriser le développement de polymères alternatifs adaptés à leur usage, mais leur utilisation pratique est encore limitée à l'heure actuelle. Les polymères biodégradables synthétiques appartiennent souvent à la famille des polyesters ou des polycarbonates et comprennent des matériaux tels que le poly(lactide) (PLA) et le poly(carbonate de triméthylène) (PTMC). Leur chimie diversifiée permet la synthèse de polymères aux propriétés physiques et mécaniques ajustables, ce qui les rend plus attrayants que les alternatives naturelles telles que les polysaccharides et les protéines.[8]

Les polyesters aliphatiques (APE) et les polycarbonates aliphatiques (APC) constituent la pierre angulaire des polymères biodégradables et sont des candidats potentiels pour des applications cliniques en raison de leur faible toxicité, de leur biocompatibilité et de leur biodégradabilité. Diverses méthodes de polymérisation sont désormais disponibles pour synthétiser des polymères avec des topologies de squelette et des fonctionnalités de chaîne latérale variées. En outre, les liaisons ester et carbonate dans les nouveaux squelettes de polymères peuvent être dégradées par voie enzymatique ou chimique, ce qui offre de nouvelles options pour le cycle de vie de ces matériaux.[9,10] Le processus de dégradation global est complexe, influencé par la cinétique de dégradation intrinsèque et les taux de diffusion de l'eau. Les facteurs affectant la diffusion de l'eau comprennent l'hydrophobicité, la forme et la surface du dispositif polymère, tandis que la cinétique de dégradation intrinsèque est déterminée par les conditions environnementales telles que le pH, la température, le poids moléculaire et les microstructures du polymère.[9,10] Cependant, les groupes ester et carbonate sont tous deux sensibles à l'hydrolyse, les polyesters subissant généralement une dégradation en masse, tandis que l'érosion de surface prédomine pour les polycarbonates (**Figure II**).[11,12] Lorsque les polymères subissent une érosion de surface, ils perdent progressivement de la masse de la surface extérieure vers l'intérieur, en conservant leur forme d'origine. En revanche, l'érosion en masse entraîne la perte de masse et la dégradation de l'ensemble du polymère, sans se limiter à la surface.[11,12] Outre leur dégradabilité, la polyvalence synthétique et le potentiel

d'introduction de diverses propriétés ont fait des APE et des APC certains des polymères les plus étudiés pour les applications biomédicales.[11]

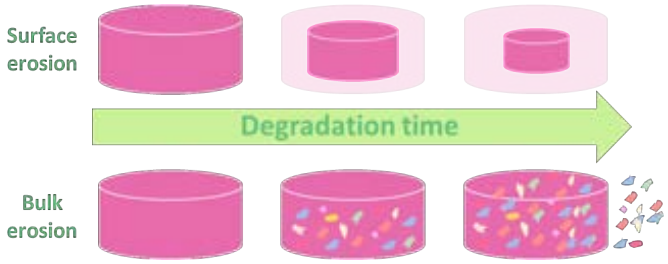

Figure II. Mécanismes de dégradation des polymères dégradables.

Les développements futurs dans ces domaines nécessitent un accès fiable à une large gamme d'APE et d'APC avec des structures diverses et bien contrôlées. L'une des méthodes permettant d'atteindre cet objectif est la copolymérisation par ouverture de cycle (ROP) de monomères fonctionnalisés, qui permet d'ajuster les propriétés du polymère en introduisant des groupes latéraux. La ROP offre la possibilité de contrôler le poids moléculaire (M_n), la distribution des poids moléculaires ($Đ$), la microstructure du polymère et la nature de ses groupes terminaux.[12-16] Une variété de catalyseurs et de monomères cycliques peuvent être adoptés, et il est possible de créer des macromolécules de poids moléculaires ajustés avec des rendements élevés en variant simplement le rapport monomère/amorceur. Initialement, la synthèse des APE et des APC utilisait des catalyseurs à base de métaux. $Sn(Oct)_2$ est l'un des catalyseurs les plus utilisés, non seulement dans l'industrie[17] pour le PLA[18] et le PTMC[19], mais aussi dans la recherche pour des monomères plus sophistiqués. Ce catalyseur polyvalent joue un rôle crucial dans les processus de polymérisation, offrant efficacité et fiabilité.[17] Par la suite, la détection de métaux résiduels dans les polymères résultants, qui induisent potentiellement des effets cytotoxiques, a nécessité le développement d'alternatives plus biocompatibles. Ces alternatives comprennent à la fois des catalyseurs sans métal et des catalyseurs enzymatiques. Malgré leur faible biocompatibilité dans certain cas, les catalyseurs métallo-organiques continuent d'être privilégiés pour leur activité catalytique élevée dans la synthèse des APE et des APC.

Pour remédier aux insuffisances des propriétés mécaniques et physiques des polymères, plusieurs stratégies impliquant des modifications physiques et chimiques ont été mises au point. Ces approches visent à améliorer les performances et la fonctionnalité des matériaux. La méthode de modification physique est relativement simple et facile à industrialiser, mais les problèmes de compatibilité et de dispersion entre les matériaux doivent encore être améliorés. D'autre part, la méthode de modification chimique consiste

à modifier le polymère par le biais de sa structure moléculaire (monomère et polymère), ce qui permet d'obtenir une conception structurelle plus stable. La modification chimique comprend principalement la copolymérisation, en particulier avec des monomères contenant de groupements fonctionnels latéraux.[20] Ces groupes latéraux peuvent établir des interactions favorables avec les ingrédients actifs, améliorant ainsi les propriétés de libération des médicaments. En outre, ils peuvent moduler les propriétés mécaniques du polymère, telles que la dureté et la résistance à la déformation, et les propriétés thermiques, telles que la température de transition vitreuse (T_g) et la température de fusion (T_m), ainsi que la vitesse de dégradation. Il est donc hautement souhaitable d'améliorer l'accès aux monomères fonctionnalisés et de développer des méthodes fiables pour leur copolymérisation contrôlée.

Les défis précédents concernant les APE fonctionnalisés, l'acide polylactique fonctionnalisé (PLA) ont démontré que les modifications de l'extrémité de la chaîne peuvent altérer les propriétés du PLA grâce à l'utilisation d'amorceurs spécialement conçus. Pour faciliter les interactions dynamiques doubles, la vanilline[21] et le 5-hydroxyméthylfurfural (HMF)[22] ont été fonctionnalisés pour induire un phénomène réversible entre les fonctions amine / imine. En contrôlant la formation des nanostructures, les parties hydrophiles d'un groupe hydroxyle à l'extrémité de la chaîne du PLA (plutôt hydrophobe) ont été mis en évidence. En conséquence, les particules s'agrègent lorsque la partie hydrophile se détache (formant un PLA à terminaison aldéhyde) après un changement de pH.[21,22] Cependant, la plage de pH inférieure à pH 2 dans l'étude précédente n'était pas pratique pour la thérapie médicale. Si l'on considère la liaison cétone-acétal, elle pourrait être engagée dans des conditions physiologiques (légèrement acides). Il a été noté qu'une liaison acétal diol-cétone à six chaînons s'hydrolysait plus rapidement qu'un cycle à cinq chaînons.[23] Par conséquent, il est intéressant de clarifier si la liaison acétal peut être hydrolysée dans des conditions physiologiques en présence de dérivés aldéhyde-hydroxyle, en tant que résidus proposés à faible toxicité.

En outre, des efforts pour modifier les APC, en particulier le poly(carbonate de triméthylène) (PTMC), ont été réalisés en fonctionnalisant les monomères avant la polymérisation. Cependant, il est important de noter que lorsque le groupe fonctionnel requis est protique (amines, acides carboxyliques et alcools), des problèmes de compatibilité chimique apparaissent, soit en désactivant le catalyseur organique ou métallique, soit en agissant comme amorceur compatible avec le ROP. Pour contourner ce problème sans compromettre l'efficacité de la polymérisation, l'une des alternatives est de fonctionnaliser les polycarbonates par modification post-polymérisation.[24,25] Par exemple, Hedrick et al. ont utilisé un monomère portant des groupes pendants d'ester

activés par le pentafluorophényle qui restent intacts pendant la polymérisation catalysée par l'acide, et ont été modifiés avec des amines et des alcools à haut rendement dans une étape de modification post-polymérisation de transesterification.[26] De même, les études de Dove et al. ont fait état de la polymérisation de monomères cycliques avec un groupe pendant allyle, modifiés par la suite avec une série de thiols par le biais de la chimie « click » thiol-ène.[27] Cette méthodologie puissante pourrait être avantageuse pour préparer une série de polycarbonates fonctionnalisés de manière aléatoire avec des propriétés adaptées.[27,28] Sur la base d'une réaction thiol-ène sur le groupe C=C, une variété de groupes fonctionnels peut être introduite le long de la chaîne polymère sans utiliser de groupe protecteur. Grâce à l'introduction de groupes fonctionnels carboxyliques (COOH) ou hydroxy (OH), des interactions privilégiées peuvent être établies avec des ingrédients actifs dans le domaine de la libération de médicaments. En outre, l'hydrophilie sera modifiée par les groupes pendants polaires, ce qui entraînera des taux de dégradation plus élevés.[29]

Il est hautement souhaitable d'élargir la polyvalence des PTMC pour inclure une gamme plus large de fonctionnalités afin de parvenir à des applications ciblées. De même, le développement des ionomères démontre le potentiel des polymères spécialisés dans les applications avancées. Un ionomère est un polymère qui incorpore un faible pourcentage d'unités ioniques (**Figure III**). Les ionomères se distinguent par l'influence profonde des forces ioniques inter-chaînes sur leurs propriétés. Bien que seule une proportion mineure de groupes ioniques liés soit présente dans la structure principale du polymère, ces groupes ont tendance à s'agréger dans la phase condensée, ce qui modifie considérablement les propriétés physiques, mécaniques, optiques et dynamiques du polymère.[30] Avec ces inspirations, il est intéressant d'inclure la liaison de coordination entre l'acétate de métal et le groupe fonctionnel carboxylate pour construire l'ionomère des dérivés du PTMC.

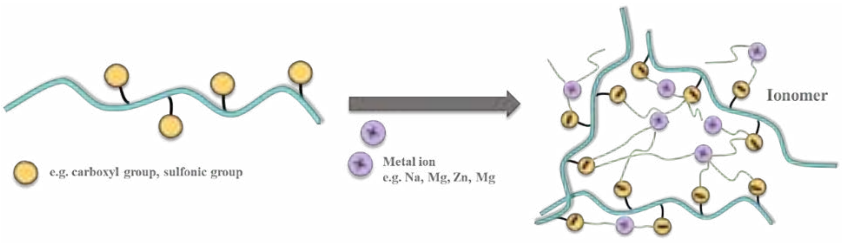

Figure III. Illustration de la formation de l'ionomère.

L'objectif de cette thèse est de se concentrer sur la conception structurelle précise de nouveaux PE et PC biodégradables comportant des groupes fonctionnels pendants, et

d'évaluer les propriétés qui pourraient avoir un impact sur leur potentiel dans diverses applications biomédicales. Selon notre stratégie, un polyester fonctionnalisé en bout de chaîne est préparé grâce à des amorceurs fonctionnalisés pour contrôler l'agrégation de particules déclenchée par le pH. Concernant les PC fonctionnalisés, nous cherchons à contrôler au mieux le caractère aléatoire de la chaîne polymère, ajustant le type, la quantité et la distribution du groupe fonctionnel. Ils seront préparés par modification pré- ou post-polymérisation pour contrôler la dégradabilité en seulement trois étapes, de la synthèse du monomère au polymère fonctionnalisé. Ces groupes fonctionnels introduits peuvent avoir un impact sur les propriétés du polymère, en particulier sur les taux de dégradation. Pour sonder la dégradabilité de ces polymères fonctionnalisés, leur dégradation a été étudiée dans des conditions hydrolytiques et enzymatiques. Enfin, pour élargir la polyvalence des PTMC, l'attention s'est portée sur les structures de réticulation via des ionomères de carboxylate de métal. Le manuscrit (**Figure IV**) est divisé donc en quatre chapitres, comme illustré ci-après :

Figure IV. Illustration générale du projet représentant la conception de structures de précision pour les APE et APC biodégradables fonctionnels.

Chapitre I *: Conception de bouts de chaîne fonctionnels de polylactides réagissant au pH pour une agrégation déclenchée*

Dans ce chapitre, de nouveaux amorceurs basés sur les unités diol-cétone acétal et vanilline ont été conçus et synthétisés, visant des applications médicales pour une utilisation à un pH d'environ 5,5-6,5 en solution aqueuse. La préparation de particules de PLA avec une unité acétal cétone à six chaînons a été réalisée pour optimiser les

performances. En outre, les taux d'agrégation des stéréocomplexes (SC) mélangés à du dioxyde de titane ont également été étudiés. Pour examiner l'agrégation, non seulement la spectroscopie UV a été réalisée pour observer le taux, mais les comportements de la morphologie de l'assemblage ont été analysés par SEM. Dans le but d'étudier l'effet du pH sur le taux d'agrégation, l'hydrolyse des liaisons acétals en fonction du poids moléculaire du polymère, de la plage de pH et de la structure de l'extrémité de la chaîne a été étudié (**Figure 1-1**). Ce travail a été publié dans : Sarisuta, K. ; Iwami, M. ; Martín-Vaca, B. ; Chanthaset, N. ; Ajiro, H. "pH Effect on Particle Aggregation of Vanillin End-Capped Polylactides Bearing a Hydrophilic Group Connected by a Cyclic Acetal Moiety". *Langmuir* **2023**, *39* (11), 3994-4004.

Figure 1-1. Préparation de PLA avec une extrémité de chaîne fonctionnelle *via* un amorceur fonctionnalisé.

Synthèses des amorceurs

Les amorceurs vanilline-6-OEG$_3$ et vanilline-6-OEG$_4$ ont été préparés selon des méthodes classiques.

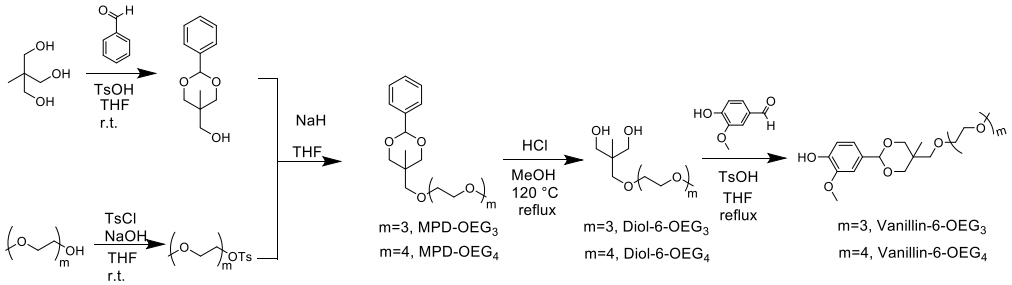

Schéma 1-1. Synthèses d'amorceurs à base de vanillineVanilline-6-OEG$_m$.

La structure chimique des nouveaux amorceurs, vanilline-6-OEG$_3$ et vanilline-6-OEG$_4$, a été confirmée par spectroscopie RMN ^{1}H (**Figure 1-2**). Les spectres ont confirmé la disparition du signal de l'aldéhyde autour de 9 ppm et l'apparition d'un signal autour de 5,6 ppm correspondant au CH de l'acétal (**Figures 1-2a** et **1-2b**). De plus, les nouveaux

amorceurs de vanilline ont été caractérisés non seulement par RMN ^{1}H mais aussi par spectrométrie de masse (**Figure 1-2c** et **1-2d**).

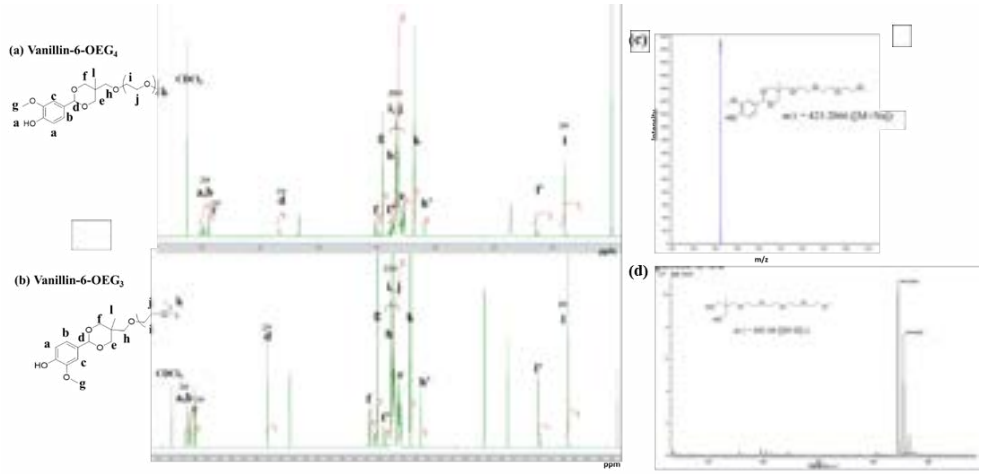

Figure 1-2. RMN 1H et rapport intégré de (a) Vanilline-6-OEG_4 et (b) Vanilline-6-OEG_3 et spectre MASS de (c) Vanilline-V6-OEG_3 et (d) Vanilline-V6-OEG_4.

Polymérisation

La polymérisation du PLA a été initiée à l'aide d'un amorceur vanilline-6-OEG_3 et catalysée par le catalyseur $Sn(Oct)_2$. La réaction s'est déroulée sur une période allant de 0,5 à 24 heures à 40°C dans du toluène 1M comme le montre le **Tableau 1-1**.

Tableau 1-1. Polymérisation de LA à l'aide du catalyseur $Sn(Oct)_2$ et d'amorceurs à base de vanilline.

Entry	Sample	Initiator	[M]/[I]	Time (h)	Yield (%)	M_n^{SECe} (kDa)	M_n^{SECf} (kDa)	DP	$Đ^e$
1[a, c]	$PLLA_{63}$-V6-OEG_3	Vanillin-6-OEG_3	20:01	24	76	4.8	3.3	63	1.8
2[a, c]	$PLLA_{61}$-V6-OEG_3	Vanillin-6-OEG_3	10:01	3	67	4.6	3.1	61	1.8
3[a, c]	$PLLA_{33}$-V6-OEG_3	Vanillin-6-OEG_3	10:01	0.5	84	2.4	1.6	33	1.3
4[a, c]	$PLLA_{34}$-V6-OEG_3	Vanillin-6-OEG_3	10:01	0.5	76	2.5	1.7	34	1.1
5[b, c]	$PLLA_{35}$-V6-OEG_3	Vanillin-6-OEG_3	5:01	2	74	2.6	1.8	35	1.2
6[b, c]	$PDLA_{35}$-V6-OEG_3	Vanillin-6-OEG_3	5:01	2	69	2.2	1.5	30	1.3
7[b, d]	$PLLA_{25}$-V6-OEG_4	Vanillin-6-OEG_4	10:01	0.5	76	1.9	1.3	25	1.2
8[b, c]	$PDLA_{23}$-V6-OEG_4	Vanillin-6-OEG_4	10:01	0.5	67	1.7	1.2	23	1.2

a) Monomer = 1.0 g; b) Monomer = 2.0 g; c) Concentration [M] Toluene = 1 mg/mL; d) Concentration [M] Toluene = 3 mg/mL; e)Determined by SEC by PS standard in THF; Catalyst = $Sn(Oct)_2$; f) Values corrected using the correction factor reported for PLA.

Pour confirmer la fixation du groupe terminal fonctionnel du PLA-V6-OEG_m, les structures ont été vérifiées par spectroscopie RMN ^{1}H, comme le montre la **Figure 1-3**.

Les spectres du PLA-V6-OEG$_3$ ont montré des signaux à 1,45-1,7, 3,2-4,2 et 5,04-5,25 ppm, correspondant au PLA et à la vanilline-6-OEG$_3$ (**Figure 1-3c**). Le signal à 4,3 ppm est attribué au groupe méthine adjacent au signal terminal du groupe CHOH du PLA (**Figure 1-3**). En outre, le signal observé à 5,60 ppm (correspondant au CH de l'acétal) et l'absence de tout signal autour de 9 ppm confirme que l'acétal est compatible avec les conditions de polymérisation. Les masses moléculaires mesurées par SEC *via* un détecteur UV à la longueur d'onde de 264 nm ont également été examinées pour s'assurer de la présence du groupe aromatique au niveau du bout de chaine.

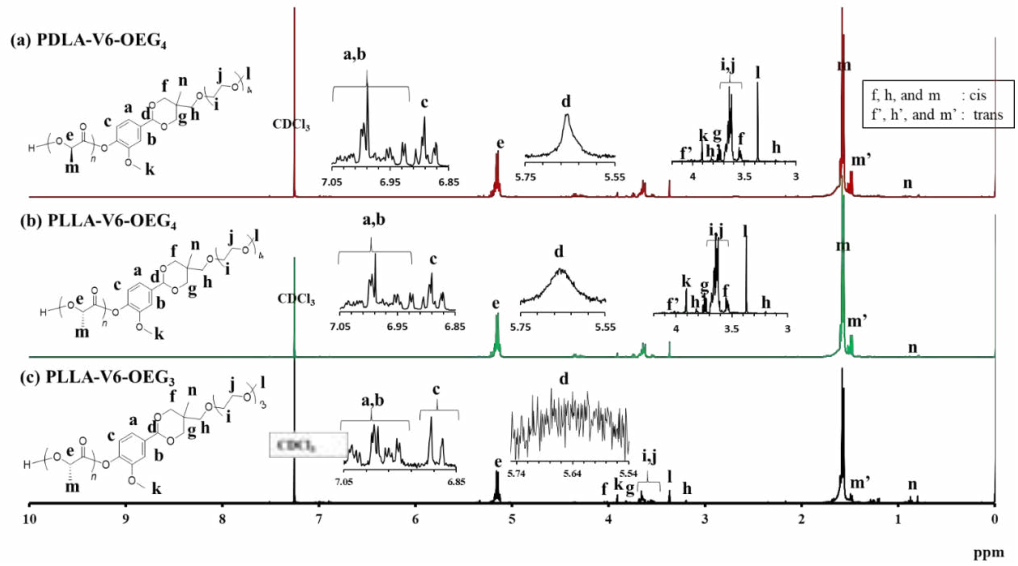

Figure 1-3. ^{1}H NMR of (a) PDLA$_{23}$-V5-OEG$_4$, (b) PLLA$_{25}$-V6-OEG$_4$ and (c) PLLA$_{33}$-V6-OEG$_3$ (400 MHz, r.t., in $CDCl_3$).

Agrégation des particules

L'agrégation des particules des polymères, provoqué par l'hydrolyse de l'acétal, a été ensuite examiné. Pour comprendre l'influence du poids moléculaire sur les taux d'agrégation, la transmision en UV (%) a été contrôlée entre 0 et 4,5 min lors du changement de pH de 7,4 à 6,2 (**Figure 1-4**).

À un pH de 7,4, les particules étaient dispersées de manière homogène dans le PBS. Après le passage du pH à 6,2 (**Figure 1-4A**) ou à 5,6 (**Figure 1-4B**), l'augmentation de la transmittance a été observé, sugérant le détachement de la liaison acétal par hydrolyse, ce qui peut induire la séparation entre les résidus hydrophiles et hydrophobes. Les résultats ont montré que les particules de poids moléculaire élevé (PLLA$_{61}$-V6-OEG$_3$, PLLA$_{63}$-V6-OEG$_3$) pouvaient présenter un taux d'agrégation lent en raison de la dépendance au M_n. Ces résultats indiquent que le poids moléculaire plus faible peut induire une séparation plus rapide entre les résidus hydrophiles et hydrophobes affectés par une

transmittance plus élevée que le poids moléculaire plus élevé. En outre, à un pH de 5,6, il a été montré que les particules $PLLA_{33}$-V6-OEG_3 étaient considérablement agrégées à partir de 1,5 min, comme le montre la pente de la **Figure 1-4Ba**, tandis qu'à un pH de 6,2, l'agrégation était constante (figure 1-4Bb). On pourrait indiquer que la force du pH pourrait influencer le taux d'agrégation; cependant, cette nouvelle découverte est prometteuse pour le contrôle dans des conditions physiologiques.

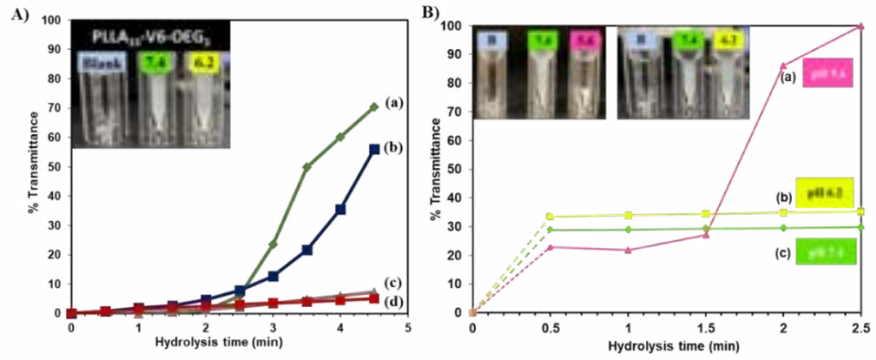

Figure 1-4. A) Agrégation des particules PLLA mesurée par UV-visible lorsque le pH passe de 7,4 à 6,2. (a) $PLLA_{33}$-V6-OEG_3, (b) $PLLA_{35}$-V6-OEG_3, (c) $PLLA_{61}$-V6-OEG_3, (d) $PLLA_{63}$-V6-OEG_3 dans un délai de 4-5 min et B) agrégation des particules $PLLA_{33}$-V6-OEG_3 (M_n 2400) mesurée par UV-visible à pH (a) pH 5,6, (b) pH 6,2, et (c) pH 7,4 en 2.5 min.

Agrégation des particules de stéréocomplexes (SC)

Dans cette partie, l'effet de l'extrémité de la chaîne a pu être discriminé avec trois types d'échantillons d'appariement comme suit :

SC (1) ; PLLA-V6-OEG_3/ PDLA-benzyl (**Figure 1-5a**).

SC (2) ; PLLA-V6-OEG_3/ PDLA-V6-OEG_3 (**Figure 1-5b**).

SC (3) ; PLLA-V6-OEG_4/ PDLA-V6-OEG_4 (**Figure 1-5c**).

Étude de l'effet de fin de chaîne

Les résultats ont montré que la SC (3) OEG_4/OEG_4 exprimait une transmittance d'environ 10 % après 3 minutes lorsque le pH passait de 7,4 à 5,6 (**Figure 1-5c**). La transmittance du SC (1) OEG_3-benzyle était d'environ 0,01 % (**Figure 1-5a**) et celle du SC (2) OEG_3/OEG_3 (**Figure 1-5b**) était d'environ 3 %. Par conséquent, on peut supposer que l'amorceur vanilline-6-OEG_4 peut induire le taux d'agrégation en raison de sa fraction plus hydrophile et de l'augmentation des molécules d'eau. En outre, le SC (3) OEG_4/OEG_4 (**Figure 1-5c**) présentait deux positions de liaison acétal avec la chaîne PLLA/PDLA, ce qui pourrait donner un potentiel d'hydrolyse dans des conditions acides. Les résultats

obtenus impliquent que l'effet de l'extrémité de la chaîne peut influencer de manière significative le taux d'agrégation.

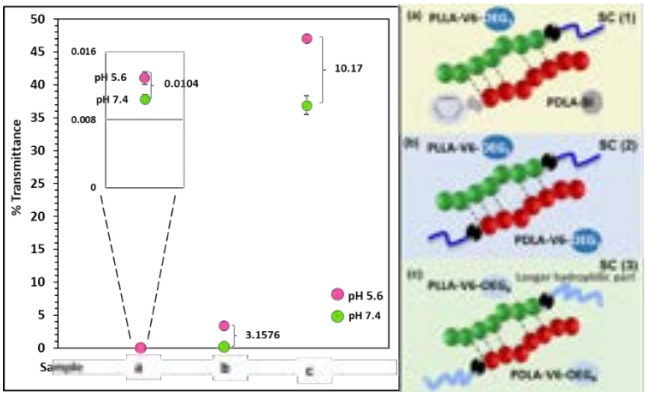

Figure 1-5 Effet de l'extrémité de la chaîne sur l'agrégation des particules de (a) une position de la liaison acétal avec OEG_3 (SC (1)), (b) deux positions de la liaison acétal avec OEG_3 (SC (2)), et (c) deux positions de la liaison acétal avec OEG_4 (SC (3)) mesuré par les spectres UV-Vis à pH5,6 à 2,5 min.

Étude de l'effet du poids moléculaire

D'après les résultats obtenus, des particules SC-PLA avec une liaison acétal (SC (1) OEG_3-benzyle) ont été formées en appariant différents poids moléculaires de PLLA-V6-OEG_3. Il a été constaté que la chaîne courte M_n 1200 g/mol présentait le taux d'agrégation le plus rapide par rapport à M_n 2400 en 2,5 min (**Figure 1-6a**).

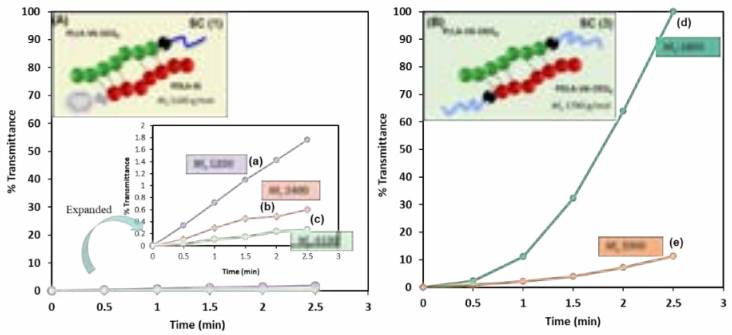

Figure 1-6. Effet de la masse moléculaire sur l'agrégation des particules SC de (A) un bras de liaison acétal avec OEG_3 (SC (1)) divers M_n de PLLA-V6-OEG_3 (a) M_n 1800 (b) M_n 24000, et (c) M_n 4100 au pH 5.6. (B) deux bras de liaison acétal avec OEG_4 (SC (3)) divers M_n de PLLA-V6-OEG_4 (d) M_n 1800, et (e) M_n 2000 au pH 5,6.

En outre, la tendance de l'effet de la masse moléculaire sur le taux d'agrégation avec deux liaisons acétals (SC (3) OEG_4/OEG_4) est présentée dans la **Figure 1-6B**. Le SC-PLA

constitué d'une chaîne courte PDLA-V6-OEG$_4$ (M_n 1700)/PLLA-V6-OEG$_4$ (M_n 1800) (SC(3)) présente le taux d'agrégation le plus rapide par rapport au SC-PLA de PLLA-V6-OEG$_4$ M_n 2000. Au vu des résultats, nous pouvons nous engager sur la relation entre le faible poids moléculaire et la mobilité moléculaire. En outre, on s'attend à ce que les groupes terminaux hydrophiles tels que les groupes hydroxyles ou carbonyles augmentent la vitesse de diffusion de l'eau et catalysent la dégradation.[31,32] En ce qui concerne l'impact de la vitesse d'agrégation, le nombre de liaisons acétals a également une influence. Par conséquent, la comparaison SC-PLA a été élucidée par des paires de PLLA-V6-OEG$_3$ (M_n 1200) / PDLA-Benzyl (M_n 5100) (SC(1)) et PLLA-V6-OEG$_4$ (M_n 1800) / PDLA-V6-OEG$_4$ (M_n 1700) (SC(3)). Il semble que le taux d'agrégation puisse être induit par le nombre de liaisons acétals, la fraction hydrophile et le poids moléculaire.

Mélange de dioxyde de titane PLLA-V6-OEG3 et SC

Les particules de PLA ont été mélangées avec du TiO_2 en faisant varier la concentration de polymère et la concentration de 2,5 mg de TiO_2 ([P] :[Ti]) (**Figure 1-7A**). L'expérience a été réalisée à une concentration de polymère de 2,5 mg/mL et une concentration variable de TiO_2 (**Figure 1-7B**). Il a été constaté que la concentration de polymère de 2,5 mg/mL pour 2,5 mg de TiO_2 était également le ratio optimal pour l'agrégation des particules dans les 3 minutes (**Figure 1-7h**). Contrairement au mélange SC TiO_2, il a été perçu que la transmittance changeait de 40 % après 30 secondes, de 41 % après 3 minutes et de 58 % après 15 minutes (**Figure 1-7Cb**). En revanche, à un pH de 7,4, la transmittance a changé de 22 % après 30 secondes et s'est maintenue même après 3 et 15 minutes (**Figure 1-7C**). Les résultats montrent que les particules SC-PLA mélangées à du TiO_2 ne s'agrègent pas dans des conditions physiologiques, ce qui semble être plus avantageux en termes de stabilité.

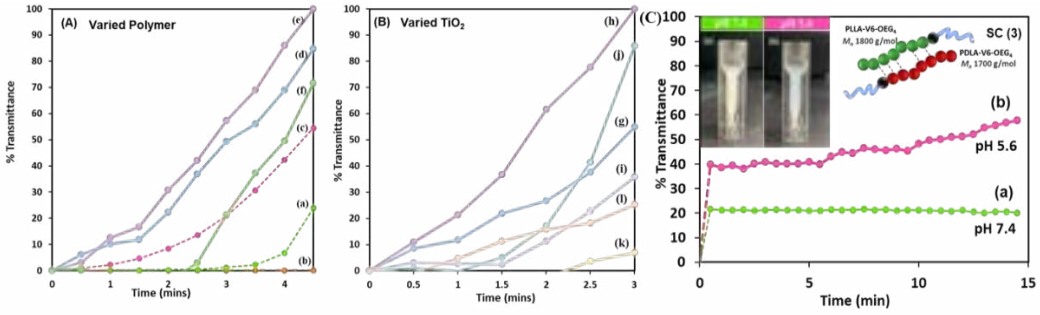

Figure 1-7. (A) Résultats UV-Vis du PLLA-V6-OEG$_3$ mélangé à une concentration de TiO_2 de 2,5 mg à un pH de 7,4 (a) 2,5P, à un pH de 5,6 (b) 2,5Ti, (c) 2,5P, (d) 1P2,5Ti, (e) 2,5P2,5Ti, et (f) 5P2,5Ti. (B) Résultats UV-Vis de PLLA-V6-OEG$_3$ de concentration 2,5 mélangé avec TiO_2 de différentes

concentrations à pH 5,6 (g)2,5P1Ti, (h) 2,5P2,5Ti, (i) 2,5P3,75Ti, (j) 2,5P5Ti, (k) 2,5P7,5Ti, et (l) 2,5P10Ti. (P = concentration de polymère (mg/mL), Ti= TiO_2 (mg)) (C) Résultats UV-Vis de l'effet du TiO_2 sur les particules de SC (a) à pH 7,4, (b) à pH 5,6.

Chapitre II : *Copolymérisation du triméthylène carbonate et 5-méthylène-1,3-dioxane-2-one : contrôle de la fonctionnalisation des copolymères aléatoires parfaits via la réaction thiol-ène*

Dans ce chapitre, l'exTMC ou un exTMC fonctionnalisé (5-((3-(benzyloxy)propyl)thio) methyl)-1,3-dioxan-2-one (TOBnTMC)) ont été choisis comme co-monomères du TMC pour accéder à des copolymères aléatoires par le choix du organocatalyseur approprié et d'un amorceur protique. Grâce à des rapports de réactivité dans les réactions de copolymérisation proche de 1, des copolymères avec des structures bien contrôlées à un haut degré d'aléatoire ($R \approx 1$) ont été préparés. La voie de synthèse des polycarbonates fonctionnalisés peut être différenciée en deux voies : (I) ROCOP du TMC et de l'exTMC suivi de la fonctionnalisation du copolymère via la réaction thio-ène. (II) Fonctionnalisation de l'exTMC *via* la réaction thio-ène suivie d'une ROCOP du carbonate fonctionnalisé résultant avec le TMC. Ces voies pourraient donner accès à des APCs avec des quantités ajustables de groupes fonctionnels uniformément distribués le long des chaînes polymères, et sans nécessiter d'étape de protection et de de protection dans le cas de la première voie. Ces travaux ont été menés à l'UPS, Toulouse, France, dans le cadre d'une collaboration avec un programme de double diplôme (**Figure 2-1**) et ont donné lieu à une publication dans : Palenzuela, M. ; Sarisuta, K. ; Navarro, M. ; Kumamoto, N. ; Chanthaset, N. ; Monot, J. ; Ajiro, H. ; Martín-Vaca, B. ; Bourissou, D. « 5-Methylene-1,3-Dioxane-2-One : A First-Choice Comonomer for Trimethylene Carbonate. » *Macromolecules* **2023**, *56* (2), 678.

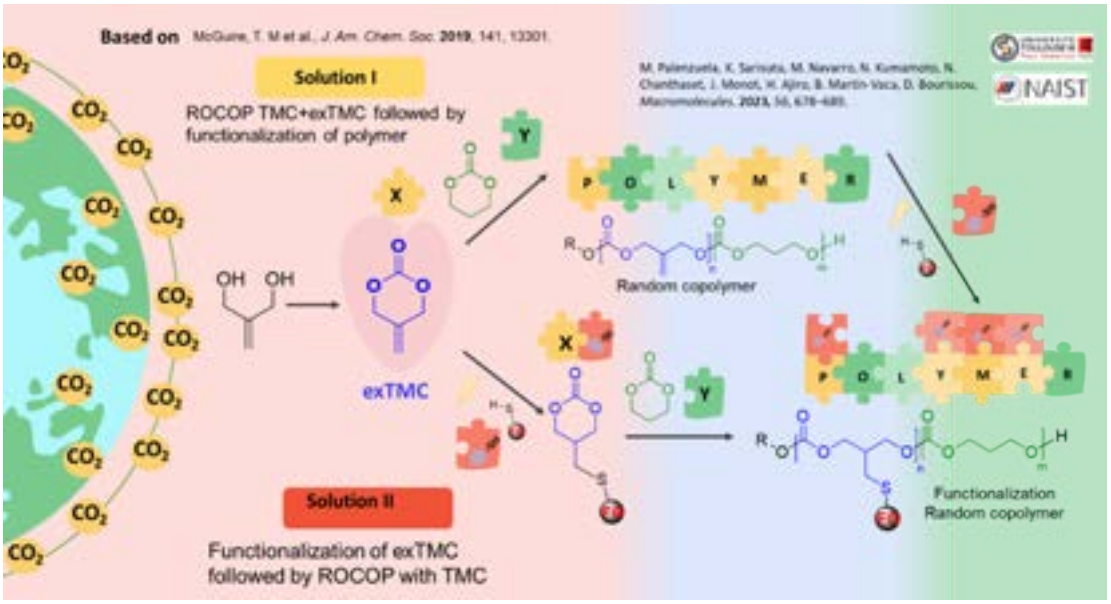

Figure 2-1. Différentes stratégies pour la préparation de copolymères aliphatiques fonctionnalisés de TMC et TOBnTMC.

Préparation de 6CCs fonctionnalisés

A la recherche d'une procédure durable pour synthétiser l'exTMC en évitant l'utilisation de dérivés du phosgène, il a été décidé de tester la méthodologie basée sur le CO_2 récemment introduite par A. Buchard et al.[33-36] La structure a été confirmée par RMN ^{1}H avec les signaux caractéristiques de (-CH_2-) à 4,86 et (=CH_2) à 5,36 ppm (**Figure 2-2**).

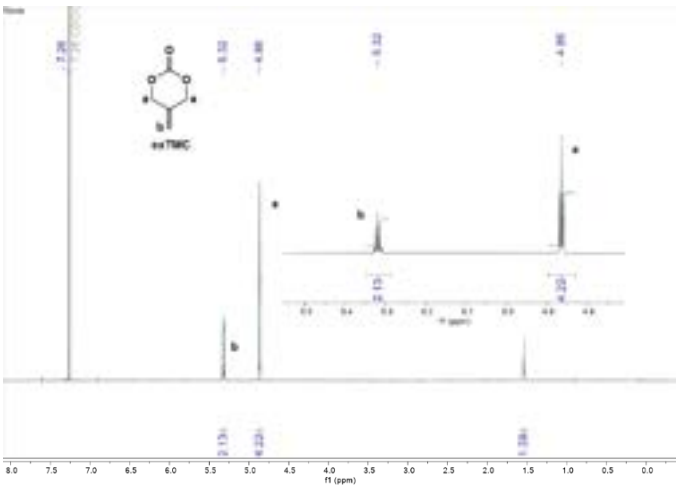

Figure 2-2. Spectre RMN ^{1}H de l'exTMC ($CDCl_3$, 300 MHz, r.t.).

Ce carbonate cyclique peut ensuite être transformé en carbonate fonctionnalisé par réaction click thiol-ène dans un processus en une étape utilisant l'irradiation de la lumière

UV (365 nm). A l'aide d'un photoamorceur DMPA à 2% p/p et 1 équivalent d'acide thiolglycolique, le nouveau monomère a été préparé. La structure a été confirmée par le spectre RMN ^{1}H (**Figure 2-3Aa**). Le signal attribué aux $=CH_2$ et OCH_2 de l'exTMC à 5,37 et 4,92 ppm ont disparu. Des nouveaux signaux à 4,55, 4,42, 3,37, 2,68 et 2,48 sont apparus et sont attribués aux groupes CH_2 et CH dérivant de l'acide thioglycolique, ce qui indique que la modification du TMC-COOH est réussie (**Figure 2-3Ab**). Cependant, il a été constaté que la polymérisation du TMC-COOH était incompatible avec le ROP organocatalysé en raison du groupe fonctionnel carboxylique, ce qui sera discuté plus loin.[26] Par conséquent, il a été nécessaire de protéger le groupe fonctionnel protique avant la polymérisation lorsque l'on travaillait avec des exTMC fonctionnalisés. Par conséquent, les dérivés thiol avec un groupe éther protégé (3-(benzyloxy)propane-1-thiol (TOBn))[37] ont finalement été choisis. La structure chimique du TOBnTMC a été confirmée par le spectre RMN ^{1}H (**Figure 2-3B**). Le signal à 5,37 ppm correspondant à la double liaison $=CH_2$ de l'exTMC a disparu. L'apparition de nouveaux signaux à 7,37 ppm, attribués au groupe phényle du 3-(benzyloxy)propane-1-thiol, indique que la modification du TOBnTMC a réussi. La présence de nouveaux signaux à 138,2, 128,4 et 127,6 ppm, attribués au groupe phényle du 3-(benzyloxy)propane-1-thiol (**Figure 2-3C**), est également confirmée par la RMN ^{13}C{^{1}H}. Le signal à 110,5 ppm correspondant à la double liaison $=CH_2$ de l'exTMC a disparu. Le TMC ayant été fonctionnalisé avec succès par la réaction thiol-ène, la prochaine étape consistera à évaluer l'homopolymérisation des TMC fonctionnalisés ainsi que leur copolymérisation avec le TMC.

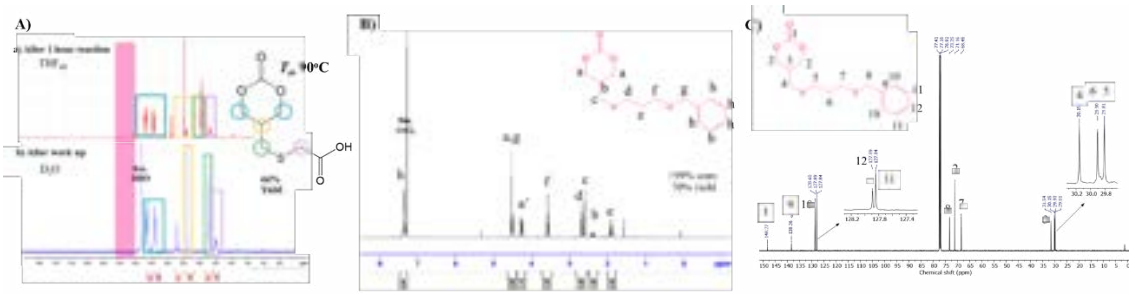

Figure 2-3. A) Spectres RMN du ^{1}H de la TMC-COOH : (a) après 1 heure de réaction dans le THF-d_8 et (b) après une réaction accélérée dans le D_2O, B) spectres RMN du ^{1}H et C) spectres RMN du ^{13}C{^{1}H} de la TOBnTMC ($CDCl_3$, 300 MHz, r.t).

Copolymérisation aléatoire de la TMC et de l'exTMC

Afin de déterminer le catalyseur approprié pour les monomères TMC et exTMC, dans le but de contrôler le caractère aléatoire du copolymère, la conversion du TMC et de

l'exTMC a été systématiquement observée en utilisant différents organocatalyseurs, à savoir TBD, TU/DMAP, DPP et MSA (**Tableau 2-1**).

Tableau 2-1. Étude de la copolymérisation exTMC/TMC avec différents organocatalyseurs[a]

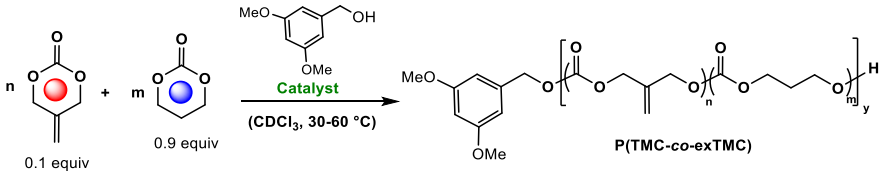

Run	Catalyst	Time(h)	$Conv_{TMC}$	$Conv_{exTMC}$	$M_n^{Theo\ (Da)}$	$M_n^{SEC,b(Da)}$	$Đ^b$
1	TBD	1	>96	>96	3267	4000	1.42
2	TU/DBU	2.5[c]	63	94	3267	4680	1.27
3	DPP	18[d]	91	94	3267	3600	1.15
4	MSA	5	>96	>96	3267	3566	1.12

[a]Reaction conditions: M/I = 30, 0.5-1 mol/L in $CDCl_3$ at 30°C. [b]In THF with calibration over PS standards, non-corrected values.

[c]Full conv exTMC, 60% conv TMC. Full conv of TMC is reached overnight. [d]60 °C

Les résultats montrent qu'avec le TBD et le TU/DBU,[38] l'exTMC est consommé plus rapidement que le TMC (TBD : 86 % de conversion après 20 min contre 50 % pour le TMC ; TU/DBU : 94 contre 63 % après 2,5h). En revanche, avec le DPP et le MSA, les conversions des deux monomères se suivent, ce qui suggère une réactivité étroite des deux monomères. L'analyse SEC montre des traces unimodales dans tous les cas, mais les distributions molaires sont plus étroites pour l'échantillon obtenu avec la DPP et la MSA (*Đ* 1,12-1,15). Comme la ROCOP avec MSA comme organocatalyseur (1,3 mol%) conduit à une incorporation plus aléatoire de deux co-monomères dans les chaînes polymères que le TBD ou le TU/DBU, tout en maintenant un bon contrôle de la polymérisation, l'étude a été poursuivie avec cet organocatalyseur. La ROCOP avec un rapport monomère exTMC/TMC de 10/90 et un DP croissant (de 15 à 120) a d'abord été étudiée à une charge de catalyseur de 1,3 % (par rapport au monomère) dans des solutions de chloroforme à 1 M. La teneur en exTMC a ensuite été augmentée à 1,3 % (par rapport au monomère) dans des solutions de chloroforme à 1 M. La ROCOP a été étudiée à 1,5 % (par rapport au monomère) dans des solutions de chloroforme. La teneur en exTMC a ensuite été augmentée à 30-50% pour un DP de 60, conduisant à des résultats proches de ceux obtenus avec une teneur de 10% en exTMC. Le ratio de fonctionnalisation peut donc être facilement ajusté. Des conversions >96% ont été observées en 2-7 h. Selon les

résultats de la **Figure 2-4a**, le spectre RMN ^{1}H d'un copolymère avec DP = 60 et un ratio monomère TMC/exTMC de 50/50 (P7, **Tableau 2-3**). L'incorporation efficace de l'amorceur difonctionnel BDM au cœur des chaînes polymères est confirmée par la présence des signaux f et g, correspondant aux groupes méthylène et aromatique de l'amorceur, à 5,16 et 7,40 ppm respectivement. Le DMBA a été utilisé afin d'observer le comportement de copolymérisation. Deux extrémités de chaîne CH_2OH différentes sont observées (b' à 3,75 ppm et d' à 4,19 ppm) correspondant aux unités terminales CH_2OH du TMC et de l'exTMC, respectivement. Les signaux sont très proches en intensité, ce qui dénote un caractère aléatoire élevé du copolymère, mais une intégration précise pour déterminer les longueurs de séquence moyennes (LexTMC et LTMC) n'a pas été possible en raison du chevauchement. Il a toutefois été possible d'utiliser la spectroscopie RMN $^{13}C\{^{1}H\}$ (**Figure 2-4b**), dans laquelle l'intégration des signaux correspondants aux homoséquences et aux hétéroséquences a été possible (après attribution des signaux par analyse RMN 2D et comparaison avec les homopolymères respectifs). Les intégrations relatives des signaux CH_2O et C=O donnent des valeurs L proches de 2 pour l'exTMC et le TMC ($L_{exTMC} = 1+I_{exTMC}/(I_{exTMC+ITCM})$, $L_{TMC} = 1+I_{exTMC}/(I_{TMC+ITCM})$), ce qui correspond à un caractère aléatoire presque parfait ($R = 1/Le_{xTMC} + 1/_{LTMC} \approx 1$).[38]

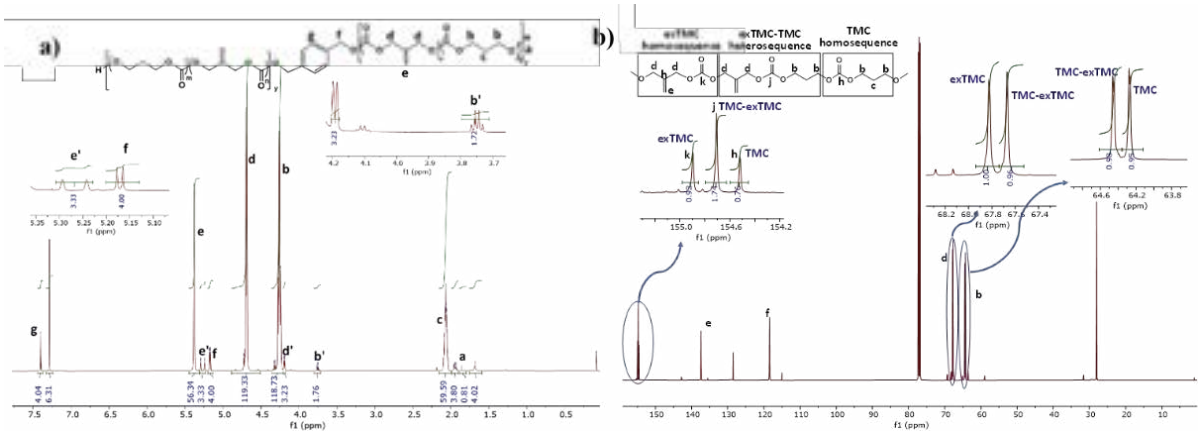

Figure 2-4. (a) Spectres RMN ^{1}H et (b) RMN ^{13}C d'un copolymère avec DP = 60 et un ratio monomère TMC/exTMC de 50/50 ($CDCl_3$, 300 MHZ, r.t).

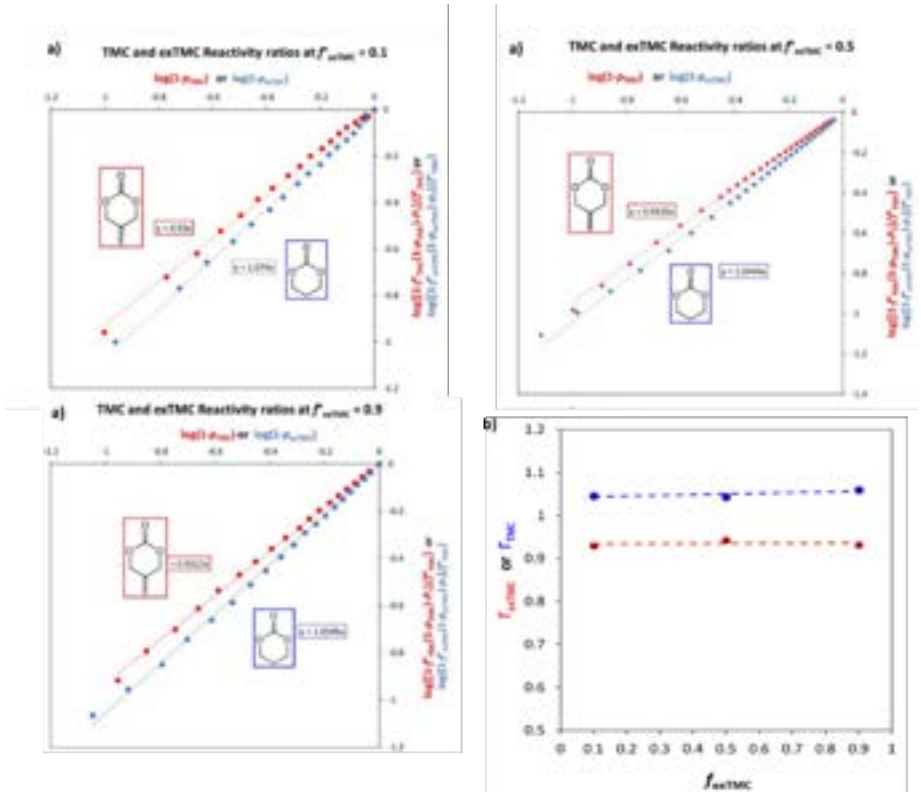

Figure 2-5. a) Détermination des rapports de réactivité des deux monomères par la méthode Beckingham-Sanoja-Lynd (BSL)[38] à partir du suivi RMN ^{1}H in situ des copolymérisations à différents rapports de monomères. Le coefficient de pente des droites (Y) représente le rapport de réactivité. b) Ajustement des rapports de réactivité déterminés à différents rapports TMC/exTMC.

Ce caractère aléatoire presque parfait du copolymère TMC/exTMC est en accord avec le suivi RMN ^{1}H des conversions de monomères. Le tracé semi-logarithmique de la réaction de copolymérisation avec un ratio monomère 50/50 et DP = 60 montre des courbes de conversion presque superposées pour les deux monomères. Pour confirmer la réactivité proche des deux monomères dans la copolymérisation, un suivi RMN ^{1}H a également été réalisé pour des copolymérisations avec des rapports monomères exTMC/TMC de 10/90 et 90/10 et DP = 60, et les rapports de réactivité relative ont été déterminés pour le TMC et l'exTMC en appliquant la méthode Beckingham-Sanoja-Lynd (BSL) à partir du suivi RMN ^{1}H in situ des copolymérisations à différents rapports de monomères (**Figure 2-5a**). Quel que soit le rapport de monomère, des rapports de réactivité de 0,95-0,98 et de 1,00-1,06 ont été obtenus pour l'exTMC et le TMC (**Figure 2-5b**),[38] respectivement, confirmant la réactivité très proche des deux monomères et étayant le caractère hautement aléatoire des copolymères obtenus.

Copolymérisation aléatoire du TMC et de l'exTMC fonctionnalisé

Tableau 2-2. Copolymérisation de TOBnTMC/TMC avec différents organocatalyseurs au DP60 avec 30 % de TOBnTMC[a]

Run	Catalyst	time(h)	$Conv^{TMC}$	$Conv^{TOBnTMC}$	M_{nSEC}[b] (kDa)	$Đ$[b]
1	TBD	4	94	99	7.1	1.62
2	TU/DBU	30	89	100	4.3	1.28
3	DPP[c]	20	99	99	4	1.46
4	MSA	5	94	96	5.2	1.15

[a]Reaction conditions: 0.5-1 M in $CDCl_3$ at 30°C. [b]In THF with PS standards calibration, non-corrected values. [c]T = 60°C.

La copolymérisation simultanée du TOBnTMC et du TMC (TMC/ TOBnTMC = 70/30) a ensuite été explorée avec le BDM comme amorceur (monomère/BDM = 60/1). Les organocatalyseurs TBD (BDM/TBD = 0,3), TU/DBU (BDM /TU/DBU = 1/1/1), DPP (BDM /DPP = 1/2) et MSA (BDM/MSA = 1/1) ont été utilisés pour établir une comparaison rapide. Toutes les réactions ont été effectuées à 30°C à l'exception de celle avec le DPP (60°C) (**Tableau 2-2**). La cinétique de conversion globale des monomères en fonction du temps montre qu'avec le TBD et le MSA, la conversion des monomères TOBnTMC et TMC peut dépasser 90% en 5 heures. Néanmoins, le taux de conversion des monomères ave le TBD était exceptionnellement rapide, atteignant une consommation de plus de 90 % en l'espace d'une heure. En revanche, le TU/DBU et le DPP se sont révélés moins actifs que le TBD et le MSA. Il faut plus de 20 heures pour atteindre une conversion de 99 %. La ROCOP de TOBnTMC/TMC avec DP 60 et des ratios croissants de TOBnTMC de 10 à 100 a d'abord été explorée à une charge de catalyseur de 1,3 % (par rapport au monomère) dans des solutions de chloroforme 1 M à 30 °C en utilisant le BDM comme amorceur bifonctionnel. Les résultats obtenus ont montré qu'une proportion croissante de TOBnTMC entraînait une diminution de M_n et un élargissement de $Đ$, en particulier pour une teneur en TOBnTMC > 30 %. Cela indique que l'utilisation d'une teneur réduite en TOBnTMC, avec le MSA comme catalyseur et le BDM comme amorceur, pourrait améliorer les résultats. Le DP a été augmenté de 30 à 120 avec 10% de TOBnTMC. Les résultats ont montré que le M_n augmentait avec le DP, mais ne pouvait pas atteindre 10 kDa en utilisant le BDM comme amorceur. Cependant, il a conservé un $Đ$ étroit (Đ < 1,12).

Le spectre RMN ^1H d'un copolymère avec DP = 60 et un rapport monomère TMC/TOBnTMC de 90/10 est illustré à la **Figure 2-6**. L'incorporation efficace de

l'amorceur difonctionnel BDM au cœur des chaînes polymères est confirmée par la présence des signaux k et l, correspondant aux groupes méthylène et aromatique de l'amorceur, à 5,16 et 7,40 ppm respectivement. Le signal (g) à 2,25 ppm est attribué aux groupements CH du TOBnTMC. Des extrémités de chaîne CH_2OH sont observées à i' à 3,75 ppm, correspondant aux unités terminales CH_2OH du TMC. Le signal a associé au groupe aromatique, le signal c associé aux groupes CH_2O du thioéther, et les signaux b, d, e et f associés au CH_2 des unités TOBnTMC, ce qui empêche une intégration précise. Les intégrales relatives des signaux h et i (correspondant aux groupements CH_2O des unités TOBnTMC et TMC, respectivement), k et l (associés à l'amorceur) s'accordent bien avec le rapport monomère initial (90/10) et l'alimentation en monomère (DP60). Les signaux i et h sont divisés en raison de la présence d'homo- et d'hétérodiades (séquences TMC-TMC, TOBnTMC-TOBnTMC et TMC-TOBnTMC).

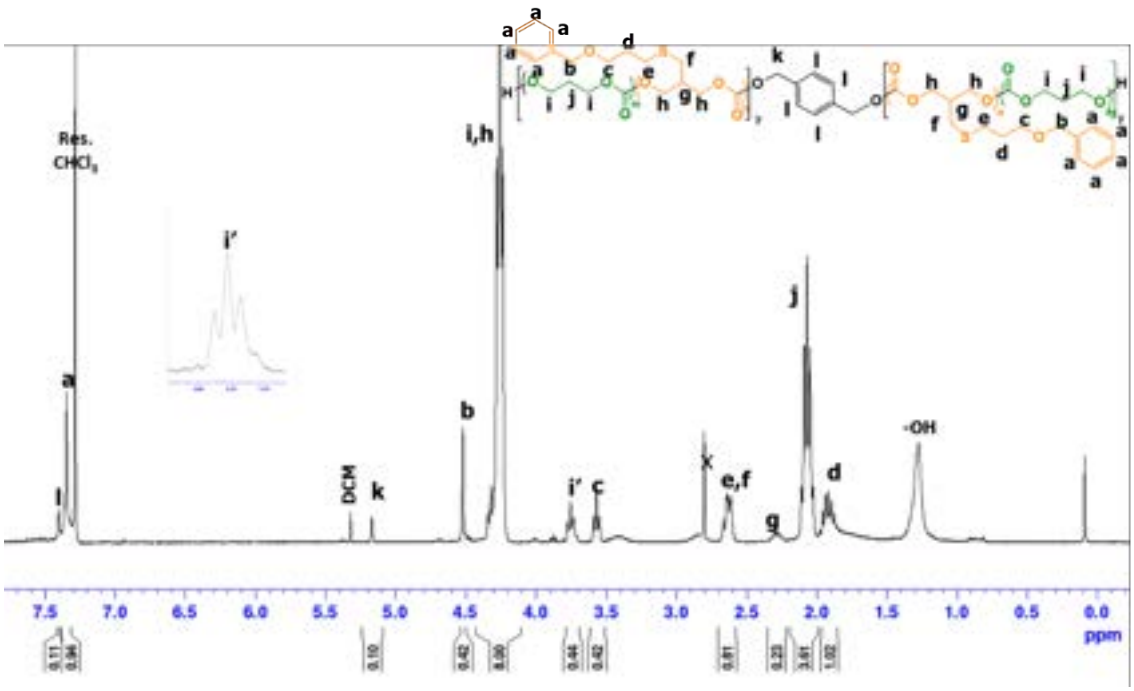

Figure 2-6. Spectres RMN ^{1}H d'un copolymère avec DP = 60 et d'un TMC/TOBnTMC ($CDCl_3$, 300 MHZ, r.t).

Le tracé semi-logarithmique de la réaction de copolymérisation, utilisant des rapports de monomères de 80/20, 50/50, et 20/80 avec DP 60, montre des courbes de conversion qui se chevauchent presque pour les deux monomères. Pour vérifier la réactivité similaire des deux monomères dans la copolymérisation, un suivi par RMN ^{1}H a été effectuée pour des copolymérisations à des rapports de monomères TOBnTMC/TMC de 80/20, 50/50 et

20/80 avec DP = 60. Les rapports de réactivité relatifs pour le TMC et le TOBnTMC ont été déterminés à nouveau à l'aide de la méthode BSL (**Figure 2-7a**), de manière similaire aux procédures utilisées pour l'exTMC. Quel que soit le rapport de monomère, des rapports de réactivité entre 0,95 et 0,99 pour le TOBnTMC et entre 1,01 et 1,05 pour le TMC ont été observés (**Figure 2-7b**), confirmant leur réactivité presque identique ($\Gamma_{TOBnTMC} \approx \Gamma_{TMC} \approx 1$) et soutenant le caractère hautement aléatoire des copolymères résultants. De plus, ces résultats suggèrent la faisabilité de la polymérisation d'un terpolymère composé de TMC, exTMC et TOBnTMC, étant donné que leurs rapports de réactivité sont proches de 1 ($\Gamma_{exTMC} \approx \Gamma_{TMC} \approx 1$ et $\Gamma_{TOBnTMC} \approx \Gamma_{TMC} \approx 1$). Cette proximité de réactivité facilite l'incorporation de deux groupes pendants complémentaires, élargissant ainsi les applications potentielles.

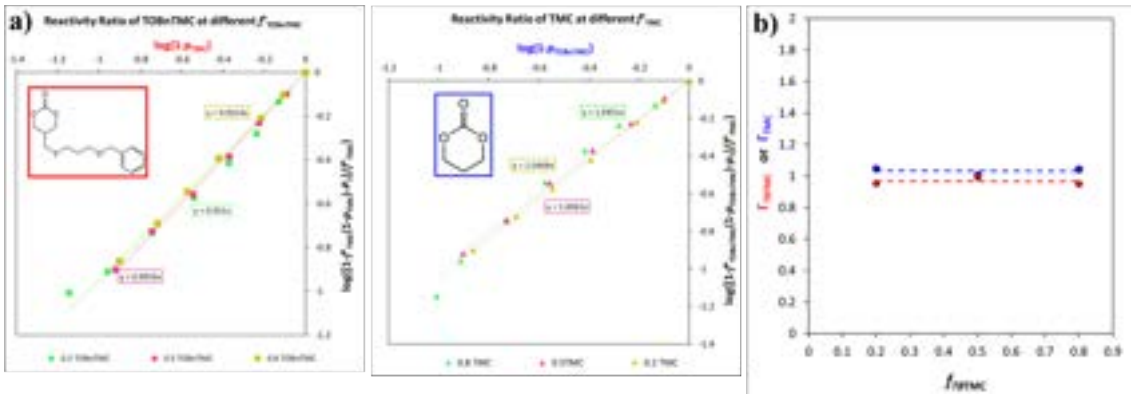

Figure 2-7. a) Détermination des rapports de réactivité des monomères TMC et TOBnTMC par la méthode BSL.[38] et b) Ajustement des rapports de réactivité déterminés à différents rapports TMC/TOBnTMC.

Tercopolymérisation du TMC, de l'exTMC et de l'exTMC fonctionnalisé

Des poly(TOBnTMC)-*ter*-Poly(TMC)-*ter*-Poly(exTMC) ont été préparés avec succès en utilisant le MSA comme catalyseur. Il a été constaté que le taux de conversion des trois monomères était presque le même, ce qui pourrait suggérer que $\Gamma_{TOBTMC} \sim \Gamma_{TMC} \sim \Gamma_{exTMC} \sim 1$. Il a donc été confirmé que le terpolymère d'exTMC, de TMC et de TOBnTMC est un terpolymère aléatoire.

Afin d'améliorer la polyvalence du tercopolymère pour l'introduction de groupes multifonctionnels protiques, les groupes fonctionnels dans les copolymères synthétisés ont été initialement protégés. Par conséquent, la déprotection ultérieure de ces groupes est cruciale. La démonstration réussie de la déprotection du groupe benzyle dans le TOBnTMC au sein du copolymère Poly(TOBnTMC)-*ter*-Poly(TMC)-*ter*-Poly(exTMC) (**Figure 2-8**), qui visait à libérer les groupes hydroxyles par une réaction d'hydrogénation

en utilisant un catalyseur Pd/C. La déprotection complète du groupe benzyle dans le TOBnTMC a été réalisée avec succès. L'élimination complète des groupes de protection benzyle (-OBn) est facilement vérifiée par la disparition de tous les signaux aromatiques appartenant au -OBn dans le spectre RMN ^{1}H, par rapport aux spectres RMN ^{1}H des copolymères protégés (**Figure 2-8a**). Bien que la débenzylation ait été réalisée en 4 heures, une hydrogénation involontaire de la double liaison dans l'exTMC a également été observée (attendue). Par conséquent, il est essentiel de modifier l'exTMC par une réaction thiol-ène afin de garantir le groupe fonctionnel voulu avant de procéder à la débenzylation à l'aide de Pd/C.

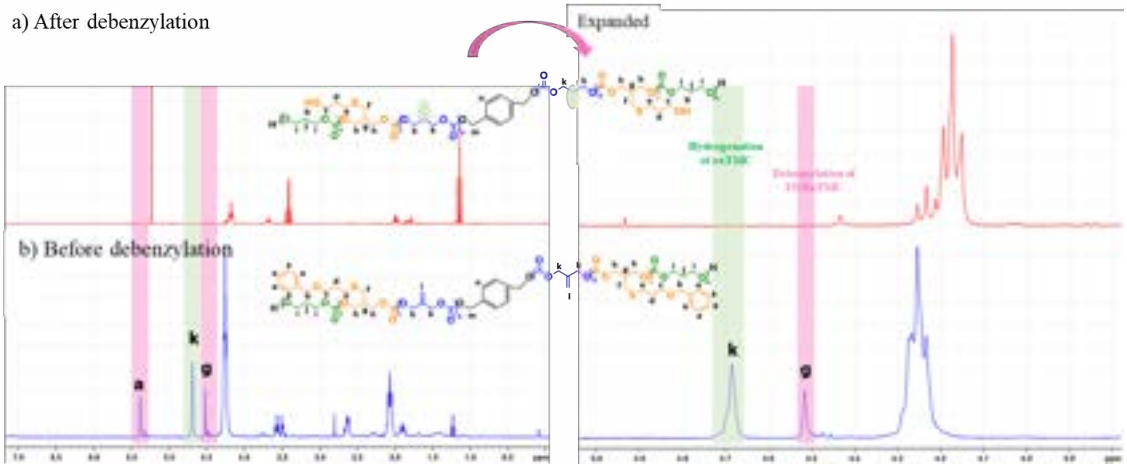

Figure 2-8. Spectres RMN ^{1}H ($CDCl_3$, 300 MHz) du Poly(TOBnTMC)-*ter*-Poly(TMC)-*ter*-Poly(exTMC) contenant 10% de TOBn ; a) après copolymère déprotégé (Hydrogénolyse), b) avant copolymère déprotégé (avec protection TOBn).

Préparation de polycarbonates fonctionnalisés par réaction thiol-ène (fonctionnalisation post-polymérisation)

Des réactions d'addition click ont été réalisées sur deux copolymères avec DP120 et différentes compositions de monomères avec des teneurs de 30 % en exTMC) dans des conditions radicalaires, en utilisant du DMPA (2,2-diméthoxy-2-phényl acétophénone) comme amorceur (2 wt%) et une irradiation à 365 nm. Après quelques heures de réaction à température ambiante, le contrôle RMN ^{1}H a montré une disparition presque complète des signaux à 4,70 et 5,40 ppm, correspondant aux séquences O-CH_2-C(=CH_2)CH_2-O des unités exTMC après modification post-polymérisation par le thiolglycérol (**Figure 2-9a**) et l'acide thioglycolique (**Figure 2-9c**), et l'apparition de nouveaux signaux de multiplets larges : (i) à 2. 80, 3,50-3,60 et 3,65-3,90 ppm correspondant aux groupes CH_2 et CH dérivant du thioglycérol (e, f et g), (ii) à 2,35 et 2,70-2,80 ppm pour les nouveaux groupes

CH et CH_2 résultant de l'addition du thio-ène à la fraction $C=CH_2$ (c et d). Toutes ces données sont cohérentes avec l'addition chimiosélective et régiosélective propre du thiol fonctionnalisé aux groupements $C=CH_2$. En outre, l'analyse SEC confirme que la réaction thiol-ène se produit sans affecter l'intégrité des chaînes polymères ni provoquer de réticulation, puisque les valeurs de M_n et Đ sont du même ordre que celles des copolymères de départ après post-modification par le thiolglycérol (**Figure 2-9b**) et l'acide thioglycolique (**Figure 2-9d**).

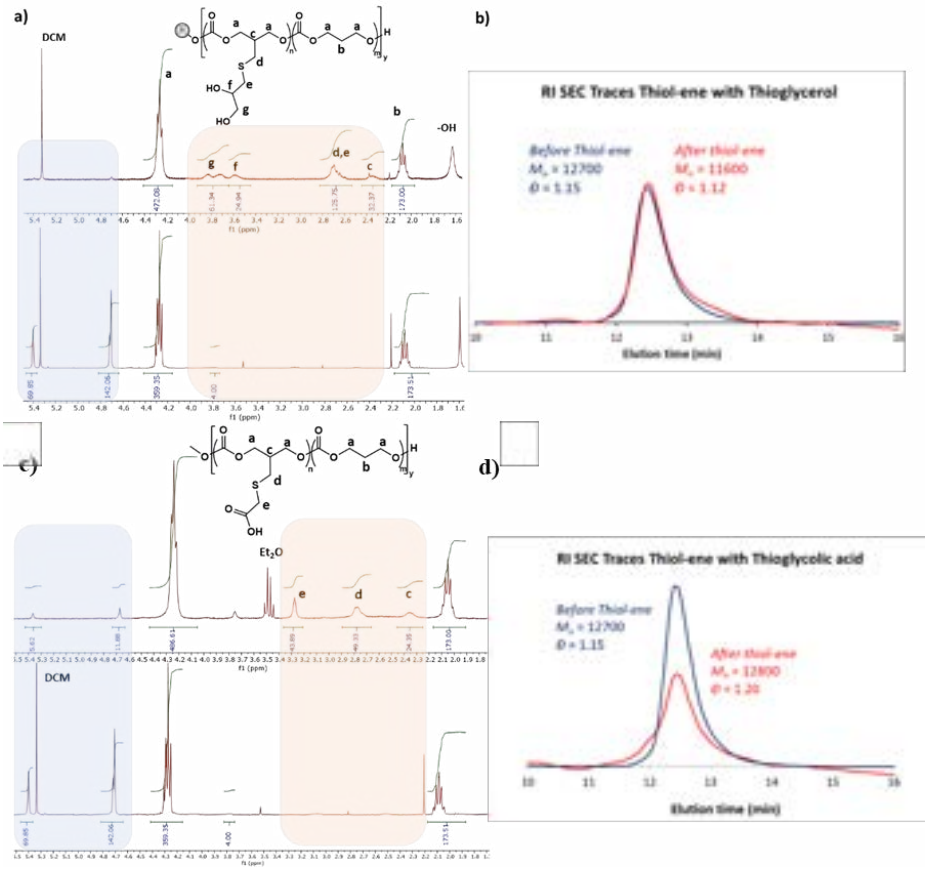

Figure 2-9. Empilement des spectres RMN 1H d'un copolymère TMC/exTMC (30% exTMC) avant (en bas) et après (en haut) la fonctionnalisation de la modification post-polymérisation par réaction thiol-ène avec a) le thioglycérol et c) l'acide thioglycolique. Traces SEC des copolymères correspondants fonctionnalisés par b) thioglycérol et d) acide thioglycolique.

Chapitre III : *Évaluation des propriétés biocompatibles des copolymères aléatoires de carbonate de triméthylène et de 5-méthylène-1,3-dioxane-2-un avec introduction contrôlée de diol et d'acide carboxylique*

Dans cette étude du chapitre III, je cherche à clarifier la relation fondamentale entre la

propriété biocompatible des polymères et la structure chimique des biomatériaux polymères. Notamment, le PTMC-*co*-PexTMC présente un potentiel considérable pour moduler le nombre de groupes fonctionnels et pour les modifier ensuite avec une gamme variée de dérivés thiols par le biais de réactions click thiol-ène, le tout sans qu'il soit nécessaire d'utiliser des groupes protecteurs. Cette étude s'étend à un examen détaillé de diverses structures de copolymères de TMC, spécifiquement conçues pour des applications dans le domaine des biomatériaux. Les copolymères synthétisés de TMC avec de l'exTMC et de TMC avec de l'exTMC fonctionnalisé par des réactions thiol-ène impliquant de l'acide thioglycolique et du thioglycérol, ont été utilisés visant de revêtements pour les biomatériaux. Des études approfondies ont été entreprises pour évaluer l'influence des variations structurelles et des groupes fonctionnels dans le PTMC-*co*-PexTMC sur plusieurs paramètres, notamment la stabilité thermique, l'angle de contact, les méchanismes de dégradation initiale, la cinétique de libération des médicaments, l'adsorption des protéines et l'adhésion des plaquettes sanguines.

Stabilité thermique

Les résultats obtenus montrent qu'après la modification post-polymérisation du PTMC-*co*-PexTMC$_{30}$ par la réaction thio-en, les polymères ont un T_{10} plus faible qu'avant la modification post-polymérisation. Cela pourrait être dû à l'incorporation de groupes fonctionnels hydroxyle ou carboxy qui contribuent probablement à la dégradation thermique des polymères après la modification post-polymérisation.[40]

Mouillabilité

En ce qui concerne les résultats, les angles de contact ont montré une tendance différente après la modification post-polymérisation via la réaction thio-ène, comme on pouvait s'y attendre. L'augmentation de la fonction protique améliore l'hydrophilie. De plus, la présence de groupes fonctionnels carboxyliques peut améliorer l'hydrophilie plus efficacement que les diols à des concentrations équivalentes.

Comportement de dégradation

Les résultats indiquent que le PexTMC-*co*-TMC$_{30COOH}$ montre le % de perte de poids le plus élevé après 90 jours à la fois dans la lipase et dans la solution PBS (100 % (**Figure 3-1b**) et 78,50 ± 5,03 % (~3,7 mg) (**Figure 3-1a**), respectivement. Il est apparu que le PTMC-*co*-PexTMC$_{30COOH}$ et le PTMC-*co*-PexTMC$_{30OH}$ subissaient une perte de poids accélérée plus rapidement que le PTMC-*co*-exTMC$_{30}$ dans la lipase, ce qui contraste avec les rapports précédents indiquant que l'augmentation de la composition du TMC dans la

chaîne du copolymère améliore la dégradation. Cela confirme la tendance plus élevée des liaisons carbonates et des surfaces hydrophobes à subir une dégradation enzymatique plus rapide que les surfaces plus hydrophiles.[41-42] Cependant, Maria et al. ont signalé que les acides carboxyliques dans la lipase peuvent catalyser des réactions d'estérification,[43] ce qui pourrait correspondre à nos résultats ; PTMC-*co*-PexTMC$_{30COOH}$ a montré la perte de poids la plus élevée en raison du pendant carboxylique qui a catalysé l'estérification de la chaîne de polymères dans la lipase.

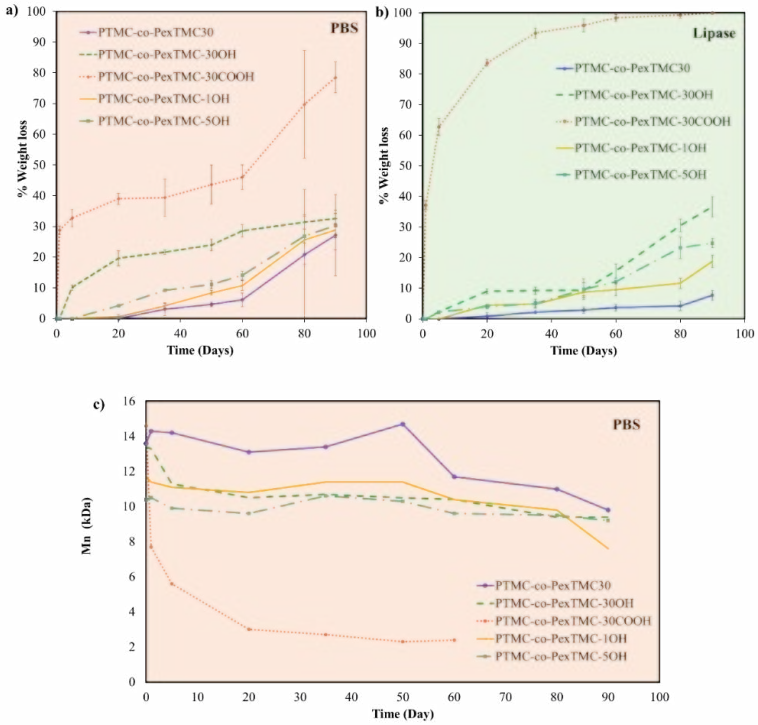

Figure 3-1 Courbe de dégradation des dérivés PTMC-*co*-PexTMC (a) % de perte de poids dans des conditions PBS, (b) % de perte de poids dans des conditions lipase, et (c) M_n après dégradation dans PBS.

En outre, le PTMC-*co*-PexTMC$_{30COOH}$ a montré une perte de poids plus rapide non seulement que le PTMC-*co*-PexTMC$_{30}$ mais aussi que le PTMC-*co*-PexTMC$_{30OH}$ dans une solution PBS. Il est bien connu que l'acide peut jouer un rôle de catalyseur de dégradation, qui accélère l'hydrolyse des liaisons ester dans le squelette du polymère.[29] En outre, les résultats obtenus pourraient impliquer que l'augmentation de la teneur en hydroxyle dans les chaînes de copolymères a entraîné une perte de poids plus élevée en raison de l'amélioration de l'hydrophilie, comme le montre la **Figure 3-1**. Il s'agit de la même tendance que celle rapportée par Amsden et ses collaborateurs, à savoir que l'augmentation de la teneur en hydroxyle dans les chaînes de copolymères a le plus grand

impact sur le taux de dégradation.[44] Par ailleurs, le M_n du polymère enrobé a été observé par SEC. Il a été constaté que le M_n du PTMC-co-PexTMC$_{30}$ et du PTMC-*co*-PexTMC$_{30OH}$ n'a pas changé de manière significative au cours de l'expérience de dégradation. En revanche, le M_n du PTMC-*co*-PexTMC$_{30COOH}$ a été réduit dès le premier jour de l'expérience dans le PBS et la solution de lipase (**Figure 3-1c**). Ces résultats pourraient indiquer que la perte de poids initiale du PTMC-*co*-PexTMC$_{30COOH}$ pourrait être due au processus d'érosion en masse du PTMC. Ils pourraient également confirmer la modification cruciale de la chaîne latérale du PTMC par une liaison éther. Cette variation pourrait s'expliquer par la présence de la fonctionnalisation.

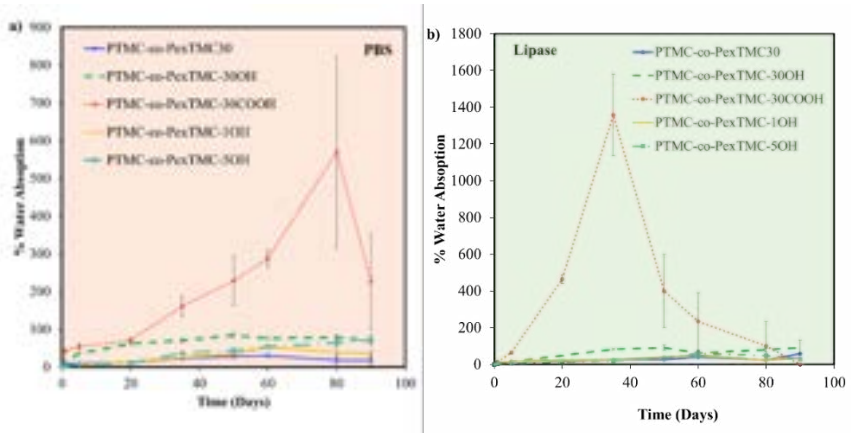

Figure 3-2 Courbe de dégradation des dérivés PTMC-*co*-PexTMC (a) % d'absorption d'eau dans des conditions PBS et (b) % d'absorption d'eau dans des conditions lipase.

L'absorption d'eau survenant au cours de la dégradation semble être un facteur important dans la dégradation du PTMC. Le PTMC-*co*-PexTMC$_{30COOH}$ a montré le % d'absorption d'eau le plus élevé à la fois dans la lipase et dans le PBS (**Figure 3-2b** et **Figure 3-2a**). Les résultats obtenus pourraient signifier que le PTMC-*co*-PexTMC$_{30COOH}$ a absorbé la plus grande quantité d'eau, soit plus de 1300 % en 35 jours et 570 % en 80 jours dans la lipase et le PBS, respectivement. Après avoir montré le % d'absorption d'eau le plus élevé, la tendance de la courbe a diminué en raison de la dégradation des chaînes de polymère, comme le montre la **Figure 3-1c**, ce qui a été confirmé par la diminution du M_n observée par analyse SEC sur le résidu solide. En conclusion, on peut indiquer qu'après la modification post-polymérisation du copolymère via la réaction thiol-en, des groupes fonctionnels hydrophiles ont été introduits dans les chaînes de polymère, de sorte que les groupes hydrophiles tels que les groupes hydroxyles ou carbonyles peuvent augmenter la vitesse de diffusion de l'eau et catalyser la dégradation.[29,45,46] Les résultats obtenus sont en accord avec des études antérieures suggérant que l'absorption d'eau pourrait contribuer

à la dégradation du copolymère. L'introduction de groupes hydrophiles dans la chaîne polymère pourrait donc entraîner une plus grande absorption d'eau, ce qui pourrait augmenter le clivage des liaisons carbonate et favoriser la dégradation autocatalytique.[47]

Libération in vitro du médicament

Comparé au PTMC-*co*-PexTMC$_{30COOH}$, le taux de libération du PTMC-*co*-PexTMC$_{30OH}$ est similaire sur une période de 1 à 14 jours. En effet, le PTMC-*co*-PexTMC$_{30COOH}$ et le PTMC-*co*-PexTMC$_{30OH}$ ont montré presque le même profil de libération après 14 jours, soit 16,4 ± 1,2 % et 15,5 ± 1,2 %, respectivement (**Figure 3-3**). Après 14 jours, le PTMC-co-PexTMC$_{30COOH}$ a présenté les profils de libération de DOX les plus élevés, soit 68,0 ± 19,6 % dans les 28 jours. D'autre part, les PTMC-*co*-PexTMC$_{30}$ et PTMC-*co*-PexTMC$_{30OH}$ ont présenté des profils de libération progressive et soutenue de l'ordre de 5,9 ± 1,3 % et 18,9 ± 2,8 % après 35 jours. Le PTMC-*co*-PexTMC$_{30COOH}$ a été brusquement libéré à plus de 126,9 ± 42,1 % en 35 jours. La possibilité d'une libération excessive de PTMC-*co*-PexTMC$_{30COOH}$ -DOX pourrait être due à la dégradation du polymère qui a affecté la transparence de la solution (**Figure 3-3**). La tendance du profil de libération du DOX était la même que celle de l'expérience de dégradation qui a montré que le PTMC-*co*-PexTMC$_{30COOH}$ a obtenu le % de perte de poids le plus élevé, ce qui pourrait signifier que le PTMC-*co*-PexTMC$_{30COOH}$ a présenté le profil de libération du DOX le plus rapide en raison de la dégradation du copolymère. Cette observation est en accord avec les travaux de Fu et al qui suggèrent que la libération du médicament implique deux mécanismes différents : la diffusion des molécules de médicament et la dégradation de la matrice polymère.[48]

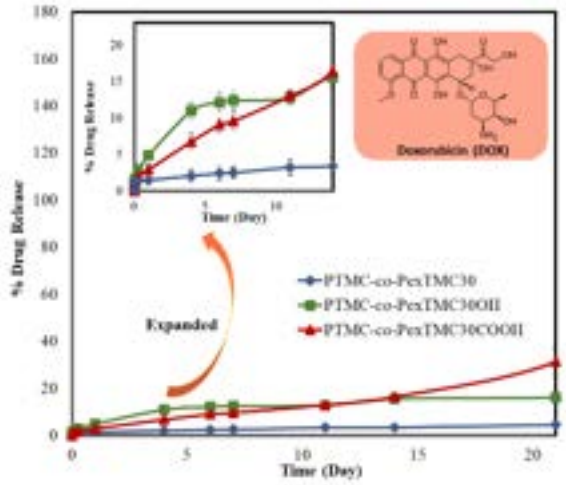

Figure 3-3. Profil de libération de la doxorubicine par le PTMC-*co*-PexTMC$_{30}$, le PTMC-*co*-PexTMC$_{30OH}$

et le PTMC-*co*-PexTMC$_{30COOH}$.

Adsorption des protéines

L'adsorption d'albumine sur de films des PTMC-*co*-PexTMCs non modifiés par post-polymérisation en faisant varier la teneur en exTMC de 1 à 30 % était de 0,64 µg/cm2 ± 0,001, 0,72 µg/cm2 ± 0,23 et 0,93 µg/cm2 ± 0,001 pour les PTMC-*co*-PexTMC$_1$, PTMC-*co*-PexTMC$_5$ et PTMC-*co*-PexTMC$_{10}$, respectivement (**Figure 3-4a**). Après modification post-polymérisation par TGA, l'adsorption de protéines a augmenté à 3,38 µg/cm2 ± 0,04, et 16,73 µg/cm2 ± 1,71 pour PTMC-*co*-PexTMC$_{1COOH}$, PTMC-*co*-PexTMC$_{5COOH}$, respectivement (**Figure 3-4a**). L'adsorption de protéines après modification post-polymérisation par TGC était de 1,68 µg/cm2 ± 0,28, 3,54 µg/cm2 ± 1,67, et 4,50 µg/cm2 ± 0,56 pour PTMC-*co*-PexTMC$_{1OH}$, PTMC-*co*-PexTMC$_{5OH}$, et PTMC-*co*-PexTMC$_{10OH}$, respectivement (**Figure 3-4a**). Le résultat est identique pour le fibrinogène (**Figure 3-4b**).

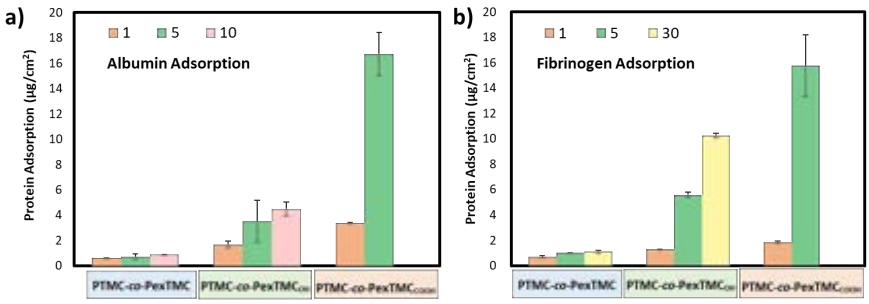

Figure 3-4. a) Adsorption des protéines de l'albumine (BSA) et b) du fibrinogène (BPF) sur PTMC-*co*-PexTMC, PTMC-*co*-PexTMC$_{OH}$ et PTMC-*co*-PexTMC$_{COOH}$.

D'après les résultats obtenus, il existe une différence marquée dans l'adsorption des protéines pour les PTMC-*co*-PexTMC fonctionnalisés en fonction de la fonction introduite sur les chaînes de polymère (groupe hydroxyle ou carboxylique). Ceci est attribué à leur grande affinité pour adsorber les protéines par rapport aux PTMC-*co*-PexTMC non fonctionnalisés dans cette étude. Il a été constaté que l'affinité des PTMC-*co*-PexTMC non fonctionnalisés pour l'adsorption des protéines n'était pas significativement modifiée par la modification de la teneur en exTMC. Cependant, les résultats ont montré que l'affinité pour l'adsorption des protéines des PTMC-*co*-PexTMC fonctionnalisés a été significativement modifiée par l'introduction de différentes teneurs en groupes hydroxy et carboxyliques. Cela a montré que l'augmentation de la teneur en groupes hydroxy et carboxylique est attribuée à sa forte affinité pour l'adsorption des protéines par rapport à une teneur plus faible en groupes fonctionnels (**Figure 3-4**).

Adhésion plaquettaire

Le nombre de plaquettes adhérant à la surface de PTMC-*co*-PexTMC$_{OH}$ était significativement inférieur à celui du verre non revêtu, de PTMC-*co*-PexTMC et de PTMC-*co*-PexTMC$_{COOH}$. Le nombre de plaquettes adhérant au substrat était de 531 cellules/mm2 ± 126, 509 cellules/mm2 ± 112, 99 cellules/mm2 ± 33, et 367 cellules/mm2 ± 136 pour le verre Bear, PTMC-co-PexTMC$_{30COOH}$, PTMC-*co*-PexTMC$_{30OH}$, et PTMC-*co*-PexTMC$_{30}$, respectivement (**Figure 3-5**). Bien que la mouillabilité du PTMC-*co*-PexTMC$_{OH}$ et du PTMC-*co*-PexTMC$_{COOH}$ soit presque similaire, les groupes fonctionnels et les charges de surface sont différents. Les groupes carboxyle (-COOH) sont chargés négativement dans le sérum sanguin et d'autres solutions protéiques aqueuses, sont hydrophiles et interagissent préférentiellement avec la fibronectine et l'albumine.49-52 La combinaison de nos résultats et de la littérature indique que le PTMC-*co*-PexTMC$_{OH}$ peut empêcher l'adhésion des plaquettes plus efficacement que le PTMC-*co*-PexTMC et le PTMC-*co*-PexTMC$_{COOH}$.

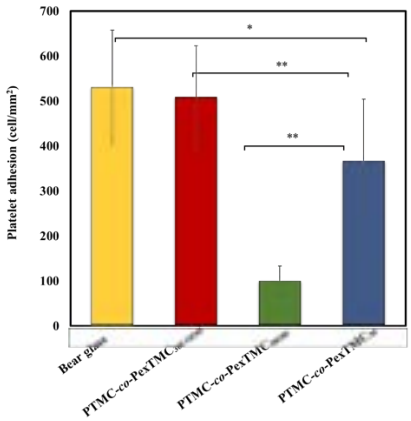

Figure 3-5. Tracé quantitatif du nombre de plaquettes adhérant à la surface des films (n = 5, *p < 0,02, **p < 0,01).

Chapitre IV *: Conception de la réticulation des chaînes latérales pour moduler les propriétés des copolymères.*

Dans ce dernier chapitre, nous abordons le domaine jusqu'ici inexploré de la fonctionnalisation du PTMC avec des groupes carboxyliques sur ses chaînes latérales pour créer des ionomères. Ce chapitre est consacré à la conception et à la réalisation d'une étude préliminaire des effets de la réticulation de l'ionomère sur les chaînes latérales du PTMC fonctionnalisé. Comme nous l'avons souligné précédemment, le PTMC-*co*-PexTMC$_{COOH}$ peut être facilement modifié pour incorporer des groupes carboxyliques

dans ses chaînes latérales sans qu'il soit nécessaire de recourir à un processus de protection. Les groupes carboxyliques sont essentiels pour positionner précisément les carboxylates métalliques, qui permettent une réticulation dynamique pour produire des ionomères. L'acétate de magnésium tétrahydraté, l'acétate de sodium trihydraté, l'acétate de fer (II) et l'acétate de zinc (II) ont été utilisés comme acétates métalliques pour générer une réticulation métallo-carboxylée, et les quantités d'acétates métalliques ont également été modifiées (avec le Zn) pour étudier leurs effets. Le comportement de dégradation, les propriétés thermiques, l'absorption d'eau et la rhéologie des réseaux réticulés par des métallo-carboxylates ont été examinés.

Préparation de l'ionomère PTMC-co-exTMC$_{30COOH}$

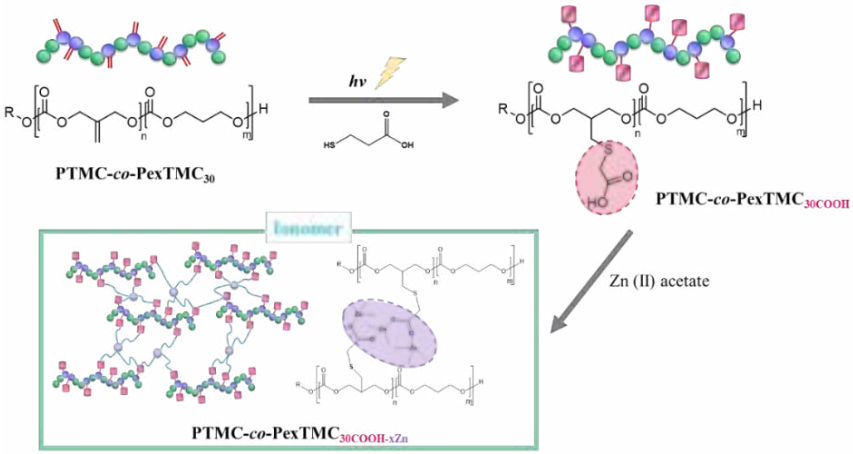

Tableau 4-1 Résumé de la stabilité M_n et thermique du PTMC-co-PexTMC$_{30}$ avant et après modification post-polymérisation par réaction thiol-ène et réticulation par l'acétate de Zn (II).

Entry	Name	M_n[a] (kDa)	$Đ$	T_g (°C)	T_d (°C)	ΔH (J/g)
1	PTMC-*co*-PexTMC$_{30}$	12.9	1.14	-	234.78	-42.39
2	PTMC-*co*-PexTMC$_{30OH}$	12.9	1.14	-2.3	166.51	-24.04
3	PTMC-*co*-PexTMC$_{30COOH}$	15.1	1.31	-4.36	177.3	-21.52
4	PTMC-*co*-PexTMC$_{30COOH-2.5Zn}$	17.3	1.58	-4.82	199.41	-15.39
5	PTMC-*co*-PexTMC$_{30COOH-5Zn}$	16.7	1.76	-5.23	212.03	-15.77
6	PTMC-*co*-PexTMC$_{30COOH-10Zn}$	17.4	2.07	-4.29	206.11	-16.82
7	PTMC-*co*-PexTMC$_{30COOH-20Zn}$	16.6	2.16	-5.53	206.4	-17.29
8	PTMC-*co*-PexTMC$_{30COOH-30Zn}$	17.8	1.81	-5.92	205.99	-16.88

[a] Determined by SEC by polystyrene (PS) standard in THF, 40 °C.

L'expérience a été définie pour différents rapports molaires entre l'acétate de Zn(II) et le

rapport molaire des groupes carboxyliques, allant de 0 à 30 %. Après la formation du PTMC-*co*-PexTMC$_{30COOH}$-xZn, l'analyse spectroscopique infrarouge à transformée de Fourier (FTIR) a montré de nouvelles absorbances caractéristiques d'élongation symétriques du carboxylate-Zn à environ 1583-1587 cm^{-1} après la formation de l'ionomère, qui se sont décalées par rapport aux élongations symétriques de l'acide carbosylique du PTMC-*co*-PexTMC$_{30COOH}$ à 1577 cm^{-1} (**Figure 4-1**). Les données SEC indiquent qu'après la formation de l'ionomère, la distribution de la masse molaire du PTMC-*co*-PexTMC$_{30COOH}$-xZn est passée à un schéma bimodal avec un M_n plus élevé par rapport au PTMC-*co*-PexTMC$_{30COOH}$, qui présentait une distribution monomodale. En outre, une augmentation de la teneur en carboxylate de Zn correspond à une augmentation de $Đ$ (**Tableau 4-1**).

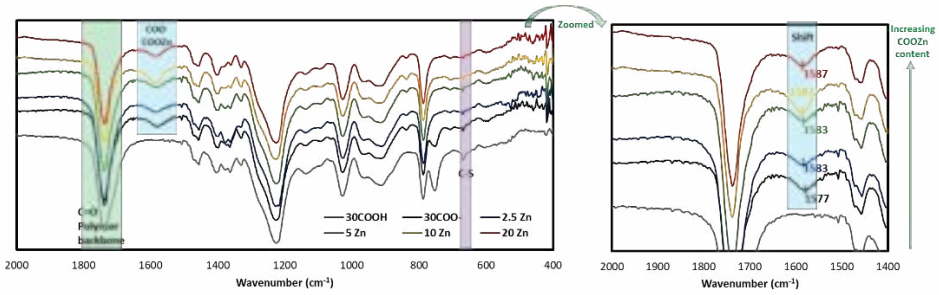

Figure 4-1. The FTIR spectra of PTMC-*co*-PexTMC$_{30COOH}$ before and after post-polymerization modification by thiol-ene reaction and crosslinked by Zn (II) acetate.

Stabilité thermique

Les résultats ont démontré que lors de la coordination du PTMC-*co*-PexTMC$_{30COOH}$ avec l'acétate de Zn(II), la stabilité thermique, comme l'indique l'augmentation des valeurs T_{10}, a été améliorée par rapport au polymère avant la coordination avec le Zn. Cette observation peut être attribuée à l'effet de réticulation des ions Zn se coordonnant avec les groupes carboxyliques, ce qui modifie probablement la structure chimique du polymère. Cette réticulation induite par la coordination améliore potentiellement les propriétés thermiques du polymère en modifiant son architecture macromoléculaire. Pour étudier l'influence de la coordination des métaux sur la stabilité thermique, une série d'ionomères à complexe métallique a été synthétisée en utilisant du sodium (I), du magnésium (II), du zinc (II) et du fer (II). Les résultats suggèrent que les variations dans le type d'ionomères à complexe métallique n'influencent pas de manière significative la stabilité thermique, comme l'indiquent les valeurs T_{10}. Ceci est probablement dû au fait que la structure de réticulation n'a pas un impact important sur le T_{10}, qui reflète

principalement les températures de dégradation thermique associées à la chaîne principale du polymère.

Mouillabilité

Les angles de contact sont de 31,5 ° ± 0,7, 44,3° ± 0,3, 45,7° ± 0,3, 50,5° ± 0,26 et 58,9° ± 0,2 pour PTMC-*co*-PexTMC$_{30COOH}$, PTMC-*co*-PexTMC$_{30COOH\text{-}2,5Zn}$, PTMC-*co*-PexTMC$_{30COOH\text{-}5Zn}$, PTMC-*co*-PexTMC$_{30COOH\text{-}10Zn}$, et PTMC-*co*-PexTMC$_{30COOH\text{-}20Zn}$, respectivement. Les résultats indiquent qu'une augmentation de la teneur en carboxylate de Zn(II) peut accroître de manière significative l'hydrophobie du PTMC-*co*-PexTMC$_{30COOH}$. Cette réduction de l'hydrophilie peut être attribuée à la formation d'un ionomère, ce qui implique une augmentation de la réticulation. Ce phénomène est probablement lié à la réduction des groupes carboxyliques disponibles, qui sont essentiels pour améliorer l'hydrophilie.

Comportement de dégradation

Les résultats obtenus indiquent que l'ionomère PTMC-*co*-PexTMC$_{30COOH\text{-}30Zn}$ a significativement réduit l'absorption d'eau de près de dix fois par rapport au PexTMC-*co*-TMC$_{30COOH}$, au cours de la même période (**Figure 4-2a**). En outre, une tendance similaire a été observée dans les expériences de perte de poids. Au cours de la même période, le PTMC-*co*-PexTMC$_{30COOH\text{-}30Zn}$ a présenté des pourcentages de perte de poids inférieurs à ceux du PTMC-*co*-PexTMC$_{30COOH}$. Les résultats indiquent que la formation de réseaux réticulés empêche efficacement la dégradation du PTMC-*co*-PexTMC$_{30COOH}$, ce qui est en accord avec des rapports précédents montrant que la réticulation du PTMC peut réduire la dégradation enzymatique.[56-58] Plus précisément, après 42 jours, le PTMC-*co*-PexTMC$_{30COOH}$ présentait une perte de poids de près de 90 % (**Figure 4-2b**), alors qu'après la réticulation avec le carboxylate de Zn(II), la perte de poids a été réduite à seulement 25 %. On peut en déduire que les groupes carboxyliques jouent un rôle en augmentant l'absorption d'eau et en agissant comme catalyseurs de dégradation,[29,45-46] ce qui accélère l'hydrolyse des liaisons ester dans le squelette du polymère. Yu et al. ont rapporté que la modification du PTMC avec un groupe carboxylique ou hydroxy pouvait accélérer l'hydrolyse plus rapidement que le PTMC non modifié.[29] Après la formation des ionomères, il peut y avoir une réduction de la disponibilité des groupes carboxyliques, qui à son tour augmente l'hydrophobie, ce qui entraîne une absorption d'eau et une perte de poids plus faibles. En outre, comme indiqué au chapitre III, la perte de poids initiale du PTMC-*co*-PexTMC$_{30COOH}$ pourrait être attribuée au processus d'érosion en masse. Toutefois, après la formation de l'ionomère PTMC-*co*-PexTMC$_{30COOH\text{-}20Zn}$, la perte de

poids initiale s'est déplacée pour ressembler au processus d'érosion de surface typique du PTMC normal.

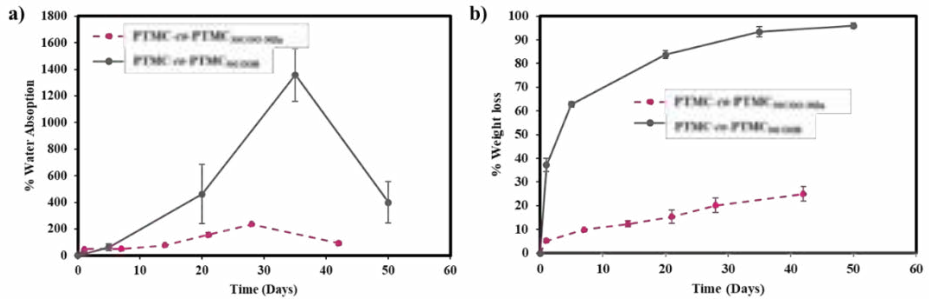

Figure 4-2. a) % d'absorption d'eau et b) % de perte de poids dans le tracé des circonstances de la lipase pour PTMC-*co*-PexTMC$_{30COOH}$ et PTMC-*co*-PexTMC$_{30COO\text{-}20Zn}$.

Adsorption des protéines

L'adsorption d'albumine des PTMC-*co*-PexTMC$_{30COOH}$, PTMC-*co*-PexTMC$_{30COOH\text{-}2,5Zn}$, PTMC-*co*-PexTMC$_{30COOH\text{-}5Zn}$, PTMC-*co*-PexTMC$_{30COOH\text{-}10Zn}$ et PTMC-*co*-PexTMC$_{30COOH\text{-}20Zn}$ revêtus sur verre était de 46. 33 µg/cm2 ± 0,03, 39,93 µg/cm2 ± 1,47, 38,77 µg/cm2 ± 2,04, 37,02 µg/cm2 ± 2,23 et 33,36 µg/cm2 ± 0,02, respectivement. Sur la base des résultats obtenus, il a été observé qu'une augmentation de la teneur en carboxylate de Zn(II) réduisait de manière significative l'adsorption des protéines.

Rhéologie

Le PTMC-*co*-PexTMC$_{30COOH}$ a toujours présenté une dominance du G'' sur le G' dans toute la gamme de températures expérimentales de 20 à 70°C (**Figure 4-3a**), ce qui pourrait signifier que le T_m (et transition sol gel) du PTMC-*co*-PexTMC$_{30COOH}$ était inférieur à 20°C et est associé à un comportement plastique. En revanche, lorsque les groupes carboxyliques du PTMC-*co*-PexTMC$_{30COOH}$ sont coordonnés avec l'acétate de Zn(II), on observe une augmentation notable de la T_m (où G' est égal à G''). Ce déplacement de la température de transition était directement corrélé à l'augmentation de la teneur en coordination métallique, atteignant des T_m plus élevés de 48°C pour PTMC-*co*-PexTMC$_{30COOH\text{-}2,5Zn}$ (**Figure 4-3b**), 59°C pour PTMC-*co*-PexTMC$_{30COOH\text{-}10Zn}$ (figure 4-3c), 61°C pour PTMC-*co*-PexTMC$_{30COOH\text{-}20Zn}$ (**Figure 4-3d**), et 70°C pour PTMC-*co*-PexTMC$_{30COOH\text{-}30Zn}$ (**Figure 4-3e**), respectivement. Ces résultats suggèrent que des ionomères à complexe métallique ont été formés et réticulés, comme indiqué par G' sur G'' après l'introduction de l'acétate de Zn(II). En outre, des concentrations plus élevées d'acétate de Zn(II) conduisent à une réticulation plus importante, qui peut maintenir le

comportement du gel à des températures plus élevées. Par conséquent, cela affecte la structure du polymère, qui à son tour influence les variations de T_d, T_{10}, T_m et l'enthalpie, comme le montrent les résultats de la DSC et de la TGA.

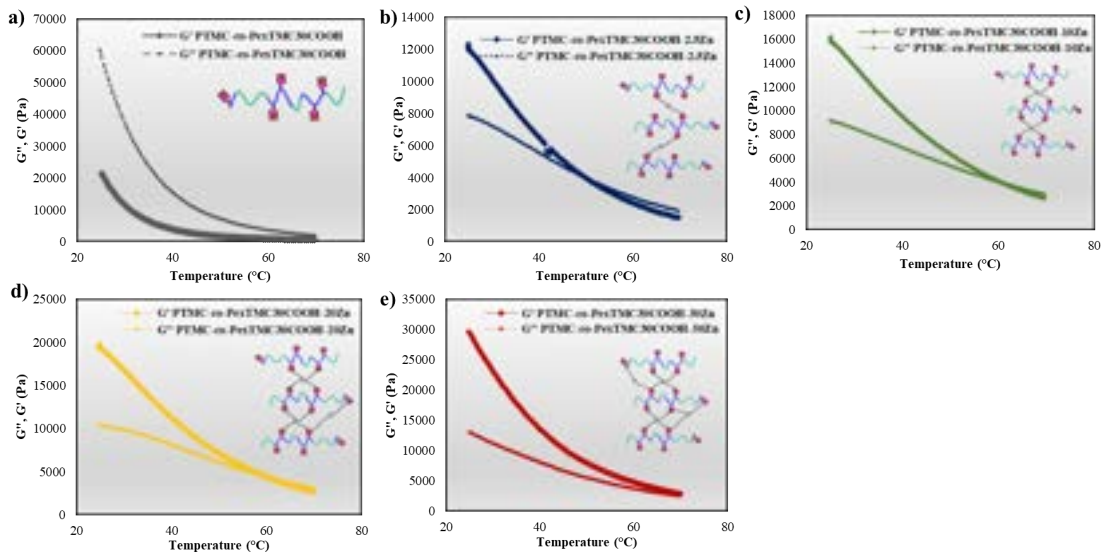

Figure 4-3. Tracé de la dépendance à la température de G' et G'' pendant le balayage dynamique isochrone de la température en fonction de la proportion d'acétate de Zn (II) ; a) PTMC-*co*-PexTMC$_{30COOH}$, b) PTMC-*co*-PexTMC$_{30COO\text{-}2,5Zn}$, c) PTMC-*co*-PexTMC$_{30COO\text{-}10Zn}$, d) PTMC-*co*-PexTMC$_{30COO\text{-}20Zn}$, et e) PTMC-*co*-PexTMC$_{30COO\text{-}30Zn}$.

Pour étudier l'impact de la coordination de différents métaux sur la rhéologie, une série d'ionomères à complexe métallique incorporant du sodium (I), du magnésium (II), du zinc (II) et du fer (II) a été étudiée. Les résultats indiquent que la variation du type de métal coordonné, au même ratio, n'a pas modifié de manière significative le T_m du PTMC-*co*-PexTMC$_{30COOH\text{-}30X}$. Pour le PTMC-*co*-PexTMC$_{30COOH\text{-}30Na}$ (**Figure 4-4a**), le PTMC-*co*-PexTMC$_{30COOH\text{-}30Mg}$ (**Figure 4-4c**) et le PTMC-*co*-PexTMC$_{30COOH\text{-}30Zn}$ (**Figure 4-4d**), G' a toujours dominé sur G'' jusqu'à environ 70°C. Cependant, le PTMC-*co*-PexTMC$_{30COOH\text{-}30Fe}$ (**Figure 4-4b**) a montré une dominance de G' sur G'' dans toute la gamme de températures expérimentales de 20 à 70 °C, ce qui suggère que le T_m du PTMC-*co*-PexTMC$_{30COOH\text{-}30Fe}$ pourrait dépasser 70 °C. En outre, les résultats suggèrent que le PTMC-*co*-PexTMC$_{30COOH\text{-}30Fe}$ présente un comportement plus élastique (G' plus élevé) que le PTMC-*co*-PexTMC$_{30COOH\text{-}30Na}$, le PTMC-*co*-PexTMC$_{30COOH\text{-}30Mg}$ et le PTMC-*co*-PexTMC$_{30COOH\text{-}30Zn}$ à la même température de mesure.

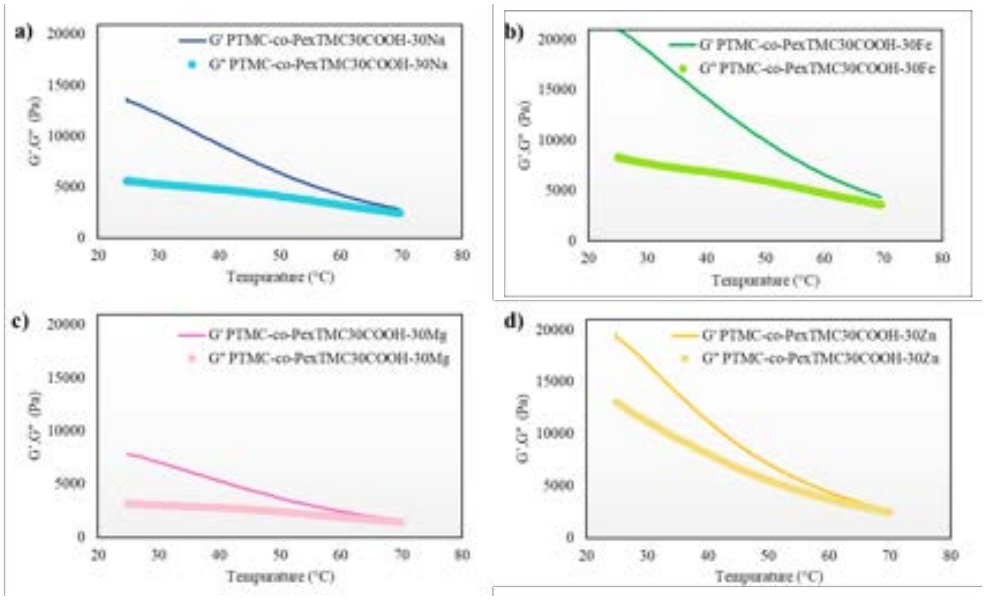

Figure 4-4. Tracé de la dépendance à la température de G' et G'' pendant le balayage dynamique isochrone de la température en faisant varier le type de coordonnées métalliques ; a) PTMC-*co*-PexTMC$_{30COO-30Na}$, b) PTMC-*co*-PexTMC$_{30COO-30Fe}$, c) PTMC-*co*-PexTMC$_{30COO-30Mg}$, et d) PTMC-*co*-PexTMC$_{30COO-30Zn}$.

Conclusion

La thèse intitulée « Synthèse et modulation des propriétés de nouveaux polymères biodégradables fonctionnels par le biais d'un contrôle fin de leur structure » visait à développer de nouvelles conceptions structurelles pour les APE et APC fonctionnels afin de contrôler précisément les propriétés cibles du niveau moléculaire au niveau macromoléculaire. Ce travail a étudié systématiquement quatre aspects clés de la conception des polymères biodégradables.

Le chapitre I a présenté le concept d'extrémité de chaîne fonctionnalisée pour développer des polyesters biodégradables fonctionnalisés par la modification de l'extrémité de chaîne. De nouveaux amorceurs à base d'acétal de vanilline ont été synthétisés pour produire des PLA fonctionnels avec fonctionnalisation précise de l'extrémité de chaîne. Ce chapitre a mis en évidence la réussite de l'incorporation d'amorceurs à base d'acétal de vanilline à l'extrémité du PLA, permettant une performance sensible au pH à l'extrémité de la chaîne fonctionnalisée conçue et facilitant l'agrégation contrôlée des particules de polymères dans des conditions physiologiques.

Le chapitre II a élucidé la stratégie de « contrôle de la structure aléatoire » par des études cinétiques détaillées, en explorant la préparation de polycarbonates avec divers groupes fonctionnels. La copolymérisation organocatalysée de CCs nouvellement fonctionnalisés avec du TMC a permis de contrôler la distribution de la séquence des monomères et

d'obtenir le caractère aléatoire souhaité. Ce chapitre a mis en évidence le contrôle réussi du caractère aléatoire et l'incorporation ajustable de groupes fonctionnels le long de la chaîne polymère, démontrant les progrès dans le développement de terpolymères pour l'introduction de groupes multifonctionnels.

Le chapitre III a étudié le comportement des copolymères biodégradables de polycarbonate fonctionnalisés par une chaîne latérale, en se concentrant sur des profils de dégradation précis, cruciaux pour les applications biomédicales. Des copolymères PTMC-*co*-PexTMC fonctionnalisés ont été synthétisés par des réactions click thiol-ène, en incorporant des groupes fonctionnels diol ou carboxyliques. L'introduction de groupes fonctionnels a renforcé l'hydrophilie et la liaison aux protéines, améliorant ainsi de manière significative les propriétés de libération des médicaments. Ces résultats soulignent le potentiel de ces copolymères conçus pour diverses applications biomédicales, mettant en évidence la capacité d'adapter les propriétés des copolymères par une fonctionnalisation stratégique.

Le chapitre IV s'est concentré sur l'utilisation des avantages du PTMC-*co*-PexTMC$_{COOH}$ pour la réticulation métal-carboxylate afin de moduler les propriétés des copolymères. Ce chapitre a démontré comment les chaînes latérales fonctionnelles facilitent la réticulation de l'ionomère, améliorant ainsi les propriétés mécaniques et la stabilité. L'ionomère synthétisé présente des propriétés thermiques supérieures et des taux de dégradation réduits, déplaçant le mécanisme de dégradation de l'érosion en masse à l'érosion en surface. Ces résultats soulignent le potentiel de transformation de l'utilisation de chaînes latérales fonctionnalisées pour la réticulation dans la conception de biopolymères, ouvrant la voie à des matériaux biodégradables avancés adaptés à des utilisations médicales spécifiques.

En résumé, cette thèse a fait progresser le domaine des polymères biodégradables en démontrant une fonctionnalisation stratégique et un contrôle précis des propriétés des polymères. Les méthodologies et les résultats présentés fournissent une base solide pour le développement de nouveaux matériaux biodégradables avec des performances améliorées dans des applications biomédicales ciblées.

References

(1) Azevedo, H.; Reis, R. Understanding the Enzymatic Degradation of Biodegradable Polymers and Strategies to Control Their Degradation Rate. *Biodegrad. Syst. Tissue Eng. Regen.Med.* **2004**, 177– 202. https://doi.org/10.1201/9780203491232.ch12

(2) Tiso, T.; Winter, B.; Wei, R.; Hee, J.; de Witt, J.; Wierckx, N.; Quicker, P.;

Bornscheuer, U. T.; Bardow, A.; Nogales, J.; Blank, L. M. The Metabolic Potential of Plastics as Biotechnological Carbon Sources – Review and Targets for the Future. *Metabolic Engineering*. **2022**, *71*, 77–98. https://doi.org/10.1016/j.ymben.2021.12.006.

(3) Künkel, A.; Becker, J.; Börger, L.; Hamprecht, J.; Koltzenburg, S.; Loos, R.; Schick, M. B.; Schlegel, K.; Sinkel, C.; Skupin, G.; Yamamoto, M. Polymers, Biodegradable. In *Ullmann's Encyclopedia of Industrial Chemistry*; Wiley-VCH GmbH: Weinheim, **2016**; pp 1– 29. https://doi.org/10.1002/14356007.n21_n01.pub2.

(4) Ghanbarzadeh, B.; Almasi, H. Biodegradable Polymers. *Biodegradation - Life of Science*; InTech, 2013. https://doi.org/10.5772/56230.

(5) Balaji, A. B.; Pakalapati, H.; Khalid, M.; Walvekar, R.; Siddiqui, H. Natural and Synthetic Biocompatible and Biodegradable Polymers. *Biodegradable and Biocompatible Polymer Composites: Processing, Properties and Applications*; Elsevier, **2017**; 3–32. https://doi.org/10.1016/B978-0-08-100970-3.00001-8.

(6) Jha, K.; Kataria, R.; Verma, J.; Pradhan, S. Potential Biodegradable Matrices and Fiber Treatment for Green Composites: A Review. *AIMS Materials Science* **2019**, *6* (1), 119–138. https://doi.org/10.3934/matersci.2019.1.119.

(7) Kunduru, K. R.; Basu, A.; Domb, A. J. Biodegradable Polymers: Medical Applications. *Encyclopedia of Polymer Science and Technology*; **2016**; 1–22. https://doi.org/10.1002/0471440264.pst027.pub2

(8) Kuperkar, K.; Atanase, L. I.; Bahadur, A.; Crivei, I. C.; Bahadur, P. Degradable Polymeric Bio(Nano)Materials and Their Biomedical Applications: A Comprehensive Overview and Recent Updates. *Polymers*. **2024**, *16*(2), 206 https://doi.org/10.3390/polym16020206.

(9) Zhang, X.; Fevre, M.; Jones, G. O.; Waymouth, R. M. Catalysis as an Enabling Science for Sustainable Polymers. *Chem. Rev.* **2017**, *118*(2), 839–885. https://doi.org/10.1021/acs.chemrev.7b00329.

(10) Tsuji, H.; Suzuyoshi, K. Environmental Degradation of Biodegradable Polyesters 1. Poly(e-Caprolactone), Poly[(R)-3-Hydroxybutyrate], and Poly(L-Lactide) Films in Controlled Static Seawater. *Polym. Degrad. Stab.* **2002**, *75*(2), 347–355. https://doi.org/10.1016/s0141-3910(01)00240-3.

(11) Anju, S.; Prajitha, N.; Sukanya, V. S.; Mohanan, P. V. Complicity of Degradable Polymers in Health-Care Applications. *Mater. Today Chem.* **2020**, *16*, 100236. https://doi.org/10.1016/j.mtchem.2019.100236.

(12) Yu, W.; Maynard, E.; Chiaradia, V.; Arno, M. C.; Dove, A. P. Aliphatic Polycarbonates from Cyclic Carbonate Monomers and Their Application as Biomaterials. *Chem. Rev.* **2021**, *121*(18), 10865–10907. https://doi.org/10.1021/acs.chemrev.0c00883.

(13) Pêgo, A. P.; Van Luyn, M. J. A.; Brouwer, L. A.; Van Wachem, P. B.; Poot, A. A.; Grijpma, D. W.; Feijen, J. *In Vivo* Behavior of Poly(1,3-Trimethylene Carbonate) and Copolymers of 1,3-Trimethylene Carbonate with *D,L*-Lactide or ε-Caprolactone: Degradation and Tissue Response. *J. Biomed. Mater. Res. A.* **2003**, *67* (3), 1044–1054. https://doi.org/10.1002/jbm.a.10121.

(14) Guillaume, S. M.; Carpentier, J. F. Recent Advances in Metallo/Organo-Catalyzed Immortal Ring-Opening Polymerization of Cyclic Carbonates. *Catal. Sci. Technol.* **2012**, *2*(5), 898–906. https://doi.org/10.1039/c2cy00507g.

(15) Dove, A. P. Controlled Ring-Opening Polymerisation of Cyclic Esters: Polymer Blocks in Self-Assembled Nanostructures. *Chem. Commun.* **2008**, *48*, 6446–6470. https://doi.org/10.1039/b813059k.

(16) Pounder, R. J.; Dove, A. P. Towards Poly(Ester) Nanoparticles: Recent Advances in the Synthesis of Functional Poly(Ester)s by Ring-Opening Polymerization. *Polym. Chem*. **2010**, *1*(3), 260–271. https://doi.org/10.1039/b9py00327d.

(17) Rittinghaus, R. D.; Herres-Pawlis, S. Catalysts as Key Enablers for the Synthesis of Bioplastics with Sophisticated Architectures. *Chem. Eur. J.* **2023**, *29*, e202202222. https://doi.org/10.1002/chem.202202222.

(18) Rao, W.; Cai, C.; Tang, J.; Wei, Y.; Gao, C.; Yu, L.; Ding, J. Coordination Insertion Mechanism of Ring-Opening Polymerization of Lactide Catalyzed by Stannous Octoate. *Chin. J. Chem.* **2021**, *39* (7), 1965–1974. https://doi.org/10.1002/cjoc.202000519.

(19) Li, X.; Chen, H.; Xie, S.; Wang, N.; Wu, S.; Duan, Y.; Zhang, M.; Shui, L. Fabrication of Photo-Crosslinkable Poly (Trimethylene Carbonate)/Polycaprolactone Nanofibrous Scaffolds for Tendon Regeneration. *Int. J. Nanomedicine.* **2020**, *15*, 6373–6383. https://doi.org/10.2147/IJN.S246966.

(20) Riley, T.; Stolnik, S.; Heald, C. R.; Xiong, C. D.; Garnett, M. C.; Illum, L.; Davis, S. S.; Purkiss, S. C.; Barlow, R. J.; Gellert, P. R. Physicochemical Evaluation of Nanoparticles Assembled from Poly(Lactic Acid)-Poly(Ethylene Glycol) (PLA-PEG) Block Copolymers as Drug Delivery Vehicles. *Langmuir* **2001**, *17*(11), 3168–3174. https://doi.org/10.1021/la001226i.

(21) Kan, K.; Akashi, M.; Ajiro, H. Polylactides Bearing Vanillin at Chain End Provided Dual Dynamic Interactions: Stereocomplex Formation and Nanostructure Control. *Macromol. Chem. Phys.* **2016**, *217* (24), 2679–2685. https://doi.org/10.1002/macp.201600395.

(22) Kan, K.; Akashi, M.; Ajiro, H. Dynamic Self-Assembly and Synthesis of Polylactide Bearing 5-Hydroxymethylfurfural Chain Ends. *ACS Appl. Polym. Mater.*

2019, *1* (2), 267–274. https://doi.org/10.1021/acsapm.8b00185.

(23) Knowles, J. P.; Whiting, A. The Effects of Ring Size and Substituents on the Rates of Acid-Catalysed Hydrolysis of Five- and Six-Membered Ring Cyclic Ketone Acetals. *European J. Org. Chem.* **2007**, *20*, 3365–3368. https://doi.org/10.1002/ejoc.200700244.

(24) Yuen, A. Y.; Bossion, A.; Veloso, A.; Mecerreyes, D.; Hedrick, J. L.; Dove, A. P.; Sardon, H. Efficient Polymerization and Post-Modification of: N -Substituted Eight-Membered Cyclic Carbonates Containing Allyl Groups. *Polym. Chem.* **2018**, *9*(18), 2458–2467. https://doi.org/10.1039/c8py00231b.

(25) Thomas, A. W.; Dove, A. P. Postpolymerization Modifications of Alkene-Functional Polycarbonates for the Development of Advanced Materials Biomaterials. *Macromol. Biosci*. **2016**, *16*(12), 1762–1775. https://doi.org/10.1002/mabi.201600310.

(26) Sanders, D. P.; Fukushima, K.; Coady, D. J.; Nelson, A.; Fujiwara, M.; Yasumoto, M.; Hedrick, J. L. A Simple and Efficient Synthesis of Functionalized Cyclic Carbonate Monomers Using a Versatile Pentafluorophenyl Ester Intermediate. *J. Am. Chem. Soc.* **2010**, *132* (42), 14724–14726. https://doi.org/10.1021/ja105332k.

(27) Tempelaar, S.; Mespouille, L.; Coulembier, O.; Dubois, P.; Dove, A. P. Synthesis and Post-Polymerisation Modifications of Aliphatic Poly(Carbonate)s Prepared by Ring-Opening Polymerisation. *Chem. Soc. Rev.* **2013**, *42*(3), 1312–1336. https://doi.org/10.1039/c2cs35268k.

(28) Shaikh, A.-A. G.; Sivaram, S. Organic Carbonates. *Chem. Rev*. **1996**, *96*(3), 951–976. https://doi.org/10.1021/cr950067i.

(29) Yu, F.; Zhuo, R. Synthesis, Characterization, and Degradation Behaviors of End-Group-Functionalized Poly(Trimethylene Carbonate)s. *Polym. J.* **2003**, *35* (8), 671–676. https://doi.org/10.1295/polymj.35.671.

(30) Zhang, L.; Brostowitz, N. R.; Cavicchi, K. A.; Weiss, R. A. Perspective: Ionomer Research and Applications. *Macromol. React. Eng.* **2014**, *8*(2), 81–99. https://doi.org/10.1002/mren.201300181.

(31) Kaneko, T.; Willner, D.; Monkovic, I.; Braslawsky, G. R.; Greenfield, R. S.; Vyas, D. M. New Hydrazone Derivatives of Adriamycin and Their Immunoconjugates—a Correlation between Acid Stability And. *Bioconjug. Chem.* **1991**, *2* (3), 133–141.

(32) Rodrigues, P. C. A.; Beyer, U.; Schumacher, P.; Roth, T.; Fiebig, H. H.; Unger, C.; Messori, L.; Orioli, P.; Paper, D. H.; Muè, R.; Kratz, F. Acid-Sensitive Polyethylene Glycol Conjugates of Doxorubicin: Preparation, In Vitro Efficacy and Intracellular Distribution. *Bioorg. Med. Chem.* **1999**, *7* (11), 2517–2524. https://doi.org/10.1016/s0968-0896(99)00209-6.

(33) McGuire, T. M.; López-Vidal, E. M.; Gregory, G. L.; Buchard, A. Synthesis of 5- to 8-Membered Cyclic Carbonates from Diols and CO2 A One-Step, Atmospheric Pressure and Ambient Temperature Procedure. *J. CO2 Util.* **2018**, *27*, 283–288. https://doi.org/10.1016/j.jcou.2018.08.009.

(34) McGuire, T. M.; Pérale, C.; Castaing, R.; Kociok-Köhn, G.; Buchard, A. Divergent Catalytic Strategies for the Cis/Trans Stereoselective Ring-Opening Polymerization of a Dual Cyclic Carbonate/Olefin Monomer. *J. Am. Chem. Soc.* **2019**, *141* (34), 13301–13305. https://doi.org/10.1021/jacs.9b06259.

(35) Tang, S.; Nozaki, K. Advances in the Synthesis of Copolymers from Carbon Dioxide, Dienes, and Olefins. *Acc Chem. Res.* **2022**, *55* (11), 1524–1532. https://doi.org/10.1021/acs.accounts.2c00162.

(36) Ngassam Tounzoua, C.; Grignard, B.; Detrembleur, C. Exovinylene Cyclic Carbonates: Multifaceted CO_2-Based Building Blocks for Modern Chemistry and Polymer Science. *Angew. Chem. - Int. Ed.* **2022**, *61*(22). https://doi.org/10.1002/anie.202116066.

(37) Hauser, A. W.; Hayward, R. C. Random Photografting of Polymers to Nanoparticles for Well-Dispersed Nanocomposites. *J. Polym. Sci. B. Polym. Phys.* **2016**, *54* (2), 152–158. https://doi.org/10.1002/polb.23803.

(38) Lynd, N. A.; Ferrier, R. C.; Beckingham, B. S. Recommendation for Accurate Experimental Determination of Reactivity Ratios in Chain Copolymerization. *Macromolecules* **2019**, *52* (6), 2277–2285. https://doi.org/10.1021/acs.macromol.8b01752.

(39) Palden, T.; Onghena, B.; Regadío, M.; Binnemans, K. Methanesulfonic Acid: A Sustainable Acidic Solvent for Recovering Metals from The Jarosite Residue of The Zinc Industry. *Green Chem.* **2019**, *21* (19), 5394–5404. https://doi.org/10.1039/c9gc02238d.

(40) Haramiishi, Y.; Kawatani, R.; Chanthaset, N.; Ajiro, H. Preparation of Block Copolymer of Poly(Trimethylene Carbonate) with Oligo(Ethylene Glycol) and The Surface Properties of The Dip Coated Film. *Polym. Test* **2020**, *86*. https://doi.org/10.1016/j.polymertesting.2020.106484.

(41) Andriani, F.; Fuoco, T. Statistical Enchainment of Ester/Ether and Carbonate Cleavable Bonds to Control Copolymers' Erosion Rate and Trigger Environment-Specific Degradation. *Eur. Polym. J.* **2022**, *178*. https://doi.org/10.1016/j.eurpolymj.2022.111457.

(42) Wu, L.; Wang, Y.; Zhao, X.; Mao, H.; Gu, Z. Investigating the Biodegradation Mechanism of Poly(Trimethylene Carbonate): Macrophage-Mediated Erosion by Secreting Lipase. *Biomacromolecules* **2023**, *24* (2), 921–928.

https://doi.org/10.1021/acs.biomac.2c01350.
(43) Domínguez de María, P.; Fernández-Álvaro, E.; ten Kate, A.; Bargeman, G. Role of Apparent PKa of Carboxylic Acids in Lipase-Catalyzed Esterifications in Biphasic Systems. *J. Mol. Catal. B. Enzym.* **2009**, *59* (1–3), 220–224. https://doi.org/10.1016/j.molcatb.2009.03.004.
(44) Mohajeri, S.; Chen, F.; De Prinse, M.; Phung, T.; Burke-Kleinman, J.; Maurice, D. H.; Amsden, B. G. Liquid Degradable Poly(Trimethylene-Carbonate- Co-5-Hydroxy-Trimethylene Carbonate): An Injectable Drug Delivery Vehicle for Acid-Sensitive Drugs. *Mol. Pharm.* **2020**, *17* (4), 1363–1376. https://doi.org/10.1021/acs.molpharmaceut.0c00064.
(45) Saha, S. K.; Tsuji, H. Effects of Molecular Weight and Small Amounts of D-Lactide Units on Hydrolytic Degradation of Poly(l-Lactic Acid)s. *Polym. Degrad. Stab.* **2006**, *91* (8), 1665–1673. https://doi.org/10.1016/j.polymdegradstab.2005.12.009.
(46) Gorrasi, G.; Pantani, R. Hydrolysis and Biodegradation of Poly(Lactic Acid). In *Adv. Polym. Sci*. **2017**, *279*, 119–151. https://doi.org/10.1007/12_2016_12.
(47) Yang, L.; Li, J.; Zhang, W.; Jin, Y.; Zhang, J.; Liu, Y.; Yi, D.; Li, M.; Guo, J.; Gu, Z. The Degradation of Poly(Trimethylene Carbonate) Implants: The Role of Molecular Weight and Enzymes. *Polym. Degrad. Stab.* **2015**, *122*, 77–87. https://doi.org/10.1016/j.polymdegradstab.2015.10.016.
(48) Fu, Y.; Kao, W. J. Drug Release Kinetics and Transport Mechanisms of Non-Degradable and Degradable Polymeric Delivery Systems. *Expert. Opin. Drug Deliv.* **2010**, *7* (4), 429–444. https://doi.org/10.1517/17425241003602259.
(49) Thevenot, P.; Hu, W.; Tang, L. Surface Chemistry Influences Implant Biocompatibility. *Current topics in medicinal chemistry* **2008**, *8* (4), 270–280. https://doi.org/10.2174/156802608783790901.
(50) Sivaraman, B.; Latour, R. A. The Adherence of Platelets to Adsorbed Albumin by Receptor-Mediated Recognition of Binding Sites Exposed by Adsorption-Induced Unfolding. *Biomaterials* **2010**, *31* (6), 1036–1044. https://doi.org/10.1016/j.biomaterials.2009.10.017.
(51) Xu, L. C.; Bauer, J. W.; Siedlecki, C. A. Proteins, Platelets, and Blood Coagulation at Biomaterial Interfaces. *Colloids Surf. B. Biointerfaces* **2014**, *124*, 49–68. https://doi.org/10.1016/j.colsurfb.2014.09.040.
(52) Schmidt, D. R.; Waldeck, H.; Kao, W. J. Protein Adsorption to Biomaterials. In *Biological Interactions on Materials Surfaces* **2009**, 1–18. https://doi.org/10.1007/978-0-387-98161-1_1.
(53) Gregory, G. L.; Williams, C. K. Exploiting Sodium Coordination in Alternating

Monomer Sequences to Toughen Degradable Block Polyester Thermoplastic Elastomers. *Macromolecules* **2022**, *55* (6), 2290–2299. https://doi.org/10.1021/acs.macromol.2c00068.

(54) Miwa, Y.; Kurachi, J.; Kohbara, Y.; Kutsumizu, S. Dynamic Ionic Crosslinks Enable High Strength and Ultrastretchability in a Single Elastomer. *Commun. Chem.* **2018**, *1* (1). https://doi.org/10.1038/s42004-017-0004-9.

(55) Kajita, T.; Tanaka, H.; Noro, A.; Matsushita, Y.; Nozawa, A.; Isobe, K.; Oda, R.; Hashimoto, S. Extremely Tough Block Polymer-Based Thermoplastic Elastomers with Strongly Associated but Dynamically Responsive Noncovalent Cross-Links. *Polymer (Guildf)* **2021**, *217*. https://doi.org/10.1016/j.polymer.2021.123419.

(56) Li, W.; Lin, M.; Wang, C.; Lu, Y.; Sui, Y.; Ni, X.; Guo, J.; Jiang, M.; Yang, L.; Cui, H. In Vitro Enzymatic Degradation of the PTMC/Cross-Linked PEGDA Blends. *Front Bioeng. Biotechnol.* **2023**, *11*. https://doi.org/10.3389/fbioe.2023.1253221.

(57) Zant, E.; Grijpma, D. W. Tough Biodegradable Mixed-Macromer Networks and Hydrogels by Photo-Crosslinking in Solution. *Acta Biomater.* **2016**, *31*, 80–88. https://doi.org/10.1016/j.actbio.2015.12.014.

(58) Hou, Z.; Hu, J.; Li, J.; Zhang, W.; Li, M.; Guo, J.; Yang, L.; Chen, Z. The in Vitro Enzymatic Degradation of Cross-Linked Poly(Trimethylene Carbonate) Networks. *Polymers (Basel)* **2017**, *9* (11). https://doi.org/10.3390/polym9110605.

Abstract

Biodegradable aliphatic polyesters (APEs) and polycarbonates (APCs) are promising candidates for clinical applications due to their low toxicity, biocompatibility, and biodegradability. Ring-opening polymerization (ROP) is widely employed to synthesize a wide range of APEs and APCs with well-controlled structures. In order to improve functionalities and expand applications in the biomedical field, this thesis focuses on the precise structural design of novel APEs and APCs featuring pendant functional groups introduced on the polymer chain or the chain ends, with the aim of evaluating properties that could enhance their potential in various biomedical applications. Our developed strategy includes on one hand, the synthesis of pH-responsive polylactides with functional chain ends using functionalized initiators to trigger aggregation. On the other hand, the copolymerization of trimethylene carbonate (TMC) and 5-methylene-1,3-dioxane-2-one (exTMC) was carried out to achieve perfect randomness in side-chain functionalization through post-polymerization thiol-ene reactions. This approach allows for adjustable types, amounts, and distributions of functional groups in a streamlined three-step process from monomer synthesis to functionalized polymer. Additionally, the investigation of various TMC and exTMC or functionalized exTMC copolymer structures for biomaterial applications was conducted. This study explored the tunability of copolymer functionality types and amounts to manage polymer properties effectively (hydrophilic/hydrophobic balance, degradability, biocompatibility …). Furthermore, precise structural design through crosslinking *via* metal-carboxylates was examined. Dynamic crosslinking to form ionomers with elastic properties was facilitated by coordinating metallic ions to the pendant carboxylate groups of PTMC-*co*-PexTMC$_{COOH}$, thereby extending the application of copolymers in appropriate biomedical fields. Overall, this thesis presents a comprehensive approach to the synthesis of functionalized biodegradable polymers, providing versatile and tunable materials for advanced biomedical applications.

Keywords: Biodegradable Polymers, Aliphatic polyesters, Aliphatic polycarbonates, Thiol-ene Reaction, Ring-opening Polymerization, Post-polymerization modification, Functionalized Polyesters, Functionalized polycarbonates, Ionomer, Crosslinking

Résumé

Les polyesters aliphatiques (APE) et les polycarbonates (APC) biodégradables sont des candidats prometteurs pour des applications cliniques en raison de leur faible toxicité, de leur biocompatibilité et de leur biodégradabilité. La polymérisation par ouverture de cycle (ROP) est largement utilisée pour synthétiser une large gamme d'APE et d'APC avec des structures bien contrôlées. Afin d'améliorer les fonctionnalités et d'étendre les applications dans le domaine biomédical, cette thèse se concentre sur la conception structurelle précise de nouveaux APE et APC comportant des groupes fonctionnels pendants introduits sur la chaîne polymère ou les extrémités de la chaîne, dans le but d'évaluer les propriétés qui pourraient améliorer leur potentiel dans diverses applications biomédicales. Notre stratégie comprend d'une part la synthèse de polylactides sensibles au pH avec des extrémités de chaîne fonctionnelles en utilisant des amorceurs fonctionnalisés pour déclencher l'agrégation. D'autre part, la copolymérisation du triméthylène carbonate (TMC) et du 5-méthylène-1,3-dioxane-2-one (exTMC) a été réalisée pour obtenir de copolymères à caractère aléatoire parfait avec la fonctionnalisation des chaînes latérales grâce à des réactions thiol-ène post-polymérisation. Cette approche permet d'ajuster les types, les quantités et les distributions de groupes fonctionnels dans un processus rationalisé en trois étapes, de la synthèse du monomère au polymère fonctionnalisé. En outre, l'étude de diverses structures de copolymères TMC et exTMC ou exTMC fonctionnalisés pour des applications de biomatériaux a été menée. Cette étude a exploré la possibilité d'accorder les types et les quantités de fonctionnalités des copolymères pour gérer efficacement les propriétés des polymères (équilibre hydrophile/hydrophobe, dégradabilité, biocompatibilité...). En outre, la conception structurelle précise par le biais de la réticulation via des carboxylates métalliques a été examinée. La réticulation dynamique pour former des ionomères aux propriétés élastiques a été facilitée par la coordination d'ions métalliques aux groupes carboxylates pendants du PTMC-co-PexTMC$_{COOH,}$ étendant ainsi l'application des copolymères dans des domaines biomédicaux appropriés. Dans l'ensemble, cette thèse présente une approche complète de la synthèse de polymères biodégradables fonctionnalisés, fournissant des matériaux polyvalents et réglables pour des applications biomédicales avancées.

Mots-clés : Polymères biodégradables, polyesters aliphatiques, polycarbonates aliphatiques, réaction thiol-ène, polymérisation par ouverture de cycle, modification post-polymérisation, polyesters fonctionnalisés, polycarbonates fonctionnalisés, ionomère, réticulation

Titre : Synthèse et Modulation des Propriétés de Nouveaux Polymères Dégradables Fonctionnels par le Contrôle Fin de Leur Structure

Mots clés : polyesters aliphatiques, copolymérisation, polycarbonates aliphatiques, modification post-polymérisation, réaction thiol-ène. polymérisation par ouverture de cycle, ionomère

Résumé : Les polyesters aliphatiques (APE) et les polycarbonates (APC) biodégradables sont des candidats prometteurs pour des applications cliniques en raison de leur faible toxicité, de leur biocompatibilité et de leur biodégradabilité. La polymérisation par ouverture de cycle (ROP) est largement utilisée pour synthétiser une large gamme d'APE et d'APC avec des structures bien contrôlées. Afin d'améliorer les fonctionnalités et d'étendre les applications dans le domaine biomédical, cette thèse se concentre sur la conception structurelle précise de nouveaux APE et APC comportant des groupes fonctionnels pendants introduits sur la chaîne polymère ou les extrémités de la chaîne, dans le but d'évaluer les propriétés qui pourraient améliorer leur potentiel dans diverses applications biomédicales. Notre stratégie comprend d'une part la synthèse de polylactides sensibles au pH avec des extrémités de chaîne fonctionnelles en utilisant des amorceurs fonctionnalisés pour déclencher l'agrégation. D'autre part, la copolymérisation du triméthylène carbonate (TMC) et du 5-méthylène-1,3-dioxane-2-one (exTMC) a été réalisée pour obtenir de copolymères à caractère aléatoire parfait avec la fonctionnalisation des chaînes latérales grâce à des réactions thiol-ène post-polymérisation. Cette approche permet d'ajuster les types, les quantités et les distributions de groupes fonctionnels dans un processus rationalisé en trois étapes, de la synthèse du monomère au polymère fonctionnalisé. En outre, l'étude de diverses structures de copolymères TMC et exTMC ou exTMC fonctionnalisés pour des applications de biomatériaux a été menée. Cette étude a exploré la possibilité d'accorder les types et les quantités de fonctionnalités des copolymères pour gérer efficacement les propriétés des polymères (équilibre hydrophile/hydrophobe, dégradabilité, biocompatibilité...). En outre, la conception structurelle précise par le biais de la réticulation via des carboxylates métalliques a été examinée. La réticulation dynamique pour former des ionomères aux propriétés élastiques a été facilitée par la coordination d'ions métalliques aux groupes carboxylates pendants du PTMC-co-PexTMCCOOH, étendant ainsi l'application des copolymères dans des domaines biomédicaux appropriés. Dans l'ensemble, cette thèse présente une approche complète de la synthèse de polymères biodégradables fonctionnalisés, fournissant des matériaux polyvalents et réglables pour des applications biomédicales avancées.

Title: Synthesis and Properties Modulation of Novel Functional Degradable Polymers by Means of Fine Tuning of Their Structure

Key words: Aliphatic polyesters, Aliphatic polycarbonates, Thiol-ene Reaction, Post-polymerization modification, Ring-opening Polymerization, Ionomer

Abstract: Biodegradable aliphatic polyesters (APEs) and polycarbonates (APCs) are promising candidates for clinical applications due to their low toxicity, biocompatibility, and biodegradability. Ring-opening polymerization (ROP) is widely employed to synthesize a wide range of APEs and APCs with well-controlled structures. In order to improve functionalities and expand applications in the biomedical field, this thesis focuses on the precise structural design of novel APEs and APCs featuring pendant functional groups introduced on the polymer chain or the chain ends, with the aim of evaluating properties that could enhance their potential in various biomedical applications. Our developed strategy includes on one hand, the synthesis of pH-responsive polylactides with functional chain ends using functionalized initiators to trigger aggregation. On the other hand, the copolymerization of trimethylene carbonate (TMC) and 5-methylene-1,3-dioxane-2-one (exTMC) was carried out to achieve perfect randomness in side-chain functionalization through post-polymerization thiol-ene reactions. This approach allows for adjustable types, amounts, and distributions of functional groups in a streamlined three-step process from monomer synthesis to functionalized polymer. Additionally, the investigation of various TMC and exTMC or functionalized exTMC copolymer structures for biomaterial applications was conducted. This study explored the tunability of copolymer functionality types and amounts to manage polymer properties effectively (hydrophilic/hydrophobic balance, degradability, biocompatibility ...). Furthermore, precise structural design through crosslinking via metal-carboxylates was examined. Dynamic crosslinking to form ionomers with elastic properties was facilitated by coordinating metallic ions to the pendant carboxylate groups of PTMC-co-PexTMCCOOH, thereby extending the application of copolymers in appropriate biomedical fields. Overall, this thesis presents a comprehensive approach to the synthesis of functionalized biodegradable polymers, providing versatile and tunable materials for advanced biomedical applications.